UNIVERSITY OF NAIROBI

COLLEGE OF BIOLOGICAL AND PHYSICAL SCIENCES

DEPARTMENT OF CHEMISTRY

PHYTOCHEMICAL INVESTIGATION OF SELECTED PLANTS IN THE FAMILIES ANACARDIACEAE AND ASTERACEAE FOR BIOACTIVE PRINCIPLES

BY:

SOUAIBOU YAOUBA

(Reg. No. I80/94474/2014)

A THESIS SUBMITTED IN FULFILMENT OF THE REQUIREMENTS FOR THE AWARD OF THE DEGREE OF DOCTOR OF PHILOSOPHY IN CHEMISTRY OF THE UNIVERSITY OF NAIROBI

2018

DECLARATION

I declare that his thesis is my original work and has not been submitted elsewhere for examination, award of a degree or publication. Where other people's work or my own work has been used, this has been properly acknowledged and referenced in accordance with the University of Nairobi's requirements.

.....Date.....03/12/2018

Souaibou Yaouba

(Reg. No: I80/94474/2014)

This PhD thesis has been submitted for examination with our approval as research supervisors

Prof. Abiy Yenesew
Department of Chemistry
University of Nairobi
.....Date 03/12/18

Dr Solomon Derese
Department of Chemistry,
University of Nairobi
.....Date 03/12/18

Dr. Eric M. Guantai
Department of Pharmacology and Pharmacognosy
University of Nairobi
.....Date 03/12/2018

DEDICATION

I dedicate this work to my family

ACKNOWLEDGEMENT

Glory be to Allah (Alhamdulillah) for the mercy He has bestowed on me to complete this PhD Degree. I express my heartfelt gratitude to my supervisors; Prof. Abiy Yenesew whose close supervision guidance and kindness are appreciated, Dr. Solomon Derese who has been very supportive and Dr. Eric M. Guantai who has always valued my research. I extend my gratitude to Prof. Mate Erdelyi (University of Gothenburg) who accepted me to carry out part of my work in his Laboratory. I can't continue without thanking Dr. Matthias Heydenreich for generating spectroscopic and spectrometric data of most my samples. I thank Prof. Dr. Dr. h.c. Michael Spiteller, Technical University of Dortmund, Germany for hosting me in his laboratory for part of my research work. I am very grateful to Intra ACP AFIMEQG project for granting me the scholarship without which this work couldn't have been achieved.

I hereby say thank you to Prof. Midiwo Jacob Ogweno for his support in supplying solvents through the International Science Program (ISP Sweden, grant KEN-02). I extend my thanks to the Swedish Research Council (Swedish Research Links, 2012-6124) for its financial support. I acknowledge Dr. Albert Ndakala for his guidance and assistance in carrying out some chemical reactions in the Laboratory. Support in this work was also received from Dr. Beatrice Irungu and is acknowledged. My sincere gratitude to Patrick Mutisso Challo for identifying my plants from the field. I happily thank all postgraduate students in the research groups at the Department of Chemistry, University of Nairobi. Dr. Negera Abdissa, Dr. Lois Mwikali Mutisya, Dr. Tsegaye Deyou, Dr. Yoseph Atilaw, Mr Marco M. Madirisha, Mr. Micheal Opata, Mr. George Kwesiga, Ms. Fozia A. Adem, Ms. Carolyne Chepkui, Ms. Maryanne W. Muhindi, Mr. Demissew and many others.

Besides, I say thank you to Prof. Nkengfack Augustin Ephrem who assisted me in coming to the University of Nairobi. To all my family members who always supported me in hard times especially to my brothers (Haman Moule, Ousmanou Yaouba, Yaya Yaouba) and sisters (Didjatou Yaouba, Aissatou Yaouba) for their support. Finally but not least, I appreciate the contribution of Prof. Hezekiah K. Chepkwony for the bioassays. Thanks to Mr Daniel S. Juma, Mr. Peter K. Muchai, Mr Gamau, Mr Njihia, who assisted me when carrying out my bioassay experiments.

TABLE OF CONTENTS

DECLARATION..... Error! Bookmark not defined.
DEDICATION ..... **iii**
ACKNOWLEDGEMENT ..... **iv**
LIST OF TABLES ..... **xi**
LIST OF FIGURES ..... **xiv**
LIST OF SCHEMES..... **xv**
LIST OF ABBREVIATIONS ..... **xvi**
LIST OF SYMBOLS..... **xviii**
LIST OF APPENDICES..... **xx**
ABSTRACT ..... **xxi**
CHAPTER ONE **1**
INTRODUCTION..... **1**
1.1 Background of the Study 1
1.2 Statement of the Problem..... 3
1.3 Objectives 4
1.3.1 General Objective 4
1.3.2 Specific Objectives 4
1.4 Justification and Significance of the Study..... 5
CHAPTER TWO **7**
LITERATURE REVIEW **7**
2.1 Causes of Common Microbial Infections 7
2.2 The Burden of Antimicrobial Resistance..... 8
2.3 Cause and Treatment of Inflammation 9
2.4 The Burden of Inflammation..... 9
2.5 Cause of Type 2 Diabetes Mellitus 10
2.6 The Burden of Type 2 Diabetes Mellitus..... 10
2.7 The Use of Plants as Antimicrobial, Anti-inflammatory and Antidiabetic Agents 11
2.7.1 Antimicrobial and antiparasitic agents from plants..... 11

2.7.2 Cytotoxic Agents from Plants 15
2.7.3 Anti-inflammatory Agents from Plants 16
2.7.4 Anti-type 2 diabetes mellitus agents from plants 18
2.8. Terpenoids 20
2.9 Biosynthesis of diterpenoids 21
2.10 The Family Anacardiaceae 22
2.10.1 The Genus *Lannea* 23
2.10.2 *Lannea rivae* (Chiov.) Sacleux 33
2.10.3 *Lannea schweinfurthii* (Engl.) Engl. 35
2.11 The Family Asteraceae 37
2.11.1 The Genus *Psiadia* 38
2.11.2 *Psiadia punctulata* Vatke (Asteraceae) 41
2.11.3 The Genus *Aspilia* 43
2.11.4 *Aspilia pluriseta* Schweinf. 47
2.11.5 *Aspilia mossambicensis* (Oliv.) Wild (Asteraceae) 49
2.11.6 Biological Activity of Compounds from the Genus *Aspilia* 51
CHAPTER THREE 52
MATERIALS AND METHODS 52
3.1 Plant Materials 52
3.2 General Methods 52
3.3 X-ray Diffraction Analyses 53
3.4 Extraction and Isolation 53
3.4.1 Extraction and Isolation of Compounds from the Root of *Lannea rivae* 53
3.4.2 Extraction and Isolation of Compounds from the Stem Bark of *Lannea rivae* 54
3.4.3 Extraction and Isolation of Compounds from the Root of *Lannea schweinfurthii* 54

3.4.4 Extraction and Isolation of Compounds from the Stem bark of *Lannea schweinfurthii* 55

3.4.5 Extraction and Isolation of Compounds from the Leaves of *Psiadia punctulata* 56

3.4.6 Extraction and Isolation of Compounds from the Stem Bark of *Psiadia punctulata* 57

3.4.7 Extraction and Isolation of Compounds from the Root of *Psiadia punctulata*.... 57

3.4.8 Extraction and Isolation of Compounds from the Root of *Aspilia pluriseta* 58

3.4.9 Extraction and Isolation of Compounds from the Aerial Part of *Aspilia pluriseta* 59

3.4.10 Extraction and Isolation of Compounds from the Root of *Aspilia mossambicensis* 59

3.4.11 Extraction and Isolation of Compounds from the Aerial Part of *Aspilia mossambicensis* 60

3.5 Procedure of Structural Modification 60

3.5.1 Methylation of Compounds **211** and **243** 60

3.5.2 Acetylation of Compounds **220** and **210** 61

3.5.3 Preparation of Compound **261** and **263** 62

3.5.4 Preparation of Compound **260** 63

3.5.5 Preparation of Compound **263** 63

3.5.6 Oxidation of Compound **207** 64

3.5.7 Preparation of Compound **268** 64

3.5.8 Hydrogenation of Compounds **240** and **243** 65

3.6 Physical Constants and Spectroscopic Data of the Isolated Compounds 66

3.6.1 Physical Constants and Spectroscopic Data of Compounds from *Lannea rivae* . 66

3.6.2 Physical Constants and Spectroscopic Data of Compounds from *Lannea schweinfurthii* 67

3.6.3 Physical Constants and Spectroscopic Data of Compounds from *Psiadia punctulata* 68

3.6.4 Physical Constants and Spectroscopic Data of Compounds from *Aspilia pluriseta* 71

3.6.5 Physical Constants and Spectroscopic Data of Compounds from *Aspilia mossambicensis* 73

3.6.6 Physical Constants and Spectroscopic Data of Synthetic Derivatives 74

3.7 Procedure for Biological Studies..... 76

3.7.1 Antimicrobial Activity 76

3.7.2 Cytotoxicity Assay..... 77

3.7.3 Anti-inflammatory Activity..... 78

3.7.4 Oral Glucose Tolerance Test..... 79

3.7.5 *In vitro* Antiplasmodial Activity 79

3.8 Theoritical Electronic Circular Dichroism Calculation..... 79

3.9 Statistical Analysis 80

CHAPTER FOUR..... 81

RESULTS AND DISCUSSION 81

4.1 Characterization of Compounds Isolated from *Lannea* species..... 81

4.1.1 Characterization of Compounds Isolated from the Roots of *Lannea rivae* 81

4.1.2 Characterization of Compounds Isolated from Stem Bark of *Lannea rivae*..... 97

4.1.3 Characterization of Compounds Isolated from Stem barks of *Lannea schweinfurthii*..... 100

4.1.4 Characterization of Compounds Isolated from Roots of *Lannea schweinfurthii* 110

4.1.5 Summary of Compounds Isolated from *Lannea* Species..... 113

4.2 Biological Activity of the Isolated Compounds from *Lannea* Species 114

4.2.1 Antimicrobial Activity of *Lannea* species 114

4.2.2 Cytotoxicity of *Lannea* species 115

4.2.3 Anti-inflammatory Activity of *Lannea* Species 116

4.3 Characterization of Secondary Metabolites Isolated from *Psiadia punctulata* 117

4.3.1 Characterization of Secondary Metabolites Isolated from Leaves of *Psiadia punctulata* 117

4.3.2 Secondary Metabolites Isolated from Stem Bark of *Psiadia punctulata*..... 149

4.3.3. Secondary Metabolites Isolated from the Roots of *Psiadia punctulata* 154

4.3.4 Summay of Compounds of *Psiadia punctulata* 162

4.3.5 Chemotaxonomic Significance on *Psiadia punctulata*..... 162

4.4 Biological Activity of the Isolated Compounds from *Psiadia punctulata* 163

4.4.1 Antimicrobial Activity of *Psiadia punctulata*..... 163

4.4.2 Cytotoxicity of *Psiadia punctulata*..... 165

4.4.3 Anti-inflammatory Activity of *Psiadia punctulata* 166

4.4.4 Oral Glucoce Tolerance Test of *Psiadia punctulata* 167

4.4.5 Antiplasmodial Activity of *Psiadia punctulata*..... 170

4.5 Characterization of Secondary Metabolites Isolated from *Aspilia pluriseta* and *Aspilia mossambicensis*..... 170

4.5.1 Characterization of Compounds Isolated from Roots of *Aspilia pluriseta*..... 171

4.5.2 Characterization of Secondary Metabolites Isolated from Aerial Parts of *Aspilia pluriseta* 192

4.5.3 Characterization of Secondary Metabolites Isolated from Roots of *Aspilia mossambicensis* 202

4.5.4 Characterization of Compounds Isolated from Aerial parts of *Aspilia mossambicensis* 209

4.5.5 Summary of Compounds from Aspilia pluriseta and *Aspilia mossambicensis*.. 215

4.6 Biological Activities of the Isolated Compounds from *Aspilia* species 215

4.6.1 Antimicrobial Activity of *Aspilia* species 215

4.6.2 Cytotoxicity on *Aspilia* Species 217
4.6.3 Anti-inflammatory Activity on *Aspilia* Species 218
4.6.4 Oral glucose Tolerance Test on *Aspilia* Species 219
4.7 Characterisation of the Synthetic Derivatives of the Isolated Compounds 221
4.7.1 Synthetic Derivatives of the Compounds from *Psiadia punctulata* 221
4.7.2 Synthetic Derivatives of Compounds from *Aspilia pluriseta* 236
4.8 Summary of the Synthetic Derivatives 243
4.9 Biological Activities of the Synthetic Derivatives 244
4.9.1 Antimicrobial Activity 244
4.9.2 Cytotoxicity of the Synthetic Derivatives 245
CHAPTER FIVE 247
CONCLUSION AND RECOMMENDATIONS 247
5.1 Conclusion 247
5.2 Recommendations 248
REFERENCES 249
APPENDICES 270

LIST OF TABLES

Table 2.1: Ethnomedicinal Uses of Plants of the Genus *Lannea* 24
Table 2.2: Some Compounds Reported from *Lannea* Species..... 27
Table 2.3: Biological Activity of Compounds Reported from *Lannea* 32
Table 2.4: Biological Activity of Compounds Reported from *Lannea rivae* 35
Table 2.5: Biological Activity of Compounds Reported from *Lannea schweinfurthii* 37
Table 2.6: Ethnobotanical Uses of *Psiadia* Species 39
Table 2.7: Reported Compounds from *Psiadia punctulata* 42
Table 2.8: Biological Activity of Compounds Reported from the Genus *Psiadia* 43
Table 2.9: Ethnobotanical uses of *Aspilia* Species..... 44
Table 2.10: Reported Compounds from the Genus *Aspilia* 45
Table 2.11: Compounds Isolated from *Aspilia pluriseta* 49
Table 2.12: Reported compounds from *Aspilia mossambicensis* 50
Table 2.13: Biological Activity of Compounds Reported from *Aspilia* Species 51
Table 4.1: ^{1}H (800 MHz) and ^{13}C (200 MHz) NMR Data of 186 ($CDCl_3$)..... 82
Table 4.2: Theoretically Calculated Coupling Constants of 186 86
Table 4.3: ^{1}H (600 MHz) and ^{13}C (150 MHz) NMR Data of 187 (CD_2Cl_2)..... 88
Table 4.4: ^{1}H NMR (600 MHz) and ^{13}C NMR (150 MHz) Data of 188 and 189 91
Table 4.5: ^{1}H (600 MHz) and ^{13}C NMR (150 MHz) Data of 190 in CD_2Cl_2 93
Table 4.6: ^{1}H (600 MHz) and ^{13}C (150 MHz) NMR Data of 191 and 192 95
Table 4.7: ^{1}H (600 MHz) and ^{13}C (150 MHz) NMR Data of 193 and 194 98
Table 4.8: ^{1}H (600 MHz) and ^{13}C (150 MHz) NMR Data of 195 (CD_2Cl_2)..... 101
Table 4.9: ^{1}H (600 MHz) and ^{13}C (150 MHz) NMR Data of 196 in CD_2Cl_2 103
Table 4.10: ^{1}H (600 MHz) and ^{13}C (150 MHz) NMR Data of 197 in CD_2Cl_2 104
Table 4.11: ^{1}H (600 MHz) and ^{13}C (150 MHz) NMR Data of 198 in CD_2Cl_2 105
Table 4.12: ^{1}H (600 MHz) and ^{13}C (150 MHz) Data of 199 in CD_2Cl_2 107
Table 4.13: ^{1}H (600 MHz) and ^{13}C NMR (150 MHz) Data of 200 in CD_2Cl_2 108
Table 4.14: ^{1}H (600 MHz) and ^{13}C NMR (150 MHz) Data of 201 in CD_2Cl_2 109
Table 4.15: ^{1}H (600 MHz) and ^{13}C (150 MHz) NMR Data of 202 and 203 111
Table 4.16: ^{1}H NMR (600 MHz) and ^{13}C (150 MHz) NMR Data of 204 in Acetone-d_6 113
Table 4.17: Antimicrobial Assay of *Lannea* Species 115
Table 4.18: Cytotoxicity of *Lannea* Species Against Mammalian Cell Lines..... 116

Table 4.19: Anti-inflammatory Activity – inhibition of carrageenan-induced paw oedema of crude extracts and compounds of *Lannea* species 117
Table 4.20: ^{1}H and ^{13}C NMR Data of 205 (CD_2Cl_2) and 206 (C_5D_5N) 120
Table 4.21: ^{1}H and ^{13}C NMR Data of 207 and 208 in $CDCl_3$ 124
Table 4.22: ^{1}H and ^{13}C NMR data of 209 in $CDCl_3$ 128
Table 4.23: ^{13}C (200 MHz) NMR Data of 210, 211 and 212 in $CDCl_3$ 129
Table 4.24: ^{1}H (800 MHz) NMR Data of 210, 211 and 212 in $CDCl_3$ 131
Table 4.25: ^{1}H (800 MHz) and ^{13}C (200MHz) NMR Data of 213 in $CDCl_3$ 133
Table 4.26: ^{1}H (800 MHz) and ^{13}C (200 MHz) NMR Data of 214 and 215 in $CDCl_3$ 135
Table 4.27: ^{1}H (800 MHz) and ^{13}C (200 MHz) NMR Data of 216 in $CDCl_3$ 139
Table 4.28: ^{1}H (800 MHz) and ^{13}C (200 MHz) NMR Data of 217 and 218 in Acetone-d_6 141
Table 4.29: ^{1}H (800 MHz) and ^{13}C (200 MHz) NMR Data of 220 and 221 in $CDCl_3$ 145
Table 4.30: ^{1}H (800 MHz) and ^{13}C (200 MHz) NMR Data of 222 in $CDCl_3$ 147
Table 4.31: ^{1}H (800 MHz) and ^{13}C (200 MHz) NMR Data of 223 and 224 in $CDCl_3$ 148
Table 4.32: ^{1}H (800 MHz) and ^{13}C (200 MHz) NMR Data of 225 in $CDCl_3$ 150
Table 4.33: ^{1}H (600 MHz) and ^{13}C (150 MHz) NMR Data of 226 and 227 in CD_2Cl_2 .. 151
Table 4.34: ^{1}H (800 MHz) and ^{13}C (200 MHz) NMR Data of 228 in $CDCl_3$ 154
Table 4.35: ^{1}H (800 MHz) and ^{13}C (200 MHz) NMR Data of 229 and 230 in acetone-d_6 155
Table 4.36: ^{1}H (600 MHz) and ^{13}C (150 MHz) NMR Data of 231 and 232 in CD_2Cl_2 .. 159
Table 4.37: ^{1}H (800 MHz) and ^{13}C NMR (200 MHz) Data of 233 in $CDCl_3$ 161
Table 4.38: Chemeotaxonommy comparison of *Psiadia punctulata* and *Psiadia arabica* 163
Table 4.39: Anti-microbial assay of *Psiadia punctulata* 164
Table 4.40: Cytotoxicity of *Psiadia punctulata* 166
Table 4.41: Anti-inflammatory of *Psiadia punctulata* 167
Table 4.42: Oral Glucose Tolerance Test (OGTT) of *Psiadia punctulata* 169
Table 4.43: Antiplasmodial Activity of *Psiadia punctulata* 170
Table 4.44. ^{1}H (800 MHz) and ^{13}C (200 MHz) NMR Data of 234 ($CDCl_3$) 171
Table 4.45: ^{1}H (800 MHz) and ^{13}C (200 MHz) NMR Data of 235 ($CDCl_3$) 175
Table 4.46: ^{1}H (800 MHz) and ^{13}C (200 MHz) NMR Data of 236 ($CDCl_3$) 178
Table 4.47: The Literature Reported NMR Data for 237, 237a and 237b and the ^{1}H (800 MHz) and ^{13}C NMR (200 MHz) Data of 237 in $CDCl_3$. 181
Table 4.48: ^{1}H (600 MHz) and ^{13}C (150 MHz) NMR data of 238 and 239 in CD_2Cl_2 .. 184
Table 4.49: ^{1}H (600 MHz) and ^{13}C (150 MHz) NMR Data of 240 and 241 in CD_2Cl_2 .. 187

Table 4.50: ^{1}H (600 MHz) and ^{13}C (150 MHz) NMR Data of 242 and 243 in CD_2Cl_2 .. 190
Table 4.51: ^{1}H (600 MHz) and ^{13}C (150MHz) NMR Data of 244 and 245 in CD_2Cl_2 .. 194
Table 4.52: ^{1}H (600 MHz) and ^{13}C (150 MHz) NMR Data of 246 and 247 in CD_2Cl_2 .. 197
Table 4.53: ^{1}H (600 MHz) and ^{13}C (150 MHz) NMR Data of 248 in CD_2Cl_2 200
Table 4.54: ^{1}H (600 MHz) and ^{13}C (150 MHz) NMR Data of 249 in CD_2Cl_2 202
Table 4.55: ^{1}H (600 MHz) and ^{13}C (150 MHz) NMR Data of 250 in CD_2Cl_2 203
Table 4.56: ^{1}H (600 MHz) and ^{13}C (150 MHz) NMR Data of 251 and 252 in CD_2Cl_2 .. 205
Table 4.57: ^{1}H (600 MHz) and ^{13}C (150 MHz) NMR Data of 253 in CD_2Cl_2 208
Table 4.58: ^{1}H (600 MHz) and ^{13}C (150 MHz) NMR Data of 254 in CD_2Cl_2 210
Table 4.59: ^{1}H (600 MHz) and ^{13}C (150 MHz) NMR Data of 255 and 256 in CD_2Cl_2 .. 212
Table 4.60: ^{1}H (600 MHz) and ^{13}C (150 MHz) NMR Data of 257 in CD_2Cl_2 215
Table 4.61: Antimicrobial results on *Aspilia* species..... 216
Table 4.62: Cytotoxicity of *Aspilia* species 218
Table 4.63: Anti-inflammatory Activity Results on *Aspilia* Species..... 219
Table 4.64: Oral Glucose Tolerance Test (OGTT) on *Aspilia* Species 220
Table 4.65: ^{1}H (600 MHz) and ^{13}C (150 MHz) NMR Data of 258 and 259 in $CDCl_3$.... 223
Table 4.66: ^{1}H (800 MHz) and ^{13}C (200 MHz) NMR Data of 260 in $CDCl_3$ 224
Table 4.67: ^{1}H (800 MHz) and ^{13}C (200 MHz) NMR Data of 261 and 262 in $CDCl_3$.... 226
Table 4.68: ^{1}H (800 MHz) and ^{13}C (200 MHz) NMR Data of 263 and 264 in $CDCl_3$... 229
Table 4.69: ^{1}H (800 MHz) and ^{13}C (200 MHz) NMR Data of 265 and 266 in $CDCl_3$.... 232
Table 4.70: ^{1}H (800 MHz) and ^{13}C (200 MHz) NMR Data of 267 in $CDCl_3$ 235
Table 4.71: ^{1}H (600 MHz) and ^{13}C (150 MHz) NMR Data of 268 (CD_2Cl_2) and 269 (Acetone-d_6) 237
Table 4.72: ^{1}H (600 MHz) and ^{13}C (150 MHz) NMR Data of 270 and 271 in CD_2Cl_2 .. 241
Table 4.73: Antimicrobial activity of the modified compounds 245
Table 4.74: Cytotoxicity of the Derivatized Compounds Against Normal and Cancer cell lines..... 246

LIST OF FIGURES

Figure 2.1: Photo of Lannea rivae 34

Figure 2.2: Photo of *Lannea schweinfurthii* 36

Figure 2.3: Photo of *Psiadia punctulata* 41

Figure 2.4: Photo of *Aspilia pluriseta* 48

Figure 2.5: Photo of Aspilia mossambicensis 50

Figure 4.1: Calculated Global Energy Minimum Geometries of Conformers of (4R,6S)-186a 83

Figure 4.2: ECD Spectra of Compound 186 84

Figure 4.3: Molecular Orbitals of 186 85

Figure 4.4: Crystal Structure Representation of Some Compounds Isolated from *Psiadia punctalata* 122

Figure 4.5: Blood Glucose Levels Reduction Graph of *Psiadia punctulata* 168

Figure 4.6: Some of the key NOE correlations observed for compound 234. 173

Figure 4.7: Crystal Structure Representation of Some Compounds Isolated from *Aspilia* Species 179

LIST OF SCHEMES

Scheme 2.1 Mevalonic Acid and Methyl Erythritol Biosynthetic Pathways of..... 21

Scheme 2.2 Cyclization of GGPP During Biosynthesis of Cyclic Diterpenoids 22

LIST OF ABBREVIATIONS

AMA	*Aspila mossambicensis* aerial part extract
AMR	*Aspila mossambicensis* aerial part extract
ANOVA	Analysis of Variance
APA	*Aspilia pluriseta* aerial part extract
APR	*Aspilia pluriseta* root extract
CC	Column Chromatography
CD	Circular Dichroism
COSY	Correlation spectroscopy
DCM	Dichloromethane
DMSO	Dimetyl sulfoxide
ECD	Electron Circular Dichroism
EIMS	Election Impact Mass Spectrometry
ESIMS	ElectroSpray Ionization Mass Spectrometry
HMBC	Heteronuclear Multiple Bond Correlation
HOMO	Highest Occupied Molecular Orbitals
HPLC	High Pressure Liquid Chromatography
HRESIMS	High Resolution Electro Spray Ionization Mass Spectrometry
HRMS	High Resolution Mass Spectrometry
HSQC	Heteronuclear Single Quantum Coherence
IR	Infra Red
LC-MS	Liquid Chromatography-Mass Spectrometry
LRR	*Lannea rivae* root extract
LRB	*Lannea rivae* stem bark extract
LSR	*Lannea schweinfurthii* root extract
LSB	*Lanne schweinfurthii* stem bark extract
LUMO	Lowest Unoccupied Molecular Orbitals
MIC	Minimum Inhibitory Concentration
MO	Molecular Orbitals
MS	Mass Spectrometry
MTT	3-[4,5-Dimethylthiazole-2-yl]-2,5-diphenyltetrazolium bromide
NMR	Nuclear Magnetic Resonance
NOE	Nucler Overhauser Effect

OD	Optical Density
OGTT	Oral Glucose Tolerance Test
Prep-HPLC	Preparative High Pressure Liquid Chromatography
PTLC	Preparative Thin Layer Chromatography
SD	Standard Deviation
T2DM	Type Two Diabetes Mellitus
TLC	Thin Layer Chromatography
UV	Ultra Violet
WHO	World Health Organization
NSAIDs	Non-Steroidal Anti-inflammatory Drugs

LIST OF SYMBOLS

$[\alpha]_D^{20}$	Specific rotation determined at the sodium D-line wavelength (589 nm) at 20 °C
$[M]^+$	Molecular ion peak
$[M+H]^+$	Protonated molecular ion peak
Ac_2O	Acetic anhydride
AcONa	Sodium acetate
br s	Broad singlet
calc.	Calculated
CC_{50}	Concentration at 50% effectiveness
d	Doublet
dd	Doublet of a doublet
ddt	Doublet of a doublet of a triplet
dL	Decilitre
dt	Doublet of a triplet
EtOAc	Ethyl acetate
EtOH	Ethanol
g	Gram
h	Hour
H_2SO_4	Sulfuric acid
HCl	Hydrochloric acid
Hz	Hertz
IC_{50}	Inhibitory Concentration at 50% effectiveness
J	Coupling constant
Kg	Kilogramme
KOAc	Potassium acetate
KOH	Potassium hydroxide
m/z	Mass to charge ratio
Me	Methyl
MeI	Methyl iodide
MeOH	Methanol
mg	Miligramme
$MgSO_4$	Magnesium sulfate

MHz	Megahertz
min	Minute
mL	Mililitre
Mult.	Multiplicity
Na_2SO_4	Sodium sulfate
$NaHCO_3$	Sodium hydro carbonate
NBS	*N*-bromosuccinimide
$NH_2OH.HCl$	Hydroxylamine hydrochloride
q	Quartet
Rel. int.	Relative intensity
s	Singlet
t	Triplet
vis	Visible
δ	Chemical shift
ΔE	Energy gap
λ_{max}	Wavelength at maximum absorption
µg	Microgramme

LIST OF APPENDICES

Appendix 1: Spectra for the Dompounds of *Lannea* Species.....270

Appendix 2: Spectra for the Compounds Isolated from *P. punctulata*.....299

Appendix 3: Spectra for the Compounds Isolated from *Aspilia* Species.....357

Appendix 4: Spectra for the Derivatized Compounds.....395

Appendix 5: Publications from this PhD work.....447

ABSTRACT

This thesis describes an investigation of two plants from Anacardiaceae plant family namely *Lannea rivae* (Chiov) Sacleux and *Lannea schweinfurthii* (Engl.) Engl. and three other plants from Asteraceae family; *Psiadia punctulata* Vatke, *Aspilia pluriseta* Schweinf. and *Aspilia mossambicensis* (Oliv.) Wild for their bioactive principles. Chromatographic separation of different extracts from the five plants led to the identification of a total of seventy six compounds among which ten were new, and fourteen derivatives obtained by chemical derivatization. Three structures wrongly reported in the literature were corrected. The structure elucidation of the compounds was performed by using Nuclear Magnetic Resonance (NMR), Ultra Violet (UV), Infra-Red (IR), Optical Rotation (OR) and Mass Spectrometric (MS) techniques. In the case of seventen compounds X-ray crystallography was used. The isolated compounds and crude extracts were tested for their cytotoxicity, antimicrobial, anti-inflammatory, antiplasmodial and antidiabetic activities. The root extract of *Lannea rivae* resulted in isolation of seven compounds of which the alkenylcyclohexanone derivatives; (4*R*,6*S*)-4,6-dihydroxy-6-((*Z*)-nonadec-14′-en-1-yl)cyclohex-2-en-1-one (**186**) and (2*S**,4*R**,5*S**)-2,4,5-trihydroxy-2-((*Z*)-nonadec-14′-en-1-yl)cyclohexanone (**187**) are new. The known compounds include taraxerol (**188**), taraxerone (**189**), *β*-sitosterol (**190**), epicatechin gallate (**191**), and 3’’,5’’-dimeyhoxy-epicatechin gallate (**192**). Epicatechin gallate showed high antimicrobial activity against *Staphylococcus aureus* and *Escherichia coli*, but most of the known compounds isolated from this plant were not effective against the two strains. From the stem bark of *L. rivae,* two known compounds were isolated, namely lupeol (**193**) and daucosterol (**194**). Roots extracts of *Lannea schweinfurthii* resulted in the identification of seven compounds namely 3-((*E*)-nonadec-16'-enyl)phenol (**195**), 1-((*E*)-heptadec-14'-enyl)cyclohex-4-ene-1,3-diol (**196**), 1-((*E)*-tridecadec-10'-enyl)cyclohex-4-en-1,3-diol (**197**), 1-((*E*)-pentadec-12'-enyl)cyclohex-4-ene-1,3-diol (**198**), 1-((*E,E*)-nonadeca-12',14'-dienyl)cyclohex-4-en-1,3-diol (**199**), 1-((*E*)-nonadec-16'-enyl)cyclohex-4-en-1,3-diol (**200**) and catechin (**201**). The stem bark of *L. schweinfurthii* resulted in the isolation of seven compounds; *4,4'-diydroxy-3-methoxy-3'-O-glucosyl-ellagic acid* (**202)**, 4,4'-dihydroxy-3-methoxy-3'-*O*-[rhamnopyranosyl-(1→2)] rhamnopyranoside ellagic acid (**203**), 3-((12'*Z*,14'*E*)-heptadeca-dienyl)phenol (**204)**, **188**, **189**, **195** and **198**.

Phytochemical study of the leaves of *Psiadia punctulata* led to the identification of twenty one compounds of which eight are new diterpene: trachyloban-17-oic acid (**205**), *ent*-17-hydroxy-trachyloban-20-oic acid (**206**), *ent*-[6β,18,19]-trihydroxy-trachyloban-2-one (**207**), normal-trachyloban-2α,18,19-triol (**208)**, normal trachyloban-2α,6α,19-triol (**209**), *ent*-15*β*,16*α*,17-trihydroxy-kauran-19-oic acid methyl ester (**214**) and compounds **219b-c**. From the stem bark of *P. punctulata*, six compounds were identified. These include *7α*-hydroxy-*ent*-trachyloban-19-oic acid (**225)**, friedelan-3β-ol (**226**), spinasterol (**227**), (*S*)-2,3-dihydroxypropyl tridecanoate (**228**) and 5-hydroxy-7,2',3',4',5'-pentamethoxy-flavone (**220**) and 5,7-dihydroxy-2',3',4',5'-tetra-methoxy-flavone (**221**). Analysis of the roots of *P. punctulata* led to the identification of six compounds; *ent*-trachylobane-*2α*,*6β*,18,19-tetraol (**229**), *ent*-kauren-16-en-2-one (**230**), friedelin (**231**), 24,25-dihydro-lanost-8(9)-en-3*β*-ol (**232**), (6*R*, 7*R*)-bisabolone (**233**) and **221**. Compounds **207** (CC_{50}=6.41±0.2 μM) and **210** (CC_{50}=3.4 ± 0.1 μM) are the most cytotoxic against Hep-G2 and DU-145 cell lines respectively. From the roots of *Aspilia pluriseta*, nine kaurene derivatives; 12*α*-methoxy-*ent*-kaura-9(11),16-dien-19-oic acid (**234**) and 16*α*-hydroxy-*ent*-kauran-19-oic acid (**235**), *9β-hydroxy*-15α-angeloyloxy-*ent*-kaur-16-en-19-oic acid (**236**), 15*α*-angeloyloxy-*ent*-kaur-16*α*,17-epoxy-*ent*-kauran-19-oic acid (**237**), methyl-9*β*-hydroxy-15*α*-angeloyloxy-*ent*-kaur-16-en-19-oate (**238**), 15α-angeloyloxy-*ent*-kaur-16-en-19-oic acid (**239**), *ent*-kaura-9(11),16-dien-19-oic (**240**), *ent*-kaura-9(11),16-dien-12-one **(241)**, methyl-*ent*-kaur-16-en-19-oate (**242**) were isolated. The seven other compounds isolated from the roots are kaurene also diterpenes derivatives (**236-242**). The aerial part of *A. pluriseta* let to the identification of seven compounds; *ent*-kaur-16-en-19-oic acid (**243**), *ent*-kaur-16-en-19-ol (**244**), *ent*-kaur-16-ene (**245**), lanosterol (**246**), stigmasta-5,22(E)-dien-3*β*-ol (**247**), 3*β*-hydroxy-olean-12-en-29-oic acid (**248**), carissone (**249**). Oral glucose tolerance test results revealed that the crude extract of *A. pluriseta* reduced the blood glucose level more than any other isolated compounds. Seven compounds namely methyl-15*α*-angeloyloxy-*ent*-kaur-16-en-19-oate (**250**), 12-oxo-*ent*-kaura-9(11),16-dien-19-oic acid (**251**), *ent*-kauran-19-oic acid (**252**), *3β*-hydroxyolean-12-en-28-oic acid (**253**), **236**, **237**, **238** were also isolated and identified from the root of *Aspilia mossambicensis* (Asteraceae). The aerial part of the same plant, *A. mossambicensis* resulted in the identification of *β*-amyrin acetate (**254**), kaura-9(11),16-diene (**255**), 15*β*-hydroxy-kaura-9(11),16-diene (**256**), methyl cinnamate (**257**), **240**, **243** and **247**.

Ten derivatives (**258**-**267**) were prepared from the isolated compounds of *Psiadia punctulata*. Four more compounds (**268**-**271**) were derivatized from the isolated compounds of *Aspilia pluriseta*. Among these derivatives, compound **265** was found to be active (CC_{50} = 16.9 ± 5.1 μM) against the growth of A549 cancer cell line. Compound **270** was the most antimicrobial against *Staphylococcus aureus*, *Escherichia. coli* and *Candida parapsilosis* having an inhibition zone of 8 mm against each strains.

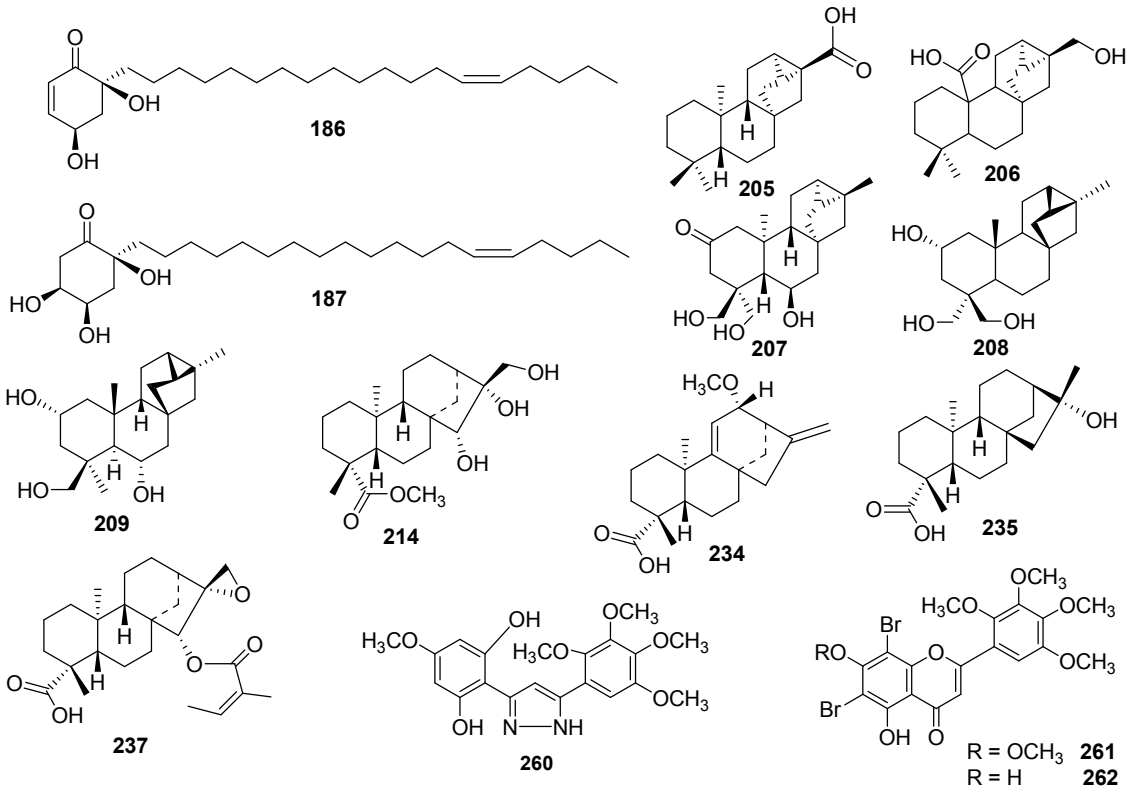

CHAPTER ONE

INTRODUCTION

1.1 Background of the Study

Plants possess the capability of producing biologically interesting and valuable chemical constituents (Yasmen *et al.*, 2018). It is estimated that over 50,000 plants, possess therapeutic value, and about 80% of the human population uses herbal medicines at least once in their life time (Kuete *et al.*, 2013). The use of medicinal plants in the treatment of human ailments and conditions including cancer, microbial infections, inflammation and diabetes is well documented (Cárdenas *et al.*, 2016). Despite the overall improvement on the use of conventional therapies to treat these ailments, the search for new lead compounds for treatment of a wide range of ailments including infectious diseases remains a high priority (González *et al.*, 2018).

Antimicrobial agents are chemicals that can be used to kill or prevent the growth of micro-organisms and are classified based on their application and spectrum of activity. The use of chemicals to cure an infectious disease without injuring the host's tissue is known as chemotherapy. There are many classes of chemotherapeutic agents in the market including antibacterial, antifungal, antiviral, antineoplastic and antiprotozoal drugs in the market. In spite of the considerable progress in synthetic chemistry, combinatorial chemistry and molecular modelling in recent years, natural products remain an important source of lead compounds, for development of new drugs (Balunas and Kinghorn, 2005; Salim *et al.*, 2008). As an example, Arteether (**1**) (trade name artemotil®) is an antimalarial drug derived from artemisinin (**2**), a sesquiterpene lactone isolated from *Artemisia annua* L. (Asteraceae). Other derivatives of artemisinin are in clinical trials as anti-malarial drugs (Van *et al.*, 1999). Another successful example of antimicrobial drugs developed from natural source includes the penicillin series (**3**).

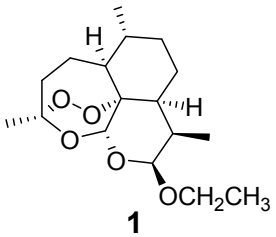

1

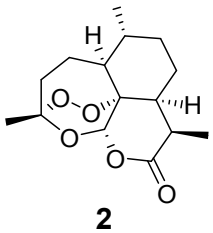

2

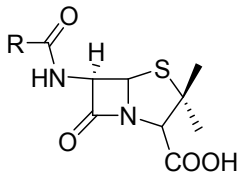

3

Plant metabolites can also be used in the treatment of non-infectious diseases. Among these, inflammation is a permeative phenomenon that occurs in response to infection, injury, and exposure to contaminants. It is a defence mechanism that is triggered by innate immune receptors (Yasmen *et al.*, 2018) and is characterized by redness, pain, heat, swelling, and loss of function in the affected area. Both steroidal and nonsteroidal anti-inflammatory drugs are used to treat inflammation (Yasmen *et al.*, 2018). For instance, there are compounds isolated from *Aesculus hippocastanum* and *Ananas comosus*drugs which are commercially available as drugs (Taylor, 2000).

Another non-infectious disease is type 2 diabetes mellitus (T2DM), which is a metabolic disease characterized by insulin deficiency resulting from inadequate β-cell insulin secretion or insulin resistance (Shams *et al.*, 2018). According to the most recent data by the International Diabetes Federation and the World Health Organization, diabetes represents one of the most important health problems, causing enormous costs, with an estimated prevalence of 350–400 million cases worldwide (Schwingshackl *et al.*, 2017).

To tackle the burden of microbial infections, cancer, inflammation and type 2 diabetes mellitus (T2DM), exploration of new cytotoxic, antimicrobial, anti-inflammatory and anti-diabetic lead compounds is crucial in order to discover various alternatives. Plant based medicines may fulfil this requirement by providing nontoxic, more potent, efficacious, and safe drugs to treat these ailments and diseases.

In the search for lead compounds for infectious and non-infectious diseases, different plants belonging to different families have been investigated and have resulted in the identification of different classes of active metabolites. In this study, selected plants from the Anacardiaceae and Asteraceae families were phytochemically investigated. Before this study was carried out, some plants of the family Anacardiaceae, including *Anacardium occidentale*

(Gonçalves and Gobbo, 2012; Santos *et al.*, 2013), *Shinus lentescifolius* (Gehrke *et al.*, 2013) and *Lannea alata* (Okoth *et al.*, 2013) were investigated and showed the presence of bioactive and structurally unique alkylcyclohexanols and alkylcyclohexanones. Similarly, plants from Asteraceae family among which *Psiadia* species (Govinden *et al.*, 2004) and *Aspilia species* (Adeniyi and Odufowora, 2000; Souza *et al.*, 2015) are known to produce diterpenoids. However, information on bioactivity of these plants is scanty. Some of these plants were investigated in this study.

1.2 Statement of the Problem

The development of antimicrobial agents is one of the most important achievements in the modern era of science and technology. However, the emergence and ever increasing number of strains of multi-drug resistant pathogenic micro-organisms to existing antimicrobial agents is a set-back to this otherwise success story (Nair and Chanda, 2005, Goud *et al.*, 2011;). In addition, a number of synthetic anti-microbial agents, impose various adverse effects including hypersensitivity and allergic reactions. These adverse side effects (hypersensitivity, allergic reactions) together with the multidrug resistance of many pathogens are a cause of concern around the globe.

Conventional management of fever and inflammation (which are associated with infections) with synthetic drugs, usually, has many side-effects and these drugs are not universally affordable (Parveen *et al.*, 2014). Many parts of the body can be affected by inflammation ranging from acute to chronic inflammation (Hunter, 2012). Chronic inflammation can be a secondary component of many diseases including autoimmune disorders, infectious diseases, rheumatoid arthritis, asthma, chronic inflammation bowel disease, neurodegenerative diseases, type 2 diabetes mellitus (T2DM) and cancer (Hunter, 2012; Fürst and Zündorf, 2014). Furthermore, chronic inflammation can play an important role in other conditions such as chronic pain, poor sleep quality, obesity, physical impairment and at the end, a decreased quality of life. Considering this broad array of negative consequences, it is evident that chronic inflammation can be a heavy burden on society (Yang *et al.*, 2013).

The need for oral type 2 *diabetes mellitus* (T2DM) agents is also growing considerably, and it accounts for over 10% of the total healthcare costs in several developed countries. Increased blood glucose levels in T2DM are closely associated with other metabolic disorders such as

hypertension, atherosclerosis, and cardiovascular disease (Shams *et al.*, 2018). The worldwide prevalence of T2DM is rapidly increasing, and the number of patients is projected to be approximately 550 million by 2030 (Shams *et al.*, 2018). Hence, treatment options for cancer, microbial infectious, inflammation, type 2 *diabetes mellitus* are still problematic, especially in the underdeveloped countries.

In Kenya, only 30% of the population has access to conventional medicine due to high cost, leaving more than 70% of the population to be under the care of traditional medical practitioners (Okoth, 2014). Phytochemical report on both Anacardiaceae and Asteraceae plant families especially those belonging to the genera *Lannea, Psiadia* and *Aspilia* is scanty; while at the same time, crude extract of some of these plant species have demonstrated anti-inflammatory, hypotensive, anti-oxidant, anti-malarial and anti-microbial activity (Achola *et al.*, 1998; Sebisubi *et al.*, 2010, Pouny *et al.*, 2011, Kuria, 2014; Okoth, 2014).

1.3 Objectives

1.3.1 General Objective

The main objective of this work is to identify bioactive principles from *Lannea rivae, Lannea schweinfurthii, Psiadia punctulata, Aspilia pluriseta* and *Aspilia mossambicensis.*

1.3.2 Specific Objectives

The specific objectives of the present study are to:

(i) Characterize the isolated compounds from the plants, *Lannea rivae, Lannea schweinfurthii, Psiadia punctulata, Aspilia pluriseta* and *Aspilia mossambicensis*;

(ii) Establish the cytotoxicity, antimicrobial, anti-inflammation, and anti-diabetes activities of crude extracts and isolated compounds from the selected plant species;

(iii) Improve the bioactivity of the isolated compounds through structural modification.

1.4 Justification and Significance of the Study

Medicinal plants are very important when it comes to solving healthcare problems and their uses are extensive around the world. In many underdeveloped countries including African countries, the use of traditional medicine by the population to solve healthcare problems is accepted as an affordable means for treatment (Abdullahi, 2011). In the young age of modern medicine, molecules with biological activity from plants have played a pivotal role in the management of diseases by providing lead compounds for development of drugs including anti-infective agents. In this exercise, folk remedies of plant origin have been tested for their anti-infective activities in experimental animal models. Several authors have reported favourable results with herbal drugs either in animal or in human studies. Continued investigations of new therapeutic approaches based on plant derivatives is therefore strongly justified (Taylor, 2000). Therefore, the results of such studies could lead to new molecules that could be developed for the management of microbial infectious, cancer, inflammation and type 2 *diabetes mellitus*.

In the search for new lead compounds, the cytotoxicity of active compounds are carried out since such compounds are intended for use as pharmaceuticals or cosmetics, in which case minimal to no toxicity is vital. The compounds which are cytotoxic may be persued further as anticancer lead compounds, in which case selective cytotoxicity to cancerous cells is crucial (McGaw *et al.*, 2014). A selective cytotoxic profile exerted on cancerous cells indicates that potential antimicrobial extract and compounds do not act as indiscriminate cellular toxins, but have a specific cell-type based cytotoxicity. In the search for anti-infective plant compounds, cytotoxicity assays help scientists to detect at an early stage antimicrobial or other activities that are likely selective against specific microbes. This process allows the identification and prioritization of test substances useful for further biological activity studies (McGaw *et al.*, 2014).

The bioactivity of many plants belonging to the Anacardiaceae and Asteraceae families including *Lannea, Psiadia* and *Aspilia* species are documented. Moreover, pharmacological activity of *Lannea barteri* (Koné *et al.*, 2011), *Lannea kerstingii* (Njinga *et al.*, 2014), *Lannea welwitschii* (Agyare *et al.*, 2013), *Psiadia terebenthina* (Gurib-Fakim *et al.*, 2003), *Psiadia*

punctulata (Gouda *et al.*, 2014), *Psiadia dentata* (Robin *et al.*, 1998) and *Aspilia* species (Rodriguez *et al.*, 1985) has been highlighted in the literature.

Therefore, it is logical to isolate and identify bioactive compounds from plants (which have low incidence of side-effects) to fight against diseases including microbial infections, inflammation and *diabetes melitius*. Although many authors have studied bioactivity of Anacardiaceae and Asteraceae species, there are few reports about the phytochemistry of these plants, especially those belonging to the genera *Lannea*, *Psiadia* and *Aspilia* growing in Kenya. The reported pharmacological activity of some of the above mentioned plant species and their use in African folk medicine suggests that these plants could furnish a variety of compounds with diverse chemical structures that possess pharmacological potential against microbial infections, inflammation and type 2 *diabetes mellitus*. Therefore, the findings of this study could lead to new compounds that could be useful (directly or after derivatization) for the management of these conditions.

CHAPTER TWO

LITERATURE REVIEW

2.1 Causes of Common Microbial Infections

There are numerous bacterial species which can cause variety of diseases in human beings. In the last decades, resistance to multiple antibiotics have been a major health problem all over the world. Many healthcare centres have considered Methycillin resistant *Staphylococcus aureus* (MRSA) as one the main challenging bacterial infections (Archibald *et al.*, 1997; Rasmussen *et al.*, 2011). *Staphylococcus aureus*, a spherical bacterium, is a Gram-positive bacteria and the main cause of Staph infection of the skin and nose. It can cause a variety of diseases including skin diseases, pneumonia, meningitis, septicaemia, oestomyelitis, endocarditis, bacterimia and sepsis. It can also cause food poisoning and many other diseases and ailments related to skin, soft tissue, respiratory track, bone and joints (Archibald *et al.*, 1997; Rasmussen *et al.*, 2011).

Another versatile opportunistic pathogen is *Escherichia coli*, a Gram-negative bacteria that can affect gall bladder, skin, surgical wound and lungs (Black *et al.*, 2000). *Salmonella typhimurium*, a Gram-negative bacteria is also a highly infectious pathogen. Most of the infections caused by this bacterium are due to ingestion of contaminated food. *Salmonella typhimurium* can infect intestines, blood stream and other body sites which can even cause death. Each year, more than 16 million people are affected worldwide with typhoid fever (World Health Organization, 2015). In 2014, WHO listed *Escherichia coli*, *Klebsiella pneumoniae* and *Staphylococcus aureus* as the three microbial species of greatest concern and are associated with both hospital and community acquired infections (Gelband *et al.*, 2015).

Fungal spores are found in air and land on skin or can be inhaled causing many types of skin infections (Mycoses) and lung infections. Out of the estimated 100,000 fungal species, only about 300 species have been identified as human pathogens; more than 75% of these micro-organisms infect primarily the skin or subcutaneous tissues. Over the years, the incidence of fungal infection has spread despite an increasing number of antifungal drugs on the global market (Laube, 2004; Moya and Llorca, 2016; O'Neill, 2016).

Fungal infections like dermatophytosis are caused by several fungal species. These infections are generally attributed to dermatophytes, a group of three types of fungi that commonly causes skin diseases in animals and humans. *Candida spp* are fungi that can cause mucocutaneous or systemic infections called candidosis. Even though other fungal species may produce diseases, particularly in immuno-compromised individuals, *Candida albicans* is the most common pathogen (Badiee and Hashemizadeh, 2014).

2.2 The Burden of Antimicrobial Resistance

Antimicrobial refer to chemical substance often produced by a micro-organisms that inhibit the growth of (or kills) other micro-organisms (Waksman, 1947). There are several terms or expressions utilized in place of the term "antimicrobials". These include "chemotherapeutics" or "anti-infectives". The word antimicrobials in a broader sense refers to substances with antibacterial, anti-fungal, or anti-parasitical activity (Kümmerer, 2009). Antimicrobials can also be effective against viruses. The term “antibiotic” was first used in 1942 by Dr. Selman A. Waksman, a soil microbiologist. He and his colleagues discovered several actinomycetes derived antibiotics (Waksman, 1947). An antibiotic in a narower sense is a chemotherapeutic agent that inhibits the growth of bacteria (Kümmerer, 2009).

Antimicrobial resistance is one of the greatest challenges to global public health and is recognized as one of the principal threats to humanity (World Health Organization, 2015). Even if resistance is a natural phenomenon, many factors have contributed to its global propagation. These factors include: misuse of antimicrobial medicines, inadequate or nonexistent programmes for infection prevention and control, use of substandard medicines and insufficient regulation of the use of antimicrobial medicines (World Health Organization, 2015).

Micro-organisms develope resistance towards the effects of antimicrobials by using genetic strategies with many variations. They can produce destructive enzymes to neutralize antimicrobial agents; modify antimicrobial targets (by mutation, so that drugs cannot recognize them), remove antimicrobial agents by pumping them out (efflux); prevent drug from entering by creating a “biofilm” or otherwise reduce permeability and create bypasses that allow them to function without the enzymes targeted by drugs (Penesyan *et al.*, 2015).

In developing countries including African countries, antimicrobial resistance remains a growing problem. According to WHO, the worldwide death toll due to infectious diseases is estimated at 52 million yearly. Although the number of new antimicrobial drugs introduced is increasing yearly, these are mostly not affordable in developing countries and their availability is limited to high-income countries, and hence they have not helprd in alleviating the global burden (Gelband *et al.*, 2015).

2.3 Cause and Treatment of Inflammation

Inflammation is triggered by the immune system in response to a physical injury or an infection. The treatment of inflammation and the resulting collateral tissue damage has not changed significantly since ancient practitioners of folk medicine (Serhan, 2017). Different approaches such as suppression, blockage and inhibition of pro-inflammatory mediators of inflammation are used for therapeutic measures. Many drugs including aspirin (**4**), paracetamol (**5**), ibuprofen (**6**), indomethacin (**7**), and non-steroidal anti-inflammatory drugs (NSAIDs) are used against inflammation. Although many of these are effective, uncontrolled inflammation can lead to different diseases, and for this reason, new therapeutic and safe lead compounds are in need of development (Koopman and Moreland, 2005). In this regards, plants remains a source of lead compound for the development of new and safe anti-inflammatory drugs.

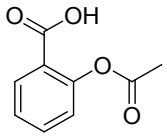

4

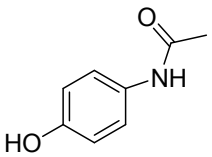

5

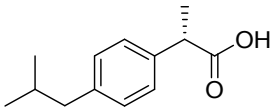

6

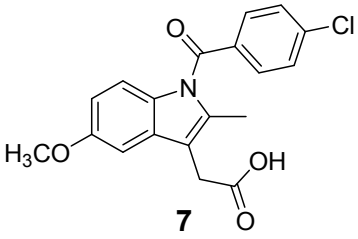

7

2.4 The Burden of Inflammation

Chronic inflammation can affect any part of the body and is often associated with microbial infections (Robbins *et al.*, 1984). Cases of diseases and conditions where chronic inflammation is involved include microbial infections, obesity, physical impairment and overall decrease in the quality of life (Robbins *et al.*, 1984). Over the last decades, the

number of patients suffering from chronic diseases (diabetes, cardiovascular diseases, autoimmune diseases, respiratory diseases and cancer) has increased rapidly. The growing rate of occurrence of these diseases indicates that chronic inflammations contributes to the their pathology (Mallbris *et al.*, 2004; Miller *et al.*, 2009; El-Gabalawy *et al.*, 2010; Kolb and Mandrup-Poulsen, 2010). Hence, a good treatment of chronic inflammation reduces the risk of many diseases including cardiovascular diseases (Mallbris *et al.*, 2004). Because of its involvement in many chronic diseases, the precise economic impact of chronic inflammation is hard to determine.

2.5 Cause of Type 2 Diabetes Mellitus

Diabetes is a chronic disease that occurs when the pancreas does not produce enough insulin (a hormone that regulates blood sugar); or when the body cannot effectively use the insulin it produces. Type 2 *diabetes mellitus* (T2DM) results from the body's ineffective use of insulin. About 90% of diabetes patients around the world have T2DM. It is largely associated with excess body weight and physical inactivity. Biguanides are one of the major classes of antidiabetic drugs, among which metformin is the most common drug used in the first line therapy for diabetes mellitus (Wu *et al.*, 2014). The thiazolidinediones (TZDs), such as ciglitazone and rosiglitazone, are representative PPARγ agonists described as potent insulin-sensitizing drugs for the treatment of T2DM (Shams *et al.*, 2018). Sulphonylureas are second line drugs agents widely used in the treatment of T2DM patients who are not severely obese. Although new anti-diabetic agents and insulin are currently used for the treatment of T2DM and have brought about promising outcomes, problems of inadequate efficacy, high cost and adverse effects still persist (Wu *et al.*, 2014).

2.6 The Burden of Type 2 Diabetes Mellitus

Diabetes mellitus is a global disease; while juvenile onset (or type 1) diabetes is an autoimmune disease that affects many children, non-insulin dependent (or maturity onset, type 2) diabetes is increasing throughout the world (Harvey, 2010). The long-term complications associated with type 2 diabetes constitute a burden of morbidity and mortality (Zimmet, 2003). In 2017, it is estimated that the number of people with type 2 diabetes will increase from about 200 million to 400 million by 2030 (Wild *et al.*, 2004; Harvey, 2010; Schwingshackl *et al.*, 2017). Usually associated with obesity ("diabesity"), this condition has

unhealthy consequences such as increased risk of cardiovascular diseases, and is becoming a major health problem globally (Harvey, 2010). Moreover, in many cases, type 2 diabetic patients die prematurely from cardiovascular illnesses. Diabetic patients are more than twice costly to treat compared to non-diabetic patients, mainly due to complications of the management of the disease (Zimmet, 2003).

2.7 The Use of Plants as Antimicrobial, Anti-inflammatory and Antidiabetic Agents

The use of medicinal plants in healthcare is not a new practice. Many drugs used today for a large number of therapeutic activities were derived from plants (Nguyen and Duez, 2008). These include steroids, cardiotonic glycosides (*Digitalis* glycosides), antimalarials (*Cinchona* alkaloids), analgesics and antitussives (*Opium*), cholinergic (physostigmine), antigout (cholchicine), anaesthetic (cocaine), skeleton muscle relaxant (tubocurarine), anticancer (*Podophyllum hexandrum*) and antimicrobial agents. The anti-inflammatory and analgesic drugs also have their origins from medicinal plants including *Salix* species (Rainsford, 2007). There are also many reports on plants that posses hypoglycaemic effect (Shams *et al.*, 2018). Medicinal plants constitute as good sources of anticancer agents by providing active substance or templates for synthesis of more active drugs (Nguyen and Duez, 2008).

2.7.1 Antimicrobial and antiparasitic agents from plants

In the fight against microbial diseases, either caused by bacteria, fungi and parasites, antimicrobials are utilized. The discovery of new lead compounds from medicinal plants in antimicrobial drug development is still an important approach in the fight against antimicrobial resistance (Newman and Cragg, 2016). The most common synthetic antibiotics prescribed include azithromycin (**8**), ciprofloxacin (**9**), trimethoprim (**10**), sulfamethoxazole (**11**), levofloxacin (**12**) doxycycline (**13**) and tedizolid (**14**) (Gelband *et al.*, 2015).

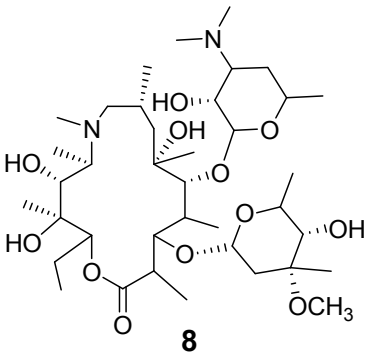

8

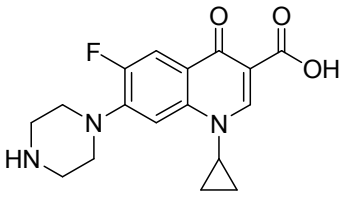

9

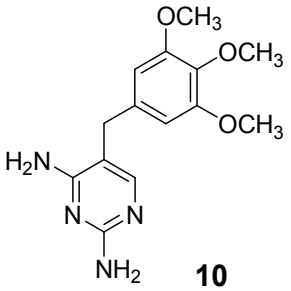

10

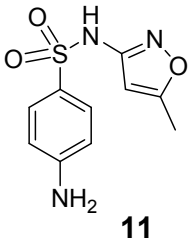

11

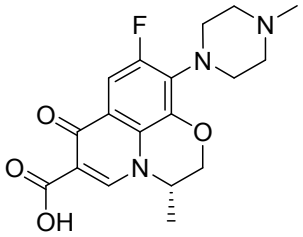

12

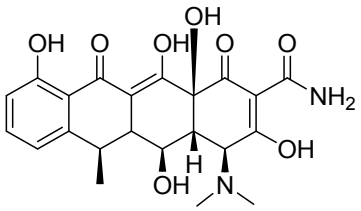

13

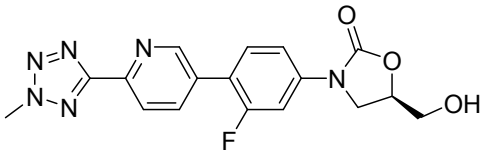

14

Active antibacterial agents derived from plants such as trometamol (**15**), fosfomycin (**16**) and tigecyclin (**17**) support the continuous use of medicinal plants as sources of antimicrobial agents (Okoth, 2014). As am example of active antibacterial compound, pyrithione (**18**) was isolated from *Polyalthea nemoralis* (Lewis and Ausubel, 2006). In the same light, there are reports on antibacterial activity of rhein (**19**), plumbagin (**20**), resveratrol (**21**), gossypol (**22**) and coumestrol (**23**) (Lewis and Ausubel, 2006). Additional plant-derived antiicrobial agents include scopoletin (**24**) isolated from tobacco and camalexin (**25**) isolated from *Arabidopsis Thaliana* (González *et al.*, 2009).

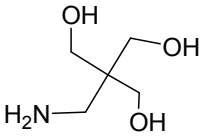

15

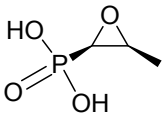

16

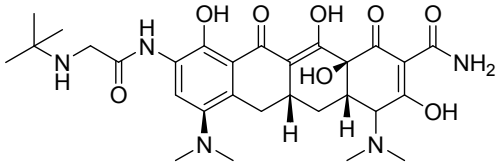

17

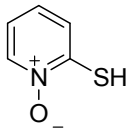

18

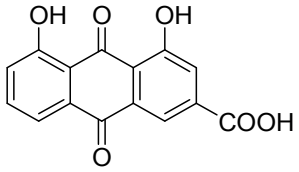

19

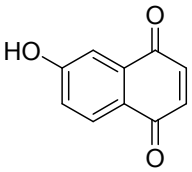

20

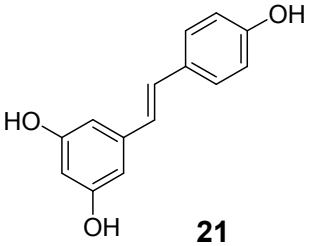

21

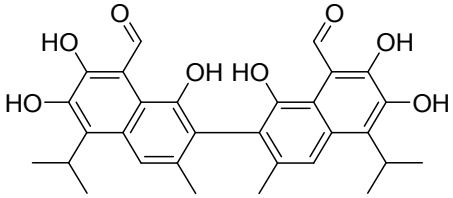

22

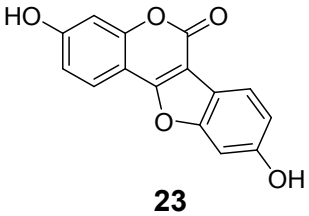

23

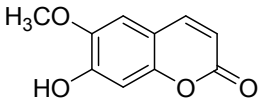

24

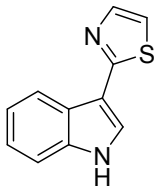

25

Chemical agents that can definitely fight against fungal infections are relatively few and information on antifungal agents from plant sources currently in use is scanty. Even though some reports are available on antifungal compounds from plants including thymol (**26**) (isolated from *Thymus vulgaris*), they are no clinically used plant based antifungal drugs (Taylor, 2000). Synthetic and semi-synthetic antifungal compounds, which are available for both oral and sometimes topical use include polyene antibiotics (nystatin and amphotericin B), azole antibiotics (imidazole and triazoles), allylamines antibiotics, glucan synthesis

inhibitors (echinocandin antibiotics), chitin synthesis inhibitors and mannan antibiotics (pradimicins and benanomycin) (Lewis, 2011).

Plants have served as sources of antiparasitic agents. New scaffolds derived from plant sources are playing an important role in the development of new antimalarial leads (Fernández *et al.*, 2016; Fröhlich *et al.*, 2018). The case of quinine (**27**) found in *Cinchona* species and used as template in the synthesis of chloroquine (**28**) is a good example of antimicrobial agent. Artemisinin (**2**) and its derivatives including atreether (**1**), artemether and sodium artesunate are used as antimalarial drugs (Okoth, 2014). Similarly, lapachol (**29**) isolated from *Tabebuia* species was used as a lead structure for the synthesis of antimalarial drug, atovaquone (**30**) (Lima *et al.*, 2004). Ajoene (**31**) along with the naturally occurring analogue allicin is active against rodent malaria and *Trypanosoma cruzi* (Fröhlich *et al.*, 2018). Miconidin (**32**) and espintanol (**33**) isolated from *Hypericum calycinum* and and gallic acid (**34**) have the ability to inhibit the proliferation of *Trypanosoma cruzi* parasite growth. It has also been shown that tetrahydrofuran lignans including grandisin (**35**) and veraguensin (**36**) have shown activity against Chagas disease (Fröhlich *et al.*, 2018). A dimeric naphthoquinone, diospyrin (**37**) isolated from *Diospyros montana* (Ebenaceae) was found to be active against *Leishmania donovani. A* naphthoquinone, benzisoquinoline-5,10-dione (**38**) which was isolated from *Psychotria camponutans*, has been identified as potential antiparasitic drug (Kayser *et al.*, 2002). Diterpenes including *ent*-kauran-16-en-19-oic acid (**39**, from *Wedelia paludosa*) and (-)-trachyloban-19-oic and (**40**, from *Viguirea aspillioides*) were found to be potent antileishmania compounds (Fröhlich *et al.*, 2018).

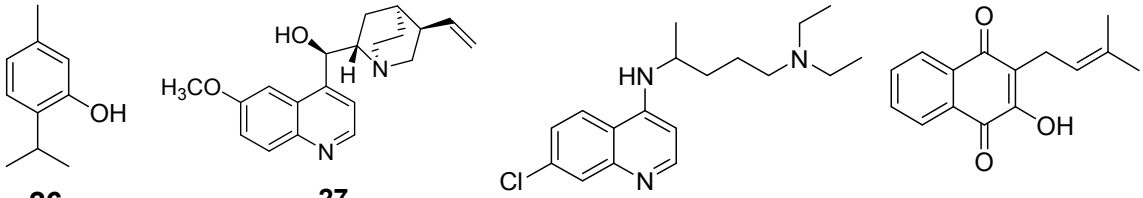

26 **27** **28** **29**

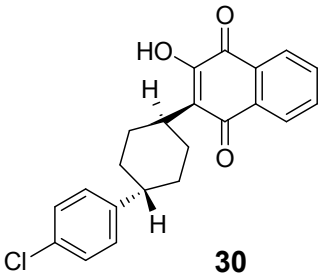

30

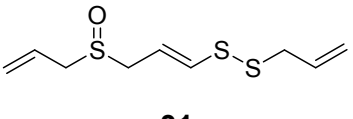

31

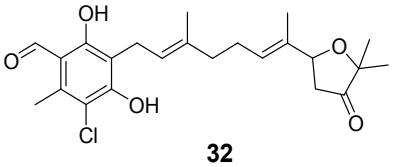

32

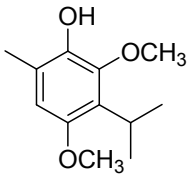

33

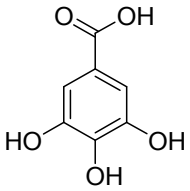

34

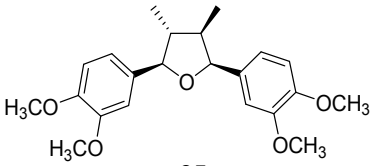

35

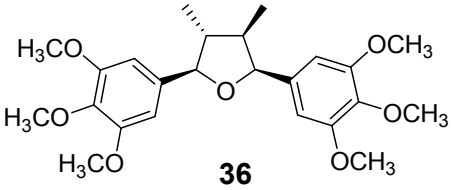

36

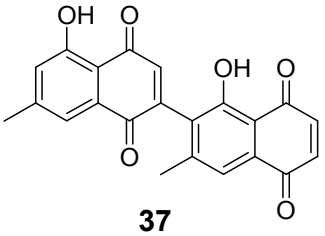

37

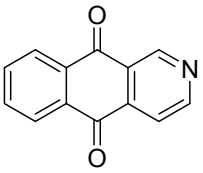

38

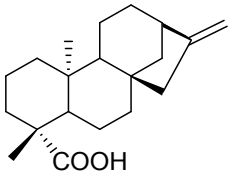

39

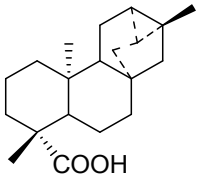

40

2.7.2 Cytotoxic Agents from Plants

Cytotoxicity literaly means toxic to cells. However, scientists are searching for cytotoxic agents with potential to treat cancer. The main objective of the search for cytotoxic compounds is to inhibit the proliferation of tumour cells. Of course not all cytotoxic compounds are potentially useful clinically. Cytotoxic substance affects living cells including normal cells. However, healthy cells can survive or repair the damage of the cytotoxic agent more easily than cancer cells. Cytotoxic compounds of interest are therefore needed to have a mediated level of toxicity which gives a chance to normal cells to survive but not cancer

cells. In other words, the search is for compounds which are selectively toxic to cancer cells without significantly affecting normal cells (Lindholm, 2005).

Numerous compounds with cytotoxic activity have been isolated from plants. Many of them have been used in the development of anticancer agents. Podophyllotoxin (**41**) isolated from *Podophyllum peltatum* has been used for many year in the treatment of tumors. However, due to its side-effects, the semi-synthetic compounds etoposide, etopophos and teniposide were developed and are being used successfully (Canel *et al.*, 2000; Cragg and Newman, 2005). The steroidal alkaloid glycoside, *β*-solamarine (**42**) is also known for its antitumor effects. The isolation and use of an anticancer compound taxol from *Taxus brevifolia* is also well documented, and more than 400 taxanoid analogs have so far been discovered (Nguyen and Duez, 2008). Recently, betulinic acid (**43**) has showed cytotoxicity against a range of cancer cell lines and formulations are being developed for clinical trials (Cragg *et al.*, 2014).

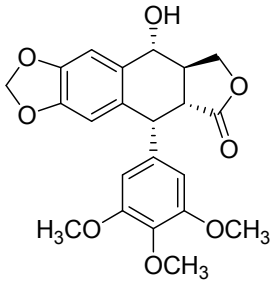

41

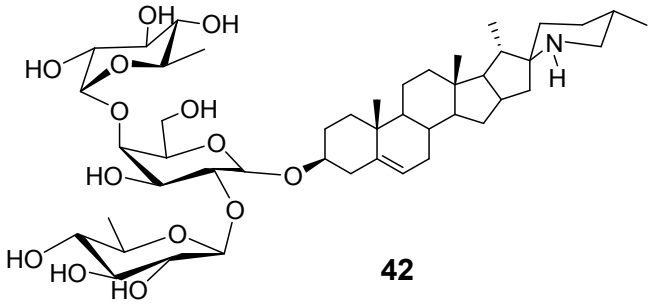

42

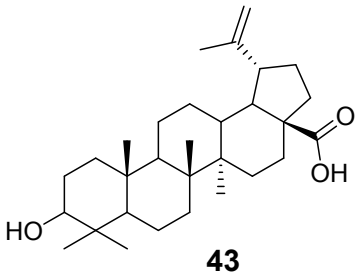

43

2.7.3 Anti-inflammatory Agents from Plants

Nonsteroidal anti-inflammatory drugs (NSAIDs) are among the most commonly prescribed drugs in modern medicine. NSAIDs are very effective in the alleviation of pain, fever and inflammation, and millions of patients worldwide have found relief from pain in their use

since the discovery of the soothing properties of Willow bark more than 3,500 years ago (Meek *et al.*, 2010). Important anti-inflammatory compounds from plants that have been tested in humans in recent years include curcumin (**44**) (from *Curcuma longa*, Zingiberaceae), colchicine (**45**) (from *Colchicum autumnale,* Colchicaceae), resveratrol (**46**, from peanuts), capsaicin (**47**) (from *Capsicum* species; Solanaceae), epigallocatechin-3-gallate (**48**) (EGCG from *Camellia sinensis,* Theaceae) and quercetin (**49) (**widely occurs in plants**)** (Fürst and Zündorf, 2014). additional anti-inflammatory agents of plant origin include luteolin (**50**), genistein (**51**), wogonin (**52**), paeonol (**53**), taxifolin (**54**), calocedrin (**55**), celastrol (**56**), reynosin (**57**) and shikonin (**58**) (Calixto *et al.*, 2004).

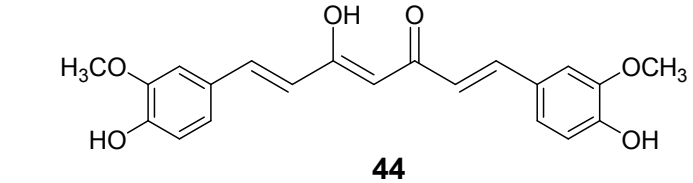

44

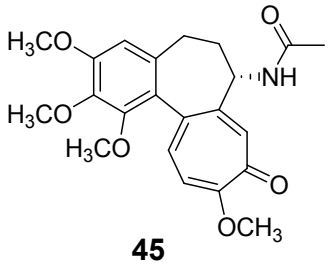

45

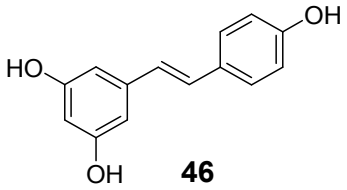

46

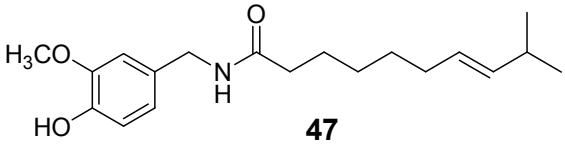

47

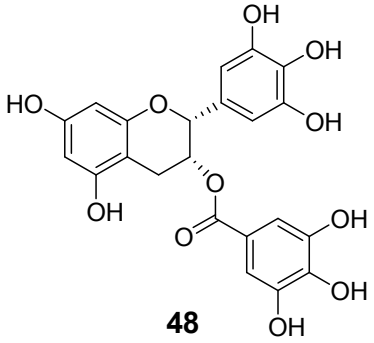

48

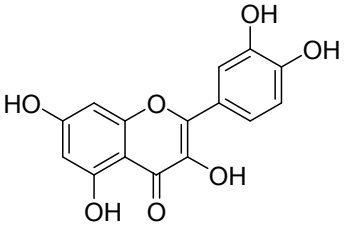

49

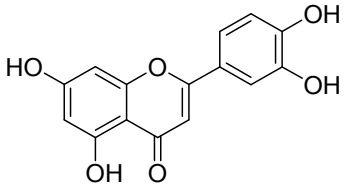

50

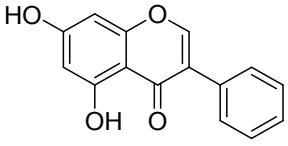

51

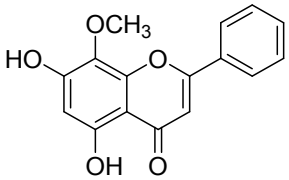

52

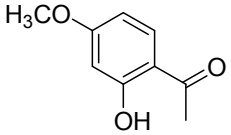

53

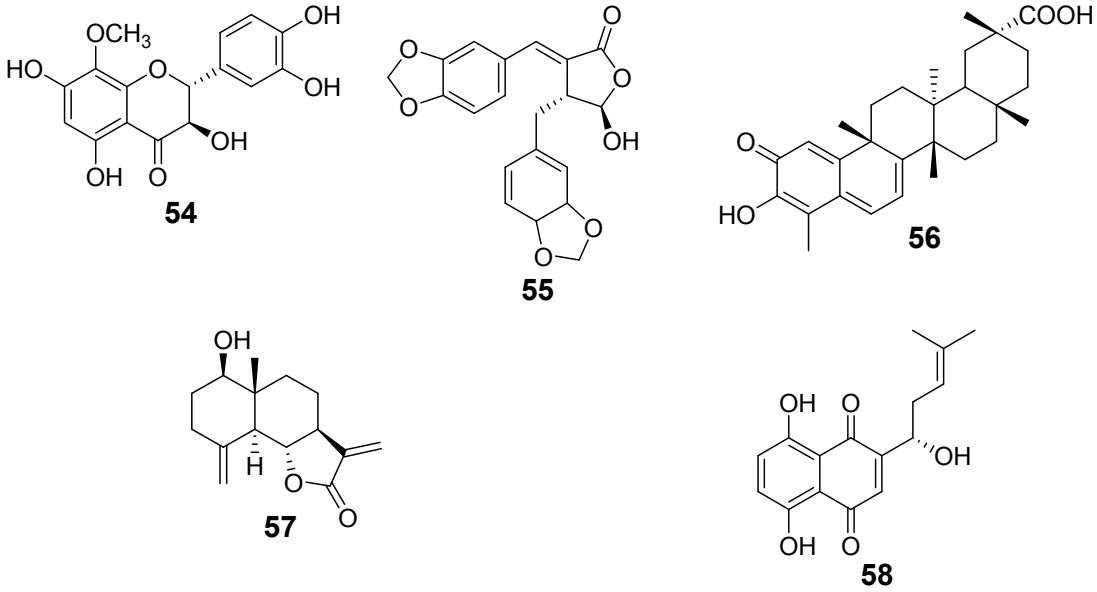

2.7.4 Anti-type 2 diabetes mellitus agents from plants

Antidiabetic agents consist of different kinds of preparation involved in the management of diabetes. The main objective of all these agents is to reduce blood sugar levels to an acceptable range and relieve symptoms of diabetes such as thirst, excessive urination, and ketoacidosis. Alternatively, antidiabetic drugs can also prevent the development of long-term complications of the disease usually faced by patients. These include neuropathy (nerve damage), nephropathy (kidney disease) and retinopathy (damage to the retina of the eye). There are two classes of anti-diabetic drugs: oral antidiabetic drugs and injectable antidiabetic drugs.

Currently, there are nine classes of drugs of oral antidiabetes medications for the treatment of T2DM. These are α-glucosidase inhibitors, biguanides, sulfonylureas, meglitinides, thiazolidinediones, di-peptydyl peptidase-4 (DPP-4) inhibitors, sodium-glucose cotransporter (SGLT)-2 inhibitors, dopamine agonists and bile acid sequestrants. Injectable antidiabetic drugs include insulin preparations and glucagon-like peptide 1 (GLP1) agonists. Known anti-diabetic agents include miglitol (**59**), mitiglinide (**60**), repaglinide (**61**), rosiglitazone (**62**) and glibenclamide (**63**).

Moreover, some natural products such as resveratrol (**64**), sulphostin (**65**), nymphayol (**66**) and berberine (**67**) can enhance insulin release (Harvey, 2010). Tecomine (**68**), isolated from the *Tecoma stans* (Bignoniaceae) has a potent stimulating effect on the basal glucose uptake rate in rats (Jung *et al.*, 2006). Besides, a kaurene diterpene, stevioside (**69**), isolated from *Stevia rebaudiana* (Asteraceae), has been used worldwide in the management of diabetes for many years. Ellagic acid (**70**) and its derivative 4-*O*-methylellagic acid and 4-(α-rhamnopyranosyl)ellagic acid (**71**) found in *Myrciaria dubia* are considered as inhibitor of aldose reductase. Castanospermine (**72**), an indol izidine alkaloid isolated from *Castanospermum australe* (Fabaceae), has hypoglycemic activity. More antidiabetic agent from plant sources include vincamine (**73**) and (-) eburnamonine (**74**) (Marles and Farnsworth, 1995).

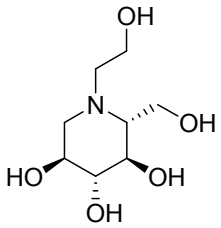

59

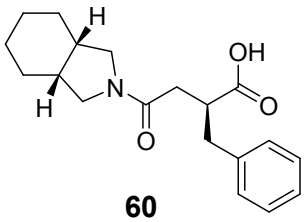

60

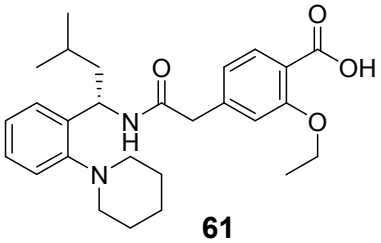

61

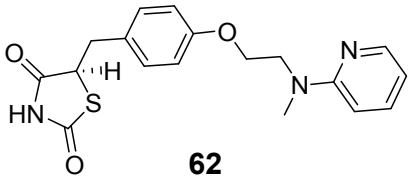

62

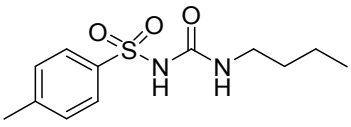

63

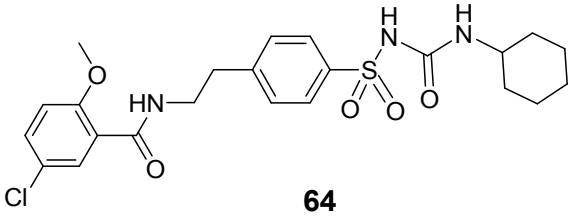

64

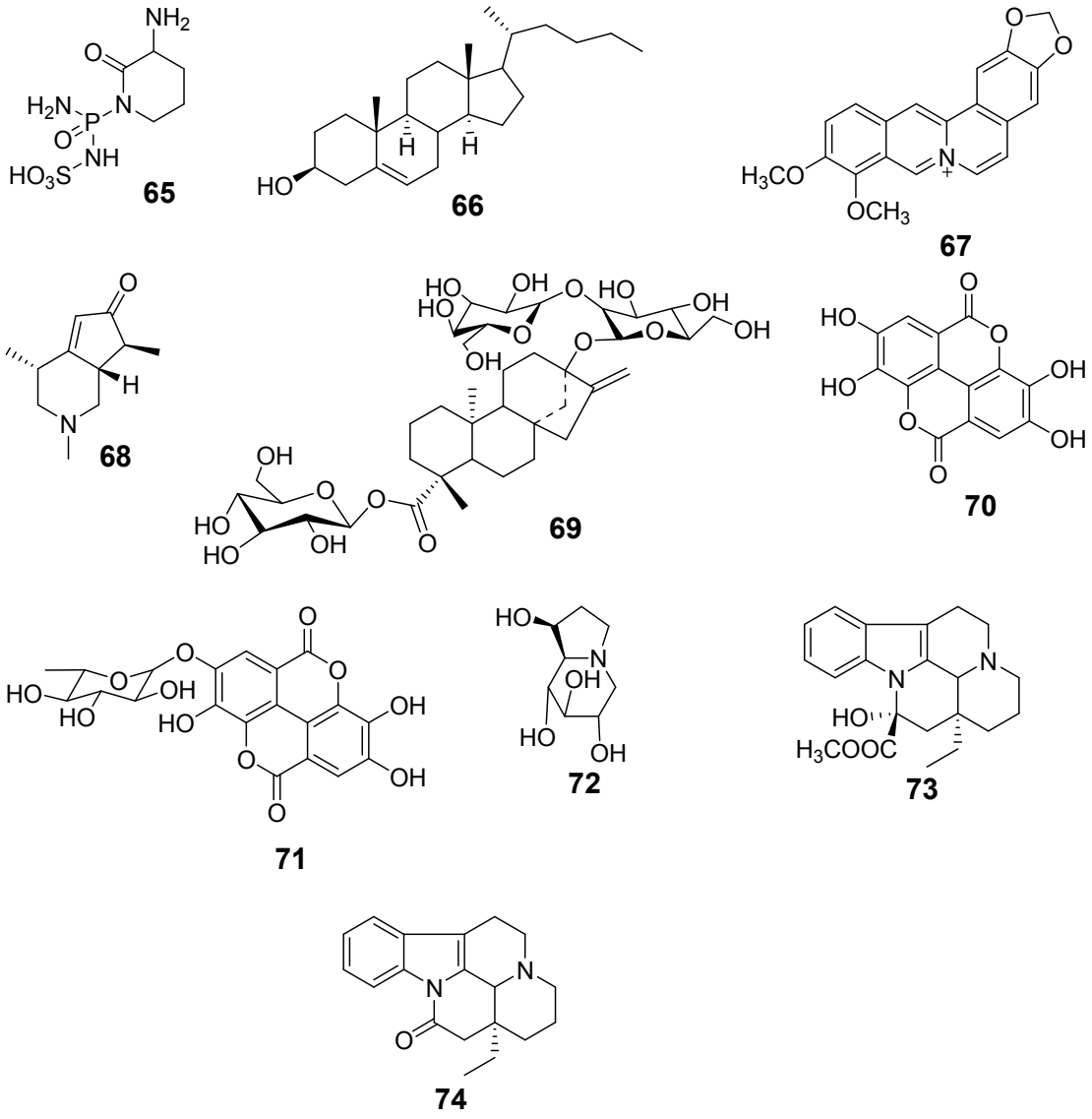

2.8. Terpenoids

Over the years, human kind has used plants containing terpenoids as medicines, incenses, foods, intoxicant and natural rubber (Fischedick, 2013). However, the modern chemistry began in the 1800's with the German chemist Otto Wallach. Regarded as the Father of terpenoids chemistry, Otto Wallach was awarded the Nobel Prize in chemistry in 1910 for his contribution in the structure elucidation of monoterpenes (Hanson, 2003; Fischedick, 2013). They are ubiquitous secondary metabolites in the plant kingdom. Many of them have a biological activity. All terpenoids are derived from fusion of branched five-carbon units based on isopentane skeleton also known as isoprene (C_5). From biosynthetic point of view,

most of terpenoids are obtained via mevalonic acid (MVA) pathway (Scheme 2.1). Nevertheless, there are few of them which are formed which are formed via methyl erythritol-4-phosphate pathway (MEP). Isoprene derived from isopentenyl-pyrophosphate (IPP) or its isomer dimethylallyl-pyrophosphate (DMAPP) by enzymatic conversion and phosphorylation from mevalonic acid (Zhang *et al.*, 2002). Although the word terpene and terpenoids can be used interchangeably, terpenes that contain at least one oxygen atom is known as terpenoids (Croteau *et al.*, 2000). Based on the number of atoms in their skeleton, terpenes and terpenoids (terpenes like) can be classified as hemiterpenes (C_5), monoterpenes (C_{10}), sesquiterpenes (C_{15}), diterpenes (C_{20}), sesterterpenes (C_{25}), triterpenes (C_{30}) and tetraterpenes (C_{40}) (Rungsimakan, 2011). Terpenes are derived from Isoprene units which are attaches one to another either by head to tail or tail to tail linkages.

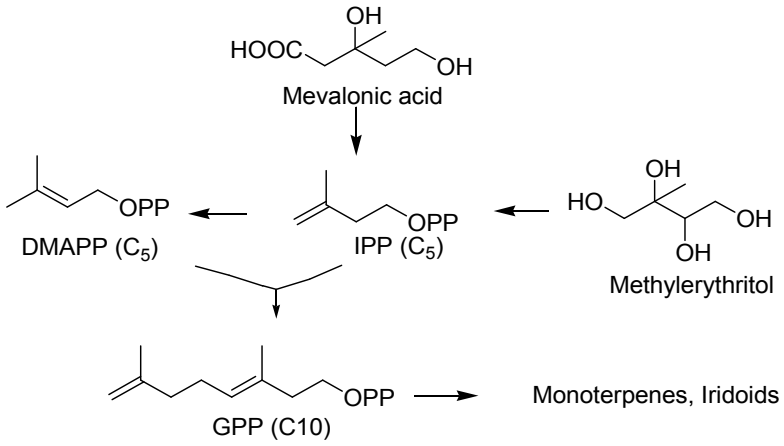

Scheme 2.1 Mevalonic Acid and Methyl Erythritol Biosynthetic Pathways of

2.9 Biosynthesis of diterpenoids

Diterpenoids are C20 molecules derived from four isoprene units joined head to tail. There are found in plants and marine animals. Geranylgeranypyrophosphate (GGPP) is the building block of all diterpenoids. Its allylic pyrophosphate group with the assistance of Mg^{2+} act as a good leaving group to generate carbocation which initiates a variety of different reaction paths (Ndunda, 2014). Depending on the bound conformation of the active site of each enzyme, a series of other reactions follow the carbocation formation. Simple enzymatic reduction of GGPP leads to formation of acyclic diterpenoids while protonation of a double

bond can initiate cyclization reactions through two main mode as shown in Scheme 2.2 (Ndunda, 2014).

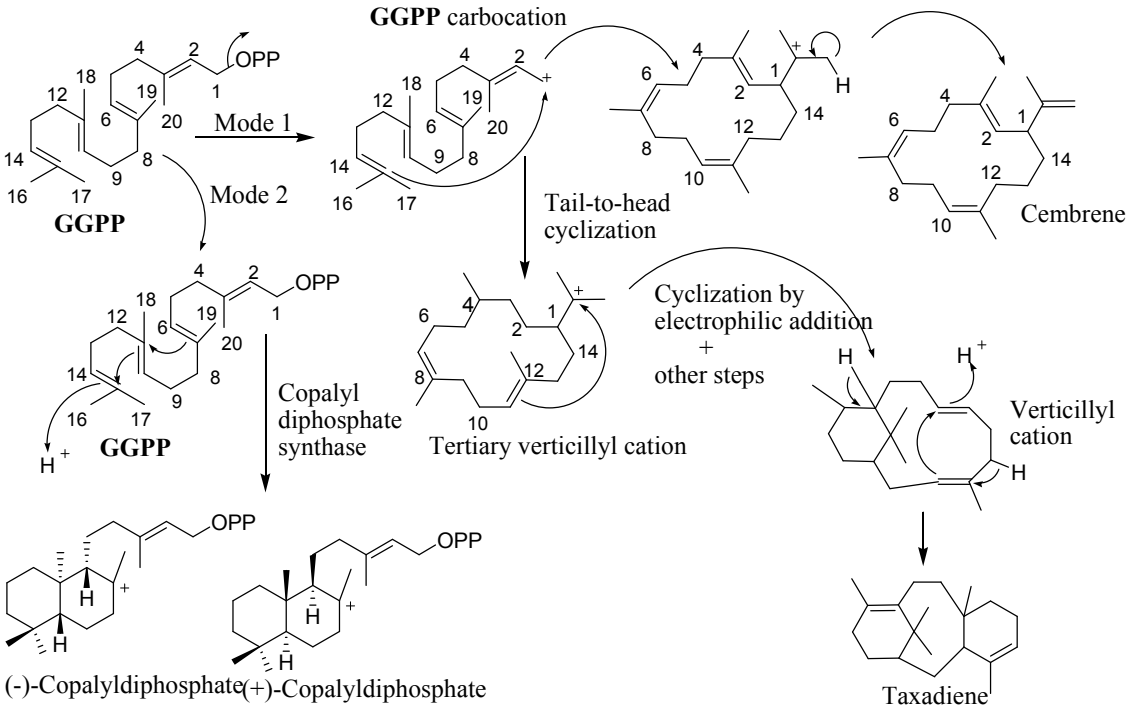

Enantiomeric carbocations from where di-, tri and tetra-cyclic diterpenoids are derived

Scheme 2.2 Cyclization of GGPP During Biosynthesis of Cyclic Diterpenoids

2.10 The Family Anacardiaceae

Two plants under the present study, namely *Lannea rivae* (Chiov) Sacleux and *Lannea schweinfurthii* (Engl.) Engl. belong to Anacardiaceae family. This family primarily includes trees, shrubs, and lianas with resin canals and clear to milky sap. Plants of this family are found in dry to moist, mostly lowland habitats, especially in the tropics and subtropics also extending into the temperate zone. The family is native to the western hemisphere (from southern Canada to Patagonia), Africa, southern Europe, temperate and tropical Asia, tropical and subtropical Australia, and most of the Pacific Islands. It is absent from northern Europe, temperate and arid Australia and New Zealand. In Kenya, the most common genera belonging to Anacardiaceae family include *Rhus, Ozoroa, Lannea, Pistacia, Pseudospondias, Sclerocarya* and *Soreindeia* (Kokwaro, 1986; 1994).

2.10.1 The Genus *Lannea*

The genus *Lannea* comprises about 40 species found in tropical Africa and Asia. Some *Lannea* species yield timber, while others are used in indigenous medicine. The most common *Lannea* species in East Africa include *Lannea edulis, L. alata, L. acida, L. barteri, L. schimperi, L. schweinfurthii, L. rivae, L. humilis,* and *L. fluccosa.* In Kenya, *L. schimperi, L. schweinfurthii, L. rivae, L. fulva, L. triphylla, L. edulis, L. humilis* are found (Kokwaro, 1994, Kindt *et al.*, 2011).

2.10.1.1 Ethnobotanical, Biological and Pharmacological Information on the Genus *Lannea*

Plants species belonging to the genus *Lannea* are used in African traditional medicine to treat many diseases and ailments including diarrhoea, gastric ulcer, liver diseases, elephantiasis, wound and snake bite (Njinga *et al.*, 2014). The traditional uses of various plants of the genus *Lannea* are summarized in Table 2.1. Several other plants in the Anacardiaceae family including those from *Rhus*, *Spondias*, Tapira, *Ozoroa* and *Anacardium* have also shown antimicrobial and radical scavenging activities because of the presenece of high levels of tanins, polyflavonoids, hydroquinones, alkylphenols and dihydroalkylhexenones (Adewusi *et al.*, 2013; Muhaisen, 2013).

Table 2.1: Ethnomedicinal Uses of Plants of the Genus *Lannea*

Plant	Plant part	Use	Biological activity	Reference
L. acida	Stem bark, roots	Diarrhoea, rheumatism, gonorrhoea, wounds gout, stomach ache, malaria, burns	Antibacterial, antioxidant, vibriocidal, cytotoxicity	Muhaisen, 2013; Ouattara *et al.*, 2011
L. alata	Stem ark, roots	Malaria, wound, snake bite, fractures, injuries	none	Okoth *et al.*, 2013
L. barteri	stem bark	Wounds, rheumatic, diarrhoea, gastritis, sterility, intestinal	Antibacterial, antifungal, antioxidant	Adoum, 2009; Allabi *et al.*, 2011; Koné *et al.*, 2011
L. coromandelica	stem ark, leave, root, Fruit	Liver disease, elephantiasis, impotence, ulcers, vaginal troubles, halitosis, heart disease, hematochezia, swellings, stomachache, dyspepsia, general debility, gout, dysentery, bruises, wounds and sores, diabetes, diarrhea, toothache, pain relief, lotion for leprous	Antioxidant, analgesic, cytotoxicity, hypotensive activity, hyperglycemic, wound healing effect, anti-atherothrombosis, antibacterial, antifungal, zoosporocidal, anti-inflammatory, antineuplasmic, anticancer, antimalarial	Imam and Moniruzzaman, 2014; Islam and Tahara, 2000; Okoth, 2014; Yun *et al.*, 2014
L. discolor	Root bark	Antimalarial, anti-fever, anti-constipation, antimenorrhagi, anti-infertility	antimalarial	Okoth, 2014
L. edulis	Root bark	Diarrhoea, diabetes, boils, sore eyes, abscesses, schistosomiasis, gonorrhoea, jaundice	Mutagenic effects, antioxidant	Okoth, 2014
L. fulva	stem bark	Antivenom, diarrhoea, icterus	Antimalaria, antidysentery	Kindt *et al.*, 2011; Kipkore *et al.*, 2014

Table 2.1 continued				
Plant	**Plant part**	**Use**	**Biological activity**	**Reference**
L. humilis	roots	Stomach pain, anaemia, nausea, general body weakness	Cytotoxicity, antitrypanosomal	Okoth, 2014
L. microcarpa	Leaves, bark, roots	Diarrhoea, gastroenteritis, malaria, bacterial infections, toothaches and wound, conjunctivis, stomatisis gingivitis, skin eruption, stomach ache, beriberi, schistosomiasis, haemorroids, rheumatism, sore throat, dysentery	Antioxidant, anti-inflammatory, antidiarrhoeic activity	Picerno *et al.*, 2006; Okoth, 2014;
L. nigritana	Stems, root bark, roots	Diarrhoea, dysentery, pulmonary troubles, mucosae, skin diseases, paralysis, epilepsy, convulsions, spasm, laxatives, stomach troubles	Cytotoxicity	Okoth, 2014
L. rivae	Roots, stem bark	Fever, colds, coughs, stomachache, bark as source of water	Antibacterial, antioxidant, antiplasmodial	Okoth *et al.*, 2016
L. schimperi	Stem bark	Gastric ulceration, dysentery, toothache, diarrhoea, chest infections, , stomach pains, mental disorders, epilepsy, snake bites, tuberculosis, skin infections, herpes simplex, herpes zoster, opportunistic infections from HIV/AIDS patients	Cytotoxicity, antimicrobial	Haule *et al.*, 2012; Okoth and Koorbanally, 2015

Table 2.1 continued				
Plant	**Plant**	**Plant**	**Plant**	**Plant**
L. schweinfurthii	Stem and root bark, leaves	Skin rashes, oral infections, stomachache, swelling of abdomen, boils, febrifuges, malaria, syphilis, cellulitis, abscesses, candidiasis, gingitivis, nasal ulcers, asthma, neurological disorder, anaemia, coughs	Neuroprotective , Anti-oxidant Antibacterial, antifungal, antiviral, amtiplasmodial, toxicity, antigiardial	Adewusi & Steenkamp 2011, Adewusi *et al.*, 2013; Seoposengwe *et al.*, 2013,; Okoth, 2014
L. stuhlmanii	roots	Antifungal, skin infections, anaemia, oral candidiasis, tonic, pain relief, herpes simplex, herpes zoster	Cytotoxicity, antitrypanosomal, anti-fungal	Okoth, 2014
L. triphylla	bark	Coughs, constipation, colds	none	Okoth, 2014
L. velutina	Bark, roots	Stomach pain, gastric ulcer, wound, skin diseases, Cell protection, diarrhoea, respiratory diseases, oedema, paralysis, epilepsy, insanity	Antioxidant, larvacidal, moluscicidal, lipoxygenase, inhibition	Ouattara *et al.*, 2011
L. welwitschii	Bark, seeds	Diarrhoea, haemorrhoids, menstrual problems, abdominal pains, epilepsy, oedema, gouts, swelling, palpitation, skin infection, ulcers, snake bites, wound, diabetes	Cytotoxicity, antibacterial, antidiarrheal, antidiabetic, antisickling activity	Okoth, 2014

2.10.1.2 Phytochemistry of the Genus *Lannea*

Various classes of compounds have been reported from the genus *Lannea*. These include terpenoids, flavonoids, alkylphenols and alkylcyclohexanones. A representive list is captured in Table 2.2.

Table 2.2: Some Compounds Reported from *Lannea* Species

Compound	Plant species	Reference
Myricadiol (**75**)	*Lannea coromandelica*	Yun *et al.*, 2014
Lupeol (**76**)	*L. coromandelica*	Okoth, 2014
β-Sitosterol (**77**)	*L. coromandelica*	Okoth, 2014
Stigmasterol (**78**)	*L. coromandelica*	Okoth, 2014
Sitosterol glucoside (**79**)	*L. coromandelica*	Okoth, 2014
6β-Hydroxy-stigmat-4-en-3-one (**80**)	*L. coromandelica*	Okoth, 2014
5α-Stigmastane-3,6-dione (**81**)	*L. coromandelica*	Okoth, 2014
Taraxerone (**82**)	*L. coromandelica*	Okoth, 2014
Taraxerol (**83**)	*L. coromandelica*	Okoth, 2014
Taraxeryl acetate (**84**)	*L. coromandelica*	Okoth, 2014
E-Lutein (**85**)	*L. rivae*	Okoth, 2014
(4S,6R)-Dihydroxy-6-[12'-Z-heptadecenyl]-cyclohex-2-enone (**86**)	*L. rivae*	Okoth *et al.*, 2016)
(4S,6R)-Dihydroxy-6-[14'-Z-nonadecenyl]-cyclohex-2-enone (**87**)	*L. rivae*	Okoth *et al.*, 2016
5-[12'(E)-Pentadecenyl]-4,5-dihydroxycyclohex-2-enone (**88**)	*L. schimperi*	Okoth and Koorbanally, 2015
5-[14'(E)-Heptadecenyl]-4,5-dihydroxycyclohex-2-enone (**89**)	*L. schimperi*	Okoth and Koorbanally, 2015
5-[16'(E)-Nonadecenyl]-4,5-dihydroxycyclohex-2-enone (**90**)	*L. schimperi*	Okoth and Koorbanally, 2015
5-[18'(E)-Heneicosenyl]-4,5-dihydroxycyclohex-2-enone (**91**)	*L. schimperi*	Okoth and Koorbanally, 2015
1-[12'(E)-Pentadecenyl]-cyclohex-3-en-1,2,5-triol (**92**)	*L. schimperi*	Okoth and Koorbanally, 2015
1-[14'(E)-Heptadecenyl]-cyclohex-3-en-1,2,5-triol (**93**)	*L. schimperi*	Okoth and Koorbanally, 2015
1-[16'(E)-Nonadecenyl]-cyclohex-3-en-1,2,5-triol (**94**)	*L. schimperi*	Okoth and Koorbanally, 2015
3-[12'(E)-Pentadecenyl]phenol (**95**)	*L. schimperi*	Okoth, 2014)
3-[14'(E)-Heptadecenyl]phenol (**96**)	*L. schimperi*	Okoth, 2014)
3-[16'(E)-Nonadecenyl]phenol (**97**)	*L. schimperi*	Okoth, 2014)
3-[18'(E)-Heneicosenyl]phenol (**98**)	*L. schimperi*	Okoth, 2014)

Table. 2.2 Continued		
Compound	**Plant species**	**Reference**
3-Pentadec-10'-Z-enylphenol (**99**)	*L. rivae*	Okoth *et al.*, 2016
3-Heptadec-12'-(Z)-enylphenol (**100**)	*L. rivae*	Okoth *et al.*, 2016
3-Nonadec-14'-(Z)-enylphenol (**101**)	*L. rivae*	Okoth *et al.*, 2016
3-Pentadecylphenol (**102**)	*L. rivae*	Okoth, 2014
4,5-Dihydroxy-4,2'-epoxy-5-[16'-Z-18'-E-heneicosenyldienne]-cyclohex-2-enone (**103**)	*L. rivae*	Okoth *et al.,* 2016)
Lanneanol (**104**)	*L. nigritana*	(Kapche *et al.,* 2007
Lanneaquinol (**105**)	*L.Bwelwitschii*	Groweiss *et al.,* 1997
2' (*R*)-Hydroxylanneaquinol (**106**)	*L. welwitschii*	Groweiss *et al.,* 1997
4α,5β-Dihydroxy-5 heptadec-8'-enylcyclohex-2-ene (**107**)	*L.welwitschii*	Groweiss *et al.,* 1997
4α,5α-Dihydroxy-5 heptadec-8'-enylcyclohex-2-ene (**108**)	*L.welwitschii*	Groweiss *et al.,* 1997
3-[14'-Nonadecenyl]phenol (Cardonol 7) (**109**)	*L. edulis*	(Queiroz *et al.,* 2003)
3-[14'-Heptadecenyl]phenol (Cardonol 13) (**110**)	*L. edulis*	Queiroz *et al*., 2003
5-[14'-Heptadecenyl]-4,5-dihydroxy-2-cyclohexenone (**111**)	*L. edulis*	Queiroz *et al.,* 2003
5-[16'-Nonadecenyl]-4,5-dihydroxy-2-cyclohexenone (**112**)	*L. edulis*	Queiroz *et al.,* 2003
5-[16'-Nonadecenyl]-4S,5S-dihydroxy-2-cyclohexenone (**113**)	*L. edulis*	Queiroz *et al.*, 2003
6,7-(2",2"-Dimethyl chromeno)-8-γ,γ-dimethyl allyl flavanone (**114**)	*L. acida*	Muhaisen, 2013
3',4'Dihydroxy-7,8 (2",2"-dimethyl chromeno)-6-γ,γ dimethyl allyl flavonol (**115**)	*L. acida*	Muhaisen, 2013
7-Methyltectorigenin (**116**)	*L. acida*	Muhaisen, 2013
Irisolidone (**117**)	*L. acida*	Muhaisen, 2013
Dihydrolanneaflavonol (**118**)	*L. alata*	Muhaisen, 2013
Lanneaflavonol (**119**)	*L. alata*	Okoth et al., 2013
(2R,3R)-(+)-4'-O-methyldihydroquercetin (**120**)	*L. coromandelica*	Islam and Tahara, 2000
7,2'-Dibuthoxy-4',5'-methylendioxyflavone **(121)**	*L. acida*	Sultana and Ilyas, 1986
5,5-Dibuthoxy- 2,2- bifuran (**122**)	*L. coromandelica*	Yun *et al.*, 2014
Physicion (**123**)	*L. coromandelica*	Reddy *et al.*, 2011

Numerous phytochemicals have been isolated from the genus *Lannea*. Myricadiol (**75**), lupeol (**76**), β-sitosterol (**77**), stigmasterol (**78**), *β*-sitosterol glucoside (**79**), 6β-hydroxy-stigmat-4-en-3-one (**80**), 5α-stigmastane-3,6-dione (**81**), taraxerone (**82**), taraxerol (**83**), taraxeryl acetate (**84**) were all isolated from *Lannea coromandelica* and others *Lannea* species. *E*-Lutein was reported from *L. rivae* (Okoth, 2014). alkenyl cyclohexanones (**86-91**, **103**, **107**, **108**, **111**, **112**, **113**) and alkenyl cyclohexanols (**92-94**, **104**) were identified from *L. schimperi*. Alkyl phenol (**95-102**, **105**, **106**, **109**, **110**) were also isolated from various *Lannea* species including *Lannea rivae*, *L. shimperi* and *L. welwitschii*. Flavonoids (**114**-**122**) and other type of compounds (**123**, **124**) were also reported from *Lannea* species (Muhaisen, 2013; Okoth, 2014).

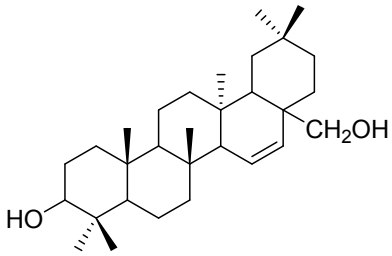

75

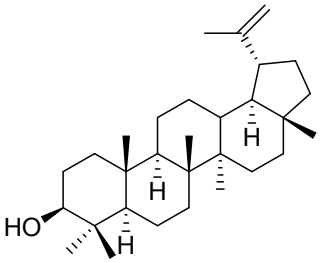

76

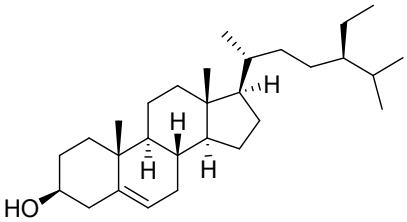

77

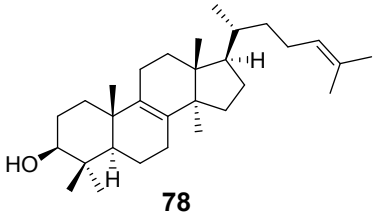

78

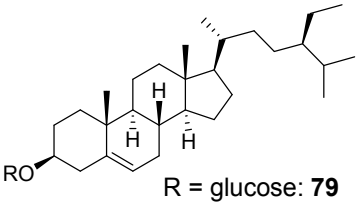

R = glucose: **79**

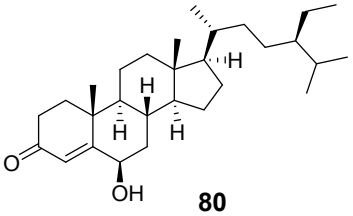

80

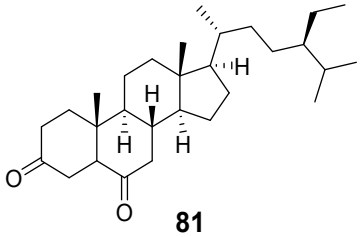

81

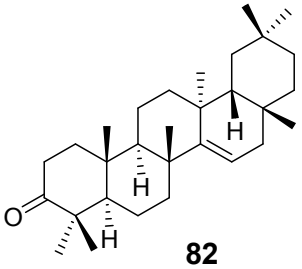

82

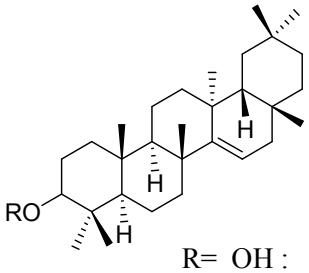

R= OH : **83**
R= Acetate: **84**

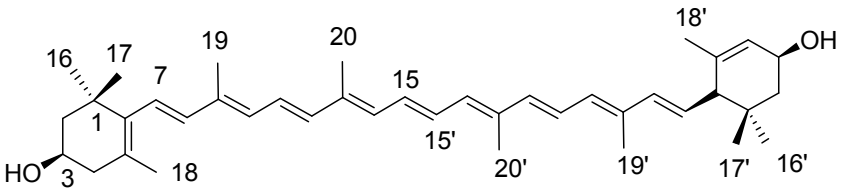

85

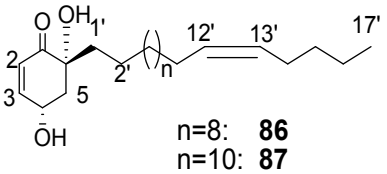

n=8: **86**
n=10: **87**

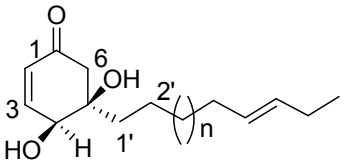

n=8: **88**
n=10: **89**
n=12: **90**
n=14: **91**

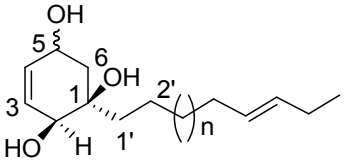

n=8: **92**
n=10: **93**
n=12: **94**

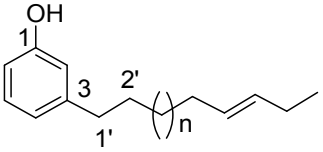

n=8: **95**
n=10: **96**
n=12: **97**
n=14: **98**

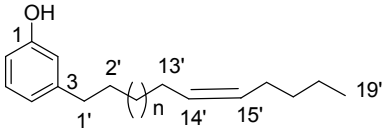

n=6: **99**
n=8: **100**
n=10: **101**

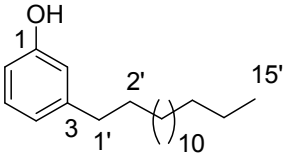

102

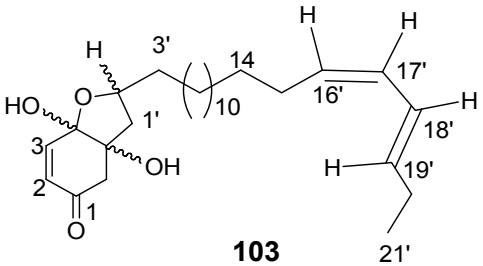

103

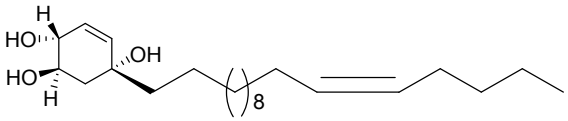

104

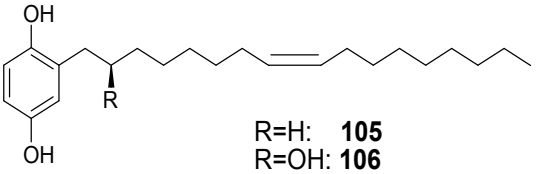

R=H: **105**
R=OH: **106**

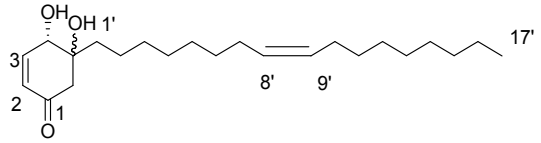

5β-OH: **107**
5α-OH: **108**

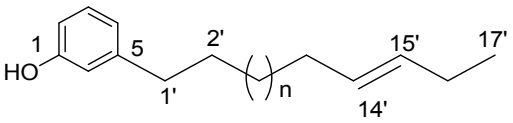

n=12: **109**
n=10: **110**

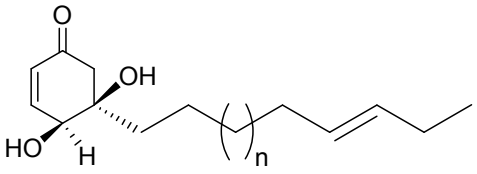

n=10: **111**
n=12: **112**

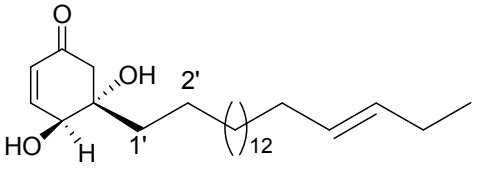

113

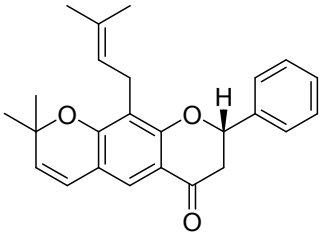

114

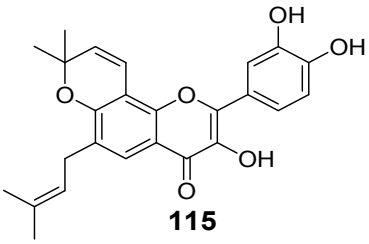

115

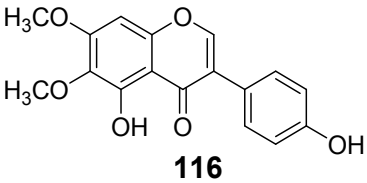

116

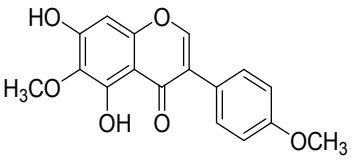

117

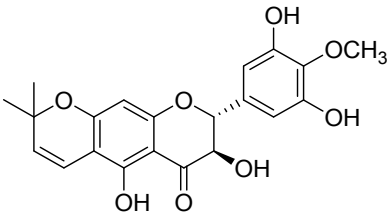

118

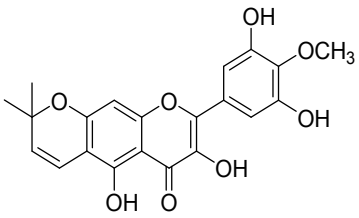

119

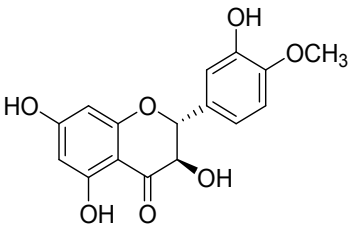

120

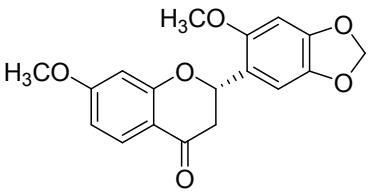

121

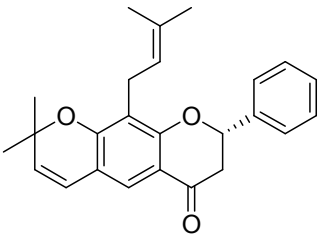

122

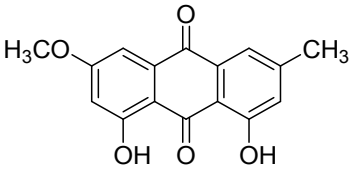

124

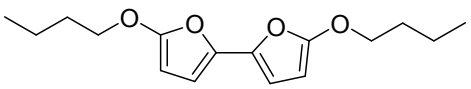

123

2.10.1.3 Biological Activity of Compounds Reported from the Genus *Lannea*

In Table 2.3, some compounds isolated from the genus *Lannea* with biological activities are listed. These activities include cytotoxicity, antiplasmodial, antimicrobial and antioxidant activity.

Table 2.3: Biological Activity of Compounds Reported from *Lannea*

Plant name	**Compounds**	**Activity reported**	**Reference**
Lannea schimperi	Mixture of 5-[12'(*E*)-pentadecenyl]-4,5-dihydroxycyclohex-2-enone (**88**), 5-[14'(*E*)-heptadecenyl]-4,5-dihydroxycyclohex-2-enone (**89**), 5-[16'(*E*)-nonadecenyl]-4,5-dihydroxycyclohex-2-enone (**90**), 5-[18'(*E*)-heneicosenyl]-4,5-dihydroxycyclohex-2-enone (**91**)	cytotoxicity	Okoth and Koorbanally, 2015
L. welwitschii	2' (*R*)-Hydroxylanneaquinol (**106**)	cytotoxicity	Groweiss *et al.,* 1997
	Lanneaquinol (**105**)	cytotoxicity	
L. rivae	2,4,5-Trihydroxy-2-[16'-Z-heneicosenyl]-cyclohexanone (**125**)	Cytotoxicity, antiplasmodial	Okoth *et al.,* 2016
	(4*S*,6*R*)-Dihydroxy-6-[12'-Z-heptadecenyl]-cyclohex-2-enone (**86**)	Antimicrobial, cytotoxicity, antiplasmodial	
	(4*S*,6*R*)-Dihydroxy-6-[140-Z-nonadecenyl]-cyclohex-2-enone (**87**)	Antimicrobial, antiplasmodial	
	Myricetin (**126**)	Antimicrobial, antiplasmodial, antioxidant	
	(-)-Epicatechin gallate (**127**)	Antimicrobial, antiplasmodial, antioxidant	
	1,2,4-Trihydroxy-4-[16'-Z-heneicosenyl]-cyclohexane (128)		
	Taraxerone (**83**)	cytotoxicity	
	Taraxerol (**82**)	cytotoxicity	

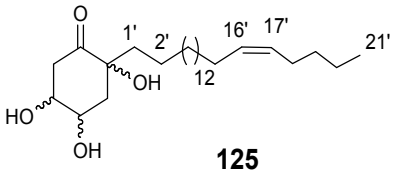

125

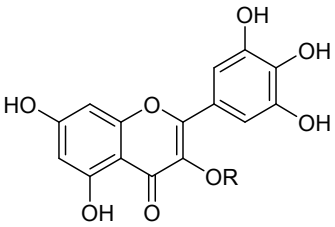

R=H: **126**

R=α-rhamnopyranoside: **129**

R= β-galactopyranoside: **130**

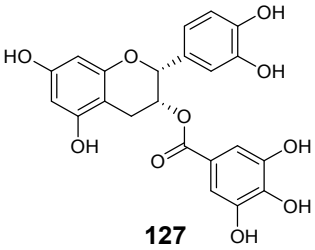

127

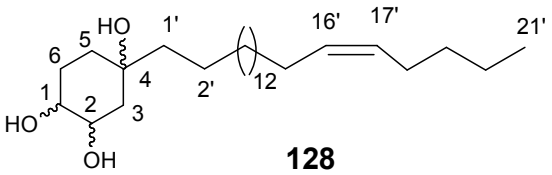

128

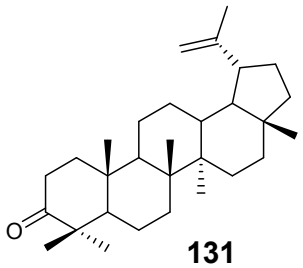

131

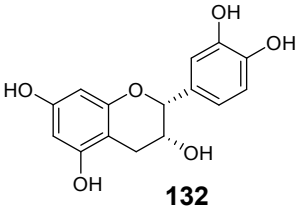

132

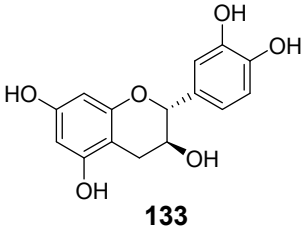

133

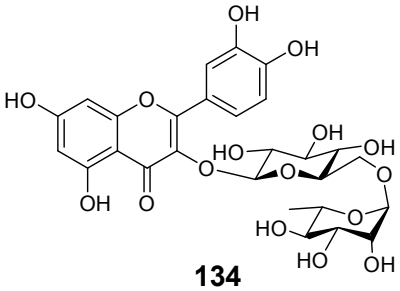

134

2.10.2 *Lannea rivae* (Chiov.) Sacleux

2.10.2.1 Botanical Description

Lannea rivae (Figure 2.1) is a deciduous shrub or small tree with a flat spreading crown; it can grow 1.5 - 9 meters tall. The plant is harvested from the wild as a local source of food, medicines and fibre. It is sometimes grown as a hedge. The plant is distributed in East tropical Africa, southern Ethiopia and Tanzania. In Kenya, the plant is found in Machakos, Marakwet, Pokot and Turkana counties (Kindt *et al.*, 2011). In Kenya, the bark and roots of *L. rivae* are used to treat coughs, colds and stomach-ache (Kipkore *et al.*, 2014). Fruits of *L. rivae* have a sweet flavor; they are often eaten by children and travellers. The inner bark is chewed for its sweet taste and as a source of water (Kokwaro, 1986).

Source: Gomedo *et al.,* 2015

Figure 2.1: Photo of Lannea rivae

2.10.2.2 Phytochemistry and Biological Activity of Compounds from *Lannea rivae*

Lannea rivae (chiov) Sacleux has been reported to have antibacterial, antioxidant and cytotoxic activity (Okoth, 2014). Previous phytochemical (Table 2.4) studies revealed the presence of alkylphenol (**99-101**), alkylcyclohexanones (**103**, **86**, **87**), alkylcyclohexanols (**92-94**, **104** and **128**) deivatives, triterpenes (**77**, **79**, **82** and **83**), flavonoids (**126**, **129**, **130** and **127**) and carotenoids (**85**).

Table 2.4: Biological Activity of Compounds Reported from *Lannea rivae*

Plant Name	Activity Reported	Reference
Taraxerol (**83**)	Cytotoxicity, antimicrobial	Okoth *et al.*, 2016
Taraxerone (**82**)	Cytotoxicity, antimicrobial	Okoth *et al.,* 2016
β-Sitosterol (**77**)	Cytotoxicity, antimicrobial	Okoth *et al.*, 2016
Sitosterol glucoside (**79**)	Cytotoxicity, antiplasmodial, antimicrobial	Okoth, 2014
E-Lutein (**85**)	Cytotoxicity, antimicrobial	Okoth *et al.,* 2016
3-Nonadec-14'-(Z)-enylphenol (**99**)	antimicrobial	Okoth *et al.*, 2016
4,5-Dihydroxy-4,2'-epoxy-5-[16'Z-18'E-heneicosenyldienne]-cyclohex-2-enone (**103**)	Cytotoxicity, antimicrobial	Okoth *et al.*, 2016
2,4,5-Trihydroxy-2-[16'-Z-heneicosenyl]-cyclohexanone (**125**)	Cytotoxicity, antimicrobial	Okoth *et al.,* 2016
(4S,6R)-dihydroxy-6-[12'-Z-heptadecenyl]-cyclohex-2-enone (**86**)	Cytotoxicity, antimicrobial, antioxidant	Okoth *et al.*, 2016
(4S,6R)-Dihydroxy-6-[14'-Z-nonadecenyl]-cyclohex-2-enone (**87**)	Cytotoxicity, antimicrobial	Okoth *et al.,* 2016
3-Pentadec-10'-Z-enylphenol (**99**)	Cytotoxicity, antimicrobial,	Okoth *et al.,* 2016
3-Heptadec-12'-Z-enylphenol (**100**)	Cytotoxicity, antimicrobial	Okoth, 2014
3-Pentadecylphenol (**102**)	Cytotoxicity, antimicrobial	
Myricetin (**126**)	Cytotoxicity, antimicrobial, antioxidant	Okoth, 2014
Myricetin-*O*-α-rhamnopyranoside (**129**)	Cytotoxicity, antimicrobial, antioxidant	Okoth, 2014
Myricetin-*O*-β-galactopyranoside (1**30**)	Cytotoxicity, antimicrobial, antioxidant	Okoth, 2014
(-)-Epigatechin-3-*O*-gallate (**127**)	Cytotoxicity, antimicrobial, antioxidant	Okoth, 2014

2.10.3 *Lannea schweinfurthii* (Engl.) Engl.

2.10.3.1 Botanical Description

Lannea schweinfurthii (Figure 2.2) is a small to medium-sized tree with drooping branches. The bark is grey, flaking to reveal a lighter underbark. Leaves are crowded at the end of branches and imparipinnate with 1-5 pairs of leaflets. Leaflets are broadly ovate or elliptic and 2-9 cm long. Terminal leaflet are larger than lateral leaflets and young leaflets densely hairy. Flowers are unisexual on different trees in axillary spikes and yellow-green. Fruits are

oblong-ellipsoid, fleshy, tipped with 4 small points (Kokwaro, 1986). *L. schweinfurthii* is distributed in Kenya, Uganda, Tanzania, Zanzibar, Malawi, Mozambique, Zambia, Zimbabwe, Swaziland and South Africa (Kokwaro, 1986, Kindt *et al.*, 2011).

Source: Dressler *et al.,* 2014

Figure 2.2: Photo of *Lannea schweinfurthii*

2.10.3.2 Ethnomedicinal Uses, Phytochemistry and Biological Activity of Compounds of *Lannea schweinfurthii*

Infusions of the roots of *Lannea schweinfurthii* (Anacardiaceae) are reported to enhance memory and are used as a sedative (Seoposengwe *et al.*, 2013). The plant is also used to treat diarrhoea, anaemia, asthma, nasal, ulcers, gingivitis, oral candidiasis, abscesses, cellulitis, malaria, syphilis, skin raches, boils, febrifuge, swelling of abdomen and coughs (Johns *et al.*, 1995; Geissler *et al.*, 2002; Maregesi *et al.*, 2007; Maregesi *et al.*, 2008; Gathirwa *et al.*, 2008; Kokwaro, 2009; Maregesi *et al.*, 2010; Ribeiro *et al.*, 2010; Adewusi and Steenkamp, 2011; Gathirwa *et al.*, 2011). The roots of *L. schweinfurthii* have showed good radical scavenging activity (Adewusi and Steenkamp, 2011). The plant also has low cytotoxic and

good neuroprotective effect on amyloid-β induced neurotoxicity in SY5Y cells (Adewusi *et al.*, 2013).

The plant was reported for various biological activities including antiplasmodial, antibacterial, antifungal, antiviral (Semliki forest virus, HIV type I and II), antimalarial, cytoxicity, antigiardial and antioxidant (Geissler *et al.*, 2002; Maregesi *et al.*, 2008; Gathirwa *et al.*, 2008; Ribeiro *et al.*, 2010, Adewusi and Steenkamp, 2011; Gathirwa *et al.*, 2011). Alkylphenol, alkylcyclohexanone and alkylcyclohenol were identified from *L. schweinfurthii* in previous phytochemical work (Okoth, 2014) and these are listed in Table 2.5 along with their biological activity.

Table 2.5: Biological Activity of Compounds Reported from *Lannea schweinfurthii*

Compounds	Activity reported	Reference
β-Sitosterol (**77**)	Cytotoxicity, antimicrobial	Okoth, 2014
Sitosterol glucoside (**79**)	Antimicrobial	
Lupenone (**131**)		
Epicatechin (1**32**)	Cytotoxicity, antimicrobial, antioxidant	
Epicatechin galate (**127**)	Cytotoxicity, antimicrobial, antioxidant	
Catechin (**133**)	Cytotoxicity, antimicrobial, antioxidant	
Rutin (**134**)	Antimicrobial	

2.11 The Family Asteraceae

The Asteraceae family is the largest family of flowering plants. A large majority of the plants in this family are herbaceous, while tree and shrubs are comparatively rare (Faleye and Ogundaini, 2012). There are about 3,000 plant species distributed in 17 tribes and 1,700 genera in the family Asteraceae (Faleye and Ogundaini, 2012). Plants from this family are distributed throughout the world and occupy a wide range of habitats. Within the family, there exist a great diversity in growth form, ranging from annual and perennial herbs to shrubs, vines or trees (Lajter, 2015).

Asteraceae (also known as Compositae) is a taxon of dicotyledonous flowering plants and the family's name Asteraceae is derived from the genus name Aster referring to the star-shaped

flower head of it members. Asteraceae is the second largest family in the division of Magnoliophyta after Orchidaceae. Common characteristics of Asteraceae plants include inflorescence (a capitulum or flower head), syngenesious anthers (stamens fused together at their edges by the anthers, forming a tube) and ovary with basal arrangement of the ovules (Walter *et al.*, 1999, Hind, 2003). The Asteraceae family is the easiest family to recognise and many of the plant species are used as ornament. The composite nature of the inflorescence of plants species from this family led the early taxonomist to call this family the Asteraceae family. Plants of this family are mostly herbaceous, shrubs, vines or trees. The family is widely distributed around the world especially in arid and semi-arid regions of subtropical and lower temperate latitude (Saeidnia *et al.*, 2011).

2.11.1 The Genus *Psiadia*

The genus *Psiadia* (Asteraceae) is an old world genus of herbaceous and woody shrubs distributed throughout Asia and surrounding continental areas of Africa and Arabian Peninsula. This phenotypically diverse group of approximately 65 species can be found in medium to high altitude mountainous habitats (Strijk *et al.*, 2012). The genus is well distributed in Madagascar and the Mascarene Islands (Rodrigues, Mauritius, Reunion) in the Indian ocean where 26 species are found (Besse *et al.*, 2003). *Psiadia* is recognised as one of the genera establishing the connection between Asian and African flora (Abou-Zaid *et al.*, 1991).

2.11.1.1 Ethnobotanical and Pharmacological Information on the Genus *Psiadia*

In general, leaves of *Psiadia* plants are used to treat cutaneous infections, bronchial infections and for stress release. In Mauritius, *Psiadia* species are traditionally used to cure bronchitis and asthma (Besse *et al.*, 2003). Table 2.6 gives some ethnobotanical and pharmacological informations on the genus *Psiadia*.

Table 2.6: Ethnobotanical Uses of *Psiadia* Species

Plant	Plant part	Uses	Biological activity	Reference
P. arabica	Leaves	Fever, injuries, colds	Antibacterial, cytotoxic	Gouda *et al.*, 2014
P. punctulata	Leaves, branches, poultine leaf	Abdominal pain, colds, fevers, removal of ectoparasites from cattle, rheumatoid arthritis, healing of broken bones, analgesic, bronchitis, asthma, cough	Analgesic, antifungal	Juma *et al.*, 2001; Juma *et al.*, 2006; Midiwo *et al.*, 1997
P. altissima	Leaves	Heamostatic, antidiarheic	Antibacterial, carminative, disinfectant	Ramanoelina *et al.*, 1994
P. terebenthina	Leaves, leaf poultine	Asthma, fever, abscesses, boils	antibacterial	Gurib-Fakim *et al.*, 2003
P. salviifolia	Leaves	Toothache, snake bite, abdominal pain, respiratory troubles, vermifuge	Antibacterial, antifungal	Dennis, 1973
P. dentata	Leaves	Abscesses	Antivirus (polyvirus type 2, perpes simplex virus type 1, HSV-1)	Robin *et al.*, 1998

2.11.1.2 Compounds from the Genus *Psiadia*

Several phytochemicals were isolated from the genus *Psiadia*; these include flavonoids (**135-147**), kaurene (**148**, **149**, **152**, **153**) and trachylobane (**150**, **151**, **154**, **155**, **156**) diterpenoids, docosyl (**157**, **158**) and eicosanyl-*p*-coumarates (**159**, **160**).

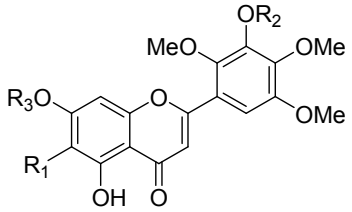

	R_1	R_2	R_3
135	OMe	H	Me
136	H	H	Me
137	H	Me	Me
138	H	H	H

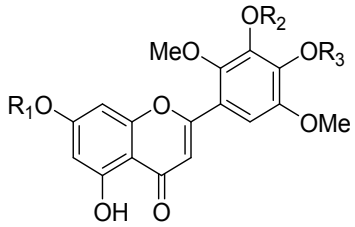

	R_1	R_2	R_3
139	H	Me	Me
140	Me	Me	H
141	H	Me	H

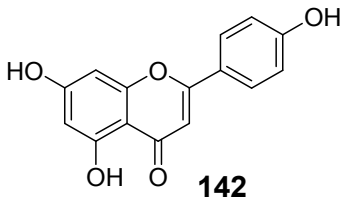

142

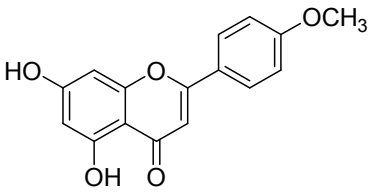

143

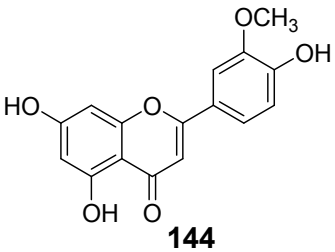

144

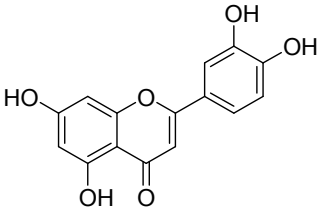

145

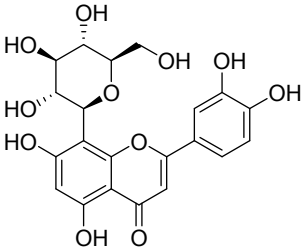

146

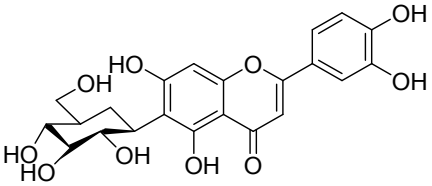

147

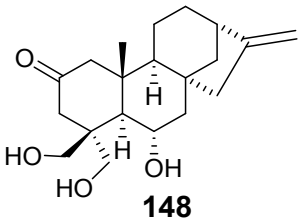

148

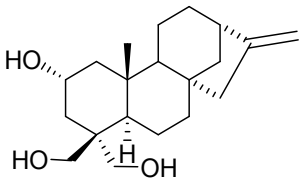

149

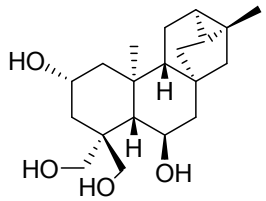

150

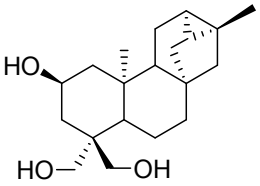

151

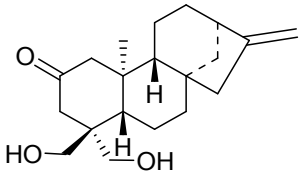

152

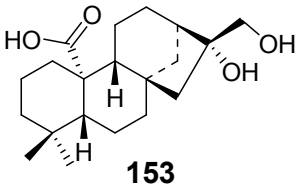

153

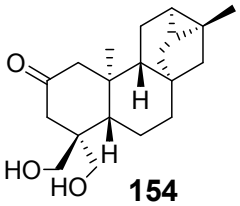

154

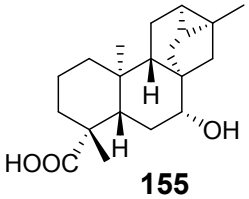

155

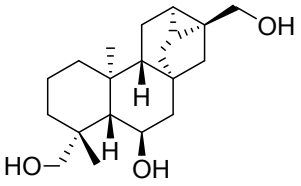

156

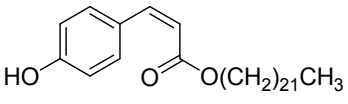

157

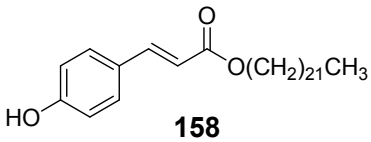

158

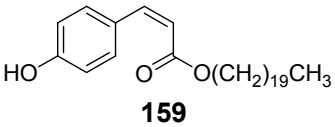

159

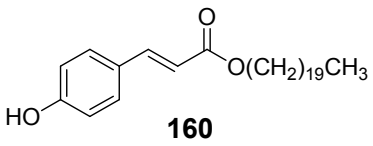

160

2.11.2 *Psiadia punctulata* Vatke (Asteraceae)

2.11.2.1 Botanical Information on *Psiadia punctulata*

Psiadia punctulata (Figure 2.3) is used in East African traditional medicine to treat colds, fevers, abdominal pain and for removal of ectoparasites from cattle (Kokwaro, 1976). The shiny look of *Psiadia punctulata*'s leaves was attributed to the presence of leaf exudate (Midiwo *et al.*, 2001). Although the plant did not show strong activity against human fungi (Midiwo *et al.*, 2001), it has shown moderate activity against *Colletotricum coffeanum* and *Fusarium oxysporum* which are coffee berry and potatoes rot fungi (Midiwo *et al.*, 2001).

Previously, *Psiadia punctulata* was considered by some taxonomists to be the same as *P. arabica*. However, some taxonomists highlighted that the two taxa are different, and phytochemical reports further support this view (Midiwo *et al*., 1997; Juma *et al.*, 2001; Juma *et al.*, 2006).

Figure 2.3: Photo of *Psiadia punctulata*

2.11.2.2 Compounds from *Psiadia punctulata*

Phytochemical report on leaf exudates of *P. punctulata* (Table 2.7) revealed that the plant contains *ent*-trachylobane (**150**, **151**, **154**, **155**, **156**) and *ent*-kaurane (**152**, **153**) type diterpenoids, flavones (**137-141**) and eicosanyl and docosyl-*p*-coumarates (Midiwo *et al.*, 1997; Juma *et al.*, 2001; Juma *et al.*, 2006). However, there is no report on other parts of the plant including the roots and the stem barks.

Table 2.7: Reported Compounds from *Psiadia punctulata*

Name of the Compound	Class of the Compound	Plant part	Reference
5,7-Dihydroxy-2',3',4',5'-tetramethoxyflavone (**139**)	Flavone	Leaf exudates	Juma *et al.*, 2001
5-Hydroxy-7,2',3',4',5'-pentamethoxyflavone (**137**)	Flavone	Leaf exudates	
5,4'-Dihydroxy-7,2',3',5'-tetramethoxyflavone (**140**)	Flavone	Leaf exudates	
5,7,4'-Trihydroxy-2',3',5'-trimethoxyflavone (**141**)	Flavone	Leaf exudates	
5,7,3'-Trihydroxy-2',4',5'-trimethoxyflavone (**138**)	Flavone	Leaf exudates	
Z-Docosyl-p-coumarate (**157**)	Phenyl propanoid	Leaf exudates	
E-Docosyl-p-coumarate (**158**)	Phenyl propanoid	Leaf exudates	
Z-Eicosanyl p-coumarate (**159**)	Phenyl propanoid	Fresh leaves	Keriko *et al.*, 1997
*E-Eicosanyl p-coumarate (**160**)*	Phenyl propanoid	Fresh leaves	Keriko *et al.*, 1997
18,19-Dihydroxy-*ent*-trachyloban-2-one (**154**)	Diterpenoid	Leaf exudates	Midiwo *et al.*, 1997
Psiadin (**152**)	Diterpenoid	Leaf exudates	
(ent)-16β,17-Dihydroxy-Kauran-20-oic acid (**153**)	Diterpenoid	Leaf exudates	
7α-Hydroxy-ent-trachyloban-19-oic acid (**155**)	Diterpenoid	Leaf exudates	
ent-Trachyloban-6β,17,19-triol (**156**)	Diterpenoid	Leaf exudates	Juma *et al.*, 2006
ent-Trachyloban-2β,6α,18,19-tetraol (**150**)	Diterpenoid	Leaf exudates	
ent-Trachyloban-2β,18,19-triol (**151**)	Diterpenoid	Leaf exudates	

2.11.2.3 Biological Activity of Some Compounds Isolated from *Psiadia*

The biological activity of some compounds reported from the genus *Psiadia* is listed in Table 2.8.

Table 2.8: Biological Activity of Compounds Reported from the Genus *Psiadia*

Plant Name	Compounds	Activity Reported	Reference
Psiadia dentata	3-Methylkaempferol	Antiviral	Robin *et al.*, 1998; Robin *et al.*, 2001
	3-Methylkaempferol and 3,4′-dimethylkaempferol	Antiviral	
P. altissima	Essential oil	Antibacterial	Ramanoelina *et al.,* 1994
P. punctulata	*ent*-Trachyloban-19-ol	Antituberculosis	Martins *et al.,* 2017
	ent-Trachylobane-2α,6β,18,19-tetraol	Antituberculosis	
	ent-Trachyloban-2β,6β,19-triol	Antituberculosis	
	ent-Trachyloban-2β,18,19-triol	Antituberculosis	
	16α,17-Dihydroxy-ent-kaur-20-oic acid	Antituberculosis	
	ent-Kaur-16-en-18,19-diol	Antituberculosis	
	18,19-Dihydroxy-ent-kaur-16-en-2-one	Antituberculosis	

2.11.3 The Genus *Aspilia*

The genus *Aspilia* consists of highly variable species with obvious overlap in their morphological characters. There are over sixty known species distributed in tropical Africa and twelve in western Africa (Adegbite and Olorode, 2003). The species are annual herbaceous weeds except for *A. africana* and *A. rudis* which are perenial (Adegbite and Olorode, 2003). *Aspilia* plants are also widely spread in south, south west and west of Kenya from the coast to the Lake Victoria. The genus *Aspilia* (Asteraceae) exhibited biological activities among which antibacterial and antifungal effects, attributed to the presence of kaurane-type diterpenoids and sesquiterpene lactones (Souza *et al.*, 2015).

2.11.3.1 Ethnobotanical and Pharmacological Information on the Genus *Aspilia*

The use of medicinal plants in the fight against diseases has been known since ancient time all over the word. Plants belonging to *Aspilia* genus are also known for their therapeutic potential. The traditional use of *Aspilia* species is summarized in Table 2.9.

Table 2.9: Ethnobotanical uses of *Aspilia* Species

Plant	Plant part	Uses	Biological activity	Reference
A. africana	Leaves	Stomach troubles, cough, to clean sores, corneal opacity, anaemia, gonorrhoea, tuberculosis, rheumatic pains, wound, insect bites	Anti-inflammatory, antiplasmodial, anti-ulcer, anti-viral, anti-fungal, anti-bacterial	Ita *et al.*, 2010; Rodriguez *et al.*, 1985; Souza *et al.*, 2015
A. holstii	Leaves	Relief for neuralgia	Anti microbial	Rodriguez *et al.*, 1985
A. mossambicensis	Leaves, roots	Alleviate menstrual cramps, cystitis, gonorrhoea, abdominal pain, backage, increase milk production, healing of wounds and ringworms, intestinal worms, respiratory problems, malaria, malaria	Antimicrobial antimalarial, galactogogue	Musyimi *et al.*, 2007, 2008; Page *et al.*, 1997
A. pluriseta	Leaves	Wound, malaria, fever,	Healing, antiplasmodial, antibacterial	Kuria, 2014; Page *et al.*, 1997; Sebisubi *et al.*, 2010
A. latissima	Leaves	Wound, malaria	Antibacterial, antifungal	Souza *et al.*, 2015

2.11.3.2 Compounds from the Genus *Aspilia*

Various classes of compounds were reported from the genus *Aspilia*. These include triterpenes (**250-254**), diterpenes (**255-267**), thiarubrines (**269**, **271**), tiophenes (**268**, **270**) and coumarine derivatives (**272-273**). Selected compounds isolated from the genus *Aspilia* are summarized in Table 2.10.

Table 2.10: Reported Compounds from the Genus *Aspilia*

Name of the Compound	Class of the Compound	Plant Part/Plant species	Reference
3*β*-*O*-[α-rhamnopyranosyl-(1→6)-β-glucopyranosyl]-Ursan-ene (**161**)	Glycosylated triterpenoid	Leaves of *A. africana* Leaves of *A. africana* Leaves of *A. africana* Leaves of *A. africana*	Faleye, 2012
3*β*-Hydroxyolean-12-ene (**162**)	Triterpenoid		
3-*β*-Acetoxyolean-12-one (**163**)	Triterpenoid		
Oleanolic acid (**165**)	Triterpenoid		
Stigmasterol (**164**)	Sterol	Root of *A. latissima*	Souza *et al.*, 2015
Kaurenoic acid (**166**)	Diterpenoid	Leaves of *A. mossambicensis* Root of *A. latissima*	Page *et al.*, 1992; Souza *et al.*, 2015
Grandiflorenic acid (**167**)	Diterpenoid	Leaves of *A. mossambicensis* Root of *A. latissima,* aerial part of *A. pluriseta*	Page *et al.*, 1992; Sebisubi *et al.*, 2010; Souza *et al.*, 2015
Ent-15*β*-senecioyloxy-16,17-epoxy-kauran-18-oic acid (**168**)	Diterpenoid	Aerial part of *A. pluriseta*	Sebisubi *et al.*, 2010
Ent-15*β*-senecioyloxy-kaur-16-en-19-oic acid (**169**)	Diterpenoid	Aerial part of *A. pluriseta*	
15*β*-Angeloyloxy-*ent*-Kaur-16-en-19-oic acid (**170**)	Diterpenoid	Root and Aerial part of *A. parvifolia,* aerial part of *A. pluriseta*	Bohlmann *et al.,* 1981; Sebisubi *et al.*, 2010
15*β*-Tigloyloxy-*ent*-kaur-16-en-19-oic acid (**171**)	Diterpenoid	Root and aerial part of *A. parvifolia,* aerial part of *A. pluriseta*	
15*α*-Tigloyloxy-ent-kaur-16-en-19-oic acid (**172**)	Diterpenoid	Root and Aerial part of *A. parvifolia*	
16,17-Epoxy-15*β*-angeloyloxy-ent-kauran-19-oic acid (**173**)	Diterpenoid	Root and aerial part of *A. parvifolia,* aerial part of *A. pluriseta*	
16,17-Epoxy-15*β*-tigloyloxy-ent-kauran-19-oic acid (**174**)	Diterpenoid	Root and aerial part of *A. parvifolia* Root of *A. latissima* Aerial part of *A. pluriseta*	Bohlmann *et al.*, 1981; Sebisubi *et al.*, 2010; Souza *et al.*, 2015
15*β*-Methy-ent-kaur-16-en-19-oate (**175**)	Diterpenoid	Root of *A. foliacea*	Ambrosio *et al.*, 2008

Table 2.10 continued			
Name of the Compound	**Class of the Compound**	**Plant Part/Plant species**	**Reference**
15*β*-Hydroxy-kaur-16-en-19 oic acid (**176**)	Diterpenoid	Root of *A. foliacea*	Ambrosio *et al.*, 2008
15*β*-Isovaleryloxy-ent-kaur-16-en-19 oic acid (**177**)	Diterpenoid	Root of *A. foliacea*	
17-Hydroxy-ent-kaur-15-en-19-oic acid (**178**)	Diterpenoid	Root of *A. foliacea*	
Thiophene A (**179**)	Polyene	Aerial part of *A. mossambicensis Root of A. parvifolia*	Bohlmann *et al.*, 1981; Norton *et al.*, 1993a
Thiarubrine A (**180**)	Polyene	Aerial part of *A. mossambicensis*	
Thiophene B (**181**)	Polyene	Aerial part of *A. mossambicensis*	
Thiarubrine B (**182**)	Polyene	Aerial part of *A. mossambicensis*	
Pentaynene (**183**)	Polyene	Aerial part of *A. mossambicensis*	
Ethyl cafeate (**184**)	Coumarines derivatives	Leaves of *A. africana*	Faleye, 2012
3-(4-hydroxyphenyl)-2-Oxo-2*H*-chromene-6-carbaldehyde (**185**)	Coumarines derivatives	Leaves of *A. africana*	

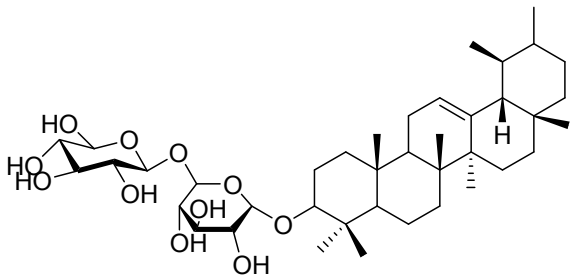

161

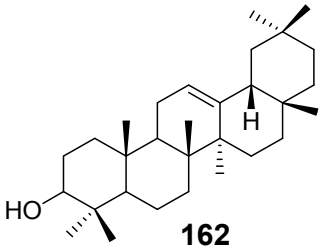

162

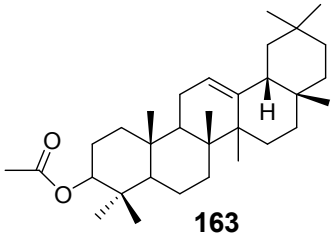

163

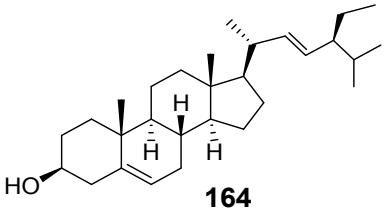

164

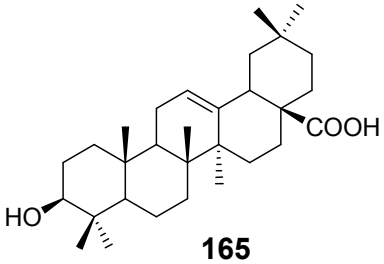

165

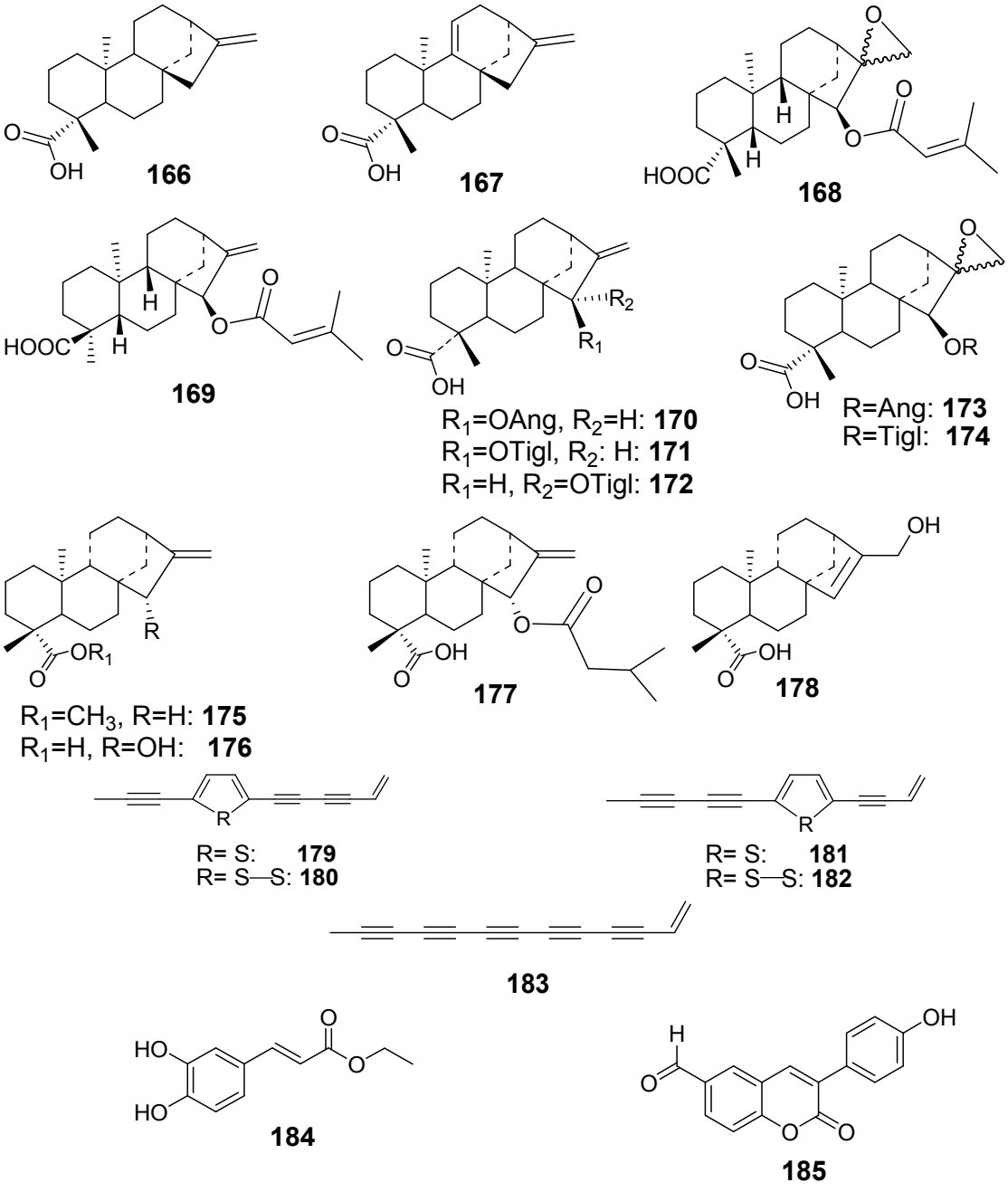

2.11.4 *Aspilia pluriseta* Schweinf.

2.11.4.1 Botanical Information on *Aspilia pluriseta*

Aspilia pluriseta (Figure 2.4) has been used in a number of traditional medicine systems to treat lacerations, bruises, burns and is reputed to aid the healing of cutaneous lesions. The

plant is found in Kenya and is commonly known as "*dwarf aspilia"* (Kuria, 2014). *A. pluriseta* is locally known in Kenya as "*Muuti"* (Kikuyu), "*Wuti"* (Kamba), "*Ol-oiyabase"* (Maasai) and "*Shilambila"* (Luhya). Many communities in the eastern (including Kenya) and southern Africa use the plant ethno-medically to treat wounds (Kuria, 2014).

Sebisubi *et al.* (2010), isolated a number of diterpenes from aerial part of *A. pluriseta*. Four of these diterpenes demonstrated moderate activity against chloroquine sensitive (D6) and chloroquine resistant (W2) *Plasmodium falciparum*. Phytochemical screening on the aqueous root bark extract of *A. pluriseta* revealed the presence of flavonols, flavones, flavonoids, chalcones, tannins, bound anthraquinones and sterols. The aqueous extract of the plant was also reported to exhibit hypoglycemic properties in mice (Piero *et al.*, 2011).

Figure 2.4: Photo of *Aspilia pluriseta*

2.11.4.2 Compounds from *Aspilia pluriseta*

Phytochemical information on *Aspilia pluriseta* in scanty. However, Sebisubi reported some diterpenes which are summarized in Table 2.11 (Sebisubi *et al.*, 2010).

Table 2.11: Compounds Isolated from *Aspilia pluriseta*

Compound Name	Class	Plant part	Reference
Grandiflorenic acid (**167**)	Diterpenoid	Aerial part	Sebisubi *et al.*, 2010
Ent-15*β*-senecioyloxy-16,17-epoxy-kauran-18-oic acid (**168**)			
Ent-15β-senecioyloxy-kaur-16-en-19-oic acid (**169**)			
15*β*-Angeloyloxy-ent-kaur-16-en-19-oic acid (**170**)			
15*β*-Tigloyloxy-ent-kaur-16-en-19-oic acid (**171**)			
16,17-Epoxy-15β-angeloyloxy-ent-kauran-19-oic acid (**173**)			
16,17-Epoxy-15β-tigloyloxy-ent-kauran-19-oic acid (**174**)			

2.11.5 *Aspilia mossambicensis* (Oliv.) Wild (Asteraceae)

2.11.5.1 Botanical Information on *Aspilia mossambicensis*

Aspilia mossambicensis (Figure 2.5) is a shrub native to central and eastern tropical Africa. The plant is found in Ethiopia, D. R. Congo, Zambia, Zimbabwe, Malawi, Mozambique, Tanzania, Uganda and Kenya (Norton *et al.*, 1993; Musyimi *et al.*, 2008). In eastern Africa, the plant is well known for the treatment of cystitis, gonorrhoea, abdominal pain, intestinal worms and skin infections (Page *et al.*, 1993; Norton *et al.*, 1993).

Phytochemical screening of the plant indicated that it contains tridecapenta-yene derivatives, thiophene derivatives, thiarubrines, flavonoids, alkaloids, steroids, saponins, anthraquinones, carbohydrates and diterpenes (Page *et al.*, 1992; Norton *et al.*, 1993; Page *et al.*, 1997; Musyimi *et al.*, 2007). Thiophenes A and B, Thiarubrines A and B were previously isolated from *Aspilia mossambicensis* (Norton *et al.*, 1993). The root of this plant also showed antibacterial activity which explains why wild chimpanzees consume the leaves of *A. mossambicensis* in self-medication (Norton *et al.*, 1993).

Source: Dressler *et al*., 2014

Figure 2.5: Photo of Aspilia mossambicensis

2.11.5.2 Compounds from *Aspilia mossambicensis*

Previous analysis of the extract of *A. mossambicensis* led to identification of thiarubrine A, B, thiophene A, B, and pentayene (Table 2.12). The structures of these compounds are illustrated in section 2.9.3.2.

Table 2.12: Reported compounds from *Aspilia mossambicensis*

Compounds	**Class**	**Plant part**	**Reference**
Kaurenoic acid (**166**)	Diterpenoid	Leaves	Page *et al.*, 1992
Grandiflorenic acid (**167**)	Diterpenoid		
Thiophene A (**179**)	Polyene	Roots	Norton *et al.*, 1993; Page *et al.*, 1997
Thiarubrine A (**180**)	Polyene		
Thiophene B (**181**)	Polyene		
Thiarubrine B (**182**)	Polyene		
Pentaynene (**183**)	Polyene		

2.11.6 Biological Activity of Compounds from the Genus *Aspilia*

The biological activity of some of the isolated compounds from the genus *Aspilia* is listed in Table 2.13. Several biological tests were conducted on different compounds. These include antimicrobial, cytotoxicity, antioxidamt and antiplasmodial activity. Among the reported compounds, some polyenes (Table 12) showed antimicrobial activity (Norton *et al.*, 1993; Page *et al.*, 1997).

Table 2.13: Biological Activity of Compounds Reported from *Aspilia* Species

Plant name	**Compound**	**Activity Reported**	**Reference**
Aspilia africana	Ethylcafeate (**184**)	Antioxidant, antimicrobial	Faleye and Ogundaini, 2012
	3-(4-Hydroxyphenyl)-2-oxo-2H-chromene-6-carbaldehyde (**185**)		
A. latissima, *A. mossambicensis, A. pluriseta*	Kaurenoic acid (**166**)	Antileishmanial, antimicrobial, uterotonic	Page *et al.*, 1992; Sebisubi *et al.*, 2010; Souza *et al.*, 2015
A. latissima *A. mossambicensis*	Grandiflorenic acid (**167**)	Antileishmanial, antimicrobial, uterotonic	Page *et al.*, 1992; Souza *et al.*, 2015
A. mossambicensis	Thiarubrine A (**180**)	Antimicrobial, cytotoxicity	Rodriguez *et al.*, 1985
A. pluriseta	15*β*-Angeloyloxy-kaur-16-en-18-oic acid (**170**)	Antimicrobial, cytotoxicity	Sebisubi *et al.*, 2010
	16,17-Epoxy-15*β*-angeloyloxy-kauran-18-oic acid (**173**)	Antimicrobial, cytotoxicity	
	ent-15*β*-Senecioyloxy-16,17-epoxy-kauran-18-oic acid (**168**)	Antimicrobial, cytotoxicity	

CHAPTER THREE

MATERIALS AND METHODS

3.1 Plant Materials

Roots and stem bark of both *Lannea rivae* and *Lannea schweinfurthii,* aerial parts and root of *Aspilia pluriseta* and *Aspilia mossambicensis,* were collected from Muthetheni location, Machakos County, Mwala Sub-County, Kenya. Leaves, stem bark and roots of *Psiadia punctulata* were collected from Ngong forest, Nairobi County, Kenya. All the plant material were collected between July 2014 and December 2015. Voucher specimens of the plants consisting of *Lannea rivae* (SY2014/01), *Lannea schweinfurthii* (SY2014/02), *Aspilia pluriseta* (SY2015/05), *Aspilia mossambicensis* (SY2015/06) and *Psiadia punctulata* (SY2014/04) were deposited at the Herbarium, School of Biological Sciences, University of Nairobi.

3.2 General Methods

Melting point of the isolated compounds was measure on Büchi Melting point B-545 instruments. Infra-Red (IR) spectra were recorded on PerkinElmer Instruments, Spectrum one FT-IR spectrophometer. The UV absorbance of the compounds was measured using a Shimadzu UV-Vis spectrometer-2700. The NMR spectra were acquired on Bruker Avance II 500, Bruker Avance II 600 and Bruker Avance III HD 800 spectrometers, using the residual solvent peaks as reference. The spectra were processed using MestReNova 10.0 software. Coupling constants (*J)* were given in Hz. LC-MS (ESI) spectra were recorded on a PerkinElmer PE SCIEX API 150 EX instrument equipped with a turbolon spray ion source and a Gemini 5 mm C-18 110 Å HPLC column using a H_2O/CH_3CN gradient (70:30 to 30:70). The spectra were recorded with 30 electronvolt ionization. The HRMS analysis (Q-TOF-MS with a lockmass-ESI source) was done by Stenhalen Analys Lab AB, Gothenburg, Sweden. EI-MS was determined by direct inlet, 70 eV on Micromass GC-TOF micro mass spectrometer (Micromass, Wythenshawe, Waters Inc., UK). ECD spectra were recorded on a J-815 CD-spektrapolarimer, serial No. Ao30261168. Optical rotations were measured on a PerkinElmer 341-LC Polarimeter. TLC analyses were carried out on Merck pre-coated silica gel 60 F_{254} plates. Prep-TLC was done on a glass plates of 20 x 20 cm dimension, pre-coated

with silica gel $60F_{254}$ having 0.25 to 1 mm thickness. Column chromatography was run on silica gel 60 Å (70-230 mesh). Gel filtration was performed on Sephadex LH-20.

3.3 X-ray Diffraction Analyses

The single crystal X-ray data were collected using Agilent Super-Nova dual wavelength diffractometer with a micro-focus X-ray source and multilayer optics monochromatized Cu-Kα (λ = 1.54184 Å) radiation. Program *CrysAlisPro* was used for the data collection and reduction. The intensities were corrected for absorption using analytical face index absorption correction method. The structures were solved with intrinsic phasing method (*SHELXT*) and refined by full-matrix least squares on F^2 with *SHELXL-2018/3*. Anisotropic displacement parameters were assigned to non-H atoms. All C-H hydrogen atoms were refined using riding models. Hydroxyl hydrogens were found from electron density maps and restrained to the proper distance from oxygen atom (0.84 Å). All hydrogen atoms were refined with U_{eq}(H) of 1.5×U_{eq}(C,O) for hydroxyl and terminal methyl groups or 1.2×U_{eq}(C) for other C-H groups. Further geometric least-squares restraints (s = 0.02) were applied to structures **238**, **269** and **239** to obtain more chemically reasonable bond distances between disordered atoms. Anisotropic displacement parameters of few disordered or terminal atoms were restrained (s = 0.01, st = 0.02) to be more equal in structures **236**, **238**, **269** and **239**.

3.4 Extraction and Isolation

The plant parts studied were extracted four time with CH_2Cl_2 /MeOH (1:1) system for 24 hours duration and four times within four days. After filtration and evaporation under reduced pressure, each crude extract was then subjected to column chromatography on Silica gel and purification was done with gel filtration on Sephadex and/or by using PTLC.

3.4.1 Extraction and Isolation of Compounds from the Root of *Lannea rivae*

The air-dried and ground roots (850 g) of *Lannea rivae* was extracted with CH_2Cl_2/MeOH (1:1), 4 x 24 hours each. The solvent was concentrated using a rotary evaporator to give 180.9 g of a brown crude extract. A portion of the crude extract (175.0 g) was partitioned between CH_2Cl_2 and H_2O, then between EtOAc and H_2O. Removal of the organic solvents gave a CH_2Cl_2 (7.8 g) and EtOAc (34.0 g) extracts. The CH_2Cl_2 extract (7.8 g) was subjected

to column chromatography on silica gel (80 g) eluting with *n*-hexane containing increasing amounts of EtOAc. The fractions eluted with 15% EtOAc in *n*-hexane were combined and further separated by column chromatography on Sephadex LH-20 (eluent: CH_2Cl_2/CH_3OH, 1:1) to yield **186** (210 mg), **187** (83 mg) and **192** (16 mg). The fractions eluted with 10% EtOAc in *n*-hexane were combined and further separated by column chromatography on silica gel using *n*-hexane and EtOAc (4:1) to give taraxerol (**188**, 56 mg), taraxerone (**189**, 47 mg) and *β*-sitosterol (**190**, 95 mg). The EtOAc extract (34 g) was subjected to column chromatography on silica gel (500 g) using *n*-hexane-EtOAc system and fractions eluted with 20% EtOAc in *n*-hexane were combined and purified on Sephadex (eluent: CH_2Cl_2/CH_3OH, 1:1) to afford epicatechin gallate (**191**, 460 mg) and taraxerol (105 mg).

3.4.2 Extraction and Isolation of Compounds from the Stem Bark of *Lannea rivae*

The powdered stem barks (980 g) of *Lannea rivae* was also extracted and partitioned as described above to give CH_2Cl_2 (7.9 g) and EtOAc (51 g) extracts. The CH_2Cl_2 extract was chromatographed on silica gel (200 g) and eluted with *n*-hexane containing increasing amounts of EtOAc. The elution with 10% EtOAc in *n*-hexane gave 3-[16'(*E*)-nonadecenyl]phenol (17 mg). The EtOAc extract was also subjected to column chromatography on silica gel (500 g) using *n*-hexane-EtOAc as solvent system. The fractions obtained by elution with 4-6% EtOAc in *n*-hexane were combined and purified on Sephadex LH-20 (eluent: CH_2Cl_2/CH_3OH, 1:1) to give daucosterol (**194**, 89 mg) and lupeol (**193**, 130 mg).

3.4.3 Extraction and Isolation of Compounds from the Root of *Lannea schweinfurthii*

The powdered roots (1.9 kg) of *Lannea schweinfurthii* was extracted with CH_2Cl_2/MeOH (1:1) as described above to give 156.7 g of crude extract. A portion of the crude extract (150.0 g) was partitioned between CH_2Cl_2 and H_2O (1:1) to afford 3.2 g of CH_2Cl_2 extract. The water layer was then extracted with EtOAc to yield 61.0 g of the EtOAc extract. The EtOAc extract was subjected to CC on silica gel (550 g) eluted with *n*-hexane containing increasing amounts of EtOAc to give three major fractions. Separation of the fraction eluted with 20% EtOAc in *n*-hexane was further purified by column chromatograph (CC) over

Sephadex (eluent: CH_2Cl_2/CH_3OH, 1:1) to afford catechin (**201**, 42 mg), 1-[10 (*E)*-tridecadienyl]cyclohex-4-en-1,3-diol (**197**) and 1-((*E*)-pentadec-12'-enyl)cyclohex-4-ene-1,3-diol (**198**, 46 mg). The CH_2Cl_2 extract (3.2 g) was also subjected to CC on silica gel (50 g) eluted with *n*-hexane containing increasing amounts of EtOAc. Taraxerol (**188**, 21 mg) and 3-((*E*)-nonadec-16'-enyl)phenol (**195**, 27 mg) were obtained from the fractions eluted with 18% and 20% EtOAc in *n*-hexane, respectively. The fraction eluted with 25% EtOAc in *n*-hexane was subjected to further purification on Sephadex (eluent: CH_2Cl_2/MeOH, 1:1) to give 1-((*E*)-heptadec-14'-enyl)cyclohex-4-ene-1,3-diol (**196**, 54 mg). The fractions eluted with 40% EtOAc in *n*-hexane was further purified by CC over Sephadex (eluent: CH_2Cl_2/CH_3OH, 1:1) to afford 4,4'-Diydroxy-3-methoxy-3'-*O*-glucosyl-ellagic acid (**202**, 25 mg) and 3-((*E*)-Heptadeca-12'*Z*,14'*E*-dienyl)phenol (**204**, 32 mg)

3.4.4 Extraction and Isolation of Compounds from the Stem bark of *Lannea schweinfurthii*

The powder stem bark (2 kg) of *L. schweinfurthii* was also extracted and partitioned as described above to obtain EtOAc and CH_2Cl_2 extracts. The EtOAc extract (56.8 g) was subjected to column chromatography on silica gel (550 g) using *n*-hexane-EtOAc system as eluent. *β*-sitosterol (**180**, 39 mg) and lupeol (**193**, 16 mg) were again isolated when eluting the column with 15% EtOAc in *n*-hexane. The fraction obtained with 30% EtOAc in *n*-hexane were combined and subjected to further purification on Sephadex LH-20 (eluent: CH_2Cl_2/MeOH, 1:1) to afford 1-((*E*)-pentadec-12'-enyl)cyclohex-4-ene-1,3-diol (**198**, 17 mg). The CH_2Cl_2 fraction from the stem barks extract of *L. schweinfurthii* led to the isolation of more amounts of taraxerol (**188**, 31 mg) and *β*-sitosterol (**180**, 15 mg). Further purification of fractions obtained in 40% EtOAc in *n*-hexane led to identification of 1-((*E*)-Heptadec-14'-enyl)cyclohex-4-en-1,3-diol (**196**, 23 mg) and 1-[(16'*E*)-nonadecenyl]cyclohex-4-en-1,3-diol (**200**, 18 mg). The fraction obtained with 20% EtOAc in *n*-hexane were combined and subjected to further purification on Sephadex using CH_2Cl_2 : CH_3OH 1:1 as an eluent to afford 1-[(11'*E, 14'E*)-heptadecadienyl]cyclohex-4-en-1,3-diol (**199**) and **203**.

3.4.5 Extraction and Isolation of Compounds from the Leaves of *Psiadia punctulata*

The air-dried and ground leaves (1 kg) of *Psiadia punctulata* were extracted with CH_2Cl_2/MeOH (1:1) by cold percolation (4 x 24 hr). The solvent was evaporated using a rotary evaporator to give gummy brown extract (220 g). A portion of the extract (80 g) was subjected to column chromatography on silica gel (800 g) and eluted with *n*-hexane containing increasing amounts of EtOAc. The fractions eluted with 4% EtOAc in *n*-hexane gave a white precipitate composed of two compounds. The two compounds were then separated by column chromatography on Sephadex LH-20 (eluted with CH_2Cl_2/MeOH; 1:1) to yield **205** (67 mg) and **206** (51 mg**)**. The fractions eluted with 5% EtOAc in *n*-hexane were combined and purified by crystallization from acetone to afford **207** (1.08 g). The fractions eluted with 20% EtOAc afforded **208** (300 mg); the fraction eluted with 30% EtOAc gave **214** (60 mg). Fractional crystallization (from acetone) of the subfractions eluted with 10% EtOAc yielded *ent*-trachyloban-2*β*,6*β*,19-triol (**210**, 600 mg) (Midiwo *et al.*, 1997) and *ent*-trachylobane-6*β*,17,19-triol (**211**, 300 mg) (Juma *et al.*, 2006).

Purification of the mother liquor on Sephadex LH-20 (eluted with CH_2Cl_2/MeOH; 1:1) yielded myristic acid (**224**, 100 mg) (Keat *et al.*, 2010) and lauric acid (**223**, 65 mg) (Nitbani *et al.*, 2016). Fractional crystallization (from acetone) of the fractions eluted with 45-50% EtOAc in *n*-hexane, in the original column afforded *ent*-trachyloban-2*β*,18,19-triol (**213**, 300 mg) (Juma *et al.*, 2006), 19-methoxycarbonyl-*ent*-trachyloban-17-oic acid (**212**, 23 mg) (Wu *et al.*, 2009) and a white solid (200 mg). Preparative HPLC separation of the lattest white solid on a chiral column led to the identification of two enantiomers; 18,19-dihydroxy-normal-kaur-16-en-2-one (**218**, 12 mg) (El-Domiaty *et al.*, 1993; Almutairi *et al.*, 2014) and 18,19-dihydroxy-*ent*-kaur-16-en-2-one (**217**, 17 mg) (Midiwo *et al.*, 1997). Elution of the main silica gel column with 55-60% EtOAc in *n*-hexane, 5-hydroxy-7,2',3',4',5'-pentamethoxyflavone (**220**, 500 mg) (Juma *et al.*, 2001) and 5,7-dihydroxy-2',3',4',5'-tetramethoxyflavone (**221**, 210 mg) (Juma *et al.*, 2001) were isolated as a yellow solid each. Purification on Sephadex LH-20 (eluted with CH_2Cl_2/MeOH; 1:1) of fractions obtained with 65% EtOAc in *n*-hexane led to the isolation of 16*β*,17-dihydroxy-*ent*-kaur-20-oic acid (**216**, 70 mg) (Midiwo *et al.*, 1997) while fractional crystallization from acetone of fractions eluted with 70% EtOAc in *n*-hexane gave 2'-hydroxyethyltridecanoate (**222**, 430 mg) (Batovska *et al.*, 2004). The fractions obtained by the elution of the main silica gel column

chromatography with 75-90% EtOAc in *n*-hexane gave a white powder. X-ray analysis of this powder led to the identification of three compounds, *vis*. 18,19-dihydroxy-trachyloban-2-one (**219a**) and kaur-16-en-2*α*,18,19-triol (**219b**), for which the X-ray crystal structures are presented in Figure 2.

3.4.6 Extraction and Isolation of Compounds from the Stem Bark of *Psiadia punctulata*

The air-dried and ground stem bark (1 kg) of *Psiadia punctulata* were extracted with CH_2Cl_2/MeOH (1:1) by cold percolation (4 x 24 hr) to afford 46 g of crude extract. A portion of the crude extract (35 g) was subjected to column chromatography on silica gel and eluted with *n*-hexane containing EtOAc with increasing polarities. The fraction eluted with 2% EtOAc in *n*-hexane was crystallized from CH_2Cl_2/MeOH mixture to give 1-*O*-(Lauroyl) glycerol (**228**, 46 mg) (Batovska *et al.*, 2004). The Fraction eluted with 5% EtOAc in *n*-hexane was subjected to column chromatography on Sephadex LH-20 (eluting with CH_2Cl_2/MeOH; 1:1) to afford friedelan-3*β*-ol (**226**, 630 mg) (Morales-Serna *et al.*, 2011) and friedelin (**231**, 35 mg) (Utami *et al.*, 2013). The fractions eluted with 10-20% EtOAc in *n*-hexane were combined and purified by fractional crystallization from CH_2Cl_2/MeOH to yield **214** (26 mg) and 7*α*-hydroxy-*ent*-trachyloban-19-oic acid (**225**, 8 mg) (Juma *et al.*, 2001) and additional amount of 5-hydroxy-7,2',3',4',5'-pentamethoxyflavone (**220**, 300 mg) and 5,7-dihydroxy-2',3',4',5'-tetramethoxyflavone (**221**, 330 mg). The mother liquor was concentrated and further purified by column chromatography on Sephadex LH-20 (eluted with CH_2Cl_2/MeOH; 1:1) to yield 11 mg of methyl-16,17-epoxy-*ent*-kauran-19-oate (**215**) (Batista *et al.*, 2007) and 32 mg of spinasterol (**227**) (Billah *et al.*, 2013). The fractions eluted with 40-50% EtOAc in *n*-hexane yielded additional amount of the new compound **207** (120 mg).

3.4.7 Extraction and Isolation of Compounds from the Root of *Psiadia punctulata*

The air-dried and ground roots (1 kg) of *Psiadia punctulata* were extracted with CH_2Cl_2/MeOH (1:1) as described for the leaves and the stem barks to afford 50 g of crude extract. A portion of this crude extract (40 g) was subjected to column chromatography on silica gel and eluted with *n*-hexane/EtOAc mixture as described above. 24,25-dihydrolanost-8(9)-en-3-ol (**232**, 121 mg) (Tuck *et al.*, 1991) was isolated as a white amorphous solid from

the fraction eluted with 5% EtOAc in *n*-hexane. the fraction eluted with 30% of EtOAc in *n*-hexane contains three spots on TLC (vanillin stame) and were separated by CC over Sephadex LH-20 (eluted with CH_2Cl_2/MeOH, 1:1) gave 16α,17-dihydroxy-*ent*-kaur-20-oic acid (**216**, 20 mg) (Midiwo *et al.*, 1997), *ent*-trachylobane-2*α*,6*β*,18,19-tetraol (**229**, 6 mg) (Juma *et al.*, 2006) and *ent*-kauren-16-en-2-one (**230**, 10 mg) (Garcez *et al.*, 2004). The eluent with 40% EtOAc in *n*-hexane gave 3-methyl-6-(6-methylhept-5-en-2-yl)cyclohex-2-enone (**233**, 27 mg) (Mathur *et al.*, 1989); while the 50% EtOAc in *n*-hexane eluent gave an additional amount of friedelin (**231**, 25 mg). The fractions eluted with 60% EtOAc was separated by column chromatography on silica gel eluting with *n*-hexane and EtOAc (6:4). The fraction eluted with 70% EtOAc afforded of normal-trachyloban-2*α*,6*α*,19-triol (**209**, 26 mg).

3.4.8 Extraction and Isolation of Compounds from the Root of *Aspilia pluriseta*

Roots powder (800 g) of *A. pluriseta* were extracted four times with CH_2Cl_2: MeOH (1:1) system for 24 hours each to afford 47g of extract. The extract was subjected to column chromatography separation on silica gel and eluted with *n*-hexane-EtOAc system. The named compound 9*β*-Hydroxy-15α-angeloyloxy-ent-kaur-16-en-19-oic acid (**236**) (22 mg) was isolated as a white crystal in hexane-20% EtOAc after purification by preparative thin layer chromatography (PTLC). The fraction eluted with *n*-hexane-8% EtOAc was purified on Sephadex column chromatography using CH_2Cl_2: MeOH (1:1) as solvent before being further purified by PTLC to give 15*α*-angeloyloxy-16β,17-epoxy-*ent*-kauran-19-oic acid (**237)** (84 mg). From the same extract, *ent*-kaura-9(11),16-dien-12-one (**241)** (27 mg) was also obtained after purification in *n*-hexane-40% EtOAc. Fractions obtained in *n*-hexane-30% EtOAc system were combined and crystallized in Acetone to afford 31 mg of methyl-9*β*-hydroxy-15*α*-angeloyloxy-*ent*-kaur-16-en-19-oate (**238**) and 89 mg of 15*α*-angeloyloxy-*ent*-kaur-16-en-19-oic acid (**239**). The same original column also afforded 80 mg of fractions in *n*-hexane-60% EtOAc. These fractions were purified on column chromatography using 15g of Sephadex to yield carissone (**249**) (34 mg).

3.4.9 Extraction and Isolation of Compounds from the Aerial Part of *Aspilia pluriseta*

Dried powder (800 g) of the aerial part of *Aspilia pluriseta* was extracted with CH_2Cl_2: MeOH (1:1) to afford 53g of crude extract. A portion of this extract (40 g) was subjected to column chromatography on silica gel and eluted with *n*-hexane-EtOAc system with increasing concentration of EtOAc. *Ent*-kaur-16-en-19-oic acid (**243**) (76 mg) and lanosterol (**246**) (41 mg) were directly isolated in *n*-hexane-2% EtOAc and *n*-hexane-6% EtOAc respectively. Similar fraction obtained in *n*-hexane-12% EtOAc were combined and purified with column chromatography on Sephadex (15 g) to afford 71 mg of stigmasta-5,22(E)-dien-3*β*-ol (**247**). In the same light, purification of subsequent fractions by PTLC resulted to isolation of *ent*-kaur-16-en-19-oic acid (**242**) (36 mg). The original column was then eluted with *n*-hexane-EtOAc 20% and fractions obtained in this system were combined as they had the same profile on TLC. After combining these fraction, *ent*- Kaur-16-ene (**245**) (73 mg) was crystallized in acetone. Fractions obtained in *n*-hexane-0-40% EtOAc were combined based on their TLC profile and separated by chromatography using a smaller size (3cmx0.7m) column on silica gel (10 g) to obtain 42 mg of 3-hydroxy-olean-12-en-29-oic acid (**248**) and an additional amount (17 mg) of lanosterol **(246)**.

3.4.10 Extraction and Isolation of Compounds from the Root of *Aspilia mossambicensis*

Dried powder (1.4 kg) of roots of *Aspilia mossambicensis* (Oliv) Wild were exactly extracted as described above to afford 92 g of crude extract. Column chromatography separation of a portion of this extract (40 g) on silica gel using *n*-hexane-EtOAc system resulted in isolation of 15*α*-angeloyloxy-16*β*,17-epoxy-*ent*-kauran-19-oic acid (**237**) (13 mg) in *n*-hexane-5% EtOAc. Fractions obtained in *n*-hexane-10% EtOAc were combined and purified by column chromatography using Sephadex and *ent*-kaura-9(11), 16-dien-19-oic acid **(240**) (218 mg) and *ent*-kauran-19-oic acid (**252**) (17 mg) were crystallized in acetone. Another fraction obtained in *n*-hexane-20% EtOAc was found to contain 3 spots corresponding to three different compounds. This fraction was then purified by column chromatography on Sephadex to afford 15*α*-angeloyloxy-*ent*-kaur-16-en-19-oic acid (**239**), stigmasta-5,22(E)-dien-3*β*-ol (**247**) and *3β*-hydroxyolean-12-en-28-oic acid (oleanolic acid; **253**).

3.4.11 Extraction and Isolation of Compounds from the Aerial Part of *Aspilia mossambicensis*

Dried powder (1 kg) of the aerial part of *A. mossambicensis* was extracted exactly as described above to yield 82 g of crude extract. A portion of this extract (40 g) was subjected to silica gel column chromatography and eluted with *n*-hexane-EtOAc with an increasing concentration of EtOAc. The fraction eluted with *n*-hexane-EtOAc 4% and 6%, compound *ent*-kaur-16-en-19-oic acid (**243**) (16 mg) and kaura-9(11),16-diene (**255**) (73 mg) directly crystallized without any further purification. While eluting the column with *n*-hexane-EtOAc 10%, 2-hydroxy-kaura-9(11),16-diene (**256**; 21 mg) was isolated after purification of the column by PTLC. Fractions obtained in *n*-hexane-15-20% EtOAc were combined and subjected to further purification on Sephadex column chromatography to result 24 mg of *β*-amyrin acetate (**254)** and 32 mg of cinnamic acid methyl ester (**257**).

3.5 Procedure of Structural Modification

3.5.1 Methylation of Compounds 211 and 243

Compound **258** (Equation 1) was prepared by using a previously described method (Boeck *et al.*, 2005). Powdered KOH (30 mg) was added to anhydrous acetone (2 ml) and the mixture was stirred for 5 minute at 25°C. Compound **220** (100 mg) was then added to the reaction followed by MeI (120 mg). the reaction was maintained at 25 °C while stirring. After 2 h, the reaction mixture was poured into water (25 ml) and extracted with ethyl acetate (3x 25 ml). the combined organic phase was washed with water (3x 25 ml), dried over $MgSO_4$ and concentrated under vacuum using a rotatory evaporator. the residue was purified by crystallization from acetone to afford 84% yield of **258**. The same procedure (Equation 2) was used on **211** to yield **265** (48% yield) and **267** (Equation 3) (57% yield). When the same method (Equation 4) was applied to compound **240**, compound **270** (65% yield) was purified.

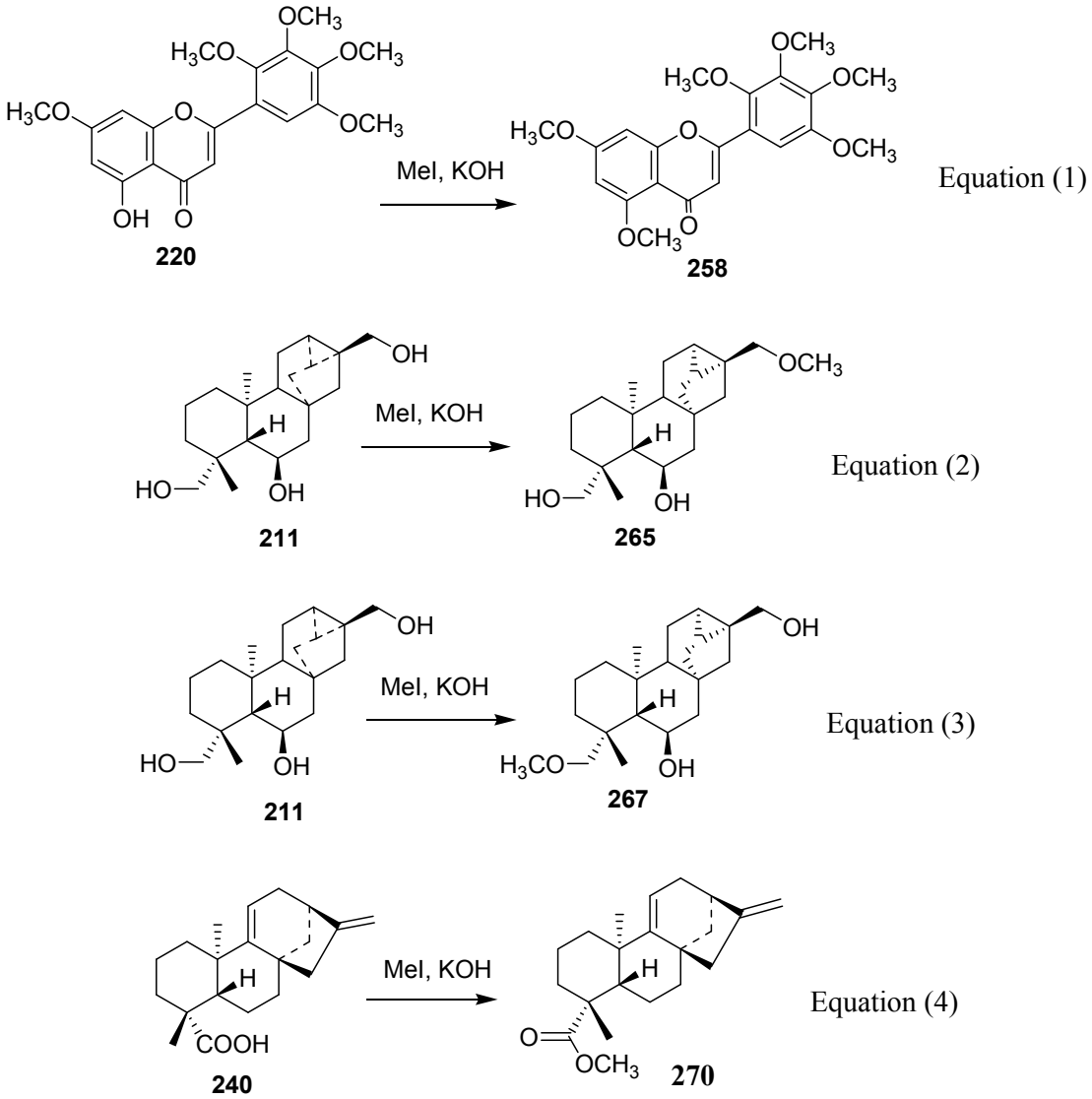

3.5.2 Acetylation of Compounds 220 and 210

In this reaction the method previously described was used by Gupta and Ali, (1999) was used. Compound **220** (10 mg) was acetylated (Equation 5) with AC_2O (3 mL) and pyridine (drops) at room temperature for 12 h. Water (10 ml) was added to the reaction mixture and extracted with EtOAc (3x10 mL), the organic phase washed with copper sulphate solution (2x10 mL) followed by saturated $NaHCO_3$ solution (3x5mL) and water (2x10mL), dried (Na_2SO_4) and concentrated to provide **259** (57% yield). The same procedure was used (Equation 6) on **210** to afford **266** (48% yield).

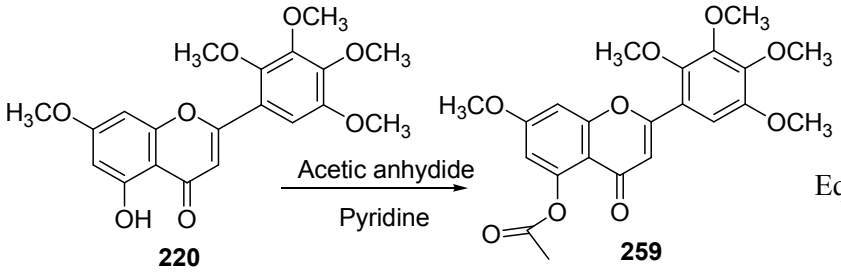

220 259

Equation (5)

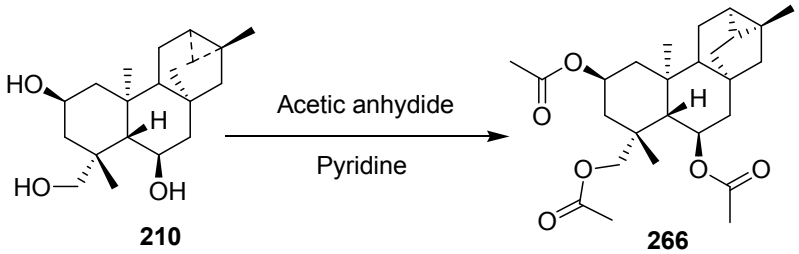

210 266

Equation (6)

3.5.3 Preparation of Compound 261 and 263

A method previously described (Nagimova *et al.*, 1996; Pan *et al.*, 2015) was used to prepare compound **261** (Equation 7). Briefly, NBS (90 mg) was added to a stirred solution of **220** (200 mg) in dichloromethane at 22°C. After completion of the reaction (3h), the mixture was dried under reduced pressure. The crude product of **261** was purified by column chromatography on Sephadex LH-20 eluting with CH_2Cl_2/CH_3OH (1:1) to yield **261** (63 % yield). The same procedure was carried out (Equation 8) on compound **221** to afford **262** with a yield of 74%.

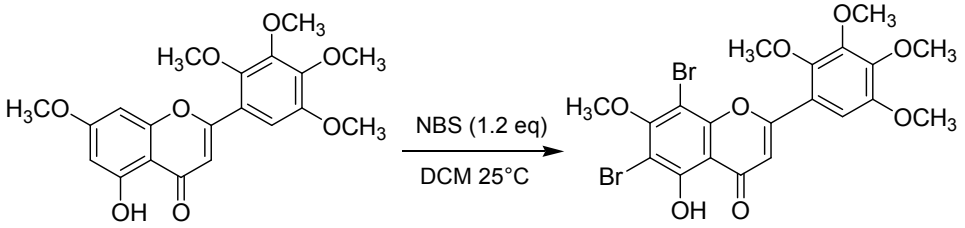

220 261

Equation (7)

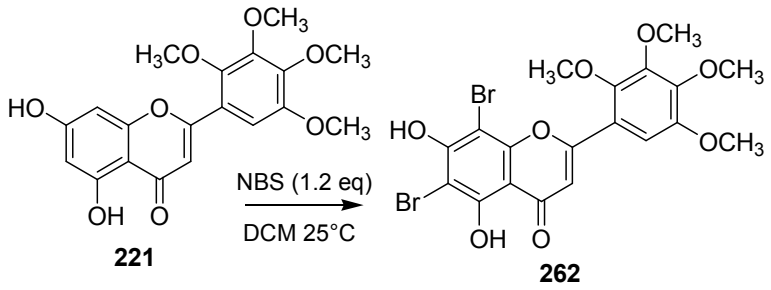

Equation (8)

3.5.4 Preparation of Compound 260

A previously described method was used to synthesise (Equation 9) compound **260** (Kenanda and Omosa, 2017). A 100 mg portion of **220** was dissolved in 10 ml ethanol and excess of hydrazine was added. The mixture was refluxed overnight. Upon cooling, crystals which were formed were then filtered and washed with ethanol to afford **260** (88% yield).

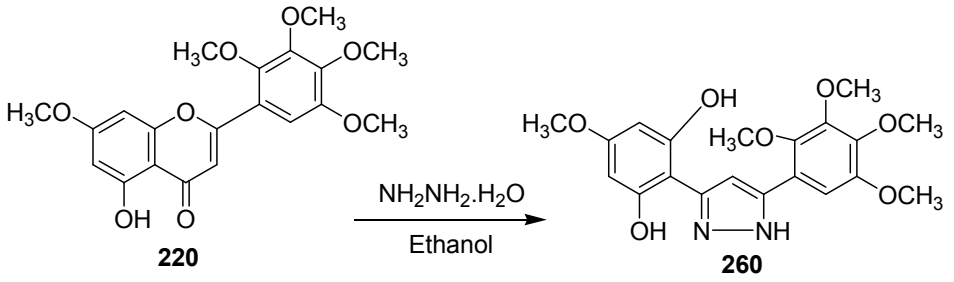

Equation (9)

3.5.5 Preparation of Compound 263

A mixture of compound **207** (100 mg), $NH_2OH{\cdot}HCl$ (50 mg) and AcONa (90 mg) in EtOH (3 mL) was prepared (Equation 10). The mixture was stirred under reflux conditions for 2h. The progress of the reaction was monitored by TLC. After completion of the reaction, H_2O (15 mL) was added and the reaction mixture was stired for a further 8 min. The product has been extracted with EtOAc (3x20 mL), dried over anhydrous Na_2SO_4. Evaporation of the solvent and purification by column chromatography of product over silica gel (*n*-hexance/EtOAc) afforded compound **263** with a yield of 67 % (Ghozlojeh and Setamdideh, 2015).

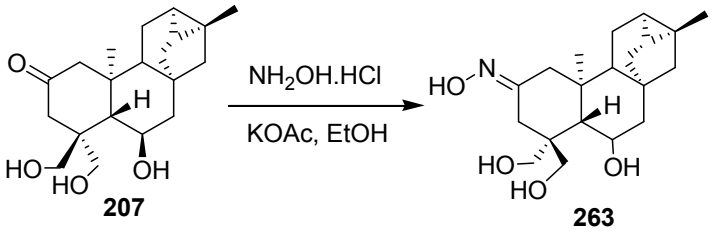

Equation (10)

3.5.6 Oxidation of Compound 207

The oxidizing agent (Equation 11) was prepared by dissolving 9.7 g (0.097 mole, 0.146 equivalents) of chromium trioxide in a mixture of 6 ml of water and 23 ml of acetic acid. A 250-ml three-necked flask was equipped with a dropping funnel, a thermometer, and a mechanical stirrer, and was charged with a solution of 0.10 mole of compounds **207** in 40 ml of acetic acid. The solution was cooled in a water bath, and the oxidizing solution was added at a rate that maintained the reaction temperature below 35°C. After completion of the addition, the reaction mixture was allowed to stand at room temperature overnight. The mixture was then extracted with 150 ml of ether, and the ethereal solution was washed four times with 100 ml portions of water to remove the bulk of the acetic acid. The ethereal solution is then washed with sodium bicarbonate solution followed by water and then dried over sodium sulfate. The ether was evaporated, and the residue purified by crystalization from acetone to afford **264** (48 % yield).

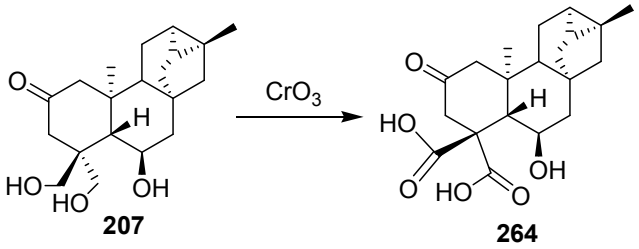

Equation (11)

3.5.7 Preparation of Compound 268

In a round bottomed flask which contained MeOH (2 mL) and concentrated H_2SO_4 (2 drops), *ent*-kaura-9(11),16-dien-19-oic acid (**240**; 0.04 g; 0.165 mmol) was added and the reaction mixture was stirred at 25 ^oC for 14 h, after which the mixture was poured into water (25 mL) and extracted with ethyl acetate (3 x 25 mL). The combined organic layer was dried over

$MgSO_4$, filtered and concentrated in a rotary evaporator to give 53% yield of **268** (Equation 12) as a pale yellow solid (Boeck *et al.*, 2005).

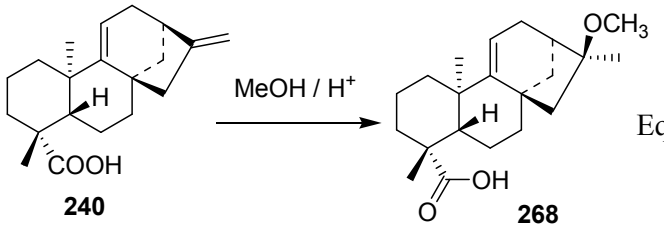

Equation (12)

3.5.8 Hydrogenation of Compounds 240 and 243

To round bottomed flask containing solution of compound **240** (100 mg) in ethanol (20 ml); 5% palladium on charcoal (30 mg) was added. The flask was corked with an air tight rubber stopper, and was bubbled with nitrogen gas to eliminate traces of air through a small syringe to make the system inert. Hydrogen gas was then bubbled into the system for 2 days at room temperature. The reaction mixture (Equation 13) was filtered and the solvent evaporated to yield compound **269** (86% yield). The same procedure (Equation 14) was carried out on **243** to afford **271** (89% yield).

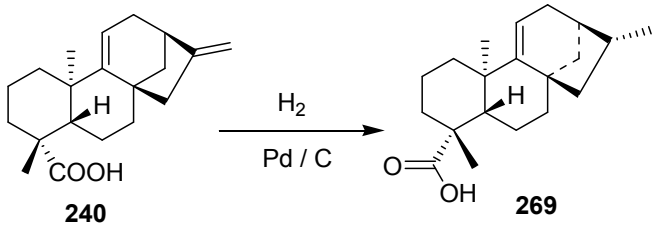

Equation (13)

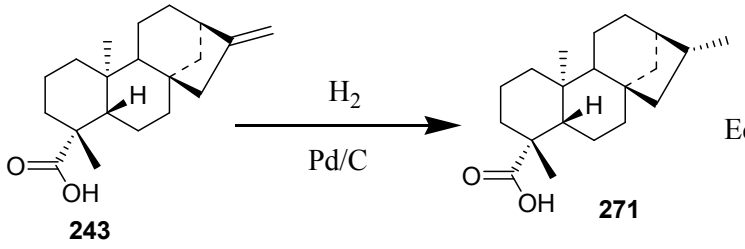

Equation (14)

3.6 Physical Constants and Spectroscopic Data of the Isolated Compounds

3.6.1 Physical Constants and Spectroscopic Data of Compounds from *Lannea rivae*

(4R,6S)-4,6-Dihydroxy-6-((Z)-nonadec-14'-en-1-yl)cyclohex-2-en-1-one (**186**). Colourless residue, $[\alpha]_D^{20}$ + 28.8° (*c* 0.5, acetone). UV λ_{max} (MeOH): 256, 336 nm. ^{1}H and ^{13}C NMR ($CDCl_3$): Table 1. EIMS *m/z* (rel. int.): 392 (6, $[M]^+$), 374 (14, $[M\text{-}H_2O]^+$), 97 (23, $[C_7H_{13}]^+$), 95 (35), 84 (100), 69 (25), 55 (52), 43 (31). HRESIMS $[M+H]^+$ *m/z*: 393.3344 ($C_{25}H_{45}O_3$ calcd. for 393.3369).

(2S,4R*,5S*)-2,4,5-Trihydroxy-2-((Z)-nonadec-14'-en-1-yl)cyclohexanone* (**187**). Colourless residue, $[\alpha]_D^{20}$ + 4.8° (*c* 0.6, acetone). UV λ_{max} (MeOH) 206 nm. ^{1}H and ^{13}C NMR (CD_2Cl_2): Table 3. EIMS *m/z* (rel. int.): 410 (4, $[M]^+$), 392 (20, $[M\text{-}H_2O]^+$), 390 (40), 374 (17, $[M\text{-}2H_2O]^+$), 339 (21), 337 (100), 139 (49), 99 (16), 97 (35, $[C_7H_{13}]^+$), 57 (33), 55 (62), 43 (12).

Taraxerol (**188**). Amorphous solid (221-222°C), ^{1}H and ^{13}C NMR (CD_2Cl_2) data, see Table 17.

Taraxerone (**189**). Amorphous solid (232-233°C), ^{1}H and ^{13}C NMR (CD_2Cl_2) data, see Table 17.

β-sitosterol (**190**). Amorphus solid (132-133°C), ^{1}H and ^{13}C NMR (CD_2Cl_2) data, see Table 18.

Epicatechin gallate (**191**). Brown solid (mp 212-213 °C). UV λmax (MeOH) 215 nm, ^{1}H and ^{13}C NMR (CD_2Cl_2) data, see Table 19.

3'', 5''-Dimethoxy-epicatechin gallate (**192**). White solid (236-237°C); ^{1}H and ^{13}C NMR (CD_2Cl_2) data, see Table 19.

Lupeol **(193)**. White solid (197-198°C), ^{1}H and ^{13}C NMR (CD_2Cl_2) data, see Table 20. EIMS *m/z* (rel. int): *m/z* 426 [M]+ (24), 43 (100), 68 (98), 55 (86), 67 (78), 81 (75), 69 (73), 95 (71), 293 (68), 41 (66), 109 (61), 121 (60), 189 (58), 207 (61), 218 (48) for $C_{30}H_{50}O$.

Daucosterol **(194).** White solid (248-249°C), ^{1}H and ^{13}C NMR (CD_2Cl_2) data, see Table 20.

3-((E)-Nonadec-16'-enyl)phenol (**195**). Colourless residue, ^{1}H and ^{13}C NMR (CD_2Cl_2) data, see Table 21.

1-((*E*)-heptadec-14'-enyl)cyclohex-4-en-1,3-diol (**196**). Colourless residue, ^{1}H and ^{13}C NMR (CD_2Cl_2) data, see Table 22.

3.6.2 Physical Constants and Spectroscopic Data of Compounds from *Lannea schweinfurthii*

1-((E)-Tridecadec-10'-enyl]cyclohex-4-en-1,3-diol (**197**). Colourless residue; $[\alpha]_D^{20}$ - 28.8° (*c* 0.5, Acetone); UV λ_{max} (MeOH) 256, 336 nm; ^{1}H and ^{13}C NMR (CD_2Cl_2) data, see Table 23. EIMS *m/z* (rel. int): 294 $[M]^+$ (6), 276 $[M - H_2O]^+$ (10), 287 (56), 261 (23), 227 (16), 211 (24), 95 (46), 70 (24), 69 (30), 55 (24), 43 (100). HRESIMS, $[M+H]^+$ *m/z*: 287.2700 for $C_{19}H_{34}O_2$.

1-((E)-Pentadec-12'-enyl)cyclohex-4-en-1,3-diol (**198**). Colourless liquid; $[\alpha]_D^{20}$ - 0.43 (*c* 1, Acetone); ^{1}H and ^{13}C NMR (CD_2Cl_2) data, see Table 24. EIMS *m/z* (rel. int): 350 $[M]^+$ (4), 333 [M - H2O]$^+$ (7), 342 (59), 307 (19), 295 (24), 193 (100), 211 (13), 97, (18), 95 (54), 84 (14), 57 (18), 43 (23). HRESIMS, $[M+H]^+$ *m/z*: 357.3078 for $C_{21}H_{38}O_2$.

1-[Nonadeca-14Z',16E'-dienyl]cyclohex-4-en-1,3-diol (**199**). Pale yellow residue, $[\alpha]_D^{20}$ - 0.26 (*c* 0.21, Acetone); ^{1}H and ^{13}C NMR (CD_2Cl_2) data, see Table 25. EIMS *m/z* (rel. int): 348 $[M]^+$ (4), 330 $[M - H_2O]^+$ (5), 340 (87), 293 (44), 223 (17), 108 (28), 95 (79), 67 (78), 57 (71), 55 (58), 43 (100). HRESIMS, $[M+H]^+$ *m/z*: 343.3314 for $C_{23}H_{40}O_2$.

1-[(16'E)-Nonadecenyl]cyclohex-4-en-1,3-diol (**200**). White solid; ^{1}H and ^{13}C NMR (CD_2Cl_2) data, see Table 26.

Catechin (**201**). Yellow solid (172-173°C), ^{1}H and ^{13}C NMR (CD_2Cl_2) data, see Table 27.

4,4'-Diydroxy-3-methoxy-3'-O-glucosyl-ellagic acid (**202**). Yellowish residue, ^{1}H and ^{13}C NMR (CD_2Cl_2) data, see Table 28.

4,4'-Dihydroxy-3-methoxy-3'-O-[rhamnopyranosyl-(1→2)] rhamnopyranoside ellagic acid (**203**). Yellowish residue, ^{1}H and ^{13}C NMR, see Table 28.

3-((12'Z,14'E)-Heptadeca-dienyl)phenol (**204**). colourless residue; ^{1}H and ^{13}C NMR (Acetone-d_6) data, see Table 29.

3.6.3 Physical Constants and Spectroscopic Data of Compounds from *Psiadia punctulata*

Trachyloban-17-oic acid (**205**). White solid (mp 213 – 215ºC), $[\alpha]_D^{20}$ = – 197 (*c* 0.005, acetone). ^{1}H and ^{13}C NMR (CD_2Cl_2) data, see Table 33. LC-MS (ESI), *m/z* (rel. int.): $[M+H]^+$ 303 (100), 285 $[M - H_2O]^+$ (35), 257 (5), 233 (7), 149 (100). HRESIMS, $[M+H]^+$ *m/z*: 303.2368 calculated for $C_{20}H_{31}O_2$, 303.2324.

17-Hydroxy-ent-trachyloban-20-oic acid (**206**). White crystals (mp 178 – 180ºC), $[\alpha]_D^{20}$ –39 (*c* 0.003, acetone). ^{1}H and ^{13}C NMR (C_5D_5N) data, see Table 33. LC-MS (ESI), *m/z* (rel. int.): $[M+H]^+$ 319 (10), 287 (100), 269 (40), 257 (30), 161 (10), 133 (7). HRESIMS, $[M+H]^+$ *m/z*: 319.2267 calculated for $C_{20}H_{31}O_3$, 319.2273.

Ent-[6β, 18, 19]-Trihydroxy-trachyloban-2-one (**207**). White solid (mp 137 – 139ºC), $[\alpha]_D^{20}$ –45 (*c* 0.004, acetone). ^{1}H and ^{13}C NMR ($CDCl_3$) data, see Table 34. LC-MS (ESI), *m/z* (rel. int.): $[M+H]^+$ 335 (50), 317 (100), 299 (60), 281 (30). HRESIMS, $[M+H]^+$ *m/z*: 335.2217 calculated for $C_{20}H_{31}O_4$, 335.2222.

Normal-trachyloban-2α,18,19-triol (**208**). White solid (mp 140 – 142ºC), $[\alpha]_D^{20}$ –36 (*c* 0.004, acetone). ^{1}H and ^{13}C NMR ($CDCl_3$) data, see Table 34. LC-MS (ESI), *m/z* (rel. int.): $[M+H]^+$ 321 (10), 303 (45), 285 (100), 267 (38), 257 (2), 187 (4). HRESIMS, $[M+H]^+$ *m/z*: 321.2438 calculated for $C_{20}H_{33}O_3$, 321.2430.

Normal trachyloban-2α,6α,19-triol (**209**). White crystals (mp 189-191ºC), $[\alpha]_D^{20}$ +56 (c 0.004, acetone). ^{1}H and ^{13}C NMR ($CDCl_3$) data, see Table 35. LC-MS (ESI), m/z (rel. int.):

$[M-H_2O]^+$ 303 (18), 285 (100), 267 (47), 205 (12), 187 (10). HRESIMS, $[M-H_2O]^+$ *m/z*:303.2320 calculated for $C_{20}H_{33}O_3$, 321.2320.

Ent-trachyloban-2β,6β,19-triol (**210**). White solid (mp 208-210 ºC); $[\alpha]_D^{20}$ -38 (*c* 0.007, Acetone); ^1H (see Table 36) and ^{13}C (see Table 36) NMR ($CDCl_3$) data. ESIMS, $[M+H]^+$ *m/z* (rel. int): 321 $[M+H]^+$ (10), 303 (100), 205 (25), 159 (22), 109 (18), 187 (12) for $C_{20}H_{32}O_3$.

Ent-trachyloban-6β,17,19-triol (**211**). White solid (mp 196-198 ºC), $[\alpha]_D^{20}$ -76 (*c* 0.006, Acetone); ^1H (see Table 36) and ^{13}C (see Table 36) NMR ($CDCl_3$) data. ESIMS, $[M+H]^+$ *m/z* (rel. int): 321 $[M+H]^+$ (4), 303 $[M-H_2O]^+$ (49), 285 (100), 267 (42), 227 (2), 205 (6), 189 (2), 153 (3), 133 (2) for $C_{20}H_{32}O_3$.

19-Methoxycarbonyl-ent-trachyloban-17-oic acid (**212**). White solid (mp 2011-212 ºC); $[\alpha]_D^{20}$- 48 (c 0.003 Acetone); ^1H (see Table 37) and ^{13}C (see Table 36) NMR ($CDCl_3$) data. ESIMS, $[M+H]^+$ *m/z* (rel. int): 347 (100), 287 (82), 269 (54), 149 (35), 213 (16) for $C_{21}H_{31}O_4$.

Ent-trachyloban-2β,18,19-triol (**213**). White solid (mp 148-149 °C); $[\alpha]_D^{20}$ - 27º (*c* 0.004, acetone); ^1H and ^{13}C NMR ($CDCl_3$) data, see Table 38. ESIMS, $[M+H]^+$ *m/z (rel. int):* 321 $[M+H]^+$ (8), 303 $[M-H_2O]^+$ (59), 285 (100), 267 (58), 255 (4), 205 (12), 227 (4) for $C_{20}H_{32}O_3$.

15α,16α,17-Trihydroxy-ent-kauran-19-oic methyl ester (**214**). White crystals (mp 198 ─ 200ºC), $[\alpha]$ + 21 (*c* 0.006, acetone). ^1H and ^{13}C NMR ($CDCl_3$) data, see Table 39. LC-MS (ESI), *m/z* (rel. int.): $[M+1]^+$ 367 (60), 349 (90), 331 (100), 313 (40), 289 (45), 271 (50), 253 (30). HRESIMS, $[M+H]^+$ *m/z*: 367.2479 calculated for $C_{21}H_{35}O_5$, 367.2448.

Methyl-16α,17-epoxy-ent-kauran-19-oate (**215**). Colourless crystals (231-232°C); ^1H and ^{13}C NMR ($CDCl_3$) data, see Table 39. ESIMS, $[M+H]^+$ *m/z* (rel. int): 333 $[M+H]^+$ (11), 331 (72), 319 (88), 313 (100), 301 (26), 271 (31), 253 (89), 255 (17).LC-MS, $[M+H]^+$ *m/z* (rel. int): 333.7 for $C_{21}H_{32}O_3$.

16α,17-Dihydroxy-ent-kaur-20-oic acid (**216**). Colourless solid (mp 198-200 ºC); $[\alpha]_D^{20}$ + 21 (*c* 0.006, acetone).^{1}H and ^{13}C NMR ($CDCl_3$) data, see Table 40. ESIMS, $[M+H]^+$ *m/z* (rel. int): 337 $[M+H]^+$ (53), 303 (94), 285 (100), 267 (48), 205 (49) for $C_{20}H_{32}O_4$.

18,19-Dihydroxy-ent-kaur-16-en-2-one (**217**). Colourless residue. ^{1}H and ^{13}C NMR (Acetone-d_6) data, see Table 41. ESIMS, *m/z* (rel. int): 319 $[M+H]^+$ (58), 301 $[M-H_2O]^+$ (100), 283 (19), 189 (22), 255 (8), 225 (5) for $C_{20}H_{30}O_3$.

18,19-Dihydroxy-normal-kaur-16-en-2-one (**218**). Colourless residue; ^{1}H and ^{13}C NMR (CD_2Cl_2) data, see Table 41. ESIMS, *m/z* (rel. int): 319 $[M+H]^+$ (58), 301 $[M-H_2O]^+$ (100), 283 (19), 189 (22), 255 (8), 225 (5) for $C_{20}H_{30}O_3$.

5-Hydroxy-7,2',3',4',5'-pentamethoxy-flavone (**220**). Yellow solid (mp 127-128 ºC); ^{1}H and ^{13}C NMR ($CDCl_3$) data, see Table 42. EIMS *m/z* (rel. int): 389 $[M+H]^+$ (100), 280 (2), for $C_{20}H_{20}O_8$.

5,7-Dihydroxy-2',3',4',5'-tetramethoxyflavone (**221**). Yellow solid (mp 125-126 ºC); ^{1}H and ^{13}C NMR ($CDCl_3$) data, see Table 42. ESIMS *m/z* (rel. int): 375 $[M+H]^+$ (100), 149 (6), 345 (2), 175 (1), 205 (1), 241 (1), 253 (1) for $C_{19}H_{18}O_8$.

2'-Hydroxyethyl-tetradecanoate (**222**). White residue; ^{1}H and ^{13}C NMR ($CDCl_3$) data, see Table 43.

Lauric acid (**223**). White solid; ^{1}H and ^{13}C NMR ($CDCl_3$) data, see Table 44.

Myristic acid (**224**). White solid; ^{1}H and ^{13}C NMR ($CDCl_3$) data, see Table 44.

7α-Hydroxy-ent-trachyloban-19-oic acid (**225**). White solid; ^{1}H and ^{13}C NMR ($CDCl_3$) data, see Table 45.

Friedelan-3β-ol (**226**). White solid (mp 270-271 ºC); ^{1}H and ^{13}C NMR (CD_2Cl_2) data, see Table 46. ESIMS, *m/z* (rel. int): *m/z* 429 $[M+H]^+$ (not observed), 221 (100), 149 (53), 203 (31), 163 (27), 279 (26) for $C_{30}H_{52}O$.

Spinasterol (**227**). White solid (mp 265-266 ºC); ^{1}H and ^{13}C NMR (CD_2Cl_2) data, see Table 46. ESIMS, *m/z* (rel. int): *m/z* 413 $[M+H]^+$ (4), 304 (2), 282 (100), 149 (30), 265 (21), 109 (19) for $C_{29}H_{48}O$.

1(*S*)-2,3-dihydroxypropyl tridecanoate (**228**). White solid (mp 51-52 ºC); ^{1}H and ^{13}C NMR ($CDCl_3$) data, see Table 47. ESIMS, $[M+H]^+$ *m/z* (rel. int): 253 $[M-2H_2O]^+$ (52), 251 $[M-H_2O]^+$ (56), 241 (51), 187 (100), 175 (64), 149 (73) for $C_{16}H_{32}O_4$.

Ent-trachylobane-2α,6β,18,19-tetraol (**229**). White solid (204-205°C) $[\alpha]_D^{20}$ – 89 (c 0.003, acetone). ^{1}H and ^{13}C NMR (Acetone-d_6) data, see Table 48. LC-MS (ESI), *m/z* (rel. int.): $[M+H]^+$ 337 (96), 319 (476), 301 (100), 283 (78), 271 (31), 253 (22), 257 (5) for $C_{20}H_{32}O_4$.

Ent-kaur-16-en-2-one (**230**). White solid; ^{1}H and ^{13}C NMR (Acetone-d_6) data, see Table 48. Molecular formula $C_{20}H_{30}O$.

Friedelin (**231**). White solid (mp 254-255 ºC); ^{1}H and ^{13}C NMR (CD_2Cl_2) data, see Table 49. EIMS *m/z* (rel. int): 426 [M]+ (21),69 (100), 55 (74), 95 (73), 81 (72), 123 (73), 41 (48), 163 (26), 205 (25), 273 (27), 246 (22), 302 (10), 411 (8), 341 (6) for $C_{30}H_{50}O$.

24,25-Dihydrolanost-8(9)-en-3β-ol (**232**). White solid (mp 247-249 ºC); ^{1}H and ^{13}C NMR (CD_2Cl_2) data, see Table 49.

(6R, 7R)-Bisabolone (**233**). White solid mp (231-233 ºC); $[\alpha]_D^{20}$-35 (c 0.004 Acetone); ^{1}H and ^{13}C NMR ($CDCl_3$) data, see Table 50. ESIMS *m/z* (rel. int): 221 $[M+H]^+$ (100), 203 (47), 163 (43), 149 (32), 165 (25) for $C_{15}H_{24}O$.

3.6.4 Physical Constants and Spectroscopic Data of Compounds from *Aspilia pluriseta*

12α-Methoxy-ent-kaura-9(11),16-dien-19-oic acid (**234**). Colourless crystal (mp 184-186 ºC); ^{1}H and ^{13}C NMR (CD_2Cl_2) data, see Table 57. LC-MS (ESI), *m/z* (rel. int.): $[M+H]^+$ 329 (12), 315 (11), 299 (100), 253 (71), 281 (10), 171 (18), 182 (3). HRESIMS, $[M-H]^+$ *m/z*: 329.2191 calculated for $C_{21}H_{29}O_3$, 303.2117.

16α-Hydroxy-ent-kauran-19-oic acid (**235**). Colourless crystal (mp 197-199 ºC); ^{1}H and ^{13}C NMR (CD_2Cl_2) data, see Table 57. LC-MS (ESI), *m/z* (rel. int.): 321 $[M+H]^+$ (8), 303 $[M-H_2O]^+$ 303 (30), 285 (100), 267 (40), 205 (10), 197 (5), 149 (5). HRESIMS, $[M+H]^+$ *m/z*: 321.2429 calculated for $C_{20}H_{31}O_2$, 321.2428.

9β-Hydroxy-15α-angeloyloxy-ent-kaur-16-en-19-oic acid (**236**). Colourless crystals (mp 256-257 ºC); ^{1}H and ^{13}C NMR (CD_2Cl_2) data, see Table 58. ESIMS, $[M+H]^+$ *m/z* (rel. int): 399 $[M-H_2O]^+$ (9), 299 (100), 253 (18), 217 (6), 203 (4), 281 (7). HRESIMS, $[M+H]^+$*m/z*: 417.1668 for $C_{25}H_{36}O_5$.

15α-Angeloyloxy-ent-kaur-16α,17-epoxy-ent-kauran-19-oic acid (**237**). White solid (242-243 ºC); ^{1}H and ^{13}C NMR (CD_2Cl_2) data, see Table 58. ESIMS, $[M+H]^+$ *m/z* (rel. int): 417 $[M+H]^+$ (100), 317 (80), 299 (71), 271 (64), 253 (23) for $C_{25}H_{36}O_5$.

Methyl-9β-hydroxy-15α-angeloyloxy-ent-kaur-16-en-19-oate (**238**). White solid (261-262°C); ^{1}H and ^{13}C NMR (CD_2Cl_2) data, see Table 59. ESIMS, $[M+H]^+$ *m/z* (rel. int): 413 $[M-H_2O]^+$ (69), 313 (100), 253 (54) for $C_{26}H_{38}O_5$.

15α-Angeloyloxy-ent-kaur-16-en-19-oic acid (**239**). White solid (256-257°C); ^{1}H and ^{13}C NMR (CD_2Cl_2) data, see Table 59. ESIMS, $[M+H]^+$ *m/z* (rel. int): 401 $[M+H]^+$ (7), 301 (100), 371 (8), 313 (11), 255 (13) for $C_{25}H_{36}O_4$.

Ent-kaura-9(11),16-dien-19-oic (**240**). White solid (253-254 ºC); ^{1}H and ^{13}C NMR (CD_2Cl_2) data, see Table 60. ESIMS, $[M+H]^+$ *m/z* (rel. int): 282 (100), 265 (13), 247 (6) for $C_{20}H_{28}O_2$.

Ent-kaura-9(11),16-dien-12-one **(241)**. White solid; ^{1}H and ^{13}C NMR (CD_2Cl_2) data, see Table 60.

Methyl-ent-kaur-16-en-19-oate (**242**). White solid (261-262 ºC); ^{1}H and ^{13}C NMR (CD_2Cl_2) data, see Table 61. ESIMS, $[M+H]^+$ *m/z* (rel. int): 317 $[M+H]^+$ (100), 251 (87), 297 (51), 175 (58), 205 (43), 149 (69), 259 (34) for $C_{21}H_{32}O_2$.

Ent-kaur-16-en-19-oic acid (**243**). White solid (247-248 ºC); ^{1}H and ^{13}C NMR (CD_2Cl_2) data, see Table 61. ESIMS, $[M+H]^+$ *m/z* (rel. int): 285 $[M-H_2O]^+$ (100), 265 (19), 247.3 (8), 212 (4) for $C_{20}H_{30}O_2$.

Ent-kaur-16-en-19-ol (**244**). White solid; ^{1}H and ^{13}C NMR (CD_2Cl_2) data, see Table 62.

Ent- kaur-16-ene (**245**). White solid; ^{1}H and ^{13}C NMR (CD_2Cl_2) data, see Table 62.

Lanosterol (**246**): White solid (137-138 ºC); ^{1}H and ^{13}C NMR (CD_2Cl_2) data, see Table 63.

Stigmasta-5,22(E)-dien-3β-ol (**247**). White solid; ^{1}H and ^{13}C NMR (CD_2Cl_2) data, see Table 63. LC-MS (ESI), $[M+H]^+$ *m/z*: 333.7 for $C_{29}H_{48}O$.

3-Hydroxy-Olean-12-en-29-oic acid (**248**). White solid; ^{1}H and ^{13}C NMR (CD_2Cl_2) data, see Table 64.

Carissone (**249**). White solid; ^{1}H and ^{13}C NMR (CD_2Cl_2) data, see Table 65. LC-MS (ESI), $[M+H]^+$ *m/z*: 333.7 for $C_{15}H_{24}O_2$.

3.6.5 Physical Constants and Spectroscopic Data of Compounds from *Aspilia mossambicensis*

Methyl-15α-angeloyloxy-ent-kaur-16-en-19-oate (**250**). Colourless crystals; ^{1}H and ^{13}C NMR (CD_2Cl_2) data, see Table 65.

12-Oxo-ent-kaura-9(11),16-dien-19-oic acid (**251**). Colourless crystals; ^{1}H and ^{13}C NMR (CD_2Cl_2) data, see Table 65.

Ent-kauran-19-oic acid (**252**). Colourless crystals; ^{1}H and ^{13}C NMR (CD_2Cl_2) data, see Table 67 ESIMS, $[M+H]^+$ *m/z* (rel. int): 305 $[M+H]^+$ (72), 282 (100), 259 (42), 247 (23), 191 (13), 287 (11), 281 (10), 149 (19) for $C_{20}H_{32}O_2$.

Oleanolic acid (**253**). White Amorphous solid; ^{1}H and ^{13}C NMR (CD_2Cl_2) data, see Table 68.

β-Amyrin acetate (**254**). White solid; ^{1}H and ^{13}C NMR (CD_2Cl_2) data, see Table 69. ESIMS, $[M+H]^+$ *m/z* (rel. int): 469 $[M+H]^+$ (not observed), 391 (38), 371 (68), 329 (63), 185 (100), 175 (88), 182 (57), 149 (98)205 (78), 251 (74), 259 (42) for $C_{32}H_{52}O_2$.

Ent-kaura-9(11),16-diene (**255**). Colourless crystals; ^{1}H and ^{13}C NMR (CD_2Cl_2) data, see Table 70.

15β-Hydroxy-ent-kaura-9(11),16-dien-19-oic acid (**256**): Colourless crystals, ^{1}H and ^{13}C NMR (CD_2Cl_2) data, see Table 70.

Methyl cinnamate (**257**). Whitish solid; ^{1}H and ^{13}C NMR (CD_2Cl_2) data, see Table 71.

3.6.6 Physical Constants and Spectroscopic Data of Synthetic Derivatives

3.6.6.1 Physical Constants and Spectroscopic Data of Synthetic Derivatives from *Psiadia punctulata*

5,7,2',3',4',5'-Hexamethoxy-flavone (**258**). White solid (mp 151-153 ºC); ^{1}H and ^{13}C NMR ($CDCl_3$) data, see Table 76, ESIMS *m/z* (rel. int): 403 $[M+H]^+$ (100), 388 (17), 373 (21), 342 (10), 327 (7) for $C_{22}H_{22}O_9$.

5-Acetyloxy-7,2',3',4',5'-pentamethoxy-flavone (**259**). White solid (mp 185-187 ºC); ^{1}H and ^{13}C NMR ($CDCl_3$) data, see Table 76, ESIMS *m/z* (rel. int): 431 $[M+H]^+$ (100), 389 (98), 416 (1), 392(1), 359(2), 267(1), 149 (1) for $C_{22}H_{22}O_9$.

3-(2,",6"-Hydroxy-4-methoxyphenyl)-5-(2',3',4',5'-methoxyphenyl)-1H-pyrazole (**260**): White yellowish crystals (mp 192-194 ºC); ^{1}H and ^{13}C NMR ($CDCl_3$) data, see Table 77. ESIMS m/z (rel. int): 403 $[M+H]^+$ (100), 388 (17), 373 (10), 370 (4) for $C_{20}H_{22}N_2O_7$.

6,8-Dibromo,5-hydroxy-7,2',3',4',5'-pentamethoxy-flavone (**261**). White solid mp (185-187 ºC); ^{1}H and ^{13}C NMR ($CDCl_3$) data, see Table 78, ESIMS *m/z* (rel. int): 549 (100), 547 (98), 483 (1), 149 (1) for $C_{20}H_{18}Br_2O_8$.

6,8-Dibromo-5,7-dihydroxy-2',3',4',5'-tetramethoxy-flavone (**262**). White solid (mp 185-187 ºC); ^{1}H and ^{13}C NMR ($CDCl_3$) data, see Table 78. ESIMS *m/z* (rel. int): 531 (53), 533 (100), 467 (6), 371 (7) 250 (4), 241 (2), 167 (2) 149 (5), 129 (4) for $C_{19}H_{16}Br_2O_8$.

6β,18,19-Trihydroxy-ent-trachyloban-2N-oxime (**263**). White yellowish solid (mp 147-149 ºC); ^{1}H and ^{13}C NMR ($CDCl_3$) data, see Table 79. ESIMS, [M+H]+ *m/z* (rel. int): 350 $[M+H]^+$ (23), 332 $[M-H_2O]^+$ (100), 314 (26). HRESIMS, $[M+H]^+$ *m/z*: 350.2331 for $C_{20}H_{31}NO_4$.

6β-Hydroxy-2-oxo-trachyloban-18,19-dioic acid (**264**). White powder (mp 147-149 ºC); ^{1}H and ^{13}C NMR ($CDCl_3$) data, see Table 79. ESIMS, [M+H]+ *m/z* (rel. int): 327 $[M+H]^+$ (8), 301 (100), 283 (12), 255 (23), 241 (7) 177 (9), 149 (17) for $C_{20}H_{26}O_6$.

17-Methoxy-trachyloban-6β,19-diol (**265**). White solid (mp 171-173 ºC); ^{1}H and ^{13}C NMR ($CDCl_3$) data, see Table 80. ESIMS ESIMS, $[M+H]^+$ *m/z* (rel. int) 335 (34), 317 (32), 299 (100), 267 (96), 287 (11), 219 (6) for $C_{21}H_{34}O_3$.

2*β*,6*β*,19-*Triacetyloxy-trachylobane* (**266**). White solid mp (142-144 ºC); ^{1}H and ^{13}C NMR ($CDCl_3$) data, see Table 80. ESIMS, $[M+H]^+$ *m/z* (rel. int) 447 (65), 387 (73), 327 (86), 267 (100), 187 (21), 173 (9) for $C_{26}H_{38}O_6$.

19-methoxy-ent-trachyloban-6β,17-diol (**267**). White solid (mp 156-158 ºC); ^{1}H and ^{13}C NMR ($CDCl_3$) data, see Table 81, ESIMS ESIMS, $[M+H]^+$ *m/z* (rel. int) 335 (32), 317 (34), 299 (100), 267 (94), 285(13), 269 (9), 219 (17), 211 (15), 187 (21) for $C_{21}H_{34}O_3$.

3.6.6.2 Physical Constants and Spectroscopic Data of Synthetic Derivatives from *Aspilia pluriseta*

16β-Methoxy-ent-kaur-9(11)-en-19 oic acid (**268**). White yellowish residue (mp 184-186 ºC); ^{1}H and ^{13}C NMR (CD_2Cl_2) data, see Table 82. ESIMS, $[M+H]^+$ *m/z* (rel. int): 347 $[M+H]^+$ (100), 315 (34), 269 (21), 287 (4), 313 (3), 229 (2), 193 (2), 149 (2). HRESIMS, $[M+H]^+$*m/z*: 447.2586 for $C_{22}H_{34}O_3$.

Ent-kaur-9(11)-en-19-oic acid (**269**). White yellowish residue (mp 128-130 ºC); ^{1}H and ^{13}C NMR (Acetone-d_6) data, see Table 82. ESIMS, $[M+H]^+$ *m/z* (rel. int): 303 $[M+H]^+$ (100), 257 (19), 287 (6), 241 (3), 175 (2). HRESIMS, $[M+H]^+$*m/z*: 303.2324 for $C_{20}H_{30}O_2$.

Methyl ent-kaura-9(11),16-dien-19 oate (**270**). White solid (185-187 ºC); ^{1}H and ^{13}C NMR (CD_2Cl_2) data, see Table 83. ESIMS, $[M+H]^+$ *m/z* (rel. int):303 $[M+H]^+$ (100), 257 (19), 287 (6), 241 (3), 175 (2). for $C_{21}H_{30}O_2$.

Ent-kauran-19-oic acid (**271**). White solid (177-179 ºC); ^{1}H and ^{13}C NMR (CD_2Cl_2) data, see Table 83. ESIMS, $[M+H]^+$ *m/z* (rel. int.): 305 $[M+H]^+$ (72), 282 (100), 259 (42), 247 (23), 191 (13), 287 (11), 281 (10), 149 (19) for $C_{20}H_{32}O_2$.

3.7 Procedure for Biological Studies

3.7.1 Antimicrobial Activity

Two complementary test methods were used in this assay, the microbroth kinetic method and the agar disc diffusion method. The microbroth kinetic method is based on continuous monitoring of changes in the optical density (OD) of microbial growth as reported previously (Esma *et al.*, 2009). Through this assay, the turbidimetric growth curves of the microorganisms in the presence of increasing concentrations of isolated compounds were determined via optical density (OD) and the percentage growth inhibition by each of the compound concentrations was determined. *Staphylococcus aureus* (NCTC 7447) and *Eshericia coli* (NCTC 12923) strains were used in this study. The stock bacterial suspension equivalent to the turbidity of 0.5 McFarland (10^8 CFU/ml) standard was prepared in Mueller Hinton Broth (MHB)and then this suspension was adjusted to 10^6 CFU/ml in the same media. All compounds and standard (gentamicin and erythromycin) were dissolved in 1.25% DMSO in analytical grade distilled water; further dilutions (80 - 320 µg/ml) were made using the same solvent. The adjusted bacterial inoculum (100 µl) was added to each well of sterile 96-well flat-bottomed microtiter plate containing the test concentrations of samples and standard (100 µl/well). The final test concentrations of the samples (compounds and standard gentamicin) were 40, 80 and160 µg/ml. Two trials were performed for each concentration of sample. Two wells containing bacterial suspension with no drug (growth control) and two wells containing only media (background control) were included in this plate. The plates were incubated at 37°C and optical densities were measured at the start of incubation and again at 4 hours using a multi-detection microplate reader at 405 nm and automatically recorded for each well. The bacterial growth in each well was quantified by determining the change in OD over the four-hour period ($\delta OD = OD_{4hr} - OD_{0hr}$) after subtraction of background ODs (ODs of microorganism-free wells). The percentage inhibition for each concentration was then calculated using the Equation 15:

$$\% \text{ growth inhibition} = [1 - (\delta OD \text{of sample well} / \delta OD \text{of the growth control well})] \times 100 \quad \text{(Equation 15)}$$

Agar disc diffusion method as described by Balouiri *et al.*, (2016) was used as a complementary method to assess the antimicrobial activity of the plant extracts and isolated compounds against *S. aureus* and *E. coli*, several species of clinical fungal isolates of *Microsporum gypseum, Trichophyton mentagrophytes* and *Cryptococcus neoformans*, environmental isolates of *Aspergilus flavus* and *Aspergilus niger*, as well as standard fungal strains of *Candida parapsilosis* (ATCC 22019) and *Candida albicans* (ATCC 90018). Twenty mL of molten agar (Mueller Hinton Agar (MHA) for bacteria and Sabouraud Dextrose Agar (SDA) for fungi) was poured into sterile Petri plates (9 cm in diameter) and allowed to set. Fifty µL of standardized inoculum was swabbed uniformly to solidified agar plates using sterile cotton swabs and allowed to dry for 5 min. Discs with a diameter of 6 mm were aseptically used. Aliquots of 20 µL of test samples at a concentration of 100 mg/mL were dispensed into respective discs using a micropipette. Gentamicin and nystatin at concentrations of 30 mg/mL were used as a positive control. Dimethyl sulphoxide (DMSO) was used as a negative control. The plates were allowed to stand on a sterile biological safety cabinet for two hours to allow proper diffusion of the extracts/test compounds into the agar and thereafter incubated at 37°C for 24 hours. Antimicrobial activity was detected by measuring zones of inhibition (to the nearest millimeter) using a transparent ruler at the end of the incubation period. All the tests were run in triplicates and in accordance with the protocols of Clinical and Laboratory Standards Institute (CLSI) formerly National Committee for Clinical Laboratory Standards (NCCLS).

3.7.2 Cytotoxicity Assay

3.7.2.1 Reagent and Cells

Human liver and lung cancer cell lines, A549 and HepG2, respectively, and immortalized normal liver LO_2, lung BEAS-2B and fibroblast-like CCD19Lu cells were all purchased from ATCC. Cells were cultured in RPMI-1640 medium supplemented with 10% fetal bovine serum and antibiotics penicillin (50 U/ml) and streptomycin (50 µg/ml; Invitrogen, U.K.). All cells were incubated at 37°C in a 5% humidified CO_2 incubator). All test compounds were dissolved in DMSO at a final concentration of 50 mM and stored at -20°C before use.

3.7.2.2 Cell Viability Assay

Cytotoxicity was assessed by using the 3-[4,5-dimethylthiazole-2-yl]-2,5-diphenyltetrazolium bromide (MTT) (5 mg/ml) assay as previously described (Wong *et al.*, 2013; Irungu *et al.*, 2014). Briefly, $5x10^3$ cells per well were seeded in 96-well plates before drug treatments. After overnight cell culture, the cells were then exposed to different concentration of the test compounds (0.19-100 μM) and incubated for 24 hours. Wells without any test compounds were used as negative control. Subsequently, 10 μL of 5 mg/mL MTT solution was added to each well and incubated at 37°C for 4 hours followed by addition of 100 μL solubilization buffer (12 mM HCl in solution of 10% sodium dodecyl sulfate). A_{570} nm was then determined in each well on the next day. The percentage of cell viability was calculated using Equation 16:

$$\text{Cell viability (\%)} = A_{treated}/ A_{control} \times 100. \qquad \text{Equation (16)}$$

3.7.3 Anti-inflammatory Activity

In vivo evaluation of the anti-inflammatory activity of isolated compounds and extracts was carried out using the carrageenan-induced rat paw oedema method (Tarkang *et al.*, 2015). Thirty five adult Wistar rats were randomly divided into seven groups. Hind paw volumes were recorded for each rat using a Mercury plethysmograph, applying the Archimedes principle of fluid displacement. Ten (10) mg/kg of vehicle (normal saline, negative control), the standard drug indomethacin (10 mg/kg) and 200 mg/kg body weight of each isolated compound or extract were administrated orally to different groups of rats. After thirty minutes, paw oedema was induced in each rat by injecting 0.1 mL of carrageenan (1% in normal saline) into the right hind paw. Paw volumes were determined and recorded at 60, 120, 180 and 240 min after carrageenan administration. The difference between the paw volume before induction of edema at each time point was taken as a measure of oedema. Evaluation of anti-inflammatory activity was done by comparison of the paw volumes in treated groups with those of the negative controls.

3.7.4 Oral Glucose Tolerance Test

Oral Glucose tolerance test was carried out using a method described by Chege *et al.*, (2015). Wistar rats of both sexes (Males and females) of seven to nine weeks old were obtained from the School of Pharmacy, University of Nairobi animal rearing unit. The animals were allowed to acclimatize to the environment for four days. All the animals were given the standard laboratory diet and water *adlibitum* except during the test where only water was given throughout the experiment. A standard antidiabetic drug, metformin (Merck), dextrose anhydrous purified (Sigma Aldrich St. Louis, Mo, USA) and a Glucometer (Expeeed^{TM} Check Blood Glucose) to measure the blood glucose levels were procured. Eighty four rats were divided into fourteen groups (labelled A, B, C, D, E, F, G, H, I, J, K, L, M, N) according to the treatment and fasted for twelve hours prior to the experiment. Group A were treated with 2 mL distilled water each, this acted as a control group of rats. Group B were treated with metformin (150 mg/kg). A dose of 200 mg/kg of the isolated compounds and extracts (as 40 mg/mL solutions in 2.5% DMSO) was administrated orally to the rats of each groups labelled C-N. Sixty minutes after administration of the test compounds, 5g/kg of dextrose was orally administrated to the rats. Blood was withdrawn from the tail vein of the rats 0, 30, 60, 90, 120, and 240 min after glucose administration and the glucose levels determined and recorded.

3.7.5 *In vitro* Antiplasmodial Activity

Culture of *Plasmodium falciparum* were carried out as described in the literature (Atilaw *et al.*, 2017). Briefly, *in vitro* parasite culture of the *P. falciparum* (strain 3D7 and D6) was maintained in RPMI 1640 medium supplemented with 10 mM Hepes, 50 μg/mL hypoxanthine and 2.5 mg/mL AlbuMAX II®. Human O+ erythrocytes were provided by Red Cross Blood Bank. The *P. falciparum* growth inhibition assay to quantify parasite growth inhibition by the various test compounds was carried out according to well-established and previously reported procedure (Atilaw *et al.*, 2017).

3.8 Theoritical Electronic Circular Dichroism Calculation

Different conformations and configurations of the studied compound with a reduced chain length were optimized at the B3LYP/6-311G** (Lee *et al.*, 1988; Becke, 1993) level of

theory without any restrictions. The ECD were computed using the Time Dependent DFT (TDDFT) (Bauernschmitt and Ahlrichs, 1996; Autschbach *et al.*, 2002) algorithm in the program package GAUSSIAN 09 (Frisch *et al.*, 2009). The 6-31G* basis set was applied. 10 singlet and 10 triplet states were solved (keyword TD (NStates = 10, 50 - 50). All GAUSSIAN results were analysed and the spectra displayed using the SpecDis 1.62 (Bruhn et al., 2014). The molecules are displayed using SYBYL-X 2.1.1 (SYBYL-X 2.1.1, 2013).

3.9 Statistical Analysis

All experiments were carried out in duplicate or triplicate, and in some cases quadruplicate and results are expressed as mean values and standard deviation (S.D.) of the mean. One-way ANOVA test was used for between-group comparisons, and a value of $p < 0.05$ was considered to be statistically significant. The programs StatgraphicsPlus5.0 and Sigmaplot 11.0 were used to perform the analysis.

CHAPTER FOUR

RESULTS AND DISCUSSION

4.1 Characterization of Compounds Isolated from *Lannea* species

The stem bark and roots of *Lannea rivae* and *Lannea schweinfurthii* were investigated and seventy three compounds were isolated from the two plants. the crude extracts and the isolated compounds were tested for their antimicrobial, anti-inflammatory, anti-T2DM and cytotoxicity activity.

4.1.1 Characterization of Compounds Isolated from the Roots of *Lannea rivae*

Seven compounds (**186-192**) were isolated from this plant part including 2 new alkenylcyclohexenone derivatives; (4*R*,6*S*)-4,6-Dihydroxy-6-((*Z*)-nonadec-14'-en-1-yl)cyclohex-2-en-1-one (**186**) and (2*S*,4*R*,5*R*)-2,4,5-trihydroxy-2-((*Z*)-nonadec-14'-en-1-yl)cyclohexanone (**187**).

4.1.1.1 (4*R*,6*S*)-4,6-Dihydroxy-6-((*Z*)-nonadec-14'-en-1-yl)cyclohex-2-en-1-one (186)

Compound **186** was isolated as a colourless paste; from HRESIMS ($[M+H]^+$ at *m/z* 393.3344) and NMR data (Table 4.1), the molecular formula $C_{25}H_{44}O_3$ was established. The presence of an α,β-unsaturated cyclohexenone moiety was evident from the UV (λ_{max} 256, 336 nm), and NMR spectral data (Table 4.1). The NMR spectra further showed that the cyclohexenone ring is substituted with two hydroxy, at C-4 (δ_H 4.62, δ_C 64.0) and C-6 (δ_C 74.5), and a C_{19} alkenyl (at C-6) group (Table 14). In the EIMS, the fragment ion at *m/z* 374 corresponding to $[M-H_2O]^+$ is in agreement with the presence of a hydroxy substituents. The identity of the alkenyl group as 14'-(Z)-nonadecenyl was deduced from the ^1H (δ_H 5.28 for H-14'/15'; δ_H 1.17 for H-3'-H-12'; δ_H 1.95 for H-13'/16', and δ_H 0.83 for H-19) and ^{13}C (δ_C 129.8/129.7 for C-14'/15; δ_C 29.8-29.2 for C-3'-C-12'; δ_C 27.1 for C-13'; 26.8 for C-16', and δ_C 13.9 for C-19') NMR spectral data (Table 14). The HRMS which showed a protonated molecular ion peak at *m/z* 393.3344 is in agreement with a $C_{19}H_{37}$ alkenyl chain. The fragment ions at *m/z* 97 ($[C_7H_{13}]^+$) resulting from allylic cleavage of hep-2-en-1-ylium is in agreement with the placement of the double bond at C-14′. The close ^{13}C NMR chemical shift values (δ_C 129.8 and 129.7) for the

olefinic carbons C-14′ and C-15' of **186** is consistent with the assignment of *Z*-configuration to the double bond at C-14′ of the alkenyl chain (David *et al.*, 1998; Queiroz *et al.*, 2003; Kapche *et al.*, 2007; Okoth and Koorbanally, 2015; Okoth *et al.*, 2016); in *E*-configured olefinic carbons (C-14′ and C-15′), the ^{13}C NMR resonances have substantially distinct values (Queiroz *et al.*, 2003; Correia *et al.*, 2006; Okoth and Koorbanally, 2015). The position of the double bond and its *cis*-configuration indicated that it is biosynthetically derived from the fatty acid [5ω]-*cis*-hexadecenoic acid, through a similar mechanism as proposed for related compounds (Correia *et al.,* 2006).

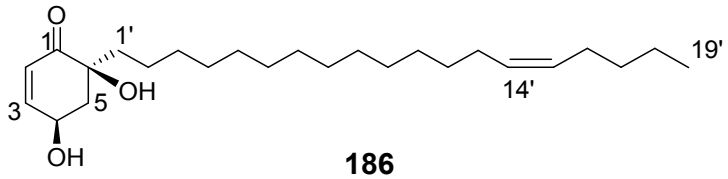

186

Table 4.1: ^{1}H (800 MHz) and ^{13}C (200 MHz) NMR Data of 186 ($CDCl_3$)

Position	δ_C	Type	δ_H (mult., *J* in Hz)	HMBC (H→C)
1	200.9	C	-	-
2	126.6	CH	5.96 (d, *J*=10.1)	C-3, C-4, C-6
3	149.4	CH	6.80 (dd, *J*=10.1, 3.6)	C-1, C-5
4	64.0	CH	4.62 (m)	C-2, C-5, C-6
5	41.0	CH_2	2.20 (dd, *J*=5.4, 14.2)	C-1, C-3
			2.15 (dd, *J*=5.4, 14.2)	C-1, C-3
6	74.5	C	-	-
1'	39.0	CH_2	1.72 (m)	C-1, C-5, C-3'
2'	22.9	CH_2	1.25 (m)	C-3'
3'-12'	29.8-29.2	10xCH_2	1.17 (br s)	C-3'-C-12', C-13'
13'	27.1	CH_2	1.95 (m)	C-12', C-15'
14' ,15'	129.8, 129.7	CH,CH	5.28 (t, *J*=4.8)	C-13', C-16'
16'	26.8	CH_2	1.95 (m)	C-14', C-18'
17'	31.8	CH_2	1.25 (m)	C-15', C-19'
18'	22.2	CH_2	1.25 (m)	C-16', C-19'
19'	13.9	CH_3	0.83 (m)	C-17'

The substitution pattern in the cyclohexenone ring was established from the HMBC experiment (Table 4.1), whereby ^{3}J correlation of H-2 (δ_H 5.96) with C-4 (δ_C 64.0) and C-6 (δ_C 74.5), H-3 (δ_H 6.80) with C-1 (δ_C 200.9) and C-5 (δ_C 41.0), and CH_2-5 (δ_H 2.20 and 2.15) with C-1 and C-3 were observed. The placement of the alkenyl group at C-6 was also supported by the HMBC correlation of CH_2-1′ (δ_H 1.71) with C-1 (δ_C 200.9) and C-5 (δ_C 41.0), as observed in related compounds (Okoth *et al.*, 2016).

The planar structure of this compound is the same as the ones reported by de Jesus Correia *et al.* (2001) and Okoth *et al*. (2016). On the basis of NMR evidence, these authors proposed (4*S**,6*S**)-**186** and (4*S**,6*R**)-**186** relative configuration, respectively. Here, in determining the absolute configuration in compound **186**, firstly, the energies of different conformations for (4*S**,6*S**)-**186a** and (4*S**,6*R**)-**186a**, where the side chain at C-6 is shorter (to reduce computational time) were calculated and the conformations with minimum energy in each case identified.

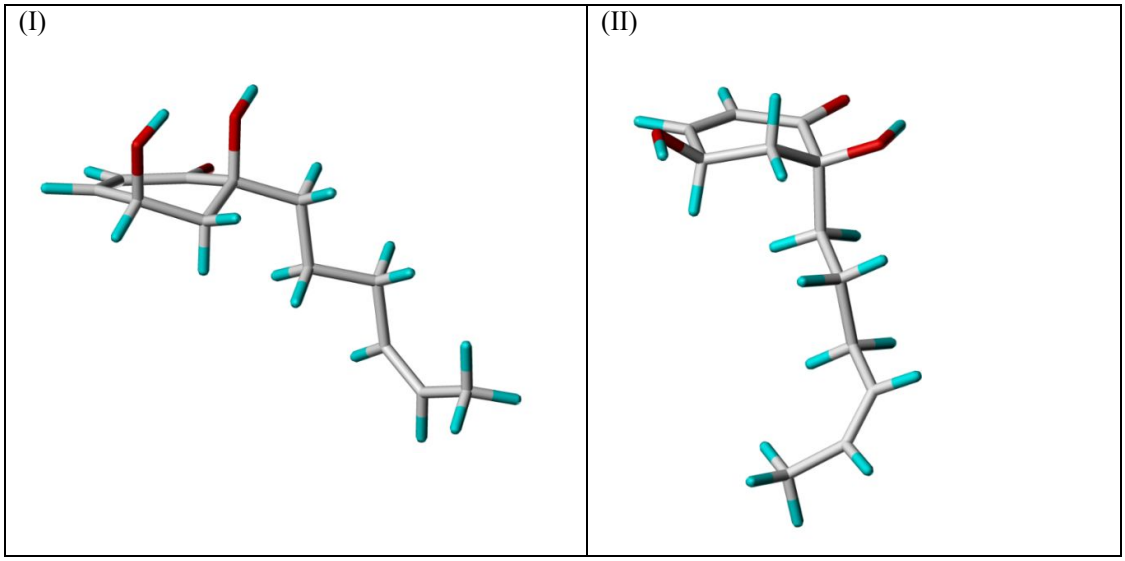

Key: conformation I: global minimum, conformation II: + 0.14 kcal/mole

Figure 4.1: Calculated Global Energy Minimum Geometries of Conformers of (4R,6S)-186a

In the case of (4*S**,6*R**)-**186a**, two conformations with ΔE = 0.14 Kcal/mol were considered (Figure 4.1, Boltzmann weighted: 55.1 for conformation I and 44.9% for II, respectively).

Hydrogen-bonding between 4-OH and 6-O (in conformation I, Figure 4.1) and between 6-OH and C=O (in conformation II, Figure 4.1) may be responsible for the stabilities of these conformers. Furthermore, it can be seen that the 5-CH_2 group in conformation I is 'down', while in conformation II this group is 'up' with respect to the other ring carbon atoms which are almost span a plane. From these calculations it is apparent that the cyclohexenone ring is not rigid, undergoing ring flipping between conformations I and II (Figure 4.1); consequently the ^3J values (5.4 Hz) observed between H-4 and both protons at C-5 is a mean value (which is in good agreement with the calculated value, Table 4.2), indicating that coupling constant and NOE interactions could not be used for conformational or configurational analyses to determine the relative configuration with certainty. It follows then that the configurational assignments proposed by de Jesus Correia *et al.* (2001), Roumy *et al.* (2009) and Okoth *et al.* (2016) on the basis of NMR evidence with the assumption of stable cyclohexenone ring, may not be reliable.

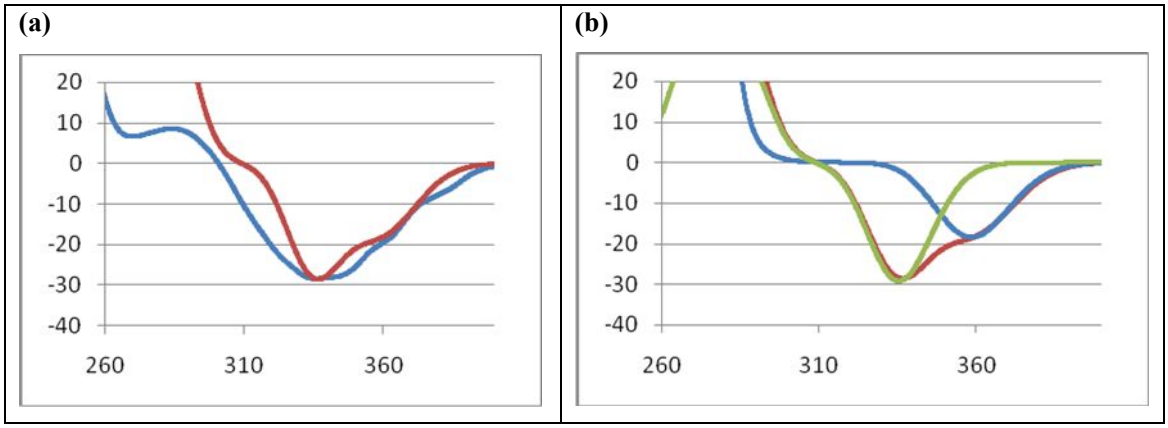

Key: (a) blue experimental, red Boltzmann weighted sum of calculated CD's for conformations I and II (55.9 and 44.1%, resp.); (b) calculated CD's, red Boltzmann weighted sum of conformations I and II, blue conformation I, and green conformation II

Figure 4.2: ECD Spectra of Compound 186

The experimental ECD spectrum of compound **186** (Figure 4.2a), which showed negative Cotton effect at λ_{max} 337 nm, was then compared with the computed ECD spectra for stable conformers of (4*S*,6*S*)-**186a**, (4*R*,6*R*)-**186a**, (4*R*,6*S*)-**186a** and (4*S*,6*R*)-**186a**. Of these, the best match was obtained for (4*R*,6*S*)-**186a** isomer where two conformations with low energies (I and II, Figure 4.1) showed negative Cotton effects at 360 and 335 nm,

respectively (Figure 4.2b). In fact the ECD spectrum of the weighed sum of these conformers is a close match with the experimental ECD (Figure 4.2a). In order to explain the long wavelength absorption position in the computed ECD spectrum of conformation I (360 nm), the most important π-π* and n-π* electron transitions were calculated and were found to be between donor MO's 54 - 56 and LUMO at 270 nm and between donor MO's 56 and 57 and LUMO at 358 nm.

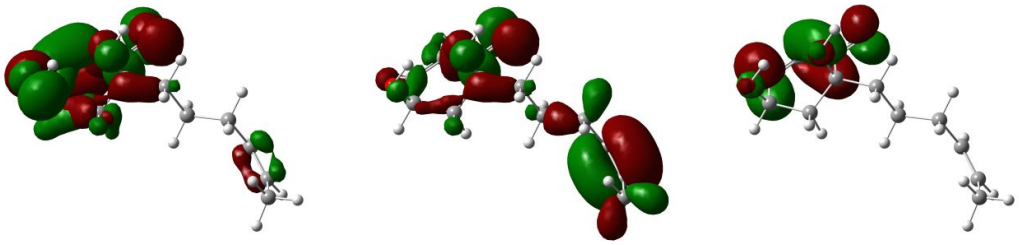

Key: Donor MO's 54 - 56 (left), donor MO's 56 and 57 (middle), and LUMO (MO 58, right) of conformation I of (4R,6S)-**186a**

Figure 4.3: Molecular Orbitals of 186

The latter one is highly influenced by the π electron system of the exocyclic double bond which transfers electrons into the LUMO which is essentially situated at the double bond of the 2-cyclohexenone ring system (Figure 4.3). However, the length of the side chain was shortened during calculations for practical reasons. Thus, the calculated wavelength may differ slightly from the actual one of (4*R*,6*S*)-**186** and may overlap with n-π* transitions from the 2-cyclohexenone ring system which are known to be in the range of approximately 330 - 340 nm. However, here the sign of the Cotton effect is much more influenced by the orientation of the 4-OH group than that of the long-chain substituent at position 6 which is much weaker (Kwit *et al.,* 2010). It follows then that the configurational assignment discussed above is reliable and consequently compound **186** was characterized as (4*R*,6*S*)-4,6-dihydroxy-6-((*Z*)-nonadec-14'-en-1-yl)cyclohex-2-en-1-one.

Table 4.2: Theoretically Calculated Coupling Constants of 186

Conformation	Dihedral angle[a]	*J* (in Hz)
I	H4-H5α (46°)	3.9
	H4-H5β (–72°)	1.9
II	H4-H5α (–53°)	5.1
	H4-H5β (–170°)	11.1
Weighted mean values (I and II)	H4-H5α	4.4
	H4-H5β	5.9
Experimental [b]	H4-H5α	5.4
	H4-H5β	5.4

Notes: Calculated coupling constants (^{3}J4H-5H) for different conformations of (4R,6S)-**186a** using the Haasnoot-de Leeuw-Altona equation (Altonia, 1996)

[a] from theoretically calculated conformations of **186a**;

[b]for compound **186**

4.1.1.2 2,4,6-Trihydroxy-2-[12'-*Z*-heptadecenyl]-cyclohexanone (187)

The second new compound (**187**) was isolated as a colourless paste from the roots of *Lannea rivae*. EIMS analysis showed a weak molecular ion peak at *m/z* 410 and a more stable fragment ion at *m/z* 392 for $[M\text{-}H_2O]^+$. Comparison of the MS and NMR data of this compound (Table 4.3) with those of compound **186** (M^+ 392, NMR: Table 4.1) indicated that compound **187** could be a hydro-derivative of **186** with a molecular formula $C_{25}H_{46}O_4$. The UV (λ_{max} 206 nm) spectrum and ^{13}C NMR chemical shift value of the carbonyl (δ_C 210.9 for C=O) did not show an α,β-unsaturated carbonyl as in compound **186**, rather the presence of a cyclohexanone ring for compound **187** was evident from the NMR spectra (Table 4.3). The NMR spectral data further showed that the cyclohexanone ring is substituted with three hydroxy groups, at C-2 (δ_C 77.3), C-4 (δ_C 68.5; δ_H4.20) and C-5 (δ_C 71.9; δ_H 4.00) and a long alkenyl chain at C-2 (Table 3). The substitution pattern in the cyclohexanone ring was established from the HMBC spectrum: correlation of CH_2-3 (δ_H 2.98 and 2.78) with C-1 (δ_C 210.9) and C-5 (δ_C 71.4); H-4 (δ_H 4.20) with C-2 (δ_C 77.3) and C-6 (δ_C 40.4); H-5 (δ_H 4.00) with C-1 (δ_C 210.9) and C-3; CH_2-6 (δ_H 2.40 and 1.72) with C-2 and C-4; and CH_2-1' (δ_H 1.79 and 2.06) with C-1 and C-3. This substitution pattern was further supported by H,H-COSY

(CH_2-3↔H-4↔H-5↔CH_2-6) spectrum. This observation indicated that two of the hydroxyl groups are located on adjacent carbon atoms at C-4 and C-5.

The NMR spectral data of **187** was similar to that of the compound previously identified from the same plant, *Lannea rivae* (Okoth *et al.*, 2016), except on the length of the side chain and that the configuration of the compound reported by Okoth *et al.* (2016) has not been determined. The side chain at C-2 in compound **187** was established to be nonadec-14-en-1-yl group from MS ($[M]^+$ at *m/z* 410) and NMR spectral data (Table 4.3). As in compound **186**, the fragment ion at *m/z* 97 ($[C_7H_{13}]^+$) formed as the result of allylic cleavage of hept-2-en-1-ylium group is consistent with the placement of the double bond at C-14'. The HMBC spectrum showed correlation of CH_3-19' (δ_H 0.94) with the sp^3 carbon atoms, C-18' (δ_C 22.4) and C-17' (δ_C 32.0), showing that the double bond is not located two bonds away from the terminal methyl group as found in some other alkenyl cyclohexenone derivatives (Queiroz *et al.*, 2003; Okoth and Koorbanally, 2015). The HMBC correlation of H-13' (δ_H 2.06) and H-16' (δ_H 2.06) with C-14' (δ_C 129.7) and C-15' (δ_C 129.8) confirmed the location of the double bond at C-14'. Comparison of the ^1H and ^{13}C NMR data with those of compound **186** and related compounds having similar long alkenyl chain suggested a *Z*-geometry at C-14' (Groweiss *et al.*, 1997; Kapche *et al.*, 2007; Okoth and Koorbanally, 2015). The two olefinic protons on the side chain, H-14' and H-15', appeared as overlapping resonances at δ_H 5.39 (t, J = 4.7 Hz) showing HMBC correlations with the allylic carbon resonances at δ_C 26.9 (C-13' and δ_C 27.2 (C-16'). These ^{13}C NMR chemical shift values are consistent with a *Z*-configuration for the double bond on the side chain, as a double bond with *E*-configuration is expected to appear at higher resonance values (*ca.* δ_C 32.0) for the allylic carbon atoms (Roumy *et al.*, 2009).

The large coupling constant between Hax-3 (δ_H 2.98, 1H, dd, *J*=12.3, 11.2 Hz) and H-4 (δ_H 4.20, ddd, *J*=11.0, 4.5, 3.1 Hz) requires that H-4 is also axial and hence OH-4 should be equatorial. On the other hand, the small coupling constant between H-4 and H-5 requires that H-5 is equatorial, making OH-5 to be axially oriented. These observations are consistent with the two hydroxy groups being *cis*-oriented. The co-occurrence of compound **187** with **186** indicated that they are biogenetically related, and it is likely that the configurations at C-2 (C-6 in compound **186**) and C-4 in compound **187** are the same as in **186**. In compound **187**

(where the cyclohexanone ring is rigid, stabilized by hydrogen bonding between C=O and OH-2), OH-4 being equatorial (*β*-oriented), OH-5 should be axial (*β*-oriented). Thus, the relative configuration of **187** is likely to be (2*S**,4*R**,5*S**). Hence the compound was characterized as (2*S**,4*R**,5*S**)-2,4,5-trihydroxy-2-((*Z*)-nonadec-14'-en-1-yl)cyclohexanone. An isomeric compound, (2*S*,4*R*,5*R*)-2,4,5-trihydroxy-2-((*Z*)-nonadec-14'-en-1-yl)cyclohexanone has been described by Chengbin *et al*., (2006).

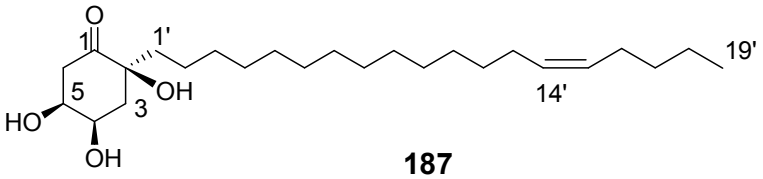

187

Table 4.3: ^{1}H (600 MHz) and ^{13}C (150 MHz) NMR Data of 187 (CD_2Cl_2)

Position	Type	δ_H (mult., *J* in Hz)	δ_C	HMBC(H→C)
1	C	-	210.9	-
2	C	-	77.3	-
3	CH_2	2.98 (dd, *J*=12.3, 11.2, H-3ax)	41.8	C-1, C-5
		2.70 (m, H-3eq)		C-1, C-2, C-4, C-5
4	CH	4.20 (ddd, *J*=11.0; 4.5, 3.1)	68.5	C-2, C-3, C-6
5	CH	4.00 (m)	71.9	C-1, C-3
6	CH_2	2.40 (dd, *J*=14.8, 4.1, H-6a)	40.4	C-1, C-2, C-4, C-5
		1.71 (dd, *J*=14.8; 3.5, H-6b)		C-2, C-4
1'	CH_2	2.06 (m)	39.5	C-1, C-3
		1.77 (d, *J*=4.4)		C-1, C-3
2'	CH_2	1.36 (m)	23.1	C-3'
3'-12'	10xCH_2	1.29 (br s)	29.8-29.3	C3'-C12', C-13'
13'	CH_2	2.06 (m)	27.2	C-14', C-15'
14', 15'	CH,CH	5.36 (m)	129.8, 129.7	C-13', C-16'
16'	CH_2	2.06 (m)	26.9	C-14', C-18'
17'	CH_2	1.36 (m)	32.0	C-15', C-19'
18'	CH_2	2.06 (m)	22.4	C-16', C-19'
19'	CH_3	0.94 (t, *J*=7.1)	13.7	C-17', C-18'

4.1.1.3 Taraxerol (188)

Compound **188** was isolated as colourless crystals from the roots of *Lannea rivae*. The ^{13}C NMR spectrum showed signals corresponding to 30 carbons including an oxygenated carbon C-3 (δ_C 78.7) and two olefinic carbons C-14 (δ_C 158.2) and C-15 (δ_C 116.7) which are characteristic of a taraxane skeleton. The ^1H NMR (Table 4.4) signals at δ_H 5.57 (H-7) and δ_H 3.19 (H-3) revealed the presence of olefinic and an oxymethine protons, respectively. Eight methyl groups; δ_H 1.13 (CH_3-26), δ_H 0.99 (CH_3-23), δ_H 0.99 (CH_3-29), δ_H 0.97 (CH_3-27), δ_H 0.95 (CH_3-25), δ_H 0.95 (CH_3-30), δ_H 0.86 (CH_3-28), δ_H 0.82 (CH_3-24), were also observed in the ^1H NMR spectrum. Comparison of the ^1H and ^{13}C NMR data of **276** with that of taraxerol in the literature (Muithya, 2010) indicated high similarity. The HMBC correlation of H-15 (δ_H 5.57) with C-8 (δ_C 38.9), C-13 (δ_C 37.9), C-17 (δ_C 35.7) and that of H-3 (δ_H 3.19) with C-1(δ_C 37.6), C-5 (δ_C 55.4), C-23 (δ_C 27.7) and C-24 (δ_C 15.2) further confirmed **188** to be taraxerol. In addition HMBC correlation between H-25 (δ_H 0.95) and C-1 (δ_C 37.6), H-30 (δ_H 0.95) and C-19 (δ_C 36.5), H-30 (δ_H 0.95) and C-20 (δ_C 72.6) were observed. Based on these observations, **188** was identified as taraxerol, a common pentacyclic triterpene in Anacardiaceae plant family.

4.1.1.4 Taraxerone (189)

Compound **189** was also isolated as colourless crystals from the roots of *Lannea rivae*. The ^1H and ^{13}C NMR data (Table 4.4) were similar to that of compound **188** with the only difference that compound **189** has a carbonyl at C-3 instead of hydroxy group as in compound **188.** In agreement with this, the HMBC spectrum of **189** showed correlations of H-23 (δ_H 1.08) and H-24 (δ_H 0.95) with C-3 (δ_C 216.8). Further HMBC corelations of H-1 with C-3 (δ_C 216.8) were observed. The ^{13}C NMR chemical shift of C-2 (δ_C 34.1) and C-4(δ_C 47.4) of compound **189** were deshilded due to the presence of a carbonyl at C-3. The NMR data of the rest of the molecule is identical to that of compound **188**. Based on these NMR data information and the literature (Muithya, 2010), compound **189** was identified as taraxerone.

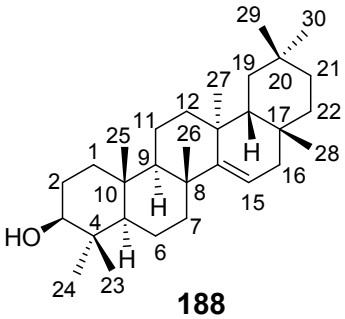
29
30
19
21
27
20
12
17
22
11
25
26
H
28
1
9
16
2
10
H
8
15
4
7
HO
H
6
24
23

188

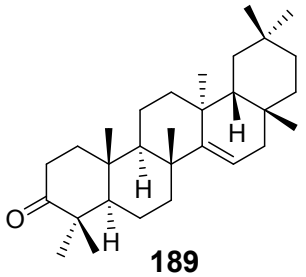
H
H
O
H

189

Table 4.4: ^{1}H NMR (600 MHz) and ^{13}C NMR (150 MHz) Data of 188 and 189

Position	**188** (CD_2Cl_2)				**189** (CD_2Cl_2)			
	δ_C	Type	δ_H (mult., *J* in Hz)	HMBC	δ_C	Type	δ_H (mult., *J* in Hz)	HMBC
1	37.6	CH_2	1.30 (d, *J*=1.7)	C-3, C-9	38.2	CH_2	1.38 (m)	C-3, C-25
			1.05 (m)	C-3, C-9				
2	27.2	CH_2	1.66 (m)	C-4	34.1	CH_2	1.69 (m)	C-4, C-10
3	78.7	CH	3.19 (m)	C-1, C-23, C-24	216.8	C	-	-
4	38.6	C	-	-	47.4	C	-	-
5	55.4	CH	0.83 (m)	C-3, C-7	55.7	CH	1.05 (m)	C-3, C-7
6	18.7	CH_2	1.61 (br s)	C-4, C-8	19.9	CH_2	1.69 (m)	C-4, C-8
7	41.3	CH_2	2.07 (dt, *J*=12.8, 3.3)	C-9, C-14	35.0	CH_2	2.11 (dt, *J*=12.9, 3.3)	C-9
8	38.9	C	-	-	38.8	C	-	-
9	49.2	CH	1.45 (m)	-	48.7	CH	1.59 (m)	C-1, C-7, C-12
10	37.6	C		-	37.6	C	-	-
11	17.4	CH_2	1.45 (m)	C-10, C-13	17.5	CH_2	1.59 (m)	C-8, C-13
12	33.6	CH_2	1.66 (m)	C-9, C-27	35.7	CH_2	1.69 (m)	C-9
13	37.9	C	-	-	37.5	C	-	-
14	158.2	C	-	-	157.7	C	-	-
15	116.7	CH	5.57 (dd, *J*=8.2, 3.2)	C-8, C-17	117.0	CH	5.60 (dd, *J*=8.2, 3.2)	C-8
16	37.5	CH_2	1.96 (ddd, *J*=14.5, 3.4, 1.1)	-	36.5	CH_2	1.12 (d, *J*=12.8)	C-14, C-18
17	35.7	C	-	-	37.7	C	-	-
18	48.6	CH	0.95 (m)	C-12, C-20	48.8	CH	1.59 (m)	C-12, C-20

Table 4.4 continued

Position	**188** (CD_2Cl_2)				**189** (CD_2Cl_2)			
	δ_C	Type	δ_H (mult., *J* in Hz)	HMBC	δ_C	Type	δ_H (mult., *J* in Hz)	HMBC
19	36.5	CH_2	1.66 (m)	C-13, C-29,	40.6	CH_2	1.38 (m)	C-17, C-21, C-30
			1.38 (m)	C-30			2.12 (m)	C-21, C-30
20	28.6	C	-	-	28.6	C	-	-
21	33.0	CH_2	1.30 (d, *J*=1.72)	C-20, C-30	33.5	CH_2	2.60 (m)	C-17, C-29
							3.33 (dd, *J*=6.3, 3.3)	C-17, C-29
22	35.0	CH_2	1.38 (m)	C-16, C-20	33.0	CH_2	1.05 (m)	-
23	27.7	CH_3	0.99 (s)	C-3, C-5	25.8	CH_3	1.08 (s)	C-3, C-5
24	15.2	CH_3	0.82 (s)	C-3, C-5	21.2	CH_3	0.95 (s)	C-3
25	15.2	CH_3	0.95 (s)	C-1, C-9	14.5	CH_3	1.12 (s)	C-1
26	25.6	CH_3	1.13 (s)	-	29.5	CH_3	0.87 (s)	-
27	21.0	CH_3	0.97 (s)	C-12, C-14	25.3	CH_3	1.18 (s)	C-12, C-14
28	29.6	CH_3	0.86 (s)	C-22	29.6	CH_3	0.95 (s)	C-22
29	33.0	CH_3	0.99 (s)	-	33.0	CH_3	0.99 (s)	-
30	29.5	CH_3	0.95 (s)	C-19, C-21	21.0	CH_3	0.95 (s)	C-19

4.1.1.5 *β*-Sitosterol (190)

The ^{13}C NMR spectrum (Table 4.5) of compound **190** showed signals corresponding to 29 carbon atoms, including two olefinic and one oxygenated carbon. The ^{1}H NMR data (Table 4.5) of **190** showed signals at δ_H 5.38 (H-6) and δ_H 3.50 (H-3) with the corresponding carbon signals appearing at δ_C 37.6 (C-3) and δ_C 37.6 (C-6), based on HSQC spectrum. In addition, six methyl groups, at δ_H 0.96 (CH_3-19), δ_H 0.90 (CH_3-24), δ_H 1.04 (CH_3-26), δ_H 0.87 (CH_3-27), δ_H 0.85 (CH_3-28) and δ_H 0.93 (CH_3-29) were also observed in the ^{1}H NMR spectrum. A close analysis of the ^{13}C NMR and the HMBC spectra allowed the identification of compound **190** as *β*-sitosterol (Okoth, 2014).

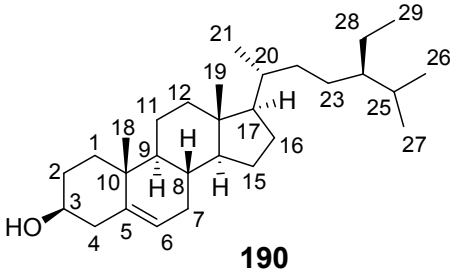

190

Table 4.5: ^{1}H (600 MHz) and ^{13}C NMR (150 MHz) Data of 190 in CD_2Cl_2

Position	δ_C	Type	δ_H	HMBC
1	37.2	CH_2	1.85 (m)	C-3, C-18
			1.21 (m)	C-3, C-5, C-18
2	31.9	CH_2	1.85 (m)	C-4, C-10
3	71.6	CH	3.50 (m)	C-1. C-5
4	42.3	CH_2	2.27 (m)	C-2, C-6, C-10
5	140.9	C	-	-
6	121.4	CH	5.38 (dt, *J*=5.37, 1.88, 1.88)	C-4, C-8, C-10
7	31.9	CH_2	2.03 (m)	C-5, C-14
8	31.7	CH	1.83 (m)	C-6, C-11, C-13
9	50.2	CH	0.97 (m)	C-7, C-12
10	36.4	C	-	-
11	21.0	CH_2	1.52 (m)	C-8, C-13
12	39.8	CH_2	1.21 (m)	C-9, C-17, C-19
			2.03 (m)	C-9, C-17, C-19
13	42.2	C	-	-

Table 4.5 continued				
Position	δ_C	Type	δ_H	HMBC
14	56.7	CH_2	1.14 (m)	C-7, C-16
15	25.9	CH_2	1.62 (m)	C-8, C-17
16	28.8	CH_2	1.85 (m)	C-13, C-14, C-20
17	56.0	CH	1.21 (m)	C-12, C-19
18	11.6	CH_3	0.73 (s)	C-1, C-5, C-9
19	18.5	CH_3	0.96 s	C-17, C-20
20	33.8	CH	1.40 (m)	C-13, C-16, C-23
21	24.2	CH_3	1.60 (s)	C-17, C-21
22	45.8	CH_2	1.0 (m)	C-21, C-24
23	23.0	CH_2	1.29 (m)	C-20, C-25, C-28
24	36.1	CH	1.40 (m)	C-22
25	29.1	CH	1.32 (m)	C-23, C-28
26	19.5	CH_3	1.04 (s)	C-24
27	19.1	CH_3	0.87 (s)	C-24
28	18.7	CH_2	0.85 (s)	C-23, C-25
29	11.7	CH_3	0.90 (s)	C-24

4.1.1.6 Epicatechin gallate (191)

Compound **191** was obtained as white amorphous solid from the roots of *Lannea rivae*. The ^{1}H NMR spectrum (Table 4.6) displayed signals characteristic of a flavan-3-ol skeleton *vis* δ_H 4.96 (1H, br s, H-2), δ_H 5.28 (1H, m, H-3), δ_H 2.86 (1H, dd, 17.3, 4.7 Hz, H-4), δ_H 2.60 (1H, dd, 17.6, 2.2 Hz, H-4) supported by the ^{13}C NMR spectrum [δ_C 76.8 (C-2), δ_C 68.5 (C-3), δ_C 26.0 (C-4), δ_C 156.8 (C-5), δ_C 156.9 (C-7)]. In ring A, two meta-coupled aromatic protons at δ_H 5.76 (1H, 2.26, H-6) and δ_H 5.86 (2.31 Hz, H-8) and the corresponding carbon signals at δ_C 95.9 (C-6) and δ_C 94.7 (C-8), respectively, indicated oxygenation at C-5 and C-7 (δ_C 156.8 and δ_C 156.9 respectively) of A-ring as expected from biogenetic point of view. A singlet at δ_H 6.75 (H-2"/H-6") and the ^{13}C NMR signals at δ_C 145.7 (C-3"), δ_C 138.9 (C-4"),δ_C 145.7 (C-5") and δ_C 162.3 (C-7") are consistent with a gallate moiety. The HMBC correlations of H-3 with C-1' and C-4a confirm the placement of the gallate moeity at C-3. The NOE effect observed between H-2 and H-3 indicated a *syn*-orientation of the two protons. Based on the above information, compound **191** was identified as epicatechin gallate.

Table 4.6: ^{1}H (600 MHz) and ^{13}C (150 MHz) NMR Data of 191 and 192

Position	**191** (DMSO-d_6)				**192** (DMSO-d_6)			
	δ_C	Type	δ_H (mult., *J* in Hz)	HMBC	δ_C	Type	δ_H (mult., *J* in Hz)	HMBC
2	76.8	CH	4.96 (br s)	C-4, C-9, C-2'	79.6	CH	4.91 (d, *J*=3.6)	C-9, C-2'
3	68.5	CH	5.28 (m)	C-10, C-2'	72.8	CH	4.35 (m)	C-10, C-2'
4	26.0	CH_2	2.86 (dd, *J*=17.28, 4.66)	C-2, C-5, C-9	28.5	CH_2	1.24 (br s)	C-5, C-9
			2.60 (dd, *J*=17.56, 2.21)	C-2, C-5, C-9				
5	156.8	C	-	-	157.7	C	-	-
6	95.9	CH	5.86 (d, *J*=2.31)	C-8, C-10	95.2	CH	5.89 (s)	C-8, C-10
7	156.9	C	-	-	155.5	C	-	-
8	94.7	CH	5.76 (d, *J*=2.26)	C-6. C-10	91.7	CH	6.05 (s)	C-6. C-10
9	155.9	C	-	-	153.6	C	-	-
10	97.6	C	-	-	96.3	C	-	-
1'	129.7	C	-	-	126.4	C	-	-
2'	114.6	CH	6.78 (d, *J*=2.08)	C-2, C-4'	114.6	CH	6.78 (d, *J*=8.04)	C-2, C-4'
3'	145.0	C	-	-	145.7	C	-	-
4'	145.1	C	-	-	144.5	C	-	-
5'	115.4	CH	6.58 (d, *J*=8.10)	C-1', C-3'	111.9	CH	6.88 (m)	C-1', C-3'
6'	117.9	CH	6.68 (dd, *J*=8.28, 2.05)	C-2, C-4'	115.4	CH		
1"	119.5	C	-	-	116.8	C	-	-
2"	108.1	CH	6.75 (s)	C-4", C-5"	108.2	CH	6.83 (s)	C-4", C-5"
3"	145.7	C	-	-	144.5	C	-	-
4"	138.9	C	-	-	138.1	C	-	-

Table 4.6 continued

Position			**191** (DMSO-d_6)				**192** (DMSO-d_6)	
	δ_C	Type	δ_H (mult., *J* in Hz)	HMBC	δ_C	Type	δ_H (mult., *J* in Hz)	HMBC
5"	145.7	C	-	-	143.8	C	-	-
6"	108.1	CH	6.75 (s)	C-4", C-7"	108.2	CH	6.83 (s)	C-4", C-7"
7"	165.5	C	-	-	163.3	C	-	-
C-3"-OCH_3	-	-	-	-	56.1	CH_3	3.76 (s)	C-3"
C-5"-OCH_3	-	-	-	-	56.1	CH_3	3.78 (s)	C-5"

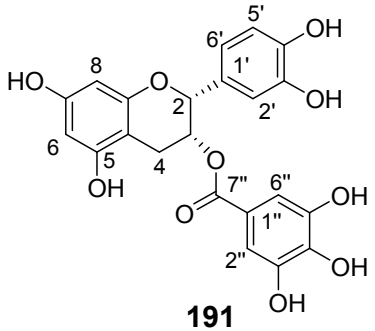

191

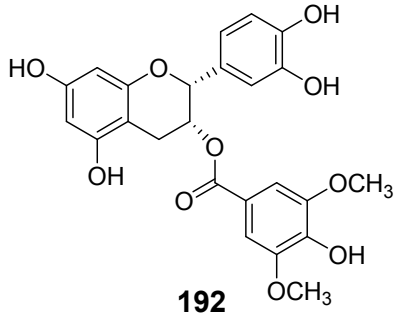

192

4.1.1.7 3'', 5''-Dimethoxy-epicatechin gallate (192)

Compound **192** was also obtained as a white amorphous solid. The ^{1}H NMR data (Table 4.6) of this compound was similar to that of **191** except that **192** has two methoxy groups at δ_H 6.78 (OCH_3-3" and OCH_3-6"). The HMBC correlation of the chemically equivalent methoxy signal at δ_H 6.78 with the carbon reonance at δ_C 144.5 (C-3") and δ_C 143.8 (C-5"), respectively, allowed the placement of these methoxy groups. The coupling constant (3.6 Hz) between H-2 and H-3 suggested the two protons are *cis*-oriented. Based on this observation and comparison with literature (Sáez *et al.*, 2013), **192** was identified as 3",5"-dimethoxy-epicatechin gallate.

4.1.2 Characterization of Compounds Isolated from Stem Bark of *Lannea rivae*

The stem bark extract of *Lannea rivae* resulted in tthe characterization of two compounds namely lupeol (**193**) and daucosterol (**194**).

4.1.2.1 Lupeol (193)

The ^{1}H and ^{13}C NMR data (Table 4.7) of compound **193** revealed that this compound is a triterpene derivative. The presence of seven methyl groups was evident from the singlet signals at δ_H 0.91 (C-23), 0.88 (C-24), 0.72 (C-25), 0.96 (C-26), 0.69 (C-27), 0.76 (C-28) and 0.90 (C-30). The oxymethine proton H-3 showed a multiplet at δ_H 3.12 and two broad singledts at δ_H 4.50 and δ_H 4.52 was indicative of olefinic protons H_2-29. Additionally, ^{13}C NMR experiment confirmed the presence of seven methyl groups [δ_C 27.3 (C-23), δ_C 14.7 (C-24), δ_C 16.0 (C-25), δ_C 15.9 (C-26), δ_C 15.2 (C-27), δ_C 17.9 (C-28) and δ_C 19.2 (C-30)] and an oxygenated carbon at δ_C 78.9 (C-3). The signal of an exomethylene group at [δ_C 109.3 (C-29)] was also evident from the spectrum. HMBC correlations were also observed between H-3 and C-23, Me-30 and C-29, C-19 and between H-25 and C-1. This information together with a comparison with the literature (Parvin *et al.*, 2011) allowed the identification of compound **193** as lupeol.

Table 4.7: ^{1}H (600 MHz) and ^{13}C (150 MHz) NMR Data of 193 and 194

Position	**193** (CD_2Cl_2)				**194** (CD_2Cl_2)			
	δ_C	Type	δ_H (mult., *J* in Hz)	HMBC	δ_C	Type	δ_H (mult., *J* in Hz)	HMBC
1	37.6	CH_2	1.59 (m)	C-3, C-25	37.2	CH_2	1.73 (m)	C-3, C-28
2	29.7	CH_2	1.85 (m)	C-4, C-10	29.1	CH_2	1.33 (dd, *J* = 10.35, 5.25)	C-4, C-10
3	78.9	CH	3.12 (d, *J*= 3.21)	C-1, C-5	77.3	CH	4.40 (dt, *J*= 11.38, 6.85, 6.85)	C-1, C-5
4	37.9	C	-	-	36.6	CH_2	1.08 (m)	
							1.73 (m)	
5	55.2	CH	0.69 (m)	C-1, C-3, C-7	140.8	C	-	-
6	18.2	CH_2	1.49 (m)	C-4, C-8	121.6	CH	5.26 (m)	C-4, C-8
7	34.2	CH_2	1.31 (m)	C-5, C-9, C-15	31.8	CH_2	1.87 (m)	C-5
8	38.7	C	-	-	31.7	CH	1.27 (m)	
9	50.3	CH	1.19 (m)	C-5, C-7, C-12	50.0	CH	0.84 (d, *J*=6.47)	C-12
10	39.9	C	-	-	42.2	C	-	-
11	20.8	CH_2	1.19 (d, *J*=7.3)	C-8, C-10, C-13	21.0	CH_2	133 (dd, *J*=10.3, 5.2)	
			1.35 (m)	C-10, C-13			1.44 (m)	
12	25.0	CH_2	1.61 (m)	C-9, C-18	38.7	CH_2	2.39 (m)	C-9, C-14
							2.06 (m)	C-9, C-14
13	38.6	CH	0.84 (d, *J*=2.0)	C-11	40.3	C	-	-
14	42.9	C	-	-	56.5	CH	0.9 (m)	C-7, C-16
15	27.3	CH_2	1.49 (d, *J*=1.7)	C-8, C-13, C-17	24.2	CH_2	1.12 (m)	
			1.53 (m)	C-8, C-13, C-17			1.18 (dd, *J*=15.8, 9.3)	
16	35.5	CH_2	1.31 (m)	C-14, C-22	28.2	CH_2	1.44 (m)	
			1.42 (m)	C-14, C-22			1.73 (m)	
17	48.2	C	-	-	55.8	CH	0.94 (m)	

Table 4.7 continued

	193 (CD_2Cl_2)				**194** (CD_2Cl_2)			
Position	δ_C	Type	δ_C	Type	δ_C	Type	δ_C	Type
18	47.9	CH	2.3 (m)	C-20, C-29	20.1	CH_3	0.77 (s)	
19	48.0	CH	2.32 (td, *J*=11.1, 11.1, 5.6)	C-29	12.1	CH_3	0.59 s	C-17, C-20
20	150.9	C	-	-	35.8	CH	1.27 (m)	
21	27.9	CH_2	1.54 (m)	C-17	19.5	CH_3	0.84 (d, *J*=6.4)	
22	37.6	CH_2	1.60 (m)		33.7	CH_2	1.34 (m)	
23	27.3	CH_3	0.91 (s)	C-3, C-5	25.8	CH_2	1.87 (m)	
24	14.7	CH_3	0.88 (s)	C-3, C-5	45.5	CH	0.77 (s)	C-22
25	16.0	CH_3	0.72 (s)	C-10	29.6	CH	1.44 (m)	C-23
26	15.9	CH_3	0.96 (s)	C-14	19.3	CH_3	0.73 (s)	
27	15.2	CH_3	0.69 (s)	-	19.0	CH_3	0.77 (s)	
28	17.9	CH_3	0.76 (s)	C-22	23.0	CH_2	1.44 (m)	
29	109.2	CH_2	4.50 d 4.52 d	C-19, C-30 C-19, C-30	12.0	CH_3	0.73 (s)	C-17
30	19.2	CH_3	0.90 s	C-29	-	-	-	-
1'	-		-	-	101.1	CH	4.15 (d, *J*=7.79)	C-3, C-5'
2'			-	-	73.8	CH	2.83 (dt, *J*=8.58, 8.56, 4.65)	C-4'
3'	-		-	-	77.1	CH	3.10 (d, *J*=4.88)	C-5'
4'	-		-	-	70.4	CH	3.01 (m)	C-2', C-6'
5'	-		-	-	77.3	CH	3.01 (m)	C-1'
6'	-		-	-	61.4	CH_2	3.58 (m)	-

4.1.2.2 Daucosterol (194)

Compound **194** was isolated as colorless powder. The NMR data (Table 4.7) of this compound **194** was almost similar to that of **190**, exception with a sugar signals. In the ^{13}C NMR spectrum, the sugar moiety was identified as D-glucopyranose. Moreover, The coupling constant (7.79 Hz) of the anomeric proton at δ_H 4.15 (C-1') signal in the ^{1}H NMR spectrum, was consistent with *β*-glycosidic linkage. The information obtained from the NMR data above and the literature (Khatun *et al.*, 2012) led to identification of compound **194** as daucosterol.

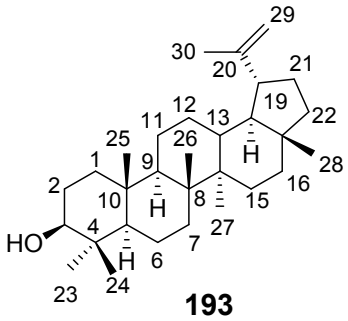

193

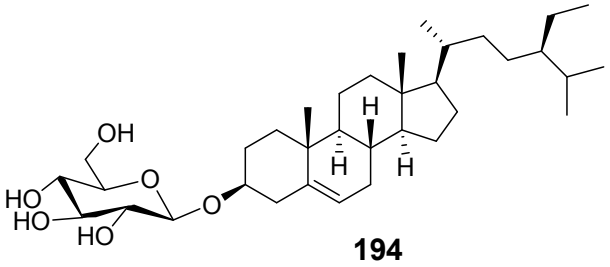

194

4.1.3 Characterization of Compounds Isolated from Stem barks of *Lannea schweinfurthii*

Phytochemical investigation of the stem bark of *Lannea schweinfurthii* afforded seven compounds including an an alkenylphenol (**195**), five alkenylcyclohexenol derivatives (**196-200**) and a flavanol (**201**).

4.1.3.1 3-((*E*)-Nonadec-16'-enyl)phenol (195)

Compound **195** was isolated as a brown paste from the stem bark extract of *Lannea schweinfurthii*. The ^{1}H and ^{13}C NMR data (Table 4.8) is consistent with compound **195** being an alkylphenolic derivative. The ^{1}H NMR signals at δ_H 6.72 (H-2), δ_H 6.80 (H-4), δ_H 7.20 (H-5) and δ_H 6.70 (H-6) indicated the presence of an aromatic ring. This was supported by the ^{13}C NMR spectrum which showed signals at δ_C 155.7 (C-1), δ_C 115.2 (C-2), δ_C 145.0 (C-3), δ_C 120.7 (C-4), δ_C 129.3 (C-5) and δ_C 112.3 (C-6), corresponding to the aromatic ring. A pseudo-triplet signal observed at δ_H 7.20 (J=7.7 Hz) in its ^{1}H NMR spectrum suggested a *meta*-substitution on the aromatic ring. This was confirmed by the presence of other aromatic

proton signals at δ_H 6.80 (H-4) and δ_H 6.70 (C-6). In addition, the signal at δ_H 5.48 (H-16'/H-17'), together with the broad singlet at 1.37 (H-4'-H-13') is consistent with a along alkenyl chain. The ^{13}C NMR signals at δ_C 35.8 (C-1'), δ_C 22.7 (C-2'), δ_C 31.4 (C-3') and δ_C 1.29.7-129-2 (C-4'-13') were assigned to sp^3 carbon atoms of the long alkenyl chain. Comparison of the ^1H and ^{13}C NMR data with those of related compounds having similar long alkenyl chain suggested an *E*-geometry at C-16' (Groweiss et al., 1997; Kapche et al., 2007; Okoth and Koorbanally, 2015). The placement of the double bond within the side chain was determined from the HMBC correlation between the terminal methyl protons H_3-19 and C-17, H-17 and C-19 and H-14 and C-17. The above information together with comparison of the data with literature (Queiroz *et al.*, 2003) allowed the identification of compound **195** as 3-((*E*)-nonadec-16'-enyl)phenol (trivial name cardonol 7). Althought this compound has been reported previously from the genus *Lannea*, this is the first time that this compound is reported from *Lannea schweinfurthii.*

Table 4.8: ^1H (600 MHz) and ^{13}C (150 MHz) NMR Data of 195 (CD_2Cl_2)

Position	δ_C	Type	δ_H (mult., *J* in Hz)	HMBC
1	155.7	C	-	-
2	115.2	CH	6.72 (br s)	C-1', C-6
3	145.0	C	-	-
4	120.7	CH	6.80 (br s)	C-1', C-6
5	129.3	CH	7.20 (dd, *J*= 7.7, 7.7)	C-1, C-3
6	112.3	CH	6.70 (br s)	-
1'	35.8	CH_2	1.61 (m, H1'a/1'b)	C-2, C-3, C-4, C-3'
2'	22.7	CH_2	2.07 (m)	C-4'/13'
3'	31.4	CH_2	2.19 (br s)	C-1', C-4'/C-13'
4'-13'	29.7-29.2	CH_2- CH_2	1.37 (br s)	C-3', C-4', C-13'
14'	31.9	CH_2	1.64 (2H, dd, *J*=4.7, 4.7)	C-4'/13', C-16'
15'	25.6	CH_2	1.64 m	C-14', C-17'
16'	129.4	CH	5.48 (m)	C-14', C-18'
17'	131.8	CH	5.48 (m)	C-15', C-19'
18'	32.6	CH_2	1.64 (m)	C-16', C-19'
19'	13.9	CH_3	1.04 (m)	C-17'

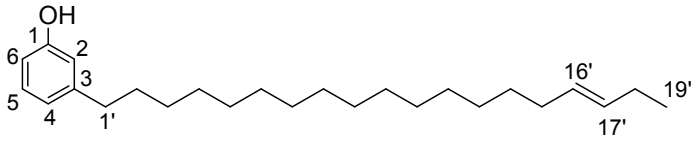

195

4.1.3.2 1-((*E*)-Heptadec-14'-enyl)cyclohex-4-en-1,3-diol (196)

Compound **196** was isolated as a colourless paste from the stem bark of *Lannea schweinfurthii.* The ^{1}H [δ_H 5.71 (H-4), 5.79 (H-5) 4.46 (H-3), 5.47 (H-14'/15')] and ^{13}C [δ_C 65.8 (C-3), δ_C125.6 (C-4), δ_C 130.7 (C-5), δ_C 129.4 (C-14'), δ_C 131.7 (C-15')] NMR data (Table 4.9) were consistent with an alkenyl cyclohexenone derivative. Comparison of the NMR data with literature revealed that it is similar with what has been reported for 1-[14'(*E*)-heptadecenyl]-cyclohex-4-en-1,3-diol (Okoth and Koorbanally, 2015), a compound identified within a mixture from *Lannea schimperi* and was claimed to be one of the precursor of cardonol by the same authors. The HMBC correlation between H-3 to C-1 and C-5 and H_2-1' to C-2 and C-6 supported the placement of the long alkenyl chain at C-1. The position of the double bond was evident from the HMBC correlation between H-15' and C-13', H-15' and C-17', and H-14' and C-12'. The ^{3}J values (7.7 Hz) observed between H-2 and H-3 which revealed an α-orientation of H-3. Furthermore, the NOESY correlation observed between H_2-1' and Hα-2 suggested that OH-1 is β-oriented. A close analyses of the NMR data along with comparison with data previously reported (Okoth and Koorbanally, 2015) guuided the identification of compound **284** as 1-((*E*)-heptadec-14'-enyl)cyclohex-4-en-1,3-diol. This is the first reported of compound **196** from *L. schweinfurthii*.

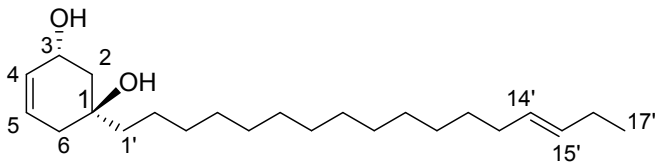

196

Table 4.9: ^{1}H (600 MHz) and ^{13}C (150 MHz) NMR Data of 196 in CD_2Cl_2

Position	δ_C	Type	δ_H (mult., *J* in Hz)	HMBC
1	72.1	C	-	-
2	43.4	CH_2	2.10 (m)	C-4, C-6, C-1'
			1.52 (dd, *J*=9.0, 7.7)	C-4, C-6, C-1'
3	65.8	CH	4.46 (ddd, *J*=7.9, 4.4, 2.2)	C-1, C-5
4	125.6	CH	5.71 (m)	C-2, C-3, C-6
5	130.7	CH	5.78 (ddd, 10.3, 2.9, 1.5)	C-1, C-3
6	42.9	CH_2	1.44 (dd, *J*=12.7, 9. 7)	C-1', C-2, C-4
1'	37.4	CH_2	2.02 (m)	C-2, C-6, C-3'
			2.19 (q, *J*=2.7, 2.7, 2.7)	C-2, C-6, C-3'
2'	22.9	CH_2	1.44 (m)	C-3'
3'-11'	29.7-29.1	CH_2- CH_2	1.31 (br s)	C-3'-C-11'
12'	32.5	CH_2	2.02 (m)	C-14'
13'	22.7	CH_2	2.02 (m)	11', C-15'
14'	129.4	CH	5.47 (m)	C-16'
15'	131.7	CH	5.47 (m)	C-13'
16'	31.9	CH_2	2.02 (m)	C-14', C-17'
17'	13.9	CH_3	1.00 (t, *J*=7.4)	C-15', C-16'

4.1.3.3. 1-[(*E*)-Tridecadec-10'-enyl]cyclohex-4-en-1,3-diol (197)

Compound **197** was obtained as a colourless paste from the stem barks of *Lannea schweinfurthii*. The NMR data (Table 4.10) suggested that **197** has the molecular formula of $C_{19}H_{34}O_2$. The NMR data for compound **197** is similar to what has been reported for an alkenyl cyclohexanol derivative (Okoth and Koorbanally, 2015), the only difference being that **197** has two less methylene groups. The remaining data of the compound including the relative configuration at C-1 and C-3 was comparable to the literature data (Okoth and Koorbanally, 2015). The coupling constant of 10.1 Hz between H-2a and H-3 revealed that H-3 is axial and hence OH-3 is α-oriented. Moreover, the ^{1}H and ^{13}C NMR data (Table 3) of **197** are similar to those of **196** described above. However, compound **197** has less carbons, having nineteen carbons in total as observed on the ^{13}C NMR spectral data. The presence of two double bonds at C4 (δ_C 124.5) and C10' (δ_C 129.2), and two oxygenated carbons (δ_H 64.9, C-1 and δ_H 70.9, C-3) was revealed from ^{13}C NMR spectrum. The HMBC correlation of the terminal methyl proton with the olefinic carbon (C-11, δ_C 131.8) suggested the double bond of the alkenyl chain to be two bonds away from the terminal methyl group (Me-13).

Comparison of the ^{1}H and ^{13}C NMR data with those of related compounds having similar long alkenyl chain suggested an *E*-geometry at C-10' (Groweiss et al., 1997; Kapche et al., 2007; Okoth and Koorbanally, 2015). Therefore, the structure of **197** was determined as 1-[(E)-tridecadec-10'-enyl]cyclohex-4-en-1,3-diol.

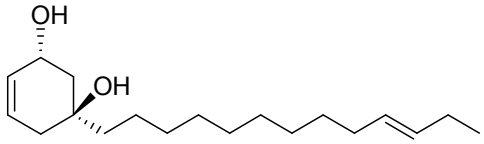

197

Table 4.10: ^{1}H (600 MHz) and ^{13}C (150 MHz) NMR Data of 197 in CD_2Cl_2

Position	δ_C	Type	δ_H (mult., *J* in Hz)	HMBC
1	70.9	C	-	-
2	43.1	CH_2	1.49 (d, 2.1)	C-4, C-6, C-1'
3	64.9	CH	4.42 (ddd, 5.9, 3.2, 2.9)	C-2, C-3, C-5
4	124.5	CH	5.56 (ddd, 10.1, 4.5, 3.5)	C-4
5	131.8	CH_2	5.71 (m)	C-1, C-3
6	37.4	CH	2.01 (d, *J*=2.01)	C-2, C-4
			2.08 (dd, *J*=2.41, 4.47)	C-2, C-4
1'	43.8	CH_2	1.49 (d, 2.1)	C-2, C-6, C-3'
2'	22.9	CH_2	1.49 (d, 2.1)	C-3'-C-9'
3'	30.2	CH_2	1.33 (d, 8.1)	C-3, C-4'
4'-6'	29.6-29.2	CH_2- CH_2	1.32 (br s)	C-4'-C-9'
7'	22.5	CH_2	1.49 (m)	-
8'	31.8	CH_2	1.33 (d, 8.1)	-
9'	32.4	CH_2	2.01 (m)	C-11'
10'-11'	129.2-131.8	CH=CH	5.44 (m)	C-15', C-16'
12'	25.4	CH_2	1.40 (dd, *J*= 2.8, 2.1)	C-9'
13'	13.5	CH_3	0.97 (t)	C-11', C-12'

4.1.3.4 1-((*E*)-Pentadec-12'-enyl)cyclohex-4-en-1,3-diol (198)

Compound **198** ($C_{21}H_{38}O_2$) was isolated as a colourless paste from the stem barks extract of *Lannea scweinfurthii.* The ^{1}H and ^{13}C NMR spectral data (Table 4.11) were consistent with this compound having an alkenyl cyclohexanol skeleton (Okoth and Koorbanally, 2015). The ^{13}C NMR spectrum displayed 21 carbons including two oxygenated carbons C-3 (δ_C 64.7)

and C-1 (δ_C 71.1). The ^{1}H NMR data (Table 4.11) revealed a triplet at δ_H 1.00 which was assigned to a terminal methyl group; two overlapping olefinic proton signals centred at δ_H 5.46 corresponding to H-12' and H-13', and the typical saturated part of the long chain alkenyl group signal (δ_H 1.36, br s). The placement of the double bond within the side chain was determined from the HMBC correlation between the terminal methyl protons (Me-15) and C-13. The large coupling constant between H-12 and H-13 revealed a *trans*-conformation of the double bond. The large ^3J coupling constant 14.2 Hz between H-2 abd H-3 revealed that H-3 is *pseudo*-axial and hence OH-3 is α-oriented. The relative configuration at C-3 was deduced from NOE effect of H_2-1' to H-3 (Okoth and Koorbanally, 2015). The ^{1}H and ^{13}C NMR data of this compound suggested an *E*-geometry at C-12' (Groweiss *et al*., 1997; Kapche *et al*., 2007; Okoth and Koorbanally, 2015). On the basis of the above information, compound **198** was characterised as 1-((*E*)-pentadec-12'-enyl)cyclohex-4-ene-1,3-diol.

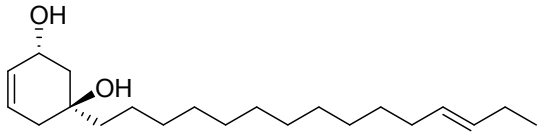

198

Table 4.11: ^{1}H (600 MHz) and ^{13}C (150 MHz) NMR Data of 198 in CD_2Cl_2

Position	δ_C	Type	δ_H (mult., *J* in Hz)	HMBC
1	71.1	C	-	-
2	40.1	CH_2	1.99 (m) 1.78 (dd, *J*= 14.2, 4.4)	C-1, C-3, C-4. C-6
3	64.7	CH	4.21 (brs)	C-1, C-5
4	126.7	CH	5.81 (dt)	C-1, C-3, C-4
5	128.5	CH_2	5.95 (m)	C-2, C-4
6	37.9	CH	2.17 (m)	C-2, C-6
1'	43.1	CH_2	1.52 (m)	C-2, C-3, C-4
2'	22.9	CH_2	1.41 (m)	C-4'
3’	30.1	CH_2	1.32 (m)	C-4'-C-5'
4’-10’	29.9-29.2	CH_2	1.32 (m)	C-4'-C-10'
11’	32.5	CH_2	1.99 (m)	C-14', C-15', C-9'
12’-13’	129.3, 131.7	CH_2, CH_2	5.46 (m)	C-10', C-14'
14’	25.6	CH_2	1.32 (m)	C-12'
15’	13.8	CH_3	1.00 (m)	C-14'

4.1.3.5 1-[Nonadeca-14'*E*,16'*E*-dienyl]cyclohex-4-en-1,3-diol (199)

Compound **199** was isolated as a pale yellow residue from the stem barks of *Lannea schweinfurthii*. The UV spectrum showed absorption band at λ_{max} = 250 nm. EIMS analysis showed a molecular ion peak at *m/z* 348 corresponding to the formula $C_{23}H_{40}O_2$. The ^1H and ^{13}C NMR data (Table 4.12) are similar to those of **196**. However, **199** has one more double bond and two more carbons as compared to **196**. A close analysis of the ^1H NMR data (Table 4.12) revealed the presence of alkenyl moiety (δ_H 1.32; H-4-10), an olefinic proton on a cyclohexene ring (δ_H 5.81, 5.95) connected to C-4 and C-5 (HSQC) and two additional pairs of olefinic protons (δ_H 5.73, 6.36) corresponding to C-14/C-15 and C-16/C-17. The assignment of the above chemical shift is further supported by the HMBC correlation of H-14 (δ_H 5.73) with C-16 (δc 128.6) and H-17 (δ_H 6.36) with C-15 (δc 130.1). The ^{13}C NMR spectrum further revealed the presence of six olefinic carbons, C-4 (δ_C 126.7), C-5 (δ_C 128.5), C-14' (δ_C 124.7), C-15' (δ_C 130.1), C-16' (δ_C 128.6), C-17' (δ_C 136.0). While H-1 did not show any NOESY correlations, the NOESY correlation of H_2-5 was comparable with that of the reported compounds which suggested that OH-1 is *β*-oriented (Okoth, 2014). Therefore, compound **199** was identified as 1-[nonadeca-14'*E*,16'*E*-dienyl]cyclohex-4-en-1,3-diol. This compound was previously reported from *L. schweinfurthii* (Okoth, 2014). However the *E,E*-congiruration of the double bonds was revised based on the NMR data which suggested that the double bonds could not have a *cis*-configuration in which case even the ^{13}C NMR chemical shift of the olefenic carbon atomes C-14' and C-15' could have been almost the same *vis* δ_C 129.7 (C-14') and δ_C 129.8 (C-15').

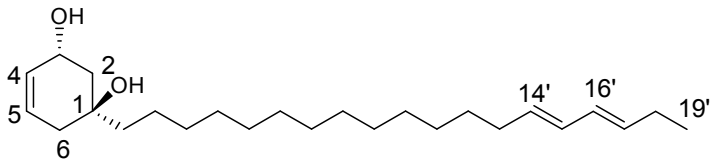

199

Table 4.12: ^{1}H (600 MHz) and ^{13}C (150 MHz) Data of 199 in CD_2Cl_2

Position	δ_C	Type	δ_H (mult., *J* in Hz)	HMBC
1	71.1	C	-	-
2	40.1	CH_2	1.78 (dd, *J*=14.2, 4.8)	C-1, C-3, C-1'
			1.54 (m)	C-1, C-3, C-1', C-14', C-15'
3	64.7	CH	4.21 (s)	C-3
4	126.7	CH	5.95 (m)	C-1, C-3, C-4, C-14'-C-15'
5	128.5	CH	5.81 (dd, 9.9, 3.7)	C-1, C-5
6	38.0	CH_2	2.17 (m)	C-14'-C15'
1'	43.1	CH_2	1.52 (m)	C-3, C-2', C-4
2'	22.9	CH_2	1.41 (m)	C-3'-C-11'
3'-11'	29.7-29.1	CH_2- CH_2	1.41 (m)	C-3'-C-11'
12'	30.1	CH_2	1.41 (d, 7.2)	C-3'-C-11'
13'	27.6	CH	2.17 (m)	C-11', C-15'
14'-15'	124.7, 130.1	CH_2, CH_2	5.73 (dd, 7.5, 4.2)	C-13', C-16'
16'-17'	128.6, 136.0	CH	6.36 (m)	C-15', C-19'
18'	25.8	CH_2	2.7 (m)	C-16'
19'	13.5	CH_3	1.05 (t, *J*=7.5)	C-17'

4.1.3.6 1-[(16'*E*)-Nonadecenyl]cyclohex-4-en-1,3-diol (200)

Compound **200** (**$C_{25}H_{46}O_2$**) was isolated as colorless paste. The ^{1}H and ^{13}C NMR spectral data (Table 4.13) revealed 25 carbons and two hydroxy groups (HO-1, HO-3). The presence of four sp2 hybridyzed carbon atoms in the ^{13}C NMR spectrum (Table 4.13) is consistent with an alkenylcyclohexen-diol skeleton as in other compounds of the genus *Lannea* (Okoth and Koorbanally, 2015). The HMBC correlation of the terminal methyl protons, CH_3-19, with the olefinic carbons (C-16, C-17) indicated that the double bond on the long chain was two bonds away from the terminal carbon. The close ^{13}C NMR chemical shift values (δ_C 129.4 and 131.8) for the olefinic carbons C-16′ and C-17' of **200** is consistent with the assignment of *E*-configuration to the double bond at C-16′ of the alkenyl chain *(David et al., 1998; Queiroz et al.,* 2003, Kapche *et al.*, 2007; Okoth and Koorbanally, 2015; Okoth *et al.*, 2016); in *E*-configured olefinic carbons (C-14′ and C-15′), the ^{13}C NMR resonances have substantially distinct values (Queiroz *et al.*, 2003, Correia *et al.*, 2006; Okoth and Koorbanally, 2015). The relative configuration at C-1 and C-3 was determined based on NOE

effect of H_2-1' with OH-3 on one hand and a large coupling constant (9.0 Hz) between H-3 and H-2β indicating an α-orientation of OH-3. Comparison of the NMR data with that of the literature (Okoth and Koorbanally, 2015) revealed compound **200** is 1-[(16'*E*)-nonadecenyl]cyclohex-4-en-1,3-diol.

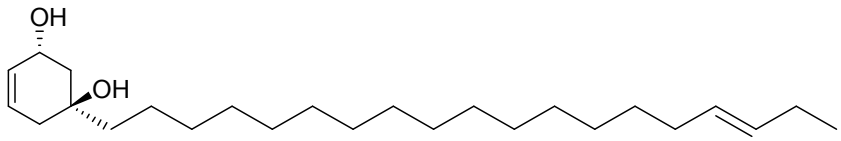

200

Table 4.13: ^{1}H (600 MHz) and ^{13}C NMR (150 MHz) Data of 200 in CD_2Cl_2

Position	δ_C	Type	δ_H (mult., *J* in Hz)	HMBC
1	72.2	C	/	/
2	43.5	CH_2	1.52 (dd, *J*=9.0, 7.7 Hz)	C-1', C-4, C-6
			2.10 (m)	C-4, C-6
3	65.8	CH	4.46 (m)	C-3, C-5
4	125.5	CH	5.71 (dd, *J*=10.1, 4.7 Hz)	C-1, C-3
5	130.7	CH	5.79 (ddd, *J*=10.1, 3.3, 1.4 Hz)	C-2, C-4
6	37.4	CH_2	2.02 (m)	C-1', C-2, C-6
			2.21 (dd, *J*=18.2, 2.7 Hz)	C-1', C-2, C-6
1'	42.9	CH_2	1.44 (ddd, *J*=13.6, 8.7, 4.9 Hz)	C-2, C-4, C-3'
			1.52 (dd, *J*= 9.0, 7.7 Hz)	C-2, C-4,
2'	22.7	CH_2	1.44 (m)	C-3
3'	32.5	CH_2	2.02 (m)	C-4'-14'
4'-14'	22.9-31.9	11xCH_2	1.32 (br s)	C-4'-C-14'
15'	22.9	CH_2	1.44 (m)	C-4'-14', C-17'
16'	129.4	CH	/	/
17'	131.8	CH	/	/
18'	25.6	CH_2	2.02 (m)	C-16'
19'	13.9	CH_3	1.0 (t, *J*=7.4 Hz)	C-17'

4.1.3.7 Catechin (201)

Compound **201** was isolated as a pale yellow solid from the stem barks of *Lannea schweinfurthii.* Typical signals of flavanol derivatives were observed at δ_H 4.91 (H-2), 4.23 (H-3), δ_H 2.88 (Ha-4), 2.27 (Hb-4). In ring B, the signals at δ_H 6.87 (H-2'), δ_H 7.08 (H-5') and

6.85 (H-6'), in the ^{1}H NMR spectral data (Table 4.14) are indicative of 3', 4'-oxygenation. This was supported by the signals at δ_C 78.5 (C-2), δ_C 66.0 (C-3), δ_C 28.1 (C-4), δ_C 156.6 (C-5), δ_C 156.7 (C-7), δ_C 144.4 (C-3') and δ_C 144.3 (C-4') in the ^{13}C NMR spectrum (Table 4.14). Based on comparison with previously reported compound (Qi *et al.*, 2003), the two aromatic protons on ring at δ_H 6.05 (H-6) and 5.95 (H-8) and the corresponding carbon signals at δ_C 95.2 (C-6) and δ_C 94.8 (C-8) were assigned (Table 4.14), and hence this compound was identified as catechin. The large coupling constant (*J*=123 Hz) between H-2 and H-3 is in agreement with trans-configuration of H-2 and H-3. The suggested structure was further supported by the HMBC correlation between H-2 with C-2', C-6' and C-4. The HMBC correlation of H-3 with C-1' and C-5 was in agreement with the proposed structure. The carbon signals at δ_C 156.6 and 156.7 were assigned to C-5 and C-7, respectively based on comparison with literature (Qi *et al.*, 2003). All the proton and carbon signals were assigned based on the HMBC and HSQC spectra. Therefore, compound **201** was identified as catechin.

Table 4.14: ^{1}H (600 MHz) and ^{13}C NMR (150 MHz) Data of 201 in CD_2Cl_2

Position	δ_C	Type	δ_H (mult., *J* in Hz)	HMBC
2	78.5	CH	4.91 (d, *J*= 12.3)	C-4, C-9, C-2'
3	66.0	CH	4.23 (ddd, *J*=11. 4, 8.2, 4.3)	C-10, C-2'
4	28.1	CH_2	2.88 (dd, *J*=16.5, 4.6)	C-2, C-5, C-9
			2.27 (dd, *J*=16.6, 3.2)	C-2, C-5, C-9
5	156.6	C	-	-
6	95.2	C	-	-
7	156.7	CH	6.05 (d, *J*=2.3)	C-8, C-10
8	94.8	C	-	-
9	156.2	CH	5.95 (d, *J*=2.3)	C-6. C-10
10	98.9	C	-	-
1'	131.3	C	-	-
2'	114.3	CH	6.87 (dd, *J*=2.0, 0.5)	C-2, C-4'
3'	144.4	C	-	-
4'	144.3	C	-	-
5'	114.6	CH	7.08 (d, *J*=7.6)	C-1', C-3'
6'	118.6	CH	6.85 (d, *J*=8.0)	C-2, C-4'

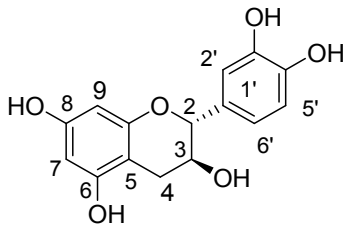

201

4.1.4 Characterization of Compounds Isolated from Roots of *Lannea schweinfurthii*

The roots extract of *Lannea schweinfurthii* yielded three compounds (**202-204**) and four other compounds (**188**, **189**, **195**, **198**) previously isolated from the roots of *Lannea rivae* (**188**, **189**) and stem bark of *Lannea schweinfurthii* (**195**, **198**).

4.1.4.1 4,4'-Dihydroxy-3-methoxy-3'-*O*-glucosyl ellagic Acid (202)

The ^{1}H and ^{13}C NMR spectral data (Table 4.15) of compound **202** is in agreement with a previously reported (Simoes, 2009) data for **202**. The presence of two carbonyl groups at C-7 (δ_C 159.5) and C-7' (δ_C 158.9) was evident from the ^{13}C NMR data (Table 4.15). The linkage of the glucose moiety at C-3' (δ_C 129.9) was established from the HMBC correlation of the anomeric proton H-1" (δ_H 4.9) with C-3' (δ_C 129.9). In its ^{1}H NMR spectrum, a signal at δ_H 3.80 corresponds to a methoxy group and was placed at C-3 based on the HMBC correlation of the methoxy protons with C-3 (δ_C 130.2). Therefore, compound **202** was identified as 4,4'-diydroxy-3-methoxy-3'-*O*-glucosylellagic acid (Simoes, 2009).

4.1.4.2. 4,4'-Dihydroxy-3-methoxy-3'-*O*-[rhamnopyranosyl-(1→2)] rhamnopyranoside ellagic Acid (203)

Compound **203** has similar ^{1}H and ^{13}C NMR spectral data (Table 4.15) to that of **202**, the only difference was that it has two sugar moieties. The ^{1}H and ^{13}C NMR spectral data are in agreement with the proposed structure for **203**. The presence of two carbonyl groups C-7 (δ_C 159.2) and C-7' (δ_C 159.2) was again evident from the ^{13}C NMR data (Table 4.15). The sugar moiety which apparently is rhamnopyranosyl-(1→2)] rhamnopyranoside was found to be linked to C-3 (δ_C 143.2) due to the HMBC correlation of an anomeric proton (δ_H 4.96) with C-3' (δ_C 158.4). In its ^{1}H NMR spectrum, a signal at δ_H 3.80 corresponds to a methoxy group (δ_H 3.80) and was placed at C-3' based on the HMBC correlation of the methoxy protons with

C-3'. Therefore, compound **203** was identified as 4,4'-dihydroxy-3-methoxy-3'-*O*-[rhamnopyranosyl-(1→2)] rhamnopyranoside ellagic acid (Simoes, 2009).

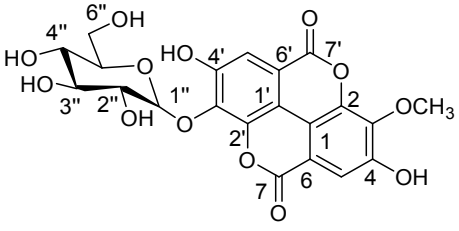

202

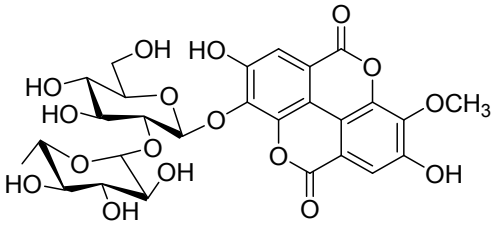

203

Table 4.15: ^{1}H (600 MHz) and ^{13}C (150 MHz) NMR Data of 202 and 203

Position	**202** (CD_2Cl_2)			**203** (CD_2Cl_2)		
	δ_C	δ_H (mult., *J* in Hz)	HMBC	δ_C	δ_H (mult., *J* in Hz)	HMBC
1	108.2	-	-	107.2	-	-
2	139.7	-	-	130.2	-	-
3	130.2	-	-	143.2	-	-
4	129.5	-	-	139.7	-	-
5	127.8	7.54 (m)	C-3, C-7	106.7	6.76 (m)	C-1, C-3
6	114.1	-	-	128.5	-	-
7	159.5	-	-	159.2	-	-
1'	103.2	-	-	126	-	-
2'	139.5	-	-	129.2	-	-
3'	129.9	-	-	158.4	-	-
4'	128.5	-	-	144.1	-	-
5'	126.2	7.25 (m)	C-3', C-7'	127.8	7.52 (d, *J*=8.75)	C-1, C-3
6'	113.6	-	-	113.6	-	-
7’	158.9	-	-	159.5	-	-
1"	100.9	4.96 (m)	C-3", C-3'	100.9	4.42, (br s)	C-3'
2"	77.0	3.68 (m)	C-4"	76.9	3.60 (d, *J*=8.7)	C-4"
3"	73.4	3.46 (m)	C-1", C-5"	68.3	3.70 (m)	C-1", C-5"
4"	72.5	3.70 (m)	C-2", C-6"	73.0	3.46 (m)	C-2", C-6"
5"	68.3	3.70 (m)	C-1", C-3"	70.2	3.46 1H (m)	C-1", C-3"
6"	17.3	1.23 (m)	C-4"	66.8	4.05 (d, *J*=3.7)	C-4"
1"'	-	-	-	101.1	4.96 (d, *J*=7.7)	C-1"
2"'	-	-	-	73.8	3.60 (d)	C-4"'
3"'	-	-	-	75.7	3.70 (m)	C-1"', C-5"'
4"'	-	-	-	70.9	3.95 (m)	C-2"', C-6"'
5"'	-	-		71.5	3.76 (m)	C-1"', C-3"'
6"'	-	-	-	17.3	1.22 (d, *J*=6.2)	C-4"'
OCH_3	54.7	3.80	C-3	54.8	3.80 (s)	C-3

4.1.4.3 3-((12'*Z*,14'*E*)-Heptadeca-dienyl)phenol (204)

Compound **204** was isolated as a brown paste from the roots of *Lannea schweinfurthii*. The ^{1}H and ^{13}C NMR data (Table 4.16) is consistent with **204** being an alkenyl phenol. The pseudo-triplet signal at δ_H 7.09 (H-5) indicated *meta*-bi-substituted aromatic ring. The aromatic ring was confirmed by ^{13}C NMR signals at δ_C 157.3 (C-1), δ_C 144.2 (C-3), δ_C 124.8 (C-5). In addition, the broad signal centred at δ_H 1.30 (H-4'/H-10'), together with the signals at δ_H 1.61 (H-1') and 2.12 (H-2'), characterised a long alkenyl chain having conjugated double bonds at C-12' (δ_C 128.8) and C-14' (δ_C 1.29.6). The placement of the double bond within the side chain was established by the HMBC correlation between the terminal methyl protons H-17' and C-15', H-15' and C-17' and H-12' and C-14'. The NMR data suggested that the double bonds of the alkenyl chain (at C-12' and C-14') could not have a *cis*-configuration in which case even the ^{13}C NMR chemical shift of the olefenic carbon atomes C-12' and C-13', C-14' and C-15' could have been almost the same *vis* δ_C 129.7. This information together with comparison of the data with literature report (Queiroz *et al.*, 2003) revealed that **204** was 3-((12'*Z*,14'*E*)-heptadeca-dienyl)phenol. This compound was isolated previously reported from *L. schweinfurthii* (Okoth, 2014). However the *E,E*-congiruration of the double bonds was revised based on the NMR data.

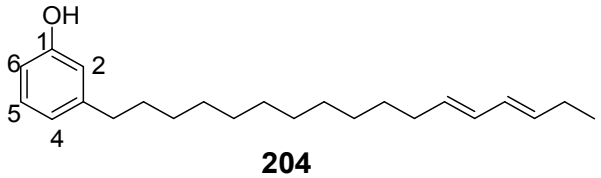

204

Table 4.16: ^{1}H NMR (600 MHz) and ^{13}C (150 MHz) NMR Data of 204 in Acetone-d_6

Position	δ_C	Type	δ_H (mult., *J* in Hz)	HMBC
1	157.3	C	-	-
2	115.2	CH	6.65 (m)	C-1', C-6
3	144.2	C	-	-
4	119.5	CH	6.70 (dd, *J*=2.2, 2.2)	C-1', C-6
5	124.8	CH	7.09 (dd, *J*=7.7, 7.7)	C-1, C-3
6	112.5	CH	6.36 (m)	-
1'	35.6	CH_2	1.61 (m, H1'a/1'b)	C-2, C-3, C-4, C-3'
2'	25.5	CH_2	2.12 (m)	C-3', C-4'/10'
3'	32.3	CH_2	2.54 (m)	C-1', C-4'/C-10'
4'-10'	29.0-29.6	CH_2	1.37 (br s)	C-4'/C-10'
11'	27.3	CH_2	1.30 (m)	C-4'/C-10', C-C-13
12'	128.8	CH	5. 35 (m)	C-4'/C-10', C-14
13'	129.6	CH	5.44 (m)	C-11', C-15'
14'	129.6	CH	5.96 (dd, *J*=10.1, 10.1)	12', C-16'
15'	135.7	CH	5.70 (m)	C-13', C-17'
16'	31.3	CH_2	1.30 (br s)	C-14'
17'	13.1	CH_3	1.0 (t, *J*=7.4)	C-15'

Taraxerol, taraxerone, 3-((*E*)-nonadec-16'-enyl)phenol and 1-((*E*)-pentadec-12'-enyl)cyclohex-4-ene-1,3-diol were also isolated from this part.

4.1.5 Summary of Compounds Isolated from *Lannea* Species

Lannea rivae afforded ten compounds (two cyclohexanones, five triterpenes, two flavanes and an ellagic acid derivative) of which two knew alkylcyclohexanones (**186** and **187**). Although most of the isolated compounds from this plant are known, some of the compounds showed good biological activity.

Phytochemical study carried out on *Lannea schweinfurthii* resulted in the isolation of nine compounds including an alkylphenol, five cyclohexanols, a flavan-3-ol and two ellagic acid derivatives.

4.2 Biological Activity of the Isolated Compounds from *Lannea* Species

Some of the isolated compounds and crude extracts of *Lannea rivae* and *Lannea schweinfurthii* were tested for their antimicrobial, cytotoxicity and antiinflammatory activity.

4.2.1 Antimicrobial Activity of *Lannea* species

The anti-microbial activity assessed using microbroth kinetic method (Table 4.17A). Only some of the compounds isolated from *Lannea rivae* showed moderate activity against *E. coli*: These are (4*R*,6*R*)-dihydroxy-6-(14'-(*Z*)-nonadecenyl)-2-cyclohexenone (**186**), taraxerol (**188**), taraxerone (**189**), β-sitosterol (**190**) and lupeol (**193**). However, these compounds did not exhibit significant activity against *S. aureus.* Only (2*S**,4*R**,5*S**)-2,4,5-trihydroxy-2-((*Z*)-nonadec-14'-en-1-yl)cyclohexanone (**187**) and *β*-sitosterol (**190**) showed activity against *S. aureus* (Table 30A). Compounds isolated from *L. schweinfurthii* were found to be inactive.

When using the disc diffusion assy (Table 4.17B), epicatechin gallate (**191**) showed strong anti-microbial activity against *Staphylococcus. aureus* exhibiting a zone of inhibition (20 mm, MIC=0.63 μg/mL) comparable with gentamicin (20 mm); however, it was inactive against other bacteria strains and fungi. This is in agreements with the literature reports (Gibbons *et al.*, 2004; Park *et al.*, 2004; Sakanaka *et al.*, 2000). The new compound, **186**, displayed weak activity against *S. aureus* and was inactive against other selected bacteria strains and fungi (Table 4.17B).

Table 4.17: Antimicrobial Assay of *Lannea* Species

A: **Microbroth kinetic system**

Bacterial strains	***E. Coli***			***S. aureus***		
Concentration (µg/ml)	**160**	**80**	**40**	**160**	**80**	**40**
Samples	**% Inhibition**			**% Inhibition**		
186	57	59	26	ne	ne	ne
187	na	ne	ne	na	44	42
188	33	33	37	ne	ne	ne
189	34	30	28	ne	ne	ne
190	52	54	61	na	29	14
193	46	32	29	ne	ne	ne
Gentamicin	62	53	50	96	97	97
Erythromycin	41	7	ne	98	98	98

B. Agar diffusion assay

Samples	**Anti bacterial assay**		**Anti fungal assay**						
	S. a	*E. c*	*M. g*	*T. m*	*C. p*	*C. a*	*A. f*	*A. n*	*C. n*
186	9	0	0	na	na	0	na	na	na
191	20 (0.63µg/mL)*	0	0	na	na	0	na	na	na
LRR	0	0	0	na	na	0	na	na	na
LSR	0	6	0	0	na	na	0	0	0
Gentamycin	20	13	-	-	-	-	-	-	-
Nystatin	-	-	13	10	16	13	15	13	18

***Key**:* *MIC value for compound **192**.
S. a = Staphylococcus aureus (ATCC 25923), *E. c = Escherichia. coli* (ATCC 25922), *M, g = Microsporum gypseum, T. m = Trichophyton mentagrophytes* (clinical isolates), *C. p = Candida parapsilosis* (ATCC 22019), *C. a = Candida albicans* (ATCC 90018), *A. f = Aspergilus flavus, A. n = Aspergilus niger* (environmental), *C. n = Cryptococcus neoformans* (clinical), na = not assessed, ne = not effective, LRR=*Lannea rivae* roots extract, LSR=*Lannea schweinfurthii* roots extract

4.2.2 Cytotoxicity of *Lannea* species

Compound **186**, Taraxerone (**189**), *β*-sitosterol (**190**), epicatechin gallate (**191**), 3-[16'(*E*) nonadecenyl] phenol (**195**), *Lannea rivae* (LRR) and *Lannea schweinfurthii* (LSR) crude

extracts were tested against DU-145 prostate cancer and Vero cell lines. Epicatechin gallate (**191**) and *β*-sitosterol (**190**) were not cytotoxic against DU-145 prostate and Vero kidney epithelial cancer cell lines (Table 4.18). Compound **186** was strongly cytotoxic against DU-145 prostate cancer cell lines with a CC_{50}value of 0.55 ± 0.08µg/mL, followed by *Lannea rivae* crude root extract (CC_{50} = 5.24 ± 0.12 µg/mL) and taraxerone (**189**, CC_{50} = 11.00 ± 0.07µg/mL) respectively. *Lannea rivae* crude extract (LRR) was found to be the most cytotoxic (CC_{50} = 5.20 ± 0.01 µg/mL) against Vero cell lines (Table 4.18) followed by *Lannea schweinfurthii* crude extracts (CC_{50}=7.36 ± 0.03 µg/mL). Among the pure compounds tested, only 3-[16'(*E*) nonadecenyl] phenol (**195**) showed significant cytotoxicity exhibiting a CC_{50} value of 16.14 ± 0.01 µg/mL (Table 4.18). The high cytotoxicity observed for the crude extracts of both plants against Vero cell lines suggests that the plant may have constituents which have strong cytotoxicity.

Table 4.18: Cytotoxicity of *Lannea* Species Against Mammalian Cell Lines

Sample	CC_{50} (µg/mL)	
	Vero cell lines	**DU-145 cell lines**
LRR[a] extract	5.20 ± 0.01	5.24 ± 0.12
LSR[b] extract	7.36 ± 0.03	74.00 ± 0.04
186	>100	0.55 ± 0.08
189	>100	11.00 ± 0.07
190	>100	>100
191	>100	>100
195	16.14 ± 0.01	49.76 ± 0.10

[a] LRR = *Lannea rivae* root; [b] LSR = *Lannea schweinfurthii* root

4.2.3 Anti-inflammatory Activity of *Lannea* Species

(4*R*,6*R*)-Dihydroxy-6-(14'-(*Z*)-nonadecenyl)-2-cyclohexenone (**186**), epicatechin gallate (**191**) and the crude extract of *Lannea rivae* (LRR) and *Lannea schweinfurthii* (LSR) were evaluated for their anti-inflammatory activity using carrageenan-induced rat paw edema method at a concentration of 200 mg/kg using indomethacin (10 mg/kg) as a standard anti-inflammatory drug.

As shown in Table 4.19, the LSR crude extracts and compound **191** were the most active at 60 min post carrageenan administration. However, at 180 min after carrageenan injection to

the rats, compound **186** was the most active, showing the smallest increase in rat paw volume at this time compared to the other test substances. Throughout the experiment, the rat group treated with the standard drug expectedly showed the most reduced inflammation. This was followed by compound **186** and LSR crude extract. In contrast epicatechin gallate (**191**) and LRR crude extract were moderately active against the carrageenan-induced inflammation.

Table 4.19: Anti-inflammatory Activity – inhibition of carrageenan-induced paw oedema of crude extracts and compounds of *Lannea* species

Treatment/ Sample	Dose	Increase in paw volumes in mL (mean ± SD, n = 5)				
	(mg/kg)	0 mn	60 min	120 min	180 min	240 min
LRR[a] extract	200	0	1.17±0.07	1.20± 0.04	1.17± 0.04	1.60 ± 0.03
LSR[b] extract	200	0	1.10± 0.04	1.16± 0.09	1.15± 0.03	1.25 ± 0.09
186	200	0	1.24± 0.03	1.21± 0.06	1.13± 0.03	1.43 ± 0.02
191	200	0	1.17± 0.07	1.17± 0.03	1.17± 0.05	1.35 ± 0.11
Normal saline	-	0	1.29± 0.07	1.32± 0.19	1.57± 0.13	1.62 ± 0.08
Indomethacin	10	0	0.84± 0.01	0.95± 0.04	0.97± 0.01	1.03 ± 0.02

[a] LRR = *Lannea rivae* roots; [b] LSR = *Lannea schweinfurthii* roots

4.3 Characterization of Secondary Metabolites Isolated from *Psiadia punctulata*

Phytochemical investigation was carried out on the leaves, stem bark and root extracts of *Psiadia punctulata.* Nineteen (**205-224**) compounds were isolated from the leaf extract, seven (**225-228**) from the stem bark extract and five (**229-233**) from the root extract.

4.3.1 Characterization of Secondary Metabolites Isolated from Leaves of *Psiadia punctulata*

The compounds isolated from the leaves of *Psiadia punctulata* include trachylobane (**205-214**) and kaurene (**215-218**) diterpenes, flavones (**220**, **221**) and fatty acid derivatives (**222-224**).

4.3.1.1 *Ent*-trachylobane Diterpenoids

Nine trachylobane diterpenes were isolated from the leaves of *Psiadia punctulata.* Of these, six (**205-209**) were new.

4.3.1.1.1 Trachyloban-17-oic acid (205)

Compound **205** was purified as a white crystals (mp 213-215 °C) from the leaves of *P. punctulata.* HRESIMS analysis showed a protonated molecular ion peak at *m/z* 303.2368 which is in agreement with a molecular formula $C_{20}H_{31}O_2$ (Calc. 303.2324). The MS and the NMR spectra (Table 4.20) indicated an *ent*-trachylobane skeleton (Midiwo *et al.*, 1997; Juma *et al.*, 2001). The ^{13}C NMR signal at δ_C 181.0 indicated the presence of an oxycarbonyl group. The presence of three methyl groups; CH_3-18 (δ_H 0.83, δ_C 33.3), CH_3-19 (δ_H 0.79, δ_C 21.6) and CH_3-20 (δ_H 0.92, δ_C 14.7) was evident from the NMR spectra leaving C-17 to be a hydroxycarbonyl group. This placement was confirmed from the HMBC correlation of H-12 (δ_H 1.94) and H-15 (δ_H 1.81) with hydroxycarbonyl (δ_C 181.0). Thus, this compound is trachyloban-17-oic acid. From the NOESY experiment (Appendix 1), it was clear that the compound has the same relative configuration as related compounds in literature (Midiwo *et al.*, 1997; Bruno-Colmenarez *et al.*, 2011). This assignment as well as the absolute configuration at the stereocenters was established on the basis of single crystal X-ray analysis (Figure 4.4). The crystal structure of this compound showed double O-H···O intermolecular hydrogen bonding motifs common for carboxylic acid groups for all four independent molecules in asymmetric unit. Therefore, this new compound (**205**) was characterised as *ent*-trachyloban-17-oic acid

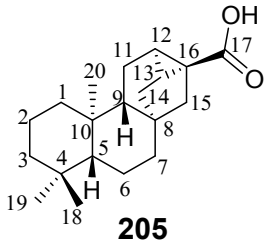

205

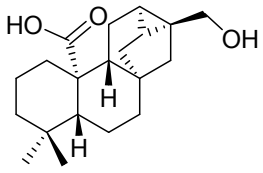

206

4.3.1.1.2 17-Hydroxy-*ent*-trachyloban-20-oic Acid (206)

HRESIMS analysis of the second new compound **206** isolated from the leaves of this plant showed a $[M+H]^+$ peak at *m/z* 319.2265 corresponding to the molecular formula $C_{20}H_{30}O_3$. The ^1H and ^{13}C NMR data (Table 4.20) indicated that this compound is also an *ent*-trachylobane diterpene. The ^{13}C NMR spectrum displayed 20 carbons including a

hydroxycarbonyl (δ_C 178.3) and an oxymethyl (δ_C 67.4; δ_H 3.89) signals. The ^{13}C NMR chemical shift values of the methyl signals (Table 4.20) indicated that, CH_3-18 (δ_C 22.0) and CH_3-19 (δ_C 32.7) are intact while CH_3-17 and CH_3-20 are oxidized into oxymethyl (δ_C 67.4) and hydroxycarbonyl (δ_C 178.3) groups respectively. HMBC correlation of the signal for oxymethyl (δ_H 3.89) with C-12 (δ_C 22.3), C-13 (δ_C 18.2), C-15 (δ_C 48.1) and C-16 (δ_C 30.2) allowed the assignment of the oxymethyl signals to CH_2-17, consequently the oxycarbonyl group was placed at C-20. The latter assignment was confirmed from HMBC correlation of CH_2-1 (δ_H 0.78 and δ_H 2.67), H-5 (δ_H 1.04) and H-9 (δ_H 1.49) to hydroxycarbonyl (δ_C 178.3). On the basis of these observations, this new compound was identified as 17-hydroxy-*ent*-trachyloban-20-oic acid (**206**).

Table 4.20: ^{1}H and ^{13}C NMR Data of 205 (CD_2Cl_2) and 206 (C_5D_5N)

	205				206			
Position	δ_C	Type	δ_H (mult., *J* in Hz)	HMBC (H→C)	δ_C	Type	δ_H (mult., *J* in Hz)	HMBC (H→C)
1	38.4	CH_2	1.49 (m)	C-2, C-9, C-20	39.0	CH_2	0.78 (m)	C-2, C-9, C-10, C-20
							2.67 (m)	C-4, C-10, C-20
2	18.0	CH_2	1.35 (m)	-	20.3	CH_2	2.43 (m)	C-3, C-9, C-10
			1.55 (m)	-			2.78 (m)	-
3	42.0	CH_2	1.13 (m)	C-2, C-14, C-18, C-19	42.6	CH_2	1.26 (m)	C-4, C-18, C-19
			1.35 (m)	-			1.39 (m)	-
4	38.3	C	-	-	33.7	C	-	-
5	55.9	CH	0.76 (dd, *J*=12.0, 1.6)	C-4, C-6, C-18, C-19, C-20	56.2	CH	1.04 (m)	C-1, C-3, C-6, C-7, C-18, C-19
6	20.0	CH_2	1.23 (m)	C-4, C-8	20.7	CH_2	1.49 (m)	C-8, C-10, C-14
			1.49 (m)	C-7, C-8, C-9			1.97 (m)	C-7, C-8
7	32.2	CH_2	1.23 (m)	C-8	38.9	CH_2	1.55 (m)	C-8, C-14, C-15
			1.94 (m)	C-8			1.65 (m)	C-8, C-9, C-14, C-16
8	40.2	C	-	-	40.7	C	-	-
9	52.2	CH	1.13 (m)	C-8, C-11, C-15, C-20	52.0	CH	1.49 (m)	C-8, C-10, C-11, C-14, C-15
10	38.9	C	-	-	49.4	C	-	-
11	19.3	CH_2	1.79 (m)	C-9, C-13, C-16	20.3	CH_2	1.55 (m)	C-8, C-10, C-14
			1.94 (m)	C-8			2.20 (m)	C-8, C-9, C-12, C-13
12	32.4	CH	1.22 (m)	C-13, C-15, C-16,	22.3	CH	1.15 (m)	C-9

Table 4.20 continued

	205				206			
	δ_C	Type	δ_C	Type	δ_C	Type	δ_C	Type
13	25.7	CH	1.79 (d, *J*=11.2)	C-8, C-16,	18.2	CH	0.94 (m)	C-12
			1.81 (m)	C-8, C-17				
14	33.0	CH_2	-	-	31.3	CH_2	1.26 (m)	C-11, C-12
							3.03 (m)	C-8, C-9, C-12, C-15, C-16
15	42.8	CH_2	1.49 (d , *J*=11.9)	C-8, C-9, C-13, C-16	48.1	CH_2	1.65 (m)	C-8, C-9, C-12, C-14, C-16
			1.81 (d, *J*=11.8)	C-16, C-17			1.97 (m)	C-7, C-8, C-9, C-13, C-16
16	29.9	C	-	-	30.2	C	-	-
17	181.0	C	-	-	66.3	CH_2	3.89 (m)	C-12, C-13, C-15, C-16
18	33.3	CH_3	0.83 (s)	C-3, C-5, C-19	22.0	CH_3	1.01 (s)	C-3, C-4, C-19
19	21.6	CH_3	0.79 (s)	C-3, C-5, C-18	32.7	CH_3	0.91 (s)	C-3, C-4, C-18
20	14.7	CH_3	0.92 (s)	C-4, C-5, C-9, C-10	178.3	C	-	-

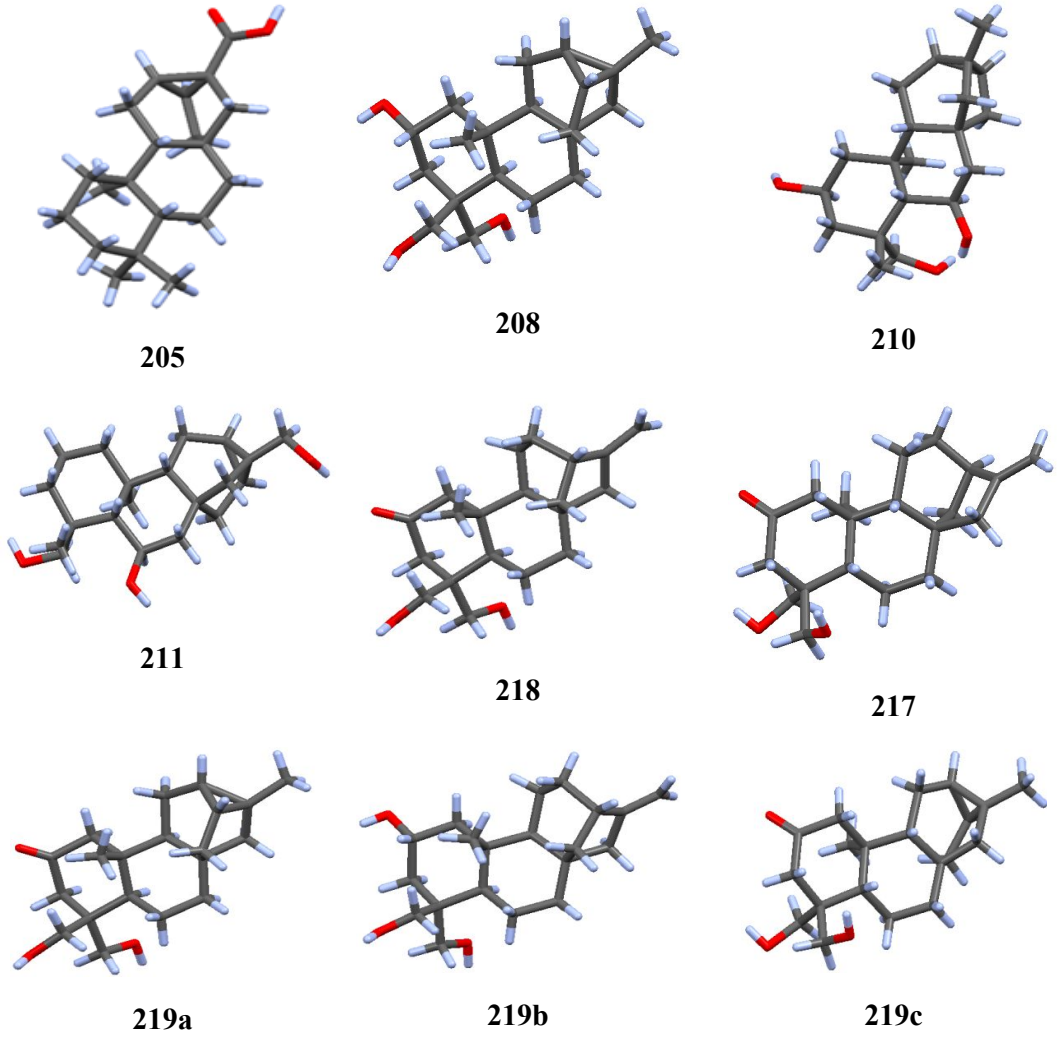

Figure 4.4: Crystal Structure Representation of Some Compounds Isolated from *Psiadia punctalata*

4.3.1.1.3 *Ent*-[6β, 18, 19]-trihydroxy-trachyloban-2-one (207)

Compound **207** was isolated as a white solid (mp 137-139 °C) from the leaves of *P. punctulata*. HRESIMS analysis which showed a molecular ion peak *m/z* 335.2185 corresponding to the molecular formula $C_{20}H_{30}O_4$ together with the ^{13}C NMR (Table 4.21) which showed 20 non-equivalent carbon signals indicated that this compound is a diterpene derivative (Midiwo *et al.*, 1997; Juma *et al.*, 2006). The ^{1}H NMR spectrum [δ_H 0.89 (dd, J = 3.1, 7.9 Hz) for H-12, 0.64 (d, J = 7.9 Hz) for H-13; 1.27 m and 1.98 (d, J = 11.9 Hz) for

CH_2-14, 1.33 m and 1.53 m for CH_2-15] and the ^{13}C NMR signals at δ_C 24.0 (C-12), 20.0 (C-13), 33.1 (C-14), 50.0 (C-15) and 22.1 (C-16) showed that the compound has an *ent*-trachylobane diterpene skeleton (Midiwo *et al.*, 1997; Juma *et al.*, 2006). In addition, the presence of a carbonyl (δ_C 211.5), an oxymethine (δ_H 4.04 m; δ_C 67.4), two oxymethyl [δ_H 3.55, d, J = 11.5 Hz, 4.00 d, J = 11.5, δ_C 64.7 and δ_H 3.55, d, J = 11.5 Hz, 3.63 d, J = 11.5, δ_C 70.3)] groups were observed in the NMR spectra (Table 34). Of the four methyl groups on *ent*-trachylobane skeleton, only two are observed in the NMR spectra *vis*. CH_3-17 (δ_H 1.15, δ_C 20.1) and CH_3-20 (δ_H 1.08, δ_C 16.9) while the other two, CH_3-18 and CH_3-19, are oxydized into oxymethylene groups.

In agreement with this assignment both oxymethylene protons showed HMBC correlation with C-3 (δ_C 46.6) and C-5 (δ_C 55.4). The oxymethine proton (δ_H 4.04) showed HMBC correlation with C-4 (δ_C 47.3), C-5 (δ_C 55.4), C-7 (δ_C 47.6), C-10 (δ_C 43.2) which is in agreement with the placement of hydroxy group at C-6. The large coupling constant (J = 10.3 Hz) between H-5 (δ_H 1.46) and H-6 (δ_H 4.04) is consistent with both protons being axial and hence OH-6 should be equatorial (β-oriented) as in the other diterpenes previously reported from this plant (Midiwo *et al.*, 1997; Juma *et al.*, 2006). Both C-1 and C-3 along with the corresponding protons are downfield-shifted indicating the placement of the carbonyl at C-2. In agreement with this, both CH_2-1 and CH_2-3 showed HMBC correlation with this carbonyl signal (δ_C 211.5). Therefore, the new compound **207** was designated as *ent*-[6*β*, 18, 19]-trihydroxy- trachyloban-2-one.

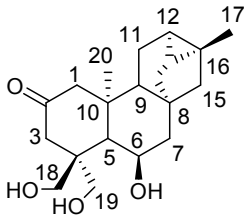

207

Table 4.21: ^{1}H and ^{13}C NMR Data of 207 and 208 in $CDCl_3$

Position	207				208			
	δ_C	Type	δ_H (mult., *J* in Hz)	HMBC (H→C)	δ_C	Type	δ_H (mult., *J* in Hz)	HMBC (H→C)
1	54.1	CH_2	1.87 (d, *J*=15.4)	C-9, C-10, C-20	47.9	CH_2	0.70 (m)	C-2, C-3, C-9, C-20
			2.26 (m)	C-3, C-10, C-20			1.94 (m)	-
2	211.5	CH	-	-	64.3	CH	3.91 (m)	-
3	46.6	CH_2	2.26 (m)	C-2, C-4, C-5, C-18, C-19	40.3	CH_2	1.30 (m)	C-1, C-4
			2.31 (m)	C-2, C-4, C-5, C-18, C-19			1.38 (m)	C-1, C-4
4	47.3	C	-	-	43.6	C	-	-
5	55.4	CH	1.46 (d, 10.3)	C-1, C-4, C-6, C-9, C-10, C-20	52.4	CH	0.95 (m)	C-4, C-7, C-19, C-18
6	67.4	CH	4.04 (m)	C-4, C-18, C-19	20.4	CH_2	1.70 (m)	C-7, C-8
							1.94 (m)	C-8
7	47.6	CH_2	1.53 (m)	C-5, C-6, C-8, C-9, C-14	40.1	CH_2	0.91 (m)	C-9
			1.76 (dd, J=12.8, 4.1)	C-5, C-6, C-8, C-9, C-14			2.36 (m)	-
8	40.4	C	-	-	39.8	C	-	-
9	51.7	CH	1.33 (m)	C-1, C-8, C-10, C-12, C-14, C-15, C-20	53.2	CH	1.25 (m)	C-10, C-12
10	43.2	C	-	-	39.6	C	-	-
11	19.7	CH_2	1.63 (m)	C-9, C-10, C-13, C-16	20.3	CH_2	0.66 (m)	-
			1.91 (m)	C-9, C-10, C-12, C-13, C-17			1.50 (m)	-

Table 4.21 continued

			207		208		207	
	δ_C	Type	δ_H (mult., *J* in Hz)	HMBC (H→C)	δ_C	Type	δ_H (mult., *J* in Hz)	HMBC (H→C)
12	24.0	CH	0.89 (dd, *J*=7.9, 3.1)	C-8, C-13, C-14, C-17	22.5	CH	1.30 (m)	C-14
13	20.0	CH	0.64 (d, *J*=7.7)	C-9, C-17	33.4	CH	2.06 (m)	C-12, C-15
14	33.1	CH_2	1.27 (m)	C-10, C-13	38.9	CH_2	1.31 (m)	C-7, C-9, C-12, C-16
			1.98 (d, J=11.9)	C-8, C-9, C-12, C-15			1.38 (m)	C-7, C-9, C-12, C-16
15	50.0	CH_2	1.33 (m)	C-9, C-13, C-14, C-16	50.3	CH_2	1.25 (m)	C-7, C-9, C-12, C-13, C-17
			1.53 (m)	C-9, C-13, C-14, C-16			1.40 (m)	C-7, C-9, C-12, C-13, C-17
16	22.1	C	-	-	24.3	C	-	-
17	20.1	CH_3	1.15 (s)	C-12, C-13, C-15, C-16	20.4	CH_3	1.12 (m)	C-12, C-15, C-16
18	64.7	CH_2	3.55 (d, *J*=11.5)	C-3, C-5, C-19	73.5	CH_2	3.42 (m)	C-3, C-5
			4.00 (d, *J*=11.5)	C-3, C-5, C-19			3.91 d (*J*=11.1)	C-3, C-5
19	70.3	CH_2	3.55 (d, *J*=11.5)	C-3, C-5, C-18	65.4	CH_2	3.74 (m)	C-3, C-5
			3.63 (d, *J*=11.3)	C-3, C-5, C-18			3.85 (m)	C-3, C-5
20	16.9	CH_3	1.08 (s)	C-1, C-5, C-9, C-10	16.1	CH_3	0.96 (s)	C-1, C-5, C-9, C-10

4.3.1.1.4 Normal-trachyloban-2*α*,18,19-triol (208)

Compound **208** was obtained as colourless crystals (mp 137-139 °C), and was assigned a molecular formula $C_{20}H_{32}O_3$ based on HRESIMS analysis ($[M+H]^+$ at *m/z*: 321.2438) and ^{13}C NMR data (Table 4.21). The ^{13}C NMR spectrum (Table 4.21) was indicative of a trachylobane diterpene skeleton as in compounds **205-207**, with an oxymethyl (δ_C 64.3) and two oxymethylene (δ_C 65.4 and δ_C 73.5) functionalities. The presence of only two methyl signals Me-17 (δ_H 1.12) and Me-20 (δ_H 0.96) in the ^1H NMR spectrum indicated that C-18 and C-19 are oxidized to oxymethylene groups. HMBC correlation of H-5 with the two oxymethylenic carbons confirmed that both C-18 (δ_C 73.5) and C-19 (δ_C 65.4) are oxymethylene groups. The placement of hydroxy group at C-2 (δ_C 64.3) was compatible with the HMBC correlation of H_2-1 with C-2. The NMR and MS data of compound **208** were identical to what has been reported for *ent*-trachylobane-2*α*,18,19-triol (Juma *et al.*, 2006). However, the crystallographic data (Figure 4.4) showed that **208** is rather the unusual normal-trachylobane diterpene. Therefore, this new compound (**208**) was identified as normal-trachyloban-2*α*,18,19-triol. In the crystalline state, compound **208** shows two independent molecules in asymmetric unit and layered structure. These hydrophilic and hydrophobic layers form when the hydrophilic ends of the molecules interact with each other through intermolecular O-H···O hydrogen bonds, donated and accepted by hydroxy groups, and hydrophobic ends through hydrophobic forces.

There are reports indicating that naturally occurring trachylobane diterpenoids belong to the *ent*-series (Block *et al.*, 2004); hence compound **208** is one of the few normal trachylobane diterpenes reported so far (Gonzalez *et al.*, 1973). It is known that, the relative configuration at the A/B ring junction (C-5 and C-10) and at ring carbon C-9 is characteristically *trans-anti* orientation, as is the case with triterpenes and sterols. However, unlike the situation in triterpenes, both the "normal" and "enantiomeric" (*enantio*- or *ent*-) absolute configuration are encountered among the natural diterpenes (Schütte, 1997).

4.3.1.1.5 Normal-trachyloban-2α,6α,19-triol (209)

Investigation of the roots of *Psiadia punctulata* resulted in the identification of a further new compound (**209**). The HRESIMS analysis ($[M-H_2O]^+$ at *m/z* 303.2320) suggested a diterpene skeleton. The NMR spectral data (Table 4.22) is similar to what has been reported for trachyloban-2β,6β,19-triol (Midiwo *et al.*, 1997). The placement of hydroxy group at C-2 was confirmed from the HMBC correlation of the H-2 (δ_H 3.70) with C-1 (δ_C 48.9), C-3 (δ_C 49.3) and C-4 (δ_C 41.4) as well as that of H_2-1 (δ_H 0.68 and δ_H 1.90) with C-2, C-3, C-4 and C-10. This was further supported by the H,H-COSY coupling of H-2 (δ_H 3.70) with H2-1(δ_H, 0.68, 1.90) and H_2-3 (δ_H, 1.01, 1.76). In the same way the chemical shift values of the methyl groups indicated that it is the C-19 methyl group which was oxidized to oxymethylene group. The placement of the third hydroxy group at C-6 was evident from the downfield shift of C-5 (δ_C 60.3) and C-7 (δ_C 50.6) in its ^{13}C NMR spectroscopic data (Table 4.22). The H,H COSY coupling constant of 11.3 Hz between H-6 and H-5 suggested a *trans*-anti orientation of both protons. This implied H-6 to be β-oriented and hence OH-6 should be α-oriented. Moreover, the relative configuration at C-2 and C-6 was established by comparison of the spectroscopic data to the related compound (Midiwo *et al.*, 1997). Whereas the compound earlier reported is levorotatory, $[\alpha]_D^{20}$ = −60, typical of *ent*-trachylobane diterpenes, the compound reported here is dextrorotatory, $[\alpha]_D^{20}$ = + 56, indicating that compound **209** is "normal" trachylobane diterpene. Being a normal trachylobane, the orientation of the two hydroxy groups at C-2 and C-6 should be α-oriented as opposed to the related compound (Midiwo *et al.*, 1997). Thus, this compound was characterized as normal-trachyloban-2α,6α,19-triol (**209**), which is new.

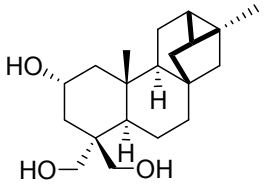

208

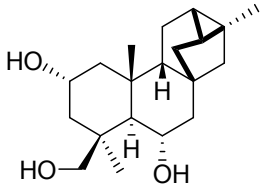

209

Table 4.22: ^{1}H and ^{13}C NMR data of 209 in $CDCl_3$

Position	δ_C	Type	δ_H (mult., *J* in Hz)	HMBC (H→C)
1	48.9	CH_2	0.68 (m)	C-3, C-9, C-20
			1.90 (m)	C-2, C-5, C-20
2	62.3	CH	3.70 (ddd, *J*=11.6, 11.6, 4.3)	C-4, C-10
3	49.3	CH_2	1.01 (m)	C-1, C-18
			1.76 (m)	C-1, C-18
4	41.4	C	-	-
5	60.3	CH	0.94 (dd, *J*=10.5, 1.8)	C-3, C-7, C-19
6	68.2	CH	4.02 (ddd, *J*=11.3, 6.2, 4.1)	C-5, C-8
				C-5, C-8
7	50.6	CH_2	1.34 (d, *J*=11.1)	C-5, C-15
			1.48 (m)	C-15
8	40.7	C	-	-
9	53.1	CH	1.21 (ddd, *J*=11.5, 8.1, 1.4)	C-1,C-7, C-12
10	40.8	C	-	-
11	19.8	CH_2	1.71 (m)	C-10, C-16
			1.90 (m)	C-10, C-16
12	24.1	CH	0.86 (dd, *J*=7.9, 3.3)	C-14, C-15
13	19.7	CH	1.21 (m)	C-8, C-12, C-17
14	33.9	CH_2	1.26 (d, *J*=11.2)	C-7, C-12, C-16
			2.19 (m)	C-12, C-16
15	48.5	CH_2	1.48 (m)	C-7, C-12, C-17
			1.64 (m)	C-7, C-13, C-17
16	22.3	C	-	-
17	20.2	CH_3	1.15 (s)	C-12, C-15
18	31.4	CH_3	1.26 (m)	C-3, C-4
19	67.6	CH_2	3.42 (dd, *J*=9.5, 4.5)	C-3, C-4, C-5
			4.02 (dd, *J*=6.2, 4.1)	C-3, C-4, C-5
20	15.9	CH_3	1.10 (s)	C-1, C-9, C-10

4.3.1.1.6 *Ent*-trachyloban-2*β*,6*β*,19-triol (210)

Compound **210** was isolated as white crystals, whose molecular formula $C_{20}H_{32}O_3$ was established based on ESIMS analysis ($[M+H]^+$ at *m/z* 321.6), and ^1H (Table 4.24) and ^{13}C (Table 4.23) NMR spectral data. The ^{13}C NMR spectrum exhibited signals for twenty carbons, three of these signals assigned to C-5 (δ_C 59.5), C-9 (δ_C 53.0) and C-13 (δ_C 20.2) and were characteristic of a trachylobane diterpene.

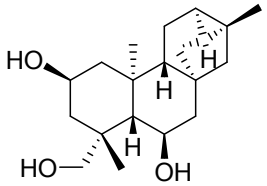

210

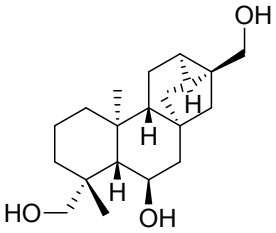

211

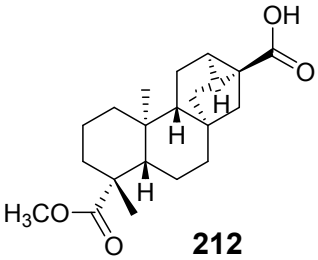

212

Table 4.23: ^{13}C (200 MHz) NMR Data of 210, 211 and 212 in $CDCl_3$

Position	210		211		212	
	δ_C	Type	δ_C	Type	δ_C	Type
1	48.6	CH_2	39.5	CH_2	39.2	CH_2
2	63.7	CH	20.2	CH_2	18.6	CH_2
3	49.4	CH_2	38.9	CH_2	38.0	CH_2
4	41.9	C	43.5	C	43.7	C
5	59.5	CH	52.6	CH_2	56.6	CH
6	69.3	CH	64.1	CH	21.6	CH_2
7	50.6	CH_2	40.3	CH_2	38.5	CH_2
8	40.9	C	48.1	C	40.2	C
9	53.0	CH	50.2	CH	51.6	CH
10	40.8	C	39.7	C	38.6	C
11	19.9	CH_2	19.9	CH_2	19.3	CH_2
12	24.1	CH_2	24.2	CH_2	25.5	CH_2
13	20.2	CH	30.6	CH	32.1	CH
14	34.1	CH	22.4	CH	32.0	CH
15	48.3	CH_2	43.8	CH_2	42.6	CH_2
16	22.5	C	33.3	C	29.8	C
17	20.3	CH_3	65.2	CH_2	181.4	C
18	31.6	CH_3	20.4	CH_3	28.6	CH_3
19	69.4	CH_2	73.1	CH_2	177.6	C
20	16.3	CH_3	15.8	CH_3	12.3	CH_3
21 (OCH_3)	-		-	-	51.2	CH_3

The ^{1}H and ^{13}C NMR spectral data (Tables 4.24 and 4.23) also showed the presence of three hydroxy substituents on a trachylobane skeleton. The placement of one of the hydroxy group at C-2 was established from the HMBC correlation of H-2 (δ_H 3.76) with C-1 (δ_C 48.6), C-3 (δ_C 49.4) and C-4 (δ_C 41.9) as well as that of H_2-1 (δ_H 0.70 and 1.89) with C-2, C-3, C-4 and C-10 (Table 36 and 37). Similarly, the HMBC spectrum allowed the placement of the second hydroxy group at C-6. The large coupling constant (10. 6 Hz) between H-6 and H-5 suggested a trans-1,2-diaxial orientation for these protons. This implied H-6 to be α-oriented and hence OH-6 should be β-oriented. Its negative specific rotation $[\alpha]_D^{20} = -60°$ indicated that this compound is an ent-trachylobane diterpene. This data was in agreement with what has been for the same compound (Midiwo *et al.*, 1997). The X-ray difractometry analysis of this compound (Figure 4.4) revealed its absolute configuration. Therefore, compound **210** was identified and its absolute configuration determined as *ent*-trachyloban-2*β*,6*β*,19-triol (Figure 9). This is the first report of the crystal structure of this compound.

4.3.1.1.7 *Ent*-trachyloban-6*β*,17,19-triol (211)

ESIMS analysis of compound **211** showed a molecular ion peak *m/z* 321.6 (corresponding to the molecular formula $C_{20}H_{32}O_3$) together with the ^{1}H (Table 4.24) and ^{13}C (Table 4.23) NMR which showed 20 non-equivalent carbon signals indicated that this compound is a diterpene derivative (Midiwo *et al.*, 1997; Juma *et al.*, 2006). The ^{13}C NMR chemical shift values of the methyl signals (Table 4.23) indicated that CH_3-18 (δ_C 31.9) and CH_3-20 (δ_C 16.8) are intact, while CH_3-17 (δ_C 63.5) and CH_3-19 (δ_C 68.3) are oxidized into oxymethyl group each. The presence of an additional hydroxyl substituent was evident from the ^{1}H NMR signal at δ_H 3.85 (δ_C 64.1) and was placed at C-6 from the HMBC correlation of H-6 with C-4 (δ_C 43.5), C-8 (δ_C 48.1) and C-10 (δ_C 39.7). The coupling constant (J = 7.8 Hz) between H-6 and H-7ax indicated H-6 is α-oriented (OH-6 then is *β*-oriented). This was supported by X-ray analysis (Figure 4.4), indicating OH-6 occupying a *β*-orientation. Hence, The absolute confiiguration of compound **211** was determined as *ent*-trachyloban-6*β*,17,19-triol.

4.3.1.1.8 19-Methoxycarbonyl-*ent*-trachyloban-17-oic Acid (212)

A close look at the ^{1}H (Table 4.24) and ^{13}C (Table 4.23) NMR spectral data of **212** ($C_{21}H_{30}O_4$) revealed that the compound consists of twenty one carbons including two carboxyls C-17 (δ_C 181.4) and C-19 (δ_C 177.6); two methyls, C-18 (δ_C 28.6) and C-20 (δ_C 12.3) and one methyl ester substituent MeO-19 (δ_C 51.2). The ^{1}H and ^{13}C NMR spectral data of **212** is in agreement with the reported data (Wu *et al.*, 2009).

Table 4.24: ^{1}H (800 MHz) NMR Data of 210, 211 and 212 in $CDCl_3$

Position	210	211	212
1	0.70 (d, *J*=11.75, 11.75)	0.91 (m)	0.78 (m)
	1.89 (m)	2.3 (m)	1.49 (m)
2	3.76 (m)	1.73 (m)	1.37 (m)
		1.97 (m)	1.78 m(m)
3	1.11 (m)	1.37 (m)	0.99 (m)
	1.69 (m)	1.42 (m)	2.13 (d, *J*=12.31)
4			
5	0.98 (d, *J*=10.59)	1.01 (m)	1.00 (m)
6	4.09 (m)	3.85 (m)	1.65 (m)
			1.82 (d, *J*=11.96)
7	1.30 (m)	0.91 (m)	1.37 (m)
	1.52 (m)	2.20 (m)	1.49 (m)
8			
9	1.19 (m)	1.42 (m)	1.12 (m)
10			
11	1.69 (m)	1.37 (m)	1.74 (m)
	1.89 (m)	1.97 (ddd, J=12.2, 4.3, 2.3)	1.94 (m)
12	0.86 (m)	0.85 (dd, J=7.8, 3.2)	1.78 (m)
13	1.12 (m)	2.21 (m)	1.94 (m)
14	1.30 (m)	1.32 (m)	1.27 (m)
	2.02 (m)		2.13 (m)
15	1.51 (m)	0.85 (dd, 7.8, 3.2)	1.49 (m)
	1.69 (m)	1.92 (ddd, 12.2, 4.3, 2.3)	1.82 (d, *J*=11.39)
16			
17	1.14 (s)	3.72 (dd, J=10.6, 3.5)	
		3.85 (m)	
18	1.30 (s)	1.16 (s)	1.15 (3H, m)
19	3.44 (d, *J*=10.20)	3.43 (d, J=7.7)	
		3.72 (dd, J=10.6, 3.5)	
20	1.10 (s)	0.99 (s)	0.75 (3H, m)
21 (OCH_3)			3.64 (3H, s)

The placement of the hydroxycarbonyl at C-17 and the methyl ester at C-19 was confirmed from HMBC spectrum which shoed correlation of methyl protons at δ_H 3.64 (Me-19) with C-19 (δ_C 177.6). Therefore, compound **212** was identified as 19-methoxycarbonyl-*ent*-trachyloban-17-oic acid.

4.3.1.1.9 *Ent*-trachyloban-2*β*,18,19-triol (213)

Compound **213** was obtained as colourless crystals, and was assigned a molecular formula $C_{20}H_{32}O_3$ based on ESIMS analysis ($[M+H]^+$ at *m/z*: 321.3) and ^{13}C NMR data (Table 4.25). The ^{13}C NMR spectrum (Table 4.25) was indicative of a trachylobane diterpene skeleton, with an oxymethine (δ_C 62.9) and two oxymethylene (δ_C 69.7 and δ_C 63.8) functionalities. The presence of only two methyl signals, Me-17 (δ_H 1.14) and Me-20 (δ_H 1.01) in the ^1H NMR spectrum indicated that C-18 and C-19 are oxidized to oxymethylene groups. HMBC correlation of H-5 with the two oxymethylenic carbons confirmed that both C-18 (δ_C 69.7) and C-19 (δ_C 63.8) are oxymethylene groups. The placement of hydroxy group at C-2 (δ_C 62.9) was compatible with the HMBC correlation of H_2-1 with C-2. The NMR and MS data of compound **213** were identical to what has been reported for *ent*-trachylobane-2*β*,18,19-triol (Juma *et al.*, 2006). The negative specific rotation ($[\alpha]_D^{20}$ = −27) of this compound indicated this compound is the same as the *ent*-trachylobane diterpene reported previously (Juma *et al.*, 2006). Therefore, compound **213** was identified as *ent*-trachyloban-2*β*,18,19-triol.

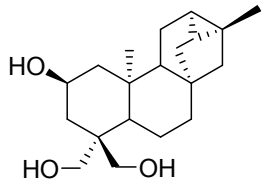

213

Table 4.25: ^{1}H (800 MHz) and ^{13}C (200MHz) NMR Data of 213 in $CDCl_3$

Position	δ_C	Type	δ_H (mult., *J* in Hz)	HMBC (H→C)
1	48.5	CH_2	0.84 (dd, *J*=7.7, 3.1)	C-2, C-3, C-9, C-20
			1.86 (d, *J*=12.2)	C-2, C-3, C-9, C-20
2	62.9	CH	3.83 (m)	C-4, C-10
3	40.5	CH_2	1.29 (d, *J*=11.2)	C-1, C-4
			1.39 (m)	C-1, C-4
4	43.9	C		/
5	53.3	CH	1.19 (m)	C-4, C-7, C-19, C-18
6	19.8	CH_2	1.76 (m)	C-7, C-8
			1.94 (m)	C-8
7	39.1	CH_2	1.08 (m)	C-9
			2.11 (m)	C-5, C-10
8	39.5	C	/	/
9	56.1	CH	1.22 (m)	C-10, C-12
10	39.4	C	/	/
11	19.8	CH_2	0.66 (m)	C-8, C-13
			1.49 (m)	C-6, C-10
12	20.4	CH	1.29 (d, *J*=11.1)	C-14
13	24.1	CH	0,84 (dd, *J*=7.3; 3.1)	C-12, C-15
14	33.2	CH_2	1.19 (m)	C-7, C-9, C-12, C-16
			2.11 (m)	C-7, C-9, C-12, C-16
15	50.3	CH_2	1.29 (m)	C-7, C-9, C-12, C-13, C-17
			1.39 (m)	C-7, C-9, C-12, C-13, C-17
16	22.2	C	/	/
17	20.0	CH_3	1.14 (3H, m)	C-12, C-15, C-16
18	69.7	CH_2	3.46 (m)	C-3, C-5
			3.63 (d, *J*=11.1Hz)	C-3, C-5
19	63.8	CH_2	3.58 (m)	C-3, C-5
			3.74 (m)	C-3, C-5
20	15.6	CH_3	1.01 (3H, s)	C-1, C-5, C-9, C-10

4.3.1.2 *Ent*-kaurene Diterpenes

Five kaurene diterpenes (**214**-**218**) were isolated from the leaves of *Psiadia punctulata.* Of these, one (**214**) was new.

4.3.1.2.1 *Methyl*-15*α*,16*α*,17-trihydroxy-*ent*-kauran-19-oate (214)

Compound **214** ($[M+1]^+$ at *m/z* 367.2466, $C_{21}H_{35}O_5$), was isolated as a white solid (mp 198-200°C) from the leaves of *P. punctulata*. The ^1H and ^{13}C NMR data (Table 4.26) of **214** indicated that this compound is an *ent*-kaurene type diterpene with three hydroxyl (Table 39) and a methyl ester substituent. Two of the hydroxyl groups were placed at C-16 (δ_C 80.6) and C-17 (δ_C 65.8) as in the case of related compounds previously reported (Shigeru *et al.*, 1990). This oxygenation pattern was confirmed from the HMBC correlations of H-13 (δ_H 3.48) to both C-15 and C-16. The third hydroxyl group was placed at C-15 (δ_C 82.0) based on the HMBC correlation of H-15 (δ_H 3.48) with C-17 (δ_C 65.8) and that of Ha/Hb-17 (δ_H 3.70/3.74) with C-15 (δ_C 82.0). The methyl ester group was located at C-19 (δ_C 177.9) based on the ^{13}C NMR resonance of C-18 (δ_C 28.7) which is in agreement with the literature (Midiwo *et al.*, 1997; Juma *et al.*, 2006). The HMBC correlation of the methyl group resonating at δ_H1.16 (CH_3-18; δ_C 28.7) with the carbonyl C-19 (δ_C 177.9) further support the assignment. The stereochemistry at C-5, C-8, C-9, C-10 (Bruno-Colmenarez *et al.*, 2011) and C-13 (Midiwo *et al.*, 1997) were determined based on the literature and NOESY spectrum. The skeleton of **214** was the same as the related compound previously reported (Bruno-Colmenarez *et al.*, 2011). This skeleton presents three six-membered rings; labeled A, B, C and a five member ring, called ring D. The substitution patterns are *trans* for A/B rings and *cis* for B/C rings. In addition, the orientation of CH_3-20 is biosynthetically an α-orientation and indirectly indicated the β-orientation of H-5 and H-9 (Qiu *et al.*, 2016). Based on this information, the methyl CH_3-20 and the proton H-5 are in *trans*-orientation. Additionally, in NOESY analysis, H-15 showed correlation with H-9 (δ_H 1.06), and HO-15b (δ_H 2.75) with HO-16 (δ_H 3.61) indicating the two hydroxy groups to be *cis*-oriented. Therefore, **214** was identified as 15α,16α,17-trihydroxy-ent-kauren-19-oic acid methyl ester.

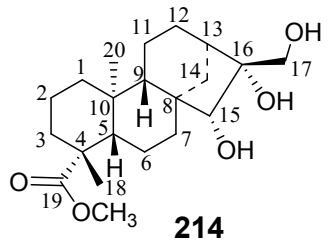

214

Table 4.26: ^{1}H (800 MHz) and ^{13}C (200 MHz) NMR Data of 214 and 215 in $CDCl_3$

Position	214			215		
	δc	δ_H (mult., *J* in Hz)	HMBC (H→C)	δ_C	δ_H (mult., *J* in Hz)	HMBC (H→C)
1	40.6	0.79 (m)	C-20, C-2, C-9, C-10	40.6	0.79 (m)	C-2, C-3, C-5, C-10, C-20
		1.89 (m)	-		1.83 (m)	C-3
2	19.0	1.44 (dd, *J*=13.1, 1.6)	C-10, C-4	19.0	1.43 (m)	C-4
		1.83 (m)	C-3, C-1, C-4		1.83 (m)	C-1, C-5
3	37.9	1.01 (d, *J*=4.4)	C-2, C-18, C-4, C-5, C-10	38.0	0.99 (m)	C-2
		2.18 (m)	C-2, C-4, C-5		2.17 (s)	C-1, C-18
4	43.7	/	-	43.8	/	/
5	56.8	1.01 (d, *J*=4.4)	C-20, C-6, C-18, C-7, C-10, C-4, C-9, C-19	56.8	1.03 (dd, *J*=12.0, 2.1)	C-6, C-7, C-9
6	21.1	1.70 (m)	C-7, C-10, C-5	22.1	1.74 (m)	C-7, C-9, C-18
		1.92 (m)	C-10, C-8, C-5		1.83 (m)	C-4
7	35.5	1.35 (dd, *J*=13.3, 3.6)	C-6, C-8, C-14, C-5, C-15	42.0	1.43 (m)	C-6, C-8, C-9, C-10, C-14, C-16
		1.80 (m)	C-13, C-8, C-9, C-15		1.61 (m)	C-5, C-6, C-13, C-14
8	47.4	-	-	44.7	/	/
9	54.6	1.06 (m)	C-15, C-8, C-20, C-11, C-6, C-12, C-7, C-10	55.7	0.99 (m)	C-1, C-8, C-10, C-11, C-12, C-14
10	39.6	-	-	39.4	/	/
11	18.7	1.35 (dd, *J*=13.3, 3.6)	C-12, C-14, C-5, C-9, C-8	18.5	1.49 (m)	C-10, C-12
		1.60 (m)	C-12, C-13, C-8		1.61 (m)	C-8, C-10, C-12, C-20
12	25.4	1.51 (m)	C-11, C-14, C-13, C-9, C-16	26.2	1.49 (m)	C-10, C-12
					1.56 (dd, *J*=14.6,1.9)	C-14

Table 4.26 continued

Position	214			215		
	δc	δ_H (mult., *J* in Hz)	HMBC (H→C)	δ_C	δ_H (mult., *J* in Hz)	HMBC (H→C)
13	43.1	2.10 (d, *J*=3.9)	C-11, C-12, C-7, C-8, C-16, C-15	45.2	2.03 (m)	/
14	35.6	1.59 (m)	C-12, C-7, C-13, C-8, C-9	37.2	1.61 (m)	C-8, C-9, C-12, C-13
		1.63 (m)	C-12, C-7, C-13, C-8, C-9		1.93 (d, *J*=11.5)	C-12, C-15
15	82.0	3.48 (s)	C-7, C-14, C-9, C-17	53.0	1.43 (m)	C-8, C-9, C-13
					1.56 (dd,*J*=14.6,1.9)	C-9, C-13, C-14
16	80.6	-	-	82.0	/	/
17	65.8	3.70 (d, *J*=12.3)	C-13, C-16, C-15	66.3	3.66 (d, *J*=11.0)	C-13
		3.74 (d, *J*=11.1)	C-13, C-15, C-16		3.78 (d, *J*=11.0)	C-15
18	28,7	1.16 (s)	C-3, C-4, C-5, C-19	28.7	1.15 (s)	C-3, C-4, C-5, C-19
19	177.9	-	-	178.1	/	/
20	15.3	0.82 (m)	C-10, C-1, C-9, C-5	15.3	0,83 (s)	C-1, C10, C-5, C-9
OCH_3	51.2	3.65 (m)	C-19	51.2	3.66 (s)	C-19
HO-15	-	2.75 (br s)	-	-	-	-
HO-16	-	3.61 (br s)	-	-	-	-
HO-17	-	2.45 (br s)	-	-	-	-

4.3.1.2.2 Methyl-16α,17-epoxy-*ent*-kauran-19-oate (215)

Compound **215** was isolated from the leaves of *P. punctulata* as a white solid. A combination of ^{1}H, ^{13}C NMR (Table 4.26) and LC-MS (molecular ion $[M+H]^+$ peak *m/z* 333.7 suggested a molecular formula $C_{21}H_{34}O_3$) and spectral data is consistant with **215** being a diterpene derivative.. A close analysis of the ^{1}H [δ_H 3.66 m, (1H, d, *J*=11.0 Hz, Ha-17), 3.78 (1H, d, *J*=11.0 Hz, Hb-17), 3.66 (3H, s, OCH_3), 2.03 (1H, m,H-13), 1.79 (1H, m, Ha-1), 1.63 (1H, m, Hb-1), 1.03 (1H, dd, *J*=12.0 Hz, 2.1 Hz, H-5), 0.99 (1H, m, H-9), δ_H 1.15 (3H, s, H-18) and 0.83 (3H, s, H-20)], and ^{13}C NMR [δ_C 178.1 (C-19), 82.0 (C-16), 66.3 (C-17), 56.8 (C-5), 55.7 (C-9), 52.2 (OCH_3), 45.2 (C-13), 44.7 (C-8), 28.7 (C-18) and 15.3 (C-20)] data (Table 4.26) and comparison with literature (Batista *et al.*, 2007; Sebisubi *et al.*, 2010) revealed an *ent*-kaurene type diterpene (Midiwo *et al.*, 1997; Juma *et al.*, 2006). Careful investigation of ^{1}H, ^{13}C NMR, HSQC and HMBC spectra allowed the assignment of each and every proton and carbon signals. The downfield chemical shift values of oxygenation of C-16 (δ_C 82.0) and C-17 (δ_C 66.3) coupled with the molecular ion peak suggested the presence of an epoxide moiety in the molecule.

The ^{13}C NMR spectrum displayed twenty one carbons including a carbonyl C-19 (δ_C 178.1) and a methoxy C-18-OCH_3 (δ_C 52.2) of a methyl ester group. HMBC correlation of the methoxy protons (δ_H 3.66) with the carbonyl C-19 (δ_C 178.1) was in agreement with an ester functionality at C-19. In addition, HMBC correlation of the methoxy protons CH_3O-19 (δ_C 3.66) with the carbonyl C-19 (δ_C 178.1) coupled with that of the methylic protons CH_3-18 (δ 1.15) with the same carbonyl confirmed that a methyl ester was located either on C-19. The relative configurations of the stereocenters of the compound **215** at C-4, C-8, C-9, C-13, C-16 were established base on comparison with literature (Batista *et al.*, 2007). The structure of **215** ($C_{21}H_{34}O_3$) which is isolated for the first time in nature from the genus *Psiadia,* was determined to be methyl-16α,17-epoxy-*ent*-kauran-19-oate (Batista *et al.*, 2007; Hueso *et al.*, 2010, Batista *et al.*, 2013).

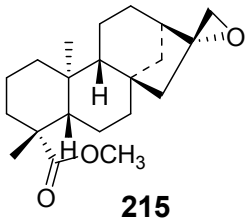

215

4.3.1.2.3 16α, 17-Dihydroxy-*ent*-kauran-20-oic Acid (216)

Compound **216** was isolated as a white solid (mp 205-207°C). The molecular formula $C_{20}H_{32}O_4$ was suggested based on the ^1H and ^{13}C NMR data (Table 4.27) and comparison with literature report (Midiwo *et al.*, 1997). The ^1H and ^{13}C NMR data indicated that this compound is an *ent*-kaurene type diterpene with two hydroxy and a carboxylic substituents (Table 4.27). The two hydroxy groups were placed at C-16 (δ_C 80.8) and C-17 C-17 (δ_C 65.6) based on the HSQC spectrum which showed that it was connected to a quaternary carbon C-16. The HMBC correlation of H_2-17 (δ_H 3.57; 3.72) with C-15 (δ_C 53.4) and C-1 (δ_C 44.9) indicated that the second hydroxy group is located at C-17 (δ_C 65.6) HMBC correlation of H2-17 with C-13, C-15 and C-16. The stereochemistry at C-5, C-8, C-9, C-10 (Bruno-Colmenarez *et al.*, 2011) and C-13 (Midiwo *et al.*, 1997) were determined based on comparison of the NMR data with literature and NOESY spectrum which showed correlation of H_2-17 (δ_H 3.57; 3.72) with H-13 (δ_H 1.90) and that of H-14 (δ_H 1.51; 2.20) with OH-16. The gross structure of **216** was the same as the compound previously reported (Midiwo *et al.*, 1997). The NOESY correlation of H_2-17 with H-9 suggested that OH-16 is α-oriented. Based on this information, compound **216** was identified as 16α,17-dihydroxy-*ent*-kauran-20-oic acid. This compound was previously isolated from the same plant (Midiwo *et al.*, 1997).

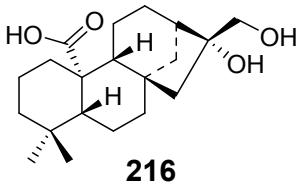

216

Table 4.027: ^{1}H (800 MHz) and ^{13}C (200 MHz) NMR Data of 216 in $CDCl_3$

Position	δc	Type	δ_H (mult., *J* in Hz)	HMBC (H→C)
1	39.4	CH_2	1.99 (ddd, *J*=12.9, 12.9, 3.6)	C-2, C-9, C-10
			2.45 (ddd, *J*=12.8, 3.3, 1.7)	-
2	20.4	CH_2	1.55 (m)	C-4, C-10
			1.51 (brs)	C-1, C-3, C-4
3	41.8	CH_2	1.55 (m)	C-2, C-4, C-5, C-10, C-18
			1.64 (m)	C-2, C-4, C-5
4	33.6	C	/	-
5	56.6	CH	1.04 (dd, *J*=12.3, 2.3)	C-4, C-6, C-9, C-10, C-18, C-19
6	20.6	CH_2	1.49 (m)	C-7, C-5, C-10
			2.42 (m)	C-5, C-8, C-10
7	42.3	CH_2	1.23 (ddd, *J*=13.3, 13.4, 3.3)	C-5, C-6, C-8, C-14, C-15
			1.38 (m)	C-8, C-9, C-13, C-15
8	48.1	C	-	-
9	54.8	CH	1.29 (m)	C-10, C-11, C-12, C-15, C-20,
10	44.6	C	-	-
11	18.4	CH_2	1.64 (m)	C-5, C-8, C-9, C-12, C-14
			2.02 (dd, *J*=15.2, 6.6)	C-8, C-12, C-13
12	24.4	CH_2	1.44 (m)	C-9, C-11, C-13, C-14, C-16
			1.49 (m)	C-9, C-11, C-13, C-14, C-16
13	44.9	CH	1.90 (m)	C-7, C-8, C-11, C-15, C-16
14	35.2	CH_2	1.51 (m)	C-7, C-8, C-9, C-12, C-13,
			2.2 (m)	C-7, C-8, C-9, C-12
15	53.4	CH_2	1.49 (m)	C-7, C-9, C-14, C-17
16	80.8	C	-	-
17	65.6	CH_2	3.57 (d, *J*=10.6)	C-13, C-15, C-16
			3.72 (d, *J*=9.2)	C-13, C-15, C-16
18	22.0	CH_3	0.84 (s)	C-3, C-4, C-5, C-19
19	32.7	CH_3	0.91 (s)	C-3, C-5, C-18
20	177.1	C	-	-

4.3.1.2.4 18,19-Dihydroxy-*ent*-kaur-16-en-2-one (217)

The ESIMS (molecular ion $[M+H]^+$ peak *m/z* 319.3), ^{1}H and ^{13}C NMR data (Table 4.28) of compound **217** suggested a molecular formula $C_{20}H_{30}O_3$. The ^{13}C NMR spectrum (Table 4.28) exhibited signals for 20 carbons which include two typical olefinic carbons [C-16 (δ_C

155.1) and C-17 (δ_C 102.8)] of an *ent*-kaurene type diterpene with two hydroxy (δ_C 66.8 and 63.5) and carbonyl (δ_C 210.4) substituents. Only one methyl group (C-20) was observed in the ^{1}H NMR spectrum (δ_H 1.08). This assignment was based on the HMBC spectrum which showed correlation of the Me-20 protons with C-5 (δ_C 47.8). This indicated that the remaining two methyl groups, C-18 (δ_C 66.8) and C-19 (δ_C 63.5), expected in the kaurene skeleton are substituted with hydroxy groups. In agreement with this, the HMBC spectrum showed correlation of CH_2-18 (δ_H 66.8) and CH_2-19 (δ_H 63.5) with C-4 (δ_C 49.7). The deshielded chemical shift of C-1 and C-3 indicated the placement of the carbonyl at C-2 (δ_C 210.4). This compound is levorotatory ($[\alpha]_D^{20}$ − 93) consistent with it being *ent*-kaurene diterpene (Midiwo *et al.*, 1997). Therefore, compound **217** was identified as 18,19-dihydroxy-*ent*-kaur-16-en-2-one.

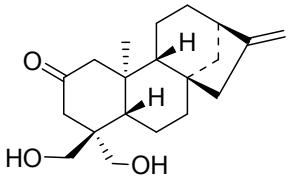

217

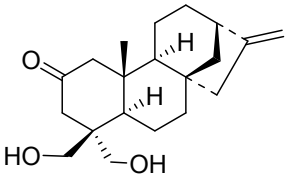

218

Table 4.28: ^{1}H (800 MHz) and ^{13}C (200 MHz) NMR Data of 217 and 218 in Acetone-d_6

Position	**217**			**218**		
	δc	δ_H (mult., *J* in Hz)	HMBC (H→C)	δc	δ_H (mult., *J* in Hz)	HMBC (H→C)
1	55.4	1.99 (m)	C-2, C-9, C-10	55.4	1.98 (m)	C-9, C-10
		2.45 (m)	-		2.44 (m)	-
2	210.4	-	-	210.5	-	-
3	43.7	2.65 (m)	C-2, C-18, C-5, C-10	43.3	2.62 (m)	C-18, C-5, C-10
		2.65 (m)	C-2, C-4, C-5		2.62 (m)	C-2, C-5
4	49.7	-	-	49.8	-	-
5	47.8	1.93 (dd, *J*=12.3, 2.3)	C-7, C-10, C-4, C-9, C-19	47.8	1.92 (dd, *J*=12.3, 2.3)	C-7, C-10, C-4, C-9, C-19
6	20.4	1.54 (m)	C-7, C-10, C-5	20.3	1.50 (m)	C-10, C-5
		1.79 (m)	C-10, C-8, C-5		1.79 (m)	C-10, C-8, C-5
7	44.0	2.42 (m)	C-6, C-14, C-5, C-15	44.1	2.44 (m)	C-6, C-14, C-5, C-15
8	42.9	-	-	42.9	-	-
9	54.7	1.40 (m)	C-8, C-11, C-6, C-12, C-7,	54.7	1.50 (m)	C-8, C-11, C-6, C-12, C-7,
10	44.1	-	-	44.1	-	-
11	18.2	1.69 (m)	C-12, C-5, C-9, C-8	18.3	1.69 (m)	C-5, C-9, C-8
		1.54 (m)	C-12, C-13, C-8		1.52 (m)	C-12, C-13, C-8
12	38.9	1.14 (m)	C-14, C-13, C-9, C-16	38.9	1.21 (m)	C-14, C-13, C-9
		1.99 (m)	C-14, C-13, C-9, C-16		1.98 (m)	C-14, C-13, C-9, C-16
13	32.7	1.70 (m)	C-11, C-12, C-7, C-8, C-15	32.7	1.69 (m)	C-12, C-7, C-8, C-15
14	40.5	1.48 (m)	C-12, C-7,C-8, C-9	40.5	1.50 (m)	C-7,C-8, C-9
		1.60 (m)	C-7, C-13, C-8, C-9		1.60 (m)	C-7, C-13, C-8, C-9
15	48.5	1.93 (m)	C-7, C-14, C-9, C-17	48.5	1.92 (m)	C-14, C-9, C-17
16	155.1	-	-	155.1	-	-

Table. 4.28 continued

Position	217			218		
	δc	δ_H (mult., *J* in Hz)		δc	δ_H (mult., *J* in Hz)	
17	102.8	4.82 (m)	C-13, C-16, C-15	102.8	4.82 (m)	C-13, C-16, C-15
		4.75 (d, *J*= 1.5)	C-13, C-16		4.75 (d, *J*= 1.5)	C-13, C-16
18	66.8	3.55 (m)	C-3, C-5	66.8	3.54 (m)	C-3, C-5
		3.62 (m)	C-3, C-5		3.62 (m)	C-3, C-5
19	63.5	3.55 (m)	C-3, C-4	63.4	3.55 (m)	C-3, C-4
		3.70 (m)	C-3, C-4		3.72 (m)	C-3, C-4
20	18.2	1.08 (3H, s)	C-1, C-9	18.2	1.08 (3H, s)	C-1, C-9

4.3.1.2.5 18,19-Dihydroxy-normal-kaur-16-en-2-one (218)

The ^{13}C NMR data (Table 4.28) of compound **218** was similar to that of **217** having two hydroxyl (δ_C 66.8 and δ_C 63.4). and a carbonyl (δ_C 210.4) substituent on a kaur-16-ene skeleton. Its ESIMS (molecular ion $[M+H]^+$ peak *m/z* 319.5) and ^1H and ^{13}C NMR data (Table 4.28) suggested a molecular formula $C_{20}H_{30}O_3$. The ^{13}C NMR data (Table 4.28) of **218** exhibited signals for 20 carbons of which two typical olefinic carbons [C-16 (δ_C 155.1) and C-17 (δ_C 102.8)] consistent with kaurene type diterpene. The placement of the only methyl group (δ_H 1.08 and 6 δ_C 18.2) at C-20 of this kaurene diterpene was established on the basis of HMBC correlation of this methyl protons (δ_H 1.08, CH_3-20) with C-5 (δ_C 47.8). The two hydroxy groups were then placed at C-18 (δ_C 66.8) and C-19 (δ_C 63.4) as in compound **217**. The deshielded chemical shift of C-1 and C-3 indicated the placement of the carbonyl at C-2 (δ_C 210.4), again as in compound **217** indicating that compounds **218** has identical gross structure as in **217**. Furthermore the NOESY spectrum (Table 41) showed that the relative configuration is the same as in compound **217**. Whereas compound **217** (which is ent-kaurene diterpene) is levorotatory (Midiwo *et al.,* 1997), compound **218** is dextrorotatory, $[\alpha]_D^{20}$ + 28, suggesting that compound **218** is a normal-kaurene diterpene, which is. is an enantiomer of **217**. Therefore, compound **218** was characterized as 18,19-dihydroxy-normal-kaur-16-en-2-one.

4.3.1.2.6 Compounds 219a, 219b and 219c

Compounds **219a**, **219b** and **219c** were minor compounds in a sample containing compound **217** and **218**. Upon X-ray analysis (Figure 4.4) of this sample, compounds **219a**, **219b** and **219c** were identified and the absolute configuration determined together with **217** and **218**.

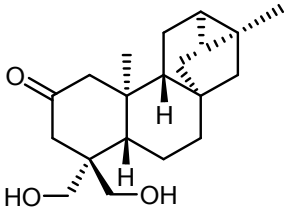

219a

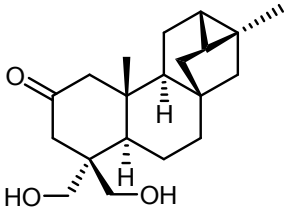

219b

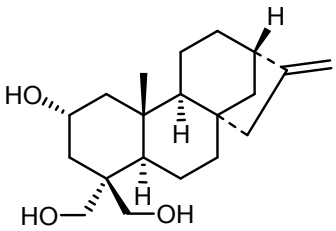

219c

4.3.1.3 Flavonoids

Two flavones (**220** and **221**) were isolated from the leaves extract of *Psiadia punctulata*. The same compounds were also isolated from the stem bark extract of the plant.

4.3.1.3.1 5-Hydroxy-7,2',3',4',5'-pentamethoxyflavone (220)

Compound **220** was isolated as a yellow solid. Based on the ^{1}H and ^{13}C NMR spectra as well as the LC-MS, which indicated $[M+H]^{+}$ at *m/z* 389.6, the molecular formula $C_{20}H_{20}O_8$ was suggested for this compound. The ^{1}H (δ_H 6.88 for H-3) and ^{13}C (δ_C 110.1 for C-3, and 182.7 for C-4) NMR data (Table 4.29) indicated that the compound is a flavone derivative (Juma *et al.*, 2001). The HMBC correlation of H-3 with C-2, C-4a, C-1' on one hand, and H-5 with C-4a and C-8 on the other hand, further support a flavone moiety. Three aromatic oxygenated carbon signals δ_C 162.5 (C-5), δ_C 164.8 (C-7), δ_C 158.0 (C-8a) in A-ring is consistent with disubstitution at C-5 (OH) and C-7 with two aromatic protons, H-6 (δ_H 6.38) and H-8 (δ_H 6.45) observed in the ^{1}H NMR spectrum (Table 4.29). In B-ring, the presence of four oxygenated carbon atoms were observed *vis* δ_C 147.7 (C-2'), δ_C 147.4 (C-3'), δ_C 149.6 (C-4') and δ_C 146.1 (C-5') in the ^{13}C NMR spectrum, leaving H-6' (δ_H 7.18) the only proton in this ring. Furthermore, there was a presence of five methoxy groups (δ_H 3.99 (OCH_3-7), δ_H 3.96 (OCH_3-2') δ_H 3.92 (OCH_3-3') δ_H 3.88 (OCH_3-4' δ_H 3.88 (CH_3-5'). Based on this data and comparison with the data published by Juma *et al.*, (2001), compound **220** was identified as 5-hydroxy-7,2',3',4',5'-pentamethoxyflavone.

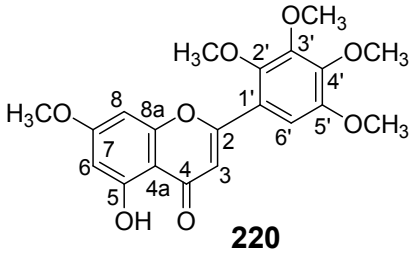

220

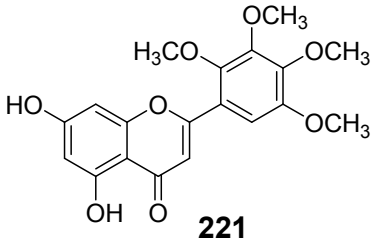

221

Table 4.29: ^{1}H (800 MHz) and ^{13}C (200 MHz) NMR Data of 220 and 221 in $CDCl_3$

Position	220				221			
	δ_C	Type	δ_H (mult., *J* in Hz)	HMBC	δ_C	Type	δ_H (mult., *J* in Hz)	HMBC
2	161.7	C	-	-	162.2	C	-	-
3	110.1	CH	6.88 (s)	C-2, C-1', C-4a	109.4	CH	6.77 (s)	C-2, C-1', C-4a
4	182.7	C	-	-	182.6	C	-	-
4a	105.6	C	-	-	104.8	C	-	-
5	162.2	C	-	-	162.0	C	-	-
6	97.9	CH	6.38 (d, *J*=2.3)	C-4a, C-8	98.7	CH	6.28 (*d*, *J*=2.1)	C-4a, C-8
7	165.5	C	-	-	163.6	C	-	-
8	92.6	CH	6.45 (d, *J*=2.2)	C-4a, C-6. C-8	94.0	CH	6.52 (d *J*=2.1)	C-4a, C-6. C-8
8a	157.9	C	-	-	158.2	C	-	-
1'	119.8	C	-	-	119.9	C	-	-
2'	147.7	C	-	-	147.8	C	-	-
3'	147.4	C	-	-	146.9	C	-	-
4'	149.5	C	-	-	149.8	C	-	-
5'	146.1	C	-	-	146.1	C	-	-
6'	106.3	CH	7.02 (s)	C-2, C-1', C-4, C-5	106.8	CH	7.17 (s)	C-2, C-1', C-4, C-5
2'-OCH_3	61.4	CH_3	3.99 (s)	C-2'	61.0	CH_3	3.94 (s)	C-2'
3'-OCH_3	61.3	CH_3	3.96 (s)	C-3'	60.9	CH_3	3.96 (s)	C-3'
4'-OCH_3	61.3	CH_3	3.92 (s)	C4'	60.6	CH_3	3.90 (s)	C-4'
5'-OCH_3	56.4	CH_3	3.88 (s)	C-5'	56.1	CH_3	3.87 (s)	C-5.
7-OCH_3	55.8	CH_3	3.88 (s)	C-7	-	CH_3	-	-

4.3.1.3.2 5,7-Dihydroxy-2',3',4',5'-tetra-methoxyflavone (221)

Compound **221** was isolated as a yellow amorphous solid. ESIMS molecular ion peak $[M+H]^+$ at *m/z* 389.6 together with the ^1H and ^{13}C NMR spectra is in agreement with the molecular formula $C_{20}H_{20}O_8$ for this compound. The ^1H and ^{13}C NMR data (Table 4.29) was similar to that of **220**; the only difference was that **221** had a total of four methoxy groups (instead of five as observed in **220**). This compound has been isolated from the same plant (Juma *et al.*, 2001) and named 5,7-dihydroxy-2',3',4',5'-tetra-methoxyflavone. The Supporting data for this claims include the presence in ^{13}C NMR spectrum of a carbonyl signal at δ_C 182.6 (C-3), three aromatic oxygenated carbon signals δ_C 162.0 (C-5), δ_C 163.6 (C-7), δ_C 158.2 (C-8a) on A-ring, and four other oxygenated aromatic carbons signals at δ_C 147.7 (C-2'), δ_C 147.4 (C-3'), δ_C 149.6 (C-4') and δ_C 146.1 (C-5') on B-ring. In addition, four ^1H NMR signals were observed at δ_H 6.77 (H-3), δ_H 6.28 (H-6), δ_H 6.52 (H-8) and δ_H 7.17 (H-6'). In comparison with compound **220**, the placement of the four methoxy groups (δ_H 3.99 (CH_3-7), δ_H 3.96 (CH_3-2') δ_H 3.92 (CH_3-3') δ_H 3.88 (CH_3-4' δ_H 3.88 (CH_3-5') was established by detailed NMR analysis and comparison with literature (Juma *et al.*, 2001). The presence of Hydrogen bonding in ^1H NMR spectrum suggested that one of the two hydroxy groups is located at C-5. Additionally, there was no HMBC correlation of any methoxy protons with C-7 and this also revealed that the hydroxy group is placed at C-7. Thus, compound **221** was identified as 5,7-dihydroxy-2',3',4',5'-tetra-methoxy-flavone (Juma *et al.*, 2001).

4.3.1.4 Fatty Acid Derivatives

Fatty acid derivatives (**222-224**) were isolated and characterised from the leaves extract of *Psiadia punctulata*.

4.3.1.4.1 2'-Hydroxyethyl tetradecanoate (222)

Compound **222** was isolated as a white amorphous solid from the leaves extract of *Psiadia punctulata.* The ^1H NMR and ^{13}C NMR spectral data (Table 4.30) indicated that is an ester of a fatty acid (Batovska *et al.*, 2004). The ^1H NMR revealed the presence of methyl protons at δ_H 0.92 (H-14) and four oxymethyl protons at δ_H 4.15 (H-1' and H-2') of a fatty ester core

structure. From the ^{13}C NMR data (Table 4.30), a carbonyl, a methyl and thirteen methylene carbon atoms were identified. Comparison of the data with that reported for a similar compound (Batovska *et al.*, 2004), led to the identification of **222** as being 2'-hydroxyethyl tetradecanoate

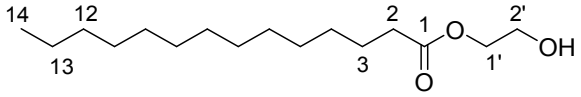

222

Table 4.30: ^{1}H (800 MHz) and ^{13}C (200 MHz) NMR Data of 222 in $CDCl_3$

Position	δ_C	Type	δ_H (mult., *J* in Hz)	HMBC
1	173.6	C	-	-
2	34.0	CH_2	2.37 (m)	C-1, C-3
3	24.9	CH_2	1.64 (m)	C-1, C-5
4-11	29.1-29.7	7xCH_2	1.30 (br s)	C-4, C-10
12	31.9	CH_2	1.30 (br s)	C-4-C-10
13	22.7	CH_2	1.31 (m)	C-4-C-10
14	13.9	CH_2	0.92 (t, *J*=7.0)	C-12, C-11
1’	68.3	CH_2	4.15 (m)	C-2’
2’	65.0	CH_3	4.15 (m)	C-1’

4.3.1.4.2 Lauric acid (223)

Compound **223** was isolated as white crystals. This compound is also a fatty acid derivative; thus broad signal at δ_H 1.28 (H-4/H-9) in ^{1}H NMR spectrum (Table 4.31) associated with the carbon signals at δ_C 29.7-29.1 (C4-C9) in ^{13}C NMR spectrum are typical for an aliphatic carboxylic acid. This was supported by the carbonyl signal at δ_C 179.6 (C-1) and a terminal methyl proton at δ_H 0.90 (H-12). The HMBC correlation between H-2 and the carbonyl C-1 and that between H-12 and C-11 is in agreement with this compound being a n-C_{12} carboxylic acid. Comparison of the data with that reported in literature (Nitbani *et al.*, 2016) revealed that **223** was lauric acid.

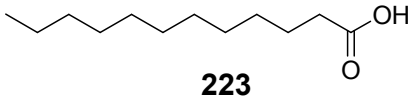

223

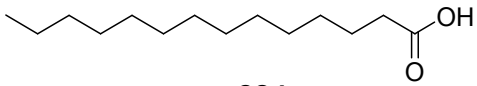

224

Table 4.31: ^{1}H (800 MHz) and ^{13}C (200 MHz) NMR Data of 223 and 224 in $CDCl_3$

Position	223			224		
	δ_C	δ_H (mult., *J* in Hz)	HMBC	δ_C	δ_H (mult., *J* in Hz)	HMBC
1	179.6	-	-	178.2	/	/
2	34.0	2.37 (m)	C-1, C-3	34.0	2.35 (m)	C-1, C-3
3	24.7	1.65 (m)	C-1, C-5	24.7	1.63 (m)	C-1, C-5
4-9	29.1-29.7	1.28 (br s)	C-4, C-10	29.1-29.6	1.25 (br s)	C-4, C-11
10	31.9	1.30 (br s)	C-4-C-10			
11	22.7	1.31 (m)	C-4-C-10			
12	14.1	0.90 (t, *J*=7.04)	C-12, C-11	31.9	1.25 (br s)	C-4-C-11, C-13, C-14
13	-	-	-	22.7	1.26 (m)	C-14, C-12
14	-	-	-	14.1	0.88 (t,*J*=2.4)	C-12

4.3.1.4.3 Myristic Acid (224)

Compound **224** was isolated as a white crystal and had similar NMR data (Table 4.31) as **223** with the only difference that **224** had 2 additional carbon signal overlapping with the signals of methyn carbons δ_C 29.7-29.1 (C4-C11). Fourteen carbon signals were observed in ^{13}C NMR spectrum; a triplet at δ_H 0.88 (H-14) in the ^{1}H NMR spectrum showed the presence of a terminal methyl proton δ_H 2.35 (H-2) coupling with a methyl group δ_H 1.63 (H-3). Comparison of the NMR data (Table 4.31) of this compound with that of a previous report (Keat *et al.*, 2010) allowed the identification of compound **224** as myristic acid.

4.3.2 Secondary Metabolites Isolated from Stem Bark of *Psiadia punctulata*

From the stem bark extract of *Psiadia punctulata*, four compounds (**225-228**) and two flavones (**220-221**) previously isolated from the leaves extract were isolated

4.3.2.1 *7α*-Hydroxy-*ent*-trachyloban-19-oic Acid (225)

Compound **225** was obtained as a white powder (mp 213-215°C) from the stem bark of *Psiadia punctulata.* The ^{1}H and ^{13}C NMR spectral data (Table 4.32) is in agreement with a molecular formula $C_{20}H_{30}O_3$. The MS and the NMR spectra (Table 4.32) further indicated a trachylobane skeleton (Midiwo *et al.*, 1997; Juma *et al.*, 2001). The ^{13}C NMR signal at δ_C 180.5 indicated the presence of an hydroxycarbonyl and hydroxy substituents. The presence of three methyl groups; CH_3-17 (δ_H 0.82, δ_C 21.7), CH_3-18 (δ_H 1.22, δ_C 28.8) and CH_3-20 (δ_H 0.89, δ_C 12.5) was evident from the ^{1}H NMR spectra. The NMR data was also similar to the one reported for 7*α*-hydroxy-*ent*-trachyloban-19-oic acid (Midiwo *et al.*, 1997). The HMBC correlation of the methyl protons at H_3-18 with the carbonyl indicated the placement of this carbonyl at C-19. The hydroxy group was placed at C-7 based on th HMBC correlation of H-7 with C-5, C-9, C-15 (Table 4.32). The stereochemistry at C-7 (Midiwo *et al.*, 1997) were determined based on the published data (Midiwo *et al.*, 1997) and NOESY spectrum where the NOE effect between H-7 and H-9 was observed. The levorotatory nature of this compound, $[\alpha]_D^{20}$ − 54, suggested an *ent*-trachylobane diterpene. Based on this, compound **225** was identified as *7α*-hydroxy-*ent*-trachyloban-19-oic acid.

1. 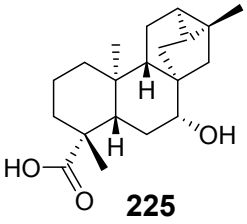

225

Table 4.32: ^{1}H (800 MHz) and ^{13}C (200 MHz) NMR Data of 225 in $CDCl_3$

Position	δ_C	Type	δ_H (mult., *J* in Hz)	HMBC (H→C)
1	37.9	CH_2	1.49 (ddd, *J*=11.0, 3.0, 3.0)	C-3, C-10, C-20
			1.49 (dd, *J*=11.0, 3.0, 3.0)	C-3, C-20
2	18.8	CH_2	0.83 (m)	C-4, C-10
			1.32 (br s)	C-4
3	32.6	CH_2	0.89 (m)	C-1
			2.09 (m)	C-1, C-5
4	42.3	C	-	-
5	56.7	CH	1.57 (m)	C-4, C-6, C-10
6	19.6	CH_2	1.37 (m)	C-8, C-10
7	67.8	CH	3.60 (m)	C-5, C-9, C-15
8	45.6	C	-	-
9	52.6	CH	1.01 (m)	C-8, C-12
10	39.3	C	-	-
11	18.6	CH_2	1.72 (m)	C-13
			1.91 (m)	C-13
12	32.6	CH	0.83 (m)	C-14, C-15
13	25.2	CH	1.50 (ddd, *J*=11.2, 3.0, 3.0)	C-8, C-11
14	22.1	CH_2	0.81 (m)	C-15
15	39.0	CH_2	1.82 (m)	C-12, C-20
16	19.9	C	-	-
17	21.7	CH_3	0.82 (s)	C-12, C-15
18	28.8	CH_3	1.22 (s)	C-3
19	180.5	C	-	-
20	12.5	CH_3	0.89 (s)	C-1, C-9, C-10

4.3.2.2 Friedelan-3*β*-ol (226)

The ^{13}C NMR spectrum (Table 4.33) and the multiplet at δ_H 0.94 (H-23) for oxymethine group in the ^{1}H NMR spectrum, revealed a friedelane-type pentacyclic triterpene skeleton (Morales-Serna *et al.*, 2011). This was further supported by the presence of the methyl proton signals in the ^{1}H NMR spectrum. The HMBC correlation of a methylene protons at δ_H 1.17 (H-30) with both C-3 (δ_C 72.7) and C-5 (δ_C 38.3) supported a friedelane-type triterpene skeleton. The HMBC correlations of H-29 (δ_H 0.94) with C-4 (δ_C 49.1) and C-6 (δ_C 41.7), and correlation of H_3-27 (δ_H 1.00) with C-16 (δ_C 36.1) and C-21 (δ_C 32.8) is consistent with this compound being a pentacyclic triterpene. Based on this data and comparison with literature (Morales-Serna *et al.*, 2011), compound **226** was identified as friedelan-3*β*-ol.

Table 4.33: ^{1}H (600 MHz) and ^{13}C (150 MHz) NMR Data of 226 and 227 in CD_2Cl_2

	226				227			
Position	δ_C		δ_H (mult., *J* in Hz)	HMBC	δ_C	Type	δ_H (mult., *J* in Hz)	HMBC
1	15.7	CH_2	1.43 (m)	C-3, C-5, C-8	37.1	CH_2	1.08 (m)	C-3, C-5, C-19
			1.54 (m)	C-5, C-3			1.81 (m)	C-3, C-5, C-9
2	35.0	CH_2	1.90 (m)	C-4, C-10	31.4	CH_2	1.40 (m)	C-4, C-10
							1.80 (m)	
3	72.7	CH	3.74 (m)	C-1, C-5	71.0	CH	3.60 (m)	C-1, C-5
4	49.1	CH	1.25 (s)	C-2,C-5,C-6	37.9	CH_2	1.08 (m)	C-2, C-6, C-10
							1.80 (m)	C-2, C-10
5	38.3	C	/	/	40.2	CH	1.40 (m	C-1, C-3, C-7
6	41.7	CH_2	1.29 (m)	C-10, C-24	29.6	CH_2	1.75 (m)	C-4, C-8, C-10
			1.73 (dt, *J*=8.4, 4.2)	C-8, C-24				
7	17.5	CH_2	1.36 (m)	C-5, C-9, C-14	117.4	CH	5.16 (m)	C-5, C-9, C-14
			1.47 (m)	C-5, C-14				
8	53.1	CH	1.28 (m)	C-13, C-11	139.5	C	/	/
9	37.1	C	/	/	49.4	CH	1.65 (m)	C-1, C-7, C-12
10	61.3	CH	0.90 (m)	C-2, C-6, C-11	34.2	C	/	/
11	35.5	CH_2	1.36 (m)	C-13, C-10	21.5	CH_2	1.48 (m)	C-10, C-13, C-8
			1.43 (m)	C-10				
12	30.6	CH_2	1.34 (m)	C-14, C-27	39.4	CH_2	2.01 (m)	C-9, C-14, C-18
13	37.8	C	/	/	43.2	C	/	/
14	39.7	C	/	/	55.1	CH	1.81 (m)	C-7,C-11, C-16

Table 4.33 continued

Position	226				227			
	δ_C			δ_C			δ_C	
15	32.1	CH_2	1.25 (m)	-	23.0	CH_2	1.40 (m)	C-8, C-13, C-17
			1.48 (m)	C-8, C-17, C-26			1.48 (m)	C-13, C-17
16	36.1	CH_2	1.34 (m)	C-14, C-22,	28.5	CH_2	1.27 (m)	C-13, C-14
				C-18, C-28			1.75 (m)	C-13, C-20
17	30.0	C	/	/	55.8	CH	1.27 (m)	C-15, C-18, C-21
18	42.8	CH	1.54 (m)	C-12, C-16	12.2	CH_3	0.80 (3H, s)	C-12. C-14
19	35.3	CH_2	-	-	13.0	CH_3	0.80 (3H, s)	C-1, C-5, C-9
20	28.2	C	/	/	40.8	CH	2.01 (d, *J*=3.1)	C-13, C-16
21	32.8	CH_2	1.48 (m)	C-17, C-30	21.4	CH_3	0.85 (3H, s)	C-17, C-22
22	39.3	CH_2	0.92 (m)	C-16, C-20, C-28	138.2	CH	5.16 (m)	C-17, C-21, C-24
			1.48 (m)	C-20, C-28				
23	11.6	CH_3	0.94 (br s)	C-3, C-5	129.4	CH	5.04 (m)	C-20, C-25, C-28
24	16.4	CH_3	0.96 (s)	C-4, C-5, C-6	51.2	CH	1.53 (m)	C-22, C-27
25	18.2	CH_3	1.01 (s)	C-10, C-11, C-8	31.8	CH	1.53 (m)	C-28, C-26
26	20.1	CH_3	0.99 (d, *J*=3.4)	C-8, C-13, C-15	21.1	CH_3	0.85 d (3H, d, *J*=3.6)	C-24, C-27
27	18.6	CH_3	1.00 (s)	C-12, C-13, C-14	18.9	CH_3	1.80 (3H, br s)	C-24, C-26
28	31.8	CH_3	0.99 (d, J=3.7)	C-16, C-22	25.4	CH_2	1.17 (m)	C-23, C-25
							1.40 (m)	C-23, C-25
29	35.2	CH_3	0.94 (br s)	C-19, C-21	12.2	CH_3	0.55 (3H, s)	C-24
30	32.3	CH_3	1.17 (s)	C-19, C-21	-	-	-	-

4.3.2.3 Spinasterol (227)

Compound **227** was purified as white crystals from the stem bark extract of *Psiadia punctulata*. The multiplet at δ_H 3.60 and a total number of 29 carbons deduced from ^1H and ^{13}C NMR spectral data (Table 4.33), respectively, were characteristic signals of a sterol skeleton. Six methyl proton signals [δ_H 0.80 (H-18), δ_H 0.80 (H-19), δ_H 0.85 (H-21), δ_H 0.85 (H-26), δ_H 1.80 (H-27) and δ_H 0.55 (H-29)] were observed in ^1H NMR spectrum. This information and comparison with published data (Billah *et al.*, 2013) led to identification of compound **227** as spinasterol.

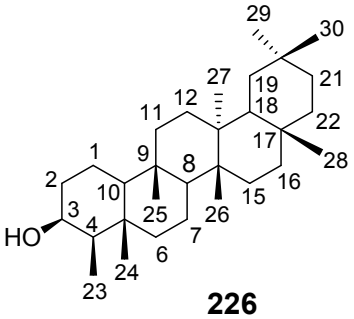

226

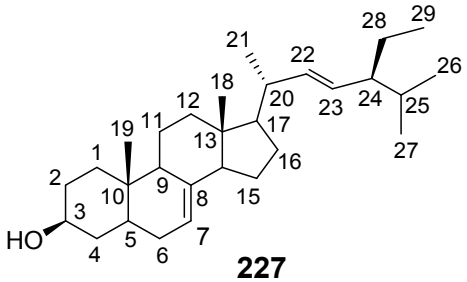

227

4.3.2.4 (*S*)-2,3-dihydroxypropyl tridecanoate (228)

Compound **228** was isolated as a white crystals from the stem bark extract of *Psiadia punctulata*. This compound is an ester of a fatty acid as evidenced from the ^1H and ^{13}C NMR data (Table 4.34). In addition, ^1H NMR spectrum revealed a methyl, a carbonyl and thirteen methyene two oxymethylene and an oxymethine signals suggested that the compound is an ester of a fatty acid. This was further supported by the ^1H NMR [at δ_H 0.88 (CH_3-13), 1.25 (H4-H10)] and ^{13}C NMR [at δ_C 29.7-29.1 (C4-C10)] spectral data (Table 4.34). The HMBC correlation of H-1' and H-2 with the carbonyl C-1 (δ_C 174.4) was also in agreement with the above information. The data was also comparable with literature report (Batovska *et al.*, 2004) and hence **228** was identified as (*S*)-2,3-dihydroxypropyl tridecanoate.

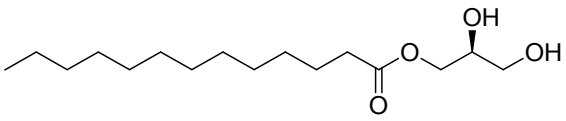

228

Table 4.34: ^{1}H (800 MHz) and ^{13}C (200 MHz) NMR Data of 228 in $CDCl_3$

Position	δ_C	Type	δ_H (mult., *J* in Hz)	HMBC
1	174.4	C	/	/
2	34.2	CH_2	2.35 (dd, *J*=7.57, 7.57)	C-1, C-3, C-4
3	24.9	CH_2	1.62 (m)	C-1, C-2C-4
4-10	29.7-29.1	CH_2	1.25 (br s)	C-4, C-10
11	31.9	CH_2	1.25 (br s)	C-4-C-10
12	22.7	CH_2	1.26 (br s)	C-4-C-10
13	14.1	CH_2	0.88 (t, *J*=7.1)	C-12, C-11
1’	65.2	CH_2	4.15 (dd, *J*=11.6, 6.2)	C-1, C-2’, C-3’
			4.21 (dd, *J*=11.6, 4.5)	C-1, C-2’, C-3’
2’	70.3	CH	3.93 (m)	C-1’, C-3’
3’	63.3	CH_2	3.60 (dd, *J*=11.5, 5.8)	C-1’, C-2’
			3.70 (dd, *J*=11.5, 4.8)	C-1’, C-2’

5-Hydroxy-7,2',3',4',5'-pentamethoxy flavone (**220)** and 5,7-dihydroxy-2',3',4',5'-tetramethoxy-flavone (**221**) were also isolated from the stem bark of this plant.

4.3.3. Secondary Metabolites Isolated from the Roots of *Psiadia punctulata*

Six compounds (**220**, **229-233**) were isolated from the roots extract of *Psiadia punctulata*. Except for compound **220**, all of these are being reported for the first time from this plant.

4.3.3.1 *Ent*-trachylobane-2*α*,6*β*,18,19-tetraol (229)

Compound **229** was obtained as colourless crystals, and was assigned a molecular formula $C_{20}H_{32}O_3$ based on ESIMS analysis ($[M+H]^+$ at *m/z*: 337.2) and ^{13}C NMR data (Table 4.35). The ^{13}C NMR spectrum (Table 4.35) was indicative of a trachylobane diterpene skeleton, with four hydroxy groups C-2 (δ_C 64.4), C-6 (δ_C 66.7), C-18 (δ_C 67.8) and C-19 (δ_C 64.9). The ^{1}H NMR data displayed two methyl signals; Me-17 (δ_H 1.14) and Me-20 (δ_H 1.04). HMBC correlation of H-5 with the two oxymethylenic carbons showed that both C-18 (δ_C 67.8) and C-19 (δ_C 64.9) are oxymethylene groups. The placement of hydroxy group at C-2 (δ_C 64.4) was compatible with the HMBC correlation of H_2-1 with C-2. The NMR and MS data of compound **229** were identical to that of *ent*-trachylobane-*2β*,*6α*,18,19-tetraol which has been reported from the leaves of this plant (Juma *et al.*, 2006).

Table 4.35: ^{1}H (800 MHz) and ^{13}C (200 MHz) NMR Data of 229 and 230 in acetone-d_6

Position	229				230			
	δ_C	Type	δ_H (mult., *J* in Hz)	HMBC (H→C)	δ_C	Type	δ_H (mult., *J* in Hz)	HMBC (H→C)
1	46.9	CH_2	1.29 (m)	C-2, C-3, C-9, C-20	47.9	CH_2	2.07 (m)	C-9, C-20
			1.48 (dd, *J*=11.0, 11.8)	C-9, C-20			2.14 (m)	C-9, C-20
2	64.4	CH	3.94 (m)	-	210.5	C	-	-
3	33.0	CH_2	1.25 (m)	C-4, C-10	43.7	CH_2	2.39 (m)	C-4, C-10
			2.14 (m)	C-10			1.45 (m)	C-10
4	43.3	C	-	-	44.1	C	-	-
5	52.8	CH	1.25 (m)	C-1, C-3, C-4, C-5, C-7	55.5	CH	2.45 (m)	C-1, C-7
6	66.7	CH	3.94 (m)	C-4, C-8, C-10	20.4	CH_2	1.80 (br s)	C-4, C-8, C-10
7	36.7	CH_2	1.33 (m)	C-5, C-15	48.5	CH_2	2.07 (m)	C-5, C-15
			1.79 (m)	C-5, C-16			2.14 (m)	C-5, C-15
8	40.5	C	-	-	49.8	C	-	-
9	50.3	CH	1.27 (m)	C-1, C-7, C-12	52.2	CH	1.48 (m)	C-1, C-7, C-12
10	36.7	C	-	-	38.9	C	-	-
11	19.2	CH_2	1.74 (m)	C-8, C-10, C-13	18.7	CH_2	1.70 (m)	C-8, C-10, C-13
			1.14 (m)	C-8, C-10, C-13			1.53 (m)	C-8, C-10, C-13
12	19.7	CH	0.63 (m)	C-1, C-4, C-5, C-9	24.0	CH_2	-	-
13	24.1	CH	0.86 (dd, *J*=7.9, 2.9)	C-13, C-15	42.9	CH	1.53 (br s)	C-15
14	20.2	CH_2	0.64 (m)	C-9, C-15, C-16	40.5	CH_2	1.59 (m)	C-9, C-15, C-16
15	47.6	CH_2	1.40 m	C-7, C-12, C-14	54.7	CH_2	1.90 (m)	C-7, C-14
			1.65 (dd, *J*=12.9, 3.8)	C-7, C-12, C-14			2.11 (m)	C-7, C-14
16	33.6	C	-	-	156.1	C	-	-
17	19.9	CH_3	1.14 (3H, s)	C-12, C-4, C-5, C-7	102.9	CH_2	4.76 (br s)	C-13, C-15
							4.83 (m)	C-13, C-15

Table 4.35 continued

Position	229				230			
	δ_C	Type	δ_H (mult., *J* in Hz)	HMBC (H→C)	δ_C	Type	δ_H (mult., *J* in Hz)	HMBC (H→C)
18	67.8	CH_2	3.45 (m)	C-1, C-15	32.7	CH_3	1.15 (3H, s)	C-1, C-5
			3.94 (m)	C-12, C-15				
19	64.9	CH_2	3.64 (m)	C-3, C-4, C-5	28.4	CH_3	2.14 (3H, s)	C-3, C-5
			4.05 (m)	C-3, C-5				
20	16.2	CH_3	1.04 (s)	C-1, C-9	18.2	CH_3	1.09 (3H, s)	C-1, C-9

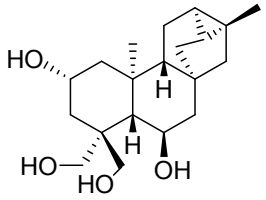

229

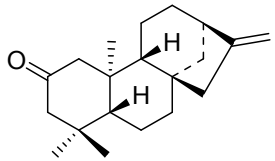

230

The stereochemistry at C-2 and C-6 were determined based on comparison with literature (Juma *et al.*, 2006) and NOESY spectrum. The specific rotation ($[\alpha]_D^{20}$ −54°) of this compound suggested an *ent*-trachylobane derivative. Therefore, compound **229** was identified as *ent*-trachylobane-2*α*,6*β*,18,19-tetraol.

4.3.3.2 *Ent*-kaur-16-en-2-one (230)

Compound **230** was isolated as a white powder from the CH_2Cl_2/MeOH extract of the roots of *Psiadia punctulata*. The NMR spectroscopic data (Table 4.35) are in agreement with the molecular formula $C_{20}H_{30}O$ assigned to **230**. The ^{1}H NMR spectrum revealed the presence of two olefinic protons; H-17a (δ_H 4.76) and 17b (δ_H 4.83) suggesting a double bond in the molecule. The ^{13}C NMR resonance of C-16 (δ_C 156.1) and C-17 (δ_C 152.9) were typical of an *ent*-kaurene skeleton. Three methyl groups Me-18 (δ_H 1.15), Me-19 (δ_H 2.14), Me-20 (δ_H 1.9) typical of a kaurene diterpenes located at C-18, C-19 and C-20 were observed in ^{1}H NMR spectrum. The HMBC correlation of methyl protons Me-18 (δ_H 1.17) with C-19 further support this claim. The HMBC correlation of H_2-1 with ketone C-2 (δ_C 210.5) suggested that the ketone is located at C-2. Furthermore, the levorotatory optical rotation ($[\alpha]_D^{20}$ −41°) nature of this compound indicated that this compound is an *ent*-kaurene diterpenoid. Therefore, compound **230** was characterised as *ent*-kaur-16-en-2-one. This compound has been previously isolated from *Guarea Kunthiana* (Garcez et 2004).

4.3.3.3 Friedelin (231)

Compound **231** was isolated as white crystals from the roots of *Psiadia punctulata*. The ^{13}C NMR spectrum summarized in Table 4.36 indicated the presence of thirty carbon signals of a triterpenoid. All the carbon atoms are sp^3, except the carbonyl, δ_C 213.3 (C-3). The ^{1}H NMR spectrum revealed the presence of eight methyls, [δ_H 0.88 (H-23), 0.71 (H-24), 0.86 (H-25), 1.01 (H-26), 1.04 (H-27), 1.18 (H-28), 0.95 (H-29) and 1.00 (H-30)] in this compound. Moreover, the carbon signal δ_C 6.82 (C-23) was typical to the pentacyclic triterpenoid skeleton, friedelane and this was evident from the HMBC correlation between H-23 and the carbonyl C-3, H-29 and C-20 between H-30 and C-20. A close comparison of the NMR data with that reported literature (Utami *et al.*, 2013) led to the identification of **231** as friedelin.

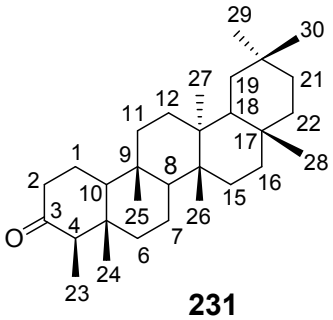

231

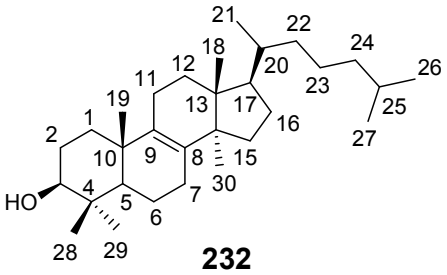

232

4.3.3.4 24,25-Dihydrolanost-8(9)-en-3*β*-ol (232)

Compound **232** was obtained as a white powder. The ^{1}H and ^{13}C NMR spectral data (Table 4.36) is in agreement with a molecular formula $C_{30}H_{52}O$. The ^{13}C NMR spectrum (Table 4.36) revealed 30 carbons including two olefinic carbons (C-8, δ_C 136.1; C-9, δ_C 139.9) and an oxygenated carbon (C-3, δ_C 79.0). Two of the olefinic carbons did not show correlation with proton signals in the HSQC spectum. This indicated a C8-C9 double bond location and suggesting a lanosterol skeleton. Based on this information and comparison of data with literature (Shingate *et al.*, 2013), compound **232** was identified as 24,25-dihydrolanost-8(9)-en-3*β*-ol.

Table 4.36: ^{1}H (600 MHz) and ^{13}C (150 MHz) NMR Data of 231 and 232 in CD_2Cl_2

Position	231				232			
	δ_C	Type	δ_H (mult., *J* in Hz)	HMBC	δ_C	Type	δ_H (mult., *J* in Hz)	HMBC
1	22.3	CH_2	1.69 (m)	C-3, C-5, C-8	38.9	CH_2	1.00 (m)	C-3, C-5, C-9
			1.97 (ddd, *J*=12.8, 7.4, 2.4)	C-3, C-5,			1.75 (m)	C-3, C-5, C-9
2	41.5	CH_2	2.30 (ddd, *J*=14.3, 7.2, 5.9)	C-4, C-10	27.4	CH_2	1.60 (m)	C-4, C-10
			2.39 (ddd, *J*=13.8, 5.0, 1.9)	C-4, C-10			1.67(m)	C-4, C-10
3	213.3	C	/	/	79.0	CH	3.23 (m)	C-1, C-5
4	58.2	CH	2.25 (q, *J*=6.7, 6.7, 6.7)	C-5, C-2, C-6	38.8	C	/	/
5	42.1	C	/	/	55.2	CH	0.71 (m)	C-7, C-3, C-19
6	41.3	CH_2	1.28 (m)	C-8, C-10, C-24	18.4	CH_2	1.40 (m)	C-4, C-8, C-10
			1.75 (ddd, *J*=13.5, 3.1, 3.1)	C-8, C-24			1.55 (m)	C-4, C-8, C-10
7	18.2	CH_2	1.37 (m)	C-5, C-9, C-14	26.4	CH_2	2.66 (m)	C-5, C-9
			1.48 (m)	C-5, C-14				
8	53.1	CH	1.55 (ddd, *J*=21.0, 12.1, 4.7)	C-6, C-13, C-11	136.1	C	/	/
9	37.4	C	/	/	139.9	C	/	/
10	59.5	CH	1.55 (m)	C-2, C-6, C-11	41.6	C	/	/
11	35.6		1.37 (m)	C-13, C-10	19.8	CH_2	1.93 (m)	C-10, C-13
							2.28 (m)	C-10, C-13
12	30.5		1.34 (m)	C-9, C-14, C-27	31.8	CH_2	1.30 (m)	C-10, C-14
13	39.6	C	/	/	49.8	C	/	/
14	38.3	C	/	/	42.0	C	/	/

Table 4.36 continued

	231				232			
Position	δ_C	Type	δ_H (mult., *J* in Hz)	HMBC	δ_C	Type	δ_H (mult., *J* in Hz)	HMBC
15	32.4	CH_2	1.28 (m)	C-8, C-17, C-26	41.7	CH_2	1.30 (m)	C-8, C-17
			1.48 (m)	C-8, C-17, C-26			1.67 (m)	C-17
16	35.9	CH_2	1.37 (m)	C-14, C-18, C-28	27.5	CH_2	2.14 (m)	C-14
			1.59 (m)	C-14, C-22, C-28			2.16 (m)	C-20
17	30.0	C	/	/	50.8	CH	1.30 (m)	C-15, C-21
18	42.8	CH	1.58 (m)	C-12, C-16, C-20	15.4	CH_3	0.79 (3H, s)	C-13, C-17
19	35.3	CH_2	1.21 (dd, *J*=13.7, 5.9)	C-13, C-21, C-29	19.1	CH_3	0.86 (3H, s)	C-3, C-5
			1.37 (m)	C-13, C-21, C-30				
20	28.2	C	/	/	49.3	CH	1.46 (m)	C-1, C-9
21	32.8	CH_2	1.28 (m)	C-17, C-30	16.2	CH_3	0.95 (3H, br s)	C-17, C-22
			1.48 (m)	C-17, C-27, C-29				
22	39.2	CH_2	0.93 (m)	C-16, C-20, C-28	33.5	CH_2	1.30 (m)	C-21, C-24
			1.48 (m)	C-16, C-20, C-28			1.54 (m	C-20
23	6.8	CH_3	0.88 (3H, s)	C-3, C-5	21.9	CH_2	1.30 (m)	C-21, C-24
							1.54 (m)	C-20
24	14.6	CH_3	0.71 (3H, s)	C-4, C-5, C-6	37.2	CH_2	/	/
25	17.9	CH_3	0.86 (3H, s)	C-10, C-11, C-8	24.0	CH	1.40 (m)	C-22
26	20.2	CH_3	1.01 (3H, s)	C-8, C-13, C-15	21.4	CH_3	1.00 (3H, s)	C-23
27	18.6	CH_3	1.04 (3H, s)	C-12, C-13, C-14	16.3	CH_3	0.86 (3H, s)	C-24
28	32.0	CH_3	1.18 (3H, s)	C-16, C-22	28.0	CH_3	1.00 (3H, s)	C-24
29	35.0	CH_3	0.95 (3H, s)	C-19, C-21	21.3	CH_3	0.95 (3H, br s)	C-3, C-5
30	31.7	CH_3	1.00 (3H, s)	C-19, C-21	14.9	CH_3	1.06 (3H, s)	C-3, C-4

4.3.3.5 (6*R*, 7*R*)-Bisabolone (233)

Compound **233** was isolated as white crystals from the roots of *Psiadia punctulata*. The ^{1}H NMR data (Table 4.37), revealed two olefinic proton signals at δ_H 5.86 (H-2) and δ_H 5.10 (H-9). Four methyl signals [δ_H 1.68 (12), δ_H 1.59 (12), δ_H 0.80 (12), δ_H 0.93 (12)] were also observed. The ^{13}C NMR spectrum revealed three signals [δ_H 201.1 (1), δ_H 127.1 (2) and δ_H 161.2 (3)] corresponding to an *αβ*-insaturated carbonyl moiety. The ^{13}C NMR spectrum revealed that this compound is a sesquiterpenoid having four olefinic carbons. The NOE correlation of H-6 with C-14 indicated their *syn*-orientation. Comparison with the data published previously (Mathur *et al.*, 1989), revealed that **233** is (6*R*, 7*R*)-Bisabolone.

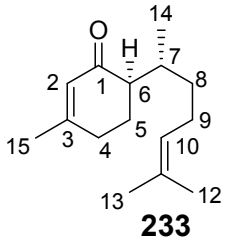

233

Table 4.37: ^{1}H (800 MHz) and ^{13}C NMR (200 MHz) Data of 233 in $CDCl_3$

Position	δ_C	Type	δ_H (mult., *J* in Hz)	HMBC
1	201.1	C	/	/
2	127.1	CH	5.86 (m)	C-1, C-4, C-6, C-15
3	161.2	C	/	/
4	30.9	CH_2	2.30 (m)	C-2, C-6, C-15
5	22.3	CH_2	1.77 (m)	C-1, C-3, C-7
			1.93 (br s)	C-1, C-3, C-7
6	49.8	CH	2.16 (ddd *J*=12.5, 4.2, 4.2)	C-2, C-4, C-8, C-14
7	17.16	CH	2.32 (m)	C-1, C-5, C-9
8	34.7	CH_2	1.29 (m)	C-6, C-14,C-10
9	26.0	CH_2	1.93 (br s)	C-7, C-11
10	124.5	CH	5.10 (m)	C-8, C-12, C-13
11	131.4	C	/	/
12	24.1	CH_3	1.68 (3H, s)	C-10, C-13
13	30.2	CH_3	1.59 (3H, s)	C-10, C-12
14	15.6	CH_3	0.80 (d *J*=6.8)	C-6, C-8
15	25.7	CH_3	1.93 (3H, br s)	C-2, C-4

5,7-Dihydroxy-2',3',4',5'-tetra-methoxyflavone (**221**) was also isolated from the roots part extract.

4.3.4 Summay of Compounds of *Psiadia punctulata*

Phytochemical investigation of *Psiadia punctula* led to the isolation of twenty two compounds among which three kaurene diterpenoids, seven trachylobane diterpenoids, two flavones, four triterpenes and one sesquiterpenoids. From this plant eight new diterpenoids (**205-209**, **214**, **219a** and **219b**) were elucidated.

4.3.5 Chemotaxonomic Significance on *Psiadia punctulata*

In this research, twenty nine compounds were isolated from *Psiadia punctulata* using chromatographic methods. To the best of our knowledge, this is the first time that **205-209**, **214**, **219b**, friedelin, 3*β*-hydroxy-friedelan, myristic acid and lauric acid are being reported from this genus. Various flavones, trachylobane and kaurene diterpenoids have been identified from the genus *Psiadia*. There have been different views on the taxonomic status of *Psiadia punctulata* and *Psiadia arabica*. Although both diterpenes and flavones have been reported from the two taxa, the particular type of class of compound varies in these taxa (Table 51). It is observed that flavones with high degree of oxygenation in A-ring are predominately found in *P. arabica*, while flavones with high oxygenated B-ring predominantly found in *Psiadia punctulata* (Table 4.38). Kaurene diterpenes predominantly found in *Psiadia arabica*, while p-coumarates, aliphatic acid, trachylobane diterpenoids predominantly found in *Psiadia punctulata*; In fact the is no p-coumarate or trachylobane diterpene that has been reported from the other *Psiadia* species including *P. arabica.* Therefore, trachylobane diterpenoids could be used as chemotaxonomic marker of *P. punctulata* to distinguish it from *P. arabica*.

It has been highlighted by Midiwo *et al*., (2005) that *Psiadia arabica* (Abou-Zaid *et al.*, 1991) and *P. punctulata* are two distinct species. The later contains flavonoids highly oxygenated on ring A and kaurene diterpenoids (Al-Yahya, 1986; El-Feraly *et al.*, 1990; Mossa *et al.*, 1992; El-Domiaty *et al.*, 1993), while the later contains flavonoids highly oxygenated on ring B, p-coumarate, kaurene diterpenoid, but also trachylobane diterpenoids

(Keriko *et al.*, 1997; Midiwo *et al.*, 1997; Midiwo *et al.*, 2001; Juma *et al.*, 2001; Juma *et al.*, 2006).

Table 4.38: Chemeotaxonommy comparison of *Psiadia punctulata* and *Psiadia arabica*

Psiadia punctulata	***Psiadia arabica***
Kaurene diterpenes	Kaurene diterpenes
Trachylobane diterpenes	Not reported
Coumarate	Not reported
Flavones with penta-oxygenation on ring B	Flavones with tri or di-oxygenation of ring B

4.4 Biological Activity of the Isolated Compounds from *Psiadia punctulata*

4.4.1 Antimicrobial Activity of *Psiadia punctulata*

When using the microbroth kinetic method, only 16α,17-dihydroxy-*ent*-kauran-20-oic acid (**216**) showed moderate activity against *E. coli*. Similarly, 5,7-dihydroxy-2',3',4',5'-tetramethoxyflavone (**221**) and **205** were moderately active against *S. aureus* (Table 4.39A). Among the compounds tested using the disc diffusion method, only the leaves (PPL), stem bark (PPB) and roots (PPR) crude extracts, 5,7-dihydroxy-2',3',4',5'-tetra-methoxy-flavone (**221**) have moderate activity against *S. aureus* and the leaves (PPL) crude extracts were active against *Microsporum gypseum* (Table 4.39B).

Table 4.39: Anti-microbial assay of *Psiadia punctulata*

A: Microbroth kinetic system

Bacterial strains	***E. Coli***			***S. aureus***		
Concentration (µg/ml)	160	80	40	160	80	40
Samples	% Inhibition			% Inhibition		
207	33	ne	ne	0.38	ne	ne
205	na	ne	ne	na	14	28
210	ne	5	ne	ne	ne	ne
211	ne	ne	ne	ne	ne	ne
216	49	29	30	ne	ne	ne
221	na	ne	6	na	40	44
226	na	ne	ne	na	ne	ne
227	na	ne	ne	na	ne	4
232	na	ne	ne	na	ne	5
Gentamicin	62	53	50	96	97	97
Erythromycin	41	7	ne	98	98	98

B. Agar disc diffusion method

					Bacterial strains			**Fungi**	
Compound	*S. a*	*E. c*	*M. g*	*T. m*	*C. p*	*C. a*	*A. f*	*A. n*	*C. n*
PPL	8	0	9.5	0	0	0	na	na	na
PPB	9	0	0	0	0	0	na	na	na
PPR	10	8	0	0	0	0	na	na	na
206	0	0	na	na	na	na	0	0	0
205	0	0	na	na	na	na	0	0	0
207	0	0	na	na	na	na	0	0	0
232	0	0	na	na	na	na	0	0	0
214	0	0	na	na	na	na	0	0	0
220	0	0	0	0	0	0	na	na	na
221	7	0	0	0	0	0	na	na	na
Gentamycin	20	13	-	-	-	-	-	-	-
Nystatin	-	-	13	10	16	13	15	13	18

Key: *S. a = Staphylococcus aureus* (ATCC 25923), *E. c = Escherichia. coli* (ATCC 25922), *M, g = Microsporum gypseum, T. m = Trichophyton mentagrophytes* (clinical isolates), *C. p = Candida parapsilosis* (ATCC 22019), *C. a = Candida albicans* (ATCC 90018), *A. f = Aspergilus flavus, A. n = Aspergilus niger* (environmental), *C. n = Cryptococcus neoformans*

(clinical), na = not assessed, ne = not effective, PPL=Leaves extracts of *Psiadia punctulata*, PPB=stem barks extracts of *P. punctulata*, PPR= roots extracts of *P. punctulata*

4.4.2 Cytotoxicity of *Psiadia punctulata*

The crude extracts from the leaves, roots and stem bark of *Psiadia punctulata* and some of the isolated compounds were evaluated for their inhibitory activity against the growth of two normal (human bronchial epithelial (BEAS-2B) and human hepatic (LO_2)) cell lines and four cancer (human prostate (DU-145), African green monkey kidney (Vero), adenocarcinomic human alveolar basal epithelial (A54) and human liver (Hep-G2)) cell lines. The results (Table 4.40) indicated that the leaves (PPL) and the stem bark (PPB) extracts were cytotoxic against Vero cell line exhibiting CC_{50} values of 2.3 ± 0.1 and 9.5 ± 0.1 µg/mL, respectively. Among the pure compounds tested, **210** was the most toxic against the Vero cell lines, exhibiting CC_{50} values of 36.0 ± 0.2 µM. This compound was also the most cytotoxic against DU-145 prostate cancer cell lines, having an CC_{50} value of 3.4 ± 0.1 µM. Compound **207** also showed strong activity against Hep-G2 human liver cancer (CC_{50} = 6.41 ± 0.2 µM) and significant activity against A549 adenocarcinomic human alveolar basal epithelial cancer (CC_{50} = 54.5 ± 3.7 µM), Vero African green monkey kidney cancer (CC_{50} = 49.2 ± 0.1 µM) and DU-145 prostate cancer (CC_{50} = 22.8 ± 0.2 µM) cell lines. PPB (CC_{50} = 14.5 ± 0.2 µM) and PPL (CC_{50} = 55.4 ± 0.1 µM) showed moderate cytotoxicity against DU-145 cell lines. Compound **221** showed moderate activity (CC_{50} = 68.7 ± 3.0 µM) against A549 cancer cell lines. Some kaurene and trachylobane diterpenes are known for their cytotoxicity (Block *et al.*, 2002; Soh *et al.*, 2013; Utami *et al.*, 2013) and anti-tumor effects (Pita *et al.*, 2012).

Table 4.40: Cytotoxicity of *Psiadia punctulata*

Samples	CC_{50} µM					
	Normal cell lines		Cancer cell lines			
	BEAS-2B	**LO_2**	**A549**	**Hep-G2**	**Vero**	**DU-145**
PPL*	-	-	-	-	2.3 ± 0.1	55.4 ± 0.1
PPB*	-	-	-	-	9.5 ± 0.1	14.5 ± 0.1
PPR*	-	-	-	-	>100	>100
206	-	-	-	-	>100	86.2 ± 0.1
207	>100	>100	54.5 ± 3.7	6.41 ± 0.2	49.2 ± 0.1	22.8 ± 0.2
208	>100	>100	>100	81.8 ± 2.3	>100	>100
209	92.0 ± 4.8	>100	>100	>100	-	-
218	>100	83.5 ± 2.9	65.1 ± 10.9	68.7 ± 2.4	-	-
217	66.2 ± 10.8	69.8 ± 1.1	52.1 ± 12.9	6.87 ± 0.3	-	-
210	>100	>100	>100	>100	36.0 ± 0.2	3.4 ± 0.1
211	64.1 ± 10.6	58.4 ± 3.8	18.1 ± 7.4	62.6 ± 1.5	52.9 ± 0.2	>100
220	70.3 ± 13.4	>100	>100	62.6 ± 2.1	-	-
221	>100	88.4 ± 1.3	68.7 ± 3.0	55.8 ± 9.7	>100	>100
216	>100	>100	>100	>100	-	-
229	>100	>100	>100	>100	-	-
212	>100	>100	>100	64.1 ± 2.3	-	-
229	90.2 ±1.9	>100	>100	>100	-	-

*CC_{50} in µg/mL for crude. PPL=Leaves extracts of *Psiadia punctulata*, PPB=stem barks extracts of *P. punctulata*, PPR= roots extracts of *P. punctulata*

4.4.3 Anti-inflammatory Activity of *Psiadia punctulata*

The anti-inflammatory activity of the constituent plant extracts and isolated compounds from *P. punctulata* at the concentration of 200 mg/kg bwt (body weight) were determined using indomethacin (10 mg/kg) as the standard drug. Results obtained from the experiment are summarized in Table 4.41 which revealed inhibition of carrageenan-induced inflammation in paw by crude extracts of all parts of the plant. In the group of rats treated with the standard drug, the paw volumes were reduced throughout the experiment as compared to the negative control. PPL and 5-hydroxy-7,2',3',4',5'-pentamethoxyflavone (**220**) exhibited a comparable

anti-inflammatory activity to that of the standard drug at the same dose of 200 mg/Kg body weght.

The significant inhibition of paw edema in rats treated with crude extracts of the plant suggested that they may contain biologically active compounds with anti-inflammatory effects. However, among the tested pure compounds, only **220** showed moderate anti-inflammatory activity. This imply the need for further phytochemical investigation of the different plant parts. In folk and modern medicine, the therapeutic benefits of medicinal plants is attributed to a synergic effect of different active constituents (Chindo *et al.*, 2003). It is evident that the present results support the traditional uses of this plant in the treatment of inflammatory conditions.

Table 4.41: Anti-inflammatory of *Psiadia punctulata*

Treatment/ Drug/sample	**Dose mg/kg**	**Carrageenan-induced oedema: in Paw volumes in mL (mean ± SD, n = 5)**				
		0 mn	60 min	120 min	180 min	240 min
PPL	200	0	1.06 ± 0.11	0.84 ± 0.07	1.12 ± 0.07	1.19 ± 0.04
PPB	200	0	0.99 ± 0.06	1.10 ± 0.05	1.19 ± 0.04	1.29 ± 0.07
PPR	200	0	1.12 ± 0.05	1.27 ± 0.07	0.72 ± 0.1	1.47 ± 0.1
207	200	0	1.19 ± 0.06	1.5 ± 0.09	1.54 ± 0.04	1.56 ± 0.04
210	200	0	1.26 ± 0.05	1.49 ± 0.08	1.58 ± 0.08	1.58 ± 0.02
220	200	0	1.14 ± 0.07	1.05 ± 0.24	1.43 ± 0.04	1.38 ± 0.08
221	200	0	1.23 ± 0.14	1.49 ± 0.08	1.57 ± 0.06	1.58 ± 0.12
Normal saline	-	0	1.29 ± 0.07	1.32 ± 0.19	1.57 ± 0.13	1.62 ± 0.08
Indomethacin	10	0	0.84 ± 0.01	0.95 ± 0.04	0.97 ± 0.01	1.03 ± 0.02

4.4.4 Oral Glucoce Tolerance Test of *Psiadia punctulata*

The results obtained in this experiment are summarized in Table 4.42. The fasting blood glucose was found to range from 105.25 ± 11.3 and 127.0 ± 12.8 mg/dL one hour after dosing the animals. The glucose was then administered orally and after 30 minutes, the blood glucose levels were found to increase to range from 156.7 ± 27.3 to 237.25 ± 25.3 mg/dL. At

this time point, the glucose levels were substantially greater in the rats treated with the isolated compounds and the crude extracts than with the standard drug Metformin.

The peak level of the blood sugar concentration observed in this experiment was 237.2 ± 25.3 mg/dL, and was reached after 30 minutes of administration of glucose in the rats group treated with compound **220**, 5-hydroxy-7,2',3',4',5'-pentamethoxyflavone (Figure 10). However, a significant decrease of the blood glucose level to 106.0 ± 8.8 mg/dL was found after 240 min of glucose administration in the same group, which was lower than that observed for the metformin group at the same timepoint (115.2 ± 7.7 mg/dL). On the other hand, all the isolated compounds, the crude extracts and the standard drug were found to decrease the concentration of glucose 90 minutes post glucose administration. *Ent*-16*β*,17-dihydroxy-*ent*-kauran-20-oic acid (**216**) was found to be the most active in lowering the blood glucose level as compared to the standard during the first hour of the experiment. At the second and fourth hour, compound **220** was the most active among the test compounds, showing activity superior to metformin at the given dose. The decrease of the blood sugar levels by these two compounds indicate their potential as hypoglycemic agents.

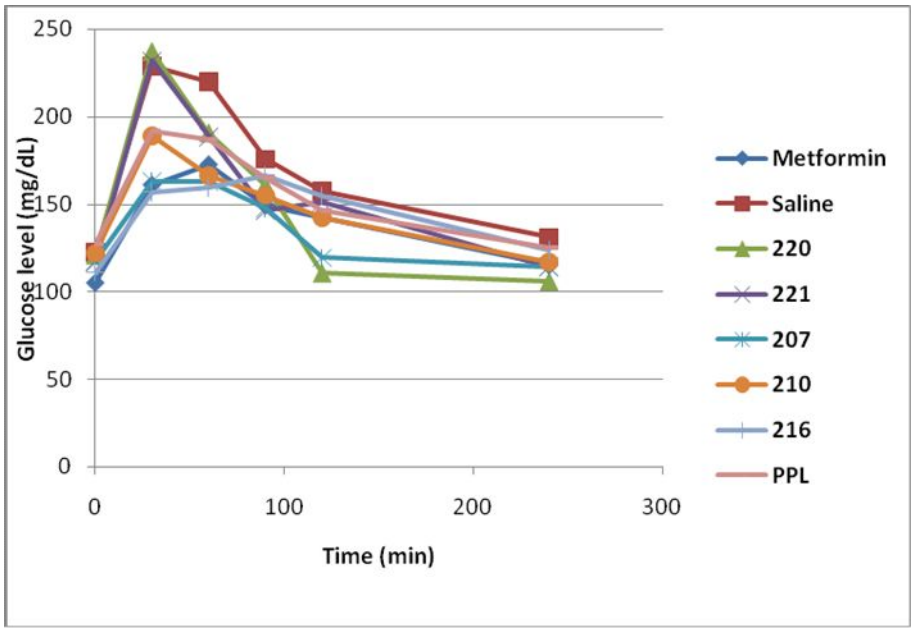

Figure 4.5: Blood Glucose Levels Reduction Graph of *Psiadia punctulata*

Table 4.42: Oral Glucose Tolerance Test (OGTT) of *Psiadia punctulata*

	Blood glucose level (mg/dL) at different times						
Group	**- 60**	**0**	**30 min**	**60 min**	**90 min**	**120 min**	**240 min**
220	121.0 ± 9.7	121.0 ± 14.1	237.2 ± 25.3	190.7 ± 28.2	161.0 ± 29.9	110.7 ± 15.0	106.0 ± 8.8
221	117.5 ± 9.9	117.2 ± 8.2	232.0 ± 47.4	188.7 ± 13.4	146.2± 21.4	151.5 ± 2.6	114.2 ± 12.2
207	107.7 ± 9.7	117.7 ± 11.2	163.0 ± 24.7	162.7 ± 16.5	148.0 ± 18.8	119.5 ± 16.8	114.2 ± 12.2
210	126.2 ± 11.9	122.2 ± 8.2	189.0 ± 17.1	166.2 ± 28.6	155.0 ± 15.7	142.5 ± 20.3	117.0 ± 9.7
216	112.7 ± 13.4	111.0 ± 8.0	156.7 ± 27.3	159.5 ± 24.4	166.5 ± 25.9	154.7 ± 17.3	123.7 ± 11.3
PPL	104.5 ± 12.1	127.0 ± 12.8	192.0 ± 31.7	187.0 ± 23.2	165.2 ± 15.7	146.5 ± 15.3	125.0 ± 12.3
Metformin	100.7 ± 14.2	105.25 ± 11.3	161.0 ± 25.2	172.5 ± 16.0	149.2 ± 19.6	142.0 ± 19.9	115.2 ± 7.7
dH_2O	112.7 ± 11.3	122.2 ± 10.1	229.0 ± 22.3	219.7 ± 25.7	175.7 ± 32.3	157.5 ± 14.3	131.0 ± 9.1

4.4.5 Antiplasmodial Activity of *Psiadia punctulata*

The antiplasmodial activity of the isolated compounds against D6 and 3D7 chloroquine sensitive-*Plasmodium falciparum* strains is summarized in Table 4.43. Compound **206** was the most active against 3D7 with IC_{50} values of 1.09 ± 0.02 μM; while compound **220** has a comparable activity against both D6 (IC_{50}= 4.01 ± 0.88 μM) and 3D7 (4.33 ± 0.63 μM) *P. falciparum* strains. Compound **207** (IC_{50} = 12.17 ± 0.27 μM) and **221** (IC_{50} = 14.31 ± 1.70 μM) were moderately active against D6 strains; however, both of the compounds did not show any activity against 3D7 strains. Compounds **205**, **206** and **214** had weak activity against D6 strains with the IC_{50} values ranging from 26.70 ± 1.56 (**214**) to 25.28 ± 0.40 (**205**). In general most of the tested compounds were ineffective against 3D7 strains except **206** and **220**. When tested against D6 strains, all compound were active except **215** which was not active against the same strains.

Table 4.43: Antiplasmodial Activity of *Psiadia punctulata*

Samples	IC_{50} (μM)	
	D6 *P. falciparum* strains	**3D7 *P. falciparum* strains**
205	25.28 ± 0.40	ne
206	26.37 ± 1.44	1.09 ± 0.02
207	12.17 ± 0.27	ne
214	26.70 ± 1.56	ne
215	ne	ne
220	4.01 ± 0.88	4.33 ± 0.63
221	14.31 ± 1.70	ne
Chloroquine	0.0086 ± 0.0013	0.0083 ± 0.0012
Mefloquine	0.0187 ± 0.0013	0.0275 ± 0.0018

Key: ne=not effective

4.5 Characterization of Secondary Metabolites Isolated from *Aspilia pluriseta* and *Aspilia mossambicensis*

Nine (**234-242**) *ent*-kaurene diterpenes of were isolated from the roots extract of *Aspilia pluriseta*. Furthermore, seven (**243-249**) additional compounds (three ent-kaurene diterpenes (**243-245**), three triterpene (**246-248**) and a sesquiterpene (**249**)) were isolated from the aerial part of *A. plurieta*. From the roots of *A. mossambicensis*, six (**236-238**, **250-252**) kaurene diterpenes and one triterpene (**253**) were isolated. The aerial part of *A. mossambicensis*

afforted four (**240**, **243**, **255**, **256**) kaurene diterpenoids, two triterpenoids (**247**, **254**) and cinamic acid (**257**).

4.5.1 Characterization of Compounds Isolated from Roots of *Aspilia pluriseta*

The roots extract of *Aspilia pluriseta* afforded nine kaurene diterpenes (**234**-**242**).

4.5.1.1 12*α*-Methoxy-*ent*-kaura-9(11),16-dien-19-oic Acid (234)

Compound **234**, $[\alpha]_D^{20}$ -88°, was isolated as a colorless crystal (m.p. 184-186 °C) from the CH_2Cl_2/MeOH (1:1) extract of the roots of *Aspilia pluriseta*. HRMS showed a $[M-H]^-$ ion peak at *m/z* = 329.2191, which is in agreement with the molecular formula $C_{21}H_{30}O_3$. The NMR spectra (Table 4.44) indicated that this compound is a kaurene diterpenoid (Souza *et al.,* 2015). The ^1H NMR spectrum further revealed the presence of three olefinic protons, namely H-11 (δ_H 5.30), H-17a (δ_H 4.84) and H-17b (δ_H 4.94), suggesting two double bonds. The ^{13}C NMR chemical shifts of C-16 (δ_C 152.9) and C-17 (δ_C 108.1) are typical of a terminal double bond in an *ent*-kaurene skeleton.

Table 4.44. ^1H (800 MHz) and ^{13}C (200 MHz) NMR Data of 234 ($CDCl_3$)

Position	δ_C Lit. [13]*	δ_C	δ_H, mult. (*J* in Hz)	HMBC (^2J, ^3J)
1	38.17	40.6	1.14 *ddd* (13.5, 9.5, 4.2)	C-2, C-3, C-10, C-20
			1.90 *ddd* (13.5, 3.5, 1.4)	C-2, C-3, C-10, C-20
2	18.35	20.0	1.43 *dddd* (14.2, 9.5, 3.9, 3.5)	C-1, C-3, C-4, C-5, C-10
			1.79 *ddddd* (14.2, 11.1, 4.2, 3.5, 1.4)	C-1, C-4, C-5
3	29.03	38.1	0.93 *ddd* (13.4, 11.1, 3.9)	C-1, C-2, C-4, C-18, C-19
			2.08 *ddd* (13.4, 3.5, 3.5)	C-1, C-4, C-5, C-7
4	43.43	44.6		
5	43.81	46.1	1.56 *dd*(11.1, 8.5)	C-4, C-7, C-9, C-10, C-18, C-19, C-20
6	20.07	18.3	1.82 *dddd* (14.2, 10.0, 8.5, 2.5)	C-3, C-4, C-5, C-7, C-10
			2.43 *dddd* (14.2, 11.1, 9.5, 3.5)	C-4, C-5, C-8
7	40.60	28.9	1.42 *ddd* (13.8, 3.5, 2.5)	C-5, C-6, C-8, C-9, C-15
			1.95 *ddd* (13.8, 10.0, 9.5)	C-6, C-8, C-9, C-14, C-15
8	44.66	43.4		
9	160.28	160.2		

Table 4.44 continued

Position	δ_C Lit. [13]*	δ_C	δ_H, mult. (*J* in Hz)	HMBC (^2J, ^3J)
10	38.94	38.9		
11	115.42	115.3	5.30 *dd* (4.3, 1.4)	C-8, C-9, C-10, C-12, C-13, C-15, C-20
12	81.79	81.7	3.38 *dd* (4.3, 2.9)	C-9, C-11, C-13, C-16, C-20, OCH_3-12
13	46.17	43.7	2.89 *dd* (2.9, 1.4)	C-10, C-11, C-12, C-15, C-16
14	40.60	40.5	1.31 *dd* (10.8, 4.3)	C-7, C-8, C-9, C-12, C-13, C-15
			1.58 *dd* (10.8, 2.5)	C-9, C-12, C-13, C-15, C-16
15	47.17	47.1	2.08 *dd* (15.4, 4.3)	C-7, C-8, C-9, C-16, C-17
			2.35 *dd* (15.4, 2.5)	C-7, C-9, C-13, C-14, C-16, C-17
16	153.00	152.9		
17	108.12	108.1	4.84 *dd* (3.0, 1.6)	C-12, C-13, C-15, C-16
			4.94 *dd* (3.0, 1.6)	C-12, C-13, C-15, C-16
18	28.22	28.2	1.17 *s*	C-3, C-4, C-5, C-8, C-19
19	182.98	183.2		
20	23.41	23.4	1.01 *s*	C-1, C-5, C-9, C-10
MeO-12	56.53	56.5	3.34 *s*	C-12

*$CDCl_3$ at 100 MHz (Ahmed *et al.,* 1991)

The second double bond was placed between C-9 (δ_C 160.2) and C-11 (δ_H5.30; δ_C115.3) by comparison of the NMR data with that of the literature [Ahmed *et al*., 1991, Li *et al*., 2016, Cai *et al*., 2017]. Signals indicating the presence of a methoxy (δ_H 3.34, δ_C56.5) and a carboxylic acid (δ_C183.2) substituent were observed. The HMBC correlations of CH_3-18 (δ_H 1.17), H-3 (δ_H 0.93) and H-5 (δ_H 1.56) with the carboxyl resonance C-19 (δ_C183.2) suggested the location of the carboxyl group (C-19) at C-4. Out of the three methyl groups expected in kaurene diterpenoid, only two, i.e. CH_3-18 (δ_H 1.17, δ_C 28.2) and CH_3-20 (δ_H 1.01, δ_C 23.4), were observed. This corroborated the suggestion of the third methyl group being oxidized to a carboxylic acid (C-19, δ_C183.2).The methoxy group OCH_3-12 (δ_H 3.34) showed HMBC correlation with C-12 (δ_C 81.7), whereas H-12 (δ_H 3.38) showed HMBC correlation with C-9 (δ_C 160.2), C-11 (δ_C 115.3), C-13 (δ_C 43.7), C-16 (δ_C 152.9) and, OCH_3-12 (δ_C 56.5). Furthermore, CH_3-20 (δ_H 1.01) showed HMBC correlation with C-1 (δ_C40.6), C-5 (δ_C46.1), the olefinic carbon C-9 (δ_C 160.2), and C-10 (δ_C 38.9). This confirmed that the second double bond in the molecule is located at C-9.

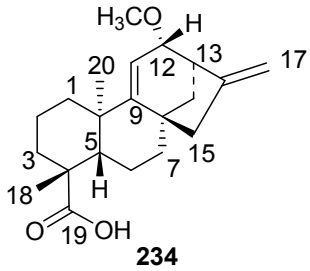

234

Moreover, the HMBC correlation of CH_2-14 (δ_H 1.31, 1.58) with a deshielded carbon C-12 (δ_C 81.7) is in agreement with OCH_3being connected to C-12. The above findings confirmed the identity of compound **234** as a C-12-methoxy substituted *ent*-kaur-9(11),16-dienoic acid derivative. The relative configuration at C-12 was deduced from the NOE of OCH_3-12 (δ_H 3.34) to H-13 (δ_H 2.89) (Figure 4.6), indicating them to

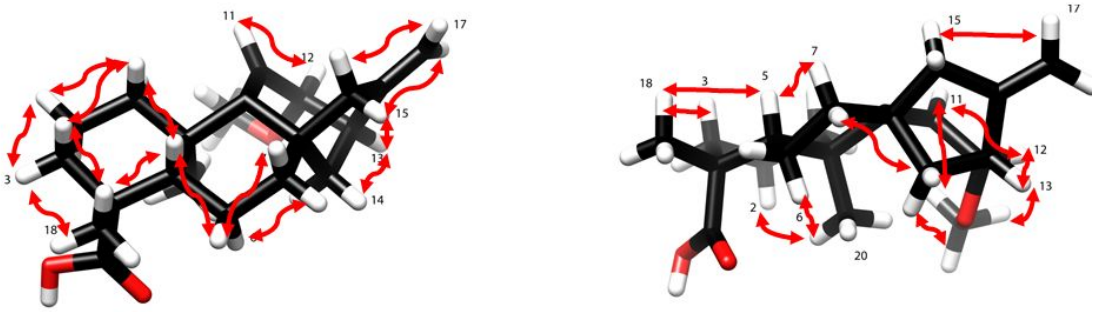

Figure 4.6: Some of the key NOE correlations observed for compound 234.

be syn-oriented, and hence OCH_3-12 to be *α*-oriented. It should be noted that H-12 (δ_H 3.38) also showed a weak NOE to H-13 (δ_H 2.89), which is expected in a strained ring system. The proposed configuration at C-12 is further corroborated by the NOE of H-12 (δ_H 3.38) with H-14b (δ_H1.58). The NOE of H-12 (δ_H 3.38 ppm) with H-17b (δ_H 4.94 ppm) supported H-12 to be *β*-oriented, and hence OCH_3-12 to be *α*-oriented. Based on the above spectroscopic evidences, compound **234**, 12*α*-methoxy-*ent*-kaur-9(11),16-dien-19-oic acid, was identified as (4*R*,4a*S*,6a*S*,9*R*,10*S*,11b*R*)-10-methoxy-4,11b-dimethyl-8-methylene-1,2,3,4,4a,5,6,7,8,9,10,11b-dodecahydro-6a,9-methanocyclohepta[*a*]naphthalene-4-carboxylic acid. This compound has previously been reported both as synthetic derivative (Ahmed *et al.,* 1991) and as natural product (Cai *et al.,* 2017; Li *et al.,* 2016). However, our NMR data assignment differsfrom that reported in the literature (Ahmed *et al.,* 1991) for its C-3 and C-7. The accuracy of the corrected assignment, given in Table 57a, is corroborated

by the HMBC correlations of H-3 and H-7 (Table 4.44), by the HSQC crosspeaks of H-3 (δ_H 0.93/2.08) to C-3 (δ_C 38.1) along with the TOCSY correlations of H-3 to H-1 (δ_H 1.14/1.90) and H-2 (δ_H 1.43/1.79), and by the HSQC crosspeaks of H-7 (δ_H 1.42/1.95) to C-7 (δ_C 28.9) along with the TOCSY correlations of H-7 to H-6 (δ_H 1.82/2.43) and H-5 (δ_H 1.56). Besides the compound having been reported earlier, it is unlikely to be an extraction artifact as the extraction (with CH_2Cl_2/MeOH, 1:1) has been performed at low temperature at neutral pH that does not promote formation of methyl ethers.

4.5.1.2 13*β*-Hydroxy-*ent*-kauran-19-oic acid (235)

Compound **235** was isolated from the root extract of *Aspilia pluriseta* as colourless crystal (mp 197-199 ºC). The molecular formula $C_{20}H_{32}O_3$, indicating five index of hydrogen deficiency was proposed based on HRMS (molecular ion peak at *m/z* = 321.2429), ESIMS (*m/z* = 303.6 corresponding to $[M - H_2O]^+$) and the NMR spectroscopic data (Table 4.45). The ^{1}H NMR spectrum revealed three methyl groups at δ_H 1.37 (H_3-17), δ_H 1.23 (H_3-18) and δ_H 0.93 (H_3-20) with the corresponding ^{13}C NMR resonances appearing at δ_C 24.4 (C-17), δ_C 28.9 (C-18) and δ_C 15.5 (C-20), respectively. Unlike compound **234**, the NMR spectra of **235** indicated the absence of a double bond at C-9 (δ_C 55.9) and C-16 (δ_C 48.8) usually observed in kaurene-type diterpenes. Furthermore, the signal at δ_C 180.7 was in agreement with the presence of a hydroxycarbonyl at C-19. This was further confirmed by the HMBC correlation of CH_3-18 (δ_H 1.23) with the carbonyl C-19 (δ_C 180.7). The methyl protons (CH_3-17) signal appearing as singlet indicated that C-16 is a quaternary carbon and hence attached to the hydroxy group (OH-16). In addition, the HMBC correlation of the methyl protons at CH_3-17 (δ_H 1.37) with C-13 (δ_C 48.8) and C-15 (δ_C 57.7) and C-16 (δ_C 79.3) established the placement of the hydroxy group at C-16. The NOESY correlation of CH_3-17 with H-9 indicated that CH_3-17 is *β*-oriented and hence, OH-16 is *α*-oriented. Compound **235** is a levorotatory ($[\alpha]_D^{20}$ −102) *ent*-kaurane diterpene and is identified as 16*α*-hydroxy-*ent*-kauran-19-oic acid.

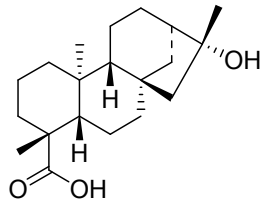

235

Table 4.45: ^{1}H (800 MHz) and ^{13}C (200 MHz) NMR Data of 235 ($CDCl_3$)

Position	δ_C	Type	δ_H, mult. (J in Hz)	HMBC (H→C)
1	40.6	CH_2	0.79 dt (13.2, 12.8, 4.3)	C-3, C-5, C-9, C-20
			1.79 d (3.1)	C-5, C-9, C-20
2	19.0	CH_2	1.43 m	C-4, C-10
			1.88 dt (13.8, 3.8, 3.8)	C-4
3	37.6	CH_2	1.62 dt (12.7, 3.2, 3.2)	C-1, C-5, C-18
			1.92 m	C-1, C-5, C-18, C-19
4	43.5	C	/	/
5	56.8	CH	1.05 dd (11.8, 2.8)	C-1, C-3, C-9, C-20
6	22.0	CH_2	1.84 m	C-4, C-8, C-10
7	41.9	CH_2	1.42 m	C-9, C-14, C-15
			1.62 dt (12.7, 3.2, 3.2)	C-14, C-15
8	45.2	C	/	/
9	55.9	CH	0.96 d (7.6)	C-7, C-12
10	39.6	C	/	/
11	18.2	CH_2	1.52 m	C-8, C-10, C-13
			1.56 m	C-8, C-13
12	26.7	CH_2	1.50 m	C-9, C-14, C-16
			1.56 m	C-9, C-14, C-16
13	48.8	CH	1.84 m	C-8
14	37.9	CH_2	1.01 td (13.6, 13.6, 4.4)	C-9, C-15
			1.01 td (13.6, 13.6, 4.4)	C-9, C-15
15	57.7	CH_2	1.55 m	C-7, C-14, C-17
16	79.3	C	/	/
17	24.4	CH_3	1.37 s	C-13, C-15
18	28.9	CH_3	1.23 s	C-3, C-5, C-19
19	180.7	C	/	/
20	15.5	CH_3	0.95 s	C-1, C-5

4.5.1.3 9*β*-Hydroxy-15*α*-angeloyloxy-*ent*-kaur-16-en-19-oic acid (236)

Compound **236** was also isolated from the root extract of *A. pluriseta*. It was isolated as pale yellow residue and the UV spectrum showed absorption band at λ_{max} 269 nm. The molecular formula ($C_{25}H_{36}O_5$) was suggested based on NMR data. The ^1H and ^{13}C NMR spectral data (Table 4.46) indicated that it is an *ent*-kaurane diterpene (Müller *et al.*, 2003). This was also supported by the HMBC correlation of the olefinic protons H_2-17 with C-13 (δ_H 41.3) and C-15 (δ_H 78.8). Of the three methyl groups expected in *ent*-kaurenes, only two (Me-18 and Me-20) were observed, with the third one (C-19) oxidized to carboxylic acid (δ_C 178.5). The HMBC correlation of CH_3-18 methyl with the oxycarbonyl (δ_C 178.5) confirmed the placement of the carboxylic acid at C-19. The presence of angeloyloxy moiety was revealed by the ^1H [δ_H 6.07 (H-3')] and ^{13}C [δ_C 167.0 (C-1'); δ_C 128.0 (C-2') and δ_C 136.2 (C-3')] NMR spectral data (Table 59) and was placed at C-15 from the HMBC correlation of H-15 (δ_H 6.10) with C-1' (δ_C 167.0). The α-rientation of this group was evident from the X-ray data (Figure 4.7). The presence of a hydroxyl group at C-9 was evidenced by a signal at δ_C 75.9. This was confirmed from the HMBC spectrum which showed correlation of H_3-20 and H_2-12 with C-9. The relative configuration at the stereocenters was established on the basis NOESY spectrum and comparison with the published data in the literature (Müller *et al.*, 2003). The single crystal X-ray diffraction analyses of compound **239** further confirmed its absolute configuration. Therefore, the known compound **236** was characterized as 9*β*-hydroxy-15*α*-angeloyloxy-*ent*-kaur-16-en-19-oic acid.

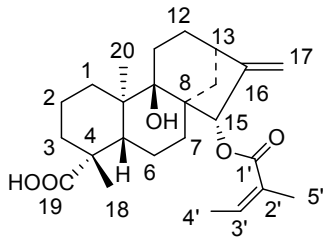

236

Table 4.46: ^{1}H (800 MHz) and ^{13}C (200 MHz) NMR Data of 236 ($CDCl_3$)

Position	δ_C	Type	δ_H (mult., *J* in Hz)	HMBC
1	32.0	CH_2	1.54 (m)	C-3, C-5, C-9, C-10
			1.87 (m)	C-2, C-3, C-5, C-10
2	19.0	CH_2	1.48 (m)	C-1, C-4, C-10
			1.96 (m)	C-11, C-3, C-4
3	37.6	CH_2	1.03 (m)	C-1, C-5, C-18, C-19
			2.11 (m)	C-1, C-5
4	44.4	C	/	/
5	49.0	CH	1.80 (dd, *J*=3.6, 3.6)	C-3, C-7, C-18, C-20
6	21.0	CH_2	1,87 (br s)	C-5, C-7, C-8, C-10
7	30.0	CH_2	1.50 (m)	C-5, C-9, C-14
			1.69 (dd, *J*=13.0, 4.8)	C-5, C-9, C-14
8	43.2	C	/	/
9	75.9	C	/	/
10	52.8	C	/	/
11	28.6	CH_2	1.33 (ddd, *J*=14.1, 13.5, 6.8)	C-8, C-9, C-12
			2.11 (m)	C-8, C-9, C-12
12	33.8	CH_2	1.60 (m)	C-9, C-14, C-16
			1.69 (dd, *J*=13.0, 4.8)	C-14
13	41.3	CH	2.78 (br s)	C-8, C-11, C-15, C-17
14	37.7	CH_2	1.03 (m)	C-7, C-9, C-12, C-15
			2.22 (m)	C-5, C-9
15	78.8	CH	6.10 (s)	C-1', C-7, C-13, C-17
16	156.6	C	/	/
17	109.2	CH_2	5.09 (d, *J*=1.23)	C-13, C-15, C-16
			5.18 (d, *J*=1.23)	C-13, C-15, C16
18	28.7	CH_3	1.22 (s)	C-3, C-5, C-19
19	184.3	C	/	/
20	17.2	CH_3	1.15 (s)	C-1, C-5, C-9
1’	167.0	C	/	/
2’	128.0	C	/	/
3’	136.2	CH	6.07 (m)	C-4', C-5'
4’	14.9	CH_3	1.96 (br s)	C-2', C-3'
5’	20.0	CH_3	1.87 (s)	C-2', C-3'

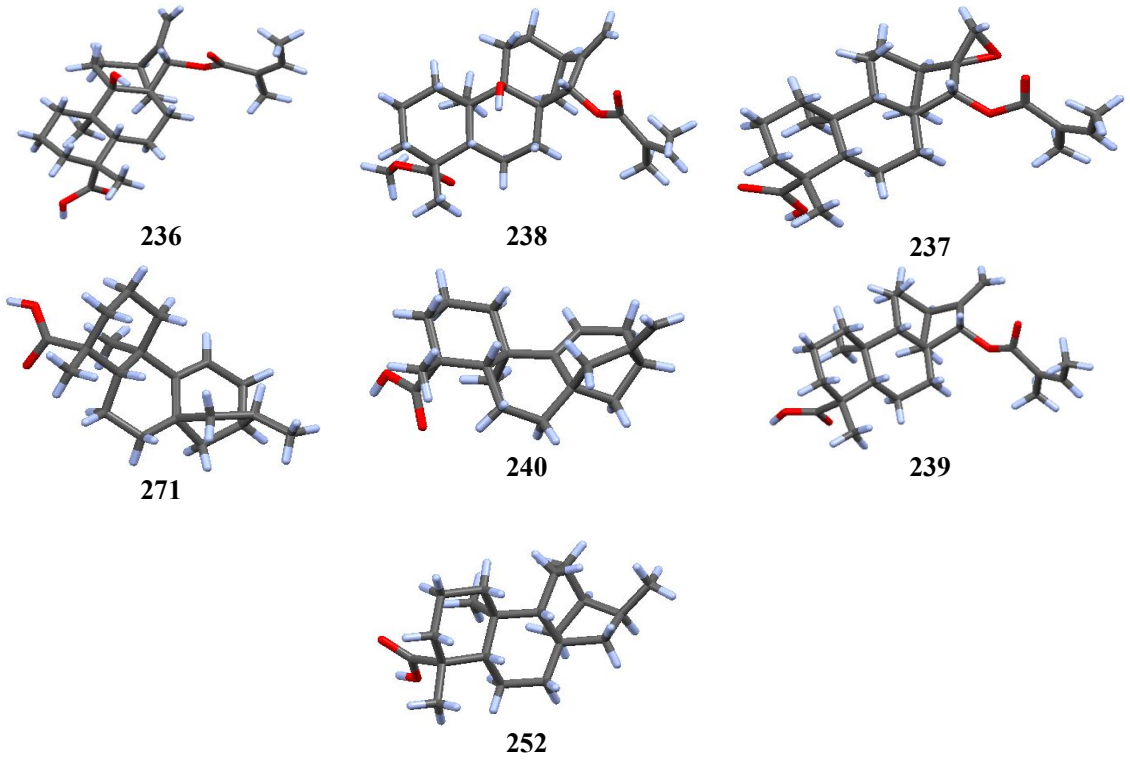

Figure 4.7: Crystal Structure Representation of Some Compounds Isolated from *Aspilia* Species

4.5.1.4 15*α*-Angeloyloxy-16*α*,17-epoxy-*ent*-kauran-19-oic Acid (237)

Compound **237** was also isolated from the root extract of *A. pluriseta*. This compound is also an *ent*-kaurane diterpene and the molecular formula $C_{25}H_{36}O_5$ was suggested based on NMR data (Table 4.47). The ^{1}H NMR spectroscopic data (Table 4.47) displayed three characteristic protons H-15 (δ_C 4.81); H_2-17 (δ_{Ha} 3.09, δ_{Hb} 2.78) and H-3' (δ_H 6.08) corresponding to the ^{13}C NMR signals for C-15 (δ_C 82.0), C-17 (δ_C 49.5) and C-3' (δ_C 137.0) respectively. Two methyl groups Me-C-19 (δ_C 1.28) and Me-C-20 (δ_C 1.03) were also observed in ^{1}H NMR spectrum. The ^{13}C NMR spectrum displayed 25 carbons including two carbonyls, C-18 (δ_C 184.2) and C-1' (δ_C 167.6); two olefinic carbons, C-2' (δ_C 128.2) and C-3' (δ_C 137.0); and three oxygenated carbons C-15 (δ_C 82.0), C-16 (δ_C 66.3) and C-17 (δ_C 49.4). Connectivity between

different protons and carbons of **237** were established based on the HSQC, ^{1}H and ^{13}C NMR, H-H COSY and HMBC experiments. HMBC spectrum showed correlation between H-17 and C-16, the correlation between H-15 and the carbonyl C-1' was also observed. The ^{13}C NMR, HSQC and HMBC data showed resonances consistent with the presence of conjugated carbonyl of an angeloyloxy moiety (at C-15), a 16*α*-17-epoxide (at C-16/C-17) and a carboxylic acid group (at C-19). Furthermore, X-ray diffraction analysis of compound **237** confirmed the gross structure and its absolute configuration. This compound was previously reported in the literature (Wafo *et al.*, 2011; Ogungbe and Setzer, 2013). Based on this information, the structure of **237** was established as showed and named 15*α*-angeloyloxy-16*α*,17-epoxy-*ent*-kauran-19-oic acid.

Some *ent*-kaurane-type diterpenoids, including 16,17-epoxy-15*β*-tigloyloxy-*ent*-kauran-18-oic acid (**237a**) and 16,17-epoxy-15*β*-senecioyloxy-*ent*-kauran-18-oic acid (**237b**), were reported earlier from *Aspilia pluriseta* (Sebisubi *et al*., 2010). These compounds were reported to have the 15*β*-tigloyloxy and 15*β*-senecioyloxy groups, respectively, occupying the less favorable orientation (Sebisubi *et al*., 2010); however, the authors have not provided evidence for these proposals. Our single crystal X-ray analyses have shown that the C-15 substituent of compounds **236**, **237, 238** and **239** is an angeloyloxy group occupying the more favourable-15*α*-position. In fact, the proposed stereochemical assignment of *ent*-kaurane-type diterpenoids reported from this genus, particularly in highly functionalized compounds, lacks evidence. We have filled this knowledge gap by determining the absolute configuration of seven *ent*-kaurane-type diterpenoids, as shown in Figure 4.7, using single crystal X-ray analyses.

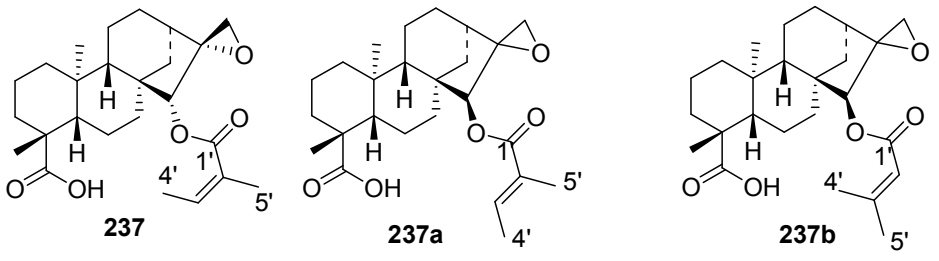

The ^{13}C NMR data of compound **237** (Table 4.47) is in close agreement to that previously reported in the literature (Wafo *et al.,* 2011), except for the chemical shift assignment of C-2

and C-12 (Table 4.47). Related structures, **237a** and **237b**, have been proposed for two compounds earlier reported (Sebisubi *et al.,* 2010) from *Aspilia pluriseta.* The ^{13}C NMR assignment (Table 4.47) for these compounds differs from our assignment, which is based on 2D NMR correlations, despite the common 16,17-epoxy-15-oxy-*ent*-kauran-18-oic acid skeleton. The ^{13}C NMR chemical shifts of C-4' (δ_C 27.4) and C-5' (δ_C 20.8) in compound **237a** do not support a tigloyloxy group at C-15 as proposed in reference (Sebisubi *et al.,* 2010); methyl carbon atoms in such group are expected to resonate at ~14 ppm (for C-4') and at ~11 ppm (for C-5'), based on chemical shift prediction (Banfi and Patiny, 2008) and previous literature (Cai *et al.,* 2017). The NMR spectra of compound **237b** that are given in the supporting information in Sebisubi *et al.,* (2010) are of low quality and do not allow confirmation of the proposed assignment. It should be noted that the numbering used in this paper does not follow the literature convention (Alvarenga *et al.,* 2005). Hence, the carboxylic group of **237b** and of its structural analogues should not be assigned as C-18, but rather as C-19, following reference (Alvarenga *et al.,* 2005). Overall, several details reported in (Sebisubi *et al.,* 2010) for these compounds appear debatable, and consequently so are the proposed structures. To avoid such uncertainties, the NMR assignments of the discussed diterpenoids are presented in Tables 4.47.

Table 4.47: The Literature Reported NMR Data for 237, 237a and 237b and the ^{1}H (800 MHz) and ^{13}C NMR (200 MHz) Data of 237 in $CDCl_3$.

	237 (Wafo *et al.,* 2011)	**237a** (Sebisubi *et al.,* 2010)	**237b** (Sebisubi *et al.,* 2010)	**237**	**237**
Position	δ_C	δ_C	δ_C	δ_C	δ_H, mult. (*J* in Hz)
1	41.2	40.6	40.6	40.6	0.80 *ddd* (7.2, 7.1, 1.3) 1.86 *dd* (2.9, 1.4)
2	28.9	19.8	19.0	19.7	1.55 *ddd* (7.3, 3.6, 2.4) 1.75 *dd* (3.7, 3.6)
3	37.7	36.7	36.4	37.6	0.96 *ddd* (13.7, 13.6, 4.3) 2.11 *dd* (13.7, 3.1)
4	43.6	46.9	47.8	43.5	
5	56.7	20.3	56.6	56.5	1.16 *dd* (9.1, 7.1)
6	19.0	41.2	20.3	20.8	1.76 *ddd* (5.7, 3.4, 2.1) 1.86* *ddd* (3.4, 3.4, 2.7)

Table 4.47 continued

237 (Wafo *et al.,* 2011)	**237a** (Sebisubi *et al.,* 2010)	**237b** (Sebisubi *et al.,* 2010)	**237**	**237**	**237** (Wafo *et al.,* 2011)
Position	δ_C	δ_C	δ_C	δ_C	δ_H, mult. (*J* in Hz)
7	35.4	47.8	41.2	35.3	1.25 *ddd* (14.4, 13.9, 4.4) 1.79 *ddd* (13.8, 13.2, 4.3)
8	47.9	52.9	43.6	47.8	
9	52.9	43.6	53.0	52.8	1.28 *dd* (13.8, 3.8)
10	39.8	56.6	39.8	39.7	
11	19.8	20.8	19.8	18.9	1.40 *ddd* (13.8, 3.4, 3.4, 3.1) 1.81 *dd* (13.8, 4.3)
12	20.8	28.9	28.9	28.8	1.50 *ddd* (13.5, 7.8, 7.2)
13	41.2	36.4	35.1	41.1	1.82 *dd* (13.8, 4.4)
14	36.5	37.7	37.7	36.4	1.68 *dd* (14.5, 3.3) 1.97 *dd* (13.1, 3.4)
15	81.9	81.2	81.2	81.9	4.73 *br s*
16	66.3	66.4	66.4	66.3	
17	49.6	49.6	49.6	49.6	2.78 *dd* (5.6, 1.3) 3.09 *dd* (5.8, 1.3)
18	28.8	28.9	28.9	28.7	1.28 *s*
19	182.3	182.6	182.6	182.7	
20	15.7	15.8	16.0	15.9	1.03 *s*
1'	167.9	166.5	166.5	167.8	
2'	128.1	129.0	115.9	128.0	
3'	137.3	137.1	156.8	137.3	5.96 *q* (7.1)
4'	15.9	27.4	20.8	15.7	1.96 *d* (1.9)
5'	20.6	20.8	27.4	20.6	*s*

4.5.1.5 Methyl-9*β*-hydroxy-15*α*-angeloyloxy-*ent*-kaur-16-en-19-oate (238)

Compound **238** was isolated as colourless crystals (mp 261-262°C). ESIMS analysis showed a protonated molecular ion peak at *m/z* 413.8 which together with the NMR spectra (Table 4.48) allowed the assignment of the molecular formula as $C_{26}H_{38}O_5$. Comparison of the NMR data with that of **236** showed that this compound is also an ent-kaurane derivative with angeloyloxy substituent at C-15. The only diference is that the carboxylic acid group is replaced by methylester group. The ^{13}C NMR spectrum indicated signals corresponding to exactly 26 carbons including two carbonyls (C-19, δ_C 177.8 and C-1' , δ_C 167.8), and two oxygenated carbons (C-9, δ_C 76.7 and C-15, δ_C 78.6). The placement of the angeloyloxy group was confirmed from the HMBC Correlation of H-15 with C-1'. Moreover, comparison

of the NMR data of **238** with the same reported compound in the literature (Winterfeldt, 1994) was in agreement with the proposed structure of **238**. Therefore, compound **238** was identified as methyl-9*β*-hydroxy-15*α*-angeloyloxy-*ent*-kaur-16-en-19-oate.

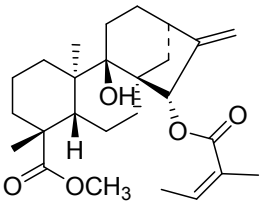

238

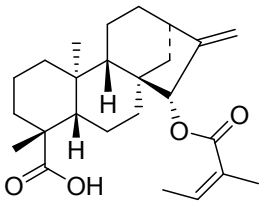

239

4.5.1.6 15*α*-Angeloyloxy-*ent*-kaur-16-en-19-oic Acid (239)

Compound **239** was purified as colourless crystals (mp 256-257°C). ESIMS analysis showed a protonated molecular ion peak at *m/z* 401.7 which together with the NMR spectra (Table 4.48) allowed the assignment of the molecular formula as $C_{25}H_{36}O_4$. The ^1H and ^{13}C NMR (Table 4.48) revealed the same signals as that of compound **236** except that this compound **239** lacked the second hydroxy substituent at C-9 (δ_C 52.9). All the other signals of compound **239** were the same as observed in compound **236**. The ^1H NMR signal at δ_H 5.37 (H-15) and the C-15 resonnating at δ_C 82.4, clearly indicated that the angeloyloxy group is located at C-15. Comparison of its ^1H and ^{13}C NMR data with the reported data for **239** showed similar values (El-Marsni *et al.*, 2015). The single crystal X-ray diffraction analysis of compound **239** (Figure 4.7) further confirmed the gross structure and allowed the establishment of its absolute configuration. Based on this information, compound **239** was characterized as 15*α*-angeloyloxy-*ent*-kaur-16-en-19-oic acid.

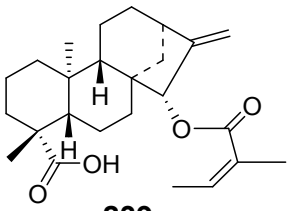

239

Table 4.48: ^{1}H (600 MHz) and ^{13}C (150 MHz) NMR data of 238 and 239 in CD_2Cl_2

Position	238				239			
	δ_C	Type	δ_H (mult., *J* in Hz)	HMBC	δ_C	Type	δ_H (mult., *J* in Hz)	HMBC
1	32.0	CH_2	1.55 (m)	C-3, C-5, C-9, C-20	40.5	CH_2	0.91 (m)	C-3, C-5, C-9, C-20
			1.88 (m)	C-2, C-3, C-5, C-20			1.93 (m)	C-2, C-3, C-5, C-20
2	19.0	CH_2	1.48 (m)	C-4, C-10	19.0	CH_2	1.55 (m)	C-4, C-10
			2.00 (m)	C-4, C-10			1.91 (br s)	C-4, C-10
3	37.8	CH_2	1.05 (m)	C-1, C-5, C-4, C-18	37.6	CH_2	1.08 (d, *J*=4.2)	C-1, C-5, C-4, C-18
			2.13 (m)	C-1, C-5, C-18			2.18 (d, *J*=13.4)	C-1, C-5, C-18
4	44.2	C	/	/	43.6	C	/	/
5	49.8	CH	1.79 (m)	C-1, C-3, C-7, C-9, C-18	56.5	CH	1.17 (m)	C-1, C-3, C-7, C-9, C-18
6	20.9	CH_2	1.90 (br s)	C-4, C-8, C-10	20.8	CH_2	1.80 (m)	C-4, C-8, C-10
7	30.0	CH_2	1.50 (m)	C-5, C-9, C-14	35.0	CH_2	1.31 (dd, *J*=10.3, 2.80)	C-5, C-9, C-14
			1.62 (dd, *J*=12.6, 2.4)	C-5, C-9, C-14, C-15			1.69 (d, *J*=10.6)	C-5, C-9, C-14, C-15
8	43.8	C	/	/	47.5	C	/	/
9	76.7	C	/	/	52.9	CH	1.32 (m)	C-1, C-5, C-7, C-12
10	52.8	C	/	/	39.8	C	/	/
11	29.1	CH_2	1.26 (m)	C-8, C-10, C-13	18.4	CH_2	1.69 (d, *J*=10.6)	C-8, C-10, C-13
			2.15 (m)	C-8, C-10, C-13				
12	33.7	CH_2	1.61 (m)	C-14, C-16	32.6	CH_2	1.55 (m)	C-14, C-16
			1.63 (dd, *J*=12.6, 2.4)	C-9, C-14, C-16			1.69 (m)	C-9, C-14, C-16
13	41.2	CH	2.82 (m)	C-8, C-11, C-17	42.6	CH	2.83 (m)	C-8, C-11, C-17

Table 4.48 contimued

Position	238				239			
	δ_C	Type	δ_H (mult., *J* in Hz)	HMBC	δ_C	Type	δ_H (mult., *J* in Hz)	HMBC
14	37.6	CH_2	1.05 (m)	C-7, C-9, C-12	37.3	CH_2	1.50 (m)	C-7, C-9, C-12
			2.22 (m)	C-9, C-12, C-16			2.04 (m)	C-9, C-12, C-16
15	78.6	CH	6.02 (s)	C-1', C-7, C-14, C-17	82.4	CH	5.37 (br s)	C-1', C-7, C-14, C-17
16	155.5	C	/	/	156.0	C	/	/
17	109.6	CH_2	5.14 (d, *J*=1.20)	C-13, C-15, C-16	109.5	CH_2	5.14 (d, *J*=1.2)	C-13, C-15, C-16
			5.16 (d, *J*=1.20)	C-13, C-15, C-16			5.17 (d, *J*=1.2)	C-13, C-15, C-16
18	28.5	CH_3	1.20 (s)	C-3, C-5, C-19	28.7	CH_3	1.27 (s)	C-3, C-5, C-19
19	177.8	C	/	/	183.7	C	/	/
20	17.0	CH_3	1.01 (s)	C-1, C-5, C-9, C-10	15.6	CH_3	1.01 (s)	C-1, C-5, C-9, C-10
1’	167.8	C	/	/	167.7	C	/	/
2’	128.2	C	/	/	128.3	C	/	/
3’	137.1	CH	6.04 (m)	C-4', C-5'	136.9	CH	6.08 (m)	C-4', C-5'
4’	15.5	CH_3	1.96 (br s)	C-2', C-3'	15.5	CH_3	1.96 (br s)	C-2', C-3'
5’	20.4	CH_3	1.87 (s)	C-2', C-3'	20.4	CH_3	1.87 (s)	C-2', C-3'
OCH_3	52.8	CH_3	3.66 (3H, s)	C-19	/		/	/

4.5.1.7 *Ent*-kaura-9(11), 16-dien-19-oic Acid (240)

ESIMS analysis (molecular ion peak at *m/z* 301.4) of compound **240**, together with the NMR spectroscopic data (Table 4.49) allowed the assignment of the molecular formula as $C_{20}H_{28}O_2$. The two signals in ^1H NMR spectrum corresponding to two terminal methylenic protons (H_2-17 δ_H 2.18, 2.67) were typical for a kaurene diterpenoid. The presence of an additional double bond at C-9(11) was shown by ^1H NMR signal at δ_H 5.33 (H-11) and ^{13}C NMR signals at δ_C 156.0 (C-9) and δ_C 114.8 (C-11). Th kaurane-type skeleton was further supported by the ^{13}C NMR signals corresponding to C-16 (δ_C 158.6), C-17 (δ_C 105.2), and C-9 (δ_C 156.0). This conpound also has a hydroxy carbonyl (δ_C 184.7) at C-19 as in other kaurene diterpenoids of this plant. Comparison of the NMR data (Table 4.49) for **240** with literature report was in agreement with this compound being a kauradien-19-oic acid (Arciniegas *et al.*, 2018; Padilla *et al.*, 2017). In addition, the X-ray diffraction analysis of compound **240** (Figure 4.7) confirmed the structure and its absolute configuration. Based on this information, **240** was identified as *ent*-kaura-9(11), 16-dien-19-oic acid. This compound is a known compound, however it is being reported for the first time from this plant.

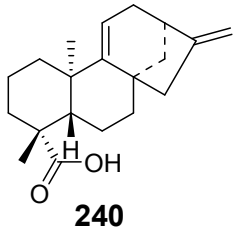

240

Table 4.49: ^{1}H (600 MHz) and ^{13}C (150 MHz) NMR Data of 240 and 241 in CD_2Cl_2

Position	240				241			
	δ_C	Type	δ_H (mult., *J* in Hz)	HMBC	δ_C	Type	δ_H (mult., *J* in Hz)	HMBC
1	40.7	CH_2	1.28 (m)	C-3, C-5, C-9, C-20	39.7	CH_2	1.32 (m)	C-3, C-5, C-9, C-20
			2.01 (m)	C-3, C-5, C-20			2.01 (s)	C-3, C-5, C-9, C-20
2	20.1	CH_2	1.55 (m)	C-4, C-10	19.9	CH_2	1.56 (m)	C-4, C-10
			1.92 (m)	C-4, C-10			2.01 (m)	C-4, C-10
3	38.1	CH_2	1.09 (m)	C-1, C-5, C-18	27.5	CH_2	1.92 (dd, *J*=11.2, 2.6)	C-1, C-5, C-18
			2.18 (m)	C-1, C-5, C-18				
4	44.7	C	/	/	40.1	C	/	/
5	46.4	CH	1.12 (m)	C-1, C-3, C-7, C-9, C-18	44.6	CH	2.47 (m)	C-1, C-3, C-7, C-9, C-18
6	18.4	CH_2	1.90 (m)	C-4, C-8, C-10	18.1	CH_2	2.01 (m)	C-4, C-8, C-10
							2.62 (m)	C-4, C-8, C-10
7	44.9	CH_2	1.49 (m)	C-5, C-9, C-14, C-15	28.7	CH_2	1.32 (m)	C-5, C-9, C-14, C-15
			2.07 (m)	C-5, C-9, C-14				
8	42.2	C	/	/	37.9	C	/	/
9	156.0	C	/	/	180.7	C	/	/
10	38.7	C	/	/	45.3	C	/	/
11	114.8	CH	5.33 (dd, 4.1, 2.9)	C-8, C-10, C-13	119.4	CH	5.67 (s)	C-10, C-13
12	37.9	CH_2	2.01 (m)	C-14, C-16	197.8	C	/	/
			2.48 (d, *J*=1.7)	C-9, C-14, C-16				
13	41.2	CH	2.81 (br s)	C-8, C-11, C-17	58.2	CH	3.29 (m)	C-8, C-11, C-17

Table 4.49 continued

Position			240				241	
	δ_C	Type	δ_H (mult., *J* in Hz)	HMBC	δ_C	Type	δ_H (mult., *J* in Hz)	HMBC
14	29.6	CH_2	1.55 (dd, *J*=10.8, 3.0)	C-7, C-9, C-12, C-16	43.9	CH_2	2.47 (m)	C-7, C-9, C-16
			2.01 (dd, *J*=19.9, 2.7)	C-7, C-9, C-16			2.62 (m)	C-7, C-9, C-16
15	50.2	CH_2	2.18 (m)	C-7, C-9, C-14	48.1	CH_2	1.84 (d, *J*=4.7)	C-7, C-9, C-13
			2.67 (m)	C-7, C-9, C-14			1.92 (dd, *J*=11.2, 2.6)	C-7, C-9, C-14
16	158.6	C	/	/	147.9	C	/	/
17	105.2	CH_2	4.83 (d, 3.1)	C-13, C-15, C-16	109.6	CH_2	4.95 (m)	C-15, C-16
			4.95 (d, 2.4)	C-13, C-15			5.13 (m)	C-13, C-15
18	28.0	CH_3	1.29 (s)	C-3, C-4, C-5, C-19	22.3	CH_3	1.28 (s)	C-3, C-5, C-19
19	184.7	C	/	/	28.6	CH_3	1.20 (d, *J*=2.6)	C-3, C-5, C-18
20	15.3	CH_3	1.07 (s)	C-3, C-5, C-20	28.3	CH_3	1.32 (m)	C-1, C-5

4.5.1.8 *Ent*-kaura-9(11),16-dien-12-one (241)

Compound **241** was isolated as colourless crystal from the roots extract of *Aspilia pluriseta*. The NMR spectroscopic data (Table 4.49) was similar to that of **240** except that this compound **241** did not have a carboxylic acid group at C-19 (δ_C 28.6) which remains a methyl group. This compound also has keto group at C-12 (δ_H 197.8). Otherwise the ^1H and ^{13}C NMR spectral data (Table 4.49) were consistent with this compound having a kaurene diterpenoid skeleton (Pinto *et al.*, 1981). Thus, the ^{13}C NMR spectrum displayed 20 carbons including three methyls C-18 (δ_C 22.3), C-19 (δ_C 28.6), C-20 (δ_C 28.3) and a carbonyl C-12 (δ_C 197.8). The HMBC correlation of H-13 with both C-11 (δ_C 119.4) and C-17 (δ_C 109.6) confirmed the placement of the carbonyl at C-12. On the basis of the above information, compound **241** was characterised as *ent*-kaura-9(11),16-dien-12-one. This compound is known (Pinto *et al.,* 1981), however, it is being reported for the first time from the genus *Aspilia.*

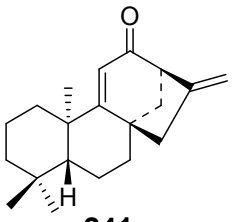

241

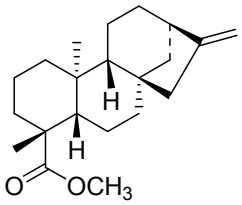

242

4.5.1.9 Methyl-*ent*-kaur-16-en-19-oate (242)

The molecular formula $C_{21}H_{32}O_2$ of compound **242** was deduced from ESIMS (molecular ion peak at *m/z* 317.8) and NMR spectroscopic data (Table 4.50). The ^1H and ^{13}C NMR data of **242** was clear that the compound is methyl-ent-kaur-16-enoate (Xavier *et al.*, 2017). Thus, ^1H NMR spectrum displayed two singlets (at δ_H 1.21 and δ_H 1.00) corresponding to two methyl groups [C-18 (δ_C 28.6) and C-20 (δ_C 15.3)]. The three proton singlet at δ_H 3.33 in ^1H NMR spectrum was assigned to the methyl protons in methyl ester group (δ_C 49.9). This was confirmed by HMBC correlation of the same protons and those of CH_3-18 with the carbonyl C-19 (δ_C 178.2). Based on these evidences and comparison with literature (Xavier *et al.*, 2017), compound **242** was identified as methyl-*ent*-kaur-16-en-19-oate.

Table 4.50: ^{1}H (600 MHz) and ^{13}C (150 MHz) NMR Data of 242 and 243 in CD_2Cl_2

Position	242				243			
	δ_C	Type	δ_H (mult., *J* in Hz)	HMBC	δ_C	Type	δ_H (mult., *J* in Hz)	HMBC
1	40.6	CH_2	1.53 (m)	C-20, C-3, C-5	40.6	CH_2	1.12 (m)	C-3, C-5, C-9, C-20
			1.90 (m)	C-20, C-3, C-5			1.87 (m)	C-2, C-3, C-5, C-20
2	19.1	CH_2	1.40 (m)	C-4,C-10	19.1	CH_2	1.41 (m)	C-4, C-10
			1.90 (m)	C-4,C-10			1.90 (m)	C-4, C-10
3	37.9	CH_2	1.07 (m)	C-1, C-18	37.9	CH_2	1.03 (d, *J*=4.2)	C-1, C-5, C-4, C-18
			2.15 (m)	C-1, C-18, C-19			2.15 (m)	C-1, C-5, C-18
4	43.8	C	/	/	43.1	C	/	/
5	56.6	CH	1.12 (m)	C-19, C-3, C-7, C-C-1	56.6	CH	1.12 (m)	C-1, C-3, C-7, C-9, C-18
6	21.8	CH_2	1.90 (m)	C-4, C-8	21.8	CH_2	1.90 (m)	C-4, C-8
7	43.1	CH_2		C-5	28.7	CH_2	1.49 (m)	C-5, C-9, C-14
							2.07 (m)	C-5, C-9, C-14
8	44.1	C	/	/	44.1	C	/	/
9	55.0	CH	1.12 (m)	C-20, C-1, C-12	55.0	CH	1.12 (m)	C-1, C-7, C-12
10	39.5	C	/	/	39.5	C	/	/
11	18.2	CH_2	1.64 (m)	C-10, C-13	18.2	CH_2	1.64 (m)	C-8, C-10, C-13
							2.63 (dd, *J*=4.2, 4.2)	C-10, C-13
12	28.4	CH_2	1.53 (d, *J*=3.8)	C-9, C-14, C-16	28.4	CH_2	1.06 (m)	C-9, C-14, C-16
			2.06 (m)	C-14, C-16				
13	41.2	CH	0.89 (m)	C-8C-15	43.8	CH	1.93 (m)	C-11, C-15, C-17
14	32.9	CH_2	1.31 (br s)	C-7, C-15, C-12	32.9	CH_2	1.76 (dd, *J*=11.7, 4.7)	C-7, C-12, C-15

							2.06 (d, *J*=10.0)	C-7, C-9, C-12

Table 4.50 continued

Position	**242**				**243**			
	δ_C	Type	δ_H (mult., *J* in Hz)	HMBC	δ_C	Type	δ_H (mult., *J* in Hz)	HMBC
15	48.8	CH_2	2.16 (m)	C-7, C-17, C-14	48.8	CH_2	2.02 (m)	C-7, C-13, C-17
							2.07 (m)	C-7, C-13, C-17
16	155.4	C	/	/	155.4	C	/	/
17	102.7	CH_2	/	/	102.9	CH_2	4.78 (m)	C-13, C-15, C-16
							4.91 (m)	C-13, C-15, C-16
18	28.6	CH_3	1.21 (s)	C-4, C-5	28.6	CH_3	1.21 (s)	C-3, C-5, C-19
19	178.2	C	/	/	178.2	C	/	/
20	15.3	CH_3	1.00 (s)	C-5, C-9	15.3	CH_3	1.00 (s)	C-1, C-5, C-9
-	49.9	OCH_3	3.33 (s)	C-19	/	/	/	/

4.5.2 Characterization of Secondary Metabolites Isolated from Aerial Parts of *Aspilia pluriseta*

The aerial part extract of *Aspilia pluriseta* led to the isolation of seven compounds including three kaurene diterpenes (**243-245**), three triterpenoids (**246-248**) and one sesquiterpene (**249**).

4.5.2.1 *Ent*-kaur-16-en-19-oic Acid (243)

Compound **243** was isolated as colourless crystals form the aerial parts extract of *Aspilia pluriseta*. The ^{13}C NMR spectral data (Table 4.50) showed twenty carbons among which two methyl groups (C-18, δ_C 28.6 and C-20, δ_C 15.3), a carbonyl (C-19, δ_C 178.2) and two olefinic carbons (C-16, δ_C 155.4 and C-17, δ_C 102.9). This compound was previously reported from the same plant (Sebisubi *et al.*, 2010; Arciniegas *et al.*, 2018; Chen *et al.*, 2018). The HMBC correlation of C-18 methyl protons (δ_C 1.21) with the carbonyl (C-19) was in agreement with the placement of the hydroxy carbonyl at C-19. Based on the above data and comparison with literature, compound **243** was elucidated as *ent*-kaur-16-en-19-oic acid. The isolation of a kaurenoic acid from Asteraceae plant species is not new. Many scientists have previously reported a similar compound (Sebisubi *et al.*, 2010; Souza *et al.*, 2015).

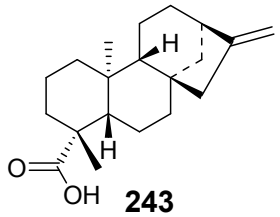

243

4.5.2.2 *Ent*-kaur-16-en-19-ol (244)

Compound **244** was isolated as a colourless paste from the areal parts of the plant *Aspilia pluriseta.* The ^{1}H and ^{13}C NMR spectroscopic data (Table 4.51) was in agreement with the molecular formula $C_{20}H_{32}O$. Comparison of the NMR spectroscopic data of this compound (Table 4.51) with the literature indicated that it is a kaurene derivative (Peña *et al.*, 2012; Cano *et al.*, 2017). An oxymethylene signal (δ_C 65.6, H_2-19) was observed in the ^{13}C NMR and its placement was based on HMBC correlation of the oxymethylene protons H_2-19 (δ_H 3.38, 3.68) with C-18 (δ_C 27.1). Furthermore, HMBC correlations of methylene protons H_2-

17 (δ_H 4.66, 4.72) with C-13 (δ_C 44.0) and C-15 (δ_C 49.1) were in agreement with its placement at C-16(17) (Cano *et al.*, 2017). The negative specific rotation ($[\alpha]_D^{20} - 89°$) is in agreement with this compound being *ent*-kaurene diterpene. On the basis of the above information, compound **244** was characterised as *ent*-kaur-16-en-19-ol.

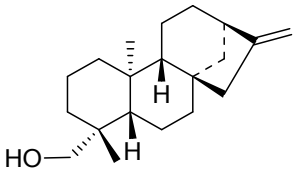

244

Table 4.51: ^{1}H (600 MHz) and ^{13}C (150MHz) NMR Data of 244 and 245 in CD_2Cl_2

Position	244				245			
	δ_C	Type	δ_H (mult., *J* in Hz)	HMBC	δ_C	Type	δ_H (mult., *J* in Hz)	HMBC
1	40.4	CH_2	0.73 (m)	C-3, C-10, C-20	40.6	CH_2	0.86 (m)	C-20, C-3, C-9
			1.70 (m)	C-3, C-10, C-20			1.98 (m)	C-20, C-3
2	20.5	CH_2	1.27 (m)	C-4, C-10	19.1	CH_2	1.41 (m)	C-4, C-10
			1.52 (m)	C-4			1.90 (m)	C-4, C-10
3	33.1	CH_2	1.40 (m)	C-1, C-5	37.9	CH_2	1.03 (m)	C-1, C-18
			1.52 (m)	C-5, C-18			2.12 (m)	C-1, C-19
4	35.6	C	/	/	43.8	C	/	/
5	56.8	CH	0.85 (m)	C-1, C-7, C-9	56.6	CH	1.07 (m)	C-19, C-7, C-20, C-3
6	18.3	CH_2	1.27, (m)	C-4, C-8, C-10	21.8	CH_2	1.88 (m)	C-4, C-8, C-10
			1.50 (m)	C-8, C-10				
7	41.6	CH_2	1.73 (m)	C-5	28.4	CH_2	1.64 (m)	C-4
			1.80 (m)	C-5, C-15				
8	44.2	C	/	/	44.1	C	/	/
9	56.2	CH	1.02 (m)	C-5, C-9, C-15	55.0	CH	1.12 (m)	C-1, C-7, C-12
10	39.7	C	/	/	39.5	C	/	/
11	18.2	CH_2	1.27 (m)	C-8, C-13	18.2	CH_2	1.64 (m)	C-10, C-13
			1.35 (m)	C-8, C-10				
12	29.7	CH_2	1.12 (m)	C-9, C-14	28.7	CH_2	-	-
13	44.0	CH	2.57, (ddd, *J*=10.7, 3.3, 3.3)	C-11, C-15	41.2	CH	1.53 (m)	C-8, C-15
14	38.7	CH_2	1.02 (m)	C-9, C-12, C-15	28.6	CH_2	-	-
			1.57 (m)	C-9, C-12, C-15				

Table 4. 51 continued

Position	244				245			
	δ_C	Type	δ_H (mult., *J* in Hz)	HMBC	δ_C	Type	δ_H (mult., *J* in Hz)	HMBC
15	49.1	CH_2	1.91 (m)	C-7, C-14, C-17	48.8	CH_2	2.03 (m)	C-14, C-17, C-9
			1.99 (m)	C-7, C-14, C-17			2.10 (m)	C-7, C-14, C-17
16	155.9	C	/	/	155.4	C	/	/
17	102.9	CH_2	4.66 (d, *J*=2.18)	C-13, C-15	102.7	CH_2	4.78 (m)	C-13, C-15
			4.72 (t, *J*=1.70)	C-13, C-15			4.80 (m)	C-13, C-15
18	27.1	CH_3	0.89 (s)	C-3, C-5, C-19	32.9	CH_3	1.19 (s)	C-3
19	65.6	CH_2	3.38 (dd, *J*=10.9, 1.2)	C-3, C-5, C-18	28.6	CH_3	1.21 (s)	C-5, C-18
			3.68 (d, *J*=10.9)					
20	18.1	CH_3	0.94 (s)	C-1, C-9, C-10	15.3	CH_3	1.00 (s)	C-1, C-9

4.5.2.3 *Ent*-kaur-16-ene (245)

The ESIMS analysis (molecular ion peak at *m/z* 273.3) of compound **245** together with the NMR spectroscopic data (Table 4.51) suggested the molecular formula $C_{21}H_{32}$. The evidence of this compound being an *ent*-kaurene diterpene was based on the ^{1}H and ^{13}C NMR data (Table 4.51) which was similar to that of **244** except that compound **245** lacks hydroxy group. The presence of three methyl groups at δ_H 1.19 (H_3-18), δ_H 1.21 (H_3-19), δ_H 1.00 (H_3-20) protons was supported in its ^{1}H NMR spectrum, together with the HMBC correlation of both H_2-17 δ_H (4.78, 4.80) with C-13 (δ_C 41.2) and C-15 (δ_C 48.8) confirmed the typical double bonds C-16(17) of a kaurene diterpene. Comparison of the NMR data of **245** to the reported NMR data for the same compound revealed that **245** is *ent*- kaur-16-ene (Xavier *et al.*, 2017). Therefore, compound **245** was a known compound and named *ent*- kaur-16-ene.

4.5.2.4 Lanosterol (246)

ESIMS analysis (molecular ion peak at *m/z* 427.4) of compound **246** (mp 132-134ºC) together with the NMR spectroscopic data (Table 4.52) revealed the molecular formula $C_{30}H_{50}O$. The ^{13}C NMR analysis displayed thirty carbons including an oxygenated carbon C-3 (δ_C 77.6). Typical olefinic carbons of lanosterol at δ_C 134.4 (C-8) and δ_C 133.3 (C-9) were observed in ^{13}C NMR spectrum. Comparison of the spectral data of this compound with literature (Zamuner *et al.*, 2005; Dias & Gao, 2009) allowed **246** to be identified as lanosterol.

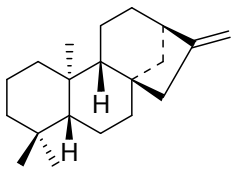

245

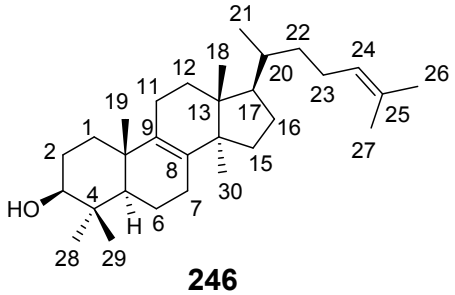

246

Table 4.52: ^{1}H (600 MHz) and ^{13}C (150 MHz) NMR Data of 246 and 247 in CD_2Cl_2

Position	246				247			
	δ_C	Type	δ_H (mult., *J* in Hz)	HMBC	δ_C	Type	δ_H (mult., *J* in Hz)	HMBC
1	35.7	CH_2			37.2	CH_2	1.06 (m)	C-3, C-10, C-19
							1.89 (ddd, *J*=13.2, 3.4, 3.4)	C-3, C-10, C-19
2	28.5	CH_2			31.7	CH_2	1.83 (m)	C-4, C-10
3	77.6	CH	3.19 (m)	35.7, 51.1	71.6	CH	3.50 (m)	C-4, C-10
4	37.1	C	/	/	42.3	C	/	/
5	51.1	CH	1.15 (m)	19.7, 27.5, 27.9, 77.6	140.9	C	/	/
6	18.8	CH_2			121.4	CH	5.39 (m)	C-4, C-8, C-10
7	27.5	CH_2			31.9	CH_2	1.83 (m)	C-5, C-9, C-14
8	134.3	C	/	/	31.9	CH	2.03 (m)	C-6, C-11, C-15
9	133.3	C	/	/	50.2	CH	0.97 (d, *J*=6.5)	C-1, C-7, C-19
10	37.1	C	/	/	36.4	C	/	/
11	21.3	CH_2			21.0	CH_2	1.57 (m)	C-8, C-10, C-13
12	30.9	CH_2	1.68 (m)	15.1, 133.3, 49.6	39.5	CH_2	2.21 (m)	C-9, C-17
			1.74 (br s)				2.03 (m)	C-9
13	44.0	C	/	/	42.1	C	/	/
14	49.6	C	/	/	56.8	CH	1.06 (m)	C-7, C-9, C-16
15	29.5	CH_2			24.3	CH_2	1.57 (m)	C-8, C-13, C-17
16	28.7	CH_2			29.6	CH_2	1.28 (m)	C-14, C-20
17	50.2	CH	1.62 (m)	18.3, 30.9, 29.5	55.9	CH	1.21 (m)	C-15, C-21, C-22

Table 4.52 continued

Position			**246**				**247**	
	δ_C	Type	δ_H (mult., *J* in Hz)	HMBC	δ_C	Type	δ_H (mult., *J* in Hz)	HMBC
18	15.1	CH_3	0.80 (s)	30.9, 50.2	12.0	CH_3	0.85 (d, *J*=7.4)	C-12, C-17
19	19.7	CH_3	1.06 (s)	51.1, 35.7	18.7	CH_3	0.97 (d, *J*=6.5)	C-1, C-5
20	35.3	CH	1.57 (m)	28.7	40.5	CH	2.03 (m)	C-13, C-23
21	18.3	CH_3	0.94 (br s)	18.3, 50.2	21.0	CH_2	1.06 (m)	C-17, C-22
22	35.2	CH_2			138.4	CH	5.20 (m)	C-17, C-21, C-24
23	24.5	CH_2			129.2	CH	5.15 (m)	C-20, C-28
24	124.0	CH	5.14 (br s)	16.8, 27.7	51.2	CH	1.57 (m)	C-22, C-25, C-29
25	134.3	C	/	/	25.4	CH	1.21 (s)	C-23, C-29
26	27.7	CH_3	1.74 (s)	124.0	11.8	CH_3	0.75 (s)	C-24
27	16.8	CH_3	1.62 (s)	124.0	29.7	CH_3	1.31 (br s)	C-24
28	27.9	CH_3	0.90 (s)	51.1, 37.1	20.8	CH_2	1.06 (m)	C-23, C-25
29	15.3	CH_3	1.01 (s)	51.1	19.1	CH_3	0.89 (m)	C-23, C-25
30	23.9	CH_3	0.94 (br s)	29.5, 134.1	/		/	/

4.5.2.5 Stigmasta-5,22(E)-dien-3*β*-ol (247)

Comparison of the ^{1}H and ^{13}C NMR (Table 4.52) spectroscopic data of **190** to that of **247** indicated that they are similar compounds except that **247** has an additional double bond at C-5 (δ 140.9). Thus, the compound was identified as stigmasta-5,22(E)-dien-3*β*-ol (**247**). This compound is very common in high plants and has been widely reported (Chaturvedula and Prakash, 2012).

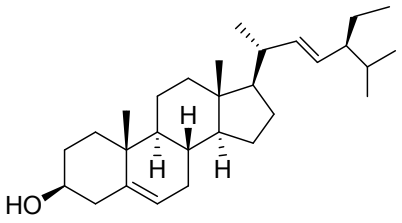

247

4.5.2.6 3*β*-Hydroxy-olean-12-en-29-oic Acid (248)

Compound **248** was purified as a white powder (mp 167-168°C). ESIMS analysis showed a protonated molecular ion peak at *m/z* 457.4 which together with the NMR spectral data (Table 4.53) suggested the molecular formula $C_{30}H_{48}O_3$. The ^{1}H and ^{13}C NMR spectral data (Table 4.53) revealed that this compound is a triterpene derivative. The ^{1}H NMR displayed seven methyl groups at δ_H 0.89 (C-23), δ_H 1.10 (C-24), δ_H 0.88 (C-25), δ_H 0.68 (C-26), δ_H 0.85 (C-27), δ_H 0,70 (C-28) and δ_H 1.23 (C-30). Signals corresponding to an oxygenated methine carbon δ_C 77.3 (C-3) and a carboxylic group at δ_C 179.1 (C-30) were also observed in the ^{13}C NMR spectrum. The presence of a double bond was evidenced by two signals (δ_C 121.7 and δ_C 144.5) in the ^{13}C NMR spectrum which were assigned to C-12 and C-13, respectively. HMBC correlation of H-30 with the carbonyl suggested the placement of the carbonyl at C-29. Based on the above discussed information, **248** was identified as the known 3β-hydroxy-olean-12-en-29-oic acid that compound was previously reported (Zhou *et al.*, 2015).

Table 4.53: ^{1}H (600 MHz) and ^{13}C (150 MHz) NMR Data of 248 in CD_2Cl_2

Position	δ_C	Type	δ_H (mult., *J* in Hz)	HMBC
1	38.8	CH_2	0.95 (m)	C-3, C-5, C-25
			1.47 (m)	C-3, C-9, C-25
2	33.4	CH_2	1.25 (m)	C-4, C-10
			1.42 (m)	-
3	77.3	CH	2.95 (m)	C-23. C-24,C-1
4	40.5	C	/	/
5	56.4	CH	0.95 (m)	C-1, C-3, C-25
6	18.4	CH_2	1.47 (m)	C-4, C-8
7	30.7	CH_2	1.57 (m)	C-5, C-9
			1.72 (m)	C-9, C-15
8	38.1	C	/	/
9	48.2	CH	1.72 (m)	-
10	37.1	C	/	/
11	19.3	CH_2	1.25 (m)	C-10, C-13
			1.80 (d, *J*=11.9)	C-10, C-13
12	121.7	CH	3.00 (m)	C-9, C-14
13	144.5	C	/	/
14	42.2	C	/	/
15	26.9	CH_2	1.42 (m)	C-8, C-17
			1.47 (m)	C-17
16	22.4	CH_2	1.72 (m)	C-22
17	45.1	C	/	/
18	41.5	CH	0.78 (m)	C-12, C-20
19	43.3	CH_2	1.34 (m)	C-29
			1.47 (m)	C-30
20	28.7	C	/	/
21	37.5	CH_2	1.47 (m)	C-17
			2.00 (m)	C-29, C-30
22	26.9	CH_2	1.42 (m)	C-22
23	29.1	CH_3	0.89 (s)	C-24, C-5
24	15.8	CH_3	1.10 (s)	C-5
25	15.7	CH_3	0.88 (s)	C-1, C-9
26	16.5	CH_3	0.69 (s)	C-9
27	15.8	CH_3	0.85 (s)	C-15
28	17.3	CH_3	0.70 (s)	-
29	179.1	C	/	/
30	24.9	CH_3	1.23 (s)	C-29

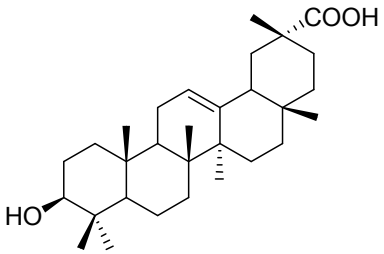

248

4.5.2.7 Carissone (249)

Compound **249** was purified as a colourless powder. ESIMS analysis of **249** showed a protonated molecular ion peak at *m/z* 237.2 which together with the NMR spectra (Table 4.54) suggested the molecular formula as $C_{15}H_{24}O_2$. It was evident from the ^{13}C NMR spectrum that this compound is a sesquiterpene exhibiting fifteen signals for fifteen carbons. The chemical shift position of the carbonyl at δ_C 196.9 (C-3) and those of two olefinic carbons δ_C 125.3(C-4) and δ_C 163.0 (C-5), suggested an *α,β*-unsaturated ketone moiety. Comparison of the NMR spectral data (Table 4.54) of **249** with a previously reported compound from *Carissa opaca* (Reisch *et al.,* 1990) allowed the identification of this compound as carissone. The identity was confirmed by HMBC experiment (Table 4.54). was compared to that of the same compound previously reported from *Carissa opaca* and similarity has been observed. HMBC correlations of both methyls CH_3-14 and CH_3-15 with C-5 further confirmed the structure. Therefore, compound **249** is being reported for the first time from the family asteracea was named carissone.

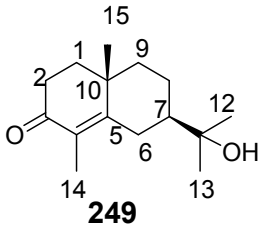

249

Table 4.54: ^{1}H (600 MHz) and ^{13}C (150 MHz) NMR Data of 249 in CD_2Cl_2

Position	δ_C	Type	δ_H (mult., *J* in Hz)	HMBC
1	53.9	CH_2	1.73 (m)	C-2, C-10, C-15
			1.94 (m)	C-10, C-15
2	35.4	CH_2	2.27 (m)	C-1, C-5
			2.35 (m)	C-1, C-5
3	196.9	C	/	/
4	125.3	C	/	/
5	163.0	C	/	/
6	34.4	CH_2	1.87 (m)	C-1, C-7
			1.98 (m)	C-1, C-11
7	48.2	CH	2.05 (m)	C-6, C-9
8	25.2	CH_2	2.35 (m)	C-5, C-11
			2.65 (m)	C-5, C-11
9	46.5	CH_2	-	-
10	42.7	C	/	/
11	78.9	C	/	/
12	27.1	CH_3	1.18 (s)	-
13	28.7	CH_3	1.23 (s)	-
14	9.9	CH_3	1.68 (3H, s)	C-1, C-2, C-10
15	23.9	CH_3	1.42 (3H, s)	C-4, C-6, C-10

4.5.3 Characterization of Secondary Metabolites Isolated from Roots of *Aspilia mossambicensis*

Phytochemical investigation of the roots of *A. mossambicensis* afforded four compounds (**250-253**) and three additional amounts of **236**, **237** and **238**.

4.5.3.1 Methyl-15*α*-angeloyloxy-*ent*-kaur-16-en-19-oate (250)

Compound **250** was isolated as a colourless crystal from the roots of *Aspilia mossambicensis*. LC-MS analysis (molecular ion peak at *m/z* 415.3) and ^{1}H and ^{13}C NMR data (Table 4.55) suggested a molecular formula $C_{26}H_{38}O_4$. The ^{1}H and ^{13}C NMR spectral data of this compound (**250**) was very similar to that of **238** and showed that it is an *ent*-kaur-16-ene derivative with methyl ester (at C-19) and an angeloyloxy (at C-15) substituents. The only difference from compound **238** was that **250** did not have a hydroxy group at C-9 (δ_C 167.7).

HMBC correlation of the methoxy protons (δ_H 3.64) with C-19 (δ_C 177.7) and that of H-15 (δ_H 5.34) with the carbonyl C-1' (δ_C 167.7) further support the placement of the mthyl ester at C-19 and angeloyloxy substituent at C-15. Therefore, compound **250** was identified as methyl-15*α*-angeloyloxy-*ent*-kaur-16-en-19-oate (Aráoz *et al.*, 2010).

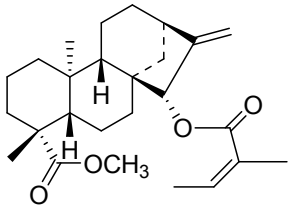

250

Table 4.55: ^{1}H (600 MHz) and ^{13}C (150 MHz) NMR Data of 250 in CD_2Cl_2

Position	δ_C	Type	δ_H (mult., *J* in Hz)	HMBC
1	40.6	CH_2	0.92 (m)	C-3, C-9, C-20
			1.90 (m)	C-3, C-9, C-20
2	19.1	CH_2	1.47 (m)	C-4, C-10
			1.66 (m)	C-4, C-10
3	37.9	CH_2	1.06 (dd, *J*=13.7, 4.1)	C-1, C-5, C-18
			1.18 (m)	C-1, C-5, C-19
4	43.6	C		
5	56.5	CH	1.10 (m)	C-7, C-18, C-19, C-20
6	20.9	CH_2	1.06 (m)	C-4, C-8, C-10
			1.9 (m)	
7	35.1	CH_2	1.31 (dd, *J*=13.2, 3.4)	C-5, C-9, C-15
			1.70 (ddd, *J*=6.2, 3.5, 3.5)	C-5, C-9, C-15
8	47.5	C		
9	53.0	CH		
10	39.6	C		
11	18.4	CH_2	1.66 (m)	C-8, C-10, C-13
			1.53 (m)	
12	32.7	CH_2	1.47 (m)	C-9, C-14, C-16
			1.60 (m)	C-9, C-14, C-16
13	42.7	CH	2.82 (br s)	C-8, C-11, C-17
14	37.3	CH_2	1.53 (m)	C-9, C-15, C-16
			2.02 (m)	C-9, C-15, C-16
15	82.5	CH	5.34 (br s)	C-1', C-9, C-13, C-17
16	156.0	C		

Table 4. 55 continued				
Position	δ_C	Type	δ_H (mult., *J* in Hz)	HMBC
17	109.5	CH_2	5.11 (s)	C-13, C-15
			5.15 (s)	C-13, C-15
18	28.4	CH_3	1.18 (3H, s)	C-4, C-5, C-19
19	177.7	C		
20	15.5	CH_3	0.88 (3H, s)	C-1, C-5
1’	167.7	C		
2’	128.4	C	/	/
3’	136.9	CH	6.07 (dddd, *J*= 8.7, 7.2, 5.8, 1.5)	C-4', C-5', C-1', C-2'
4’	15.0	CH_3	1.99 (br s)	C-2'
5’	20.5	CH_3	1.90 (br s)	C-2', C-3' C-1'
OCH_3	50.9	CH_3	3.64 (3H, s)	C-19

4.5.3.2 12-Oxo-*ent*-kaura-9(11),16-dien-19-oic Acid (251)

Compound **251** was isolated as colourless paste from the roots of both plants *Aspilia pluriseta* and *Aspilia mossambicensis*. EIMS analysis showed an intense molecular ion peak at *m/z* 315.3 which together with NMR data (Table 4.56) was in agreement with the molecular formula $C_{20}H_{26}O_3$. Comparison of the MS and NMR (Table 4.56) data of this compound with those reported in literature indicated that compound **251** is a kaurene derivative (Qiu *et al.*, 2014, Huang *et al.*, 2016). The ^{13}C NMR chemical shift value of a carbonyl C-12 (δ_C 200.1 for C=O) indicated an α,β-unsaturated carbonyl. The HMBC correlation oh H-11 (δ_H 5.76) with C-9 (δ_C 180.2) and C-12 (δ_C 200.1) revealed that the double bond was located at C-9(11). Furthermore, HMBC correlations of methynic protons H_2-17 (δ_H 5.76) with C-13 (δ_C 45.5) and C-15 (δ_C 48.5) were in agreement with this compound being a kaurene diterpene. the placement of the hydroxycarbonyl at C-19 (δ_C 180.1 for C=O) was evidenced by the HMBC correlation of CH_3-18 with C-19. Furthermore, the optical rotation ($[\alpha]_D^{20}$ −66) of this compound indicated that this compound belongs to a *ent*-kaurene diterpene series. On the basis of the above information, compound **251** was characterised as 12-oxo-*ent*-kaura-9(11),16-dien-19-oic acid. This compound is reported in literature (Huang *et al*., 2016), however, tt is being reported from this plant for the first time.

Table 4.56: ^{1}H (600 MHz) and ^{13}C (150 MHz) NMR Data of 251 and 252 in CD_2Cl_2

Position	251				252			
	δ_C	Type	δ_H (mult., *J* in Hz)	HMBC	δ_C	CH_2	δ_H (mult., *J* in Hz)	HMBC
1	39.8	CH_2	1.28 (m)	C-3, C-10, C-20	40.6	CH_2	1.85 (m)	C-3, C-10, C-20
			1.94 (m)	C-3, C-10, C-20				C-3, C-10, C-20
2	19.9	CH_2	1.63 (m)	C-4, C-10	19.0	CH_2	1.38 (m)	C-4, C-10
			1.94 (m)	C-4				C-4, C-10
3	38.1	CH_2	1.04 (m)	C-1, C-5, C-18, C-19	38.0	CH_2	1.71 (m)	C-5, C-18
			2.22 (d, *J*=13.2)	C-5, C-18			2.12 (m)	C-5, C-18
4	40.4	C	/	/	43.1	C	/	/
5	58.2	CH	3.39 (m)	C-1, C-3, C-7, C-9	56.6	CH	1.52 (m)	C-1, C-3, C-7
6	18.3	CH_2	1.79 (dd, *J*=11.2, 4.8)	C-4, C-8, C-10				
			2.14 (m)	C-4, C-8, C-10	22.1	CH_2	1.86 (m)	C-5, C-9, C-15
7	28.9	CH_2	1.69 (m)	C-5, C-9, C-15	26.7	CH_2	1.42 (m)	C-5, C-9, C-15
			2.09	C-5, C-9, C-15				
8	44.6	C	/	/	45.1	C	/	/
9	180.2	C	/	/	56.1	CH	1.01 (m)	C-1, C-12, C-20
10	45.2	C	/	/	39.5	C	/	/
11	120.0	CH	5.76 (s)	C-9, C-12	18.1	CH_2	1.58 (m)	C-9, C-12
12	200.1	C	/	/	29.3	CH_2		
13	45.5	CH	1.63 m	C-8, C-11, C-17	42.1	CH	1.52 (m)	C-11, C-17
14	44.2	CH_2	2.40 (ddd, *J*=15.9, 2.9, 2.9)	C-9, C-12, C-15	37.3	CH_2		
			2.53 (d, *J*=4.7)	C-9, C-12, C-15			1.86 (m)	C-9, C-12, C-15

Table 4.56 continued

Position	251				252			
	δ_C	Type	δ_H (mult., *J* in Hz)	HMBC	δ_C	CH_2	δ_H (mult., *J* in Hz)	HMBC
15	48.5	CH_2	1.79 (d, *J*=4.8)	C-7, C-14, C-17	48.5	CH_2	1.86 (m)	
			1.94 (m)	C-7, C-14, C-17				
16	146.6	C	/	/	29.5	CH		
17	11.2	CH_2	5.00 (br s)	C-13, C-15	23.9	CH_3	1.33 (3H, s)	C-13, C-15
			5.25 (br s)	C-13, C-15				
18	28.2	CH_3	1.26 (s)	C-3, C-5, C-19	28.3	CH_3	1.20 (3H, s)	C-3, C-5, C-19
19	181.4	C	/	/	177.9	C	/	
20	22.8	CH_3	1.17 (s)	C-1, C-9, C-10	15.2	CH_3	1.01 (3H, s)	

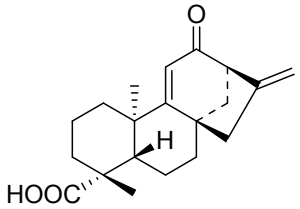

251

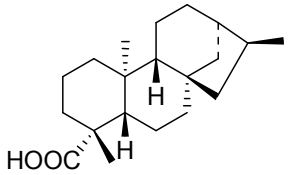

252

4.5.3.3 *Ent*-kauran-19-oic Acid (252)

Compound **252** was isolated as a colourless amorphous solid. ESIMS ([M+H]+ at *m/z* 389.6) together with the ^{1}H and ^{13}C NMR spectral data (Table 4.56) is in agreement with the molecular formula $C_{20}H_{32}O_2$ for this compound. The ^{1}H and ^{13}C NMR data (Table 67) indicated a kaurene diterpene skeleton. However there was no signals for the olefinic carbon on ^{13}C NMR spectrum. Besides, three methyl signals assigned to C-17 (δ_C 23.9), C-18 (δ_C 28.3) and C-20 (δ_C 15.2) were observed on ^{1}H NMR spectrum and a carbonyl at C-19 (δ_C 177.9) was evidenced on ^{13}C NMR spectrum. This suggested that the C-16 (17) double bond which is common in kaurene was reduce into a methine CH-16 (δ_C 29.5) and a methyl CH_3-17 (δ_C 23.9) instead. was hydrogenated and hence a methyl group at CH_3-17 instead. HMBC correlation of CH_3-18 protons with the hydroxy carbonyl at C-19, and that of CH_3-17 protons with both C-13 and C-15 further support the proposed structure. Based on this evidence and similarity of the NMR spectral data to that reported in literature (Tincusi *et al.*, 2002), it was evident that **252** is *ent*-kauran-19-oic acid. This compound is being reported for the first time from the genus *Psiaidia*.

4.5.3.4 Oleanolic Acid (253)

Compound **253** was isolated from the root extract of *Aspilia mossambicensis* and showed a $[M+H]^+$ peak at *m/z* 457.4 corresponding to the molecular formula $C_{30}H_{48}O_3$. The ^{1}H and ^{13}C NMR data (Table 4.57) indicated that this compound was a triterpene showing signals of seven methyls, two olefinic carbons, a hydroxy carbonyl and a n oxymethine carbon atoms. HMBC correlation of H_2-22 with the hydroxy carbonyl revaealed the placement of this hydroxy carbonyl at C-28. The placement of the double bond at C-12 was indicated by HMBC correlation of H_2-11 with C-12. Comparison of of the NMR spectroscopic data with literature (Seebacher *et al.*, 2003) allowed the identification of compound **253** as oleanolic acid.

Table 4.57: ^{1}H (600 MHz) and ^{13}C (150 MHz) NMR Data of 253 in CD_2Cl_2

Position	δ_C	Type	δ_H (mult., *J* in Hz)	HMBC
1	38.6	CH_2	0.98 (d, *J*=6.6)	C-3, C-5, C-25
			1.62 (m)	C-3, C-9, C-25
2	29.2	CH_2	1.32 (m)	C-4, C-10
3	77.1	CH	3.17 (dd, *J*=11.3, 4.7)	C-23. C-24,C-1
4	39.3	C	/	/
5	55.9	CH	0.81 (m)	C-1, C-3, C-25
6	18.2	CH_2	1.44 (m)	C-4, C-8
			1.57 (m)	C-4, C-8
7	33.6	CH_2	1.22 (m)	C-5, C-9
			1.44 (m)	C-9, C-15
8	38.4	C	/	/
9	47.6	CH	1.62 (m)	-
10	36.9	C	/	/
11	23.2	CH_2	1.91 (dd, *J*=8.9, 3.6)	C-10, C-13
			1.90 (m)	C-10, C-13
12	122.1	CH	5.26 (dd, *J*=3.7, 3.7)	C-9, C-14
13	140.0	C	/	/
14	41.6	C	/	/
15	27.8	CH_2	1.10 (m)	C-8, C-17
			1.76 (m)	C-17
16	23.0	CH_2	1.62 (m)	C-22
			2.05(m)	C-22
17	46.9	C	/	/
18	41.4	CH	2.90 (m)	C-12, C-20
19	46.9	CH_2	1.17 (m)	C-29
			1.76 (m)	C-30
20	30.4	C	/	/
21	32.8	CH_2	1.32 (m)	C-17
			1.54 (m)	C-29, C-30
22	32.5	CH_3	1.62 (m)	C-22
			1.76 (m)	C-22
23	27.5	CH_3	1.01 (3H, s)	C-24, C-5
24	15.4	CH_3	0.80 (3H, s)	C-5
25	14.9	CH_3	0.96 (3H, s)	C-1, C-9
26	16.7	CH_3	0.82 (3H, s)	C-9
27	25.4	CH_3	1.19 (3H, s)	C-15
28	177.9	C	/	/
29	32.5	CH_3	0.94 (3H, s)	C-30
30	22.9	CH_3	0.96 (3H, s)	C-29

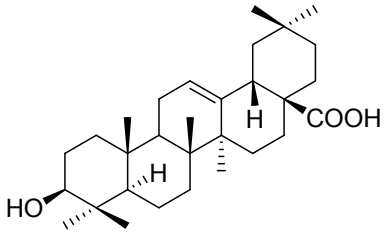

253

9*β*-Hydroxy-15*α*-angeloyloxy-*ent*-kaur-16-en-19-oic acid (**236**), 15*α*-Angeloyloxy-*ent*-kaur-16α,17-epoxy-*ent*-kauran-19-oic acid (**237**), Methyl-9*β*-hydroxy-15*α*-angeloyloxy-*ent*-kaur-16-en-19-oate (**238**) were also isolated from the root parts.

4.5.4 Characterization of Compounds Isolated from Aerial parts of *Aspilia mossambicensis*

The aerial part extract od *A. mossambicensis* yieded four compounds (**254-257**) and additional amount of three compounds (**240**, **243**, **247**).

4.5.4.1 *β*-Amyrin Acetate (254)

Compound **254** was isolated as amorphous solid. ESIMS ($[M]^+$ at *m/z* 469.4) and NMR spectral data (Table 4.58) suggested the molecular formula $C_{32}H_{52}O_2$ of this compound. The ^{1}H NMR spectrum revealed nine methyls. The presence of an acetate group was evidenced by HMBC correlation of H-3 with the carbonyl. This was further justified by the presence of exactly 32 carbon signals observed on ^{13}C NMR spectrum. Based on the above evidence and comparison of the NMR spectral (Table 4.58) data of **254** with literature the compound was identified as *β*-amyrin acetate, previously isolated from *Aspilia africana* (Faleye, 2012).

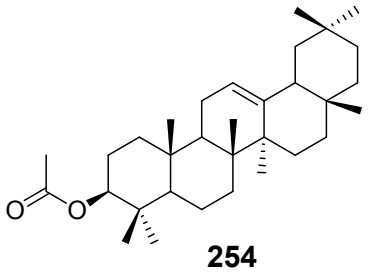

254

Table 4.58: ^{1}H (600 MHz) and ^{13}C (150 MHz) NMR Data of 254 in CD_2Cl_2

Position	δ_C	Type	δ_H (mult., *J* in Hz)	HMBC
1	38.2	CH_2	1.26 (m)	C-3, C-5, C-25
			1.47 (m)	C-3, C-9, C-25
2	28.3	CH_2	1.32 (m)	C-4, C-10
3	81.3	CH	4.50 (m)	C-1, C-1', C-23, C-24,
4	40.4	C	/	/
5	55.8	CH	0.92 (m)	C-1, C-3, C-25
6	18.8	CH_2	1.47 (m)	C-4, C-8
			1.59 (m)	C-4, C-8
7	33.6	CH_2	1.39 (td, *J*=14.4, 14.0, 3.5)	C-5, C-9
			1.59 (m)	C-9, C-15
8	37.7	C	/	/
9	48.1	CH	1.65 (m)	-
10	37.4	C	/	/
11	24.2	CH_2	1.65 (m)	C-10, C-13
			1.92 (m)	C-10, C-13
12	122.3	CH	5.23 (br)	C-9, C-14
13	146.7	C	/	/
14	42.3	C	/	/
15	27.5	CH_2	1.76 (m)	C-8, C-17
16	24.2	CH_2	1.65 m)	C-22
			1.92 (m)	C-22
17	47.3	C	/	/
18	38.8	CH	1.99 (m)	C-12, C-20
19	47.8	CH_2	1.16 (m)	C-29
			1.65 (m)	C-30
20	35.3	C	/	/
21	33.0	CH_2	1.59 (m)	C-29, C-30
			1.39 (m)	C-22
22	28.7	CH_2	1.59 (m)	C-22
			0.88 (3H, s)	C-24, C-5
23	17.0	CH_3	1.01 (3H, s)	C-5
24	15.9	CH_3	1.02 (3H, s)	C-1, C-9
25	17.2	CH_3	0.91 (3H, s)	C-9
26	26.7	CH_3	1.19 (3H, s)	C-15
27	24.0	CH_3	0.91 (3H, s)	C-16, C-22
28	33.1	CH_3	0.93 (3H, s)	C-30
29	26.3	CH_3	1.19 (3H, s)	C-29
30	35.3	CH_3	1.38 (m)	C-17
1'	171.2	C	/	/
2'	21.6	CH_3	2.06 (s)	C-1'

4.5.4.2 *Ent*-kaura-9(11),16-diene (255)

Compound **255** was isolated as a colourless solid from the aerial part extract of *Aspilia mossambicensis*. The ^{1}H and ^{13}C NMR spectroscopic data (Table 4.59) and a molecular ion peak at *m/z* 271.2 observed in ESIMS, are in agreement with the molecular formula $C_{20}H_{30}$. Unlike in compound **240**, this compound (**255)** did not show any signal of a carbonyl. This being the only difference observed in NMR spectral data (Table 4.59), the structure of **255** was proposed and identified as *ent*-kaura-9(11),16-diene. The isolation of *ent*-kaura-9(11),16-diene from the Asteraceae family is documented (Zhang *et al.*, 2001).

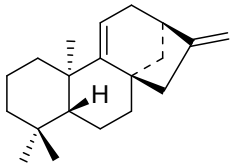

255

Table 4.59: ^{1}H (600 MHz) and ^{13}C (150 MHz) NMR Data of 255 and 256 in CD_2Cl_2

Position	255				256			
	δ_C	Type	δ_H (mult., *J* in Hz)	HMBC	δ_C	Type	δ_H (mult., *J* in Hz)	HMBC
1	40.7	CH_2	0.87 (m)	C-5, C-20	40.7	CH_2	1.24 (m)	C-3, C-9
			2.01 (m)	C-3, C-20			1.95 (m)	C-3, C-20
2	18.4	CH_2	1.65 (m)	C-4	18.3	CH_2	1.51 (m)	C-4, C-10
			2.50 (m)	C-4, C-10			1.95 (m)	C-4, C-10
3	38.1	CH_2	1.07 (dd, *J*=11.3, 5.1)	C-1, C-18	38.3	CH_2	1.05 (m)	C-1, C-5, C-18
			2.50 (dd, *J*=11.4, 2.3)	C-1, C-5, C-19			2.14 (m)	C-1, C-5, C-19
4	42.2	C	/	/	43.1	C	/	/
5	56.9	CH	1.14 (m)	C-3, C-18, C-20	56.5	CH	1.173 (m)	C-7, C-18, C-20
6	20.2	CH_2	1.53 (m)	C-4, C-8	20.1	CH_2		
			1.92 (m)				2.63 (m)	C-8, C-10
7	46.4	CH_2	1.74 (m)	C-5, C-9, C-15	48.9	CH	1.24 (m)	C-5, C-9
							1.95 (m)	C-5, C-9
8	44.9	C	/	/	46.8	C	/	/
9	158.6	C	/	/	153.5	C	/	/
10	38.8	C	/	/	39.7	C	/	/
11	114.8	CH	5.29 (br s)	C-13, C-8	118.1	CH	5.27 (m)	C-8, C-10
12	29.6	CH_2	1.53 (m)	C-9, C-16	38.3	CH_2	1.95 (m)	C-14, C-16
			2.02(m)	C-9, C-16			2.31 (m)	C-9, C-14, C-16
13	41.3	CH	1.53 (m)	C-11, C-17	45.7	CH	2.76 (br s)	C-11, C-17

Table 4.59 continued

Position			**255**				**256**	
	δ_C	Type	δ_H (mult., *J* in Hz)	HMBC	δ_C	Type	δ_H (mult., *J* in Hz)	HMBC
14	37.9	CH_2	2.23 (ddd, *J*=15.6, 2.6, 2.6)	C-7, C-16	27.7	CH_2	1.51 (m)	C-9, C-15, C-16
			2.67 (m)	C-7			2.08 (m)	C-9, C-16
15	50.2	CH_2	2.08 (m)	C-9, C-17	72.2	CH	3.89 (m)	C-9, C-13, C-17
16	156.0	C	/	/	158.5	C	/	/
17	106.2	CH_2	4.83 (m)	C-13	107.2	CH_2	4.78 (m)	C-13, C-15
			4.96 (m)	C-13			4.91 (m)	C-13
18	23.4	CH_3	1.07 (3H, s)	C-5, C-19	23.02	CH_3	1.23 (3H, s)	C-4, C-5
19	28.0	CH_3	1.29 (3H, s)	C-4	28.5	C	/	/
20	14.5	CH_3	0.99 (3H, s)	C-1, C-9	13.6	CH_3	1.09 (3H, s)	C-5, C-9

4.5.4.3 15*α*-Hydroxy-kaura-9(11),16-diene (256)

Compound **256** was obtained as white solid from the aerial parts of *Aspilia mossambicensis*. The ^{1}H and ^{13}C NMR spectroscopic data (Table 4.58) of this compound was similar to that of **240** except that **256** has an additional hydroxy group at C-15 (δ_C 72.2). HMBC corelation of H_2-17 (δ_H 4.78) and H_2-7 (δ_H 1.24) with C-15 (δ_C 72.2) indicated the location of hydroxy at C-15. These evidences suggested a molecular formula $C_{20}H_{30}O$ for **256** and identified as 15*β*-hydroxy-kaura-9(11),16-diene. This compound was previously reported in the literature (Nagashima *et al.*, 2005).

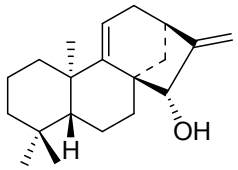

256

4.5.4.4 Methyl Cinnamate (257)

Compound **257** was isolated as colourless solid from the roots *Aspilia mossambicensis*. The molecular formula $C_{10}H_{10}O_2$ was suggested based on ^{1}H and ^{13}C NMR spectroscopic data (Table 4.60). The ^{1}H NMR data revealed a monosubstituted benzene protons at δ_H 7.78 (C-2), δ_H 6.88 (C-3), δ_H 6.96 (C-4), δ_H 7.78 (C-5), δ_H 6.96 (C-6) and a methyl ester goup at δ_C 166.9 (C-9). In addition to that, ^{13}C NMR spectrum displayed olefinic carbons at δ_C 114.4 (C-7) and δ_C 115.8 (C-8). HMBC correlations of the methoxy protons (δ_H 3.73) with the carbonyl C-9 further support that it is a methyl ester of cimmic acid (Gao *et al.*, 2012; Guzman, 2014). Hence, compound **257** was identified as methyl cinnamate and it is being reported for the first time from the genus *Aspilia*.

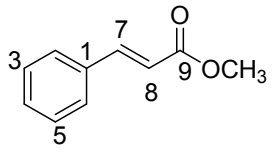

257

Table 4.60: ^{1}H (600 MHz) and ^{13}C (150 MHz) NMR Data of 257 in CD_2Cl_2

Position	δ_C	Type	δ_H (mult., *J* in Hz)	HMBC
1	130.8	C	/	/
2	115.5	CH	7.78 (d, *J*=8.6)	C-4
3	117.4	CH	6.88 (d, *J*=8.6)	C-1, C-5
4	121.6	CH	6.96 (d, *J*=8.6)	C-2
5	115.8	CH	7.78 (d, *J*=8.6)	C-1
6	114.4	CH	6.96 (d, *J*=8.6)	-
7	144.8	CH	6.32 (d, *J*=15.6)	C-9
8	126.6	CH	7.56 (d *J*=15.6)	-
9	166.9	C	/	/
OCH_3	50.6	CH_3	3.73 (3H, s)	C-9

Ent-kaur-16-en-19-oic acid (**243**), *ent*-kaura-9(11)-16-dien-19-oic acid (**240**) and stigmasta-5,22(E)-dien-3β-ol (**247**) were also isolated from the roots of *A. mossambicensis.*

4.5.5 Summary of Compounds from Aspilia pluriseta and *Aspilia mossambicensis*

A total of fourteen compounds have been isolated from *Aspilia pluriseta*. In addition, this is the first time that compounds **234**, **235**, **238, 241, 242, 246, 243** and **249** are being reported from this plant. From *Aspilia mossambicensis*, all the compounds are reported for the first time from the plant except **255**. Besides, four kaurene derivative were prepared by semi-synthetic reaction, among which two were new.

4.6 Biological Activities of the Isolated Compounds from *Aspilia* species

4.6.1 Antimicrobial Activity of *Aspilia* species

Both *Aspilia mossambicensis* aerial parts (AMA) and roots (AMR) extracts showed considerable antibacterial activity against *E. coli* when using microbroth dilution method (Table 4.61A), followed by *ent*-kaur-16-en-19-oic acid (**243**), lanosterol (**246**) and 9*β*-hydroxy-15*α*-angeloyloxy-*ent*-kaur-16-en-19-oic acid (**236**). In contrast, 15*α*-angeloyloxy-16β,17-epoxy-*ent*-kauran-19-oic acid (**237**) was inactive against *E. coli*, but moderately active against *S. aureus*. In this kinetic method, *ent*-kaura-9(11),16-dien-19-oic acid (**240**) showed slight activity against both *S. aureus* and *E. coli.*

The roots (APR) and aerial part (APA) extracts of *Aspilia pluriseta* showed the highest activity against *S. aureus, E. coli* and *M. gypseum* in the Agar disc diffusion assay (Table 4.61B). Compound **252** exhibited activity against *C. parapsilosis* displaying an inhibition zone of 7 mm. The other compounds assayed did not show considerable activity against this panel of bacteria strains and fungi.

Table 4.61: Antimicrobial results on *Aspilia* species

A: Microbroth Kinetic System

	E. coli			***S. aureus***		
Concentration (µg/ml)	**160**	**80**	**40**	**160**	**80**	**40**
Samples	**% Inhibition (405 nm)**			**% Inhibition**		
Gentamicin	61	53	50	96	97	97
Erythromycin	41	7	ne	98	98	98
Aspilia pluriseta						
238	30	ne	ne	ne	ne	ne
236	29	8	19	ne	1	ne
237	ne	ne	3	33	30	25
245	ne	ne	2	ne	3.34	16
243	43	7	10	ne	ne	ne
240	10	7	5	7	3.89	25
246	27	24	28	ne	ne	ne
249	6	ne	ne	ne	ne	ne
Aspilia mossambicensis						
257	ne	ne	ne	ne	ne	ne
253	ne	ne	ne	ne	ne	ne
247	ne	ne	ne	ne	ne	ne
254	ne	ne	7	ne	ne	ne
255	ne	ne	ne	ne	ne	ne
AMR	52	55	68	ne	ne	7
AMA	52	51	50	ne	ne	ne

B: **Agar Diffusion Method**

	Antibacterial assay		*Antifungal assay*						
Compounds	*S. a*	*E. c*	*M. g*	*T. m*	*C. p*	*C. a*	*A. f*	*A. n*	*C. n*
236	0	0	na	na	na	na	0	0	0
241	0	0	na	na	na	na	0	0	0
248	0	0	na	na	na	na	0	0	0
237	0	0	na	na	na	na	0	0	0
252	0	0	0	0	7	0	na	na	na
APA	11	7	8	0	0	0	na	na	na
APR	10	8	11	0	0	0	na	na	na
Gentamycin	20	13	-	-	-	-	-	-	-
Nystatin	-	-	13	10	16	13	15	13	18

Key: *S. a = Staphylococcus aureus* (ATCC 25923), *E. c = Escherichia. coli* (ATCC 25922), *M, g = Microsporum gypseum, T. m = Trichophyton mentagrophytes* (clinical isolates), *C. p = Candida parapsilosis* (ATCC 22019), *C. a = Candida albicans* (ATCC 90018), *A. f = Aspergilus flavus, A. n = Aspergilus niger* (environmental), *C. n = Cryptococcus neoformans (clinical), na = not accessed, ne = not effective*), APA = *Aspilia pluriseta* arial parts extracts, APR = *A. pluriseta* roots extracts, AMA = *A. mossambicensis* aerial parts extracts, AMR = *A. mossambicensis* roots extracts

4.6.2 Cytotoxicity on *Aspilia* Species

Results of cytotoxicity against two normal (BEAS-2B, LO_2) cell lines and three cancer (A549, Hep-G2, Vero) cell lines is summarized in Table 4.62. Of the tested compounds, 12α-methoxy-*ent*-kaura-9(11),16-dien-19-oic acid (**234**), 9β-hydroxy-15α-angeloyloxy-*ent*-kaur-16-en-19-oic acid (**236**), 15α-angeloyloxy-16β,17-epoxy-*ent*-kauran-19-oic acid (**237**),12-oxo-*ent*-kaura-9(11),16-dien-19-oic acid (**251**), *ent*-kauran-19-oic acid (**252**) showed cytotoxicity against different cell lines, exhibiting CC_{50} values of less than 100 µM (Table 4.62). When tested against DU-145 cancer cell lines, only *ent*-kauran-19-oic acid (**252**) showed moderate cytotoxicity with a CC_{50} value of 69.4 ± 0.1 µM. The remaining compounds did not show any activity against DU-145 cell lines. Compound **236** (CC_{50} = 30.7 ± 1.70 µM) was the most active against A549 cancer cell line. Moreover, **237** was toxic against Hep-G2, LO_2 and BEAS-2B and LO_2 with CC_{50} values of 24.7 ± 2.8, 57.2 ± 1.2 and

89.9 ± 2.0 μM, respectively. This indicate a low selectivity as it is also cytotoxic against normal cells. However, the selectivity can be improve by structural modification.

Table 4.62: Cytotoxicity of *Aspilia* species

Compound	CC_{50} (μM)					
	Normal cell lines		Cancer cell lines			
	BEAS-2B	LO_2	A549	Hep-G2	Vero	DU-145
234	>100	>100	>100	27.3 ± 1.9	-	-
235	>100	>100	>100	>100	-	-
236	>100	>100	30.7 ± 1.70	>100	-	-
237	89.9 ± 2.0	57.2 ± 1.2	>100	24.7 ± 2.8	-	-
238	>100	>100	>100	>100	-	-
239	>100	>100	>100	>100	-	-
240	>100	>100	>100	>100	-	-
241	>100	75.3 ± 2.8	>100	>100	-	-
242	>100	>100	>100	>100	-	-
243	>100	>100	>100	>100	>100	>100
247	>100	>100	>100	>100	-	>100
248	>100	>100	>100	>100	-	-
251	38.6 ± 2.5	30.0 ± 1.7	80.5 ± 1.8	81.3 ± 0.3	-	-
252	-	-	-	-	-	69.4 ± 0.1

4.6.3 Anti-inflammatory Activity on *Aspilia* Species

The results of the anti-inflammatory activity test (Table 4.63) showed that the crude extract of *Aspilia pluriseta* and 15*α*-angeloyloxy-*ent*-kaur-16-en-19-oic acid (**239**) were weakly active. The compoumds *ent*-kaura-9(11),16-dien-19-oic acid (**240**), methyl-*ent*-kaur-16-en-19-oate (**242**) and *ent*-kaur-16-en-19-oic acid (**243**) were inactive at 400 mg/Kg body weight. Although, there was no significant anti-inflammatory activity observed for the isolated compounds, further work should be done on this plant to identify the compounds responsible for the anti-inflammatory activity observed for the crude extract.

Table 4.63: Anti-inflammatory Activity Results on *Aspilia* Species

Treatment/ Drug	Dose mg/Kg	Carrageenan-induced oedema: in Paw volumes (mean ± SD, n = 5) in mL				
		0 mn	60 min	120 min	180 min	240 min
Normal saline	-	0	1.29 ± 0.07	1.32 ± 0.19	1.57 ± 0.13	1.62 ± 0.08
Indomethacin	10	0	0.84 ± 0.01	0.95 ± 0.04	0.97 ± 0.01	1.03 ± 0.02
239	400	0	1.16 ± 0.07	1.22 ± 0.03	1.23 ± 0.05	1.25 ± 0.11
240	400	0	1.43 ± 0.03	1.45 ± 0.15	1.48 ± 0.03	1.70 ± 0.07
242	400	0	1.34 ± 0.10	1.38 ± 0.03	1.34 ± 0.03	1.37 ± 0.09
243	400	0	1.26 ± 0.04	1.29 ± 0.04	1.31 ± 0.12	1.16 ± 0.03
APA	400	0	1.08 ± 0.09	1.33 ± 0.06	1.40 ± 0.01	1.42 ± 0.15
APR	400	0	1.19 ± 0.07	1.48 ± 0.11	1.55 ± 0.12	1.56 ± 0.05

Key: APA = *Aspilia pluriseta* arial parts extracts, APR = *A. pluriseta* roots extracts

4.6.4 Oral glucose Tolerance Test on *Aspilia* Species

Oral glucose tolerance test results summarised in Table 4.64 revealed that the cude extract of aerial part of *A. mossambicensis* (AMA) reduced the blood glucose level more than any isolated compounds. Figure 4.8 shows that the peak of blood glucose was reached 30 min after administration of glucose in all rat groups with the glucose level ranging from 138.7 ± 11.4 to 229.0 ± 22.3 mg/dL (Table 4.64). At 30 and 60 minutes, *ent*-kaura-9(11),16-dien-12-one (**241**) showed comparable lowering of blood glucose to metformin. 15α-angeloyloxy-16β,17-epoxy-*ent*-kauran-19-oic acid (**237**) was comparable to metformin at 60, 90 and 120 minutes, while *ent*-kaur-16-en-19-oic acid (**243**) was comparable to metformin at 120 and 240 minutes. These were the three most active compounds.

Table 4.64: Oral Glucose Tolerance Test (OGTT) on *Aspilia* Species

	Bloog glucose level (mg/dL) at different time						
Group	**-60**	**0**	**30 min**	**60 min**	**90 min**	**120 min**	**240 min**
Metformin	100.7 ± 14.2	105.2 ± 11.3	161.0 ± 25.2	172.5 ± 16.0	149.2 ± 19.6	142.0 ± 19.9	115.2 ± 7.7
Saline	112.7 ± 11.3	122.2 ± 10.1	229.0 ± 22.3	219.7 ± 25.7	175.7 ± 32.3	157.5 ± 14.3	131.0 ± 9.1
240	138.5 ± 15.8	148.2 ± 17.2	183.5 ± 20.6	185.5 ± 20.6	157.2 ± 15.8	161.5 ± 17.9	139.7 ± 17.1
243	118.0 ± 14.6	113.2 ± 8.6	203.2 ± 29.3	169.2 ± 13.9	162.7 ± 19.6	134.7 ± 15.9	115.5 ± 12.6
241	141.0 ± 14.3	129.0 ± 13.7	155.7 ± 14.5	166.2 ± 10.2	163.2 ± 15.6	160.7 ± 16.5	140.2 ± 13.2
237	125.0 ± 9.2	188.7 ± 15.3	209.0 ± 38.8	155.5 ± 16.9	128.0 ± 30.5	127.7 ± 15.6	140.2 ± 13.2
239	114.2 ± 15.6	112.5 ± 11.9	194.5 ± 57.9	168.7 ± 27.9	155.2 ± 23.7	148.2 ± 18.8	125.5 ± 21.8
AMA	103.0 ± 7.9	107.0 ± 6.9	138.7 ± 11.4	135.0 ± 13.5	141.2 ± 12.6	145.5 ± 15.2	118.0 ± 10.0

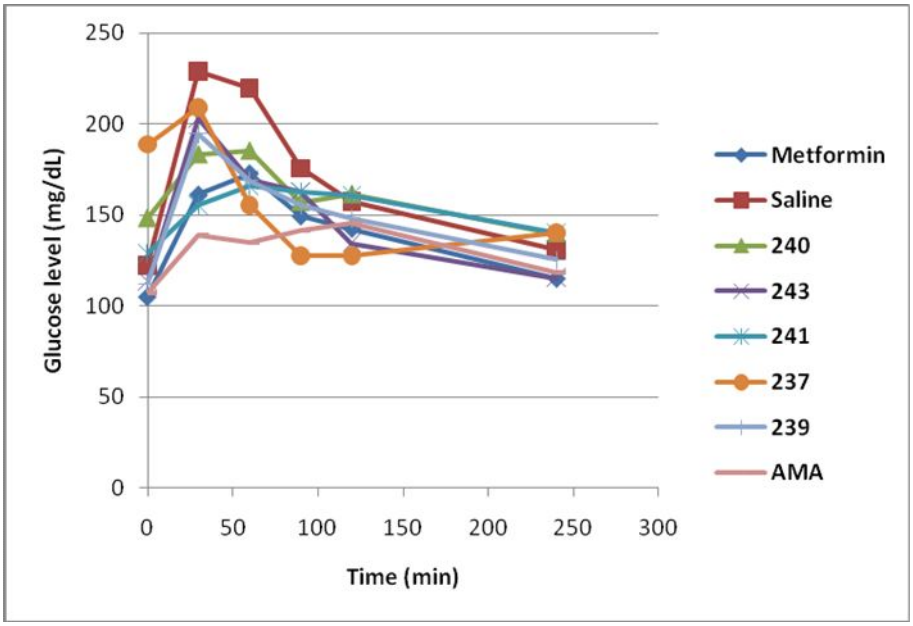

Figure 4.8: Blood Glucose Levels Reduction Graph of *Aspilia* Species

4.7 Characterisation of the Synthetic Derivatives of the Isolated Compounds

4.7.1 Synthetic Derivatives of the Compounds from *Psiadia punctulata*

4.7.1.1 5,7,2',3',4',5'-Hexamethoxyflavone (258)

Methylation reaction carried out on 5-hydroxy,7,2',3',4',5'-pentamethoxy-flavone led to yellow powder of compound **258**. ESIMS spectrum displayed an intense molecular ion m/z 403.3 peak, Based on this and its ^{1}H and ^{13}C NMR spectra, the molecular formula $C_{21}H_{22}O_8$ was suggested for this compound. The ^{1}H and ^{13}C NMR data (Table 4.65) indicated similarity between this compound and the starting material. Three aromatic oxygenated carbon signals δ_C 160.8 (C-5), δ_C 164.0 (C-7) and δ_C 158.5 (C-8a) on A-ring and four others, δ_C 147.7 (C-2'), δ_C 146.9 (C-3'), δ_C 149.6 (C-4') and δ_C 145.6 (C-5') on B-ring were observed from the ^{13}C NMR spectrum. This observation was in agreement with the presence of four ^{1}H NMR signals at δ_H 6.88 (H-3), δ_H 6.38 (H-6), δ_H 6.45 (H-8) and δ_H 7.02 (H-6'). Furthermore, the presence of six methoxy groups [δ_H 3.92 (CH_3O-5), δ_H 3.88 (CH_3O-7), δ_H 3.97 (CH_3O-2'), δ_H 3.95 (CH_3O-3'), δ_H 3.95 (CH_3O-4'), δ_H 3.93 (CH_3O-5')] suggested that all the hydroxyl

groups were methylated. The HMBC correlation between H-3 and C-2, C-4a, C-1' on one hand and between H-5 and C-4a, C-8 on the other hand, further support a flavone moiety. Based on this data and the comparison of the data to that of the starting material, compound **258** was found to be 5,7,2',3',4',5'-hexamethoxy-flavone.

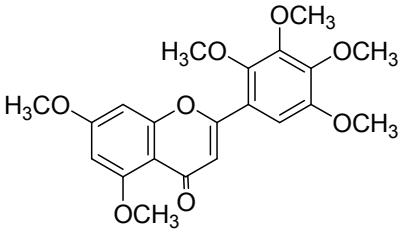

258

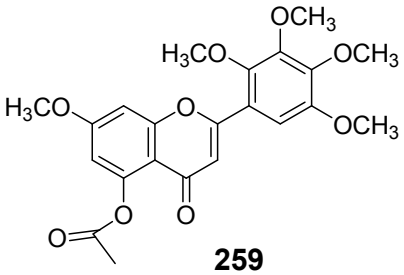

259

4.7.1.2 5-Acetyloxy-7,2',3',4',5'-pentamethoxyflavone (259)

Compound **259** was obtained by acetylating 5-hydroxy-7,2',3',4',5'-pentamethoxy-flavone. Based on the ^{1}H and ^{13}C NMR spectra, the molecular formula $C_{22}H_{22}O_9$ was suggested for this compound. The ^{1}H and ^{13}C NMR data (Table 4.65) indicated similarity between this compound and the starting material. Three aromatic oxygenated carbon signals δ_C 159.8 (C-5), δ_C 150.7 (C-7) and δ_C 163.5 (C-8a) on A-ring and four others, δ_C 147.7 (C-2'), δ_C 146.9 (C-3'), δ_C 149.9 (C-4') and δ_C 146.0 (C-5') on B-ring were observed from the ^{13}C NMR spectrum. This observation was in agreement with the presence of four ^{1}H NMR signal at δ_H 6.67 (H-3), δ_H 6.71 (H-6), δ_H 6.11 (H-8) and δ_H 7.27 (H-6'). Furthermore, the presence of five methoxy groups (δ_H 3.99 (CH_3O-7), δ_H 3.96 (CH_3O-2'), δ_H 3.95 (CH_3O-3'), δ_H 3.94 (CH_3O-4'), δ_H 3.90 (CH_3O-5') suggested that all the hydroxyl groups were methylated except for that at position C-5. The presence of an additional carbonyl and methyl group revealed that the compound was acetylated successfully. The HMBC correlation between H-3 and C-2, C-4a, C-1' on one hand and between H-5 and C-4a, C-8 on the other hand, further support a flavone moiety. Based on this data and the comparison of the data to that of the starting material, compound **259** was found to be 5-acetyloxy-7,2',3',4',5'-pentamethoxy-flavone.

Table 4.65: ^{1}H (600 MHz) and ^{13}C (150 MHz) NMR Data of 258 and 259 in $CDCl_3$

Position	258				259			
	δ_C	Type	δ_H (mult., *J* in Hz)	HMBC	δ_C	Type	δ_H (mult., *J* in Hz)	HMBC
2	160.0	C	-	-	158.9	C	-	-
3	113.3	CH	6.88 (s)	C-2, C-1', C-4a	111.9	CH	6.67 (s)	C-2, C-1', C-4a
4	177.1	C	-	-	175.4	C	-	-
4a	109.0	C	-	-	110.9	C	-	-
5	160.8	C	-	-	159.8	C	-	-
6	95.9	CH	6.38 (d, *J*=2.27)	C-4a, C-8	107.9	CH	6.71 (d, *J*=2.5)	C-4a, C-8
7	164.0	C	-	-	163.5	C	-	-
8	92.8	CH	6.45 (d, *J*=2.24)	C-4a, C-6. C-8	99.00	CH	6.11 (d, *J*=2.5)	C-4a, C-6. C-8
8a	158.5	C	-	-	150.7	C	-	-
1'	120.1	C	-	-	120.0	C	-	-
2'	147.7	C	-	-	147.7	C	-	-
3'	146.9	C	-	-	146.9	C	-	-
4'	149.6	C	-	-	149.9	C	-	-
5'	145.6	C	-	-	146.0	C	-	-
6'	106.3	CH	7.02 (s)	C-2, C-1', C-4, C-5	107.0	CH	7.27 (s)	C-2, C-1', C-4, C-5
C-2'-OCH_3	61.2	CH_3	3.97 (3H,s)	C-2'	60.7	CH_3	3.99 (3H, s)	C-2'
C-3'-OCH_3	61.0	CH_3	3.95 (3H, s)	C-3'	60.7	CH_3	3.96 (3H, s)	C-3'
C-4'-OCH_3	56.3	CH_3	3.95 (3H, s)	C4'	60.4	CH_3	3.95 (3H, s)	C4'
C-5'-OCH_3	56.2	CH_3	3.93(3H, s)	C-5'	55.9	CH_3	3.94 (3H, s)	C-5'
C-7-OCH_3	55.8	CH_3	3.88 (3H, s)	C-7	55.8	CH_3	3.90 (3H, s)	C-7
C-5-OCH_3	61.2	CH_3	3.92 (3H, s)	C-5	168.5	C=O	-	-
/	/	/	/	/	55.8	CH_3	3.90 (3H, s)	C-7

4.7.1.3 3-(2,'',6''-Hydroxy-4-methoxyphenyl)-5-(2',3',4',5'-methoxyphenyl)-1*H*-pyrazole (260)

A reaction treatment of 5-hydroxy-7,2',3',4',5'-pentamethoxyflavone (**220**) with an excess of hydrazine led to identification of **260**. Basically, the ^{1}H and ^{13}C NMR of **260** resemble to that 5-hydroxy-7,2',3',4',5'-pentamethoxy-flavone (**220**) with a difference that compound **220** lost a carbonyl at C-4. The NMR spectroscopic data (Table 4.66) agreed with a molecular formula $C_{20}H_{22}N_2O_7$ for this compound. The ^{13}C NMR spectrum display 20 carbons including five methoxy groups (δ_C 60.7 (CH_3O-7), δ_C 60.4 (CH_3O-2'), δ_C 55.9 (CH_3O-3'), δ_C 55.8 (CH_3O-4'), δ_C 60.7 (CH_3O-5')) support the similarity. However, the missing carbonyl observed on ^{13}C NMR spectrum confirmed that the reaction had taken place leading to a flavone pyrazole. Based on this information and the absence of chelation on ^{1}H NMR spectrum, compound **260** was identified as 3-(2,",6"-hydroxy-4-methoxyphenyl)-5-(2',3',4',5'-methoxyphenyl)-1*H*-pyrazole.

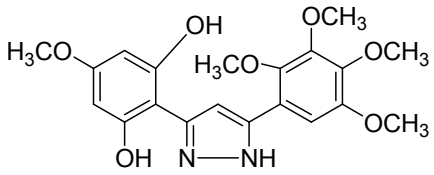

260

Table 4.66: ^{1}H (800 MHz) and ^{13}C (200 MHz) NMR Data of 260 in $CDCl_3$

Position	δ_C	Type	δ_H (mult., *J* in Hz)	HMBC
1	139.1	C	/	/
2	105.5	CH	7.14 (s)	C-4, C-1'
3	149.5	C	/	/
4	117	C	/	/
5	160.3	C	/	/
6	93.4	CH	6.11, (s)	C-4, C-8
7	160	C	/	/
8	93.4	CH	6.11 (s)	C-4, C-6
9	160.3	C	/	/
1'	99	C	/	/
2'	143.6	C	/	/
3'	144.8	C	/	/

Table 4.66 continued				
Position	δ_C	Type	δ_H (mult., *J* in Hz)	HMBC
4'	147.7	C	/	/
5'	150.2	C	/	/
6'	104.5	CH	7.48 (s)	C-1, C-4'
C-7-OCH_3	60.7	CH_3	3.75 (3H, s)	C-7
C-2'-OCH_3	60.4	CH_3	3.92 (3H, s)	C-2'
C-3'-OCH_3	55.9	CH_3	3.89 (3H, s)	C-3'
C-4'-OCH_3	55.8	CH_3	3.87 (3H, s)	C-4'
C-5'-OCH_3	60.7	CH_3	3.96 (3H, s)	C-5'

4.7.1.4 6,8-Dibromo-5-hydroxy-7,2',3',4',5'-pentamethoxyflavone (261)

Bromination of 5-hydroxy,7,2',3',4',5'-pentamethoxy-flavone (**220**) led to yellow powder of compound **261**. ESIMS spectrum displayed an isotopic molecular ion m/z 547.6 peak, Based on this and its the ^1H and ^{13}C NMR spectroscopic data (Table 4.67), the molecular formula $C_{20}H_{18}Br_2O_8$ was suggested for this compound. The deshielded ^{13}C NMR chemical shift (Table 78) of C-5 (δ_C 145.6) and C-7 (δ_C 145.6) indicated a successful bromination at these two aromatic carbons. Observation of three aromatic oxygenated carbon signals δ_C 158.0 (C-5), δ_C 159.9 (C-7) and δ_C 152.4 (C-8a) on A-ring and four others, δ_C147.5 (C-2'), δ_C 146.7 (C-3'), δ_C 149.5 (C-4') and δ_C 148.2 (C-5') on B-ring from the ^{13}C NMR spectrum indicated that the remaining part of the molecule remained intact. From the ESIMS, the presence of bromine isotopes were evident from the peaks observed at *m/z* 545.5, 547.5, 544.5. Furthermore, the presence of five methoxy groups [δ_H 3.94 (CH_3O-7), δ_H 3.89 (CH_3O-2'), δ_H 3.88 (CH_3O-3'), and δ_H 3.84 (CH_3O-4')] suggested that only the hydroxyl groups on B-ring were methylated. Therefore, compound **261** was found to be 6,8-dibromo-5-hydroxy-7,2',3',4',5'-pentamethoxyflavone.

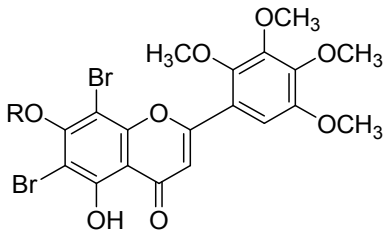

R = OCH_3: **261**
R = OH: **262**

Table 4.67: ^{1}H (800 MHz) and ^{13}C (200 MHz) NMR Data of 261 and 262 in $CDCl_3$

Position	261				262			
	δ_C	Type	δ_H (mult., *J* in Hz)	HMBC	δ_C	Type	δ_H (mult., *J* in Hz)	HMBC
2	161.6	C	-	-	161.3	C	-	-
3	105.9	CH	7.23 (s)	C-2, C-4, C-4a, C-1'	109.6	CH	7.18 (s)	C-2, C-4, C-4a, C-1'
4	182.5	C	-	-	182.2	C	-	-
4a	108.5	C	-	-	105.9	C	-	-
5	158.0	CH	13.64 (br s, OH)	C-4a, C-5, C-6	157.7	CH	13.74 (br s, OH)	C-4a, C-5, C-6
6	100.9	C	-	-	93.3	C	-	-
7	159.9	C	-	-	155.0	C	-	-
8	95.0	C	-	-	86.3	C	-	-
8a	152.4	C	-	-	152.6	C	-	-
1’	118.0	C	-	-	118.2	C	-	-
2’	147.5	C	-	-	147.9	C	-	-
3’	146.7	C	-	-	146.6	C	-	-
4’	149.5	C	-	-	149.5	C	-	-
5’	148.2	C	-	-	148.1	C	-	-
6’	109.7	CH	7.37 (s)	C-2, C-1’, C-4, C-5	105.9	CH	7.34 (s)	C-2, C-1’, C-4, C-5
C-2’-OCH_3	61.3	CH_3	3.94 (3H, s)	C-2’	61.3	CH_3	3.94 (3H, s)	C-2’
C-3’-OCH_3	61.2	CH_3	3.89 (3H, s)	C-3’	61.3	CH_3	3.89 (3H, s)	C-3’
C-4’-OCH_3	61.1	CH_3	3.88 (3H, s)	C4’	61.1	CH_3	3.88 (3H, s)	C4’
C-5’-OCH_3	56.1	CH_3	3.84 (3H, s)	C-5’	56.1	CH_3	3.84 (3H, s)	C-5’
C-7-OCH_3	61.3	CH_3	3.94 (3H, s)	C-7	/	/	/	/

4.7.1.5 6,8-Dibromo-5,7-dihydroxy-7,2',3',4',5'-pentamethoxyflavone (262)

Bromination of 5,7-dihydroxy,2',3',4',5'-tetramethoxyflavone (**221**) led to compound **262**. ESIMS spectrum displayed an isotopic molecular ion m/z 533.4 peak, Based on this and its ^{1}H and ^{13}C NMR spectroscopic data (Table 4.67), the molecular formula $C_{19}H_{16}Br_2O_8$ was suggested for this compound. The dishielded ^{13}C NMR chemical shift (Table 4.67) of C-5 δ_C (147.7) and C-7 (δ_C 155.0) indicated a successful bromination at these two aromatic carbons. Observation of three aromatic oxygenated carbon signals δ_C 155.7 (C-5), δ_C 155.0 (C-7) and δ_C 152.6 (C-8a) on A-ring and four others, δ_C 147.9 (C-2'), δ_C 146.6 (C-3'), δ_C 149.5 (C-4') and δ_C 148.1 (C-5') on B-ring from the ^{13}C NMR spectrum indicated that the remaining part of the molecule remained intact. From the ESIMS, the presence of bromine isotopes were evident from the peaks observed at *m/z* 535.5, 533.4, 537.3. Furthermore, the presence of four methoxy groups [δ_H 3.94 (CH_3O-7), δ_H 3.89 (CH_3O-2'), δ_H 3.88 (CH_3O-3'), δ_H 3.84 (CH_3O-4'), δ_H 3.94 (CH_3O-5')] suggested that all the hydroxyl groups were methylated except MeO-5. Therefore, compound **262** was found to be 6,8-dibromo- 5,7-dihydroxy-7,2',3',4',5'-pentamethoxyflavone.

4.7.1.6 6*β*,18,19-Trihydroxy-*ent*-trachyloban-2*N*-oxime (263)

Reaction of 6*β*,18,19-trihydroxy-*ent*-trachyloban-2-one (**207**) with hydroxylamine hydrochloride ($HONH_2.HCl$) led to compound **263**. HRESIMS of **263** showed a protonated molecular ion peak at *m/z* 350.2331 corresponding to the molecular formula $C_{20}H_{31}NO_4$. In agreement with this, the ^{13}C NMR spectrum showed 20 non-equivalent carbon signals which further indicated that this compound is also a diterpene derivative. The ^{1}H and ^{13}C NMR spectra (Table 4.68), once again showed that the compound has a trachylobane diterpene skeleton. In addition, the presence of a shielded carbon (δ_C 206.5) indicated the presence of an oxime functionality at C-2 (δ_C 206.5). Only two methyl signals were observed in the NMR spectra vis. CH_3-17 (δ_H 1.19; δ_C 19.7) and CH_3-20 (δ_H 1.03; δ_C 13.6). This revealed that only the carbonyl at C-2 of the starting compound was transformed into an oxime group. The large coupling constant (J = 14.5 Hz) between H-5 (δ_H 2.25) and H-6 (δ_H 4.32) is consistent with both protons being axial and hence OH-6 should be equatorial (β-oriented) as in the starting isolated compound reported from this plant, namely 6*β*,18,19-trihydroxy-*ent*-trachyloban-2-one. Both C-1 and C-3 along with the corresponding proton signals are downfield-shifted

confirming the placement of the oxime at C-2. Therefore, the new compound **263** was characterized as 6*β*,18,19-trihydroxy-*ent*-trachyloban-2*N*-oxime.

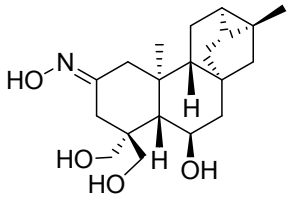

263

Table 4.68: ^{1}H (800 MHz) and ^{13}C (200 MHz) NMR Data of 263 and 264 in $CDCl_3$

Position	263				264			
	δ_C	Type	δ_H (mult., *J* in Hz)	HMBC (H→C)	δ_C	Type	δ_H (mult., *J* in Hz)	HMBC
1	49.9	CH_2	1.37 (m)	C-10, C-20	55.3	CH_2	2.10 (m)	C-2, C-3, C-10, C-20
			1.47 (m)	C-3, C-10, C-20			2.25 (m)	C-2, C-3, C-10, C-20
2	155.7	C	-	-	206.5	C	/	/
3	48.0	CH_2	1,47 (m)	C-2, C-5, C-18, C-19	42.2	CH_2	1.73 (d, *J*=11.6)	C-1, C-5
			1.70 (m)	C-2, C-4, C-18, C-19			1.97 (m)	C-1
4	41.3	C	-	-	41.3	C	/	/
5	56.0	CH	1.18 (m)	C-4, C-6, C-9, C-10, C-20	56.3	CH	2.25 (dd, *J*=14.5, 5.1)	C-1, C-3, C-7, C-18, C-19
6	66.5	CH	3.95 (m)	C-18, C-19	75.6	CH	4.32 (m)	C-4, C-8
7	35.9	CH_2	2.14 (m)	C-6, C-8, C-9, C-14	42.8	CH_2	1.73 (m)	C-9, C-15
			2.25 (m)	C-6, C-9, C-14			1.97 (m)	C-9, C-15
8	40.5	C	-	-	37.2	C	/	/
9	51.6	CH	1.36 (m)	C-1, C-8, C-12, C-15, C-20	49.8	CH	1.73 (m)	C-1, C-7, C-12
10	38.2	C	-	-	37.9	C	/	/
11	19.6	CH_2	1.77 (m)	C-10, C-13, C-16	22.2	CH_2	1.58 (m)	C-8, C-13, C-16
			2.00 (m)	C-10, C-12, C-13			1.73 (m)	C-8, C-13
12	24.0	CH	0.88 (m)	C-8, C-13, C-17	24.3	CH	0.99 (br s)	C-14, C-16, C-17
13	19.7	CH	0.67 (m)	C-9, C-17	18.4	CH	0.67 (m)	C-8, C-11, C-15
14	32.8	CH_2	1.28 (m)	C-13	33.5	CH_2	1.32 (m)	C-12, C-15, C-16
			1.93 (m)	C-9, C-12, C-15			2.05 (br s)	C-12, C-15, C-16
15	30.5	CH_2	1.64 (m)	C-9, C-14, C-16	50.1	CH_2	1.32 (m)	C-5, C-7, C-13
			2.25 (m)	C-9, C-14, C-16			1.41 (m)	C-7, C-13, C-17
16	21.8	C	-	-	19.5	C	/	/

Table 4.68 continued

Position	**263**	**264**	Position	**263**	**264**	Position	**263**	**264**
	δ_C	Type	δ_H (mult., *J* in Hz)	HMBC (H→C)	δ_C	Type	δ_H (mult., *J* in Hz)	HMBC
17	20.2	CH_3	1.16 (3H, s)	C-12, C-13, C-16	19.7	CH_3	1.19 (s)	C-12, C-15
18	63.8	CH_2	3.63 (m)	C-3, C-5, C-19	175.3	C	/	/
			3.95 (m)	C-3, C-5, C-19				
19	69.4	CH_2	3.47 (m)	C-5, C-18	175.3	C	/	/
			3.67 (m)	C-5, C-18				
20	16.3	CH_3	1.05 (3H, s)	C-1, C-5, C-9, C-10	13.6	CH_3	1.03(s)	C-1, C-9
-	-	OH	9.38 (br s	C-2	-	-	-	-

4.7.1.7 6*β*-Hydroxy-2-oxo-*ent*-trachyloban-18,19-dioic Acid (264)

Oxidation of 6*β*,18,19-trihydroxy-*ent*-trachyloban-2-one led to **264**. The ^{1}H and ^{13}C NMR data summarized in Table 4.68 revealed similarity with the starting molecule except that this compound has two extra carbonyl and missed one methyl group. based on comparison of the spectroscopic data , a molecular formula of $C_{20}H_{26}O_6$ was suggested. Observation of the ^{1}H and ^{13}C NMR spectroscopic data (Table 4.68) revealed two methyl groups (δ_C 19.7 (C-17); δ_C 13.6 (C-20)), two identical carbonyl signals (δ_C 175.3 for each C-18 and C-19) and a ketone signal (δ_C 206.5 (C-2)). This information confirmed that CH_2-18 and CH_2-19 were oxidized to a carboxylic acid groups each. Therefore, the new compound **264** was identified as 6*β*-hydroxy-2-oxo-*ent*-trachyloban-18,19-dioic acid.

4.7.1.8 17-Methoxy-*ent*-trachyloban-6*β*,19-diol (265)

Compound **265** was derivatized from *ent*-trachyloban-6β,17,19-triol (**211**) by methylation reaction. The ^{1}H and ^{13}C NMR spectroscopic data (Table 4.69) corroborate a mono-methylated derivative of the starting molecule and hence agreed with the molecular formula of **265** to be $C_{21}H_{34}O_3$. The ^{1}H and ^{13}C NMR data (Table 4.69) indicated that this compound is also an *ent*-trachylobane diterpene. The ^{13}C NMR spectrum displayed 21 carbons including a methoxy group (δ_C 58.9) and three oxygenated carbon signals at δ_C 60.01 (C-6), δ_C 79.9 (C-17) and δ_C 68.9 (C-19). Each assignment was confirmed from HMBC correlation and comparison of the data to that of *ent*-trachyloban-6*β*,17,19-triol. On the basis of this observation, compound **265** was identified as 17-methoxy-ent-trachyloban-6*β*,19-diol.

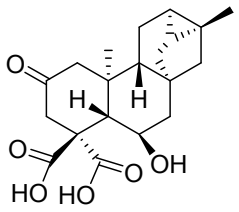

264

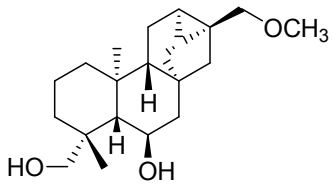

265

Table 4.69: ^{1}H (800 MHz) and ^{13}C (200 MHz) NMR Data of 265 and 266 in $CDCl_3$

Position	265				266			
	δ_C	Type	δ_H (mult., *J* in Hz)	HMBC	δ_C	Type	δ_H (mult., *J* in Hz)	HMBC
1	40.3	CH_2	-	-	43.8	CH_2	0.91 (m)	C-3, C-20
			-	-			1.75 (m)	C-3, C-20, 2-CO
2	19.1	CH_2	1.56 (m)	C-4, C-10	19.6	CH_2	1.15 (m)	C-4, C-10
			1.76 (m)	C-10			1.94 (m)	C-10
3	38.7	CH_2	-	-	43.0	CH_2	1.20 (m)	C-1, C-5
							1.94 (m)	C-1, C-5
4	47.6	C	-	-	38.8	C	/	/
5	59.4	CH	0,72 (m)	C-3, C-7	57.4	CH	1.46 (m)	C-3, C-7
6	61.2	CH	3.59 (m)	C-4, C-8	66.9	CH	4.09 (m)	C-4, C-8, 6-CO
7	47.3	CH_2	-	C-5, C-9	50.2	CH_2	1.35 (m)	C-5, C-9
							1.47 (m)	C-9
8	45.2	C	-	-	40.3	C	/	/
9	51.2	CH	1.04 (m)	C-15, C-20	52.2	CH	1.35 (m)	C-15, C-20
10	39.6	C	-	-	41.5	C	/	/
11	18.7	CH_2	1.07 (m)	C-10, C-16	20.3	CH_2	1.16 (m)	C-10, C-16
12	22.9	CH	0.72 (m)	C-14, C-15	20.9	CH	1.75 (m)	C-14, C-15
							1.92 (m)	C-14, C-15
13	18.6	CH	0.49 (m)	-	23.9	CH	0.90 (m)	-
14	32.8	CH_2	1.19 (m)	C-7, C-15	33.4	CH_2	1.35 (m)	C-7, C-15
			1.92 (m)	C-7, C-15			2.08 (m)	C-7, C-15

Table 4.69 continued

Position	265				266			
	δ_C	Type	δ_H (mult., *J* in Hz)	HMBC	δ_C	Type	δ_H (mult., *J* in Hz)	HMBC
15	49.5	CH_2	1.19 (m)	C-14, C-17	44.8	CH_2	1.21 (m)	C-14, C-17
			1.33 (m)	C-14, C-17			1.93 (m)	C-14, C-17
16	47.9	C	-	-	22.1	C	/	/
17	66.9	CH_2	3.79 (m)	C-12, C-15	70.4	CH_2	5.15 (m)	C-12, C-15
			3.90 (m)	C-12, C-15				
18	30.6	CH_3	1.10 (3H, s)	C-3, C-5	30.3	CH_3	1.22 (3H, s)	C-3, C-5
19	77.3	CH_2	3.90 (m)	C-3, C-5	66.6	CH_2	4.95 (m)	19-CO
			3.15 (m)	C-3, C-5				
20	14.9	CH_3	0.92 (3H, s)	C-1	15.9	CH_3	1.17 (3H, s)	C-1
OCH_3	57.2	CH_3	3.20 (3H, s)	C-17	-	-	-	-
CH_3					19.9	CH_3	1.98 (3H, s)	C=O
C=O					170.2	C	/	/
CH_3					19.8	CH_3	2.01 (3H, s)	C=O
C=O					169.5	C	/	/
CH_3					19.7	CH_3	2.04 (3H, s)	C=O
C=O					169.2	C	/	/

4.7.1.9 2*β*-6*β*,19-Tri-acetyloxytrachylobane (266)

Compound **266** was purified after acetylation of *ent*-trachyloban-6*β*,17,19-triol (**211**).^{1}H and ^{13}C NMR spectra agree with the molecular formula $C_{26}H_{38}O_6$ for this compound. The ^{1}H and ^{13}C NMR data (Table 4.69) was similar to that of *ent*-trachyloban-2α,6α,19-triol except that, this compound has six extra methyls equivalent to triacelylation and a carbonyl group. Supporting data for this claims include the presence in ^{13}C NMR spectrum of three carbonyl signals at δ_C 169.4 (2-CO), δ_C 169.2 (6-CO), δ_C 170.2 (19-CO) and three methyl carbon signals δ_C 19.7 (2-CO-CH_3), δ_C 19.8 (6-CO-CH_3) and δ_C 20.0 (19-CO-CH_3). In addition, three ^{1}H NMR signals were observed at δ_H 1.98 (2-CO-CH_3), δ_H 2.01 (6-CO-CH_3) and δ_H 2.04 (19-CO-CH_3) corresponding to the three methyl of the acetyloxy groups. The HMBC correlation between each methyl with its adjacent carbonyl further supported the structure. Based on this data and the comparison of the data to that of *ent*-trachyloban-2α,6α,19-triol, the new compound **266** was named 2*β*,6*β*,19-triacethyloxy-*ent*-trachylobane.

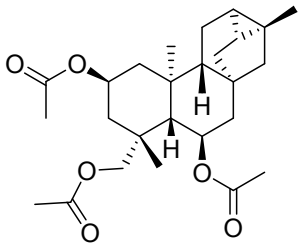

266

4.7.1.10 19-Methoxy-e*nt*-trachyloban-6*β*,17-diol (267)

Compound **267** was derivatized by methylation of *ent*-trachyloban-6β,17,19-triol. The ^{1}H and ^{13}C NMR data (Table 4.70) corroborate a mono-methylated derivative of the starting molecule and hence agreed with the molecular formula of **267** being $C_{21}H_{34}O_3$. The ^{1}H and ^{13}C NMR data (Table 4.70) indicated that this compound is also an *ent*-trachylobane diterpene. The ^{13}C NMR spectrum displayed 21 carbons including a methoxy group (δ_C 58.9) and three oxygenated carbon signals at δ_C 60.01 (C-6), δ_C 79.9 (C-17) and δ_C 68.9 (C-19). Each assignment was confirmed from HMBC correlation and comparison of the data to that of *ent*-trachyloban-6β,17,19-triol. On the basis of these observations, this new compound **267** was identified as 19-methoxy-e*nt*-trachyloban-6*β*,17-diol.

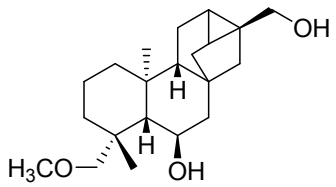

267

Table 4.70: ^{1}H (800 MHz) and ^{13}C (200 MHz) NMR Data of 267 in $CDCl_3$

Position	δ_C	Type	δ_H (mult., *J* in Hz)	HMBC
1	47.4	CH_2	1.50 (m)	C-3, C-20
			1.65 (m)	C-3, C-20
2	20.3	CH_2	1.83 (m)	C-4, C-10
			2.05 (d, *J*=11.05)	C-10
3	40.8	CH_2	1.20 (m)	C-1, C-5
4	34.1	C	/	/
5	50.6	CH	1.32 (m)	C-3, C-7
6	60.0	CH	0.93 (m)	C-4, C-8
7	50.6	CH_2	1.50 (m)	C-5, C-9
8	40.0	C	/	/
9	49.8	CH	1.65 (m)	C-15, C-20
10	41.7	C	/	/
11	22.5	CH_2	1.12 (m)	C-10, C-16
12	24.2	CH	0.93 (d, *J*=10.7)	C-14, C-15
13	30.6	CH	2.05 (d, J=11.9)	C-11, C-15
14	31.9	CH_2	1.16 (m)	C-7, C-15
			1.26 (m)	C-7, C-15
15	48.7	CH_2	0.66 (m)	C-14, C-17
			1.83 (d, *J*=1.3)	C-14, C-17
16	29.1	C	/	/
17	79.9	CH_2	3.13 (m)	C-12, C-15
			3.8 (d, *J*=9.3)	C-12, C-15
18	31.2	CH_3	1.24 (3H, s)	C-3, C-5
19	68.9	CH_2	3.97 (m)	19-OCH_3
20	16.0	CH_3	1.09 (3H, s)	C-1
19-OCH_3	58.9	CH_3	3.37 (3H, s)	C-7

4.7.2 Synthetic Derivatives of Compounds from *Aspilia pluriseta*

4.7.2.1 16*β*-Methoxy-*ent*-kaur-9(11)-en-19 oic Acid (268)

Compound **268** (mp 148-150ºC) was derivatized from *ent*-kaura-9(11),16-dien-19-oic acid using a method previously reported (Boeck *et al.*, 2005). The molecular formula $C_{21}H_{32}O_3$ was suggested based on NMR spectroscopic data (Table 4.71). The ^{1}H NMR spectrum displayed three characteristic protons H-11 (δ_H 5.21), CH_3O-16 (δ_H 3.16) and H-17 (δ_H 1.02) corresponding to C-11 (δ_C 114.2), CH_3O (δ_C 49.4) and C-17 (δ_C 23.2) respectively. Three methyl groups Me-17 (δ_C 1.02), Me-19 (δ_C 1.24) and Me-20 (δ_C 1.27) were also observed in ^{1}H NMR spectrum. The ^{13}C NMR spectrum displayed 21 carbons including a carbonyl groups C-18 (δ_C 178.2), two olefinic carbons C-9 (δ_C 157.5) and C-11 (δ_C 114.2) and a quaternary oxygenated carbon C-16 (δ_C 87.2). HMBC spectrum showed correlations between the methoxy protons and C-16 (δ_C 87.2), H-19 (δ_H 1.24) and the carbonyl C-1' (δ_C 178.2), H-20 (δ_H 1.27) and C-1 (δ_C 43.4) and between H-5 (δ_H 1.75) and both C-1 (δ_C 43.4) and C-18 (δ_C 178.2). The ^{13}C NMR and HMBC data showed resonances consistent with the presence of a carboxylic acid group at C-19 and a methoxy group located on C-16. NOESY data and comparison of the NMR data with that of the related compounds previously reported led to establishment of the relative configuration of **357**. Based on this information, the structure of **268** was established and named 16*β*-methoxy-*ent*-kaur-9(11)-en-19 oic acid.

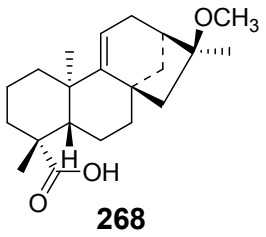

268

Table 4.71: ^{1}H (600 MHz) and ^{13}C (150 MHz) NMR Data of 268 (CD_2Cl_2) and 269 (Acetone-d_6)

Position	268				269			
	δ_C	Type	δ_H (mult., *J* in Hz)	HMBC	δ_C	Type	δ_H (mult., *J* in Hz)	HMBC
1	43.4	CH_2	1.48 (m)	C-3, C-5	41.1	CH_2	1.28 (m)	C-3, C-20
			1.91 (m)	C-20			1.98 (m)	C-20
2	18.4	CH_2	1.48 (m)	C-4, C-10	18.6	CH_2	1.44 (m)	C-4, C-10
			1.91 (dd, *J*=16.5, 6.9)	C-10				
3	38.2	CH_2	1.05 (m)	C-1, C-5	38.2	CH_2	1.09 (m)	C-1, C-5
			2.15 (m)	C-1, C-5			2.17 (m)	C-1, C-5
4	42.6	C	/	/	42.4	C	/	/
5	56.0	CH	1.75 (m)	C-1, C-3, C-20	46.6	CH	1.73 (m)	C-1, C-3, C-20
6	20.2	CH_2	1.48 (m)	C-4, C-8	20.2	CH_2	1.53 (ddd, *J*=14.1, 3.5, 3.5)	C-4, C-8
			1.91 (m)	C-8			1.92 (m)	C-8
7	41.0	CH_2	1.25 (m)	C-5	29.8	CH_2	2.17 (m)	C-5
			1.98 (m)	C-5				
8	44.6	C	/	/	44.7	C	/	/
9	157.5	C	/	/	158.3	C	/	/
10	38.7	C	/	/	38.7	C	/	/
11	114.2	CH	5.21 (m)	C-10, C-13	115.0	CH	5.24 (dd, *J*=3.5, 3.5)	C-10, C-13
12	30.2	CH_2	1.48 (m)	C-9, C-14	30.2	CH_2	1.43 (dd, *J*=11.1, 3.7)	C-9, C-14
							1.92 (m)	C-9, C-14
13	41.7	CH	2.22 (m)	C-14, C-16	46.0	CH	1.50 (m)	-
14	30.9	CH_2	2.05 (m)	C-7, C-12	37.8	CH_2	2.36 (m)	C-7, C-12

			2.28 (m)	C-7, C-12			1.39 (m)	C-7, C-12

Table 4.71 continued

Position	**268**				**269**			
	δ_C	Type	δ_H (mult., *J* in Hz)	HMBC	δ_C	Type	δ_H (mult., *J* in Hz)	HMBC
15	46.5	CH_2	1.65 (m)	C-9, C-16, C-17	49.8	CH_2	1.40 (m)	C-9, C-16, C-17
							1.82 (m)	C-9, C-16, C-17
16	87.2	C	/	/	37.1	CH	2.44 (m)	C-8, C-12
17	23.3	CH_3	1.02 (3H, s)	C-13, C-15	23.2	CH_3	1.06 (d, *J*=8.3)	C-13, C-15
18	28.0	CH_3	1.24 (3H, s)	/	28.0	CH_3	1.26 (3H, s)	C-3, C-18
19	178.2	C	/	C-3, C-18	184.8	C	/	/
20	21.5	CH_3	1.27 (3H, s)	C-1, C-5	18.5	CH_3	1.02 (3H, s)	C-1, C-5
-	49.4	OCH_3	3.16 (3H, s)	C-16	-	-	-	-

4.7.2.2 *Ent*-kaur-9(11)-en-19-oic Acid (269)

Compound **269** (mp 160-162ºC) was obtained by hydrogenation of *ent*-kaura-9(11),16-dien-19-oic acid (**240**)**.** The NMR spectroscopic data (Table 4.71) corresponded to $C_{20}H_{30}O_2$. This compound displayed the same NMR spectroscopic data (Table 82) as that of **240** except that it lacked one double bond. Observation of H-11 (δ_H 5.24) signal on ^{1}H NMR spectrum revealed that the C-9(11) double bond was not hydrogenated. In contrast, the absence of the signals of the C-16-C-17 in both proton and carbon spectra indicated that this double bond was hydrogenated. The NMR spectroscopic data (Table 4.71) were consistent with this compound being a kaurene type diterpene with a carbonyl at C-19 (δ_C 184.8). The ^{13}C NMR spectrum displayed 20 carbons including two olefinic carbons C-9 (δ_C 158.3). and C-11(δ_C 115.0). The HMBC correlation of H_3-18 and C-19 on one hand and between H-11 (δ_H 5.24) and C-8 (δ_C 44.7) further confirmed this compound as having a kaurene skeleton. The relative configuration at C-16 was deducted from NOESY spectrum and the literature (Braca *et al.*, 2005). On the basis of the above information, compound **269** was characterised as *ent*-kaur-9(11)-en-19-oic acid.

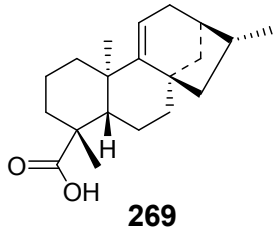

269

4.7.2.3 Methyl-*ent*-kaura-9(11),16-dien-19-oate (270)

The ESIMS analysis (molecular ion peak at *m/z* 315.2) of compound **270**, together with its NMR spectroscopic data (Table 4.72) agreed with the molecular formula $C_{21}H_{30}O_2$. The ^{1}H and ^{13}C NMR spectroscopic data (Table 4.72) of compound **270** was similar to that of **240**. However a close observation indicated that **270** has an additional methoxy group resonating at δ_C 51.1 and corresponding to the signal (δ_H 3.16) observed on ^{1}H NMR spectrum. This was further confirmed when the ^{13}C NMR displayed 21 carbons including four olefinic (C-9, δ_C 156.1; C-11, δ_C 114.8; C-16, δ_C 158.5 and C-17, δ_C 106.3) carbons and a carbonyl (C-18, δ_C 177.6). Observation of only two methyl groups at C-19 (δ_C 27.9) and C-20 (δ_C 23.3)

coupled with the presence of two double bonds were in agreement with a kauradiene diterpene skeleton. HMBC correlation of the methoxy with the carbonyl revealed an ester moiety. The suggested structure was then confirmed when comparing the ^{1}H and ^{13}C NMR spectroscopic data to that of the same compound previously isolated. Compound **270** was therefore identified as methyl-*ent*-kaura-9(11),16-dien-19-oate.

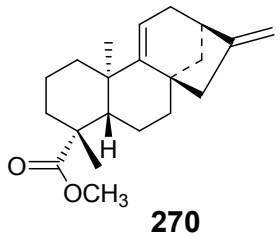

270

Table 4.72: ^{1}H (600 MHz) and ^{13}C (150 MHz) NMR Data of 270 and 271 in CD_2Cl_2

Position	270				271			
	δ_C	Type	δ_H (mult., *J* in Hz)	HMBC	δ_C	Type	δ_H (mult., *J* in Hz)	HMBC
1	38.4	CH_2	1.05 (dd, *J*=13.3, 13.3)	C-3, C-5, C-20	40.6	CH_2	0.85 (m)	C-3, C-20
			2.18 (m)	C-3, C-5, C-20			1.05 (m)	C-20
2	20.3	CH_2	1.51 (m)	C-4, C-10	19.1	CH_2	1.46 (m)	C-4, C-10
			1.98 (m)	C-4, C-10			1.65 (m)	C-4, C-10
3	37.9	CH_2	1.98, (m)	C-1, C-5, C-18	38.0	CH_2	1.04, (m)	C-1, C-5
			2.45 (m)	C-1, C-5			2.14 (m)	C-1, C-5
4	42.2	C	/	/	34.3	C	/	/
5	46.5	CH	1.65 (m)	C-1, C-3, C-18, C-19, C-20	56.7	CH	1.09 (m)	C-1, C-3, C-20
6	18.5	CH_2	1.89 (m)	C-4, C-8	22.2	CH_2	1.52 (m)	C-4, C-8
			2.45 (m)	C-4, C-8			1.56 (m)	C-8
7	29.7	CH_2	1.51 (m)	C-5, C-9, C-15	40.0	CH_2	1.85 (ddd, *J*=11.6, 3.3, 3.3)	C-5
			1.98 (m)	C-5, C-9, C-15			2.01 (m)	C-5
8	44.9	C	/	/	44.7	C	/	/
9	156.1	C	/	/	56.5	CH	1.01 (br s)	C-1, C-7, C-12
10	38.6	C	/	/	39.5	C	/	/
11	114.8	CH	2.21 (m)	C-8, C-9, C-13	18.7	CH_2	1.41 (m)	C-10, C-13
12	44.7	CH_2	1.51 (m)	C-9, C-16	25.7	CH_2	1.46 (m)	C-9, C-14
			1.65 (m)	C-9, C-16			1.65 (m)	C-9, C-14

Table 4.72 continued

Position	270				271			
	δ_C	Type	δ_H (mult., *J* in Hz)	HMBC	δ_C	Type	δ_H (mult., *J* in Hz)	HMBC
13	41.3	CH	2.79 (br s)	C-14, C-14, C-16	43.1	CH	-	-
14	40.8	CH_2	1.25 (m)	C-7, C-9, C-12, C-16	40.7	CH_2	1.46 (m)	C-7, C-12
			2.98(m)	C-7, C-12, C-16			1.58 (m)	C-7, C-12
15	50.2	CH_2	2.21 (m)	C-7, C-9, C-13, C-16, C-17	48.7	CH_2	0.99 (m)	C-9, C-16, C-17
			2.65 (m)	C-9, C-13, C-16, C-17			1.65 (m)	C-9, C-16, C-17
16	158.5	C	/	/	42.1	CH	1.85 (m)	C-8, C-12
17	106.3	CH_2	4.81 (3H, s)	C-13, C-15	15.3	CH_3	1.03 (d, 8.6)	C-13, C-15
			4.94 (m)	C-13, C-15				
18	27.9	CH_3	1.20 (3H, s)	C-3, C-5, C-19	28.4	CH_3	1.20 (s)	C-3, C-18
19	177.6	C	-	-	178.2	C	-	-
20	23.3	CH_3	0.96 (3H, s)	C-1, C-5	15.2	CH_3	1.01 (s)	C-1, C-5
-	51.1	OCH_3	3.16 (3H, s)	C-18	-	-	-	-

4.7.2.4 *Ent*-kauran-19-oic Acid (271)

The molecular formula $C_{20}H_{32}O_2$ of compound **271** was proposed based on its its NMR spectroscopic data (Table 4.72). The ^{1}H NMR spectrum revealed three methyl groups at δ_H 1.03 (C-17), δ_H 1.20 (C-18) and δ_H 1.01 (C-20) corresponding to the signals at δ_C 15.3 (C-17) δ_C 28.4 (C-18) δ_C 15.2 (C-20) in ^{13}C NMR spectrum, respectively. Observation of the carbonyl at δ_C 178.2 (C-19) on ^{13}C NMR spectrum further confirmed the product of hydrogenation of **243**. In addition, HMBC correlation of methyl protons at C-17 (δ_H 1.03) with C-13 (δ_C 43.1) and C-15 (δ_C 48.7) on one hand and that of C-18 (δ_C 1.20) methyl protons with C-19 (δ_C 178.2) confirmed the structure of compound **271**. Connectivity of H-16 (δ_H 1.85) to the corresponding carbon C-16 (δ_C 42.1) was also observed on HSQC spectrum. Based on this evidence and comparaison with the spectral data of the starting material (**208**), compound **271** was elucidated as *ent*-kauran-19-oic acid.

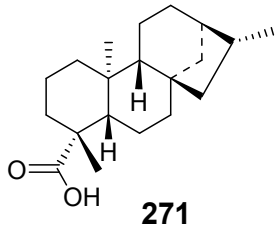

271

4.8 Summary of the Synthetic Derivatives

Some isolated compound from *Psiadia punctulata* were modified by chemical reactions to afford new derivatives. From 5-hydroxy-7,2',3',4',5'-pentamethoxy-flavone (**220**), four compounds namely 5,7,2',3',4',5'-hexamethoxyflavone (**258**), 5-acetyloxy-7,2',3',4',5'-pentamethoxyflavone (**259**), 3-(2",6"-hydroxy-4-methoxyphenyl)-5-(2',3',4',5'-methoxyphenyl)-1*H*-pyrazole (**260**), 6,8-dibromo-5-hydroxy-7,2',3',4',5'-pentamethoxy-flavone (**261***)* were generated. Moreover, 5,7-dihydroxy-2',3',4',5'-tetramethoxyflavone (**221**) was modified to afford 6,8-dibromo- 5,7-dihydroxy-7,2',3',4',5'-pentamethoxyflavone (**262**). Among the trachylobane diterpenoids which have been isolated, *ent*-[6β, 18, 19]-trihydroxy trachyloban-2-one (**207**) afforded two compounds including 6*β*,18,19-trihydroxy-*ent*-trachyloban-2*N*-oxime (**263**) and 6*β*-hydroxy-2-oxo-trachyloban-18,19-dioic acid (**264**). The trachylobane diterpenoid *ent*-trachyloban-6*β*,17,19-triol (**211**) was derivatized to three

different compounds namely 17-methoxy-*ent*-trachyloban-6*β*,19-diol (**265**), 2*β*,6*β*,19-triacetyloxy-*ent*-trachylobane (**266**) and 19-methoxy-*ent*-trachyloban-6β,17-diol (**267**).

Two compounds which were isolated from *Aspilia pluriseta* were modified chemically. compound *ent*-kaur-9(11),16-dien-19-oic acid (**240**) was derivatized to three compounds including 16*β*-methoxy-*ent*-kaur-9(11)-en-19 oic acid (**268**), e*nt*-kaur-9(11)-en-19-oic acid (**269**) and methyl-*ent*-kaura-9(11),16-dien-19-oate (**270**). Furthermore, *ent*-kaur-16-en-19-oic acid (**243**) was derivatized to *ent*-kauran-18-oic acid (**271**).

4.9 Biological Activities of the Synthetic Derivatives

4.9.1 Antimicrobial Activity

Among the tested derivatives, 5,7,2',3',4',5'-hexamethoxy-flavone (**258**) and 6*β*-hydroxy-2-oxo-*ent*-trachyloban-18,19-dioic acid (**264**) showed moderate activity against only *S. aureus* with the agar disc diffusion method. Both had an inhibition zone of 7 mm (Table 4.73) . It is noteworthy that the precursors to these two compounds were not active against the same bacteria before modification of their structure. This indicates that the reaction carried on the two compounds has improved their anti bacterial activity against *S. aureus*. Methyl-*ent*-kaura-9(11),16-dien-19-oate (**270**) exhibited moderate activity against *S. aureus, E. coli* and *C. parapsilosis* with inhibition zones of 8 mm.

Table 4.73: Antimicrobial activity of the modified compounds

Zone of Inhibition (mm)									
	Bacterial strains		Fungi						
Compound	*S. a*	*E. c*	*M. g*	*T. m*	*C. p*	*C. a*	*A. f*	*A. n*	*C. n*
260	0	0	0	0	0	0	na	na	na
259	0	0	0	0	9	0	na	na	na
258	7	0	0	0	0	0	na	na	na
264	7	0	0	0	0	0	na	na	na
268	0	0	7	0	0	0	na	na	na
270	8	8	0	0	8	0	na	na	na
Gentamycin	20	13	-	-	-	-	-	-	-
Nystatin	-	-	13	10	16	13	15	13	18

Key: *S. a = Staphylococcus aureus* (ATCC 25923), *E. c = Escherichia. coli* (ATCC 25922), *M, g = Microsporum gypseum, T. m = Trichophyton mentagrophytes* (clinical isolates), *C. p = Candida parapsilosis* (ATCC 22019), *C. a = Candida albicans* (ATCC 90018), *A. f = Aspergilus flavus, A. n = Aspergilus niger* (environmental), *C. n = Cryptococcus neoformans (clinical), na = not accessed, ne = not effective*

4.9.2 Cytotoxicity of the Synthetic Derivatives

Modification reaction performed on *ent*-[6β, 18, 19]-trihydroxy-trachyloban-2-one (**207**) to 6*β*,18,19-trihydroxy-*ent*-trachyloban-2*N*-oxime (**263**) did not improve the cytotoxicity against the tested cells (Table 4.74). In contrast, it increased the cytotoxicity against the normal BEAS-2B cells. Similarly, 2,6,18-triacethyloxy-*ent*-trachylobane (**266**) obtained from*ent*-trachyloban-2*α*,6*α*,19-triol (**210**) and 17-methoxy-ent-trachyloban-6*β*,19-diol (**265**) obtained from *ent*-trachyloban-6*β*,17,19-triol(**211**) did not show improved cytotoxicity against the tested cancer cells. However, bromination of 5,7-dihydroxy-2',3',4',5'-tetra-methoxy-flavone (**221**) to get 6,8-dibromo-5,7-dihydroxy-7,2',3',4',5'-pentamethoxy-flavone (**262**) suppressed the cytotoxicity against normal cells and improved its activity against Hep-2 cancer cells (CC_{50} = 34.4±8.1 μM).

Table 4.74: Cytotoxicity of the Derivatized Compounds Against Normal and Cancer cell lines

Samples	CC_{50} (µM)					
	Normal cell lines		Cancer cell lines			
	BEAS-2B	**LO_2**	**A549**	**Hep-G2**	**Vero**	**DU-145**
263	5.8 ± 0.6	>100	>100	62.4 ± 0.8	-	-
266	25.5 ± 2.0	26.7 ± 3.0	17.6 ± 1.4	64.1 ± 3.6	-	-
265	25.5 ± 2.6	26.7 ± 2.0	16.9 ± 5.1	37.7 ± 10.6	>100	>100
267	63.9 ± 12.1	67.1 ± 1.5	52.1 ± 10.4	>100	-	-
259	65.1 ± 2.4	31.4 ± 1.8	>100	>100	>100	>100
261	57.1 ± 8.1	>100	70.3 ± 5.3	>100	-	-
260	>100	>100	>100	>100	-	-
258	36.9 ± 4.5	>100	46.7 ± 6.3	65.6 ± 2.3	58.8± 0.2	>100
262	>100	>100	>100	34.4 ± 8.1	-	-
268	>100	>100	>100	>100	-	-
269	>100	>100	>100	>100	-	-

CHAPTER FIVE

CONCLUSION AND RECOMMENDATIONS

5.1 Conclusion

Phytochemical and bioactivity studies were carried out on two *Lannea* species (*Lannea rivae* and *Lannea schweinfurthii*), one *Psiadia* species (*Psiadia punctulata*) and two *Aspilia* species (*Aspilia pluriseta* and *Aspilia mossambisencis*). A total of seventy six compounds among which ten new ones were identified. Furthermore, fourteen derivatives were prepared by chemical reactions.

The roots extract of *Lannea rivae* resulted in isolation of seven compounds of which two alkenylcyclohexanone derivatives (**186** and **187**) were new. Epicatechin gallate (**191**) and the crude extract of *Lannea rivae* were active against *S. aureus,* while compound **186** showed moderate activity against *E. coli*. From the stem bark of *Lannea rivae,* two compounds were isolated, namely lupeol (**193**) and daucosterol (**194**). Root extracts of *Lannea schweinfurthii* resulted in the identification of six alkylcyclohehexanone derivatives (**196**, **197**, **198**, **199**, **200**, **201**), one alkylphenol (**195**) and one flavonoid (**201**). The stem bark of *Lannea schweinfurthii* resulted in isolation of eleven compounds including two triterpenes (**188**, **189**), two ellagic acid derivatives (**202**, **203**), two alkylphenol (**195**, **204**) and five alkylcyclohexanol (**196-200**) derivatives. More interestingly, the isolated new compound **186** was strongly cytotoxic against the DU-145 cancer cell line (CC_{50} = 0.55 ± 0.08 µg/mL).

Phytochemical study of the leaves of *Psiadia punctulata* led to the isolation and characterization of twenty one compounds of which six were new trachylobane diterpenoids (**205-209, 219a**) and three new kaurene diterpenoids (**214**, **219b, 219c**). Furthermore, additional known compounds were isolated from the leaves; these include four trachylobane diterpenoids (**210-213**), four kaurene diterpenoids (**215-218**), two flavones (**220** and **221**) and three fatty acid derivatives (**222-224**). From the stem bark of *P. punctulata*, two triterpenes (**226** and **227),** one trachylobane diterpene (**225**), one aliphatic compound (**228**) and a flavonoid (**221**) were isolated. Phytochemical ivestigation of the roots of *Psiadia punctulata* led to identification of five compounds (**229-233**) and a flavone (**220**) previously isolated from the stem bark of this plant.

From the roots of *Aspilia pluriseta*, nine kaurene diterpenes derivatives (**234-242**) were characterized. The aerial part of *Aspilia pluriseta* let to the identification of three kaurene diterpenoids (**243-245**),

two triterpenoids (**246** and **248**), one steroid (**247**) and one monoterpenoid (**249**). In the oral glucose tolerance test, the crude extract of *Aspilia pluriseta* reduced the blood glucose level more than any other isolated compound. Four compounds (**250-253)**, and three (**236-238**) others which were isolated from *A. pluriseta* were also isolated from the root of *Aspilia mossambicensis*. The aerial part of the same plant, *A. mossambicensis* resulted in the identification of compounds **254-257**, **243**, **240** and **247**.

Ten derivatives including **258-267** were prepared from the compounds isolated from *Psiadia punctulata*. Four more compounds (**268-271**) were derivatized from the compounds isolated from *Aspilia pluriseta*. Among these derivatives, compound **265** was found to be the most active (CC_{50} =16.9±5.1 μM) against the growth of adenocarcinomic human alveolar basal epithelial (A54) cancer cell line. Compound **270** showed the most antimicrobial activity against *Staphylococcus aureus*, *Escherichia coli* and *Candida parapsilosis* having a zone of nhibition of 8 mm against each strain.

5.2 Recommendations

i. More compounds isolated from *Lannea rivae* and *Lannea schweinfurthii* should be tested against different micro-organisms and cancer cell lines. This is because roots extracts from these plants showed strong cytotoxicity (CC_{50} 5.24 ± 0.12 μg/mL for LRR and 74.00 ± 0.04 μg/mL for LSR).

ii. The trachylobane diterpenes should be investigated against other cancer cell lines in addition to A549, Hep-G2, Vero and DU-145 cancer cell lines which were used in this work. The reason being that the crude extract from the leaves, roots and stem bark of *Psiadia punctulata* and some of the isolated compounds showed moderate to strong cytotoxicity. To support the taxonomic difference between *Psiadia punctulata* and *Psiadia arabica*, more chemical variation studies should be carried out.

iii. The aerial parts and roots of *Aspilia pluriseta* and *Aspilia mossambicensis* should also be investigated phytochemically to support the claims of their use in traditional medicine. The roots and aerial part of *Aspilia pluriseta* showed moderate antibacterial activity against Gram positive *S. aureus*. This indicates that the plant contain antimicrobial compounds. The tested compounds from both *A. pluriseta* and *A. mossambicensis* also revealed moderate anti-inflammatory and blood glucose reducing potential. This suggested further bioassay on more isolated compounds.

REFERENCES

Abdullahi, A. A. (2011). Trends and challenges of traditional medicine in Africa. *African Journal of Traditional, Complementary and Alternative Medicines* **8**, 115-123.

Abou-Zaid, M. M., El-Karemy, Z., EI-Negoumy, S. I., Altosaar, I. and Saleh, N. A. (1991). The flavonoids of *Psiadia punctulata*. *Bulletin of the Chemical Society of Ethiopia* **5**, 37-40.

Achola, K., Indalo, A. and Munenge, R. (1998). Pharmacological activities of *Psiadia punculata*. *Pharmaceutical Biology, 36*, 88-92.

Adegbite, A. and Olorode, O. (2003). Hybridization studies in the genus *Aspilia thouars* (Asteraceae) in Nigeria. I: Hybrid between *A. Kotschyi* and *A. Helianthoides*. *Compositae Newsletter* **39**, 27-40.

Adeniyi, B. and Odufowora, R. (2000). *In-vitro* antimicrobial properties of *Aspilla africana* (Compositae). *African Journal of Biomedical Research* **3**, 167-170.

Adewusi, E. A. and Steenkamp, V. (2011). *In vitro* screening for acetylcholinesterase inhibition and antioxidant activity of medicinal plants from Southern Africa. *Asian Pacific Journal of Tropical Medicine* **4**, 829-835.

Adewusi, E. A., Foucheb, G. and Steenkamp, V. (2013). Effect of four medicinal plants on amyloid-β induced neurotoxicity in SHSY5Y cells. *African Journal of Traditional, Complementary and Alternative Medicines* **10**, 6-11.

Adoum, O. (2009). Determination of toxicity levels of some savannah plants using brine shrimp test (BST). *Bayero Journal of Pure and Applied Sciences* **2**, 135-138.

Agyare, C., Bempah, S. B., Boakye, Y. D., Ayande, P. G., Adarkwa-Yiadom, M. and Mensah, K. B. (2013). Evaluation of antimicrobial and wound healing potential of *Justicia flava* and *Lannea welwitschii*. *Evidence-Based Complementary and Alternative Medicine* **13**, 1-10.

Ahmed, M., Jakupovic, J. and Castro, V. (1991). Kaurene derivatives from *Lasianthea fruticosa*, revision of stereochemistry of related compounds. *Phytochemistry* **30**, 1712-1714.

Al-Yahya, M. (1986). Phytochemical studies of the plants used in traditional medicine of Saudi Arabia. *Fitoterapia* **57**, 179-182.

Allabi, A. C., Busia, K., Ekanmian, V. and Bakiono, F. (2011). The use of medicinal plants in self-care in the Agonlin region of Benin. *Journal of Ethnopharmacology* **133**, 234-243.

Almutairi, S., Edrada-Ebel, R., Fearnley, J., Igoli, J. O., Alotaibi, W., Clements, C. J., Gray, A. I. and Watson, D. G. (2014). Isolation of diterpenes and flavonoids from a new type of propolis from Saudi Arabia. *Phytochemistry Letters* **10**, 160-163.

Alvarenga, S. A., Ferreira, M. J., Rodrigues, G. V. and Emerenciano, V. P. (2005). A general survey and some taxonomic implications of diterpenes in the Asteraceae. *Botanical Journal of the Linnean Society* **147**, 291-308.

Ambrosio, S. R., Furtado, N. A., de Oliveira, D. C., da Costa, F. B., Martins, C. H., de Carvalho, T. C., Porto, T. S. and Veneziani, R. (2008). Antimicrobial activity of kaurane diterpenes against oral pathogens. *Journal of Natural Sciences C* **63**, 326-330.

Aráoz, M. V. C., Mercado, M. I., Grau, A. and Catalán, C. A. (2010). *Ent*-kaurane derivatives from the root cortex of *Yacon* and other three *Smallanthus* species (Heliantheae, Asteraceae). *Biochemical Systematics and Ecology* **38**, 1042-1048.

Archibald, L., Phillips, L., Monnet, D., McGowan, J. E., Tenover, F. and Gaynes, R. (1997). Antimicrobial resistance in isolates from inpatients and outpatients in the United States: Increasing importance of the intensive care unit. *Clinical Infectious Diseases* **24**, 211-215.

Arciniegas, A., Pérez-Castorena, A. L., Meléndez-Aguirre, M., Ávila, J. G., García-Bores, A. M., Villaseñor, J. L. and Romo de Vivar, A. (2018). Chemical composition and antimicrobial activity of *Ageratina deltoidea*. *Chemistry and Biodiversity* **15**, 1-10.

Atilaw, Y., Duffy, S., Heydenreich, M., Muiva-Mutisya, L., Avery, V. M., Erdélyi, M. and Yenesew, A. (2017). Three chalconoids and a pterocarpene from the roots of *Tephrosia aequilata*. *Molecules* **22**, 318-329.

Autschbach, J., Ziegler, T., Van-Gisbergen, S. J. and Baerends, E. J. (2002). Chiroptical properties from time-dependent density functional theory. I. Circular dichroism spectra of organic molecules. *The Journal of Chemical Physics* **116**, 6930-6940.

Badiee, P. and Hashemizadeh, Z. (2014). Opportunistic invasive fungal infections: Diagnosis and clinical management. *The Indian Journal of Medical Research* **139**, 195-204.

Banfi, D. and Patiny, L. (2008). www.nmrdb.org: Resurrecting and processing NMR spectra on-line *Chimia*, **62**, 280-281.

Balouiri, M., Sadiki, M. and Ibnsouda, S. K. (2016). Methods for in vitro evaluating antimicrobial activity: A review. *Journal of Pharmaceutical Analysis* **6**, 71-79.

Balunas, M. J. and Kinghorn, A. D. (2005). Drug discovery from medicinal plants. *Life Sciences* **78**, 431-441.

Batista, R., García, P. A., Castro, M. A., Corral, J. M. M. d., Sanz, F., Speziali, N. L. and Oliveira, A. B. D. (2007). Methylent-16*β*,17-epoxykauran-19-oate. *Acta Crystallographica Section E Structure Reports Online* **63**, 932-933.

Batista, R., García, P. A., Castro, M. A., del Corral, J. M. M., Speziali, N. L., Varotti, F. D. P., de Paula, R. C., García-Fernández, L. F., Francesch, A. and San Feliciano, A. (2013). Synthesis, cytotoxicity and antiplasmodial activity of novel *ent*-kaurane derivatives. *European Journal of Medicinal Chemistry* **62**, 168-176.

Batovska, D. I., Tsubota, S., Kato, Y., Asano, Y. and Ubukata, M. (2004). Lipase-mediated desymmetrization of glycerol with aromatic and aliphatic anhydrides. *Tetrahedron: Asymmetry* **15**, 3551-3559.

Bauernschmitt, R. and Ahlrichs, R. (1996). Treatment of electronic excitations within the adiabatic approximation of time dependent density functional theory. *Chemical Physics Letters, 256*, 454-464.

Becke, A. D. (1993). Density-functional thermochemistry. III. The role of exact exchange. *The Journal of Chemical Physics* **98**, 5648-5652.

Besse, P., Da-Silva, D., Humeau, L., Govinden-Soulange, J., Gurib-Fakim, A. and Kodja, H. (2003). A genetic diversity study of endangered *Psiadia* species endemic from Mauritius Island using PCR markers. *Biochemical Systematics and Ecology* **31**, 1427-1445.

Billah, A. M., Hussain, M. M., Dastagir, M. G., Ismail, M. and Quader, A. (2013). Isolation of α-spinasterol from *Amaranthus spinosus* stems. *Latin American and Caribbean Bulletin of Medicinal and Aromatic Plants* **12**, 15-17.

Black, S., Shinefield, H., Fireman, B., Lewis, E., Ray, P., Hansen, J. R., Elvin, L., Ensor, K. M., Hackell, J. and Siber, G. (2000). Efficacy, safety and immunogenicity of heptavalent pneumococcal conjugate vaccine in children. *The Pediatric infectious Disease Journal* **19**, 187-195.

Block, S., Baccelli, C., Tinant, B., Van Meervelt, L., Rozenberg, R., Jiwan, J.-L. H., Llabres, G., De Pauw-Gillet, M.-C. and Quetin-Leclercq, J. (2004). Diterpenes from the leaves of *Croton zambesicus*. *Phytochemistry* **65**, 1165-1171.

Block, S., Stevigny, C., De Pauw-Gillet, M.-C., de Hoffmann, E., Llabres, G., Adjakidjé, V. and Quetin-Leclercq, J. (2002). *Ent*-trachyloban-3*β*-ol, a new cytotoxic diterpene from *Croton zambesicus*. *Planta Medica,* **68**, 647-649.

Boeck, P., Sá, M. M., Souza, B. S. d., Cercená, R., Escalante, A. M., Zachino, S. A., Cechinel Filho, V. and Yunes, R. A. (2005). A simple synthesis of kaurenoic esters and other derivatives and evaluation of their antifungal activity. *Journal of the Brazilian Chemical Society* **16**, 1360-1366.

Bohlmann, F., Ziesche, J., King, R. M. and Robinson, H. (1981). Eudesmanolides and diterpenes from *Wedelia trilobata* and an *ent*-kaurenic acid derivative from *Aspilia parvifolia*. *Phytochemistry* **20**, 751-756.

Braca, A., Abdel-Razik, A. F., Mendez, J. and Morelli, I. (2005). A new kaurane diterpene dimer from *Parinari campestris*. *Fitoterapia* **76**, 614-619.

Bruno-Colmenarez, J., de Delgado, G. D., Peña, A., Alarcón, L., Usubillaga, A. and Delgado-Méndez, P. (2011). Structure of *ent*-15*α*-hydroxykaur-16-en-19-oic acid. *Advances in Chemistry* **6**, 16-20.

Cai, C.; Zhang, Y.; Yang, D.; Hao, X. and Li, S. (2017**).** Two new kaurane-type diterpenoids from *Wedelia chinensis* (Osbeck.) Merr. *Natural Products Research* **31**, 2531-2536.

Calixto, J. B., Campos, M. M., Otuki, M. F. and Santos, A. R. (2004). Anti-inflammatory compounds of plant origin. Part II. Modulation of pro-inflammatory cytokines, chemokines and adhesion molecules. *Planta Medica* **70**, 93-103.

Canel, C., Moraes, R. M., Dayan, F. E. and Ferreira, D. (2000). Podophyllotoxin. *Phytochemistry* **54**, 115-120.

Cano, B. L., Moreira, M. R., Goulart, M. O., dos Santos Gonçalves, N., Veneziani, R. C. S., Bastos, J. K., Ambrósio, S. R. and dos Santos, R. A. (2017). Comparative study of the cytotoxicity and genotoxicity of kaurenoic acid and its semi-synthetic derivatives methoxy kaurenoic acid and kaurenol in CHO-K1 cells. *Food and Chemical Toxicology* **102**, 102-108.

Cárdenas, A. V. C., Hernández, L. R., Juárez, Z. N., Sánchez-Arreola, E. and Bach, H. (2016). Antimicrobial, cytotoxic, and anti-inflammatory activities of *Pleopeltis polylepis*. *Journal of Ethnopharmacology* **194**, 981-986.

Chaturvedula, V. S. P. and Prakash, I. (2012). Isolation of stigmasterol and *β*-sitosterol from the dichloromethane extract of *Rubus suavissimus*. *International Current Pharmaceutical Journal* **1**, 239-242.

Chege, I. N., Okalebo, F. A., Guantai, A. N., Karanja, S. and Derese, S. (2015). Management of type 2 diabetes mellitus by traditional medicine practitioners in Kenya-key informant interviews. *Pan African Medical Journal* **22**, 1-12.

Chen, Q., Lin, H., Wu, X., Song, H. and Zhu, X. (2018). Preparative separation of six terpenoids from *Wedelia prostrata* Hemsl. By two-step high-speed counter-current chromatography. *Journal of Liquid Chromatography & Related Technologies* **41**, 408-414.

Chengbin, C., Changwei, L., Bing, C. and Bing, H., (2006). Isolation of polysubstituted saturated cyclohexanone compounds as antitumor agents. From *Faming Zhuanli Shenqing 2006*, CN 187238 A 20061206.

Chindo, B., Amos, S., Odutola, A., Vongtau, H., Abbah, J., Wambebe, C. and Gamaniel, K. (2003). Central nervous system activity of the methanol extract of *Ficus platyphylla* stem bark. *Journal of Ethnopharmacology* **85**, 131-137.

Correia, S. d. J., David, J. P. and David, J. M. (2006). Secondary metabolites from species of Anacardiaceae. *Quimica Nova* **29**, 1287-1300.

Cragg, G. M., Grothaus, P. G. and Newman, D. J. (2014). New horizons for old drugs and drug leads. *Journal of Natural Products* **77**, 703-723.

Cragg, G. M. and Newman, D. J. (2005). Plants as a source of anti-cancer agents. *Journal of Ethnopharmacology* **100**, 72-79.

Croteau, R., Kutchan, T. M. and Lewis, N. G. (2000). Natural Products (secondary metabolites). *Biochemistry and molecular biology of plants* **24**, 1250-1319.

David, J. M., Chávez, J. P., Chai, H.-B., Pezzuto, J. M. and Cordell, G. A. (1998). Two new cytotoxic compounds from *Tapirira guianensis*. *Journal of Natural Products* **61**, 287-289.

Dennis, R. (1973). Essential oil of *Psiadia salviifolia*. *Phytochemistry* **12**, 2705-2708.

Dias, J. R. and Gao, H. (2009). ^{13}C Nuclear Magnetic Resonance data of lanosterol derivatives. Profiling the steric topology of the steroid skeleton via substituent effects on its ^{13}C NMR. *Spectrochimica Acta Part A: Molecular and Biomolecular Spectroscopy* **74**, 1064-1071.

Dressler, Schmidt, M. and Zizka, G. (2014). African plants: A photo guide. *URL: http://www. africanplants. senckenberg. de* (Available on 12-06-2018).

El-Domiaty, M. M., El-Feraly, F. S., Mossa, J. S. and McPhail, A. T. (1993). Diterpenes from *Psiadia arabica*. *Phytochemistry* **34**, 467-471.

El-Feraly, F. S., Mossa, J. S., Al-Yahya, M. A., Hifnawy, M. S., Hafez, M. M. and Hufford, C. D. (1990). Two flavones from *Psiadia arabica*. *Phytochemistry* **29**, 3372-3373.

El-Gabalawy, H., Guenther, L. C. and Bernstein, C. N. (2010). Epidemiology of immune-mediated inflammatory diseases: Incidence, prevalence, natural history, and comorbidities. *The Journal of Rheumatology Supplement* **85**, 2-10.

El-Marsni, Z., Torres, A., Varela, R. M., Molinillo, J. M., Casas, L., Mantell, C., Martinez de la Ossa, E. J. and Macias, F. A. (2015). Isolation of bioactive compounds from Sunflower leaves (*Helianthus annuus* L.) extracted with supercritical carbon dioxide. *Journal of Agricultural and Food Chemistry* **63**, 6410-6421.

Esma G. K., Özbilge, H. and Albayrak, S. (2009). Determination of the effect of gentamicin against *Staphylococcus aureus* by using microbroth kinetic system. *Ankem Derg* **23**, 110-114.

Faleye, F. J. (2012). Terpenoid constituents of *Aspilia africana* [Pers] C.D. Adams leaves. *International Journal of Pharmaceutical Sciences Review and Research* **13**, 138-142.

Faleye, F. J. and Ogundaini, O. A. (2012). Evaluation of antioxidant and antimicrobial activities of two isolates from *Aspilia africana* (Pers) C.D Adams. *International Research Journal of Pharmacy* **655**, 135-138.

Fernández, A. l. E., Hong, W. D., Nixon, G. L., O'Neill, P. M. and Calderón, F. l. (2016). Antimalarial chemotherapy: Natural product inspired development of preclinical and clinical candidates with diverse mechanisms of action: Miniperspective. *Journal of Medicinal Chemistry* **59**, 5587-5603.

Fischedick, J. (2013). *Terpenoids for medicine*: Doctoral Thesis, Leiden University, Leiden, Netherlands, 1-182.

Frisch, M., Trucks, G., Schlegel, H., Scuseria, G., Robb, M., Cheeseman, J., Scalmani, G., Barone, V., Mennucci, B. and Petersson, G. (2009). Fox D. J. Gaussian 09, revision A. 02. Gaussian. *Inc., Wallingford, CT*.

Fröhlich, T., Hahn, F., Belmudes, L., Leidenberger, M., Friedrich, O., Kappes, B., Couté, Y., Marschall, M. and Tsogoeva, S. B. (2018). Synthesis of artemisinin-derived dimers, trimers and dendrimers: Investigation of their antimalarial and antiviral activities including putative mechanisms of action. *Chemistry–A European Journal* **24**, 8103-8113

Fürst, R. and Zündorf, I. (2014). Plant-derived anti-inflammatory compounds: Hopes and disappointments regarding the translation of preclinical knowledge into clinical progress. *Mediators of Inflammation* **10**, 1-9

Gao, L., Xu, X., Nan, H., Yang, J., Sun, G., Wu, H. and Zhong, M. (2012). Isolation of cinnamic acid derivatives from the root of *Rheum tanguticum* Maxim. Ex Balf. and its significance. *Journal of Medicinal Plants Research* **6**, 929-931.

Garcez, F. R., Garcez, W. S., Silva, A. F. G. d., Bazzo, R. d. C. and Resende, U. M. (2004). Terpenoid constituents from leaves of *Guarea kunthiana*. *Journal of the Brazilian Chemical Society* **15**, 767-772.

Gathirwa, J., Rukunga, G., Mwitari, P., Mwikwabe, N., Kimani, C., Muthaura, C., Kiboi, D., Nyangacha, R. and Omar, S. (2011). Traditional herbal antimalarial therapy in Kilifi district, Kenya. *Journal of Ethnopharmacology* **134**, 434-442.

Gathirwa, J., Rukunga, G., Njagi, E., Omar, S., Mwitari, P., Guantai, A., Tolo, F., Kimani, C., Muthaura, C. and Kirira, P. (2008). The in vitro anti-plasmodial and in vivo anti-malarial efficacy of combinations of some medicinal plants used traditionally for treatment of malaria by the Meru community in Kenya. *Journal of Ethnopharmacology* **115**, 223-231.

Gehrke, I. T., Neto, A. T., Pedroso, M., Mostardeiro, C. P., Da Cruz, I. B., Silva, U. F., Ilha, V., Dalcol, I. I. and Morel, A. F. (2013). Antimicrobial activity of *Schinus lentiscifolius* (Anacardiaceae). *Journal of Ethnopharmacology* **148**, 486-491.

Geissler, P. W., Harris, S. A., Prince, R. J., Olsen, A., Achieng'Odhiambo, R., Oketch-Rabah, H., Madiega, P. A., Andersen, A. and Mølgaard, P. (2002). Medicinal plants used by Luo mothers and children in Bondo district, Kenya. *Journal of Ethnopharmacology* **83**, 39-54.

Gelband, H., Molly Miller, P., Pant, S., Gandra, S., Levinson, J., Barter, D., White, A. and Laxminarayan, R. (2015). The state of the world's antibiotics 2015. *Wound Healing Southern Africa* **8**, 30-34.

Gemedo, D. T., Maass, B. L. and Isselstein, J. (2005). Plant biodiversity and ethnobotany of Borana pastoralists in Southern Oromia, Ethiopia. *Economic Botany* **59**, 43-65.

Ghozlojeh, N. P, and Setamdideh, D. (2015). Synthesis of oximes from the corresponding of organic carbonyl compounds with $NH_2OH.HCl$ and oxalic acid. *Oriental Journal of Chemistry* **31**, 1823-1825.

Gibbons, S., Moser, E. and Kaatz, G. W. (2004). Catechin gallates inhibit multidrug resistance (MDR) in *Staphylococcus aureus*. *Planta Medica* **70**, 1240-1242.

Gonçalves, G. M. S. and Gobbo, J. (2012). Antimicrobial effect of *Anacardium occidentale* extract and cosmetic formulation development. *Brazilian Archives of Biology and Technology* **55**, 843-850.

Gonzalez, A., Fraga, B., Hernandez, M. and Luis, J. (1973). New diterpenes from *Sideritis canariensis*. *Phytochemistry* **12**, 1113-1116.

González, L. R., Mitchell, G., Gattuso, M., Diarra, M. S., Malouin, F. and Bouarab, K. (2009). Plant antimicrobial agents and their effects on plant and human pathogens. *International Journal of Molecular Sciences* **10**, 3400-3419.

González, M. L., Joray, M. B., Laiolo, J., Crespo, M. I., Palacios, S. M., Ruiz, G. M. and Carpinella, M. C. (2018). Cytotoxic activity of extracts from plants of central Argentina on sensitive and multidrug-resistant Leukemia cells: Isolation of an active principle from *Gaillardia megapotamica*. *Evidence-Based Complementary and Alternative Medicine* **10**, 1-13

Goud, R., Gupta, S., Neogi, U., Agarwal, D., Naidu, K., Chalannavar, R. and Subhaschandra, G. (2011). Community prevalence of methicillin and vancomycin-resistant *Staphylococcus aureus* in and around Bangalore, Southern India. *Journal of the Brazilian Society of Tropical Medicine* **44**, 309-312.

Gouda, Y. G., Abdallah, Q. M., Elbadawy, M. F., Basha, A. A., Alorabi, A. K., Altowerqe, A. S. and Mohamed, K. M. (2014). Cytotoxic and antimicrobial activities of some compositae plants growing in Taif area, Saudi Arabia. *International Journal of Pharmaceutical Science Invention* **3**, 43-48.

Govinden-Soulange, J., Magan, N., Gurib-Fakim, A., Gauvin, A., Smadja, J. and Kodja, H. (2004). Chemical composition and in vitro antimicrobial activities of the essential oils from endemic *Psiadia* species growing in Mauritius. *Biological and Pharmaceutical Bulletin, 27*, 1814-1818.

Groweiss, A., Cardellina, J. H., Pannell, L. K., Uyakul, D., Kashman, Y. and Boyd, M. R. (1997). Novel cytotoxic, alkylated hydroquinones from *Lannea welwitschii*. *Journal of Natural Products* **60**, 116-121.

Gupta, J. and Ali, M. (1999). Phytochemical investigation of *Mangifera indica* root bark. *Indian Journal of Chemistry* **38**, 1093-1098.

Gurib-Fakim, A., Marie, D. and Narod, F. (2003). The pharmacological properties of the isolated bioactive compounds from endemic medicinal plants of Mauritius. *Paper presented at the III WOCMAP Congress on Medicinal and Aromatic Plants*. *Bioprospecting and Ethnopharmacology* **1**, 133-137.

Guzman, J. D. (2014). Natural cinnamic acids, synthetic derivatives and hybrids with antimicrobial activity. *Molecules* **19**, 19292-19349.

Hanson, J. R. (2003). *Natural products: The Secondary Metabolites* (Vol. 17): The Royal Society of Chemistry, 1-147.

Harvey, A. L. (2010). Plant natural products in anti-diabetic drug discovery. *Current Organic Chemistry* **14**, 1670-1677.

Haule, E. E., Moshi, M. J., Nondo, R. S., Mwangomo, D. T. and Mahunnah, R. L. (2012). A study of antimicrobial activity, acute toxicity and cytoprotective effect of a polyherbal extract in a rat ethanol-HCl gastric ulcer model. *BMC Research Notes* ***5***, 1-9.

Hind, D. N. (2003). Flora of Grão-Mogol, Minas Gerais: Compositae (Asteraceae). *Botany Bulletin of the University of São Paulo* **21**, 179-234.

Huang, W., Liang, Y., Wang, J., Li, G., Wang, G., Li, Y. and Chung, H. Y. (2016). Anti-angiogenic activity and mechanism of kaurane diterpenoids from *Wedelia chinensis*. *Phytomedicine* **23**, 283-292.

Hueso, F. I., Girón, N., Velasco, P., Amaro-Luis, J. M., Ravelo, A. G., de las Heras, B., Hortelano, S. and Estevez-Braun, A. (2010). Synthesis and induction of apoptosis signaling pathway of *ent*-kaurane derivatives. *Bioorganic & Medicinal Chemistry* **18**, 1724-1735.

Hunter, P. (2012). The inflammation theory of disease: The growing realization that chronic inflammation is crucial in many diseases opens new avenues for treatment. *EMBO Reports* **13**, 968-970.

Imam, M. Z., and Moniruzzaman, M. (2014). Antinociceptive effect of ethanol extract of leaves of *Lannea coromandelica*. *Journal of Ethnopharmacology* **154**, 109-115.

Irungu, B. N., Orwa, J. A., Gruhonjic, A., Fitzpatrick, P. A., Landberg, G., Kimani, F., Midiwo, J., Erdélyi, M. and Yenesew, A. (2014). Constituents of the roots and leaves of *Ekebergia capensis* and their potential antiplasmodial and cytotoxic activities. *Molecules* **19**, 14235-14246.

Islam, M. T. and Tahara, S. (2000). Dihydroflavonols from *Lannea coromandelica*. *Phytochemistry* **54**, 901-907.

Ita, B., Koroma, L. and Kormoh, K. (2010). Isolation and characterization of inositol from the ethanolic leaf extract of *Aspilia africana*. *Journal of Chemical and Pharmaceutical Research,* **2**, 1-6.

Johns, T., Faubert, G. M., Kokwaro, J. O., Mahunnah, R. and Kimanani, E. K. (1995). Anti-giardial activity of gastrointestinal remedies of the Luo of East Africa. *Journal of Ethnopharmacology* **46**, 17-23.

Juma, B. F., Yenesew, A., Midiwo, J. O. and Waterman, P. G. (2001). Flavones and phenylpropenoids in the surface exudate of *Psiadia punctulata*. *Phytochemistry* **57**, 571-574.

Juma, B. F., Yenesew, A., Midiwo, J. O., Waterman, P. G., Matthias, H. and Martin, P. G. (2006). Three *ent*-trachylobane diterpenes from the leaf exudates of *Psiadia punctulata*. *Phytochemistry* **67**, 1322–1325.

Jung, M., Park, M., Lee, H. C., Kang, Y.-H., Kang, E. S. and Kim, S. K. (2006). Antidiabetic agents from medicinal plants. *Current Medicinal Chemistry* **13**, 1203-1218.

Kapche, G., Laatsch, H., Fotso, S., Kouam, S., Wafo, P., Ngadjui, B. and Abegaz, B. (2007). Lanneanol: A new cytotoxic dihydroalkylcyclohexenol and phenolic compounds from *Lannea nigritana* (Sc. Ell.) Keay. *Biochemical Systematics and Ecology* **35**, 539-543.

Kayser, O., Kiderlen, A. F. and Croft, S. L. (2002). Natural products as potential antiparasitic drugs. *Studies in natural products chemistry* **26**, 779-848.

Keat, N. B., Umar, R. U., Lajis, N. H., Chen, T. Y., Li, T. Y., Rahmani, M. and Sukari, M. A. (2010). Chemical constituents from two weed species of *Spermacoce* (Rubiaceae). *Malaysian Journal of Analytical Sciences* **14**, 6-11.

Kenanda, E. O. and Omosa, L. K. (2017). Pyrazole, isoxazoline and bypyrimidine derivatives from *Polygonum senegalense* and *Psiadia punctulata* flavonoids and their anti-microbial activities. *Pharmacognosy Communications* **7**, 47-52.

Keriko, J. M., Nakajima, S., Baba, N. and Iwasa, J. (1997). Eicosanyl *p*-coumarates from a Kenyan plant, *Psiadia punctulata*: Plant growth inhibitors. *Bioscience, Biotechnology and Biochemistry* **61**, 2127-2128.

Khatun, M., Billah, M. and Quader, M.A., (2012). Sterols and sterol glucoside from *Phyllanthus* species. *Dhaka University Journal of Science* **60**, 5-10.

Kindt, R., van Breugel, P., Lilleso, J., Bingham, M., Demissew, S., Dudley, C., Friis, I., Gachathi, F., Kalema, J. and Mbago, F. (2011). Potential natural vegetation of Eastern Africa. Volume 2: Description. *Forest & Landscape Working Paper* **1**, 1-193.

Kipkore, W., Wanjohi, B., Rono, H. and Kigen, G. (2014). A study of the medicinal plants used by the Marakwet community in Kenya. *Journal of Ethnobiology and Ethnomedicine* **10**, 1-22.

Kokwaro, J. O. (1976). *Medicinal plants of East Africa*. East African Literature Bureau, 1st edition, Nairobi, 1-470.

Kokwaro, J. O. (1986). *Flora of tropical East Africa-Anacardiaceae*: *CRC Press*, Rotterdam, 1-350.

Kokwaro, J. O. (1994). *Flowering plant families of east africa:* An introduction to plant taxonomy: East African Publishers. Nairobi, 1-292.

Kokwaro, J. O. (2009). *Medicinal plants of East Africa*. East African Literature Bureau, 3rd edition, Nairobi, 1-169.

Kolb, H. and Mandrup-Poulsen, T. (2010). The global diabetes epidemic as a consequence of lifestyle-induced low-grade inflammation. *Diabetologia* **53**, 10-20.

Koné, W., Soro, D., Dro, B., Yao, K. and Kamanzi, K. (2011). Chemical composition, antioxidant, antimicrobial and acetylcholinesterase inhibitory properties of *Lannea barteri* (Anacardiaceae). *Australian Journal of Basic and Applied Sciences* **5**, 1516-1523.

Koopman, W. J. and Moreland, L. W. (2005). Arthritis and allied conditions: *A textbook of rheumatology*. Volume 1, 13 edition, Lippincott Williams & Wilkins, *Amazon*, 1-2100.

Kuete, V., Seo, E.-J., Krusche, B., Oswald, M., Wiench, B., Schröder, S., Greten, H. J., Lee, I.-S. and Efferth, T. (2013). Cytotoxicity and pharmacogenomics of medicinal plants from traditional Korean medicine. *Evidence-Based Complementary and Alternative Medicine* **13**, 1-14

Kümmerer, K. (2009). Antibiotics in the aquatic environment: A review. Part I. *Chemosphere* **75**, 417-434.

Kuria, J. M. (2014). *Efficacy of Aspilia pluriseta schweinf in cutaneous wound healing in a mouse model.* MSc, thesis, University of Nairobi, Nairobi, 1-75.

Lajter, I. (2015). *Biologically active secondary metabolites from Asteraceae and Polygonaceae species*. PhD Thesis, University of Szeged, Hungary, 1-61.

Laube, S. (2004). Skin infections and ageing. *Ageing Research Reviews* **3**, 69-89.

Lee, C., Yang, W. and Parr, R. G. (1988). Development of the colle-salvetti correlation-energy formula into a functional of the electron density. *Physical Review B* **37**, 785-789.

Lewis, K. and Ausubel, F. M. (2006). Prospects for plant-derived antibacterials. *Nature Biotechnology, 24*, 1504.

Lewis, R. E. (2011). *Current concepts in antifungal pharmacology*. Paper presented at the Mayo Clinic Proceedings **86**, 805-817.

Li, S.F., Ding, J. Y., Li, Y. T., Hao, X. J. and Li, S. L. (2016**)**. Antimicrobial Diterpenoids of *Wedelia trilobata* (L.) Hitchc. *Molecules*, **21**, 457.

Lima, N. M., Correia, C. S., Leon, L. L., Machado, G., Madeira, M. d. F., Santana, A. E. G. and Goulart, M. O. (2004). Antileishmanial activity of lapachol analogues. *Memories of the Oswaldo Cruz Institute* **99**, 757-761.

Lindholm, P. (2005). *Cytotoxic compounds of plant origin–biological and chemical diversity*. Acta Universitatis Upsaliensis, Uppsala, 1-71.

Mallbris, L., Akre, O., Granath, F., Yin, L., Lindelöf, B., Ekbom, A. and Ståhle-Bäckdahl, M. (2004). Increased risk for cardiovascular mortality in psoriasis inpatients but not in outpatients. *European Journal of Epidemiology* **19**, 225-230.

Maregesi, Ngassapa, O. D., Pieters, L. and Vlietinck, A. J. (2007). Ethnopharmacological survey of the Bunda district, Tanzania: Plants used to treat infectious diseases. *Journal of Ethnopharmacology* **113**, 457-470.

Maregesi, Pieters, L., Ngassapa, O. D., Apers, S., Vingerhoets, R., Cos, P., Berghe, D. A. V. and Vlietinck, A. J. (2008). Screening of some Tanzanian medicinal plants from Bunda district for antibacterial, antifungal and antiviral activities. *Journal of Ethnopharmacology* **119**, 58-66.

Maregesi, Van Miert, S., Pannecouque, C., Haddad, M. H. F., Hermans, N., Wright, C. W., Vlietinck, A. J., Apers, S. and Pieters, L. (2010). Screening of Tanzanian medicinal plants against *Plasmodium falciparum* and human immunodeficiency virus. *Planta Medica* **76**, 195-201.

Marles, R. J. and Farnsworth, N. R. (1995). Antidiabetic plants and their active constituents. *Phytomedicine* **2**, 137-189.

Martins, C. H. G., Midiwo, J. O., Parreira, R. L. T. and Heleno, V. C. (2017). Study of anti-tuberculosis activity behaviour of natural kaurane and trachylobane diterpenes compared with structural properties obtained by theoritical calculations. *Natural Product Communications* **12**, 763-769.

Mathur, J., Ahuja, P. S., Lal, N. and Mathur, A. K. (1989). Propagation of *Valeriana wallichi*i D. C. Using encapsulated apical and axial shoot buds. *Plant Science* **60**, 111-116.

McGaw, L. J., Elgorashi, E. E. and Eloff, J. N. (2014). *Cytotoxicity of African medicinal plants against normal animal and human cells*. *Toxicological Survey of African Medicinal Plants*. 1st Edition, Elsevier, Amsterdam, 1-744.

Meek, I. L., Van de Laar, M. A. and E Vonkeman, H. (2010). Non-steroidal anti-inflammatory drugs: An overview of cardiovascular risks. *Pharmaceuticals* **3**, 2146-2162.

Midiwo, J., Owuor, F., Juma, B. and Waterman, P. (1997). Diterpenes from the leaf exudate of *Psiadia punctulata*. *Phytochemistry* **45**, 117-120.

Midiwo, J., Yenesew, A., Juma, B., Omosa, K. L., Omosa, I. L. and Mutisya, D. (2001). *Phytochemical evaluation of some Kenyan medicinal plants.* Paper presented at the 11th NAPRECA Symposium Book of Proceedings, Antananarivo, Madagascar, 311-323.

Miller, A. H., Maletic, V. and Raison, C. L. (2009). Inflammation and its discontents: The role of cytokines in the pathophysiology of major depression. *Biological Psychiatry* **65**, 732-741.

Morales-Serna, J. A., García-Ríos, E., Madrigal, D., Cárdenas, J. and Salmón, M. (2011). Constituents of organic extracts of *Cuphea hyssopifolia*. *Journal of the Mexican Chemical Society* **55**, 62-64.

Mossa, J. S., El-Domiaty, M. M., Al-Meshal, I. A., El-Feraly, F. S., Hufford, C. D., McPhail, D. R. and McPhail, A. T. (1992). A flavone and diterpene from *Psiadia arabica*. *Phytochemistry* **31**, 2863-2868.

Moya, L. F. and Llorca, L. L. V. (2016). Omics for investigating chitosan as an antifungal and gene modulator. *Journal of Fungi* **2**, 1-11.

Muhaisen, H. M. (2013). Chemical constituents from the bark of *Lannea acida* Rich (Anacardiaceae). *Der Pharma Chemica* **5**, 88-96.

Muithya, J. N. (2010). *Phytochemical and in vitro anti-microbial screening of Echinops hispidus Fresen. and Grewia similis k. Schum.* PhD Thesis, School of Pure and Applied Science, Kenyatta University, Nairobi, 1-107.

Müller, S., Tirapelli, C. R., de Oliveira, A. M., Murillo, R., Castro, V. and Merfort, I. (2003). Studies of *ent*-kaurane diterpenes from *Oyedaea verbesinoides* for their inhibitory activity on vascular smooth muscle contraction. *Phytochemistry* **63**, 391-396.

Musyimi, D., Ogur, J. and Muema, P. (2007). Effects of leaf and root extracts of *Aspilia* plant (*Aspilia mossambicensis*) Oliv. wild. On some selected micro-organisms. *International Journal of Biological Chemistry* **1**, 213-220.

Musyimi, D., Ogur, J. and Muema, P. (2008). Phytochemical compounds and antimicrobial activity of extracts of Aspilia plant (*Aspilia mossambicensis*) Oliv. wild. *International Journal of Botany* **4***,* 56-61.

Nagashima, F., Kondoh, M., Fujii, M., Takaoka, S., Watanabe, Y. and Asakawa, Y. (2005). Novel cytotoxic kaurane-type diterpenoids from the New Zealand Liverwort *Jungermannia* species. *Tetrahedron* **61**, 4531-4544.

Nagimova, A., Zhusupova, G. and Erzhanova, M. (1996). Synthesis of biologically active bromine derivatives of quercetin. *Chemistry of Natural Compounds* **32**, 695-697.

Nair, R. and Chanda, S. (2005). Anticandidal activity of *Punica granatum*. Exhibited in different solvents. *Pharmaceutical Biology* **43**, 21-25.

Ndunda, B. (2014). *Phytochemistry and Bioactivity Investigations of Three Kenyan Croton species*. Doctoral dissertation, PhD Thesis, University of Nairobi, Nairobi, 1-307.

Newman, D. J. and Cragg, G. M. (2016). Natural products as sources of new drugs from 1981 to 2014. *Journal of Natural Products* **79**, 629-661.

Nguyen, A.-T. and Duez, P. (2008). Cytotoxic anticancer drugs from medicinal plants. *Phytochemistry Research Progress. New York: Nova Science Publishers Inc* **1**, 193-208.

Nitbani, F. O., Siswanta, D. and Solikhah, E. N. (2016). Isolation and antibacterial activity test of lauric acid from crude Coconut oil (*Cocos nucifera* L.). *Procedia Chemistry* **18**, 132-140.

Njinga, N., Sule, M., Pateh, U., Hassan, H., Ahmad, M., Abdullahi, S., Danja, B. and Bawa, B. (2014). Phytochemical and antimicrobial activity of the leaves of *Lannea kerstingii* Engl and K. Krause (Anacadiaceae). *Nitte University Journal of Health Science* **4**, 4-9.

Norton, R., Huang, D. and Rodriguez, E. (1993). *Aspilia mossambicensis*: In vitro propagation and production of antibiotic polyacetylenes by root cultures. *Medicinal and Aromatic Plants* **5**, 54-63.

O'Neill, J. (2016). Tackling drug-resistant infections globally: Final report and recommendations. *The Review on Antimicrobial Resistance* **1**, 1-71.

Ogungbe, I. V. and Setzer, W. N. (2013). In-silico Leishmania target selectivity of antiparasitic terpenoids. *Molecules* **18**, 7761-7847.

Okoth, D. A. (2014). *Phytochemistry and bioactive natural products from Lannea alata, Lannea rivae, Lannea schimperi and Lannea schweinfurthii (Anacardiaceae)*. PhD Thesis, University of Kwazulu-Natal, 1-668.

Okoth, D. A., Akala, H. M., Johnson, J. D. and Koorbanally, N. A. (2016). Alkyl phenols, alkenyl cyclohexenones and other phytochemical constituents from *Lannea rivae* (Chiov) sacleux (Anacardiaceae) and their bioactivity. *Medicinal Chemistry Research* **25**, 690-703.

Okoth, D. A., Chenia, H. Y. and Koorbanally, N. A. (2013). Antibacterial and antioxidant activities of flavonoids from *Lannea alata* (Engl.) engl.(Anacardiaceae). *Phytochemistry Letters* **6**, 476-481.

Okoth, D. A. and Koorbanally, N. A. (2015). Cardanols, long chain cyclohexenones and cyclohexenols from *Lannea schimperi* (Anacardiaceae). *Natural Product Communications* **10**, 103-106.

Ouattara, L., Koudou, J., Zongo, C., Barro, N., Savadogo, A., Bassole, I., Ouattara, A. and Traore, A. S. (2011). Antioxidant and antibacterial activities of three species of *Lannea* from Burkina Faso. *Journal of Applied Science* **11**, 157-162.

Padilla, G. G. F., Diazgranados, M., Ccana-Ccapatinta, G., Casoti, R. and Da Costa, F. B. (2017). Caffeic acid derivatives and further compounds from *Espeletia barclayana* Cuatrec.(Asteraceae, Espeletiinae). *Biochemical Systematics and Ecology* **70**, 291-293.

Page, J. E., Balza, F., Nishida, T. and Towers, G. N. (1992). Biologically active diterpenes from *Aspilia mossambicensis,* a Chimpanzee medicinal plant. *Phytochemistry* **31**, 3437-3439.

Page, J. E., Huffman, M., Smith, V. and Towers, G. (1997). Chemical basis for *Aspilia* leaf-swallowing by Chimpanzees: A reanalysis. *Journal of Chemical Ecology* **23**, 2211-2226.

Pan, G., Yang, K., Ma, Y., Zhao, X., Lu, K. and Yu, P. (2015). Synthesis of 6-or 8-bromo flavonoids by regioselective mono-bromination and deprotection protocol from flavonoid alkyl ethers. *Bulletin of the Korean Chemical Society* **36**, 1460-1466.

Park, K. D., Park, Y. S., Cho, S. J., Sun, W. S., Kim, S. H., Jung, D. H. and Kim, J. H. (2004). Antimicrobial activity of 3-*O*-acyl-(-)-epicatechin and 3-*O*-acyl-(+)-catechin derivatives. *Planta Medica* **70,** 272-276.

Parveen, A., Shaheen, K., Qamer Shaik, M., Ali, S., Hussain, M. and Ali, S. (2014). Prescribing patterns of antibiotics in post operative patients in a teaching Hospital. *Indo-American Journal of Pharmeutical Research* **4**, 527-532.

Parvin, S., Kader, M. A., Muhit, M. A., Haque, M. E., Mosaddik, M. A. and Wahed, M. I. I. (2011). Triterpenoids and phytosteroids from stem bark of *Crataeva nurvala* Buch Ham. *Journal of Applied Pharmaceutical Science* **1**, 47-50.

Peña, A., Alarcón, L., Baptista, J. G., Aparicio, R., Villasmil, T. and Usubillaga, A. (2012). A phytochemical analysis of *Espeletia nana* Cuatrec. A midget *Espeletiinae* from Paramo Ortiz, Venezuela. *Avances en Quimica* **7**, 187-192

Penesyan, A., Gillings, M. and Paulsen, I. T. (2015). Antibiotic discovery: Combatting bacterial resistance in cells and in biofilm communities. *Molecules* **20**, 5286-5298.

Picerno, P., Mencherini, T., Loggia, R. D., Meloni, M., Sanogo, R. and Aquino, R. (2006). An extract of *Lannea microcarpa*: Composition, activity and evaluation of cutaneous irritation in cell cultures and reconstituted Human epidermis. *Journal of Pharmacy and Pharmacology* **58**, 981-988.

Piero, N. M., Joan, M. N., Kibiti, C. M., Ngeranwa, J., Njue, W. N., Maina, D. N., Gathumbi, P. and Njagi, E. N. (2011). Hypoglycemic activity of some Kenyan plants traditionally used to manage diabetes mellitus in Eastern province ***2***, 1-6.

Pinto, A. C., Prado, S. K. and Pinchin, R. (1981). Two kaurenes from *Vellozia caput-ardeae*. *Phytochemistry* **22**, 2017-2019.

Pita, J. C. L. R., Xavier, A. L., Sousa, T. K. G. d., Mangueira, V. M., Tavares, J. F., Júnior, R. J. d. O., Veras, R. C., Pessoa, H. D. L. F., Silva, M. S. D. and Morelli, S. (2012). In *vitro* and in *vivo* antitumor effect of trachylobane-360, a diterpene from *Xylopia langsdorffiana*. *Molecules* **17**, 9573-9589.

Pouny, I., Vispe, S., Marcourt, L., Long, C., Vandenberghe, I., Aussagues, Y., Raux, R., Chalo Mutiso, P. B., Massiot, G. and Sautel, F. (2011). Four new carvotanacetone derivatives from *Sphaeranthus ukambensis*, inhibitors of the ubiquitin-proteasome pathway. *Planta Medica* **77**, 1605-1609.

Qi, S.-H., Wu, D.-G., Ma, Y. B. and Luo, X.-D. (2003). A novel flavane from *Carapa guianensis*. *Acta Botanica Sinica-Chinese Edition* **45**, 1129-1132.

Qiu, Q., Wu, X., Li, G., Li, Y., and Wang, G. (2014). Chemical constituents from *Wedelia chinensis. Zhong Cheng Yao* **36**, 1000-1004.

Qiu, M., Yang, B., Cao, D., Zhu, J., Jin, J., Chen, Y., Zhou, L., Luo, X. and Zhao, Z. (2016). Two new hydroxylated *ent*-kauranoic acids from *Pteris semipinnata*. *Phytochemistry Letters* **16**, 156-162.

Queiroz, E. F., Kuhl, C., Terreaux, C., Mavi, S. and Hostettmann, K. (2003). New dihydroalkylhexenones from *Lannea edulis*. *Journal of Natural Products, 66*, 578-580.

Rainsford, K. (2007). Anti-inflammatory drugs in the 21st century *Inflammation in the Pathogenesis of Chronic Diseases*-Springer **1**, 3-27.

Ramanoelina, P. A., Rasoarahona, J. R., Masotti, V., Viano, J., Gaydou, E. M. and Bianchini, J.-P. (1994). Chemical composition of the leaf oil of *Psiadia altissima* (Compositeae). *Journal of Essential Oil Research* **6**, 565-570.

Rasmussen, R. V., Fowler Jr, V. G., Skov, R. and Bruun, N. E. (2011). Future challenges and treatment of *Staphylococcus aureus* bacteremia with emphasis on MRSA. *Future Microbiology* **6**, 43-56.

Reddy, A. K., Joy, J. M. and Kumara, C. A. (2011). *Lannea coromandelica*: The Researcher's Tree. *Journal of Pharmacy Research* **4**, 577-579.

Ribeiro, A., Romeiras, M. M., Tavares, J. and Faria, M. T. (2010). Ethnobotanical survey in Canhane village, district of Massingir, Mozambique: Medicinal plants and traditional knowledge. *Journal of Ethnobiology and Ethnomedicine* **6**, 1-10.

Robbins, S., Cotran, R. and Kumar, V. (1984). *Pathologic basis of disease (Philadelphia, PA: Saunders)*. 8th Edition, Saunders, 1-1464

Robin, V., Boustie, J., Amoros, M. and Girre, L. (1998). In-vitro antiviral activity of seven *Psiadia* species, Asteraceae: Isolation of two antipoliovirus flavonoids from *Psiadia dentata*. *Pharmacy and Pharmacology Communications* **4**, 61-64.

Robin, V., Irurzun, A., Amoros, M., Boustie, J. and Carrasco, L. (2001). Antipoliovirus flavonoids from *Psiadia dentata*. *Antiviral Chemistry and Chemotherapy* **12**, 283-291.

Rodriguez, E., Aregullin, M., Nishida, T., Uehara, S., Wrangham, R., Abramowski, Z., Finlayson, A. and Towers, G. N. (1985). Thiarubrine a, a bioactive constituent of *Aspilia* (Asteraceae) consumed by wild Chimpanzees. *Experientia* **41**, 419-420.

Roumy, V., Fabre, N., Portet, B., Bourdy, G., Acebey, L., Vigor, C., Valentin, A. and Moulis, C. (2009). Four anti-protozoal and anti-bacterial compounds from *Tapirira guianensis*. *Phytochemistry* **70**, 305-311.

Rungsimakan, S. (2011). *Phytochemical and biological activity studies on Salvia viridis L.* PhD Dissertation, University of Bath, United Kingdom, 1-403.

Saeidnia, S., Gohari, A., Mokhber-Dezfuli, N. and Kiuchi, F. (2011). A review on phytochemistry and medicinal properties of the genus *Achillea*. *DARU: Journal of Faculty of Pharmacy, Tehran University of Medical Sciences* **19**, 173-186.

Sáez, A. M., Fernández-Pérez, M. P., Chazarra, S., Mchedlishvili, N., Tárraga-Tomás, A. and Rodríguez-López, J. N. (2013). Factors influencing the antifolate activity of synthetic Tea-derived catechins. *Molecules* **18**, 8319-8341.

Sakanaka, S., Juneja, L. R., and Taniguchi, M. (2000). Antimicrobial effects of green Tea polyphenols on thermophilic spore-forming bacteria. *Journal of Bioscience and Bioengineering,* **90**, 81-85.

Salim, A., Chin, Y. and Kinghorn, A. (2008). *Bioactive molecules and medicinal plants*. Ramawat K. G., Merillon J. M., eds: *Springer* **1**, 1-24

Santos, F. O., Angélico, E. C., da Costa, J. G. M., Rodrigues, F. F., Rodrigues, O. G. and de Medeiros, R. S. (2013). Antibacterial evaluation of *Anacardium occidentale* Linn. (Anacardiaceae) in semiarid Brazil. *African Journal of Biotechnology* **12**, 4836-4840

Schütte, H. R. (1997). Secondary plant substances. Diterpenes. *Progress in Botany* - Springer,1, 255-277.

Schwingshackl, L., Lampousi, A., Portillo, M., Romaguera, D., Hoffmann, G. and Boeing, H. (2017). Olive oil in the prevention and management of type 2 diabetes mellitus: A systematic review and meta-analysis of cohort studies and intervention trials. *Nutrition & Diabetes* **7**, 1-6.

Sebisubi, F. M., Odyek, O., Anokbonggo, W. W., Ogwal-Okeng, J., Carcache-Blanco, E. J., Ma, C., Orjala, J. and Tan, G. T. (2010). Antimalarial activity of aspilia pruliseta, a medicinal plant from Uganda. *Planta Medica* **76**, 1870-1873.

Seebacher, W., Simic, N., Weis, R., Saf, R. and Kunert, O. (2003). Complete assignments of ^{1}H and ^{13}C NMR resonances of oleanolic acid, 18α-oleanolic acid, ursolic acid and their 11-oxo derivatives. *Magnetic Resonance in Chemistry* **41**, 636-638.

Seoposengwe, K., van Tonder, J. J. and Steenkamp, V. (2013). *In vitro* neuroprotective potential of four medicinal plants against rotenone-induced toxicity in SH-SY5Y neuroblastoma cells. *BMC Complementary and Alternative Medicine* **13**, 2-11.

Serhan, C. N. (2017). Treating inflammation and infection in the 21st century: New hints from decoding resolution mediators and mechanisms. *The FASEB Journal* **31**, 1273-1288.

Shams, E. S. M., Radwan, M. M., Wanas, A. S., Habib, A.-A. M., Kassem, F. F., Hammoda, H. M., Khan, S. I., Klein, M. L., Elokely, K. M. and ElSohly, M. A. (2018). Bioactivity-guided isolation of potential antidiabetic and antihyperlipidemic compounds from *Trigonella stellata*. *Journal of Natural Products* **81**, 1154-1161.

Shigeru, S., Toshio, M., Kaoru, U. and Akira, U. (1990). Kaurene-type diterpenes from *Adenostemma lavenia* O. Kuntze. *Chemical and Pharmaceutical, Bulletin* **38**, 1308-1312.

Shingate, B. B., Hazra, B. G., Salunke, D. B., Pore, V. S., Shirazi, F. and Deshpande, M. V. (2013). Synthesis and antimicrobial activity of novel oxysterols from lanosterol. *Tetrahedron* **69**, 11155-11163.

Simoes, A. C. (2009). *Investigation of antiplasmodial compounds from various plant extracts.* PhD Thesis, University of Geneva, Geneva, 1-226.

Soh, D., Nkwengoua, E., Ngantchou, I., Nyasse, B., Denier, C., Hannaert, V., Shaker, K. H. and Schneider, B. (2013). Xylopioxyde and other bioactive kaurane-diterpenes from *Xylopia aethiopica* Dunal (Annonaceae). *Journal of Applied Pharmaceutical Science* **3**, 13-19.

Souza, J. M., Chang, M. R., Brito, D. Z., Farias, K. S., Damasceno-Junior, G. A., Turatti, I. C., Lopes, N. P., Santos, E. A. and Carollo, C. A. (2015). Antimicrobial activity of *Aspilia latissima* (Asteraceae). *Brazilian Journal of Microbiology* **46**, 1103-1110.

Srinivasa, R. V., Einstein J. W., Das, K. (2014). Hepatoprotective and Antioxidant Activity of *Lannea coromandelica*. *International Letters of Natural Sciences* **8**, 30-43.

Strijk, J. S., Noyes, R. D., Strasberg, D., Cruaud, C., Gavory, F., Chase, M. W., Abbott, R. J. and Thébaud, C. (2012). In and out of Madagascar: Dispersal to peripheral Islands, insular speciation and diversification of Indian Ocean daisy trees (*Psiadia*, Asteraceae). *PloS one* **7**, 1-17.

Sultana, S. and Ilyas, M. (1986). A flavanone from *Lannea acida*. *Phytochemistry* **25**, 963-964.

Tarkang, P. A., Okalebo, F. A., Siminyu, J. D., Ngugi, W. N., Mwaura, A. M., Mugweru, J., Agbor, G. A. and Guantai, A. N. (2015). Pharmacological evidence for the folk use of Nefang: Antipyretic, anti-inflammatory and antinociceptive activities of its constituent plants. *BMC Complementary and Alternative Medicine* **15**, 12-11.

Taylor, L. (2000). Plant based drugs and medicines. *Raintee Nutrition Inc* **1** , 1-8.

Tincusi, B. M., Jiménez, I. A., Bazzocchi, I. L., Moujir, L. M., Mamani, Z. A., Barroso, J. P., Ravelo, A. G. and Hernandez, B. V. (2002). Antimicrobial terpenoids from the oleoresin of the Peruvian medicinal plant *Copaifera paupera*. *Planta medica* **68**, 808-812.

Tuck, S., Patel, H., Safi, E. and Robinson, C. (1991). Lanosterol 14 alpha-demethylase (P45014DM): Effects of P45014DM inhibitors on sterol biosynthesis downstream of lanosterol. *Journal of Lipid Research* **32**, 893-902.

Utami, R., Khalid, N., Sukari, M. A., Rahmani, M. and Dachriyanus, A. (2013). Phenolic contents, antioxidant and cytotoxic activities of *Elaeocarpus floribundus* blume. *Pak. Journal of Pharmaceutical Science,* **26**, 245-250.

Van A. M. A., Eggelte, T. A. and van Boxtel, C. J. (1999). Artemisinin drugs in the treatment of malaria: From medicinal herb to registered medication. *Trends in Pharmacological Sciences,* **20**, 199-205.

Wafo, P., Kamdem, R. S., Ali, Z., Anjum, S., Begum, A., Oluyemisi, O. O., Khan, S. N., Ngadjui, B. T., Etoa, X. F. and Choudhary, M. I. (2011). Kaurane-type diterpenoids from *Chromoleana odorata*, their X-ray diffraction studies and potent α-glucosidase inhibition of 16-kauren-19-oic acid. *Fitoterapia,* **82**, 642-646.

Waksman, S. A. (1947). What is an antibiotic or an antibiotic substance? *Mycologia* **39**, 565-569.

Walter, S., Campbell, C., Kellogg, E. and Stevens, P. (1999). *Plant systematics. A phylogenetic approach.* 4th edition, Smaver Associates Inc, 226-271.

Wild, S., Roglic, G., Green, A., Sicree, R. and King, H. (2004). Global prevalence of diabetes: Estimates for the year 2000 and projections for 2030. *Diabetes Care* **27**, 1047-1053.

Winterfeldt, E. (1994). Ferdinand Bohlmann (1921-1991) and his scientific work. *Liebig's Annals of Chemistry* **5**, 1-34.

Wong, V. K. W., Zhang, M. M., Zhou, H., Lam, K. Y. C., Chan, P. L., Law, C. K. M., Yue, P. Y. K. and Liu, L. (2013). Saikosaponin-d enhances the anticancer potency of TNF-α via overcoming its undesirable response of activating NF-Kappa B signalling in cancer cells. *Evidence-Based Complementary and Alternative Medicine* **13**, 1-14

World Health Organization (2015). Worldwide country situation analysis: Response to antimicrobial resistance. Repport, Geneva, 1-42.

Wu, Ding, Y., Tanaka, Y. and Zhang, W. (2014). Risk factors contributing to type 2 diabetes and recent advances in the treatment and prevention. *International Journal of Medical Sciences* **11**, 1185-1200.

Wu, Lu, C. H. and Shen, Y. M. (2009). Three new *ent*-trachylobane diterpenoids from co-cultures of the calli of *Trewia nudiflora* and *Fusarium* sp. Wxe. *Helvetica Chimica Acta* **92**, 2783-2789.

Xavier, J. F. H., Maciuk, A., Rochelle do Vale Morais, A., Alencar, E. D. N., Garcia, V. L., Tabosa do Egito, E. S. and Vauthier, C. (2017). Development of a gas chromatography method for the analysis of Copaiba oil. *Journal of Chromatographic Science* **55**, 969-978.

Yang, Y. C., McClintock, M. K., Kozloski, M. and Li, T. (2013). Social isolation and adult mortality: The role of chronic inflammation and sex differences. *Journal of Health and Social Behavior* **54**, 183-203.

Yasmen, N., Aziz, M., Tajmim, A., Akter, M., Hazra, A. K. and Rahman, S. (2018). Analgesic and anti-inflammatory activities of diethyl ether and *n*-hexane extract of *Polyalthia suberosa* leaves. *Evidence-Based Complementary and Alternative Medicine* **18**, 1-8.

Yun, X.-j., Shu, H.-m., Chen, G.-y., Ji, M.H. and Ding, J.-y. (2014). Chemical constituents from barks of *Lannea coromandelica*. *Chinese Herbal Medicines* **6**, 65-69.

Zamuner, M., Cortez, D. A., Dias Filho, B. P., Lima, M. I. S. and Rodrigues-Filho, E. (2005). Lanostane triterpenes from the fungus *Pisolithus tinctorius*. *Journal of the Brazilian Chemical Society* **16**, 863-867.

Zhang, H., Wynne, G. and Mander, L. N. (2001). Synthesis of *ent*-9α,15α-cyclokaurene from grandiflorenic acid. *ARKIVOC* **8**, 40-58.

Zhang, H., Qiu, M., Chen, Y., Chen, J., Sun, Y., Wang, C. and Fong, H. H. (2002). Plant terpenes. *Phytochemistry and Pharmacognosy. Encyclopedia of Lyfe Support Systems* 1-239.

Zhou, Y., Yang, B., Liu, Z., Jiang, Y., Liu, Y., Fu, L., Wang, X. and Kuang, H. (2015). Cytotoxicity of triterpenes from green walnut husks of *Juglans mandshurica* Maxim in HepG-2 cancer cells. *Molecules* **20**, 19252-19262.

Zimmet, P. (2003). The burden of type 2 diabetes: Are we doing enough? *Diabetes & Metabolism* **29**, 6S9-6S18.

APPENDICES

Appendix 1: Spectra for the Dompounds of *Lannea* Species

Appendix 1A: The ^{1}H NMR spectrum (600 MHz) of (4*R*,6*S*)-4,6-dihydroxy-6-((*Z*)-nonadec-14'-en-1-yl)cyclohex-2-en-1-one (**186**) in $CDCl_3$, *J* in Hz, δ in ppm.

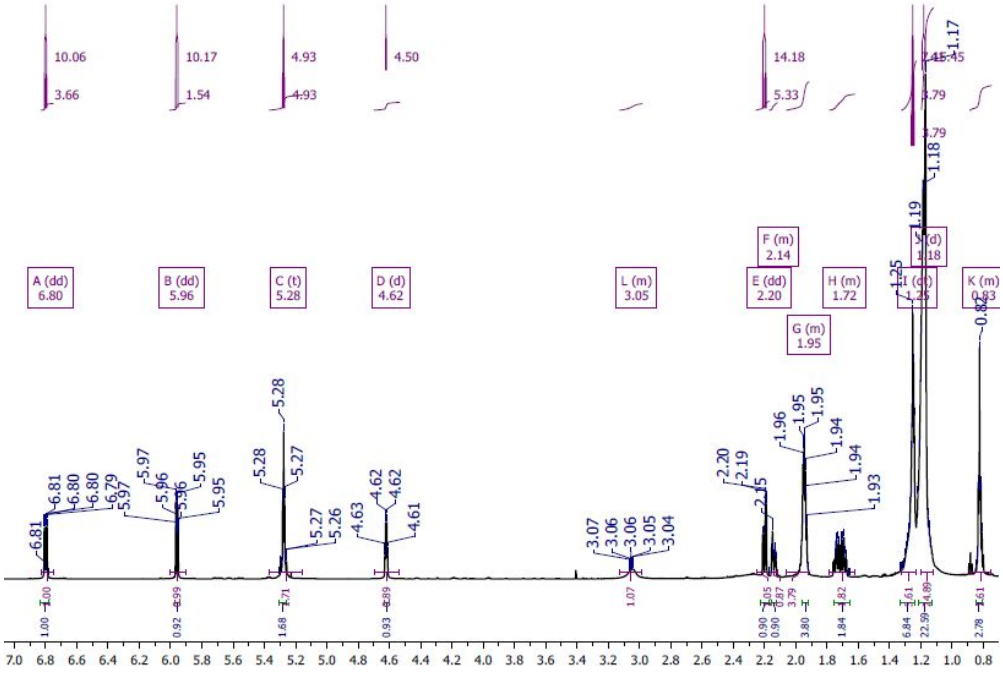

Appendix 1B: The ^{13}C NMR spectrum (200MHz) of (4*R*,6*S*)-4,6-dihydroxy-6-((*Z*)-nonadec-14'-en-1-yl)cyclohex-2-en-1-one (**186**) in $CDCl_3$.

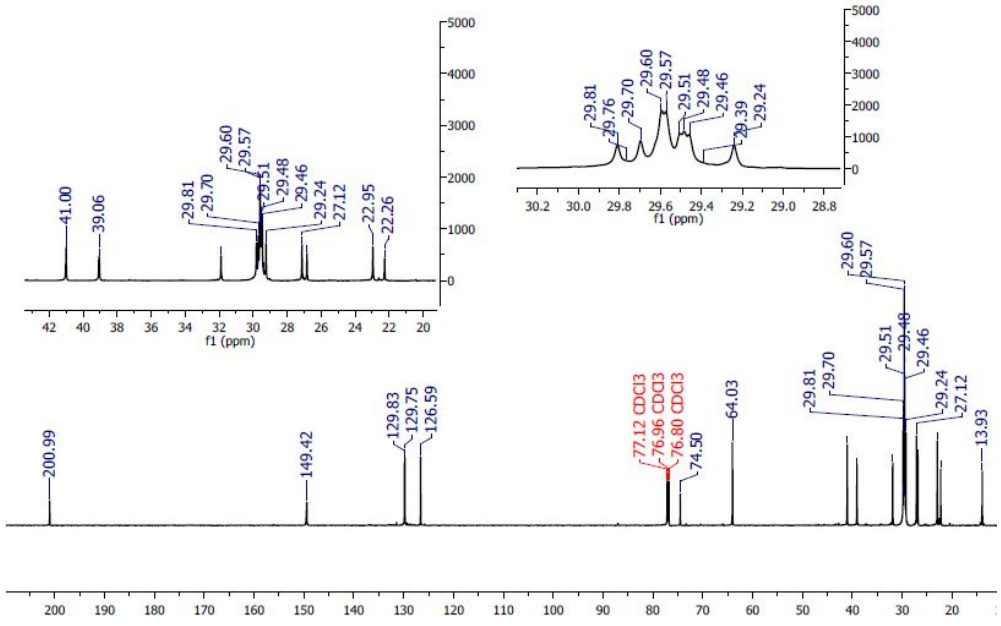

Appendix 1C: The H-H COSY spectrum of (4*R*,6*S*)-4,6-dihydroxy-6-((*Z*)-nonadec-14'-en-1-yl)cyclohex-2-en-1-one (**186**) in $CDCl_3$

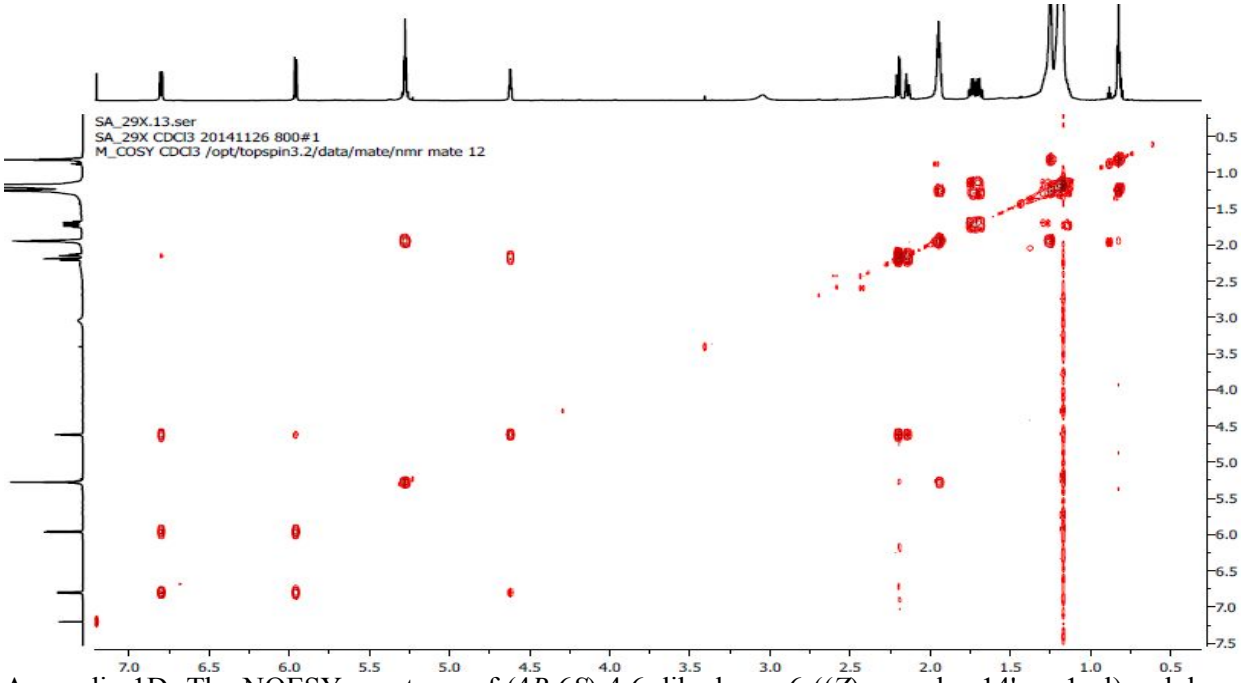

Appendix 1D: The NOESY spectrum of (4*R*,6*S*)-4,6-dihydroxy-6-((*Z*)-nonadec-14'-en-1-yl)cyclohex-2-en-1-one (**186**), in $CDCl_3$

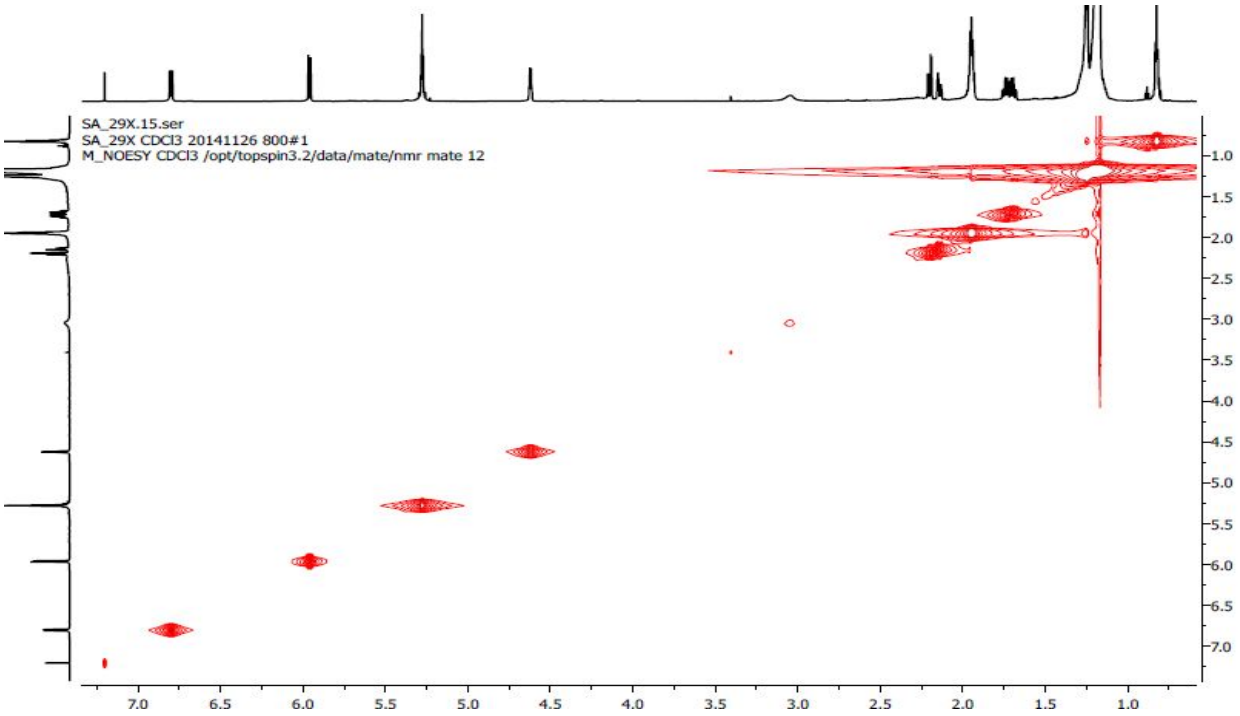

Appendix 1E: The HSQC spectrum of (4*R*,6*S*)-4,6-dihydroxy-6-((*Z*)-nonadec-14'-en-1-yl)cyclohex-2-en-1-one (**186**) in $CDCl_3$

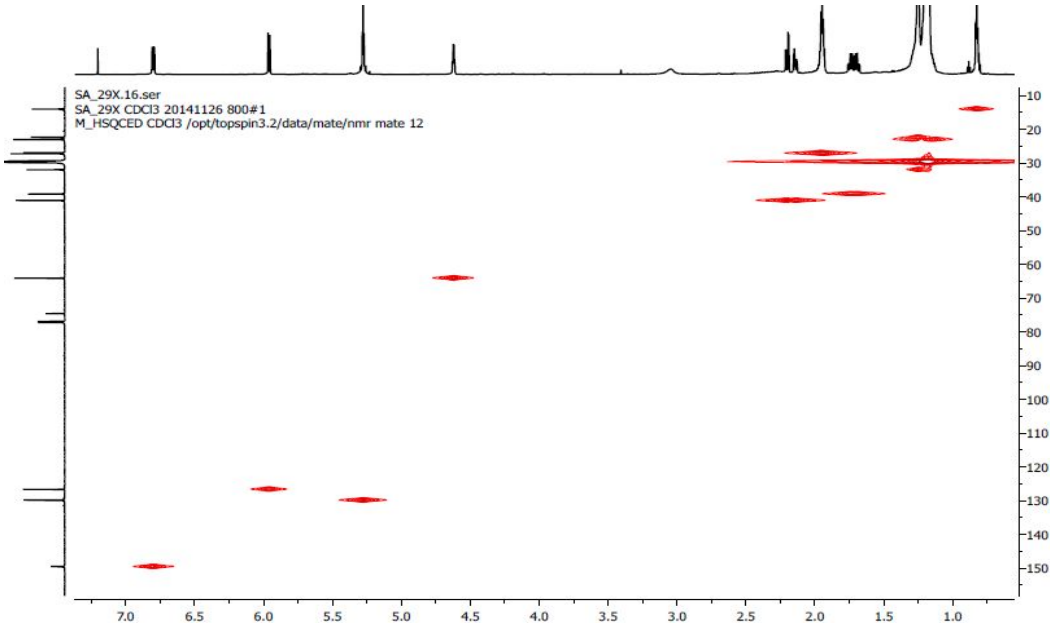

Appendix 1F: The HMBC spectrum of (4*R*,6*S*)-4,6-dihydroxy-6-((*Z*)-nonadec-14'-en-1-yl)cyclohex-2-en-1-one (**186**) in $CDCl_3$

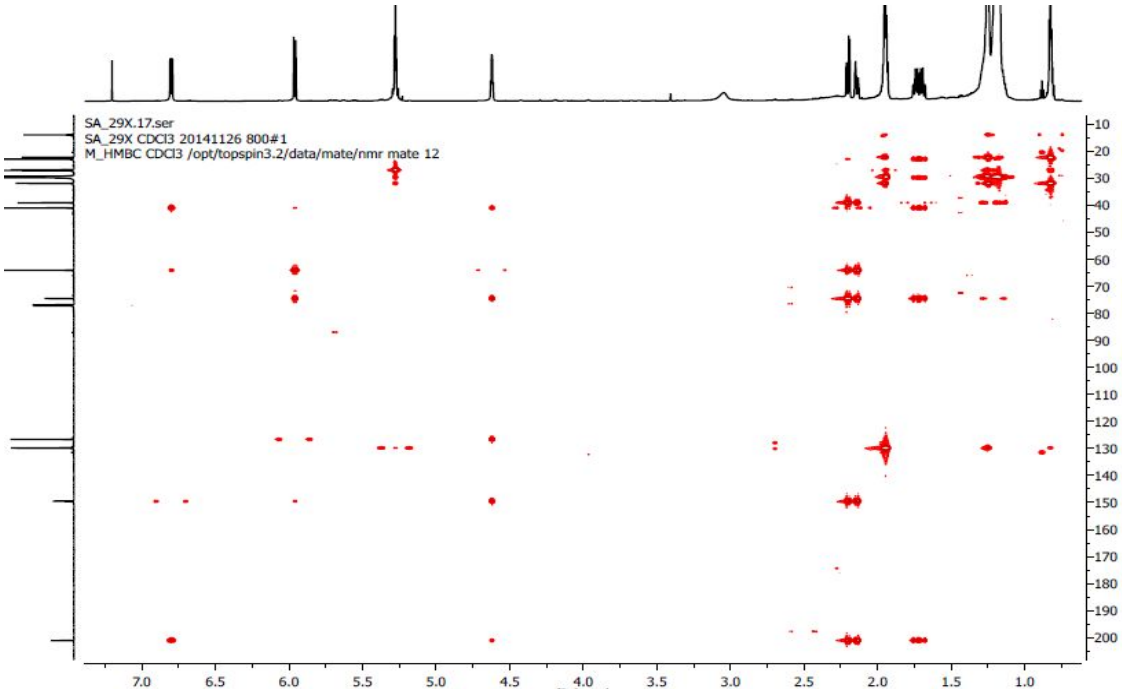

Appendix 1G: The HRESIMS spectrum of (4*R*,6*S*)-4,6-dihydroxy-6-((*Z*)-nonadec-14'-en-1-yl)cyclohex-2-en-1-one (**186**)

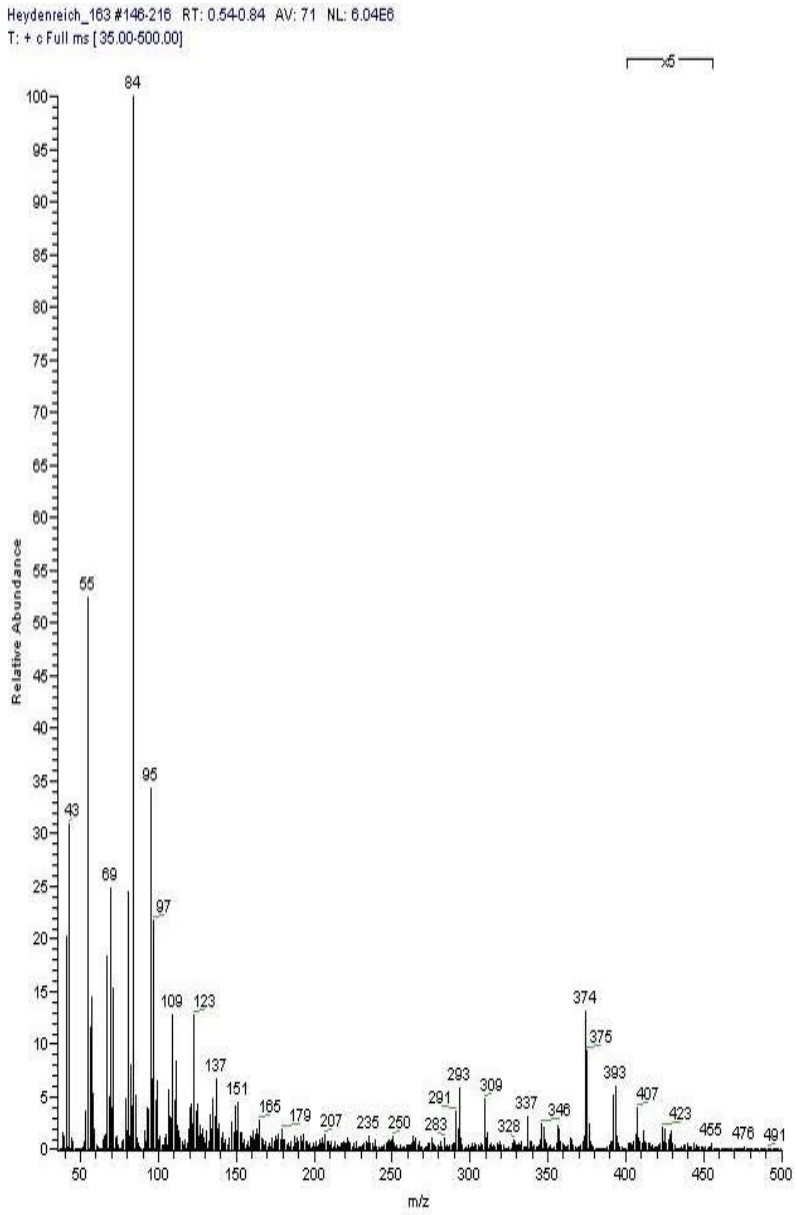

Appendix 1H: The UV graph of (4*R*,6*S*)-4,6-dihydroxy-6-((*Z*)-nonadec-14'-en-1-yl)cyclohex-2-en-1-one (**186**)

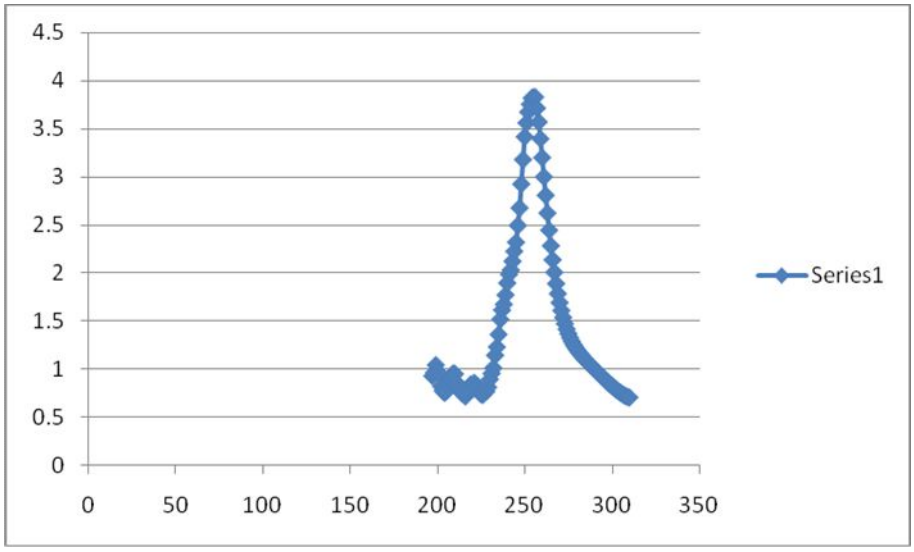

Appendix 2A: The ^{1}H NMR spectrum (800 MHz) of (2*S*,4*R*,5*R*)-2,4,5-trihydroxy-2-((*Z*)-nonadec-14'-en-1-yl)cyclohexanone (**187**) in Acetone-d_6.

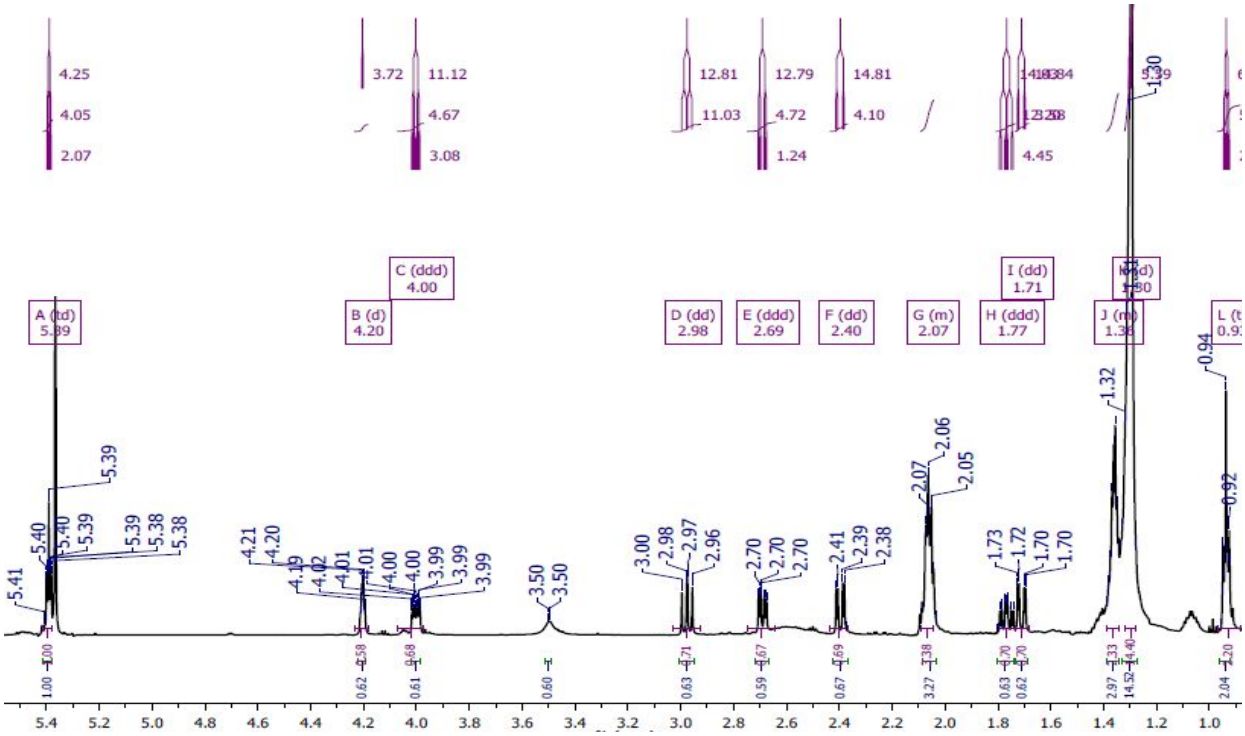

Appendix 2B: The ^{13}C NMR spectrum (200MHz) of (2*S*,4*R*,5*R*)-2,4,5-trihydroxy-2-((*Z*)-nonadec-14'-en-1-yl)cyclohexanone (**275**) in Acetone-d_6.

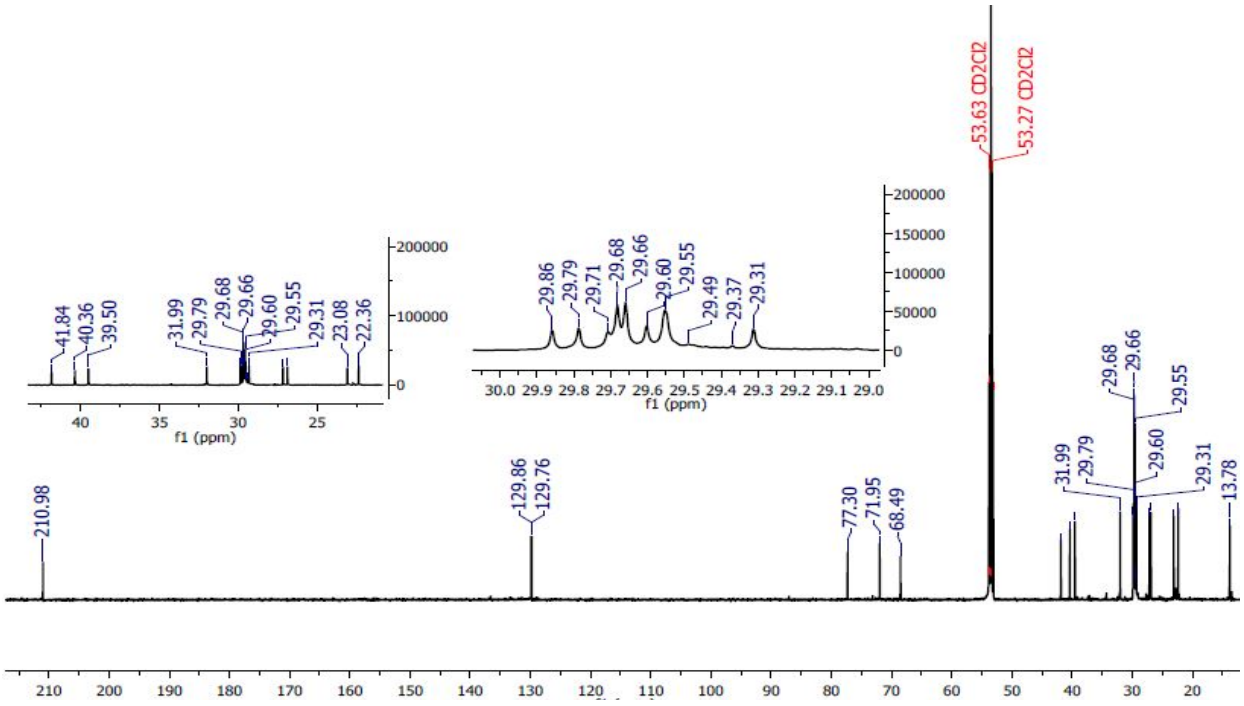

Appendix 2C: The H-H COSY spectrum of (2*S*,4*R*,5*R*)-2,4,5-trihydroxy-2-((*Z*)-nonadec-14'-en-1-yl)cyclohexanone (**187**) in Acetone-d_6

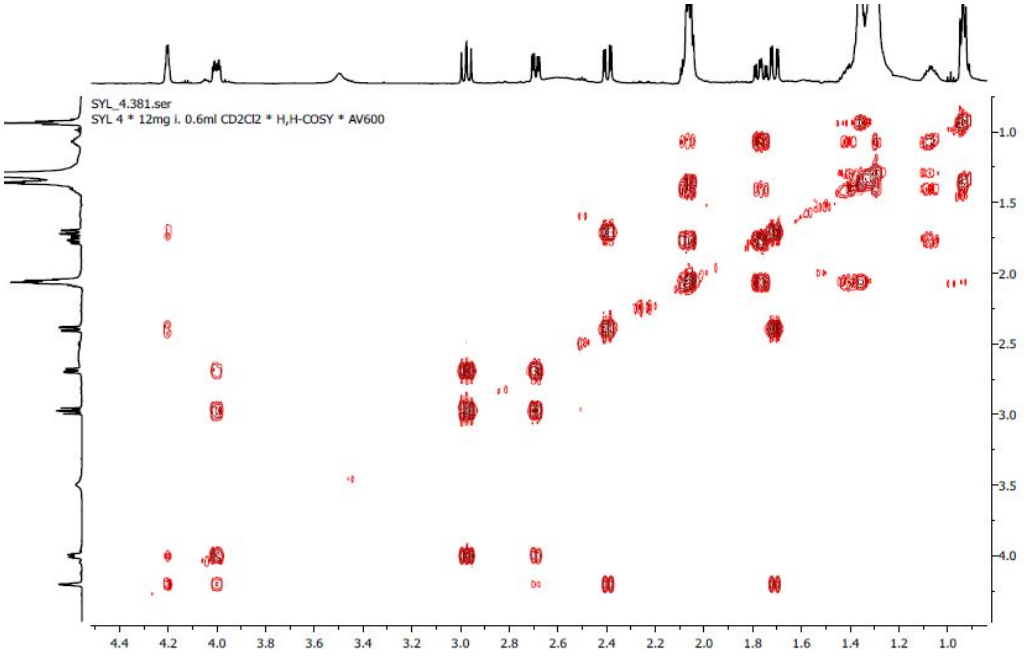

Appendix 2D: The HSQC spectrum of (2*S*,4*R*,5*R*)-2,4,5-trihydroxy-2-((*Z*)-nonadec-14'-en-1-yl)cyclohexanone (**187**) in Acetone-d_6

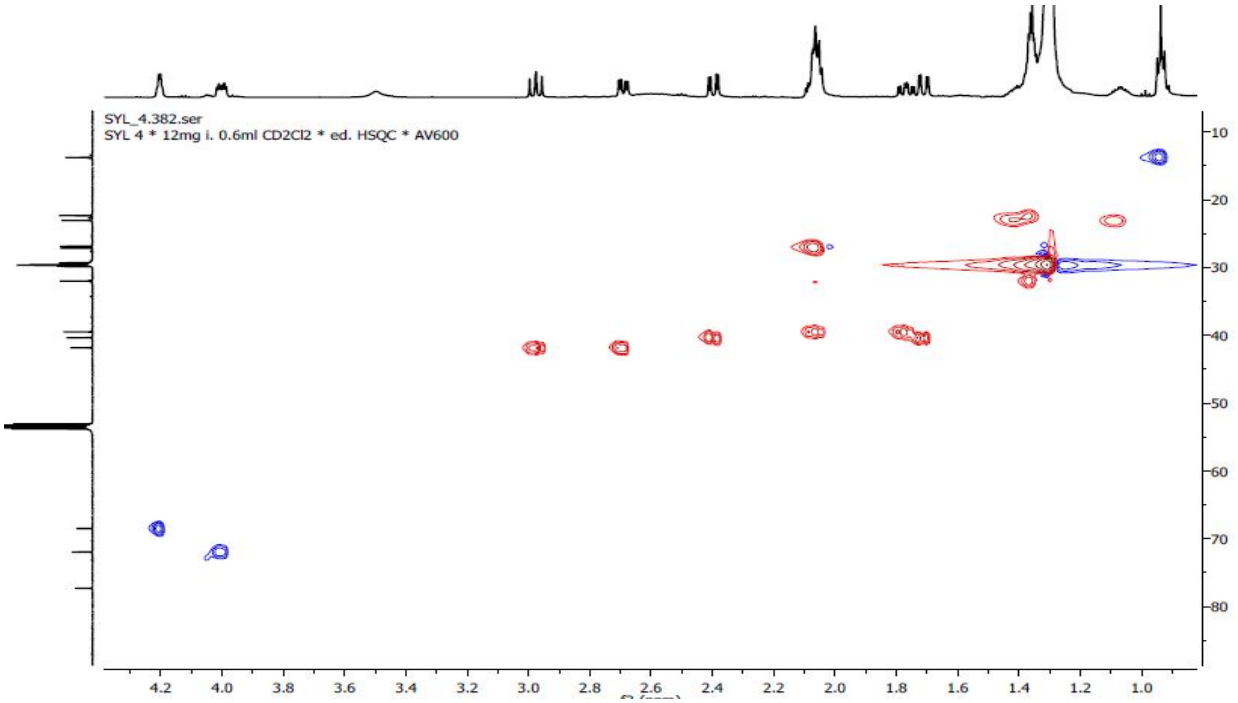

Appendix 2E: The HMBC spectrum of (2*S*,4*R*,5*R*)-2,4,5-trihydroxy-2-((*Z*)-nonadec-14'-en-1-yl)cyclohexanone (**187**) in Acetone-d_6.

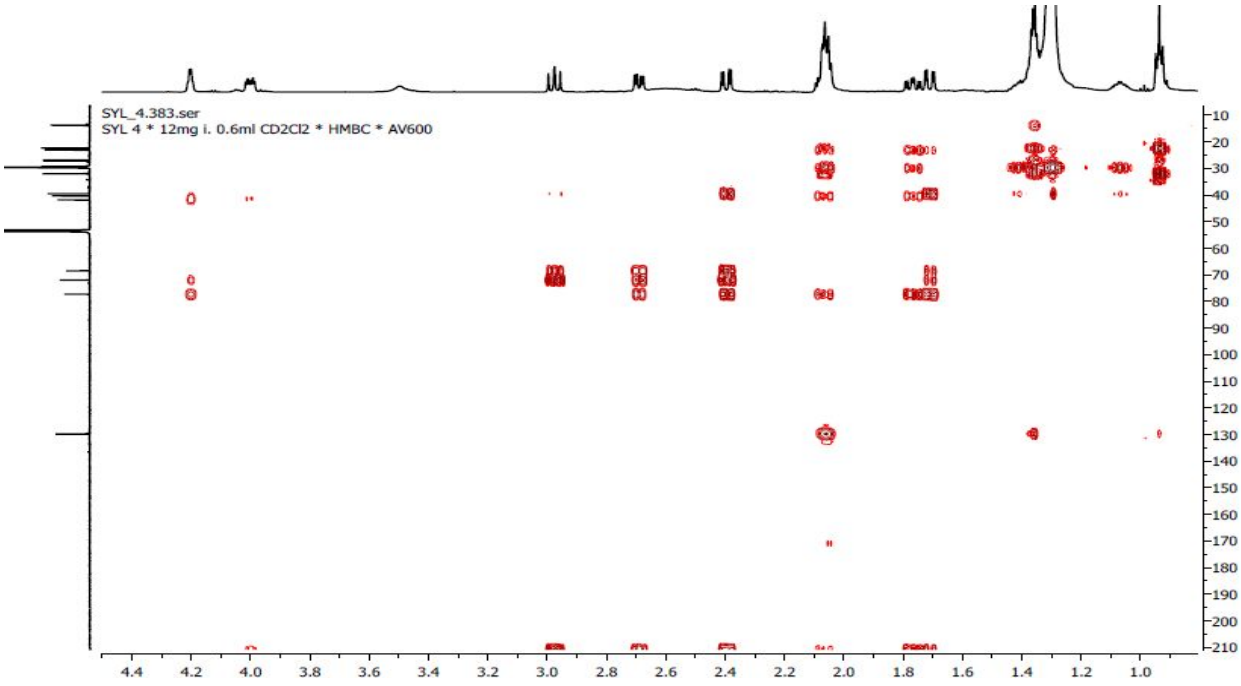

Appendix 2F: The HRMS spectrum of (2*S*,4*R*,5*R*)-2,4,5-trihydroxy-2-((*Z*)-nonadec-14'-en-1-yl)cyclohexanone (**187**)

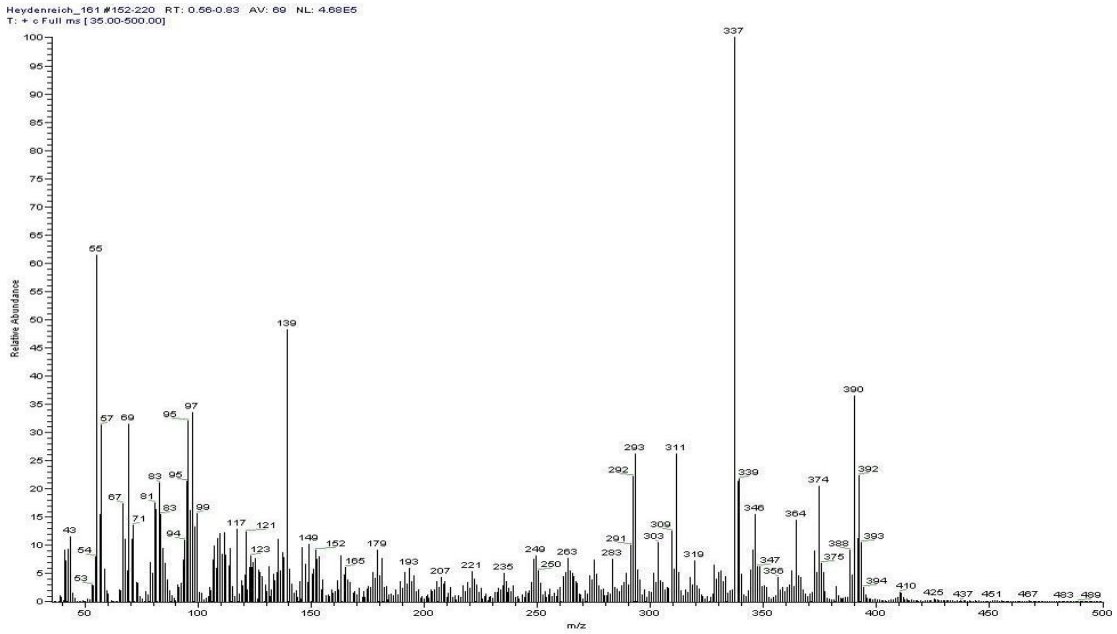

Appendix 2G: The UV graph of (2*S*,4*R*,5*R*)-2,4,5-trihydroxy-2-((*Z*)-nonadec-14'-en-1-yl)cyclohexanone (**187**)

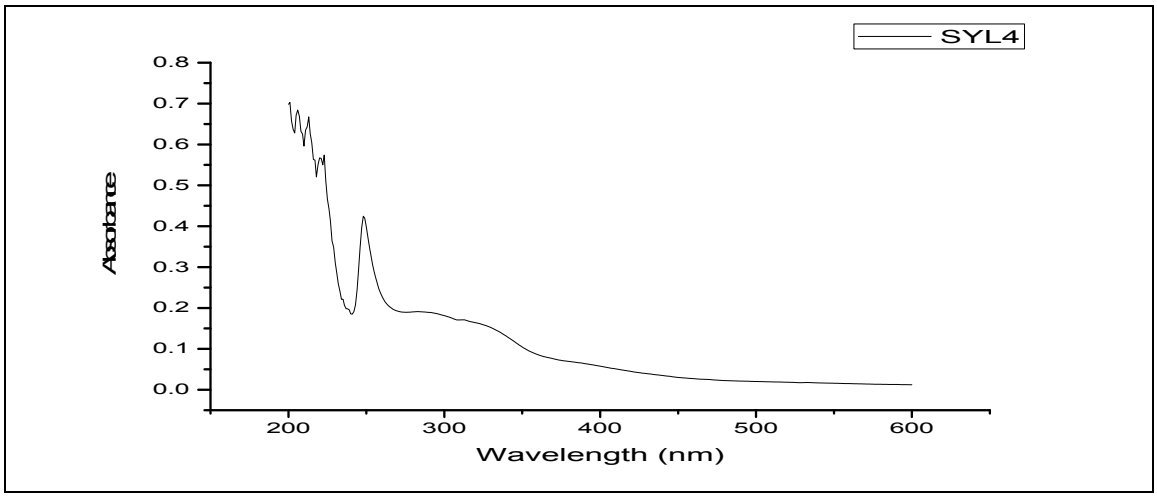

Appendix 3A: The ^{1}H NMR spectrum (600 MHz) of Taraxerol (**188**) in CD_2Cl_2

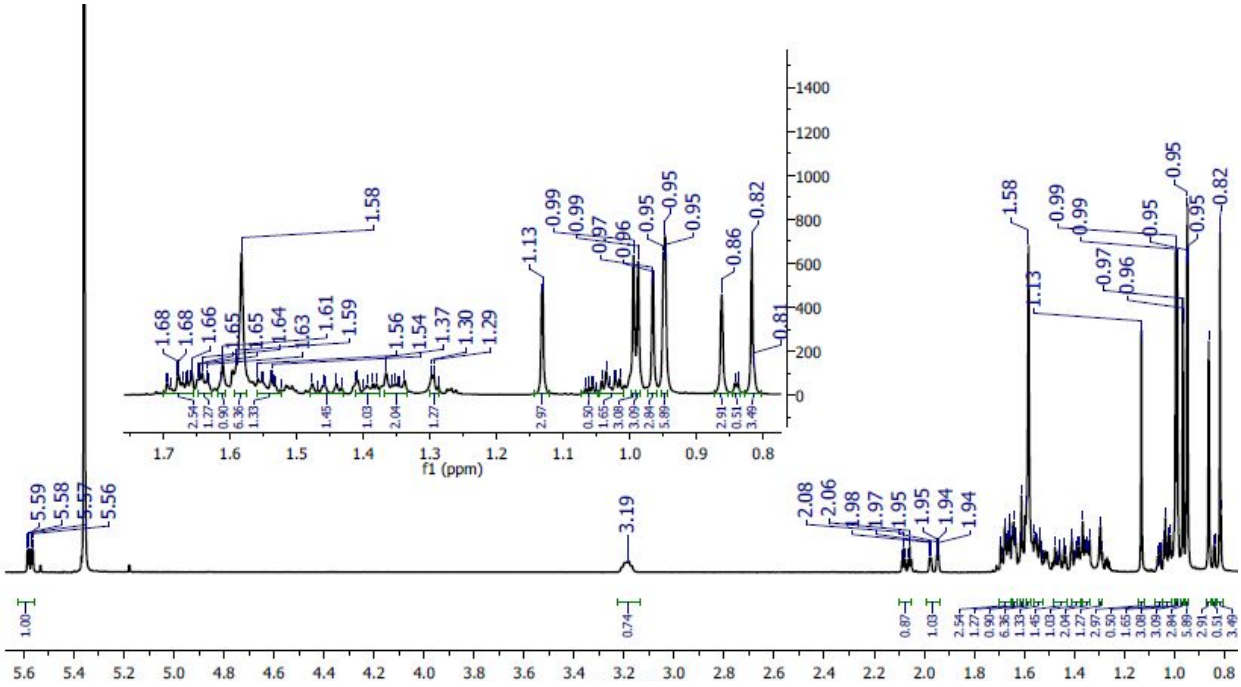

Appendix 3B: The ^{13}C NMR spectrum (150MHz) of Traxerol (**188**) in CD_2Cl_2

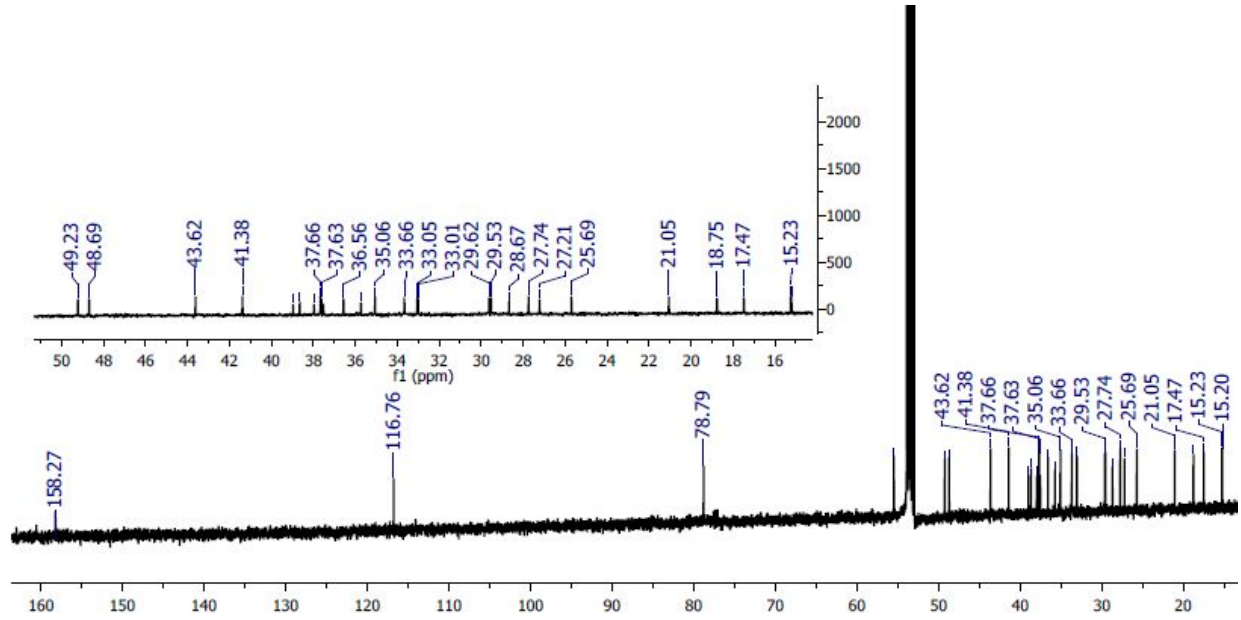

Appendix 4A: The ^{1}H NMR spectrum (600 MHz) of taraxerone (**189**) in CD_2Cl_2

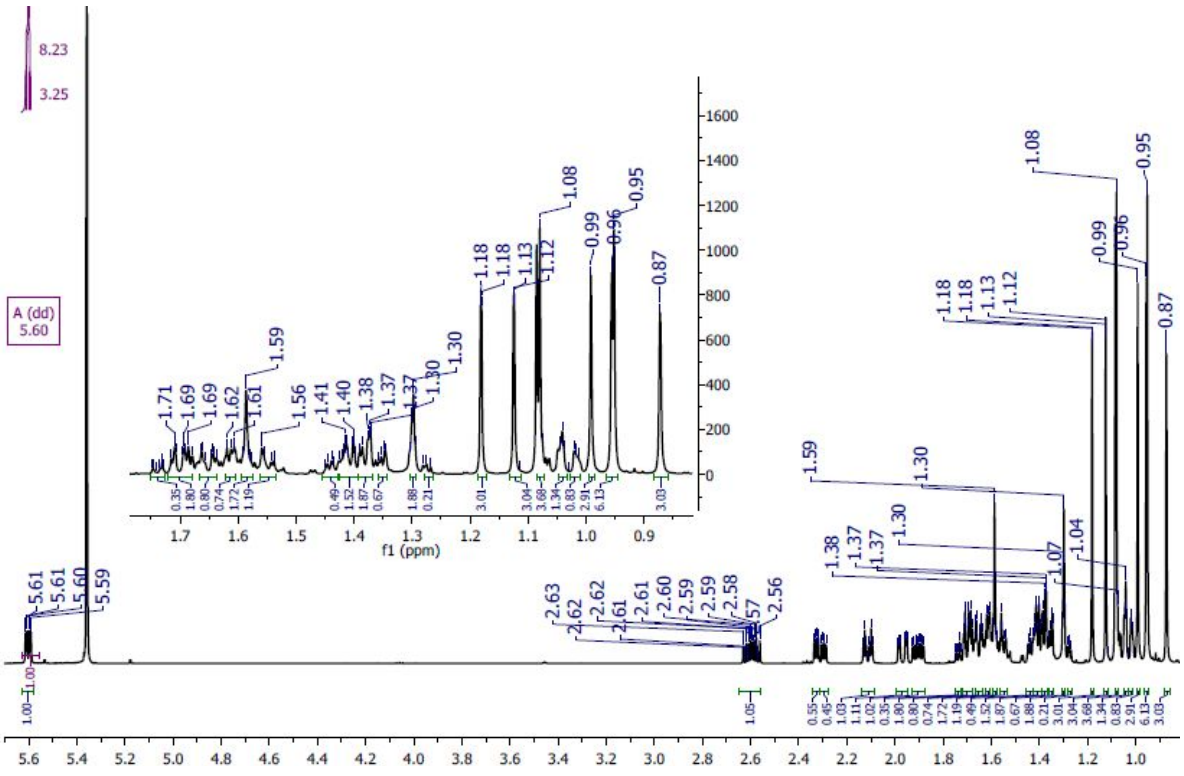

Appendix 4B: The ^{13}C NMR spectrum (150MHz) of taraxerone (**189**) in CD_2Cl_2

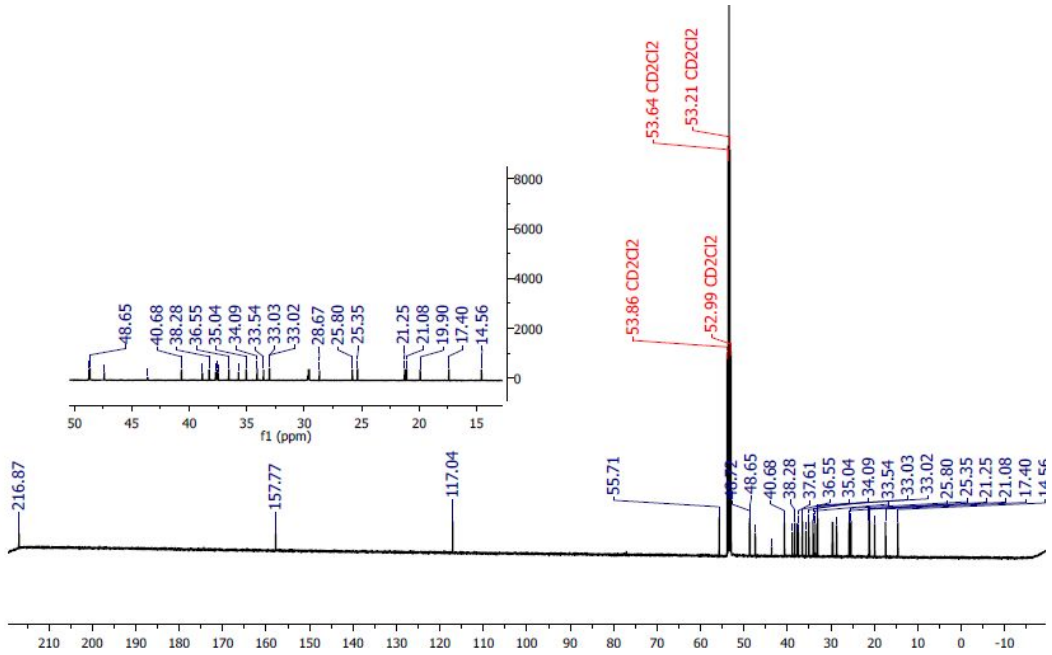

Appendix 5A: The ^{1}H NMR spectrum (600 MHz) of *β*-sitosterol (**190**) in CD_2Cl_2

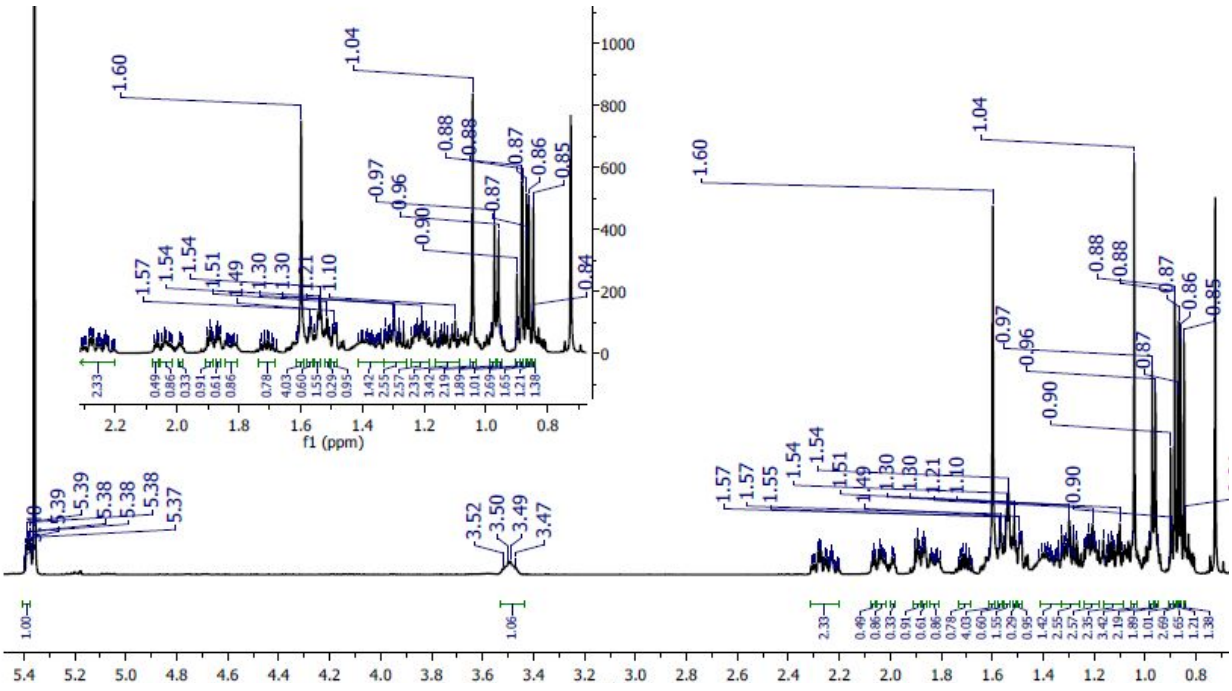

Appendix 5B: The ^{13}C NMR spectrum (150MHz) of β-sitosterol (**190**) in CD_2Cl_2

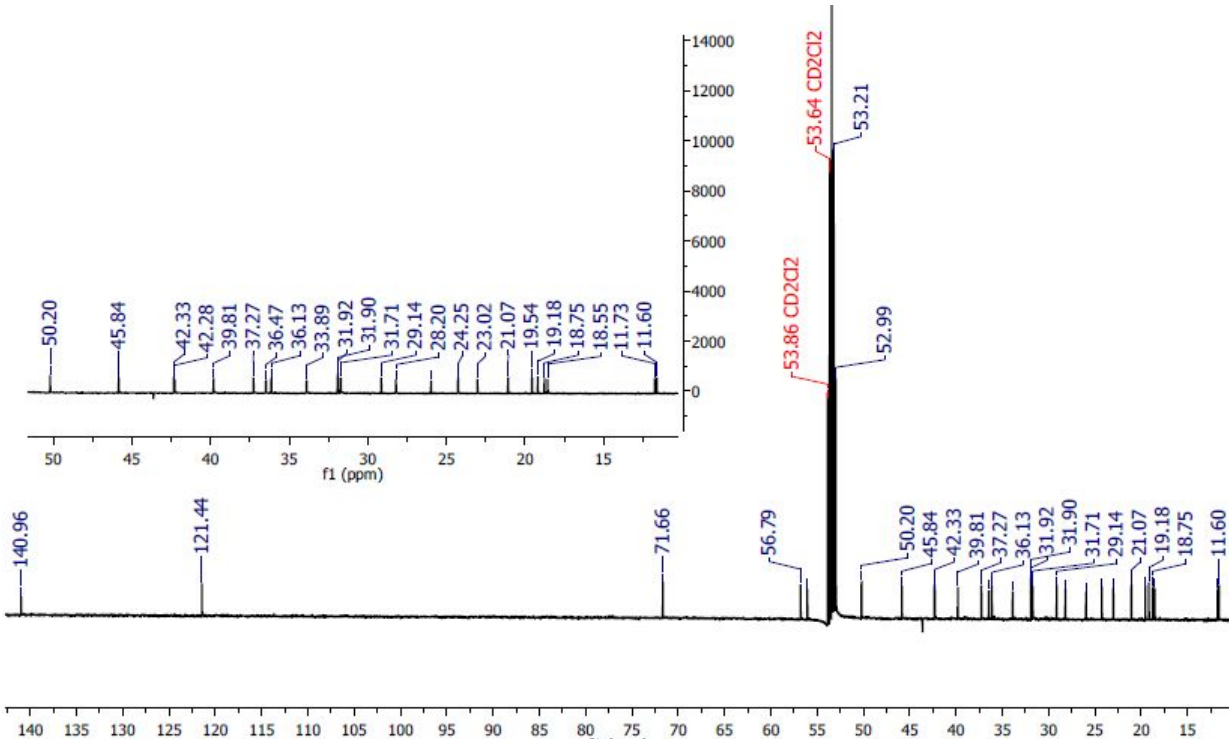

Appendix 6A: The ^{1}H NMR spectrum (800 MHz) of epicatechin gallate (**191**) in DMSO

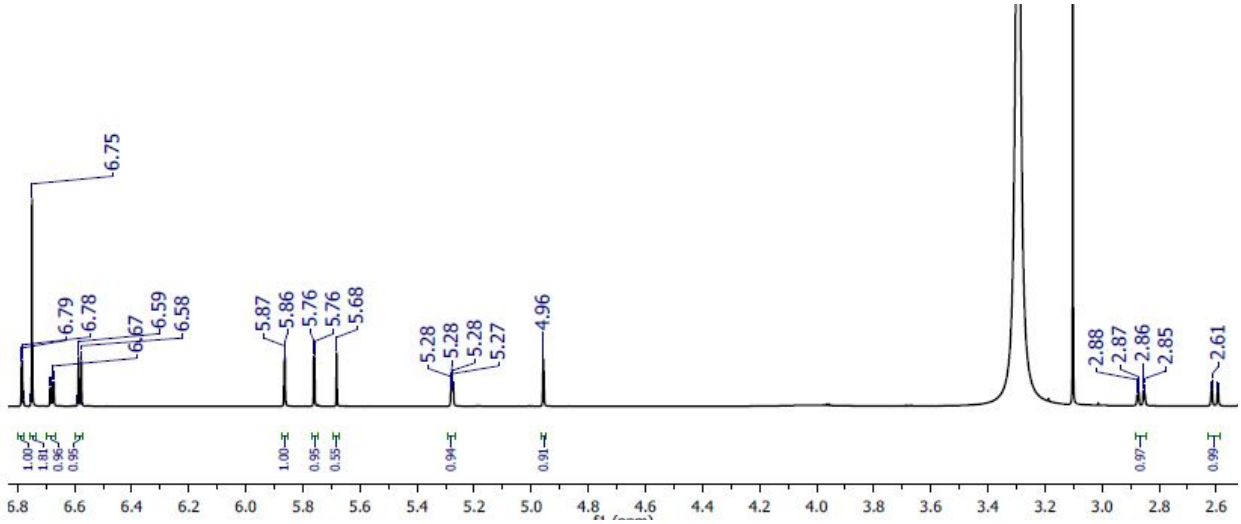

Appendix 6B: The ^{13}C NMR spectrum (200MHz) of epicatechin gallate (**191**) in DMSO

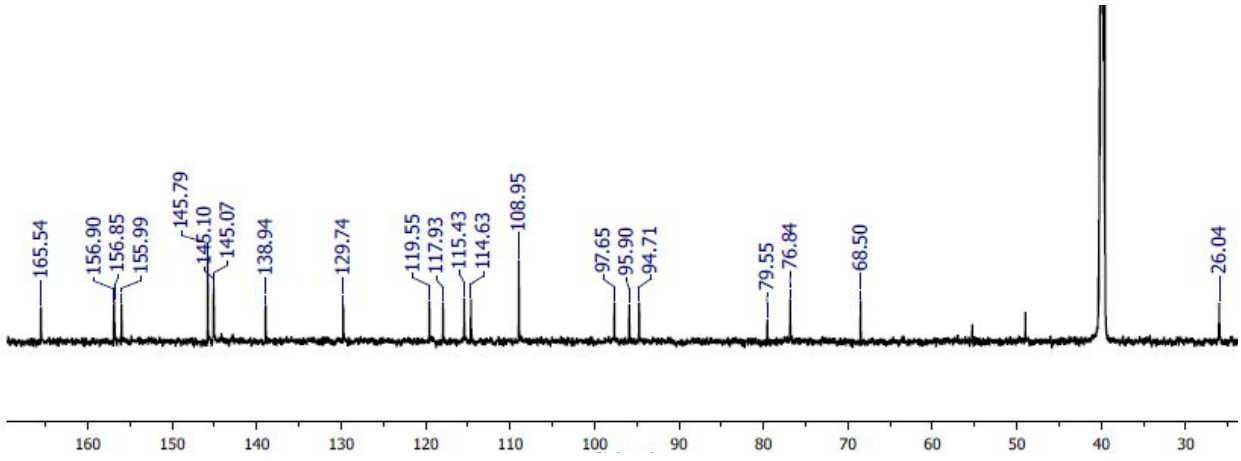

Appendix 7A: The ^{1}H NMR spectrum (800 MHz) of 3",5"-dimethoxy-epicatechin gallate (**192**) in DMSO

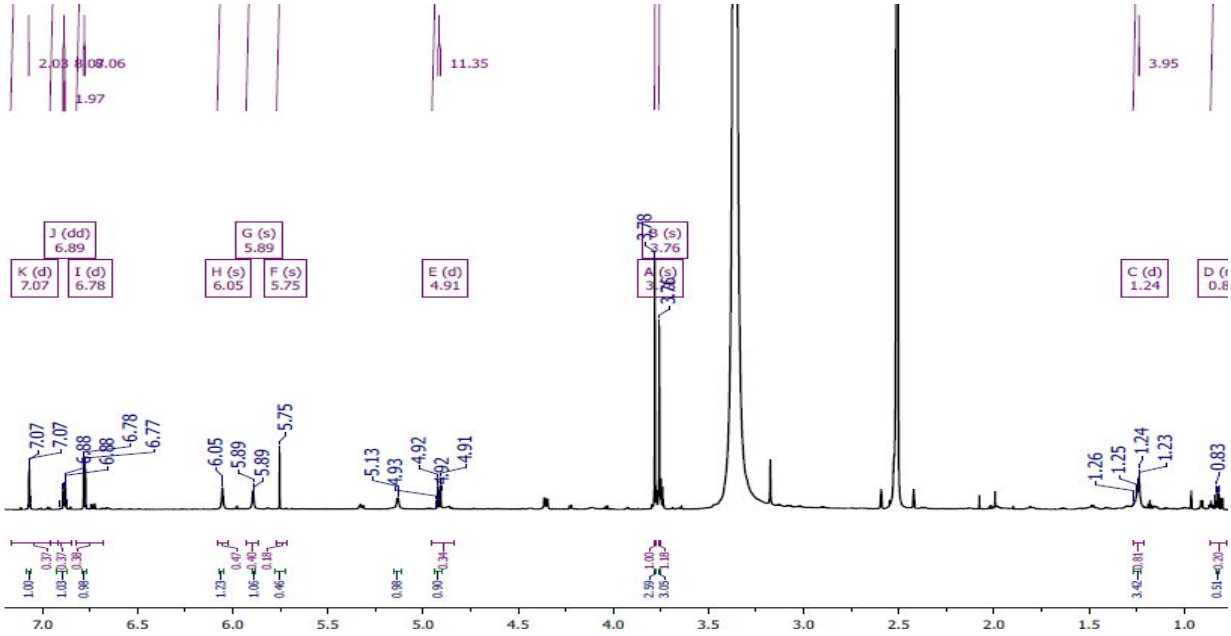

Appendix 7B: The ^{13}C NMR spectrum (200MHz) of 3",5"-dimethoxy-epicatechin gallate (**192**) in DMSO

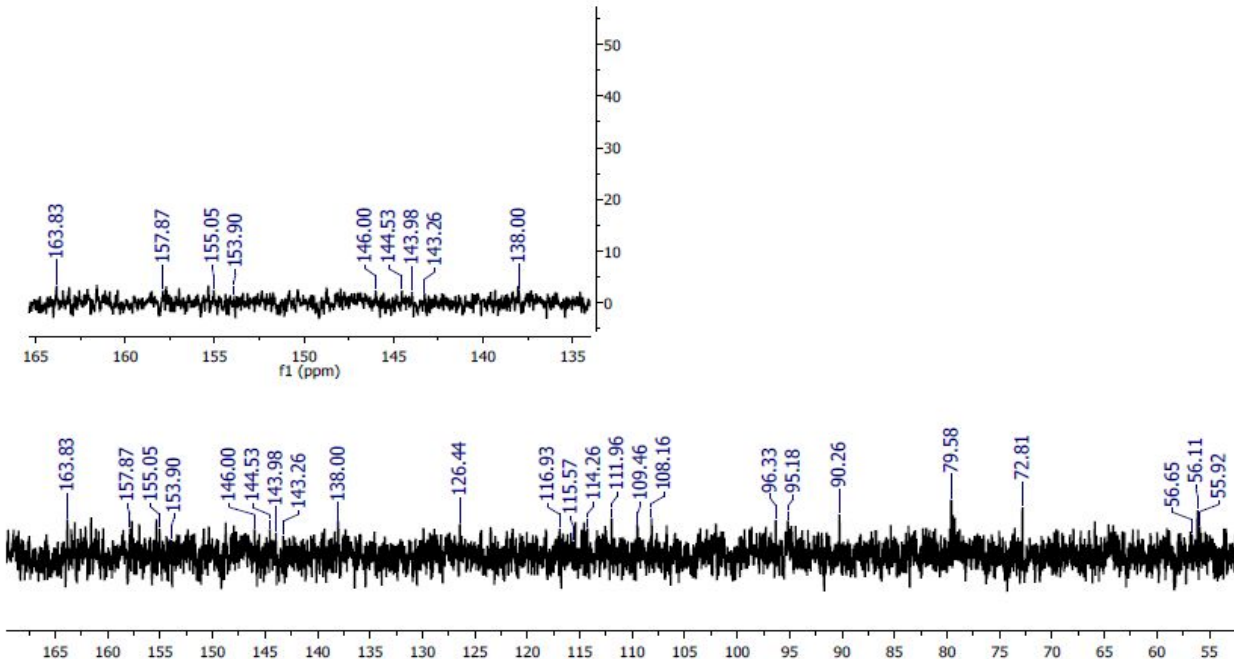

Appendix 8A: The ^{1}H NMR spectrum (800 MHz) of lupeol (**193**) in $CDCl_3$

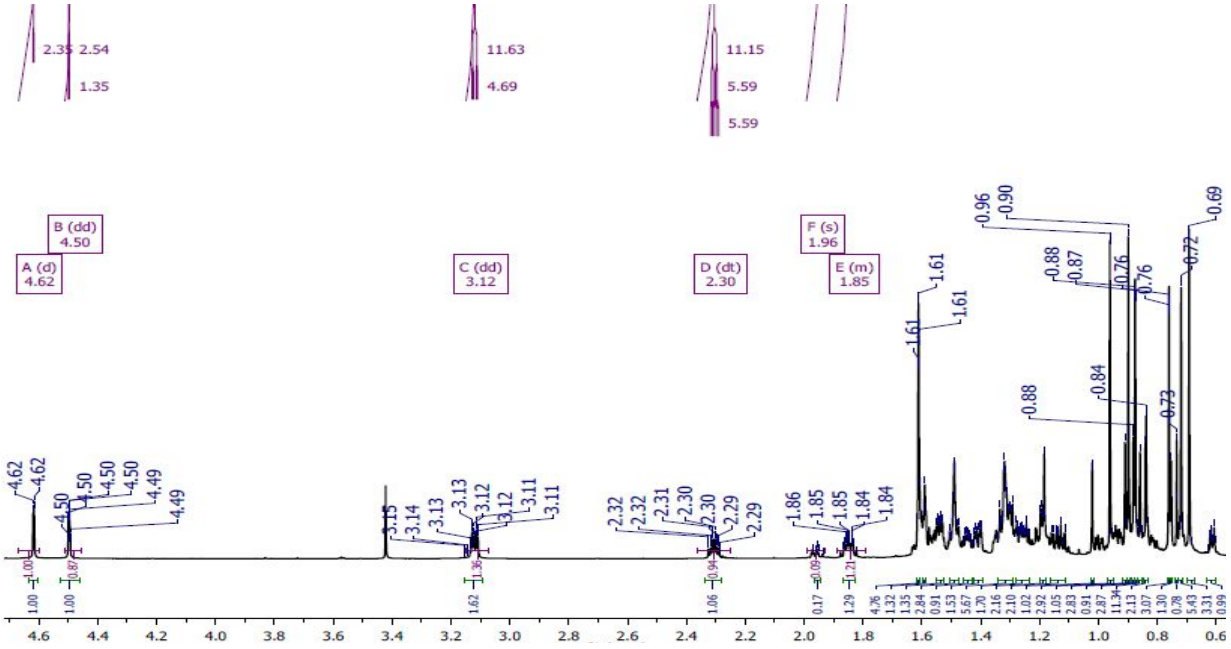

Appendix 8B: The ^{13}C NMR spectrum (200MHz) of lupeol (**193**) in $CDCl_3$

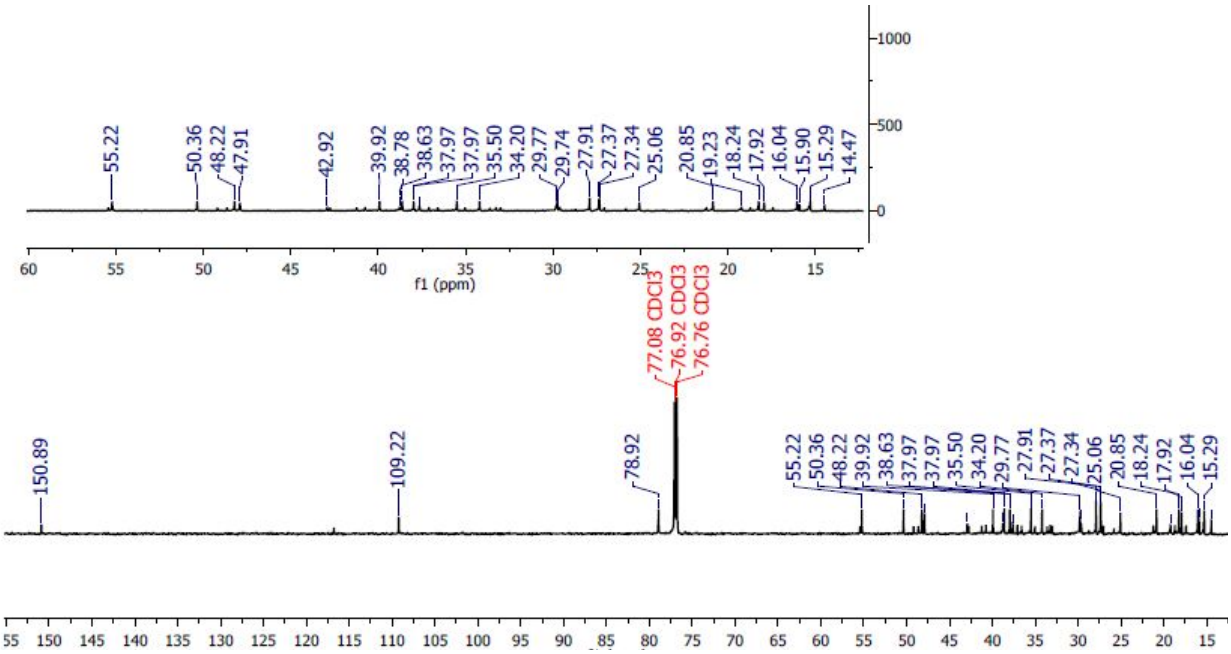

Appendix 9A: The ^{1}H NMR spectrum (800 MHz) of daucosterol (**194**) in DMSO

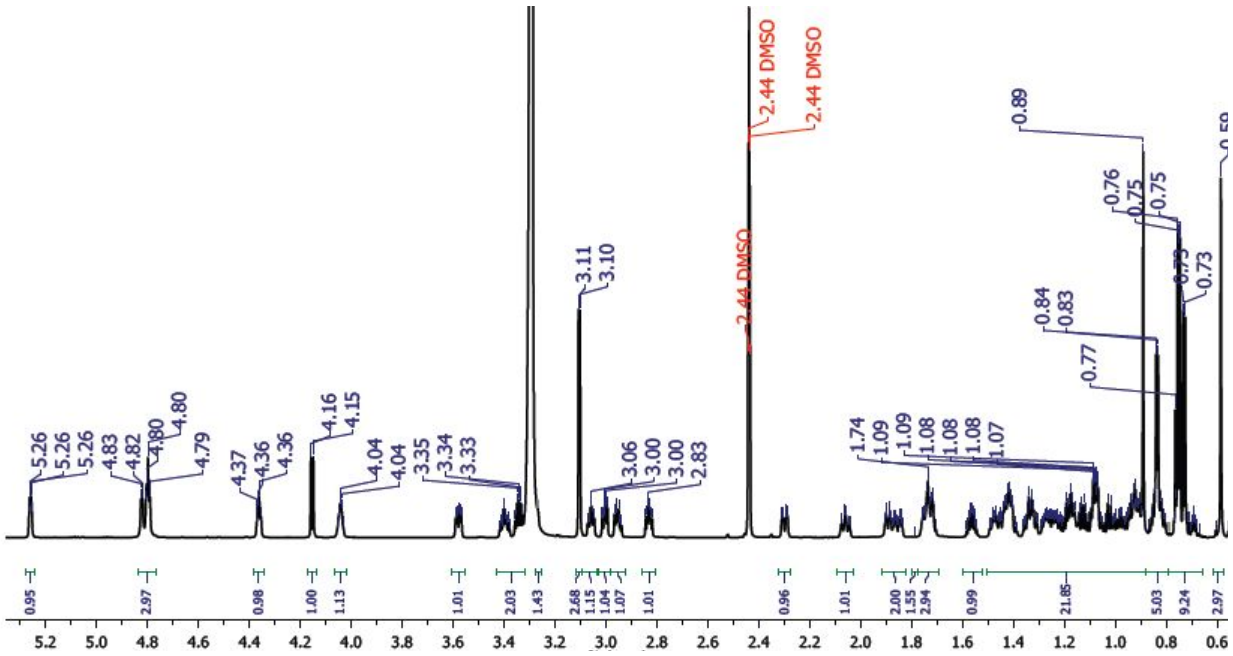

Appendix 9B: The ^{13}C NMR spectrum (150MHz) of daucosterol (**194**) in DMSO

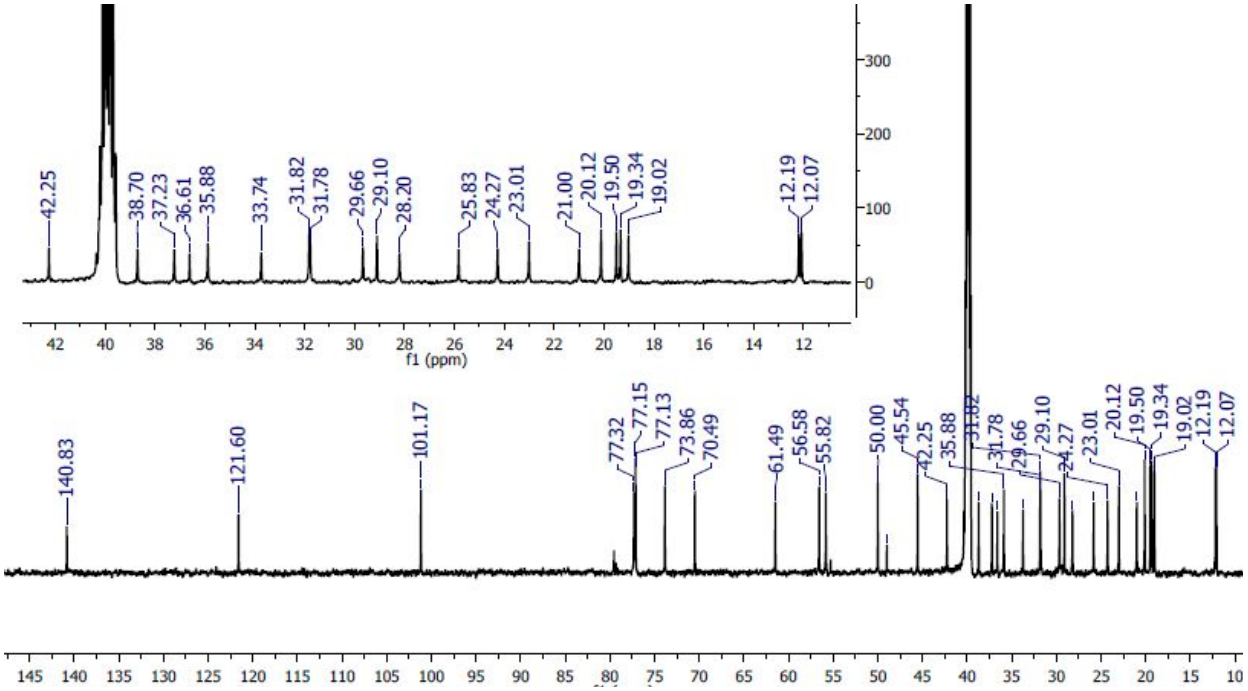

Appendix 10A: The ^{1}H NMR spectrum (600 MHz) of 3-((*E*)-nonadec-16'-enyl)phenol (**195**) in CD_2Cl_2

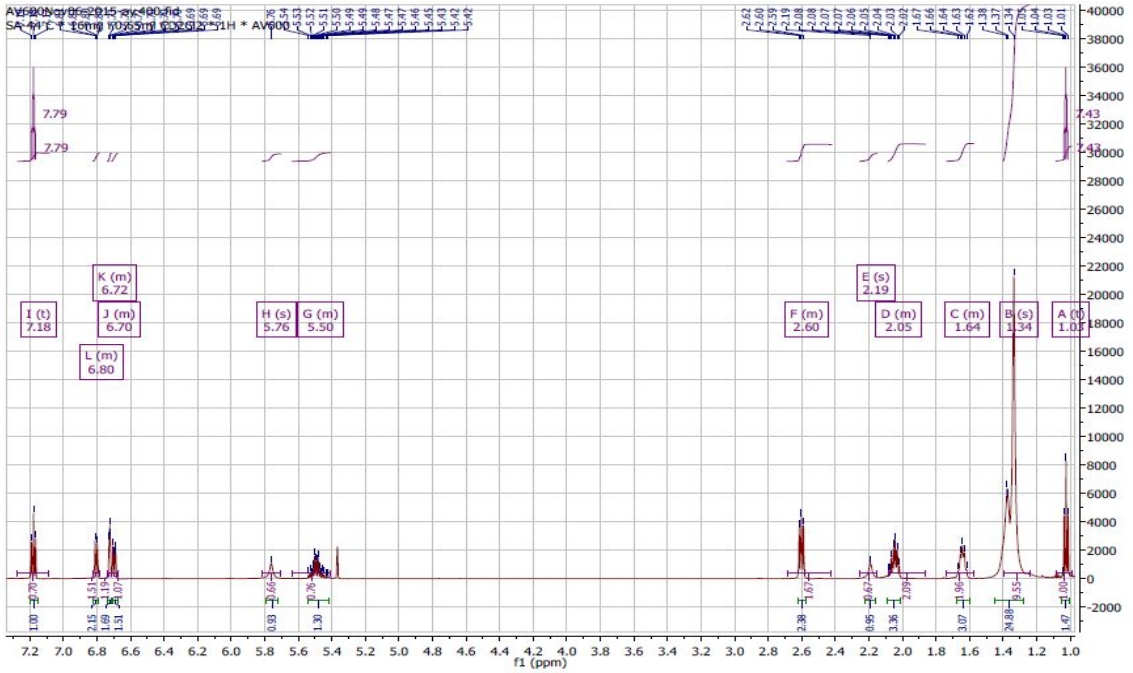

Appendix 10B: The ^{13}C NMR spectrum (150MHz) of 3-((*E*)-nonadec-16'-enyl)phenol (**195**) in CD_2Cl_2

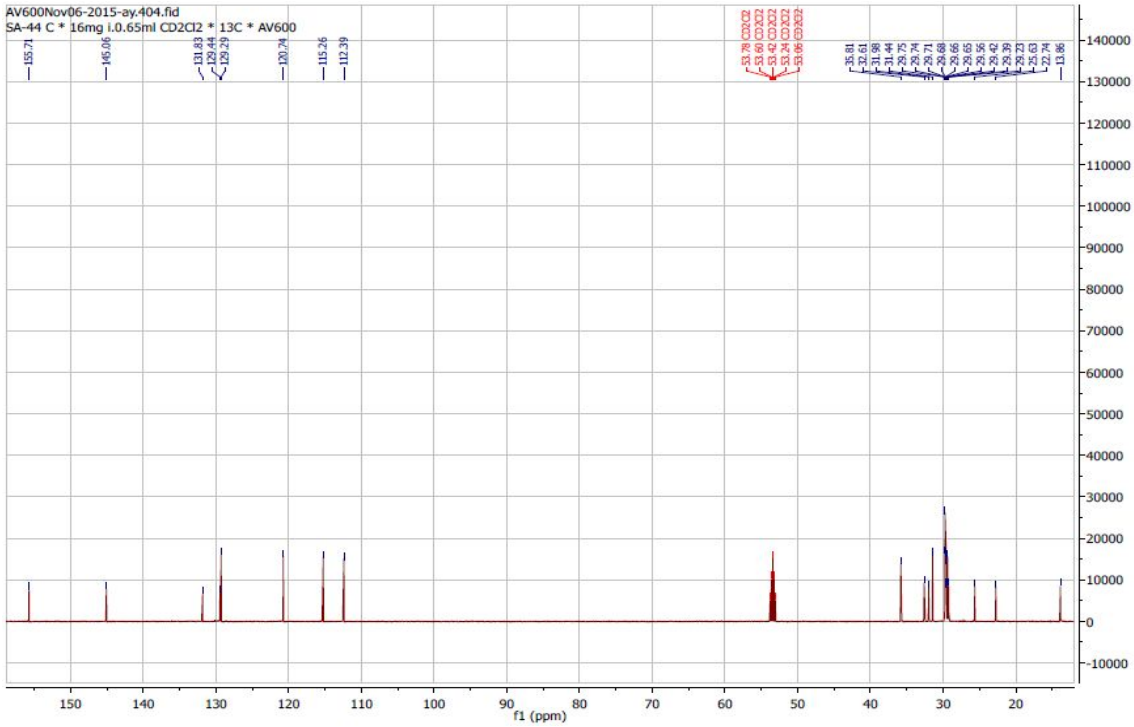

Appendix 10C: The UV spectrum of 3-((*E*)-nonadec-16'-enyl)phenol (**195**)

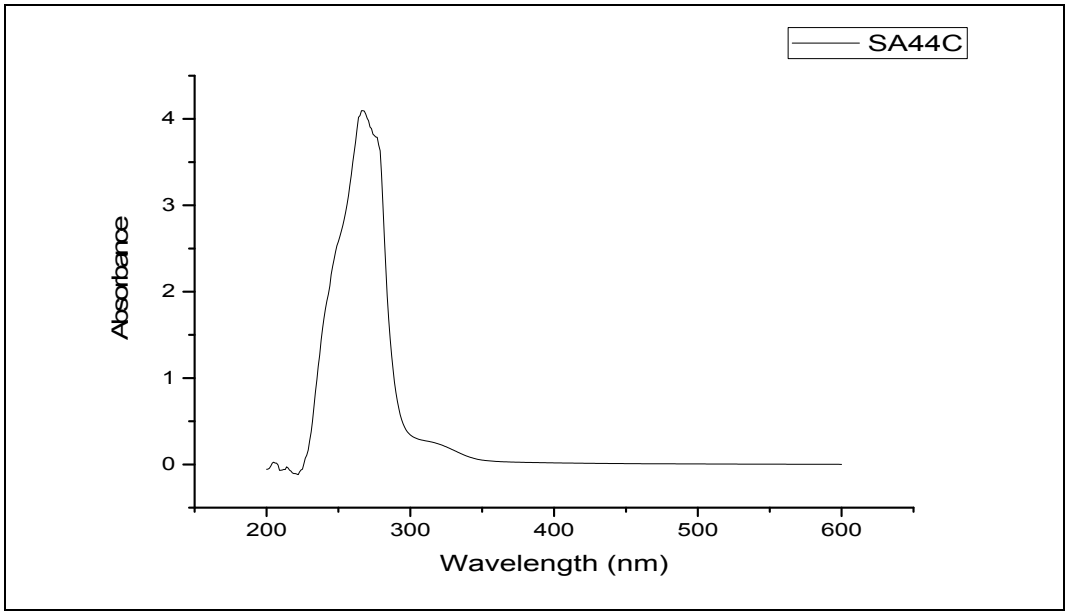

Appendix 11A: The ^{1}H NMR spectrum (600 MHz) of 1-((*E*)-heptadec-14'-enyl)cyclohex-4-en-1,3-diol (**196**) in CD_2Cl_2

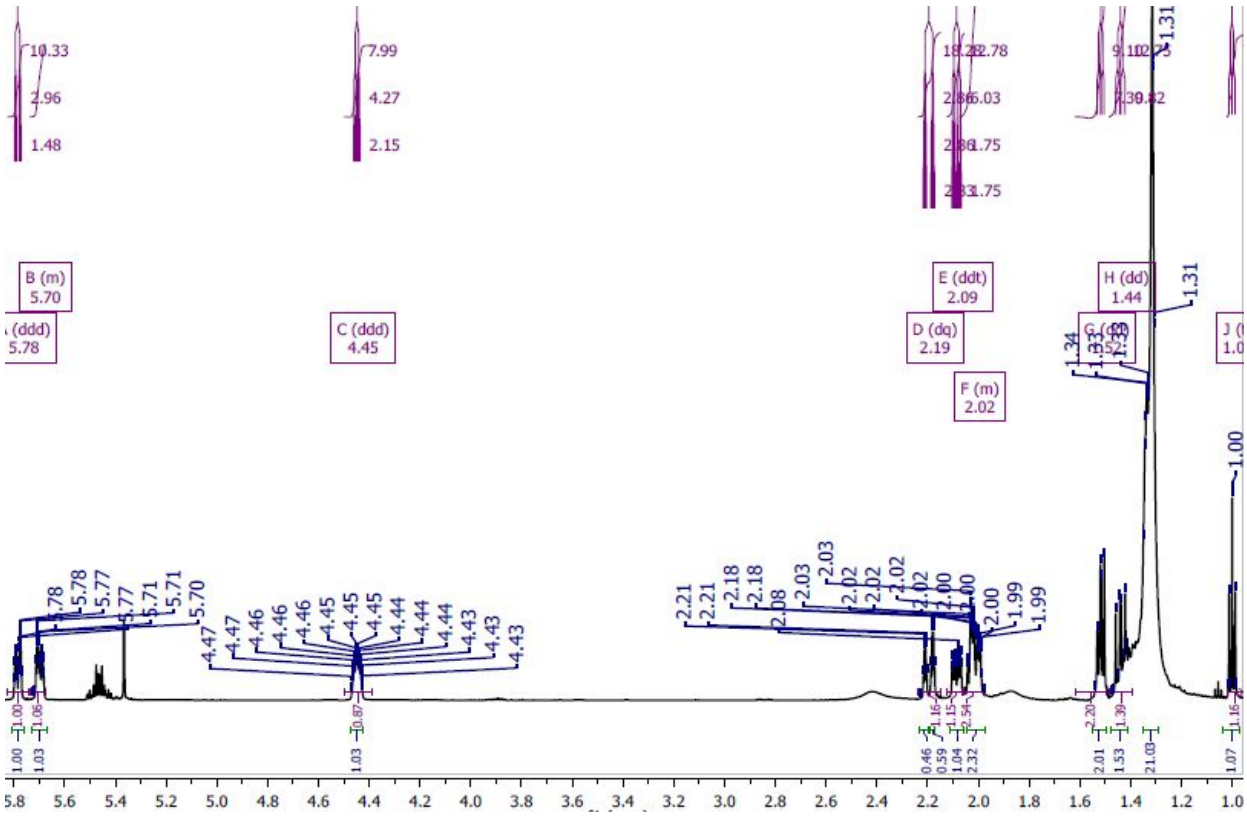

Appendix 11B: The ^{13}C NMR spectrum (150 MHz) of 1-((*E*)-heptadec-14'-enyl)cyclohex-4-en-1,3-diol (**196**) in CD_2Cl_2

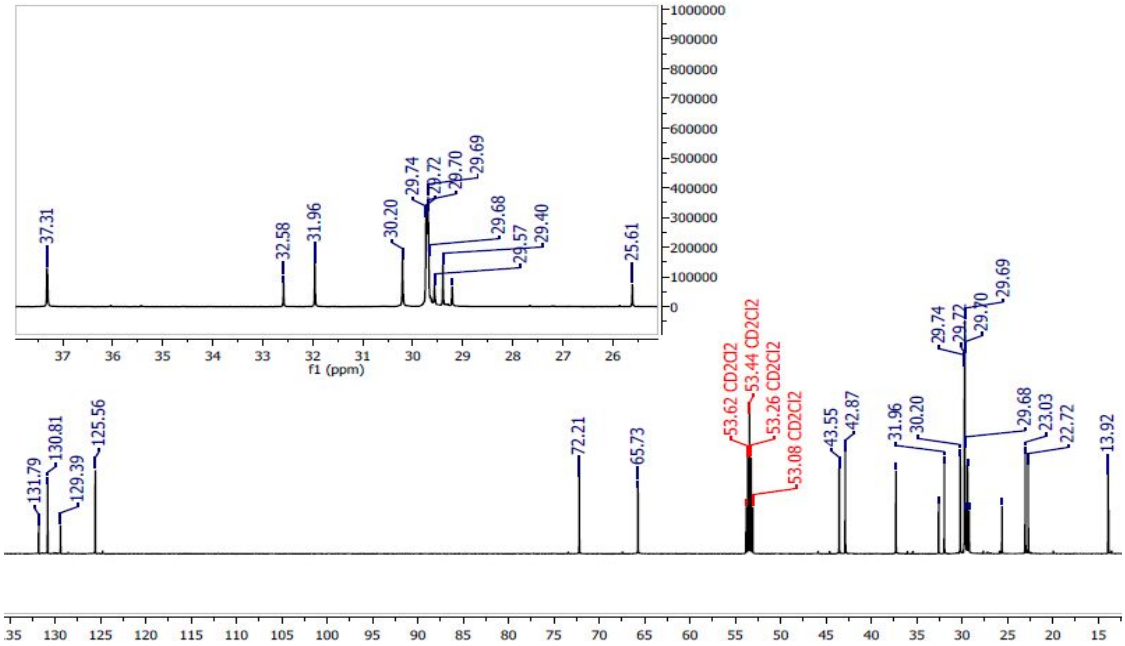

Appendix 12A: The ^{1}H NMR spectrum (600 MHz) of 1-[(E)-tridecadec-10'-enyl]cyclohex-4-en-1,3-diol (**197**) in Acetone-d_6

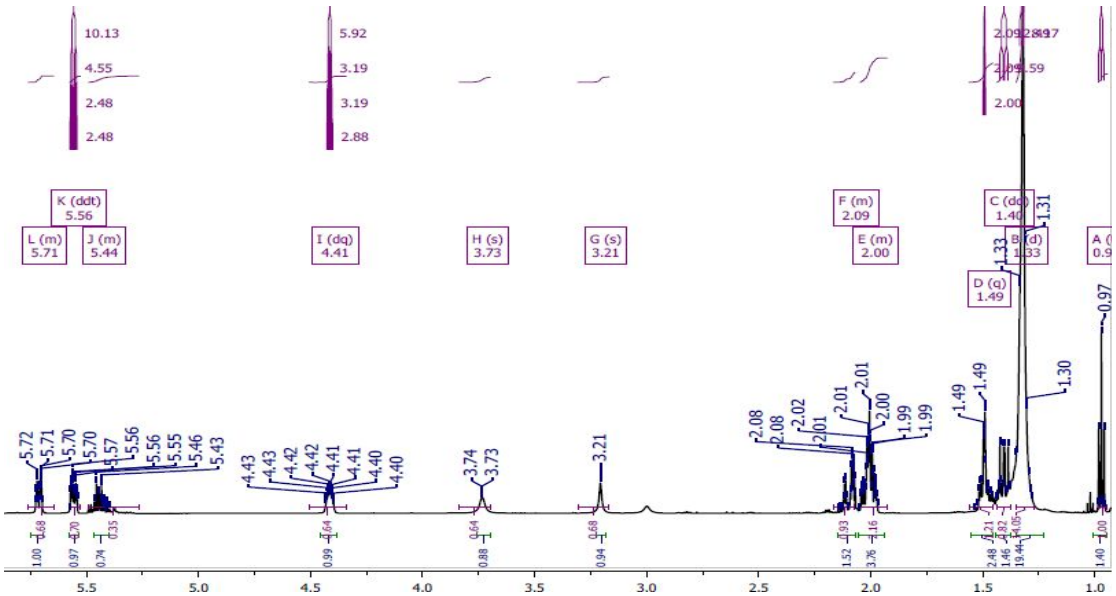

Appendix 12B: The ^{13}C NMR spectrum (150MHz) of 1-[(E)-tridecadec-10'-enyl]cyclohex-4-en-1,3-diol (**197**) in Acetone-d_6

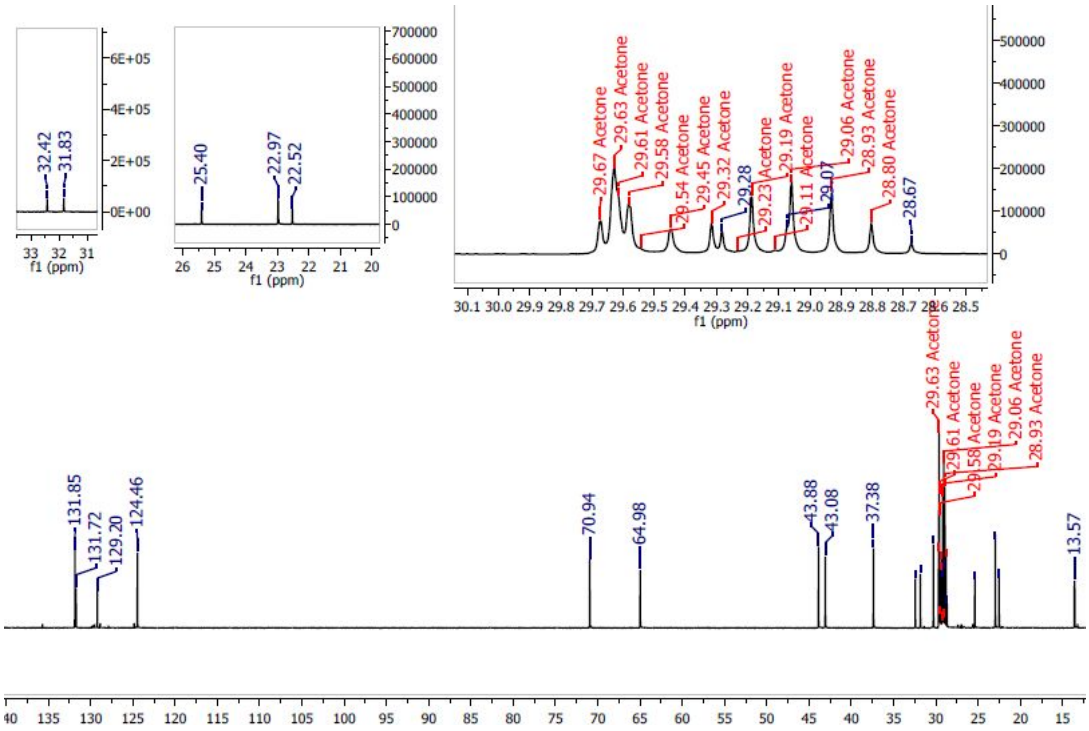

Appendix 12C: The UV graph of 1-[(E)-tridecadec-10'-enyl]cyclohex-4-en-1,3-diol (**197**)

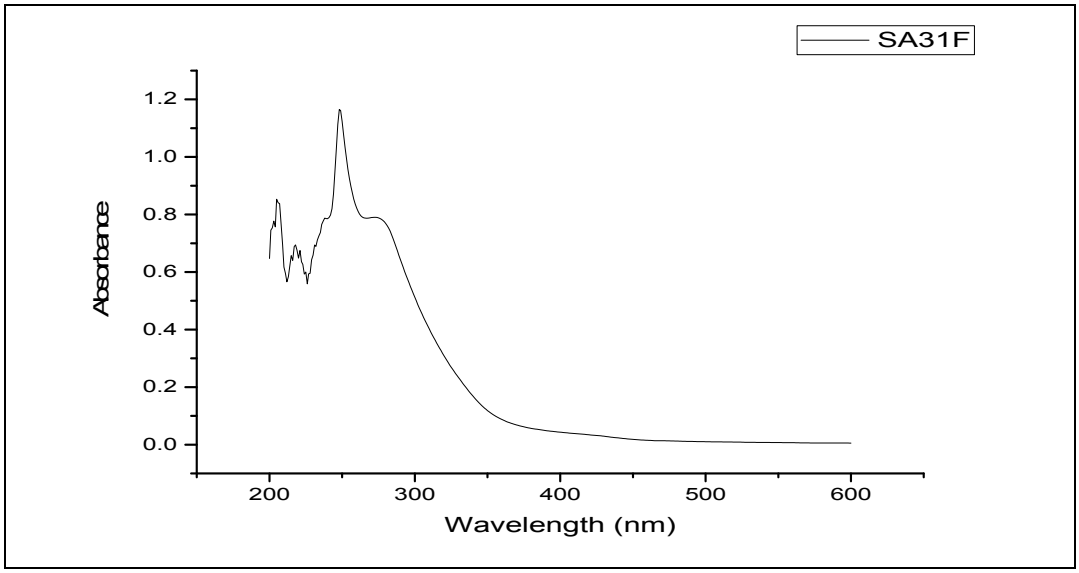

Appendix 13A: The ^{1}H NMR spectrum (600 MHz) of 1-((*E*)-pentadec-12'-enyl)cyclohex-4-ene-1,3-diol (**198**) in CD_2Cl_2

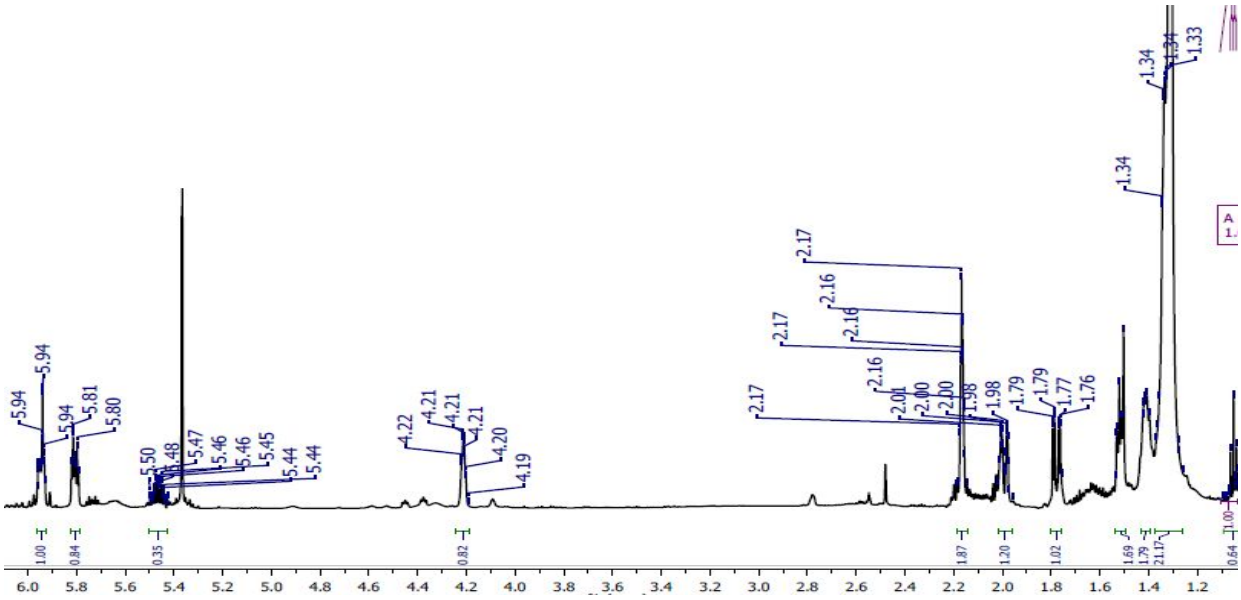

Appendix 13B: The ^{13}C NMR spectrum (150MHz) of 1-((*E*)-pentadec-12'-enyl)cyclohex-4-ene-1,3-diol (**198**) in CD_2Cl_2

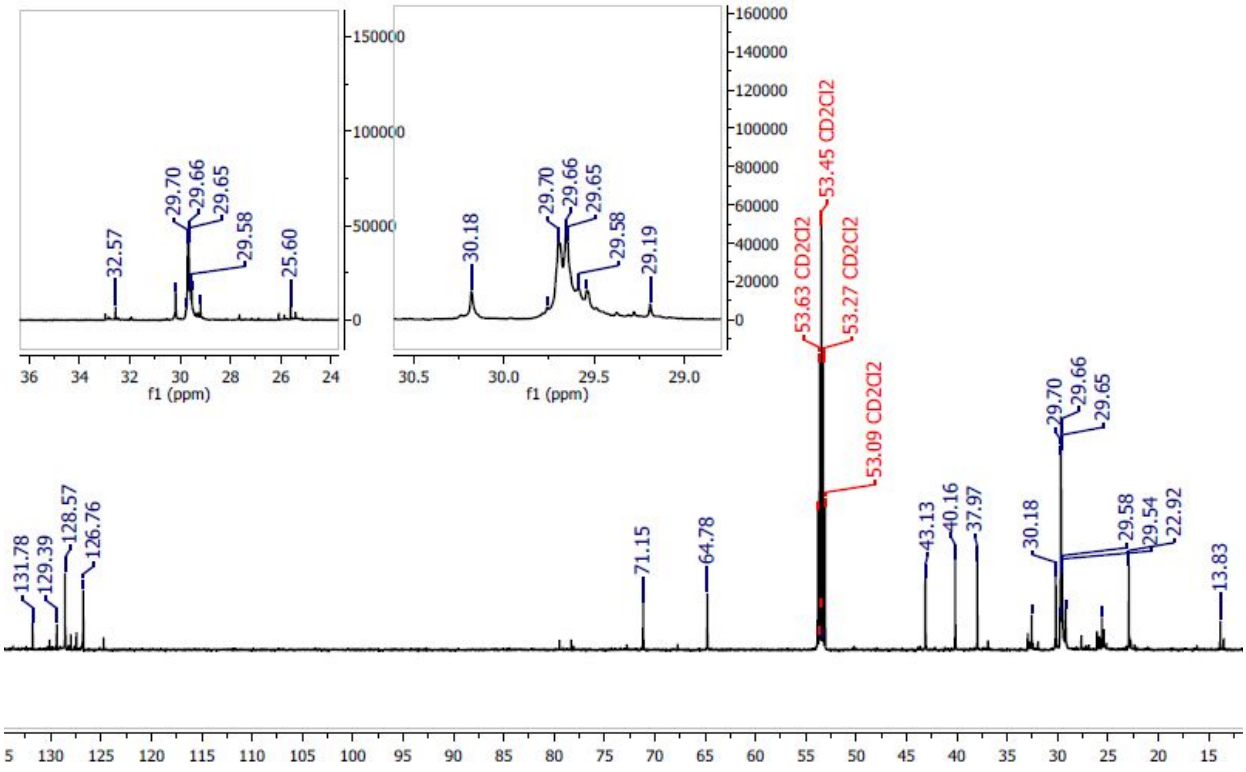

Appendix 13C: The UV graph of 1-((*E*)-pentadec-12'-enyl)cyclohex-4-ene-1,3-diol (**198**)

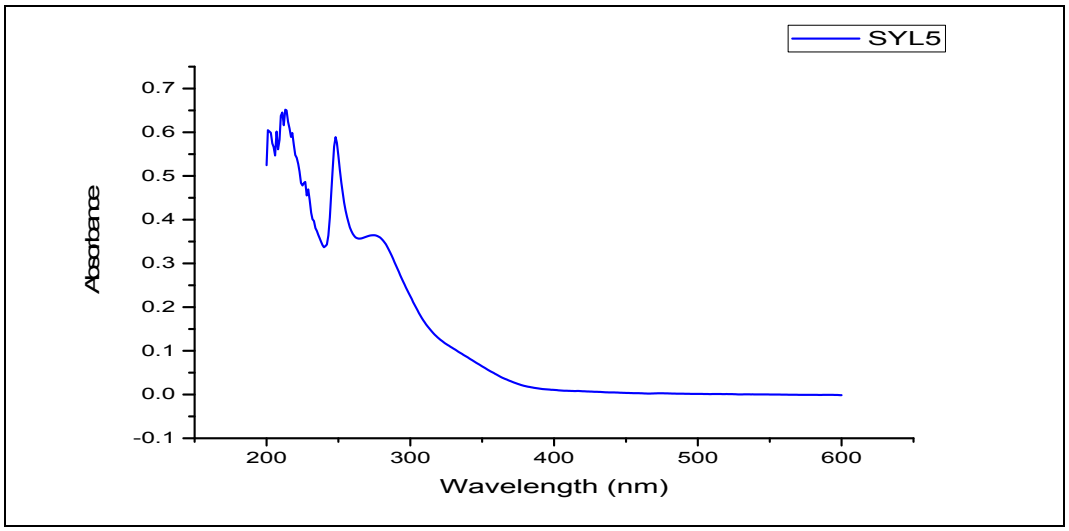

Appendix 14A: The ^{1}H NMR spectrum (600 MHz) of 1-[(11'*E, 14'E*)-nonadecadienyl]cyclohex-4-en-1,3-diol (**199**) in CD_2Cl_2

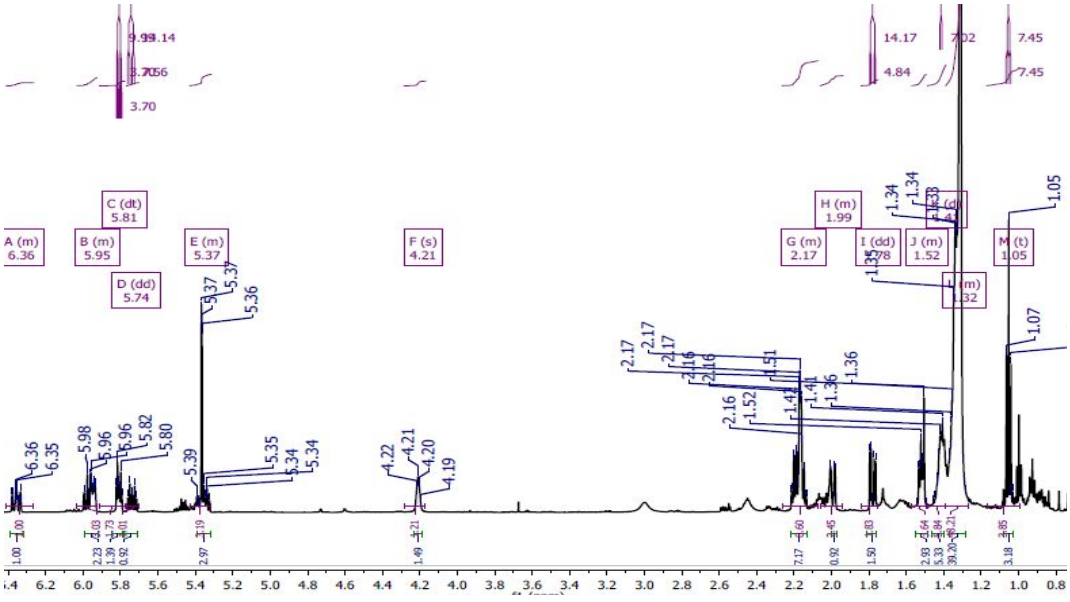

Appendix 14B: The ^{13}C NMR spectrum (150MHz) of 1-[(11'*E, 14'E*)-nonadecadienyl]cyclohex-4-en-1,3-diol (**199**) in CD_2Cl_2

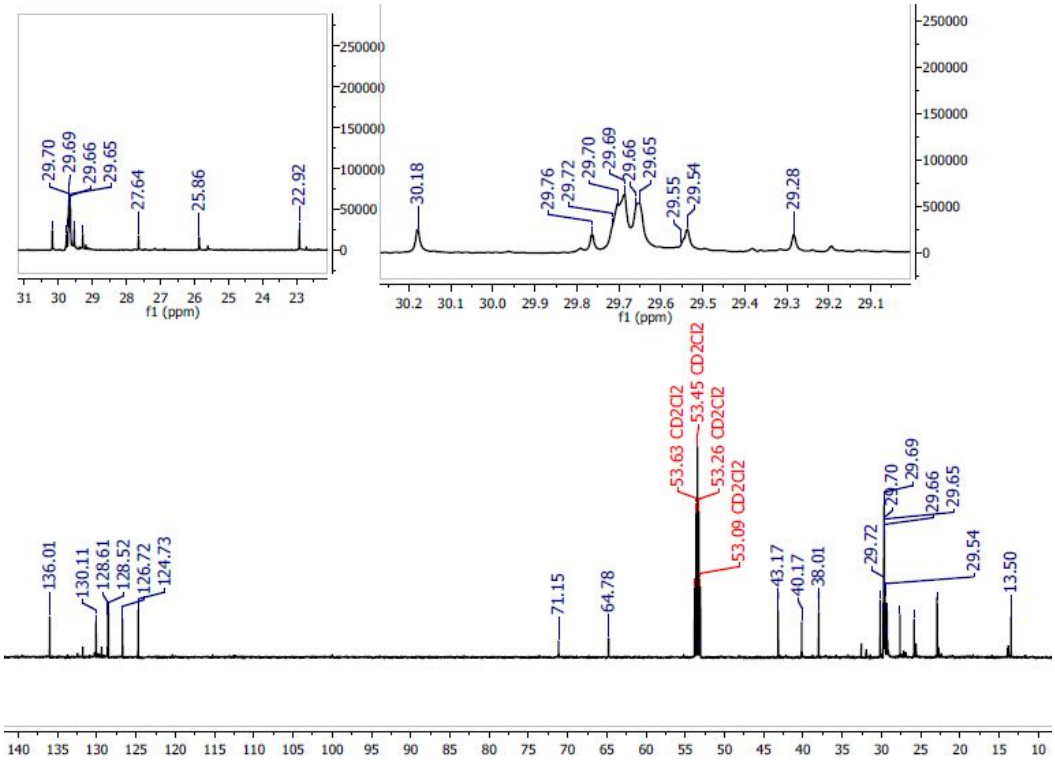

Appendix 14C: The UV graph of 1-[(11'*E, 14'E*)-nonadecadienyl]cyclohex-4-en-1,3-diol (**199**)

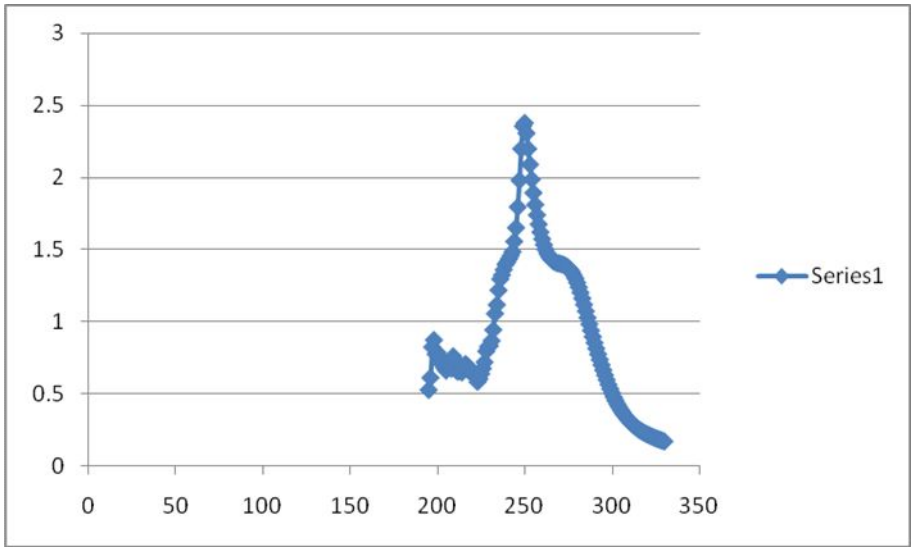

Appendix 15A: The ^{1}H NMR spectrum (600 MHz) of 1-[(16'*E*)-nonadecenyl]cyclohex-4-en-1,3-diol (**200**) in CD_2Cl_2

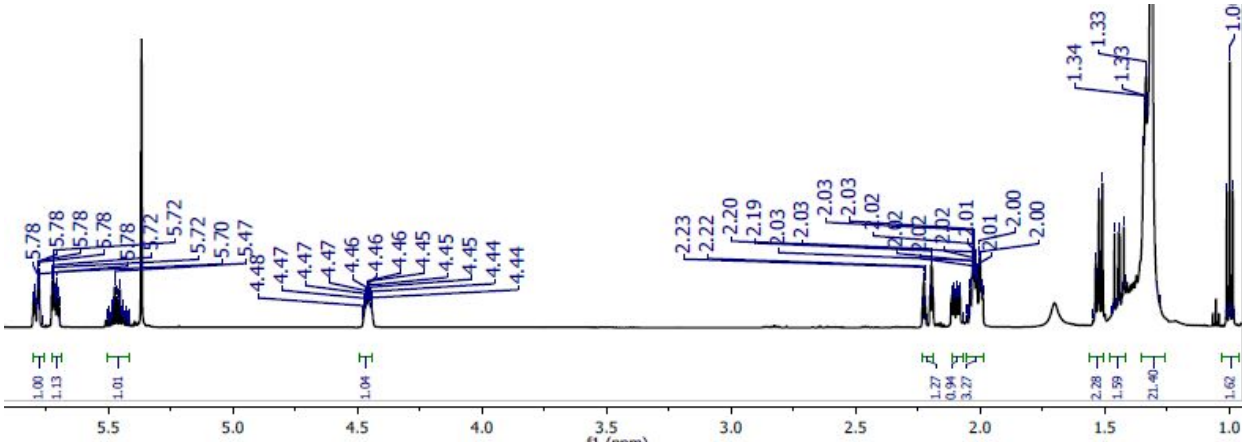

Appendix 15B: The ^{13}C NMR spectrum (150MHz) of 1-[(16'*E*)-nonadecenyl]cyclohex-4-en-1,3-diol (**200**) in CD_2Cl_2

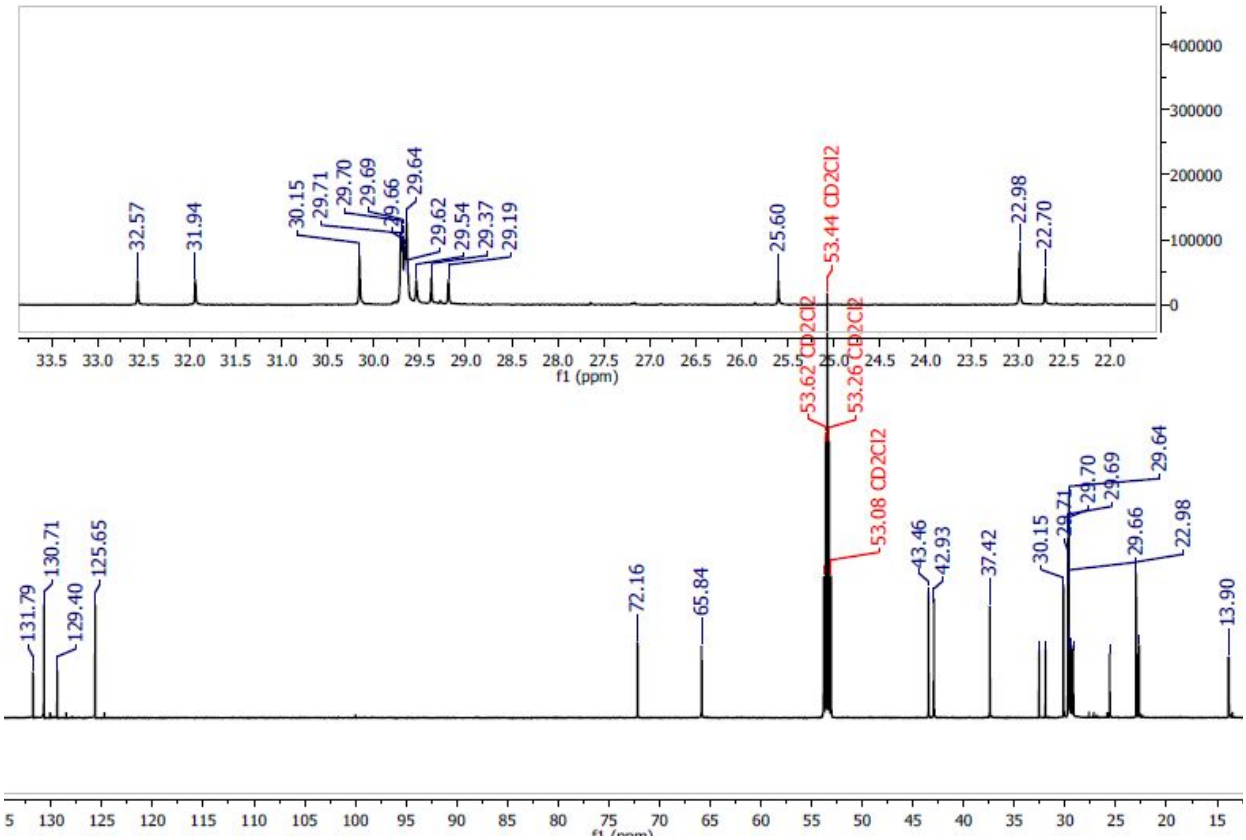

Appendix 16A: The ^{1}H NMR spectrum (600 MHz) of catechin (**201**) in Acetone-d_6

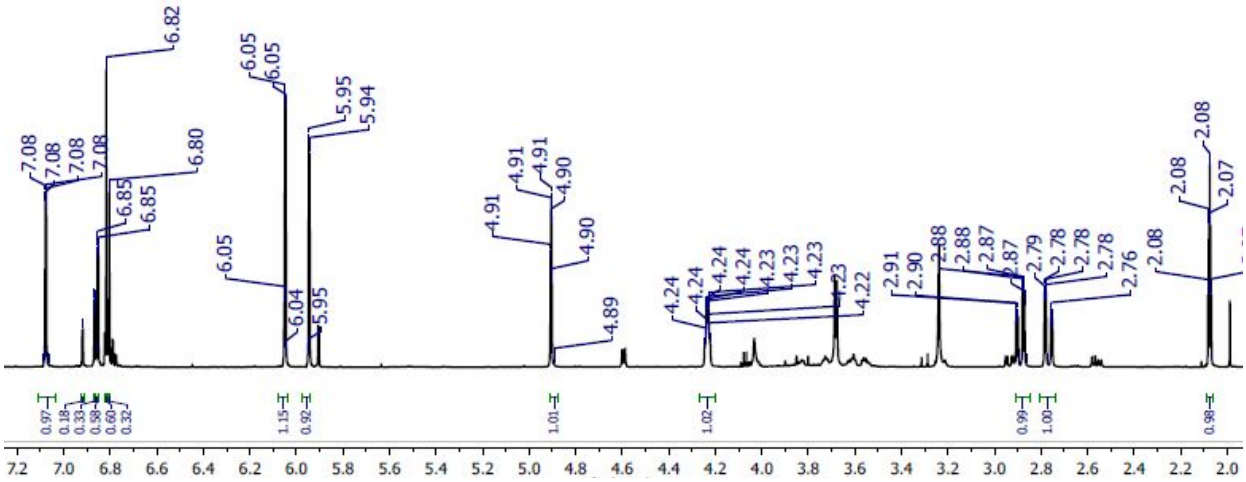

Appendix 16B: The ^{13}C NMR spectrum (150MHz) of catechin (**201**) in Acetone-d_6

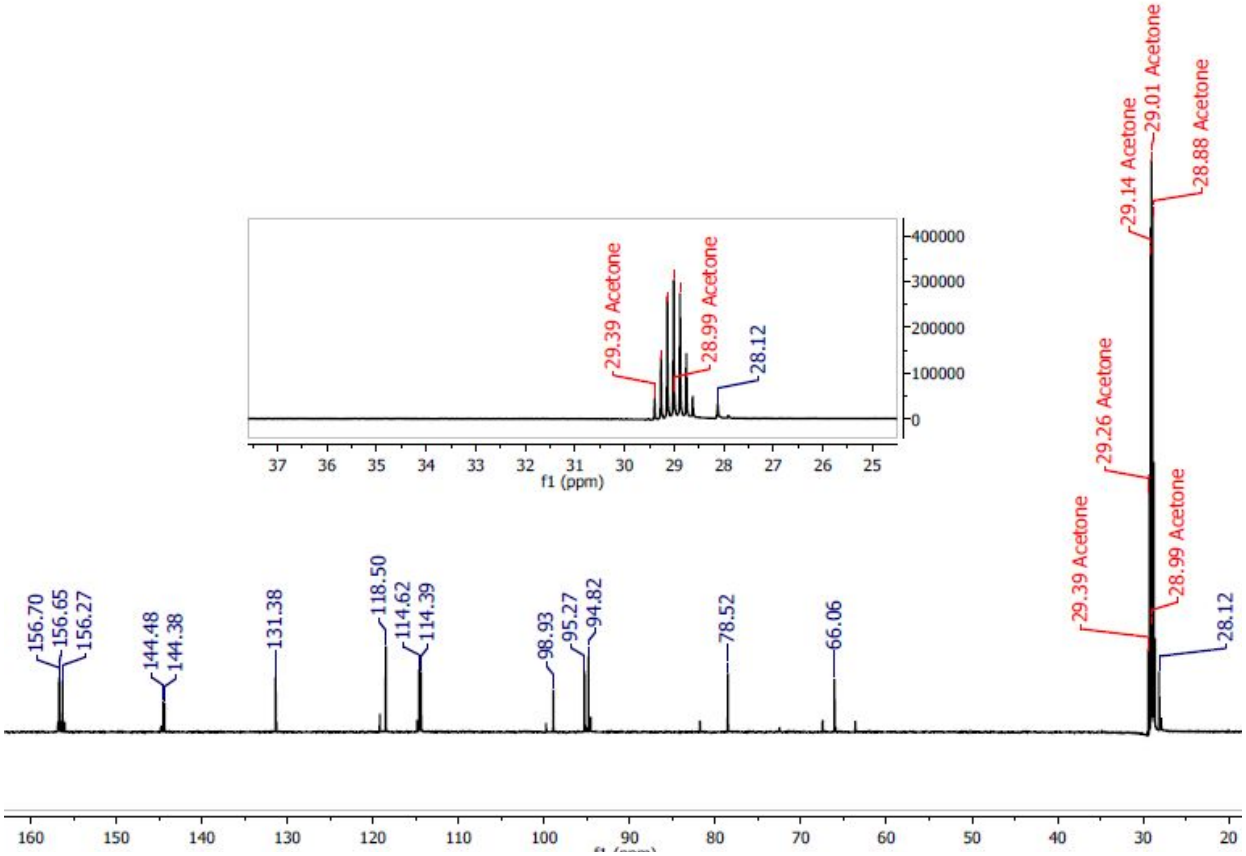

Appendix 17A: The ^{1}H NMR spectrum (600 MHz) of 4,4'-diydroxy-3-methoxy-3'-*O*-glucosyl-ellagic acid (**202**) in Acetone-d_6

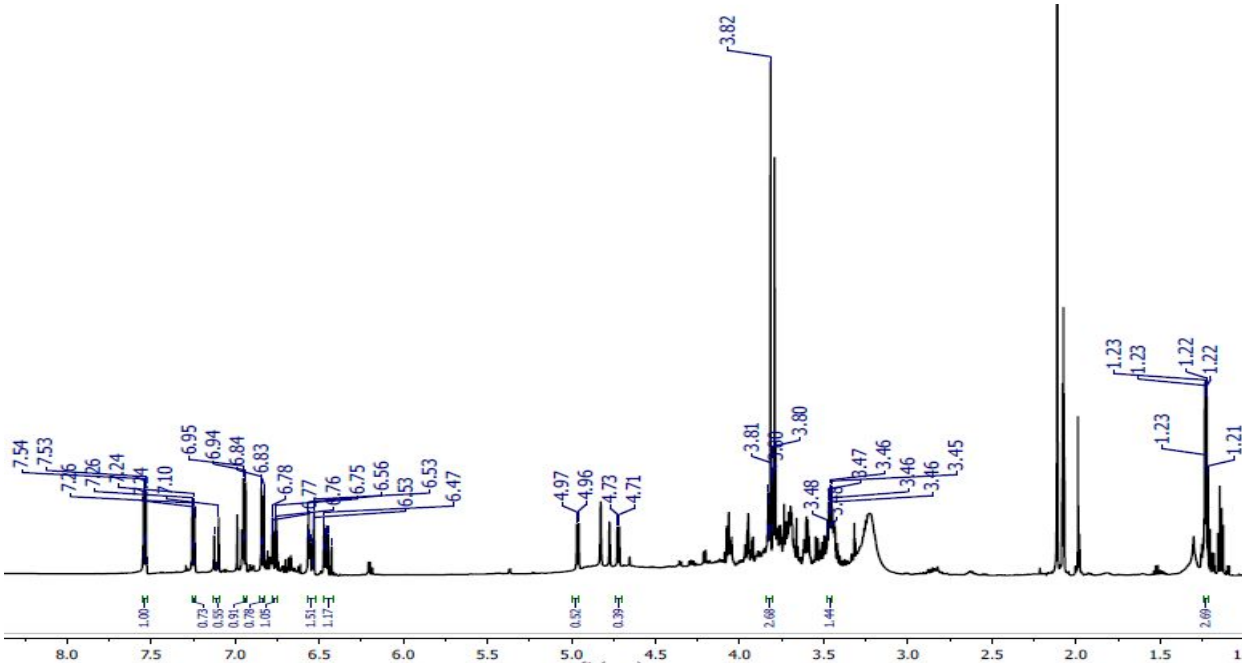

Appendix 17B: The ^{13}C NMR spectrum (150MHz) of 4,4'-diydroxy-3-methoxy-3'-*O*-glucosyl-ellagic acid (**202**) in Acetone-d_6

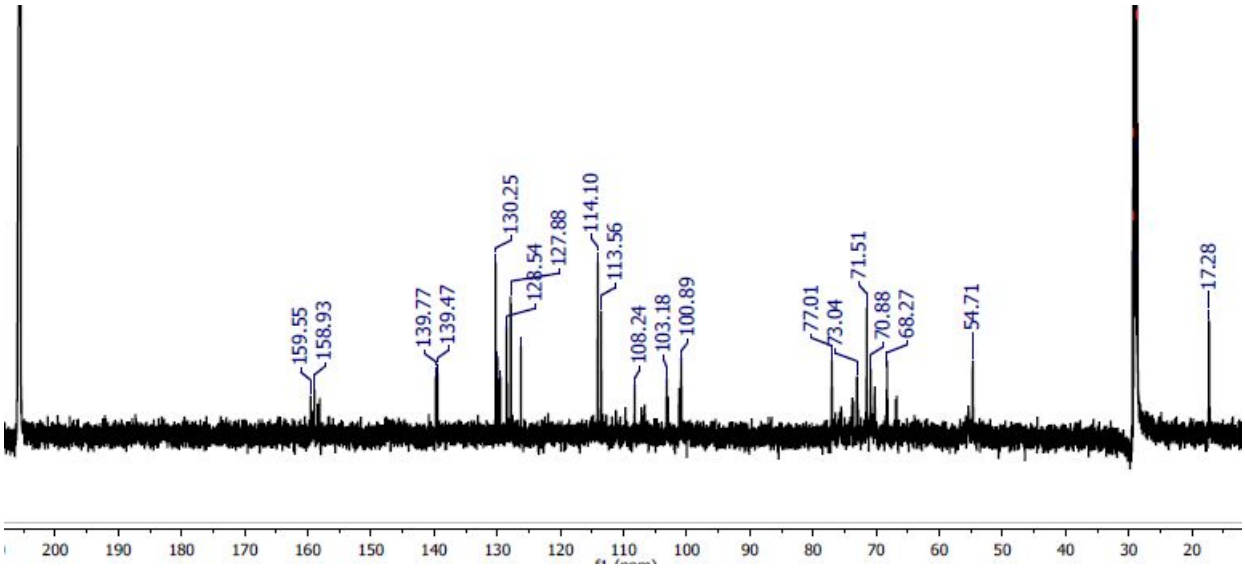

Appendix 18A: The ^{1}H NMR spectrum (600 MHz) of 3'-*O*-methylellagic acid 4-*O*-[rhamnopyranosyl-(1→2)] rhamnopyranoside (**203**) in Acetone-d_6

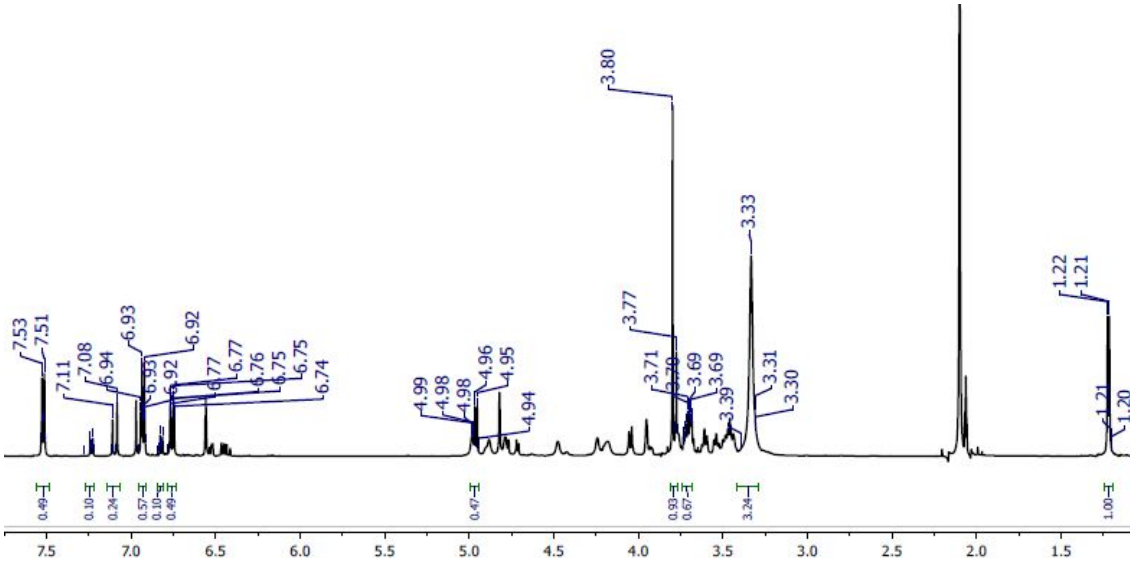

Appendix 18B: The ^{13}C NMR spectrum (200MHz) of 3'-*O*-methylellagic acid 4-*O*-[rhamnopyranosyl-(1→2)] rhamnopyranoside (**203**) in Acetone-d_6

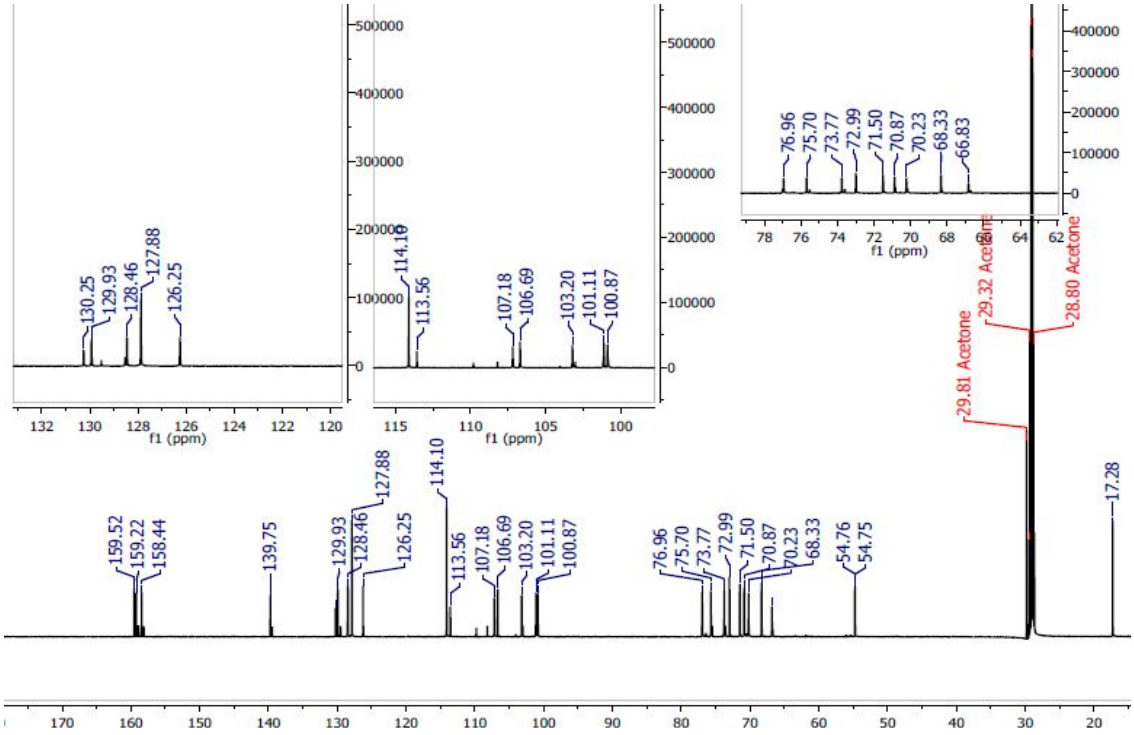

Appendix 19A: The ^{1}H NMR spectrum (600 MHz) of 3-((*E*)-heptadeca-12',14'-dieenyl)phenol (**204**) in $CDCl_3$

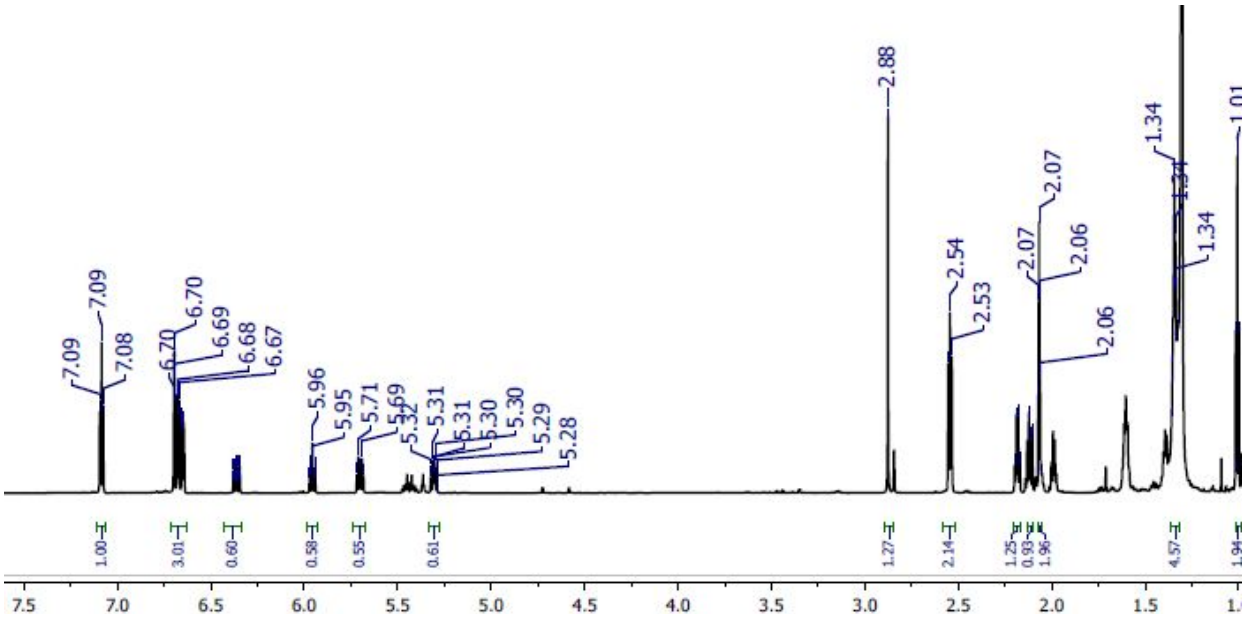

Appendix 19B: The ^{13}C NMR spectrum (200MHz) of 3-((*E*)-heptadeca-12',14'-dieenyl)phenol (**204**) in $CDCl_3$

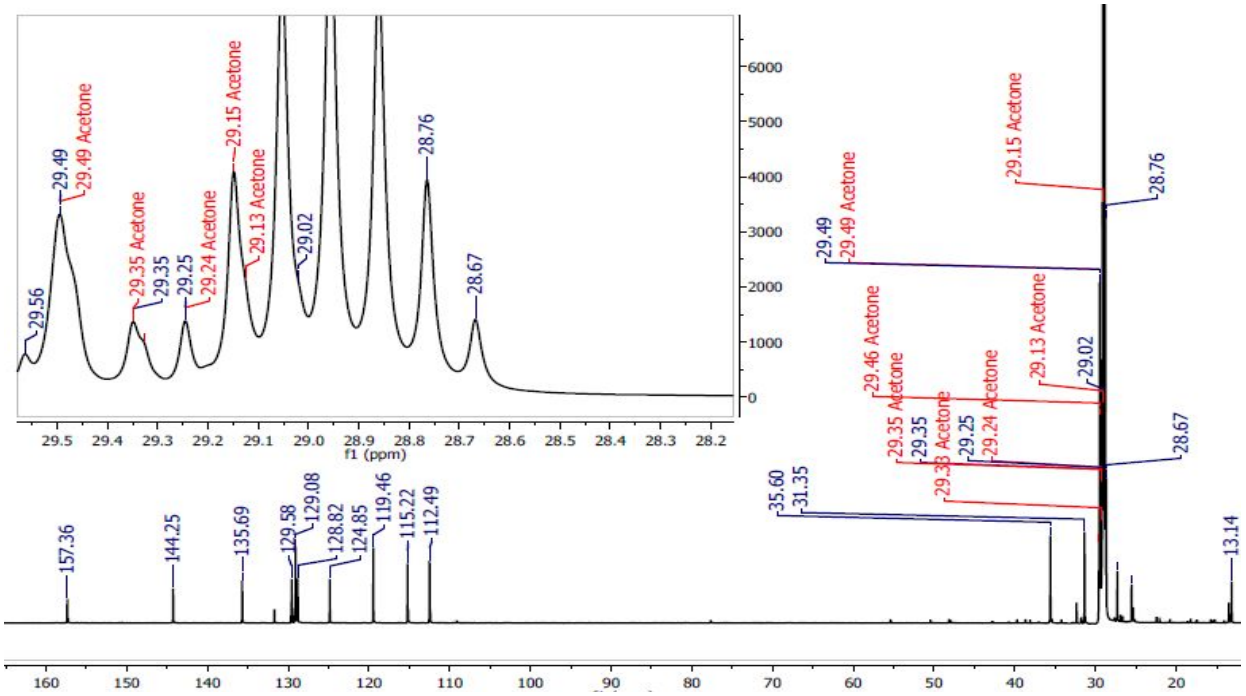

Appendix 2: Spectra for the Compounds Isolated from P. punctulata

Appedix 20A. The ^{1}H NMR spectrum of trachyloban-17-oic acid (293) observed at 600 MHz for $CDCl_3$ solution at 25 °C.

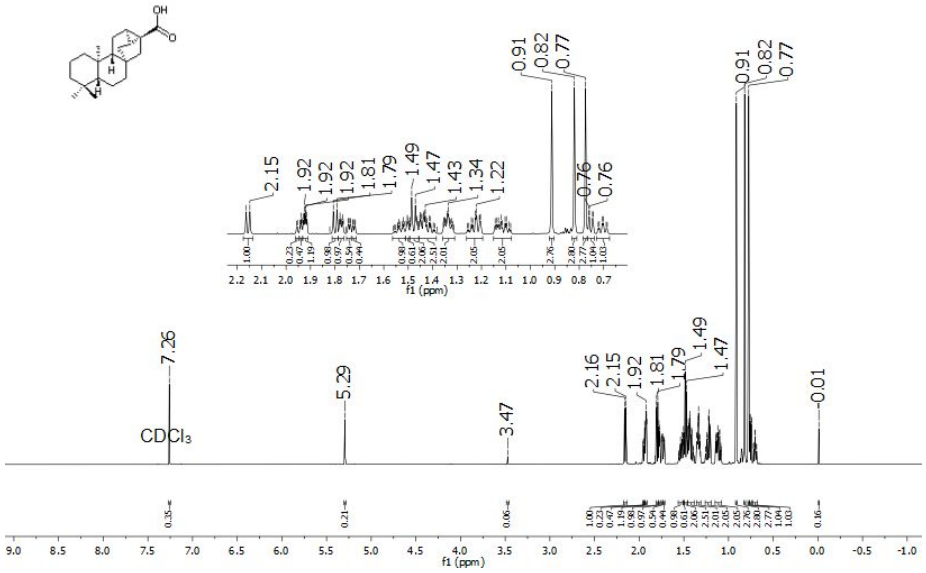

Appendix 20B. The ^{13}C NMR spectrum of trachyloban-17-oic acid (**205**) observed at 200 MHz for $CDCl_3$ solution at 25 °C.

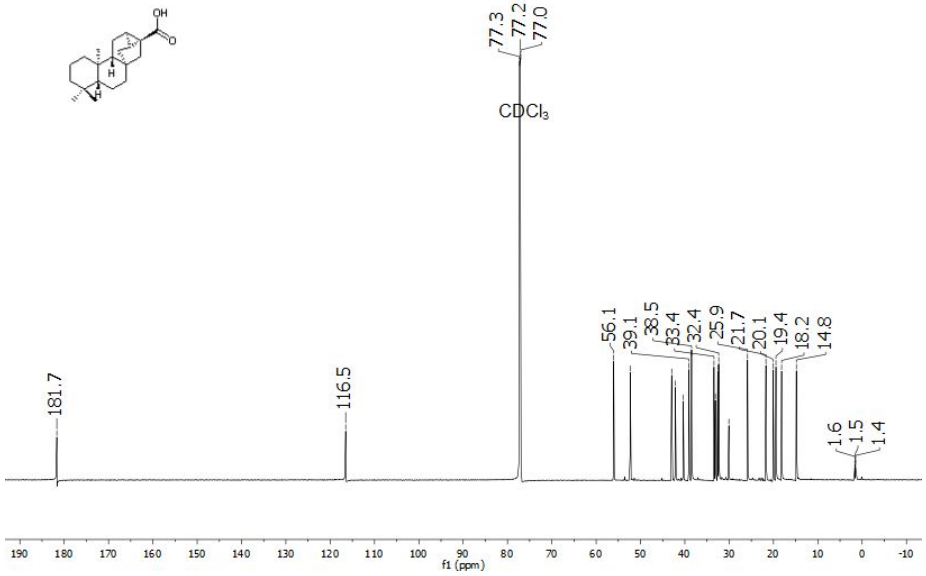

Appendix 20C. The ^{1}H-^{1}H COSY spectrum of trachyloban-17-oic acid (**205**) observed at 600 MHz for $CDCl_3$ solution at 25 °C.

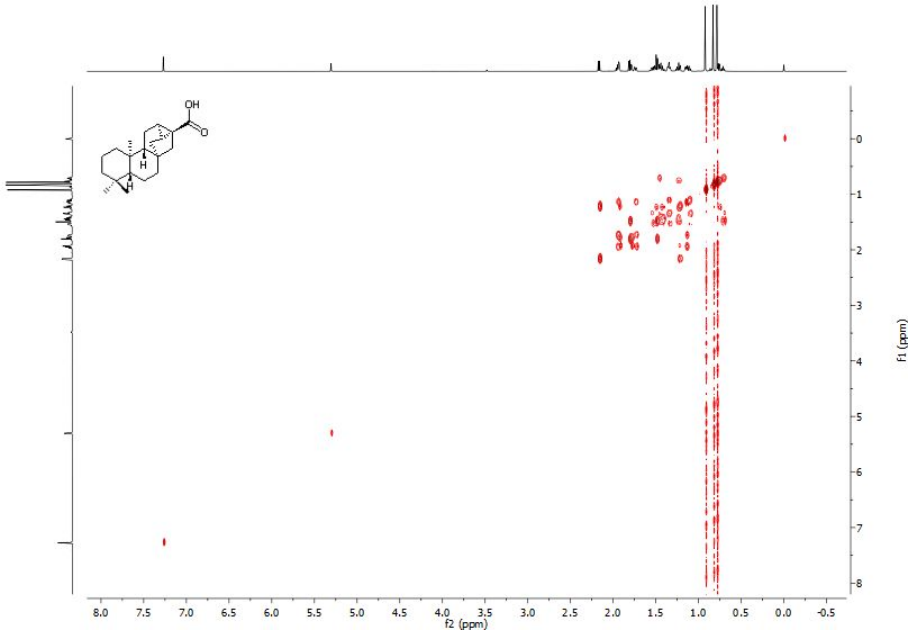

Appendix 20D. The ^{1}H-^{1}H NOESY NMR spectrum of trachyloban-17-oic acid (**205**) observed at 600 MHz for $CDCl_3$ solution at 25 °C.

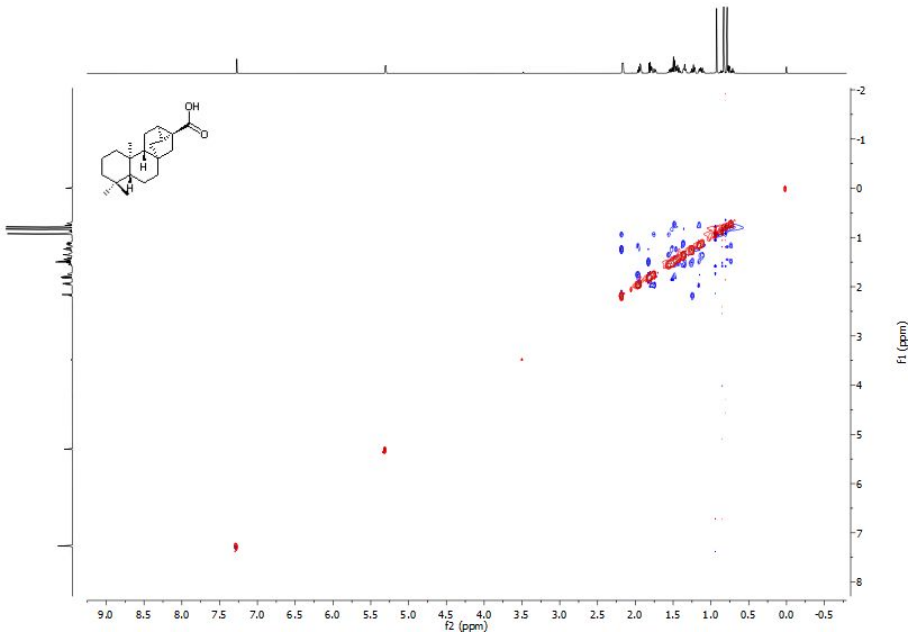

Appendix 20E. The ^{1}H-^{13}C HSQC NMR spectrum of trachyloban-17-oic acid (**205**) observed at 600 and 200 MHz for $CDCl_3$ solution at 25 °C.

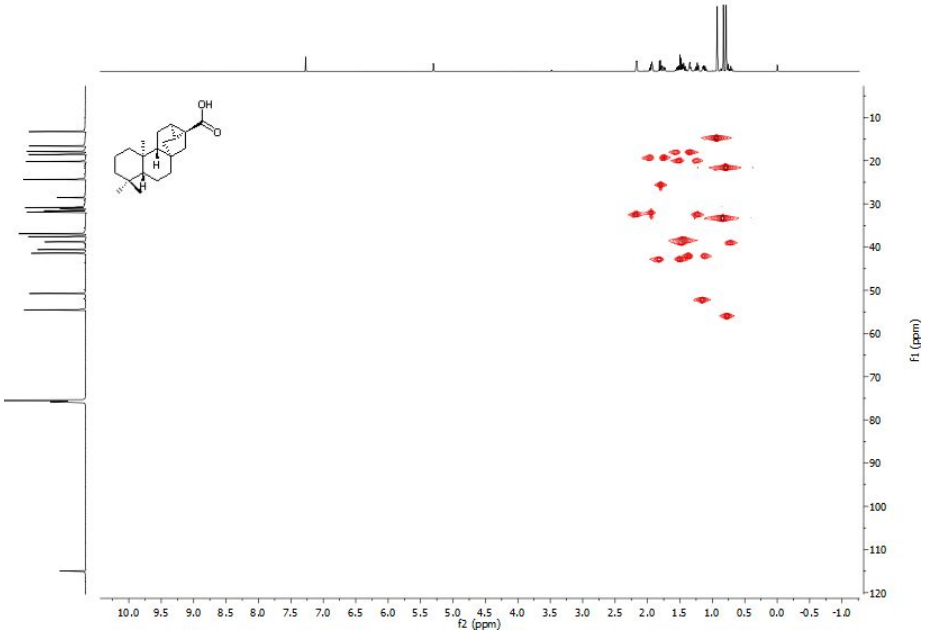

Appendix 20F. The ^{1}H-^{13}C HMBC NMR spectrum of trachyloban-17-oic acid (**205**) observed at 600 and 200 MHz for $CDCl_3$ solution at 25 °C.

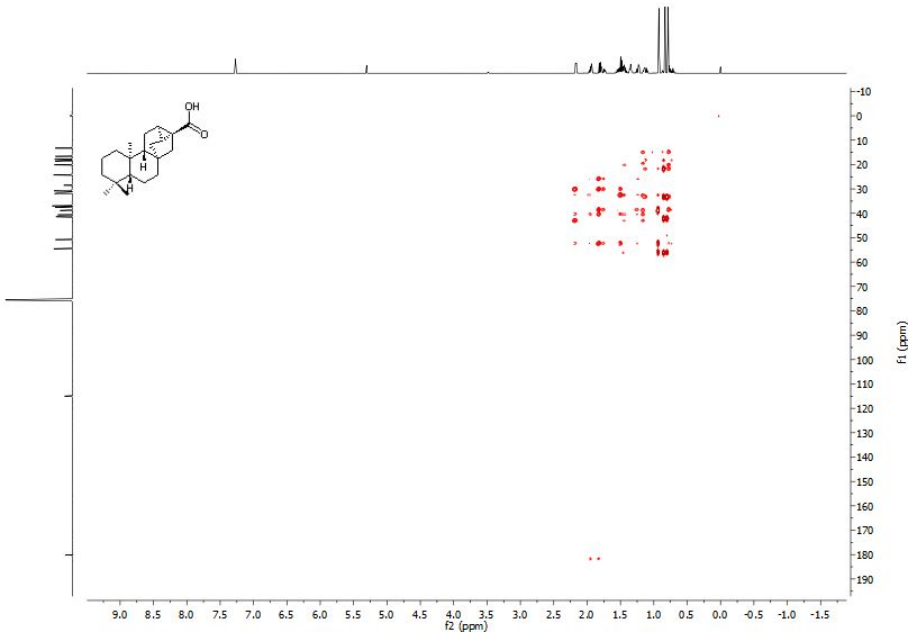

Appendix 20G. The HRMS (ESI) spectrum of trachyloban-17-oic acid (**205**).

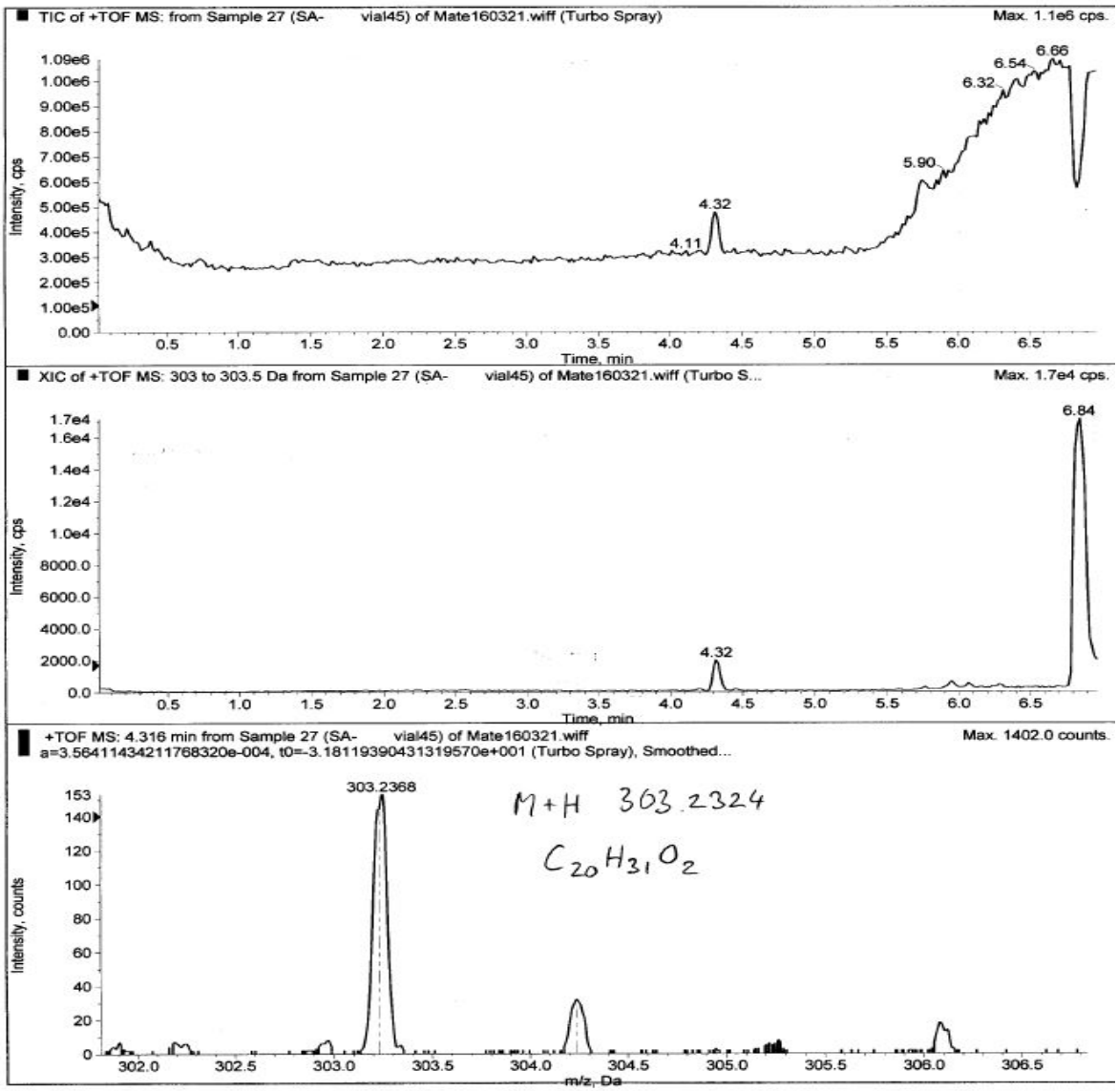

Appendix 21A. The ^{1}H NMR spectrum of 17-hydroxy-*ent*-trachyloban-20-oic acid (**206**) observed at 800 MHz for C_5D_5N solution at 25 °C.

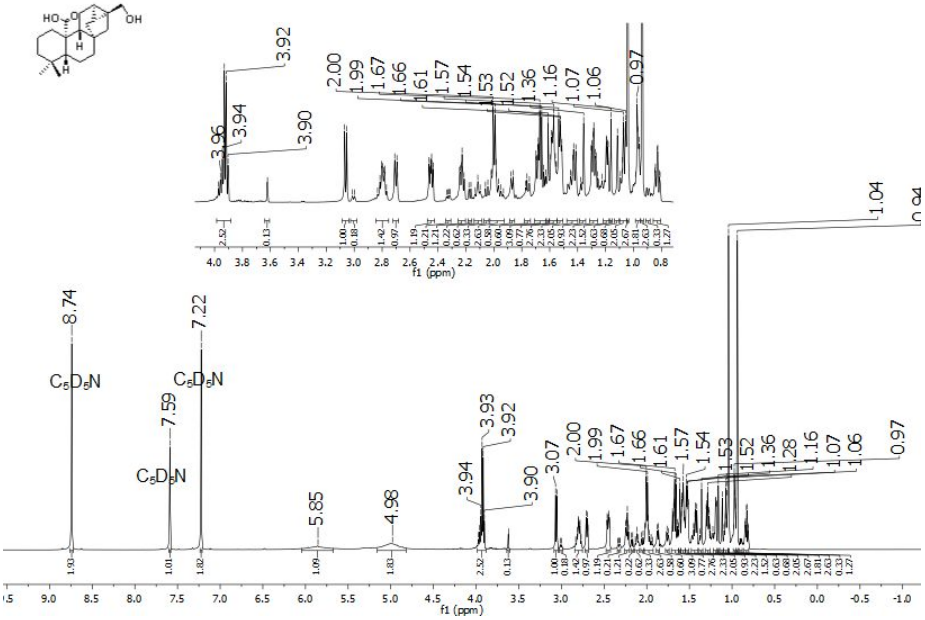

Appendix 21B. The ^{13}C NMR spectrum of 17-hydroxy-*ent*-trachyloban-20-oic acid (**206**) observed at 200 MHz for C_5D_5N solution at 25 °C..

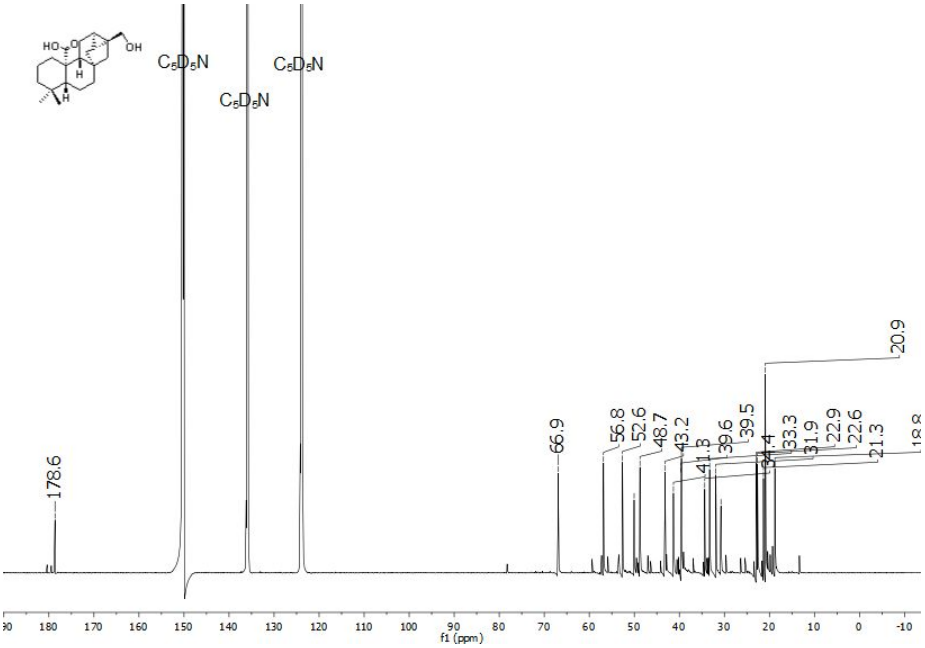

Appendix 21C. The ^{1}H-^{1}H COSY NMR spectrum of 17-hydroxy-*ent*-trachyloban-20-oic acid (**206**) observed at 800 MHz for C_5D_5N solution at 25 °C.

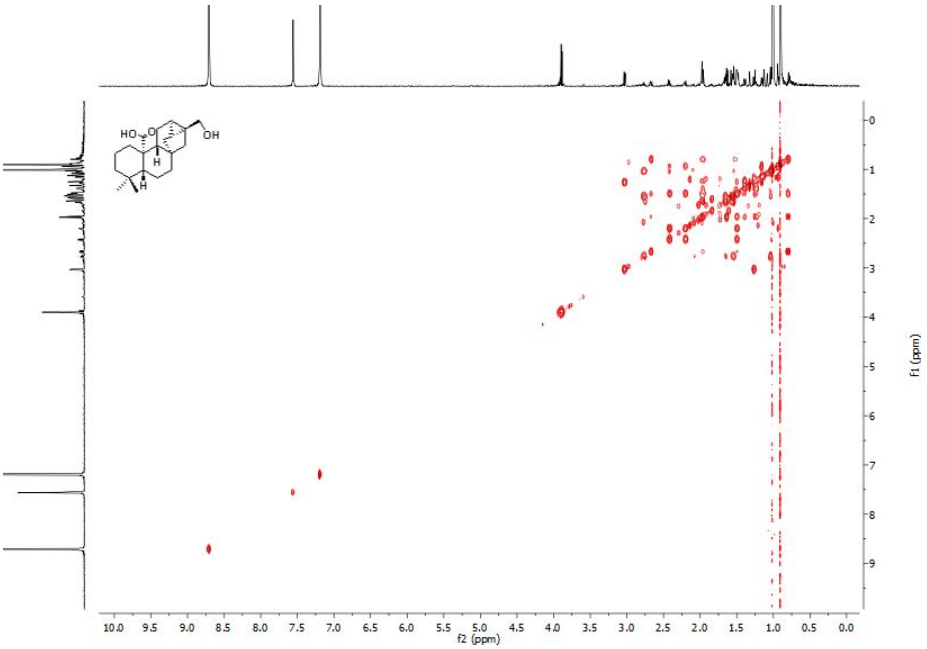

Appendix 21D. The ^{1}H-^{1}H NOSEY NMR spectrum of 17-hydroxy-*ent*-trachyloban-20-oic acid (**206**) observed at 800 MHz for C_5D_5N solution at 25 °C.

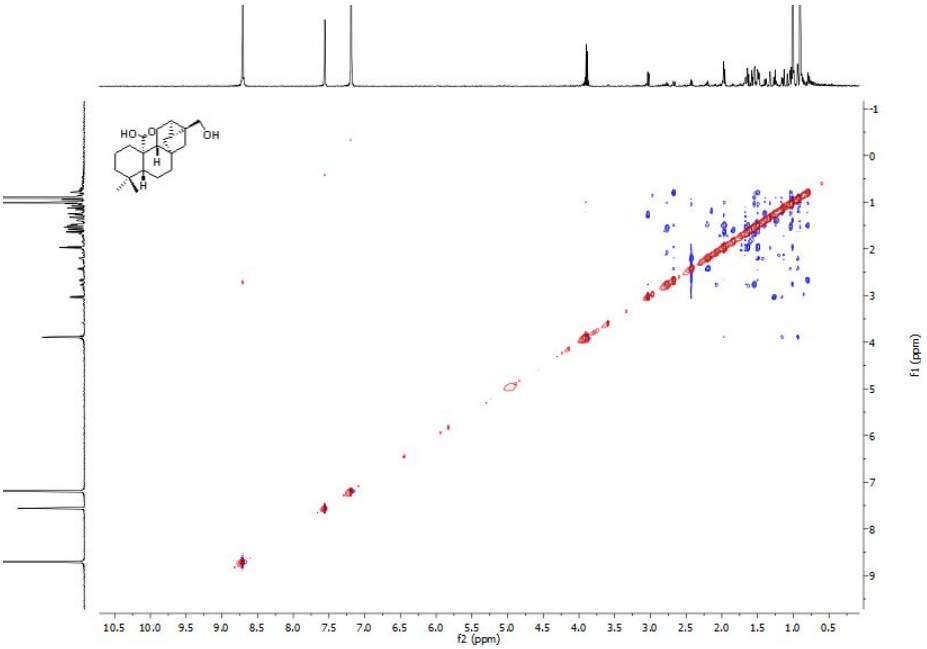

Appendix 21E. The ^{1}H-^{13}C HSQC NMR spectrum of 17-hydroxy-*ent*-trachyloban-20-oic acid (**206**) observed at 800 and 200 MHz for C_5D_5N solution at 25 °C.

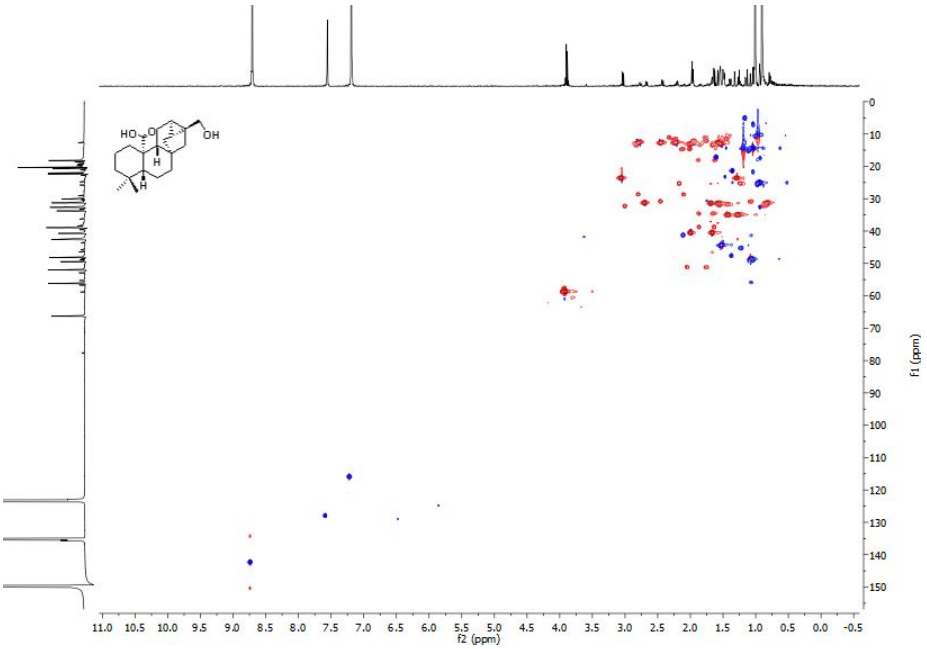

Appendix 21F. The ^{1}H-^{13}C HMBC NMR spectrum of 17-hydroxy-*ent*-trachyloban-20-oic acid (**206**) observed at 800 and 200 MHz for C_5D_5N solution at 25 °C.

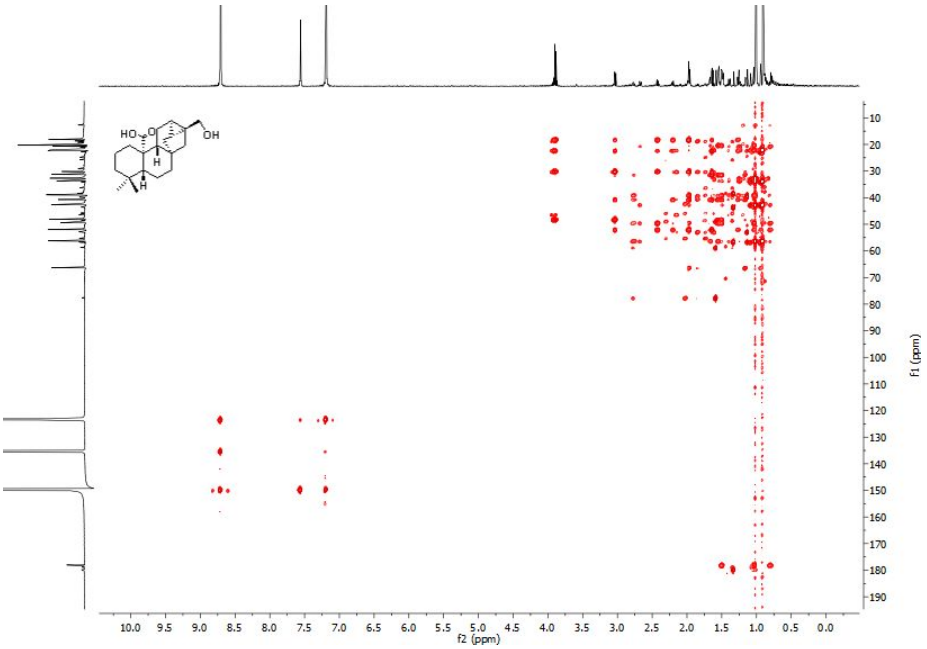

Appendix 21G. The HRMS (ESI) spectrum of 17-hydroxy-*ent*-trachyloban-20-oic acid (**206**).

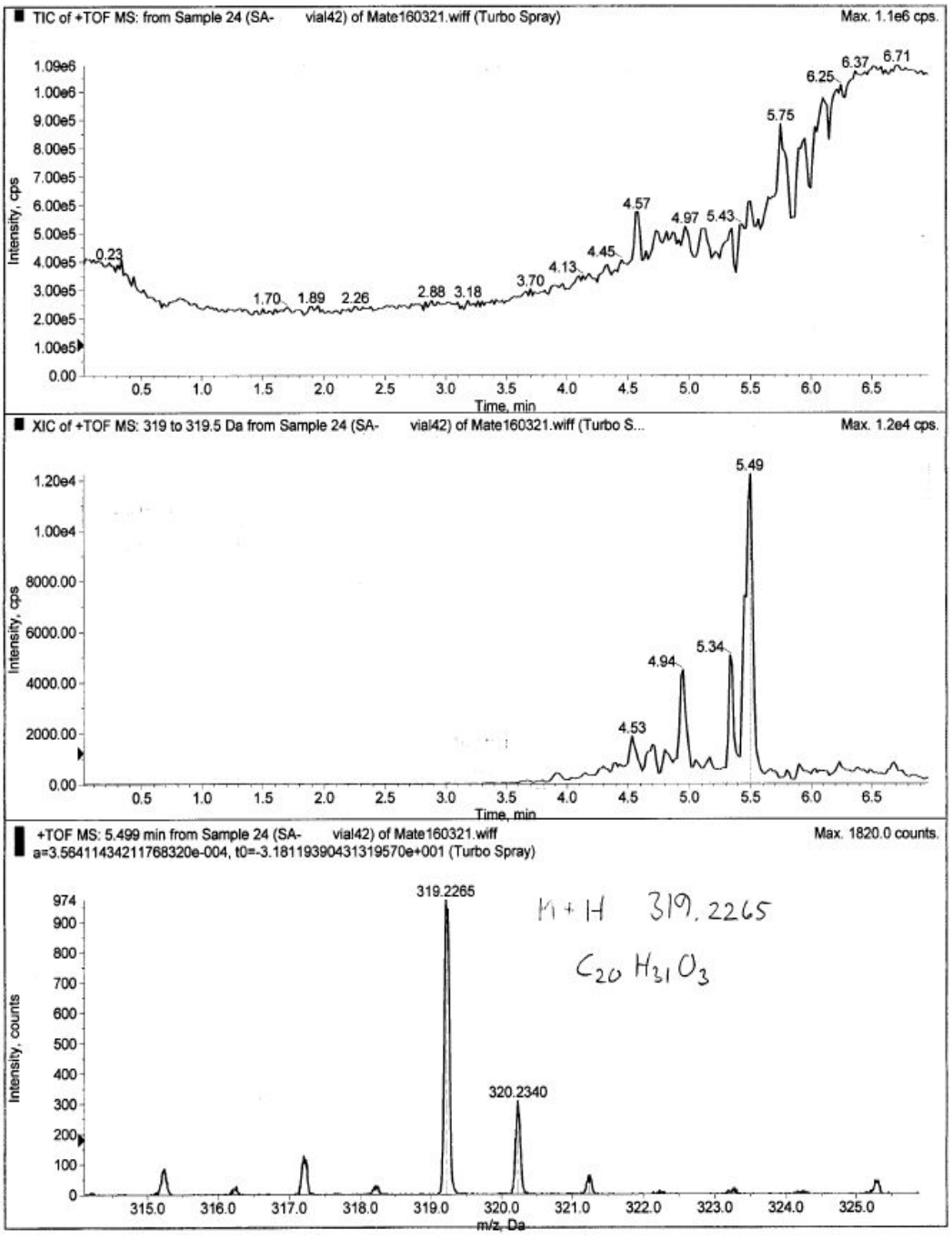

Appendix 22A. The ^{1}H NMR spectrum of *ent*-[6β, 18, 19]-trihydroxy- trachyloban-2-one (**207**) observed at 800 MHz for $CDCl_3$ solution at 25 °C.

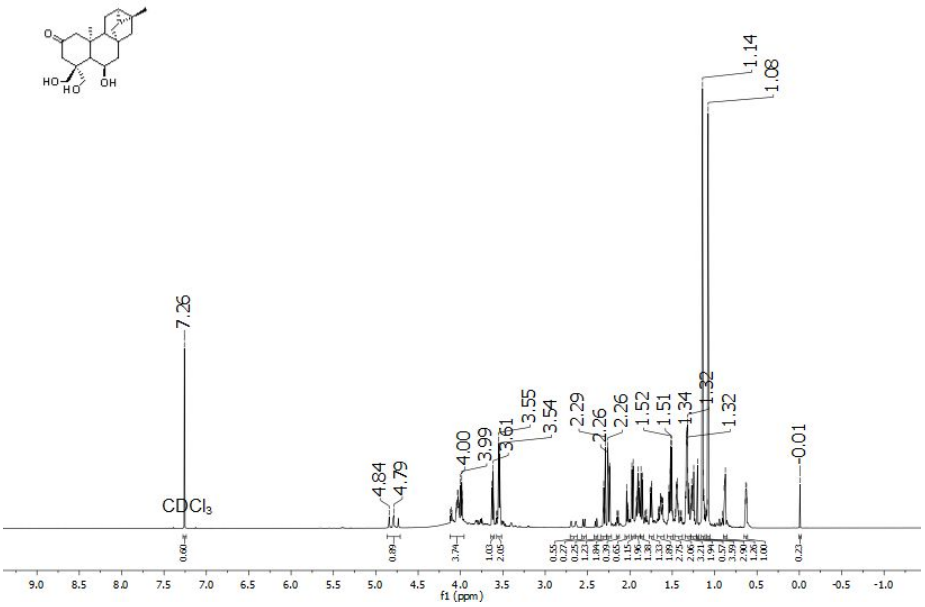

Appendix 22B. The ^{13}C NMR spectrum of *ent*-[6β, 18, 19]-trihydroxy- trachyloban-2-one (**207**) observed at 200 MHz for $CDCl_3$ solution at 25 °C.

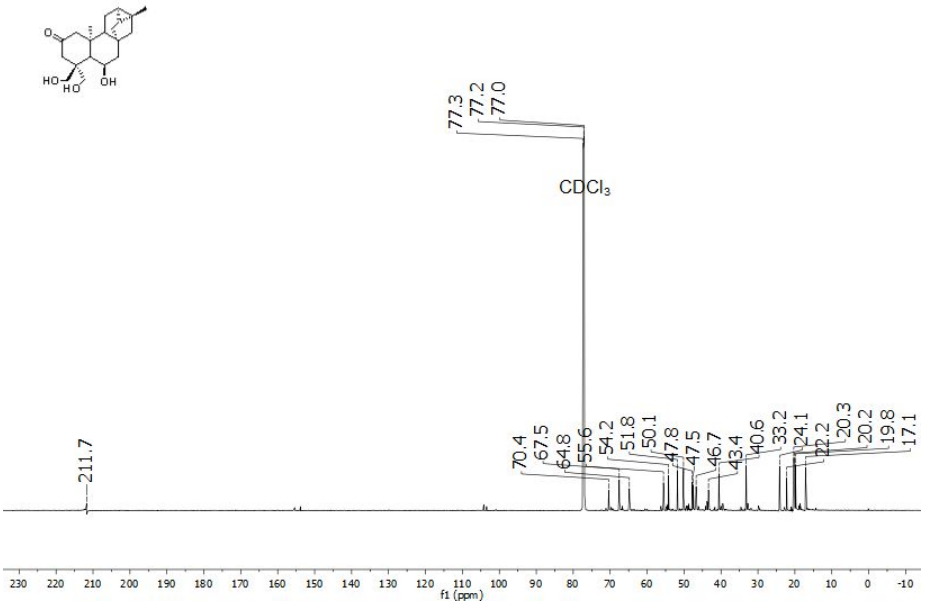

Appendix 22C. The ^{1}H-^{1}H COSY NMR spectrum of *ent*-[6β, 18, 19]-trihydroxy-trachyloban-2-one (**207**) observed at 800 MHz for $CDCl_3$ solution at 25 °C.

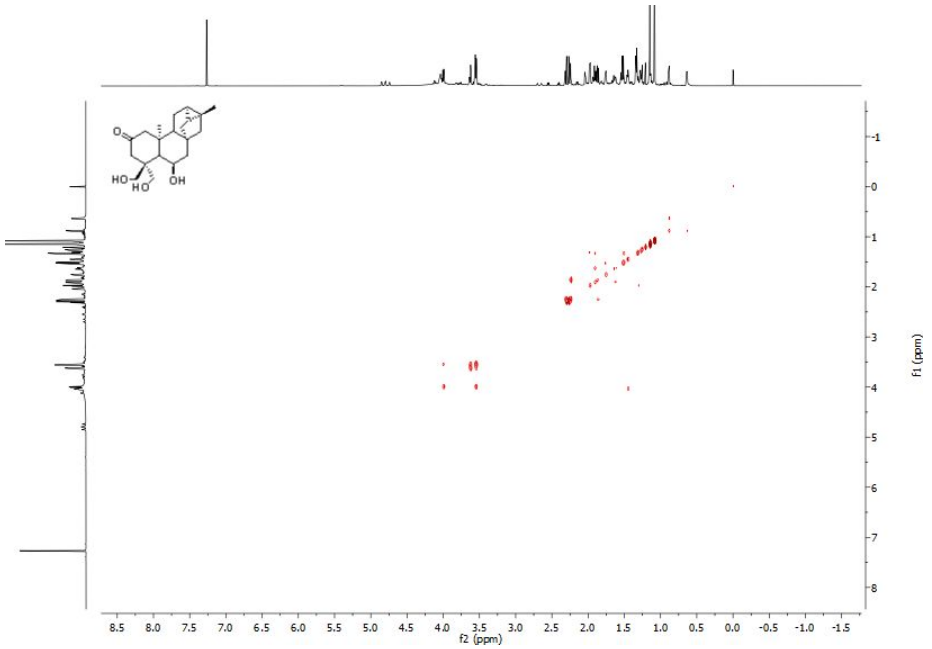

Appendix 22D. The ^{1}H-^{1}H NOSEY NMR spectrum of *ent*-[6β, 18, 19]-trihydroxy-trachyloban-2-one (**207**) observed at 800 MHz for $CDCl_3$ solution at 25 °C.

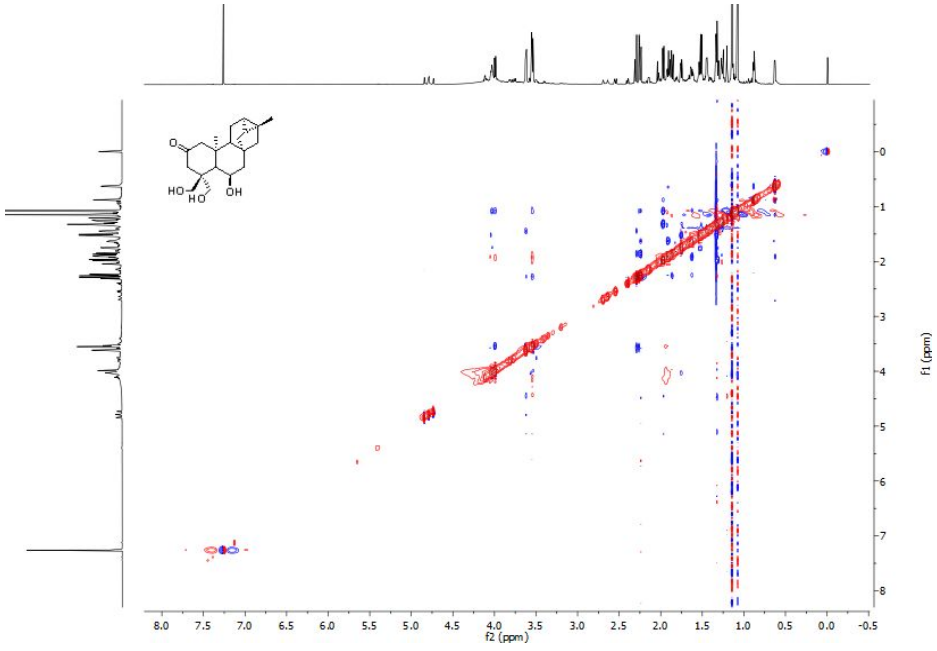

Appendix 22E. The ^{1}H-^{13}C HSQC NMR spectrum of *ent*-[6β, 18, 19]-trihydroxy-trachyloban-2-one (**207**) observed at 800 and 200 MHz for $CDCl_3$ solution at 25 °C.

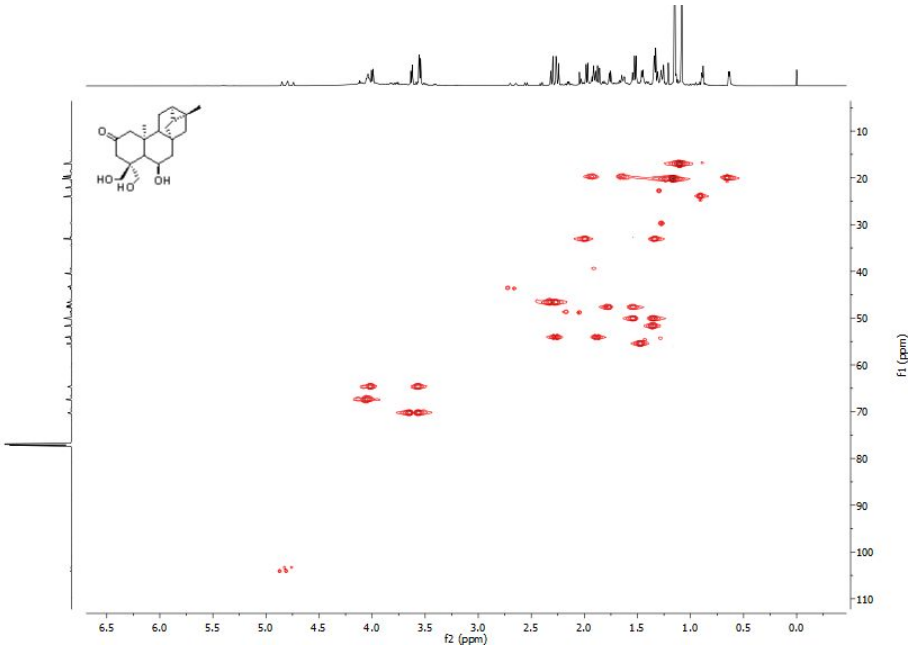

Appendix 22F. The ^{1}H-13C HMBC NMR spectrum of *ent*-[6β, 18, 19]-trihydroxy-trachyloban-2-one (**207**) observed at 800 and 200 MHz for $CDCl_3$ solution at 25 °C.

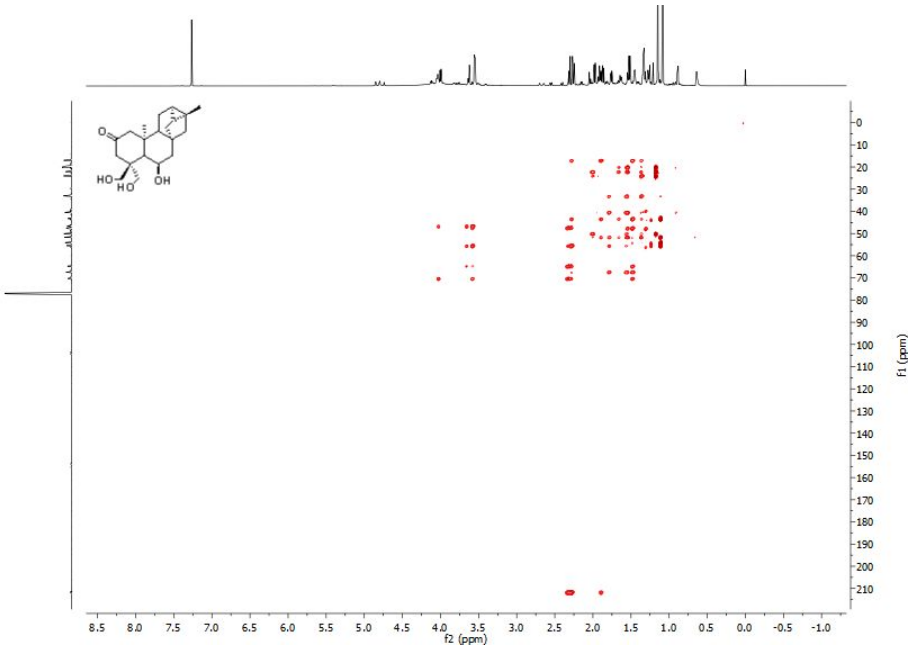

Appendix 22G. The HRMS (ESI) spectrum of *ent*-[6β, 18, 19]-trihydroxy- trachyloban-2-one(**207**).

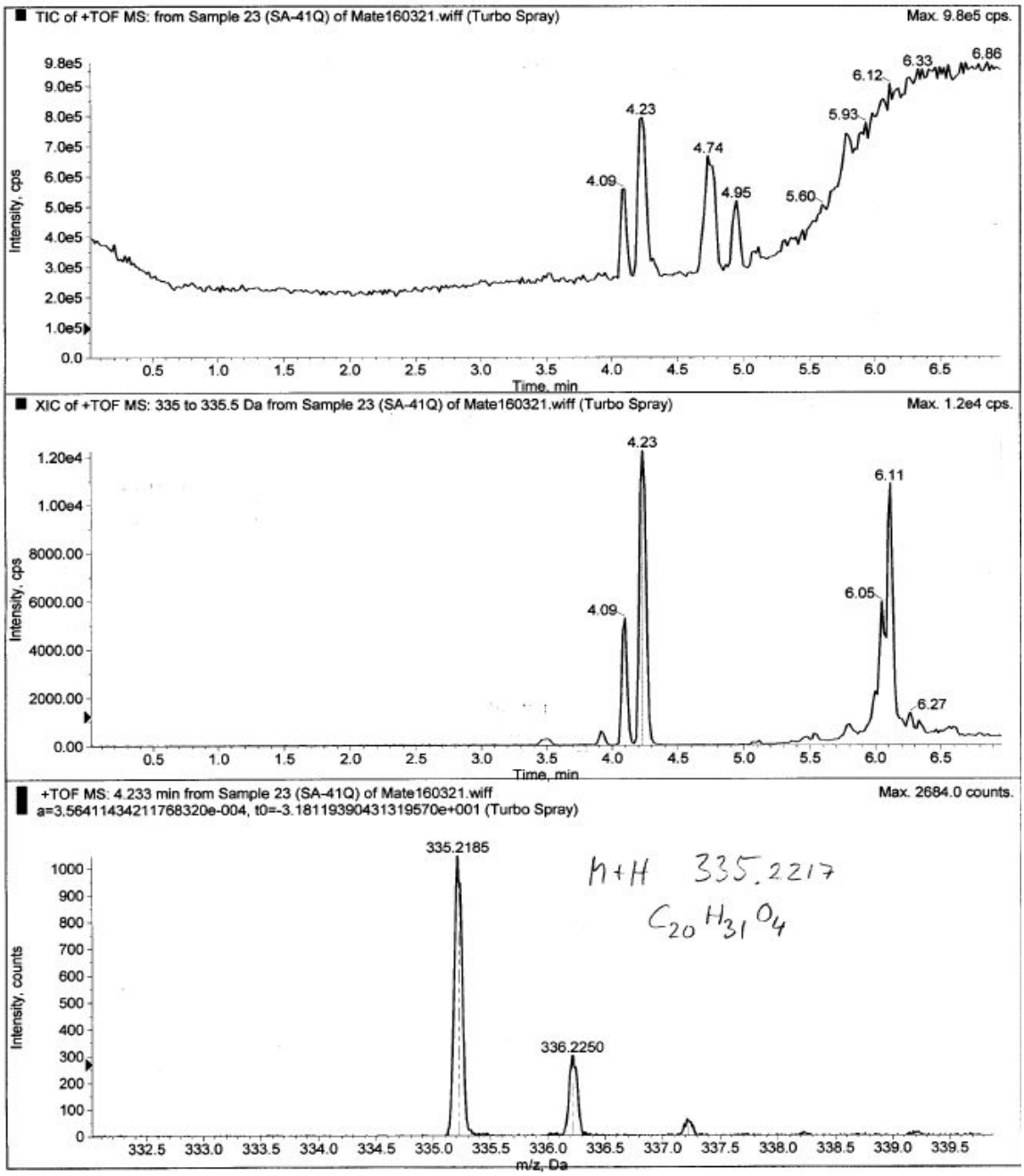

Appendix 23A. The ^{1}H NMR spectrum of normal-trachyloban-2α,18,19-triol (**208**) observed at 600 MHz for $CDCl_3$ solution at 25 °C.

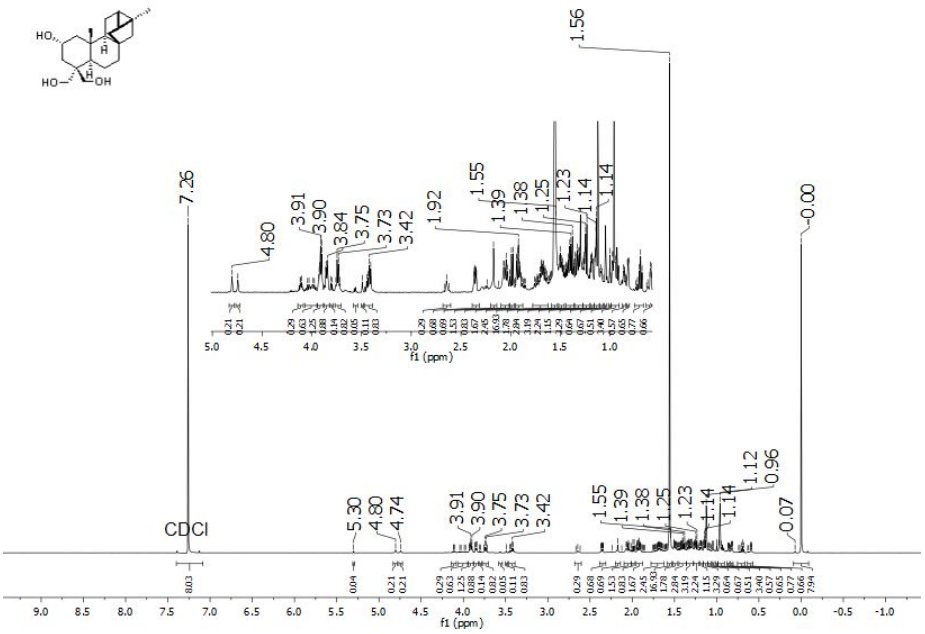

Appendix 23B. The ^{13}C NMR spectrum of normal-trachyloban-2α,18,19-triol (**208**) observed at 200 MHz for $CDCl_3$ solution at 25 °C.

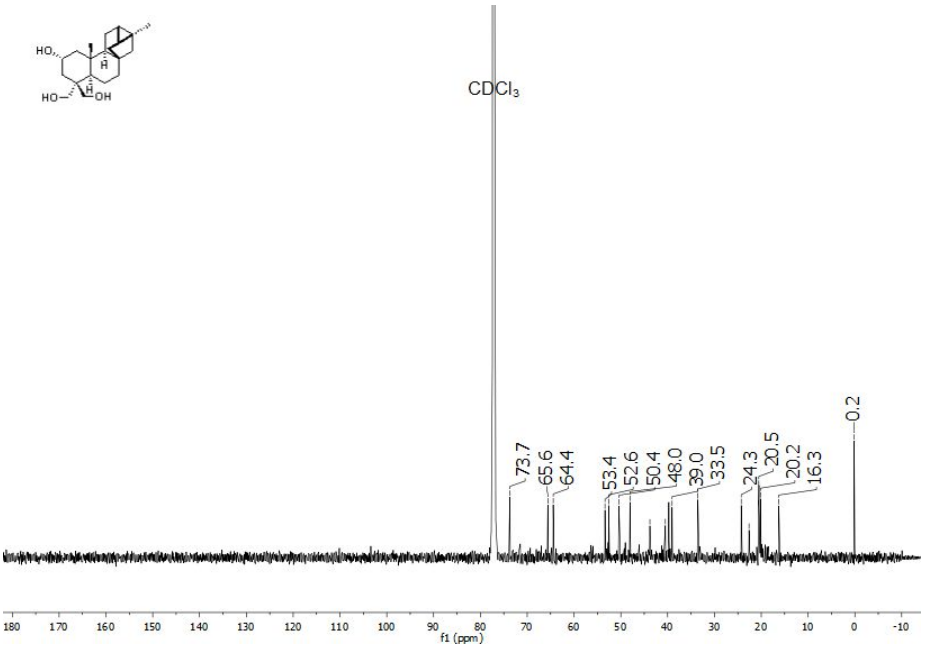

Appendix 23C. The ^{1}H-^{1}H COSY NMR spectrum of normal-trachyloban-2α,18,19-triol (**208**) observed at 600 MHz for $CDCl_3$ solution at 25 °C.

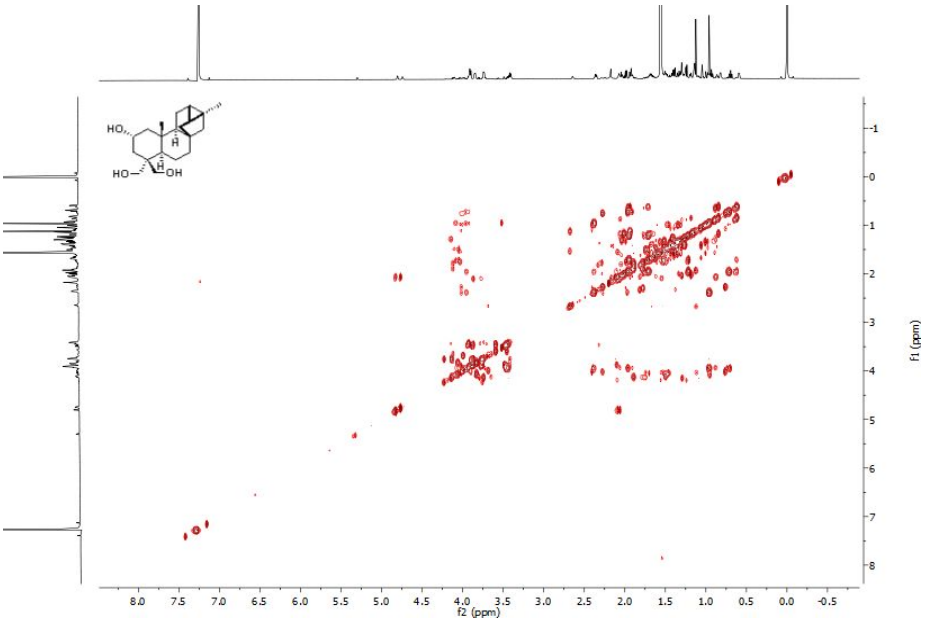

Appendix 23D. The ^{1}H-^{1}H NOSEY NMR spectrum of normal-trachyloban-2α,18,19-triol (**208**) observed at 600 MHz for $CDCl_3$ solution at 25 °C.

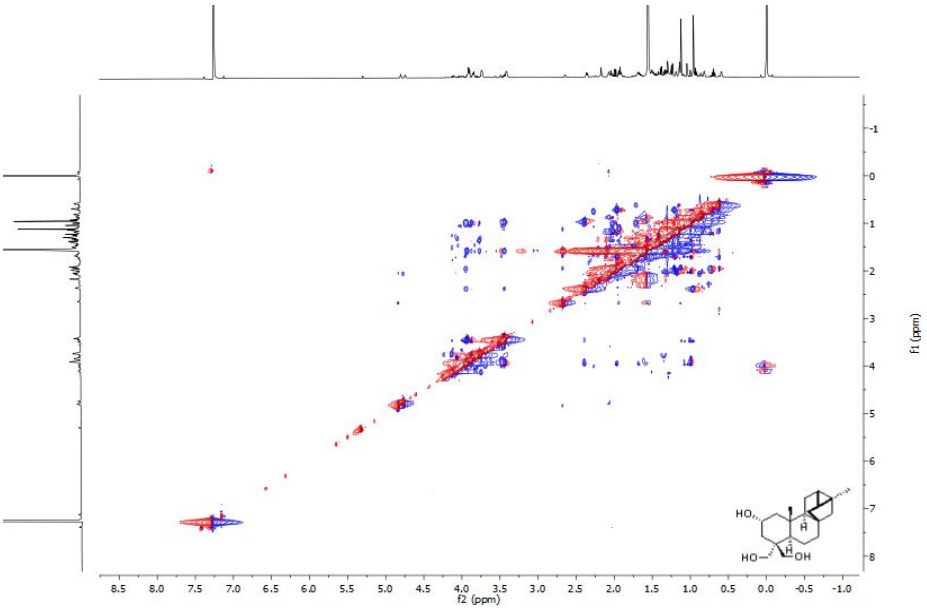

Appendix 23E. The ^{1}H-^{13}C HSQC NMR spectrum of normal-trachyloban-2α,18,19-triol (**208**) observed at 600 and 200 MHz for $CDCl_3$ solution at 25 °C.

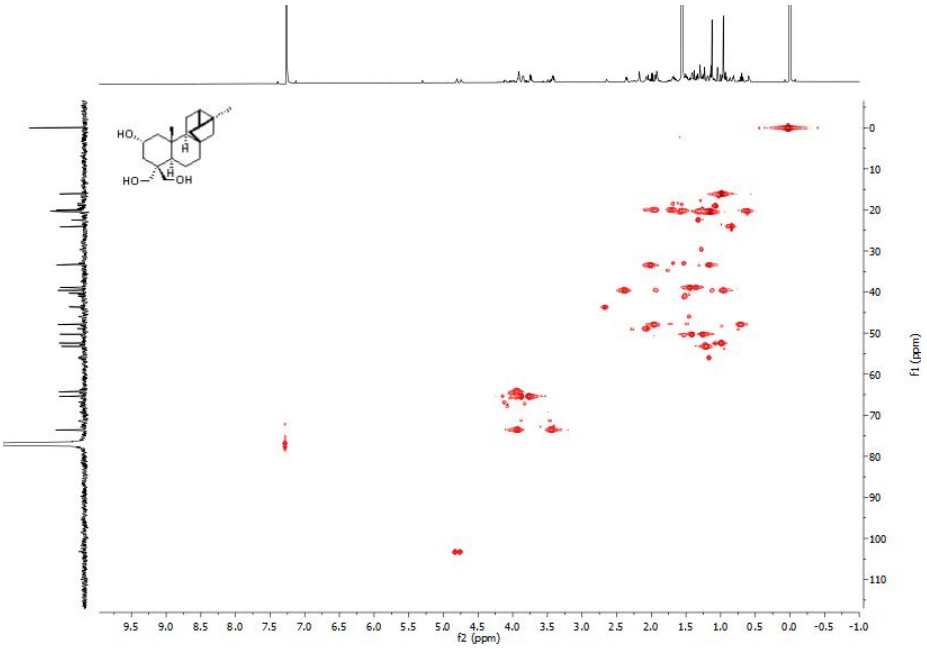

Appendix 23F. The ^{1}H-^{13}C HMBC NMR spectrum of normal-trachyloban-2α,18,19-triol (**208**) observed at 600 and 200 MHz for $CDCl_3$ solution at 25 °C.

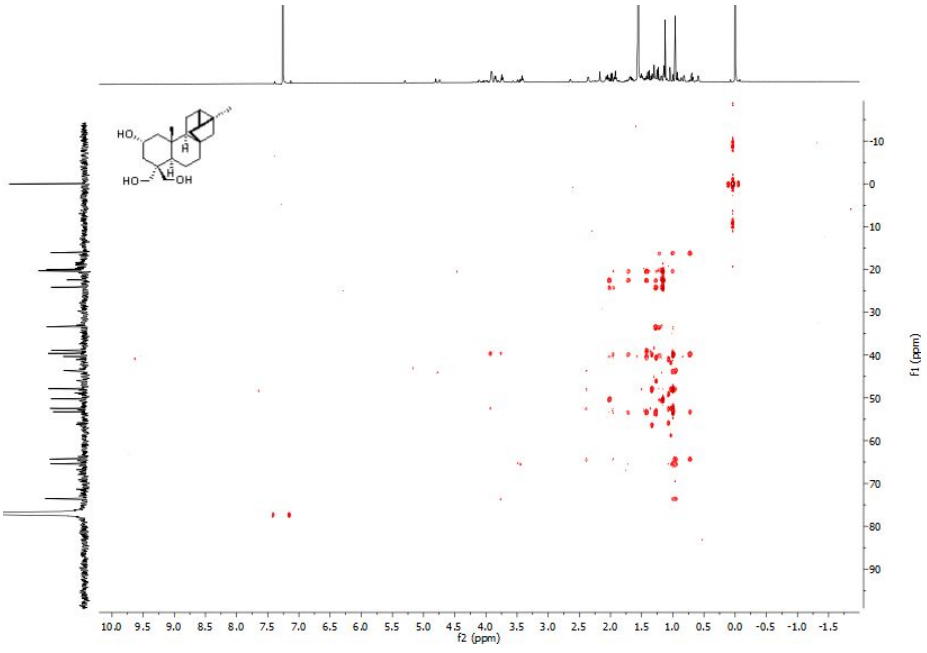

Appendix 23G. The HRMS (ESI) spectrum of normal-trachyloban-2α,18,19-triol (**208**).

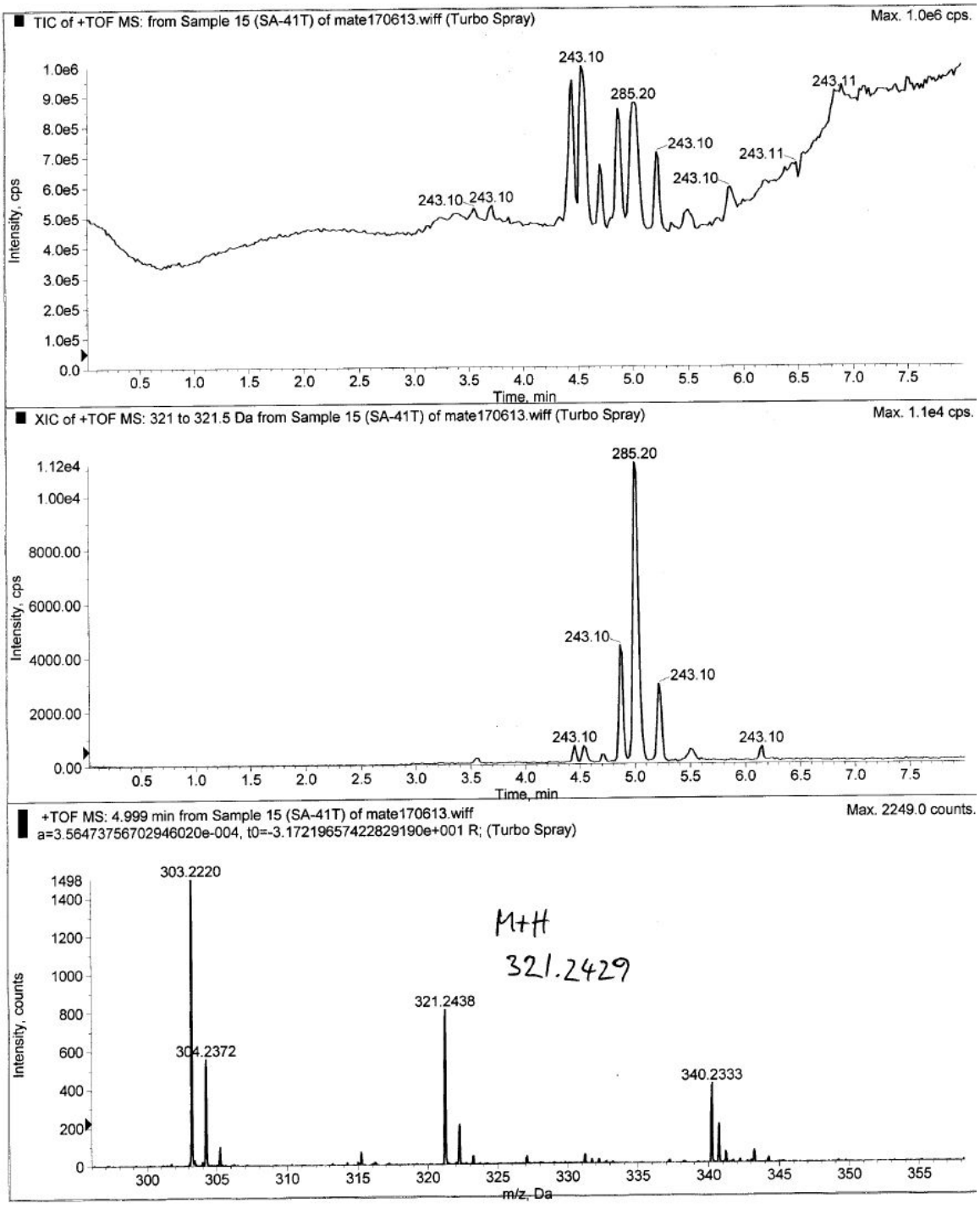

Appendix 24A. The ^{1}H NMR spectrum of normal-trachyloban-2α,6α,19-triol (**209**) observed at 800 MHz for Acetone-d_6 solution at 25 °C.

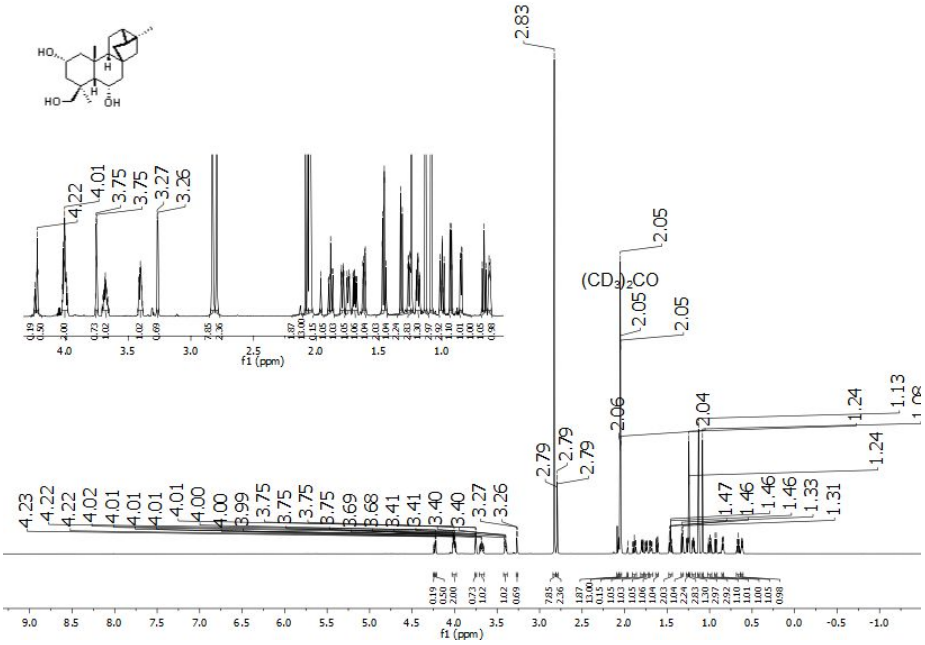

Appendix 24B. The ^{13}C NMR spectrum of normal-trachyloban-2α,6α,19-triol (**209**) observed at 200 MHz for Acetone-d_6 solution at 25 °C.

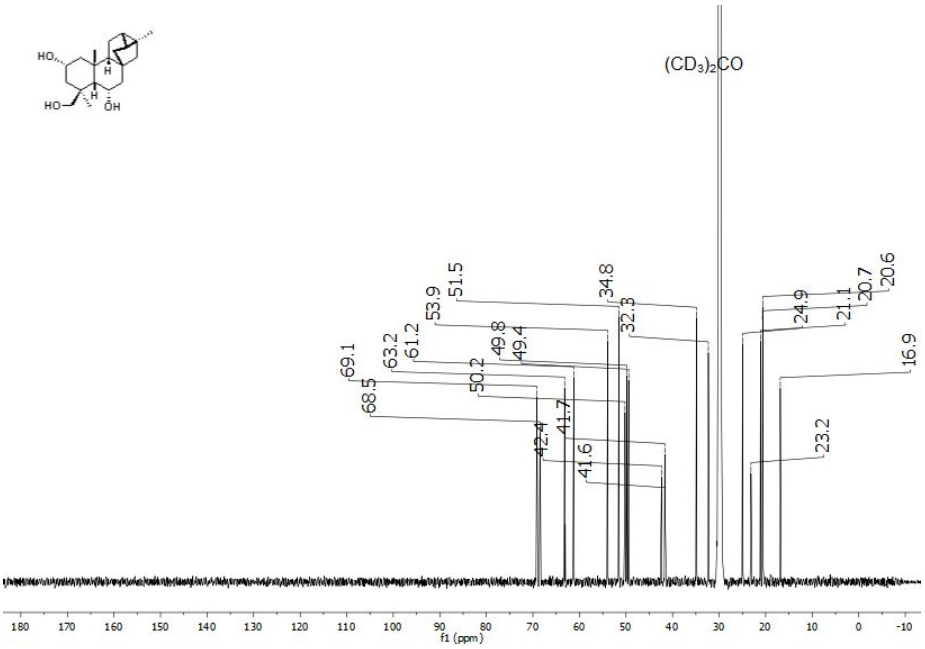

Appendix 24C. The ^{1}H-^{1}H COSY NMR spectrum of normal-trachyloban-2α,6α,19-triol (**209**) observed at 800 MHz for Acetone-d_6 solution at 25 °C.

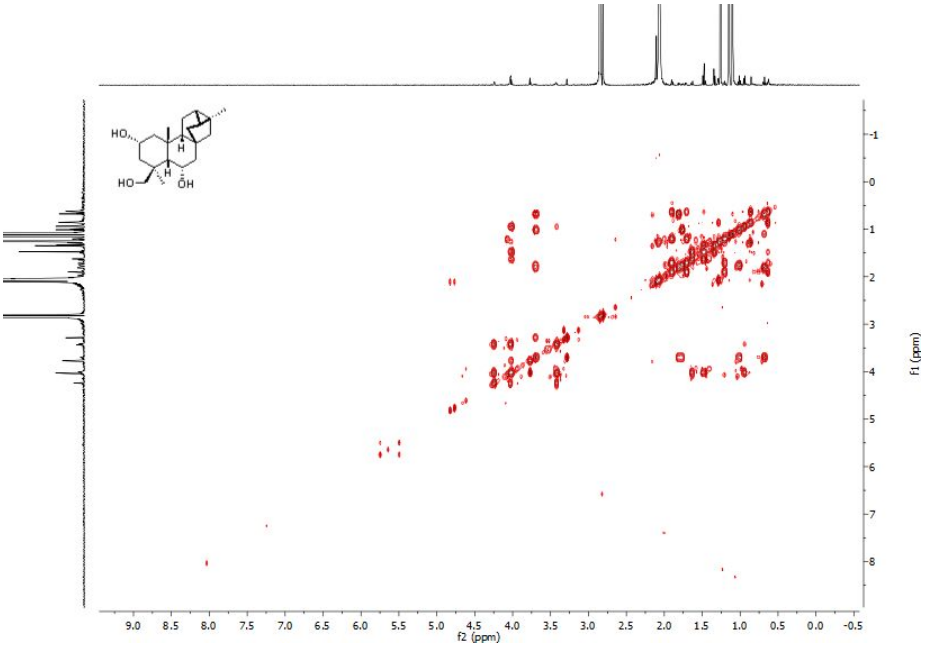

Appendix 24D. The ^{1}H-^{1}H NOESY NMR spectrum of normal-trachyloban-2α,6α,19-triol (**209**) observed at 800 MHz for Acetone-d_6 solution at 25 °C.

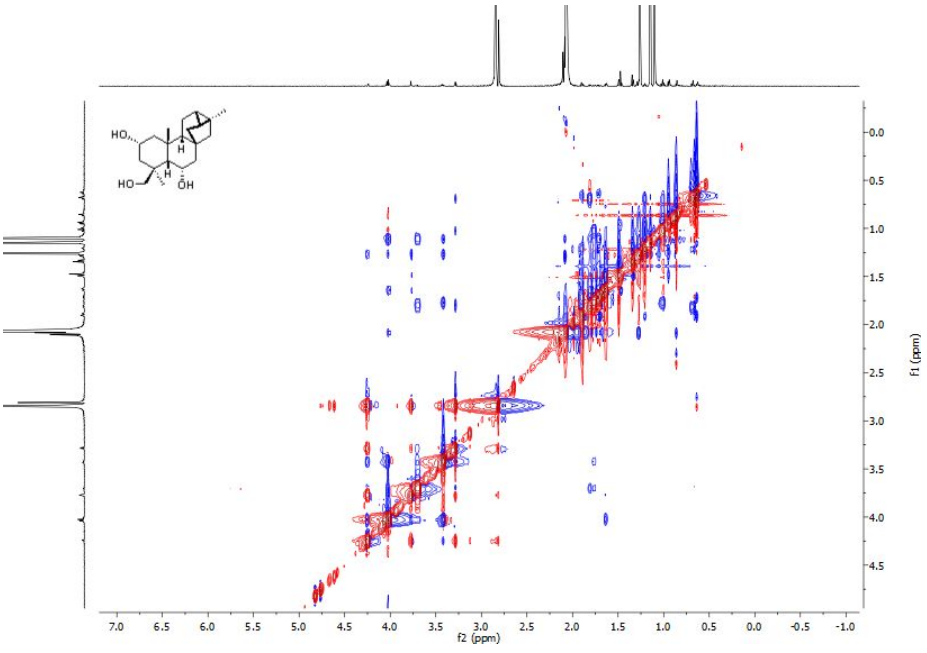

Appendix 24E. The ^{1}H-^{13}C HSCQ NMR spectrum of normal-trachyloban-2α,6α,19-triol (**209**) observed at 800 and 200 MHz for Acetone-d_6 solution at 25 °C.

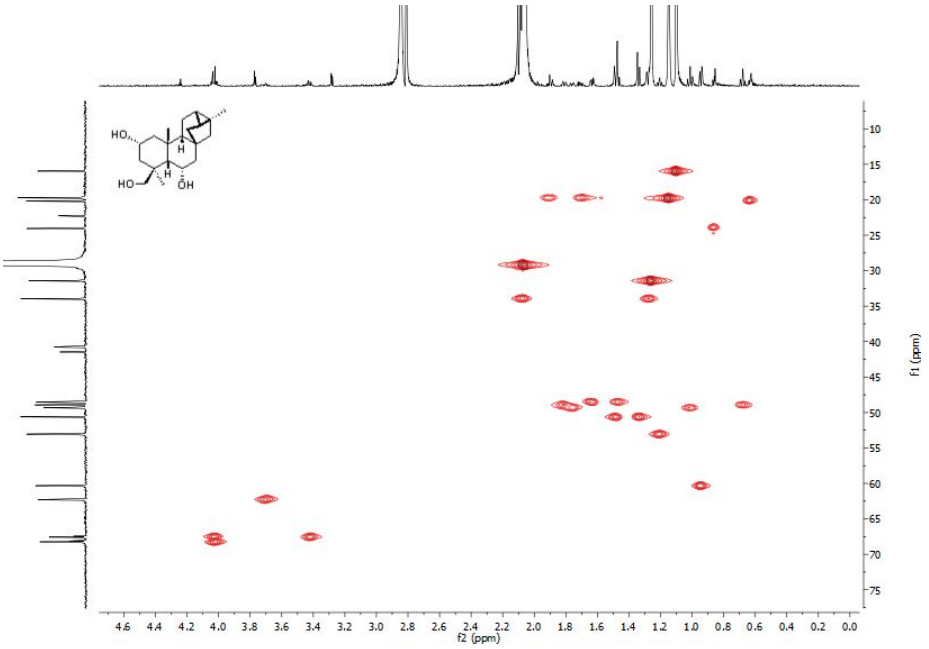

Appendix 24F. The ^{1}H-^{13}C HMBC NMR spectrum of normal-trachyloban-2α,6α,19-triol (**209**) observed at 800 and 200 MHz for Acetone-d_6 solution at 25 °C.

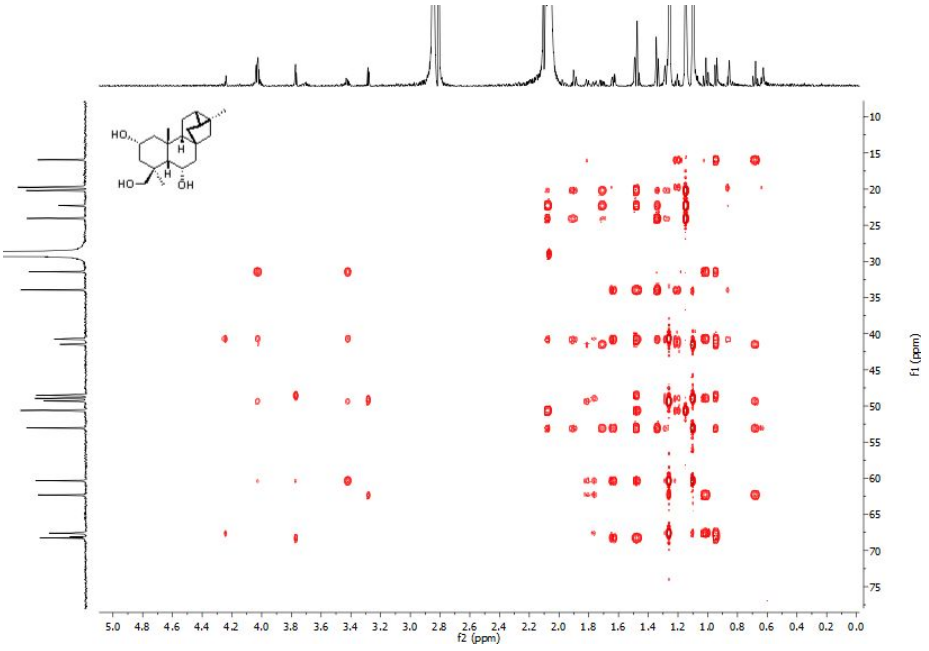

Appendix 24G. The HRMS (ESI) spectrum of normal-trachyloban-*2α*,*6α*,19-triol (**209**).

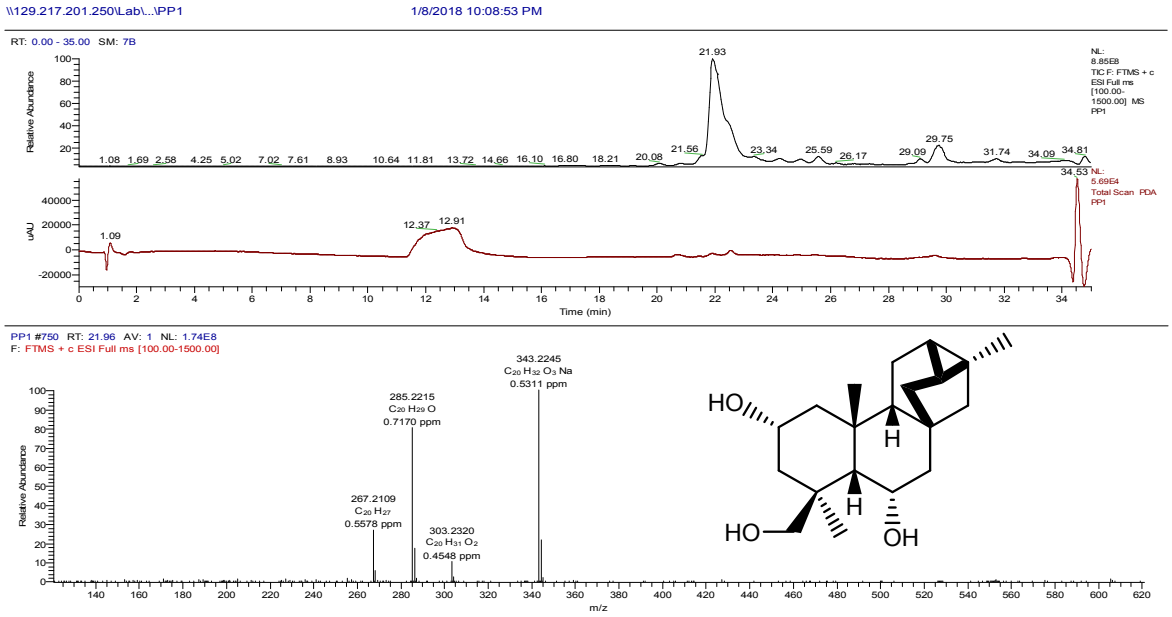

Appendix 25A. The ^{1}H NMR spectrum of *ent*-trachyloban-2β,6β,19-triol (**210**) observed at 600 MHz for $CDCl_3$ solution at 25 °C.

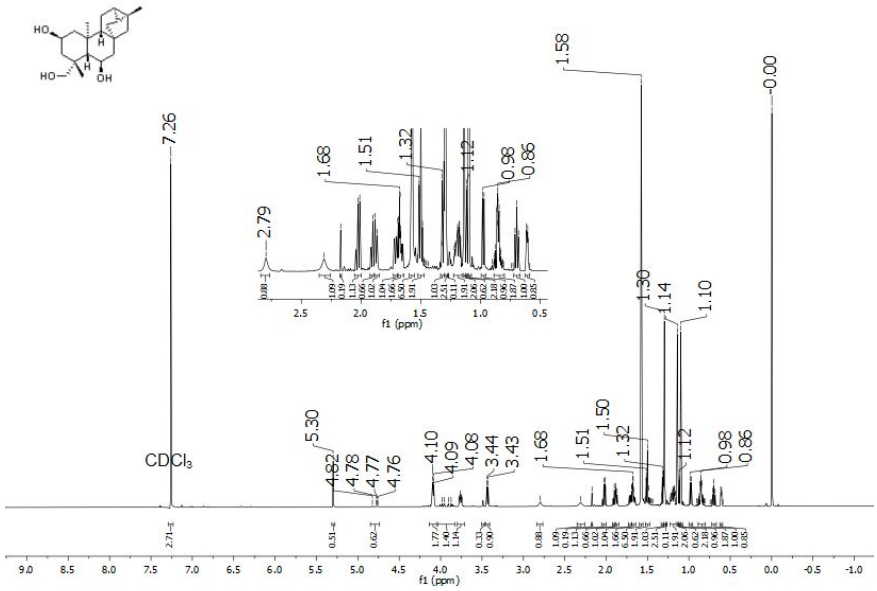

Appendix 25B. The ^{13}C NMR spectrum of *ent*-trachyloban-2β,6β,19-triol (**210**) observed at 200 MHz for $CDCl_3$ solution at 25 °C.

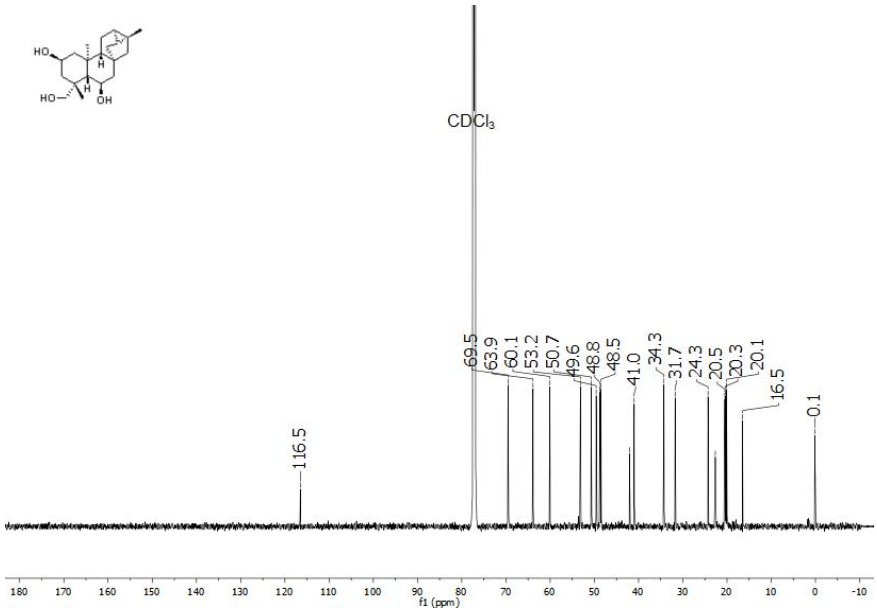

Appendix 25C. The HRMS (ESI) spectrum of *ent*-trachyloban-2β,6β,19-triol (**210**).

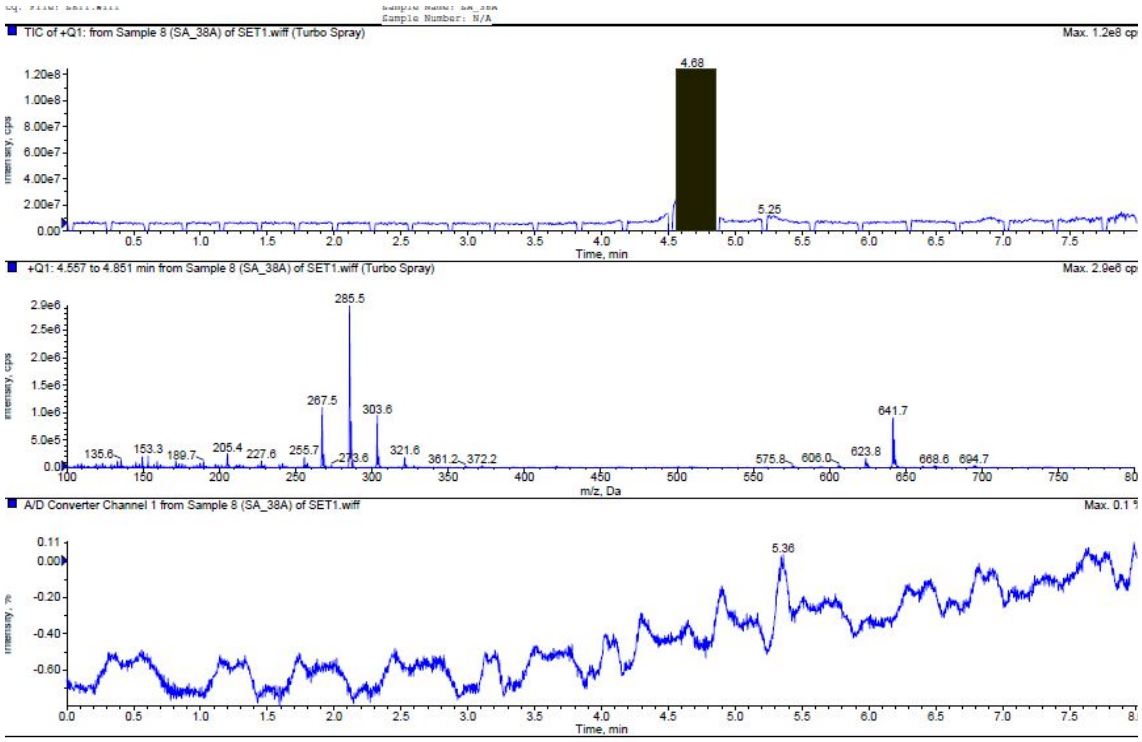

Appendix 26A. The ^{1}H NMR spectrum of *ent*-trachyloban-6β,17,19-triol (**211**) observed at 600 MHz for CD_2Cl_2 solution at 25 °C.

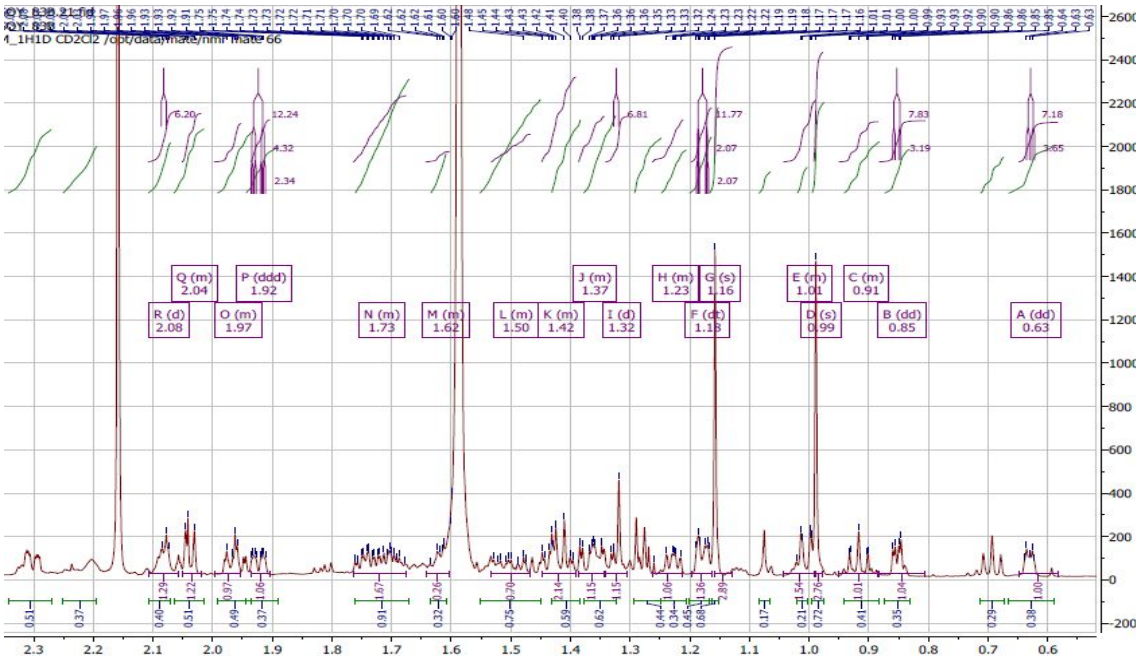

Appendix 26B. The ^{13}C NMR spectrum of *ent*-trachyloban-6β,17,19-triol (**211**) observed at 200 MHz for CD_2Cl_2 solution at 25 °C.

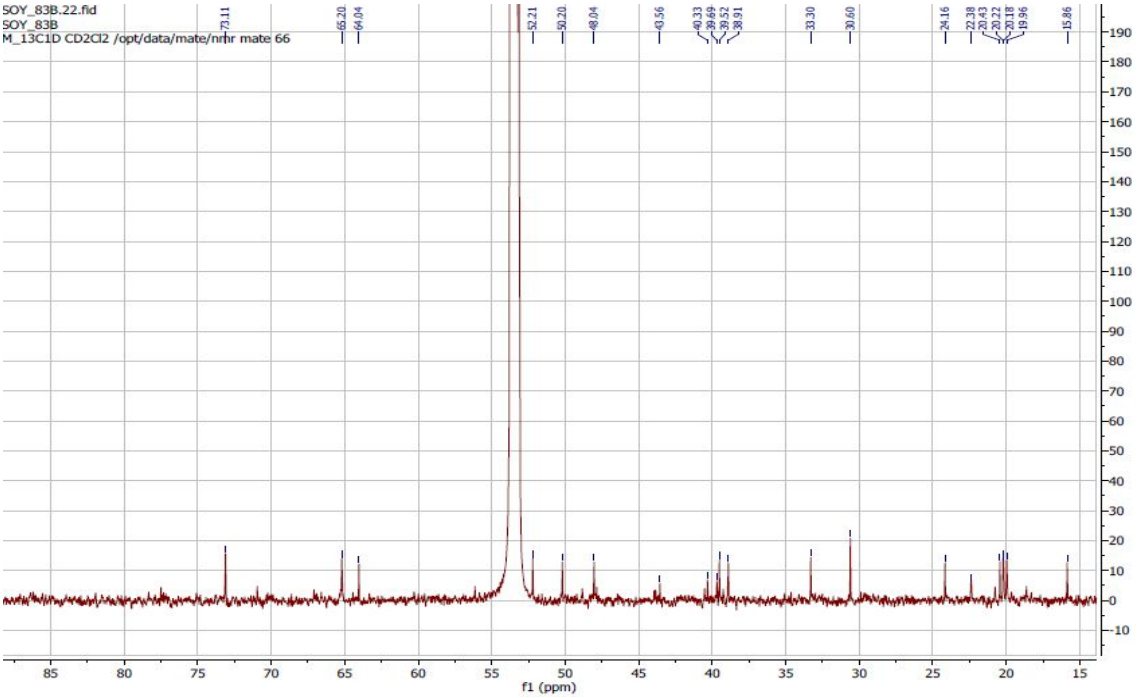

Appendix 26C. The HRMS (ESI) spectrum of *ent*-trachyloban-6β,17,19-triol (**211**).

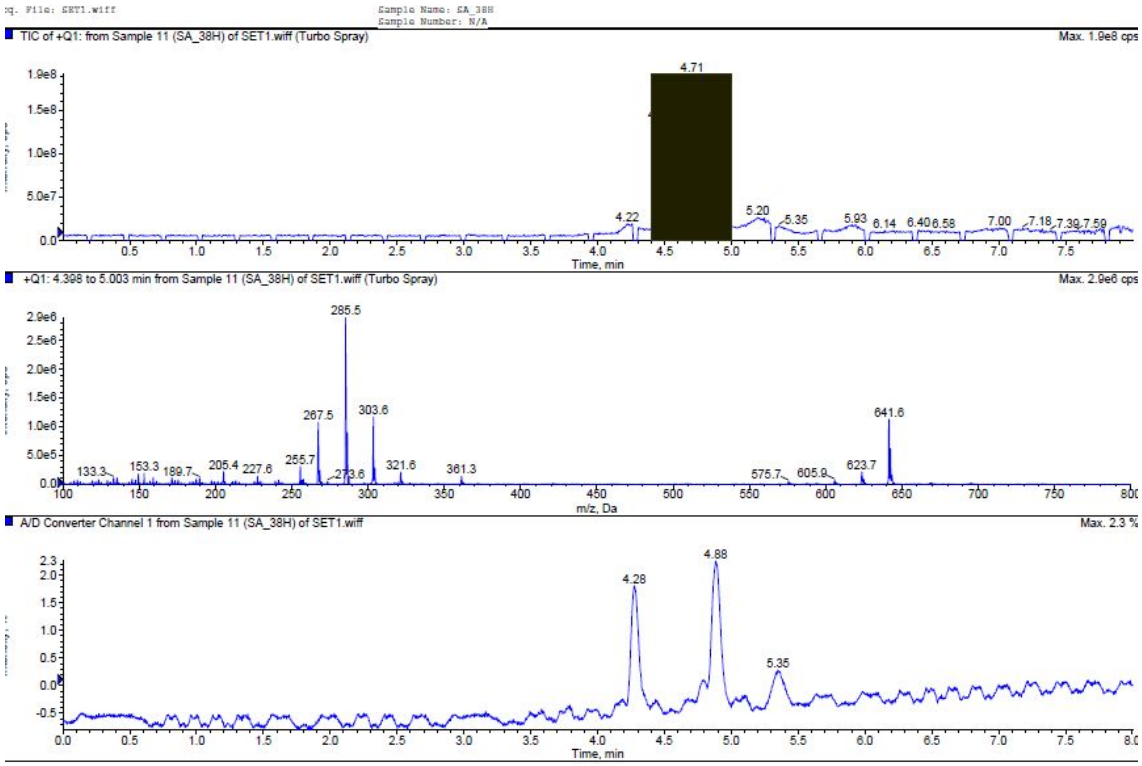

Appendix 27A. The ^{1}H NMR spectrum of 19-methoxycarbonyl-*ent*-trachyloban-17-oic acid (**212**) observed at 600 MHz for $CDCl_3$ solution at 25 °C.

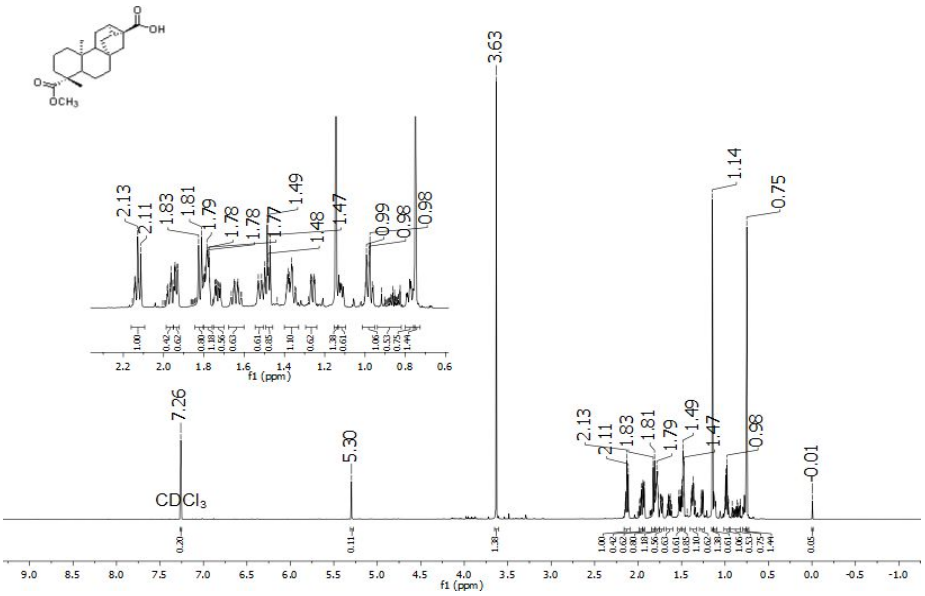

Appendix 27B. The ^{13}C NMR spectrum of 19-methoxycarbonyl-*ent*-trachyloban-17-oic acid (**212**) observed at 200 MHz for $CDCl_3$ solution at 25 °C.

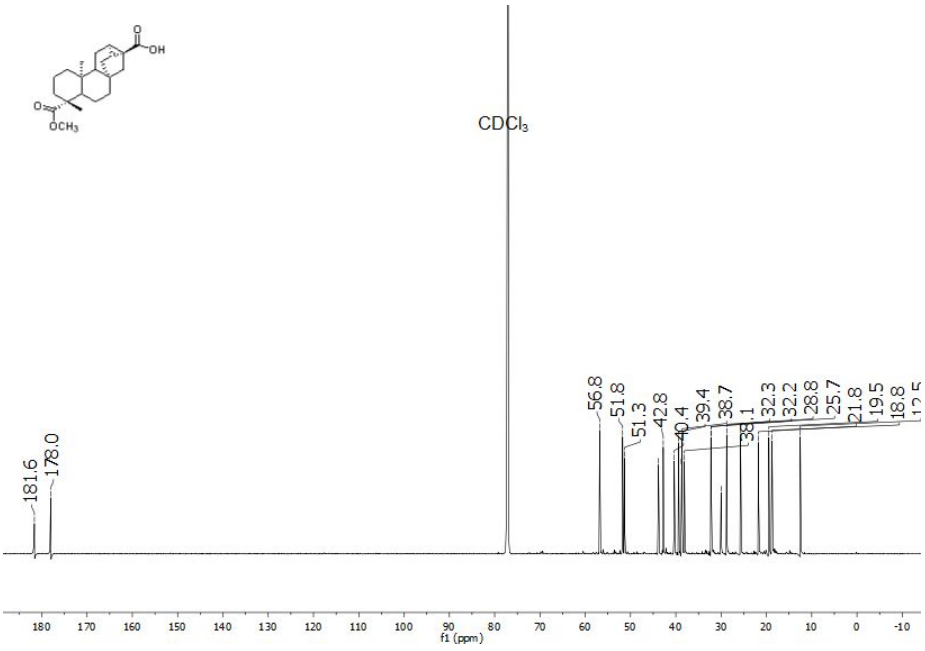

Appendix 27C. The HRMS (ESI) spectrum of 19-methoxycarbonyl-*ent*-trachyloban-17-oic acid (**212**)

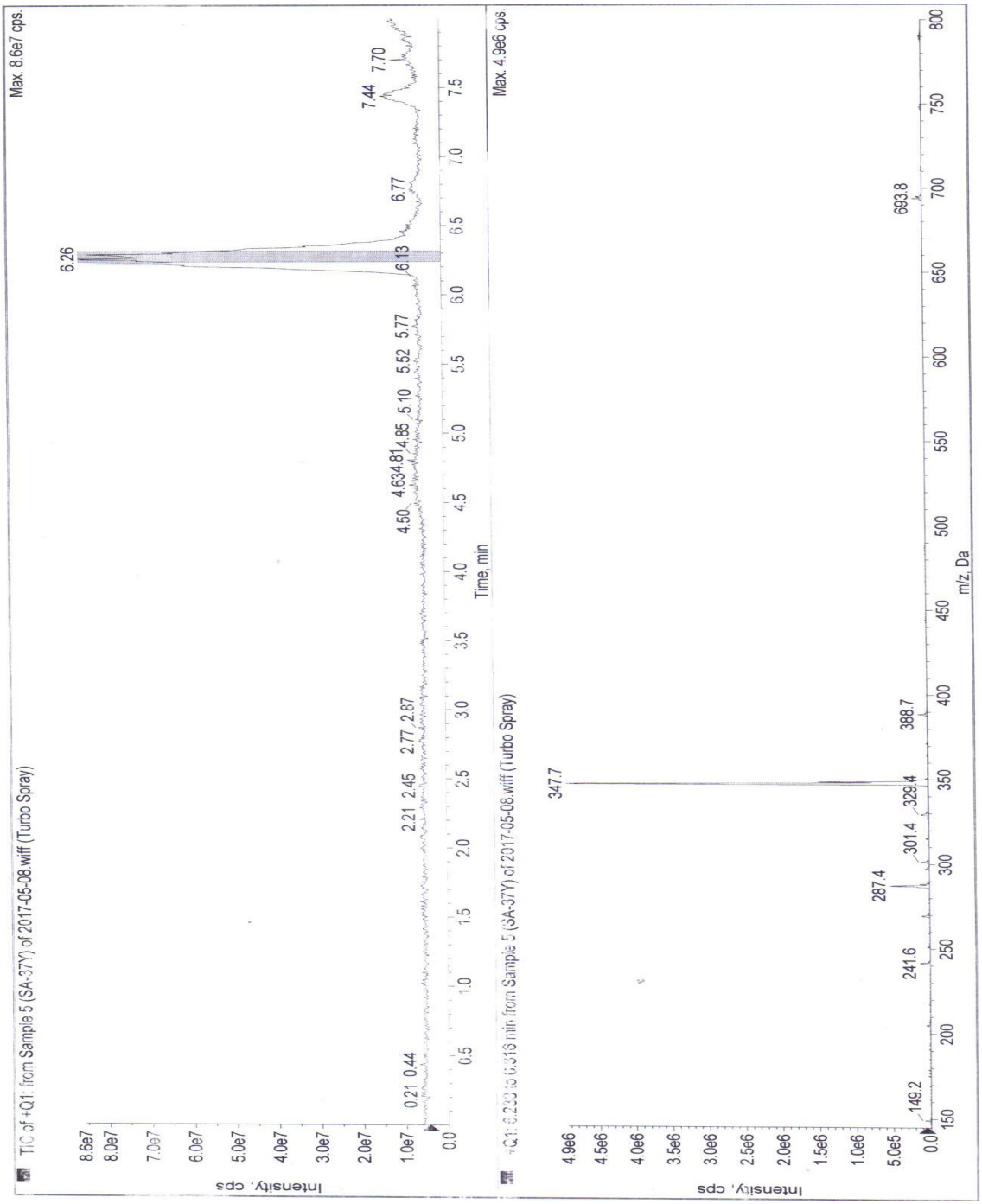

Appendix 28A. The ^{1}H NMR spectrum of *ent*-trachyloban-2β,18,19-triol (**213**) observed at 600 MHz for Acetone-d_6 solution at 25 °C.

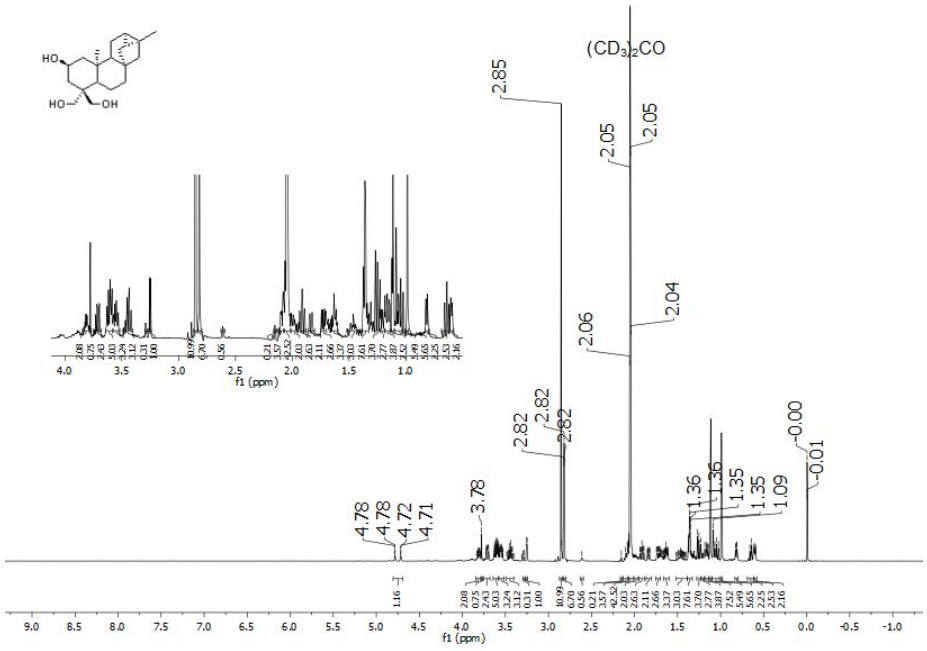

Appendix 28B. The ^{13}C NMR spectrum of *ent*-trachyloban-2β,18,19-triol (**213**) observed at 200 MHz for Acetone-d_6 solution at 25 °C.

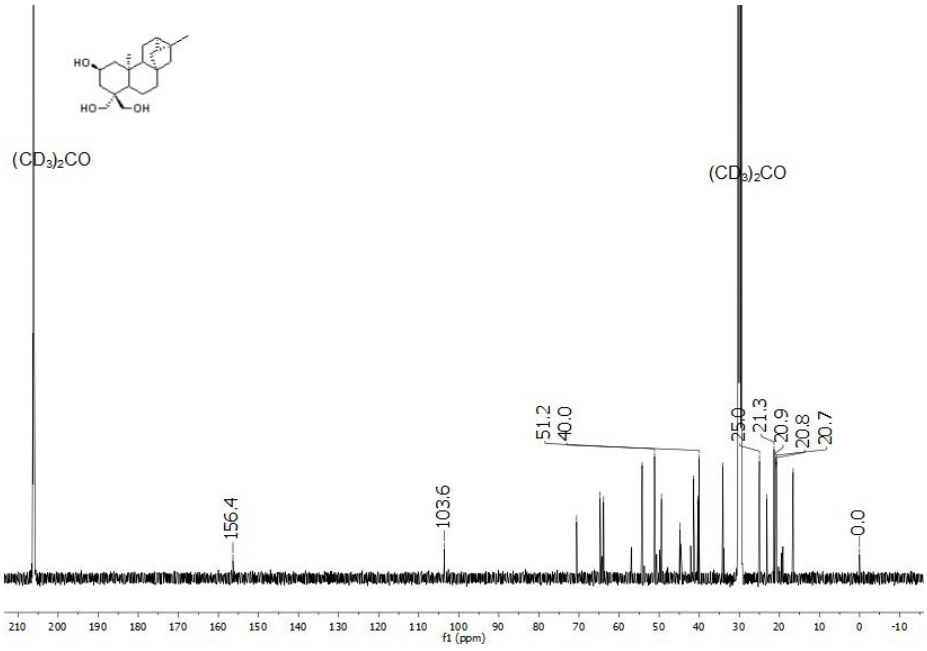

Appendix 53C. The ESIMS spectrum of *ent*-trachyloban-2β,18,19-triol (**213**)

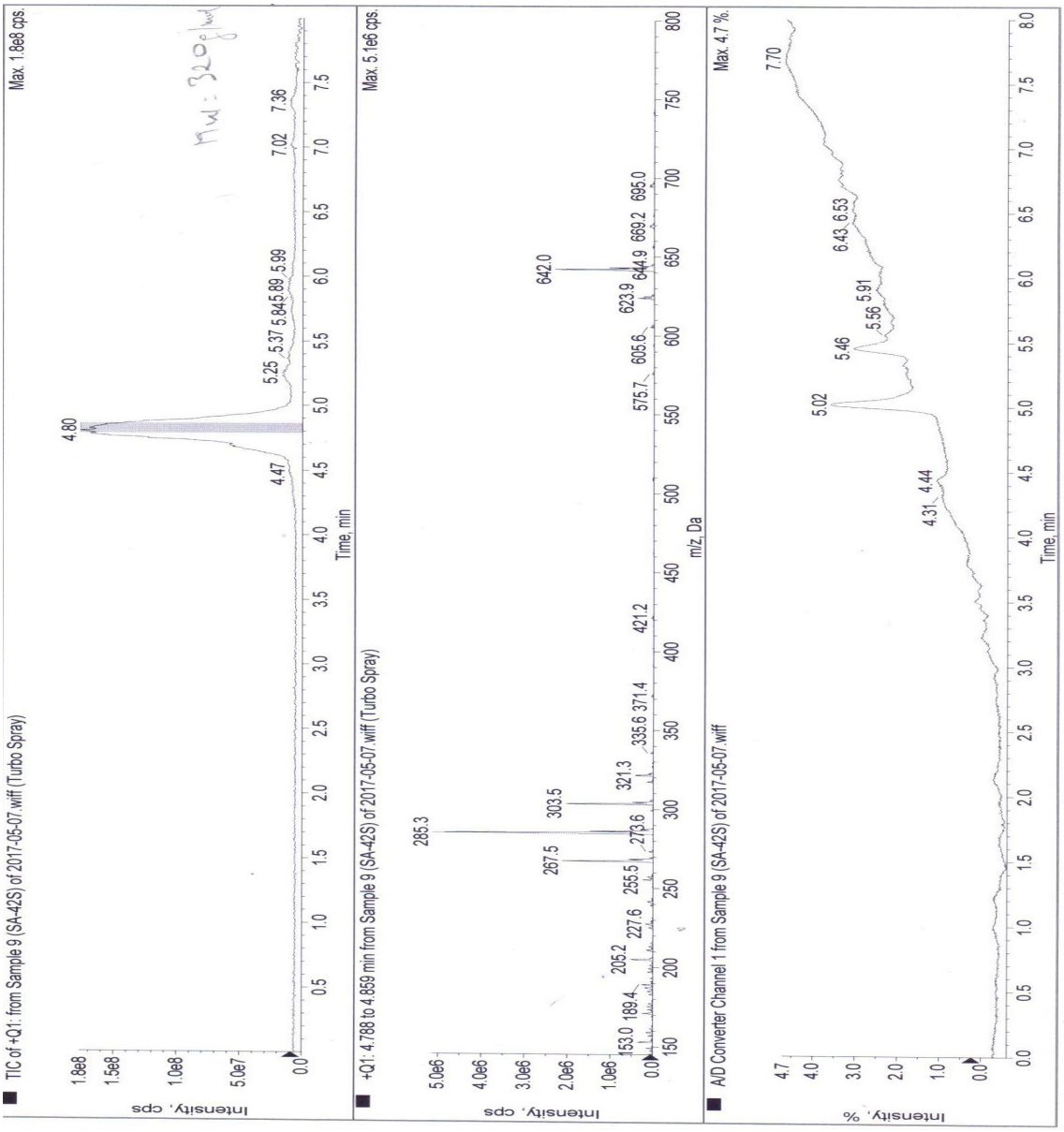

Appendix 29A. The ^{1}H NMR spectrum of methyl-15α,16α,17-trihydroxy-ent-kauran-19-oate (**214**) observed at 800 MHz for $CDCl_3$ solution at 25 °C.

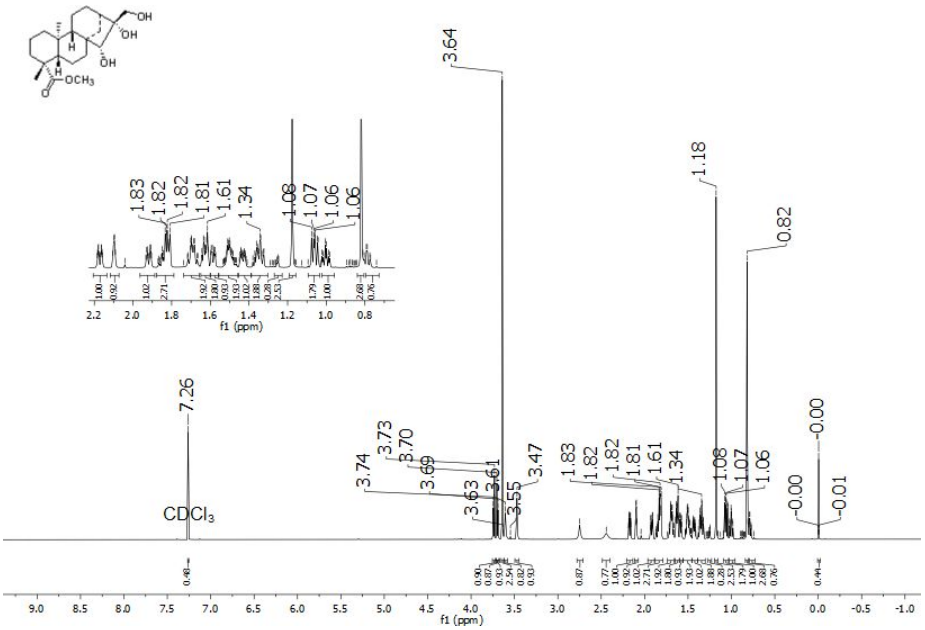

Appendix 29B. The ^{13}C NMR spectrum of methyl-15α,16α,17-trihydroxy-ent-kauran-19-oate (**214**) observed at 200 MHz for $CDCl_3$ solution at 25 °C.

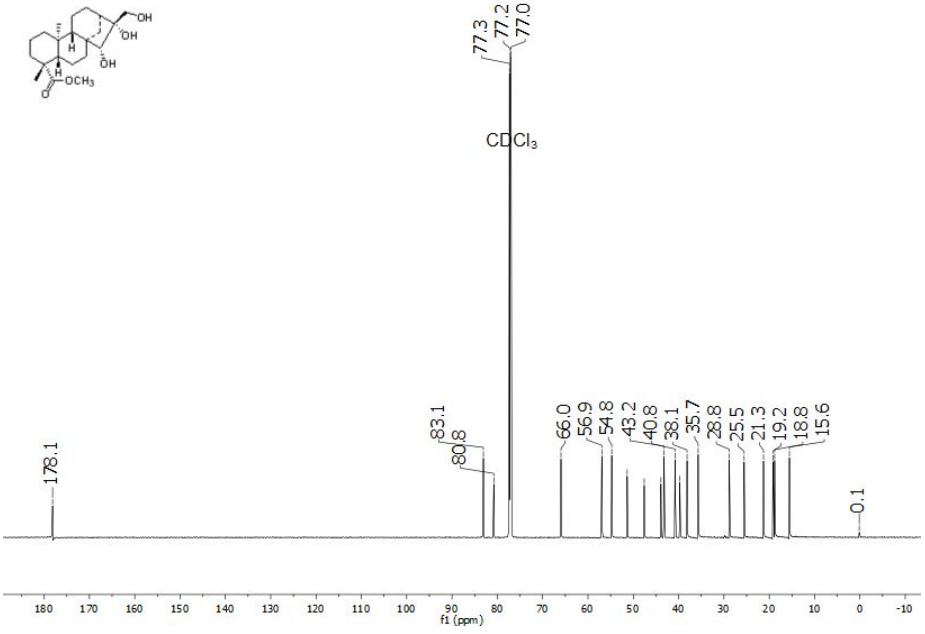

Appendix 29C. The ^{1}H-^{1}H COSY NMR spectrum of methyl-15α,16α,17-trihydroxy-ent-kauran-19-oate (**214**) observed at 800 MHz for $CDCl_3$ solution at 25 °C.

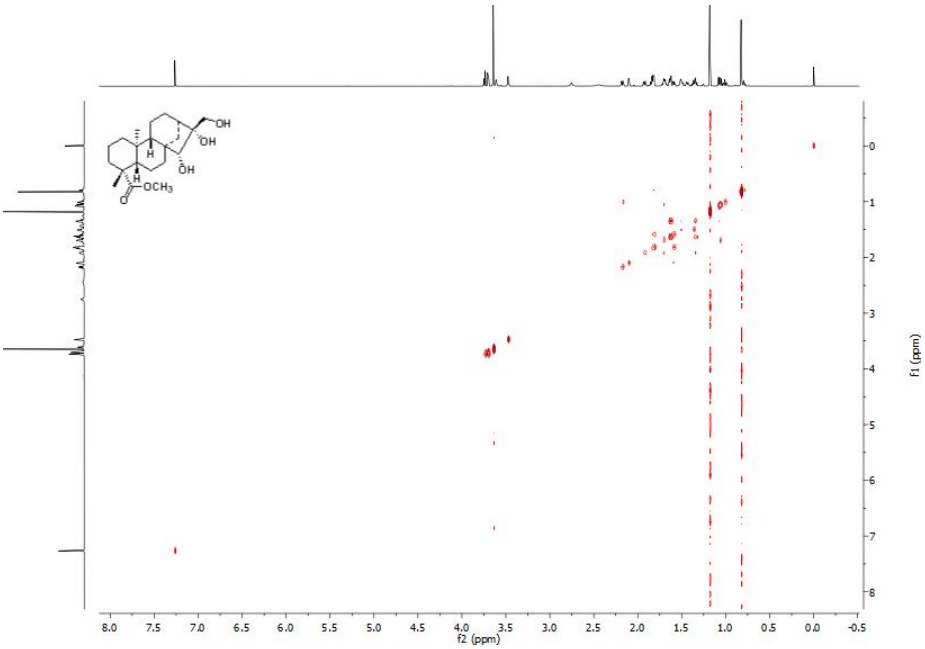

Appendix 29D. The ^{1}H-^{1}H NOSEY NMR spectrum of methyl-15α,16α,17-trihydroxy-ent-kauran-19-oate (**214**) observed at 800 MHz for $CDCl_3$ solution at 25 °C.

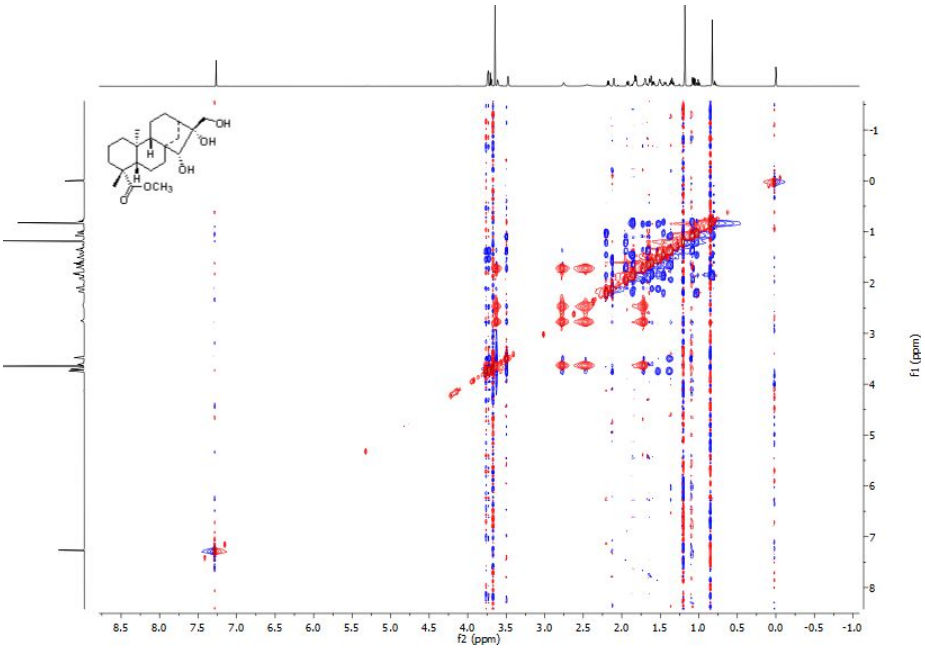

Appendix 29E. The ^{1}H-^{13}C HSQC NMR spectrum of methyl-15α,16α,17-trihydroxy-ent-kauran-19-oate (**214**) observed at 800 and 200 MHz for $CDCl_3$ solution at 25 °C.

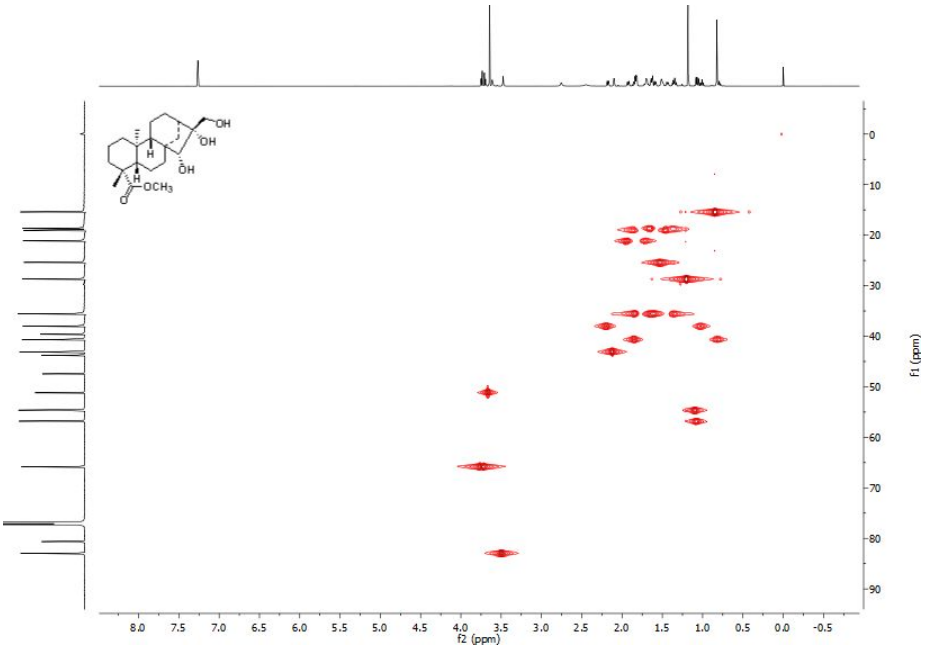

Appendix 29F. The ^{1}H-^{13}C HMBC NMR spectrum of methyl-15α,16α,17-trihydroxy-ent-kauran-19-oate (**214**) observed at 800 and 200 MHz for $CDCl_3$ solution at 25 °C.

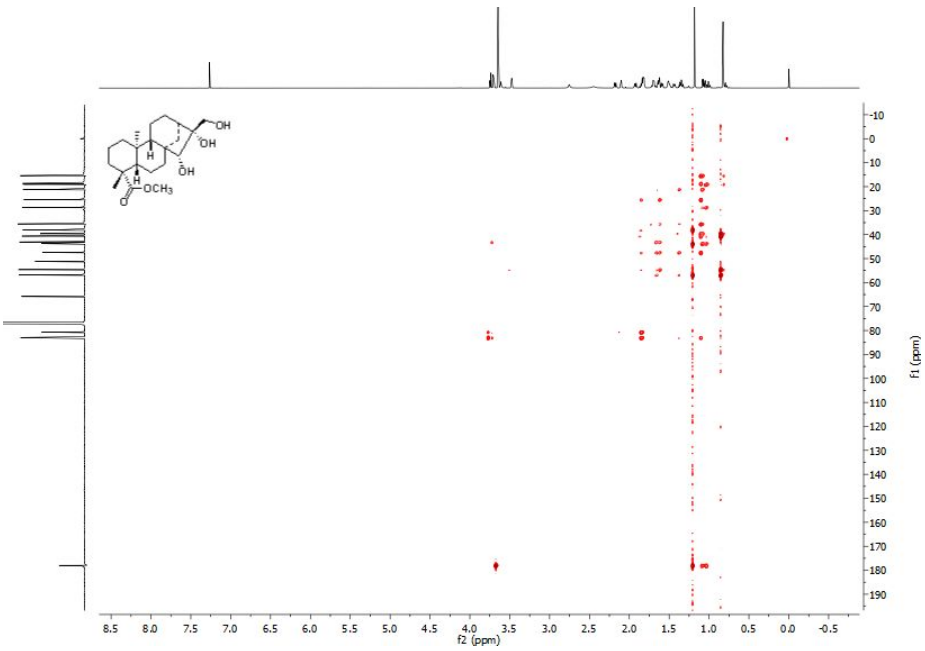

Appendix 29G. The HRMS (ESI) spectrum of methyl-15α,16α,17-trihydroxy-ent-kauran-19-oate (**214**).

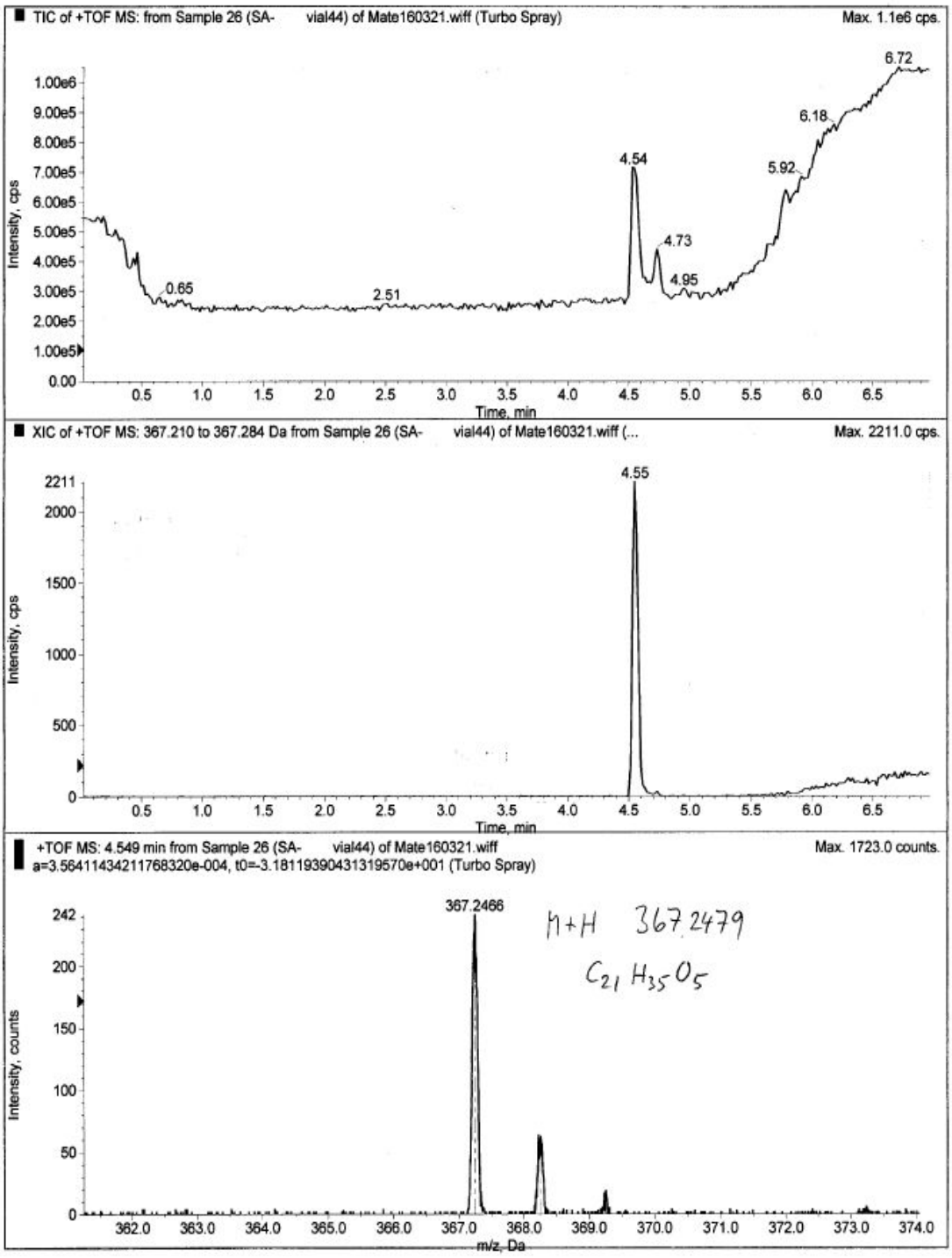

Appendix 30A. The ^{1}H NMR spectrum of methyl-16α,17-epoxy-*ent*-kauran-19-oate (**215**) observed at 800 MHz for $CDCl_3$ solution at 25 °C.

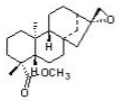

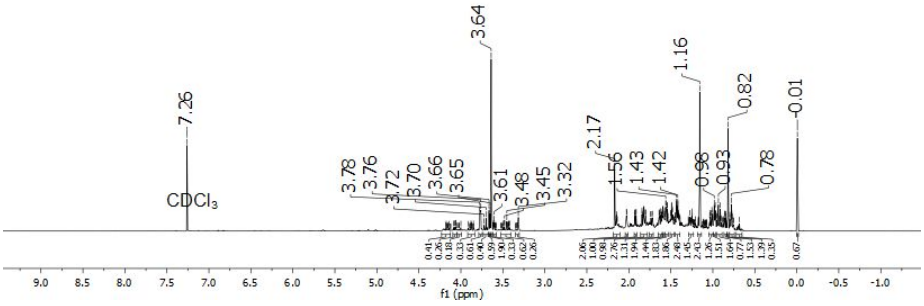

Appendix 30B. The ^{13}C NMR spectrum of methyl-16α,17-epoxy-*ent*-kauran-19-oate (**215**) observed at 200 MHz for $CDCl_3$ solution at 25 °C.

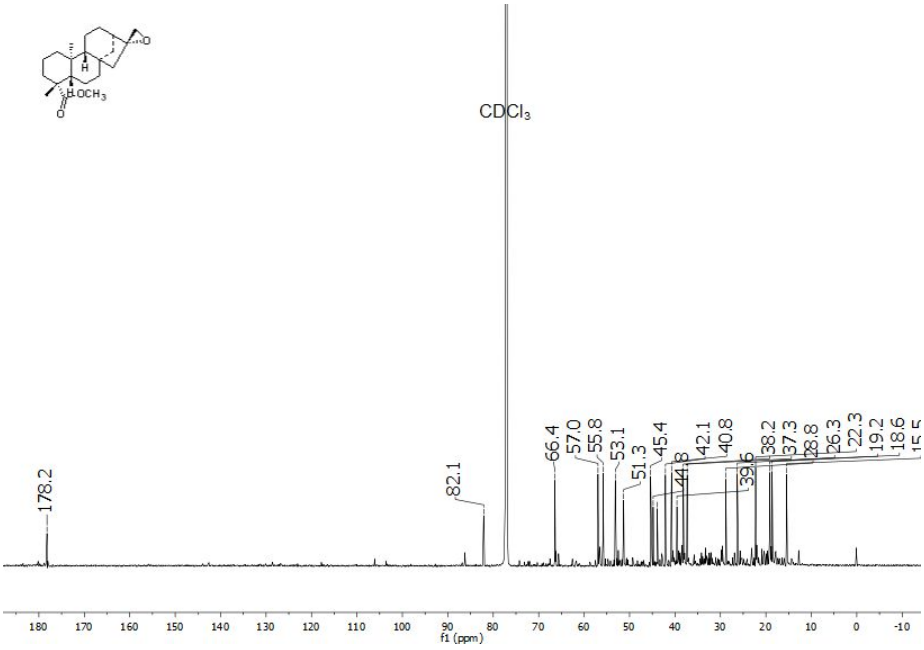

Appendix 31A. The ^{1}H NMR spectrum of 16α,17-dihydroxy-*ent*-kaur-20-oic acid (**216**) observed at 800 MHz for Acetone-d_6 solution at 25 °C.

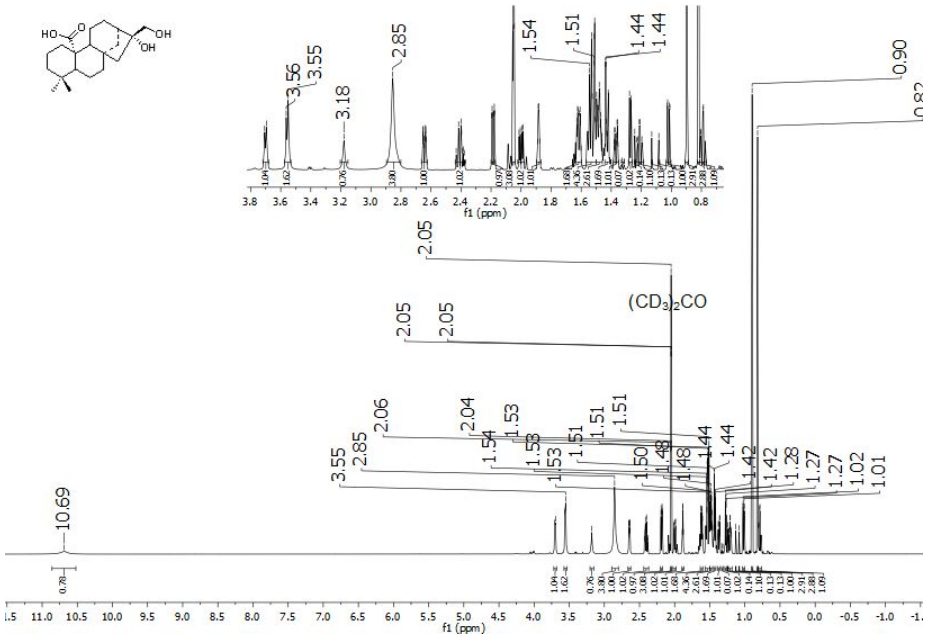

Appendix 31B. The ^{13}C NMR spectrum of 16α,17-dihydroxy-*ent*-kaur-20-oic acid (**216**) observed at 200 MHz for Acetone-d_6 solution at 25 °C.

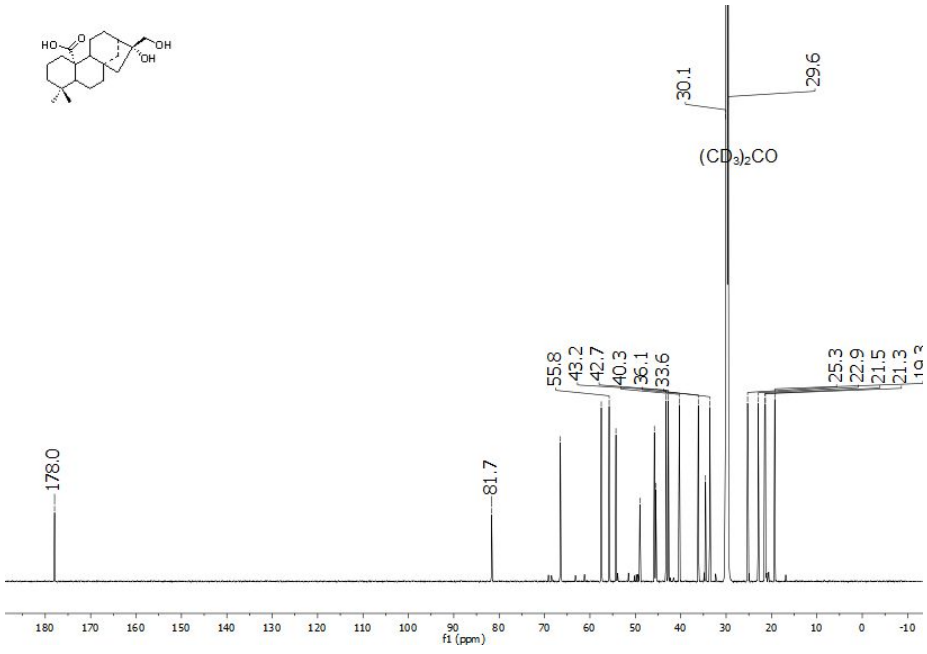

Appendix 31C. The ESIMS spectrum of 6β,18,19-16α,17-dihydroxy-*ent*-kaur-20-oic acid (**216**)

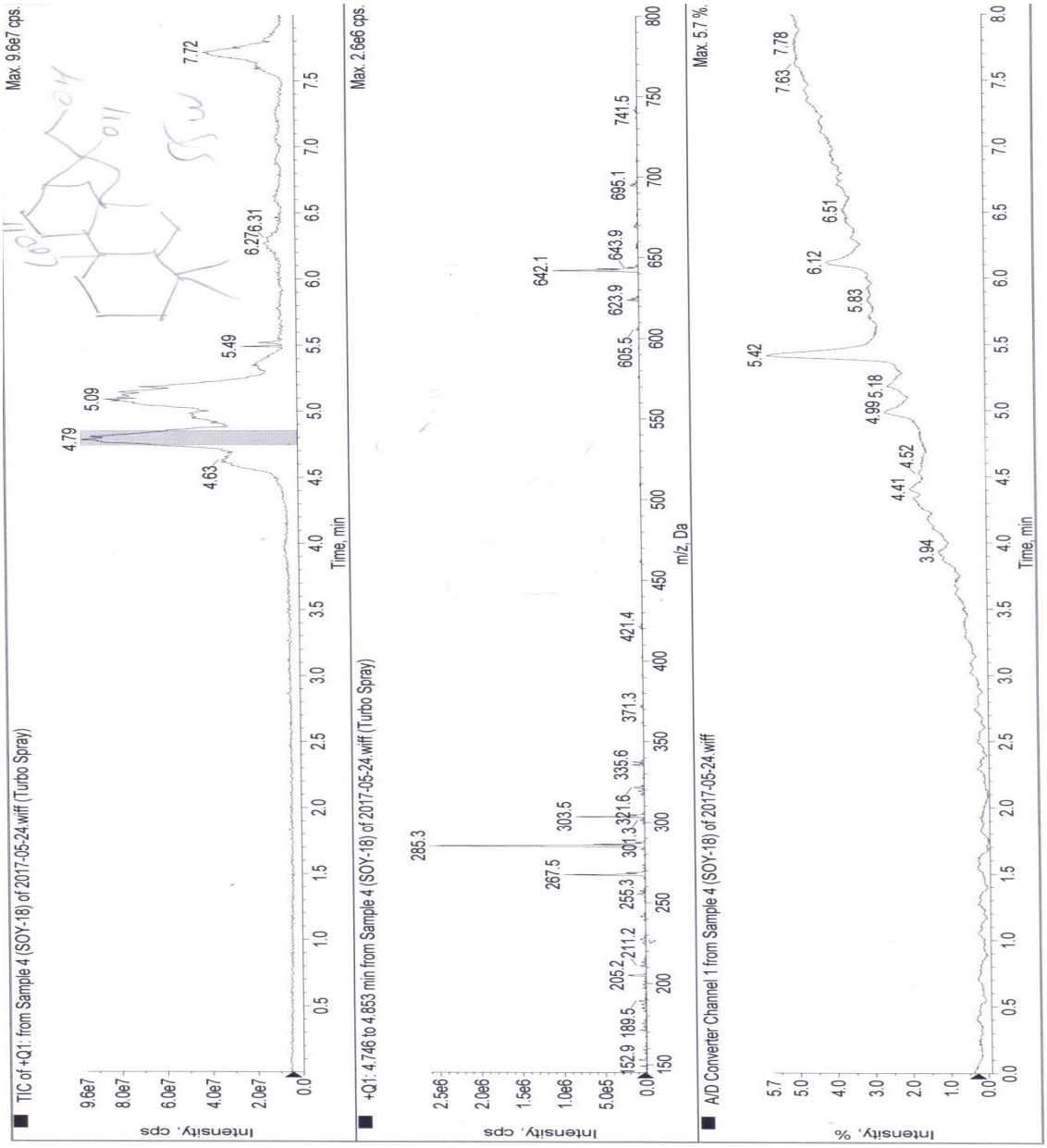

Appendix 32A. The ^{1}H NMR spectrum of 18,19-dihydroxy-*ent*-kaur-16-en-2-one (**217**) observed at 800 MHz for Acetone-d_6 solution at 25 °C.

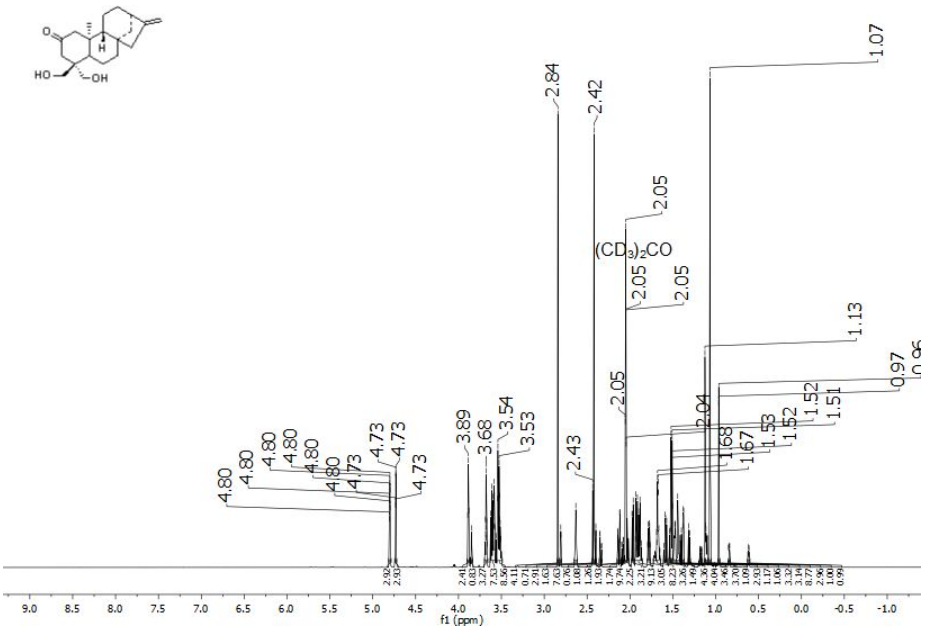

Appendix 32B. The ^{13}C NMR spectrum of 18,19-dihydroxy-*ent*-kaur-16-en-2-one **(217)** observed at 200 MHz for Acetone-d_6 solution at 25 °C.

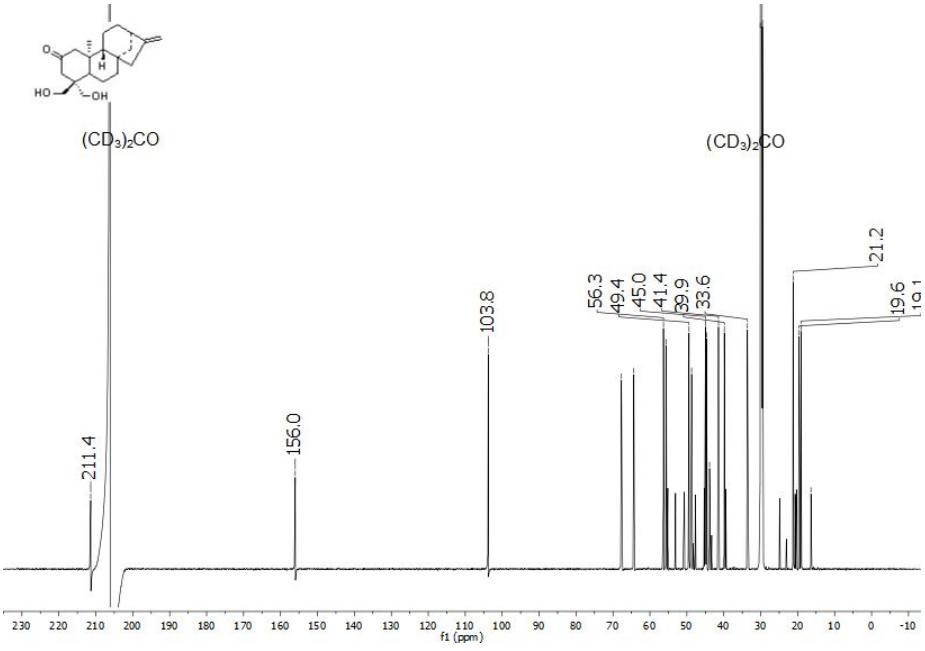

Appendix 32C. The ESIMS spectrum of 18,19-dihydroxy-*ent*-kaur-16-en-2-one **(217)**

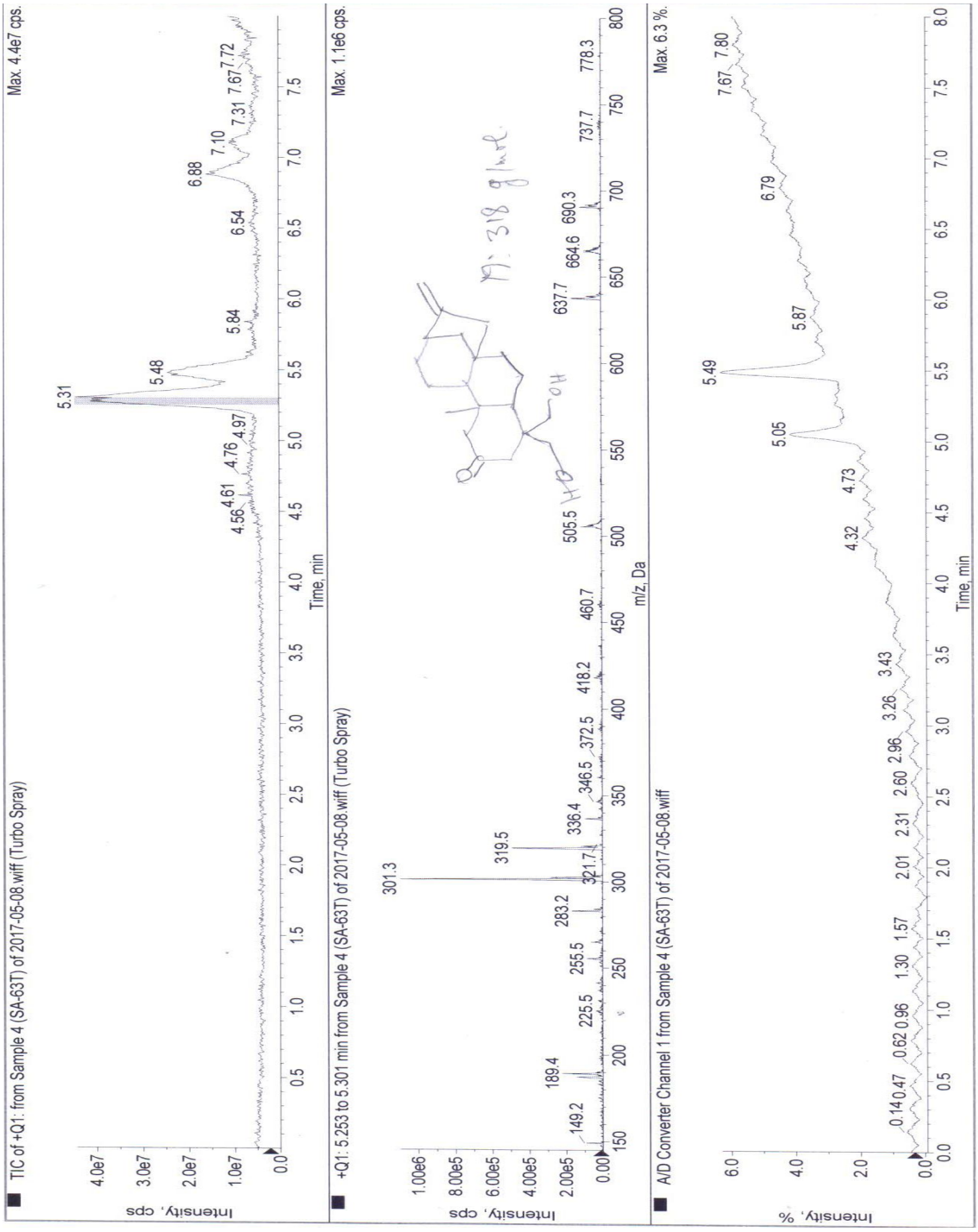

Appendix 33A. The ^{1}H NMR spectrum of 18,19-Dihydroxy-normal-kaur-16-en-2-one (**218**) observed at 800 MHz for Acetone-d_6 solution at 25 °C.

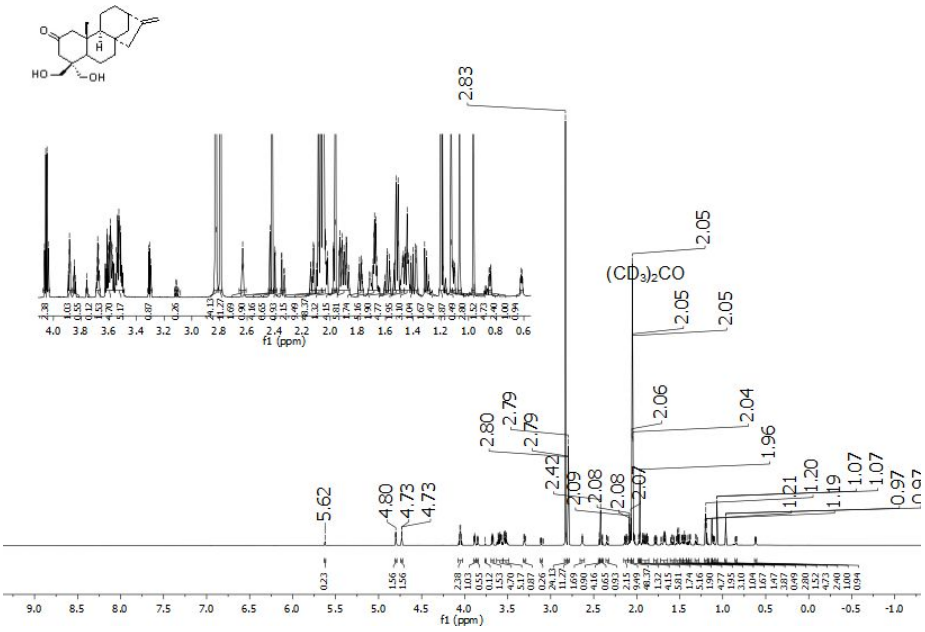

Appendix 33B. The ^{13}C NMR spectrum of 18,19-Dihydroxy-normal-kaur-16-en-2-one **(218)** observed at 200 MHz for Acetone-d_6 solution at 25 °C.

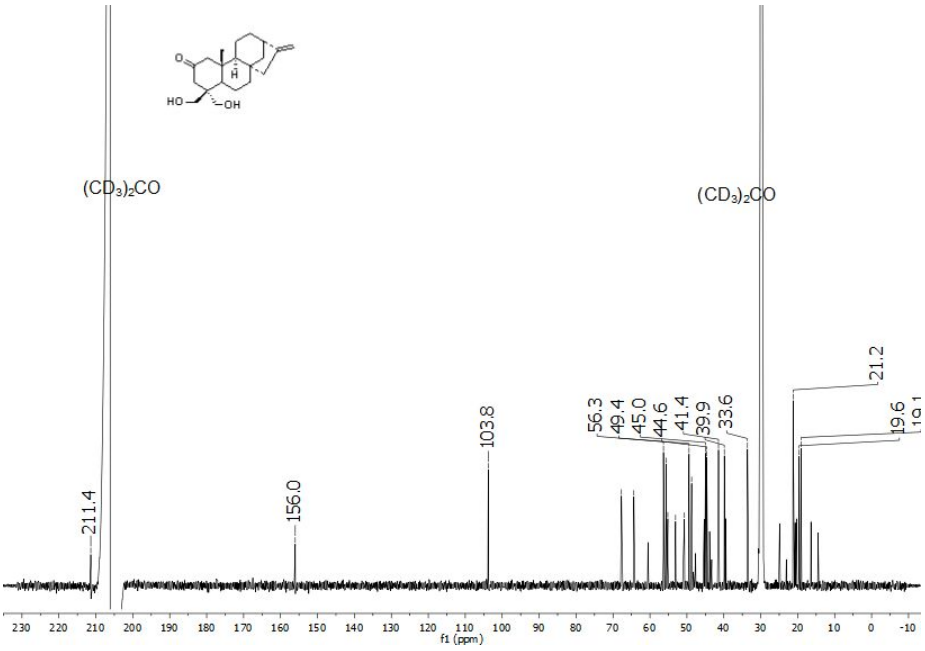

Appendix 29G. The HRMS (ESI) spectrum of 18,19-Dihydroxy-normal-kaur-16-en-2-one (**218**).

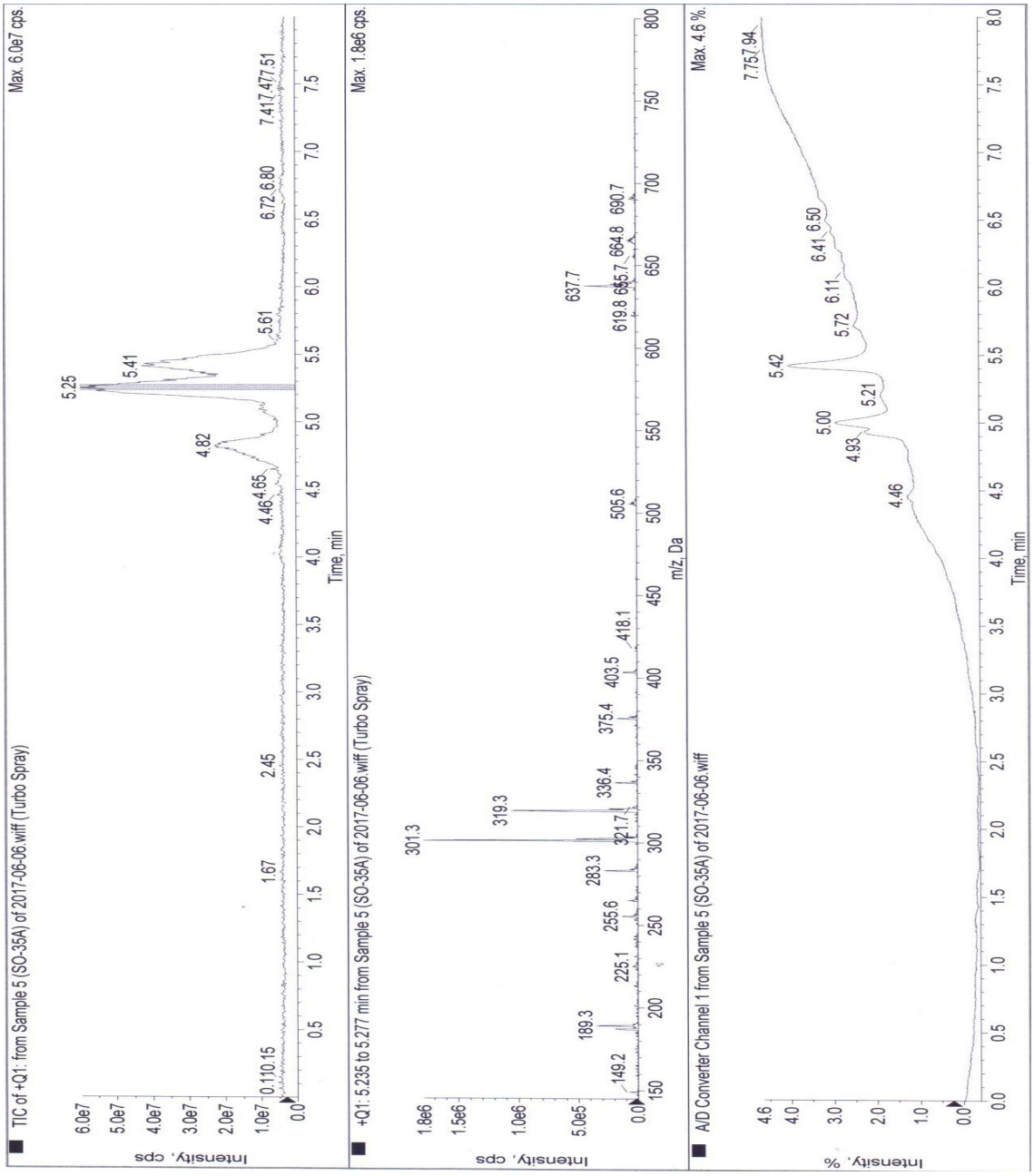

Appendix 34A. The ^{1}H NMR spectrum of 5-hydroxy-7,2',3',4',5'-pentamethoxy-flavone **(220)** observed at 600 MHz for $CDCl_3$ solution at 25 °C.

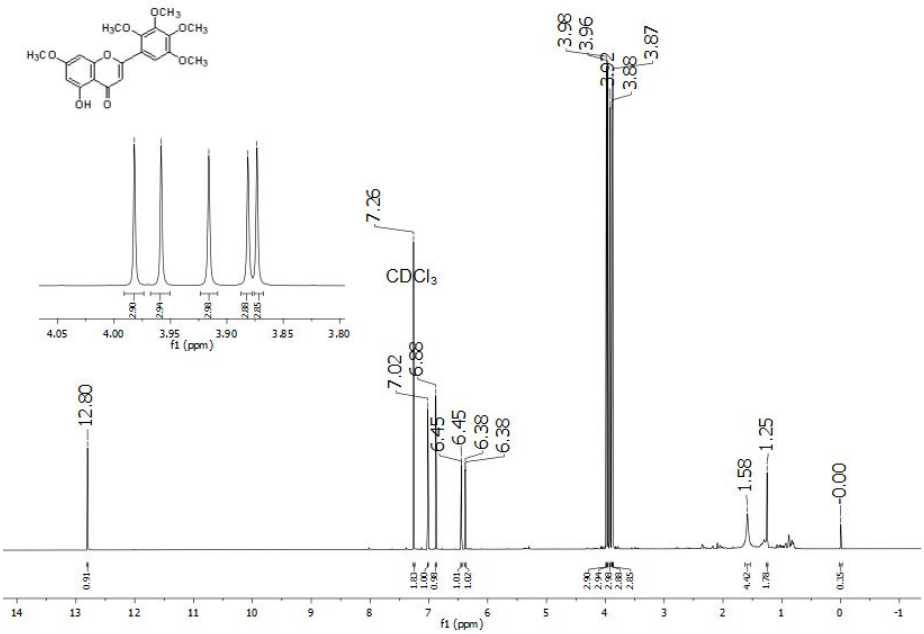

Appendix 34B. The ^{13}C NMR spectrum of 5-hydroxy-7,2',3',4',5'-pentamethoxy-flavone **(220)** observed at 200 MHz for $CDCl_3$ solution at 25 °C.

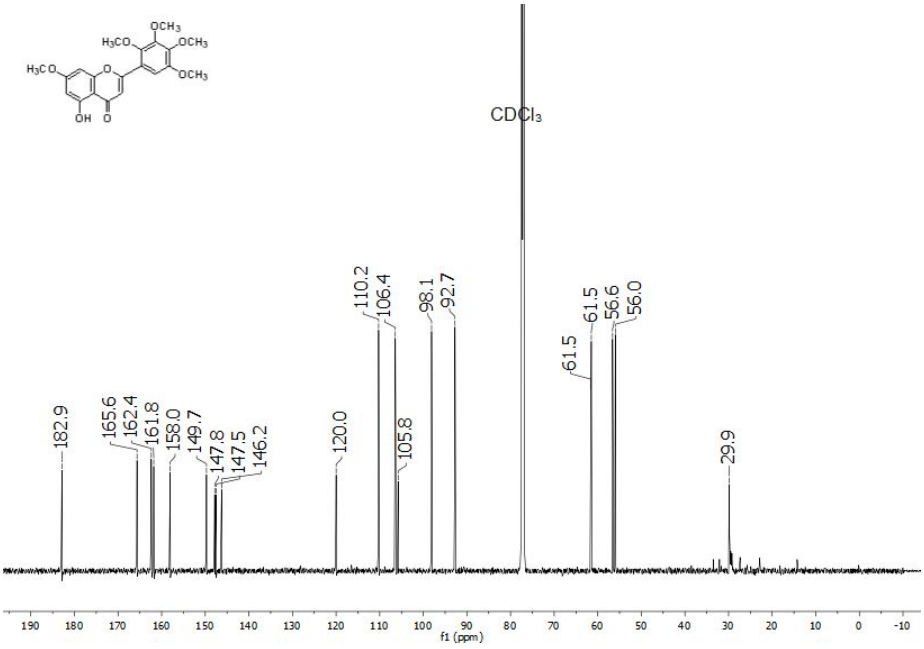

Appendix 34C. The HRMS (ESI) spectrum of 5-hydroxy-7,2',3',4',5'-pentamethoxy-flavone (**220**).

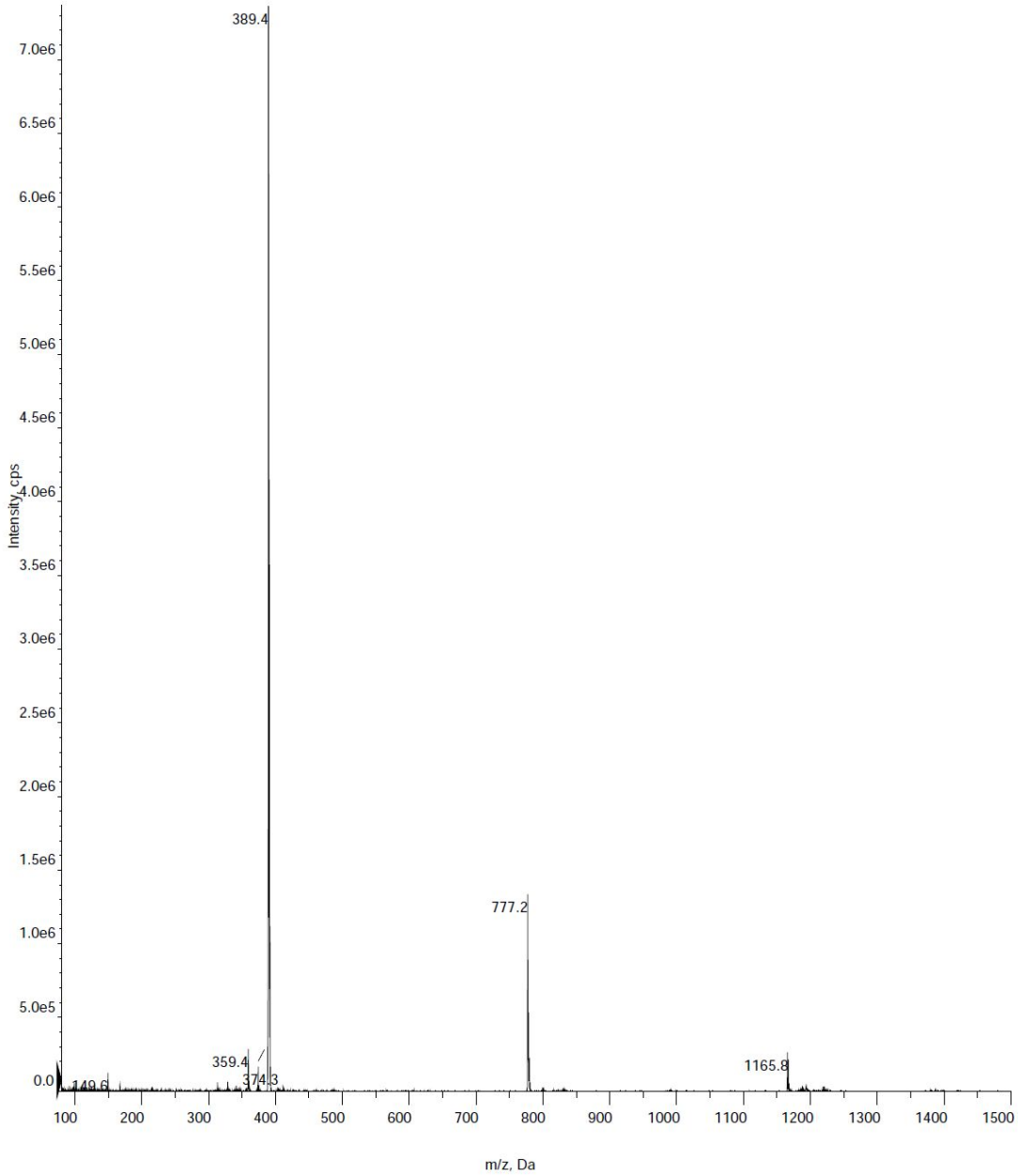

Appendix 35A. The ^{1}H NMR spectrum of 5,7-dihydroxy-2',3',4',5'-tetramethoxyflavone **(221)** observed at 600 MHz for CD_3CN solution at 25 °C.

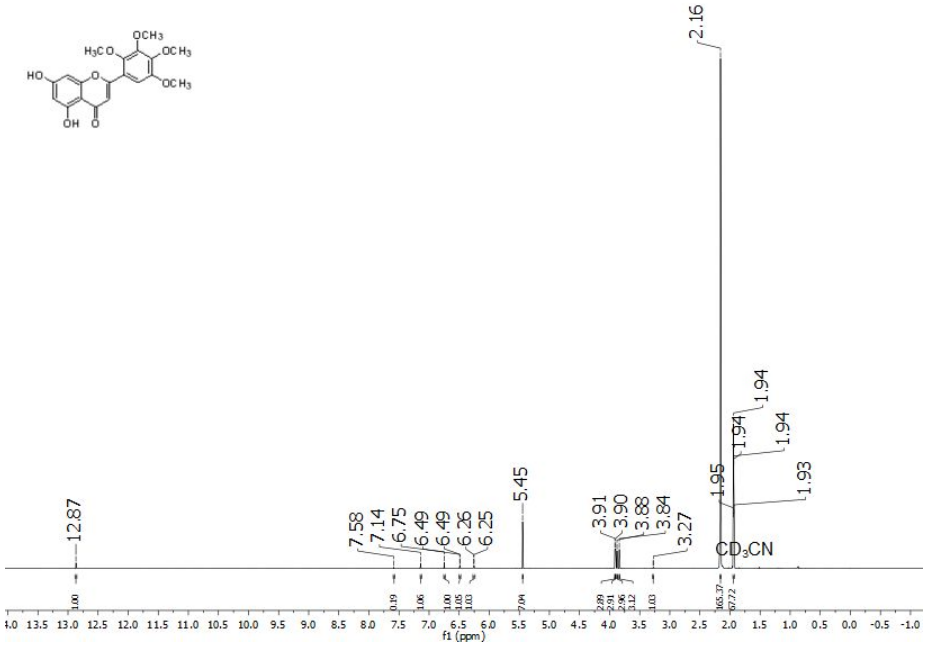

Appendix 35B. The ^{13}C NMR spectrum of 5,7-dihydroxy-2',3',4',5'-tetramethoxyflavone **(221)** observed at 200 MHz for CD_3CN solution at 25 °C.

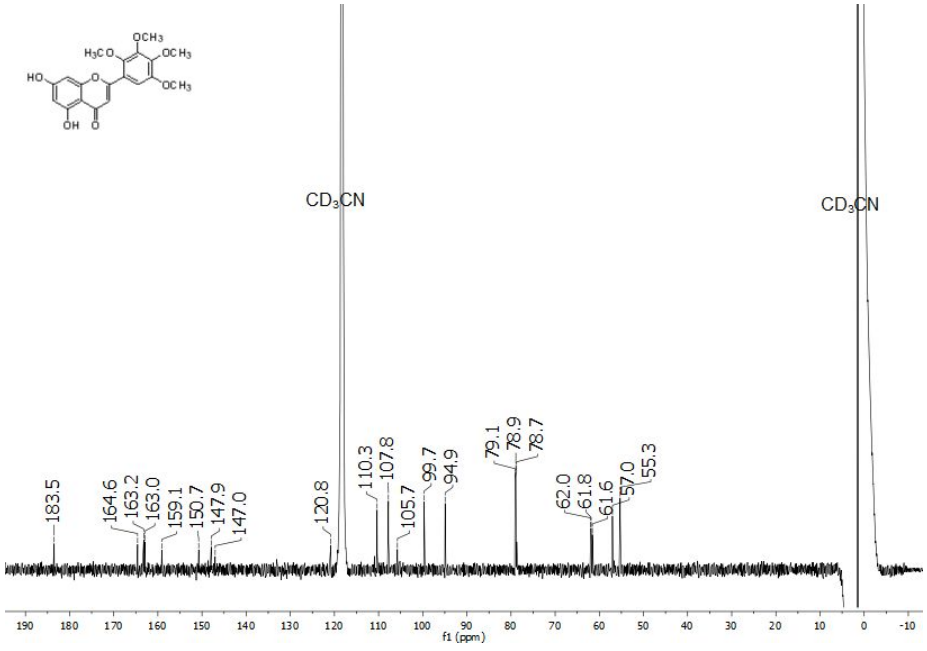

Appendix 35C. The HRMS (ESI) spectrum of 5,7-dihydroxy-2',3',4',5'-tetramethoxyflavone (**221**) observed at 600 MHz for CD_3CN solution at 25 °C.

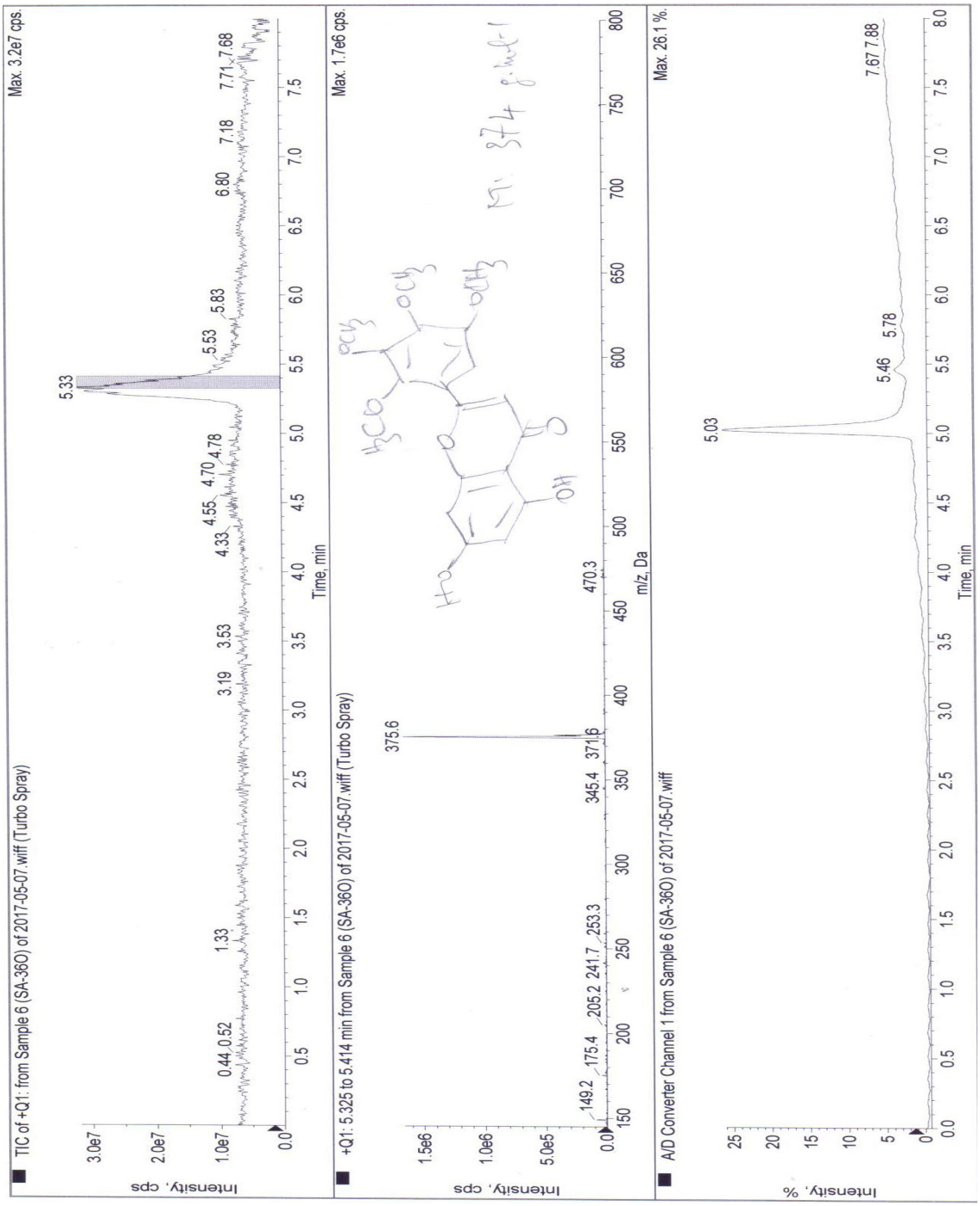

Appendix 36A. The ^{1}H NMR spectrum of 2'-hydroxyethyl-tetradecanoate (**222**) observed at 600 MHz for CD_2Cl_2 solution at 25 °C.

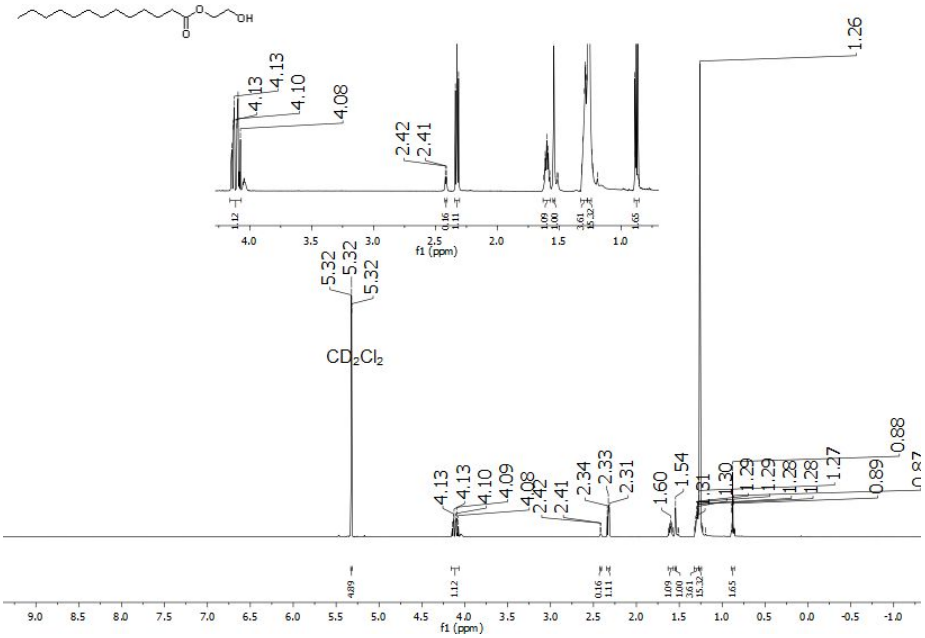

Appendix 36B. The ^{13}C NMR spectrum of 2'-hydroxyethyl-tetradecanoate (**222**) observed at 200 MHz for CD_2Cl_2 solution at 25 °C.

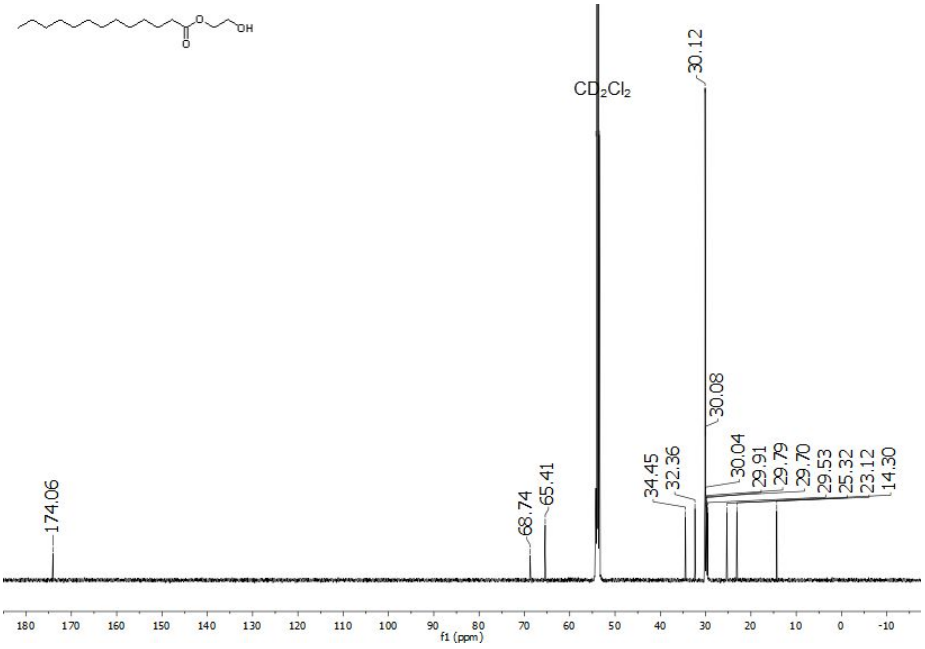

Appendix 37A. The ^{1}H NMR spectrum of lauric acid **(223)** observed at 600 MHz for $CDCl_3$ solution at 25 °C.

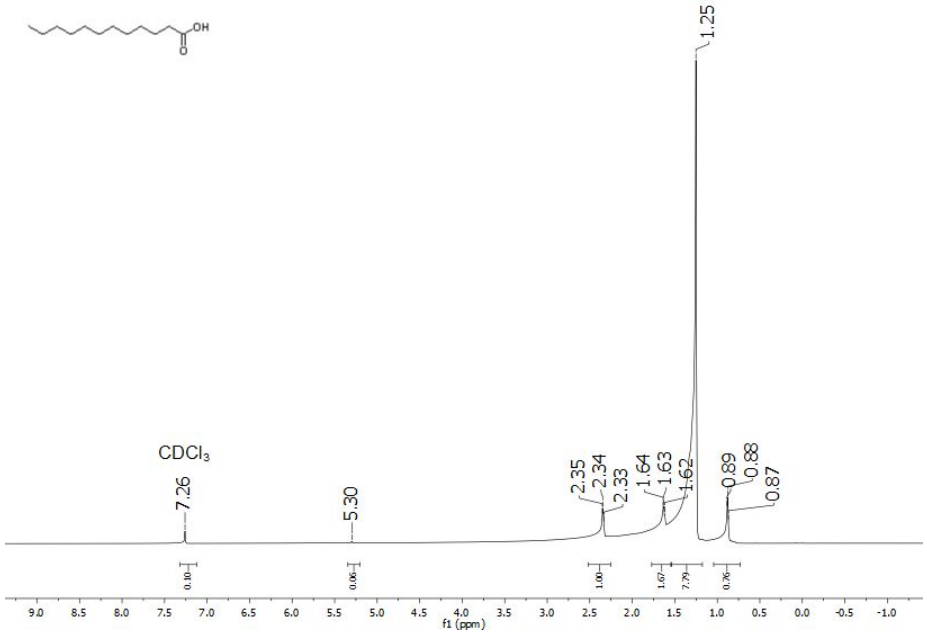

Appendix 37B. The ^{13}C NMR spectrum of lauric acid **(223)** observed at 200 MHz for $CDCl_3$ solution at 25 °C.

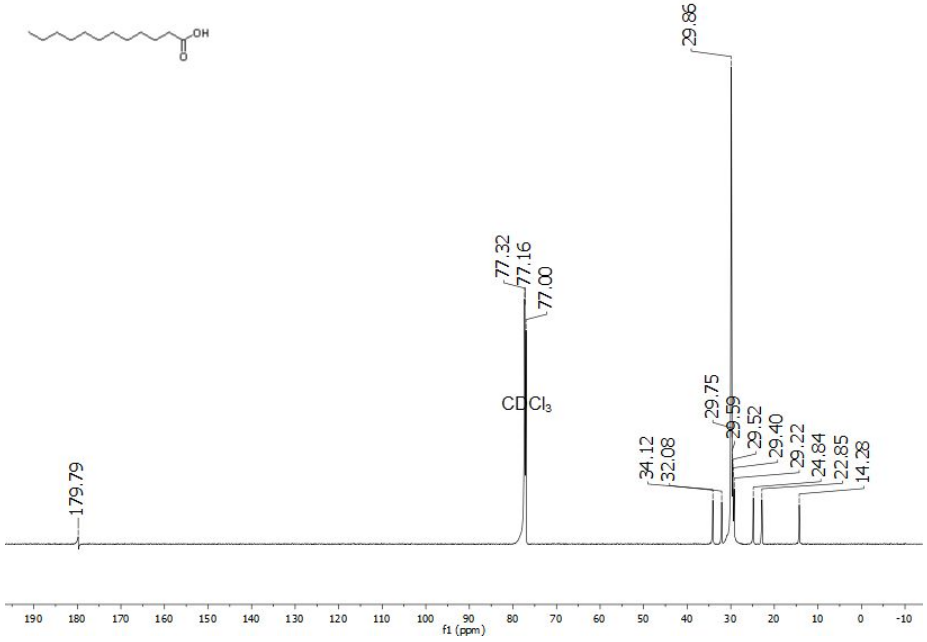

Appendix 38A. The ^{1}H NMR spectrum of myristic acid **(224)** observed at 600 MHz for $CDCl_3$ solution at 25 °C.

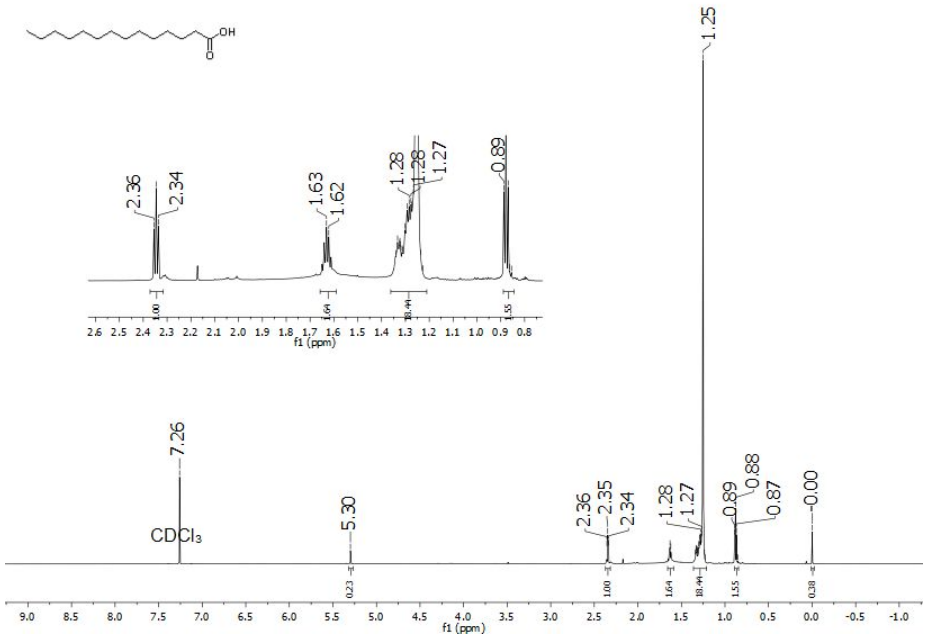

Appendix 38B. The ^{13}C NMR spectrum of myristic acid **(224)** observed at 200 MHz for $CDCl_3$ solution at 25 °C.

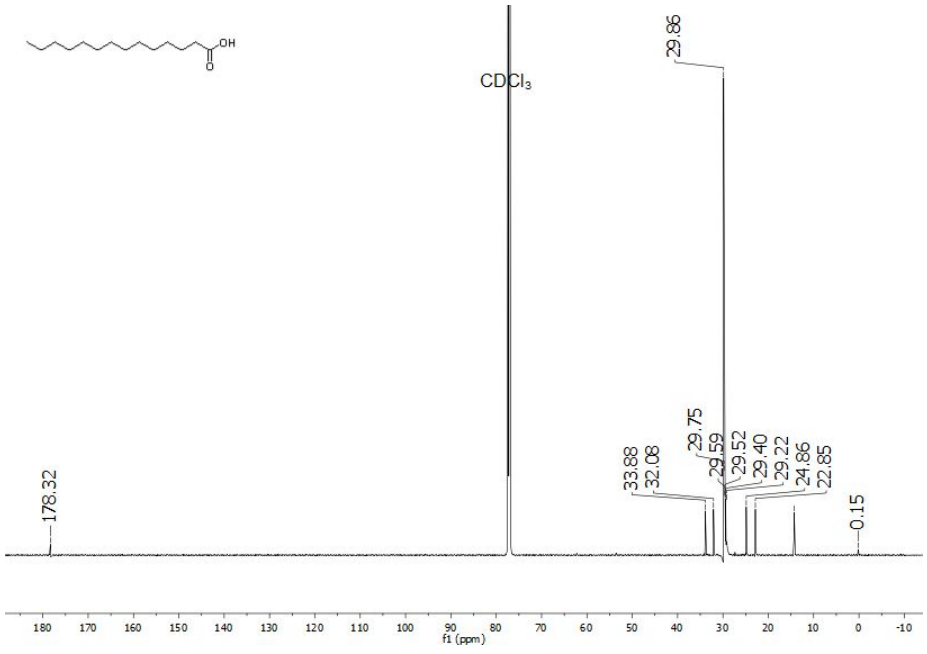

Appendix 39A. The ^{1}H NMR spectrum of 7α-hydroxy-*ent*-trachyloban-19-oic acid (**225**) observed at 800 MHz for $CDCl_3$ solution at 25 °C.

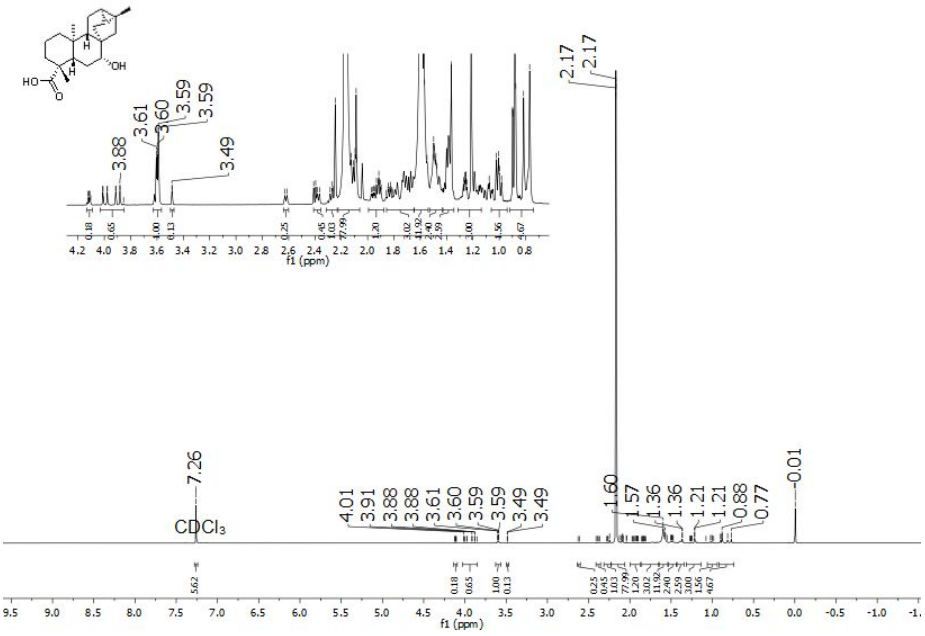

Appendix 39B. The ^{13}C NMR spectrum of 7α-hydroxy-*ent*-trachyloban-19-oic acid (**225**) observed at 200 MHz for $CDCl_3$ solution at 25 °C.

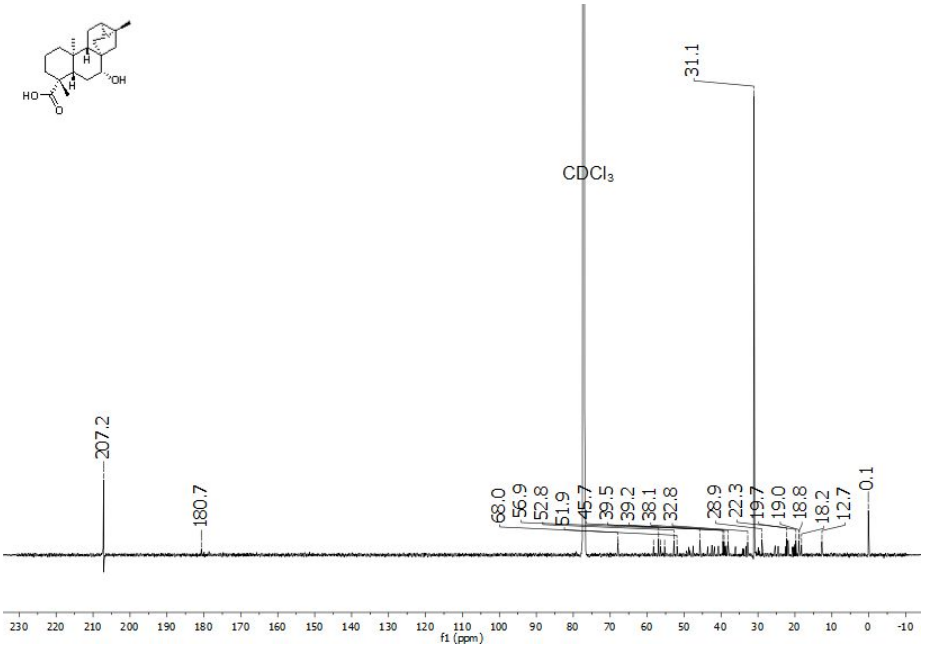

Appendix 40A. The ^{1}H NMR spectrum of friedelan-3β-ol (**226**) observed at 600 MHz for $CDCl_3$ solution at 25 °C.

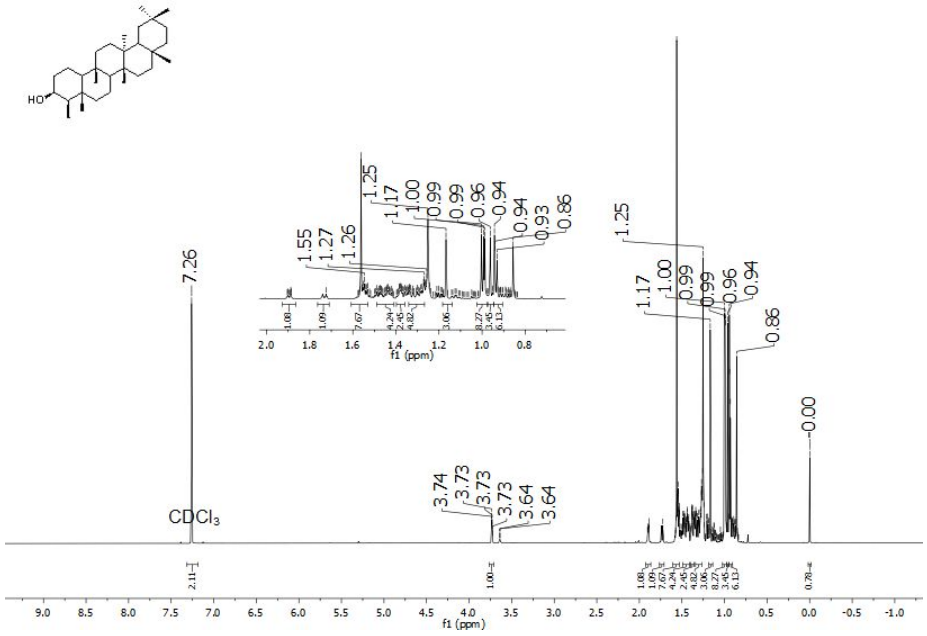

Appendix 40B. The ^{13}C NMR spectrum of friedelan-3β-ol (**226**) observed at 200 MHz for $CDCl_3$ solution at 25 °C.

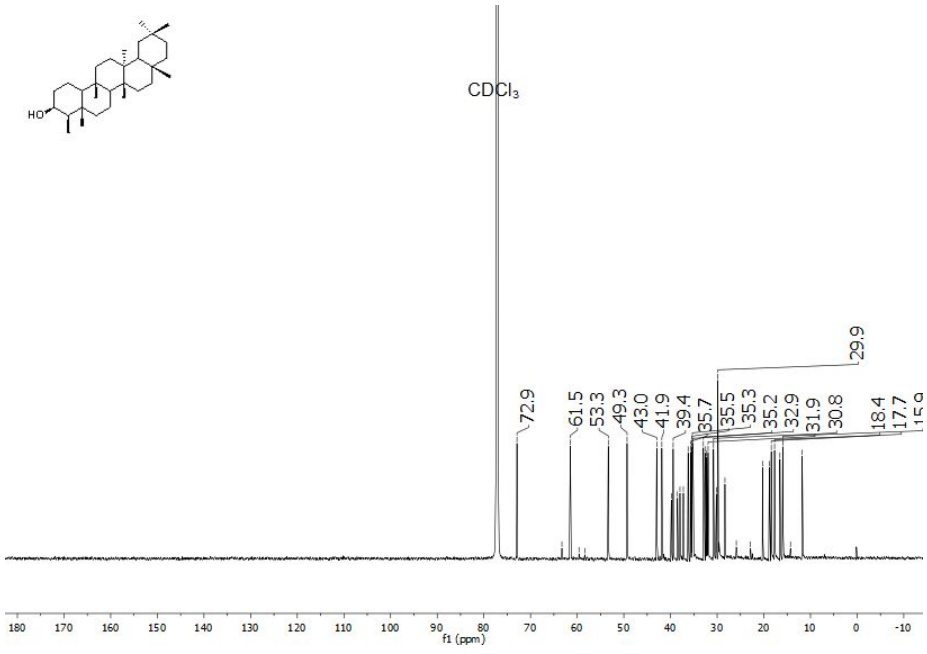

Appendix 41A. The ^{1}H NMR spectrum of spinasterol (**227**) observed at 600 MHz for $CDCl_3$ solution at 25 °C.

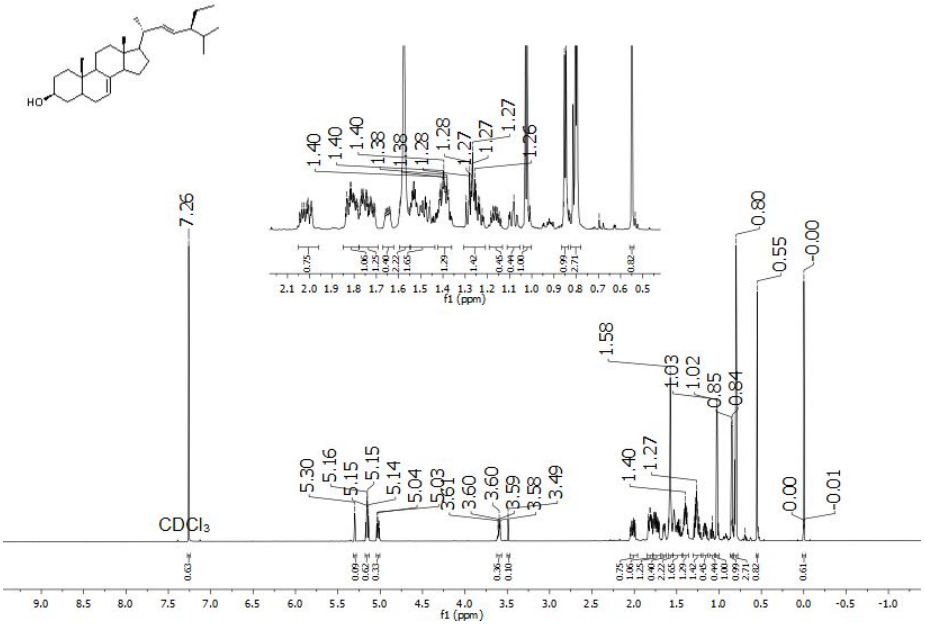

Appendix 41B. The ^{13}C NMR spectrum of spinasterol (**227**) observed at 200 MHz for $CDCl_3$ solution at 25 °C.

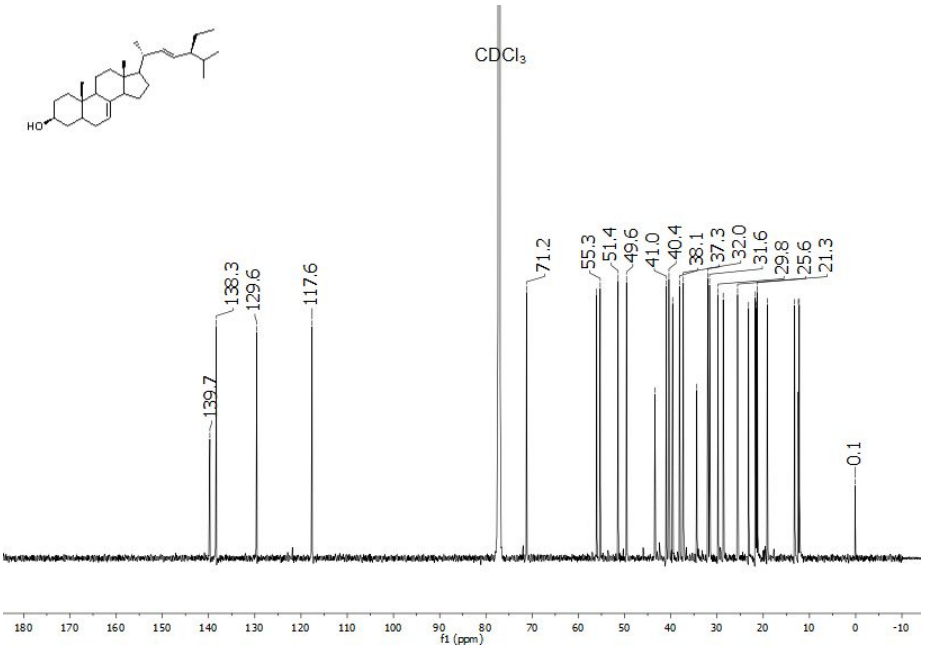

Appendix 41C. The HRMS (ESI) spectrum of spinasterol (**227**).

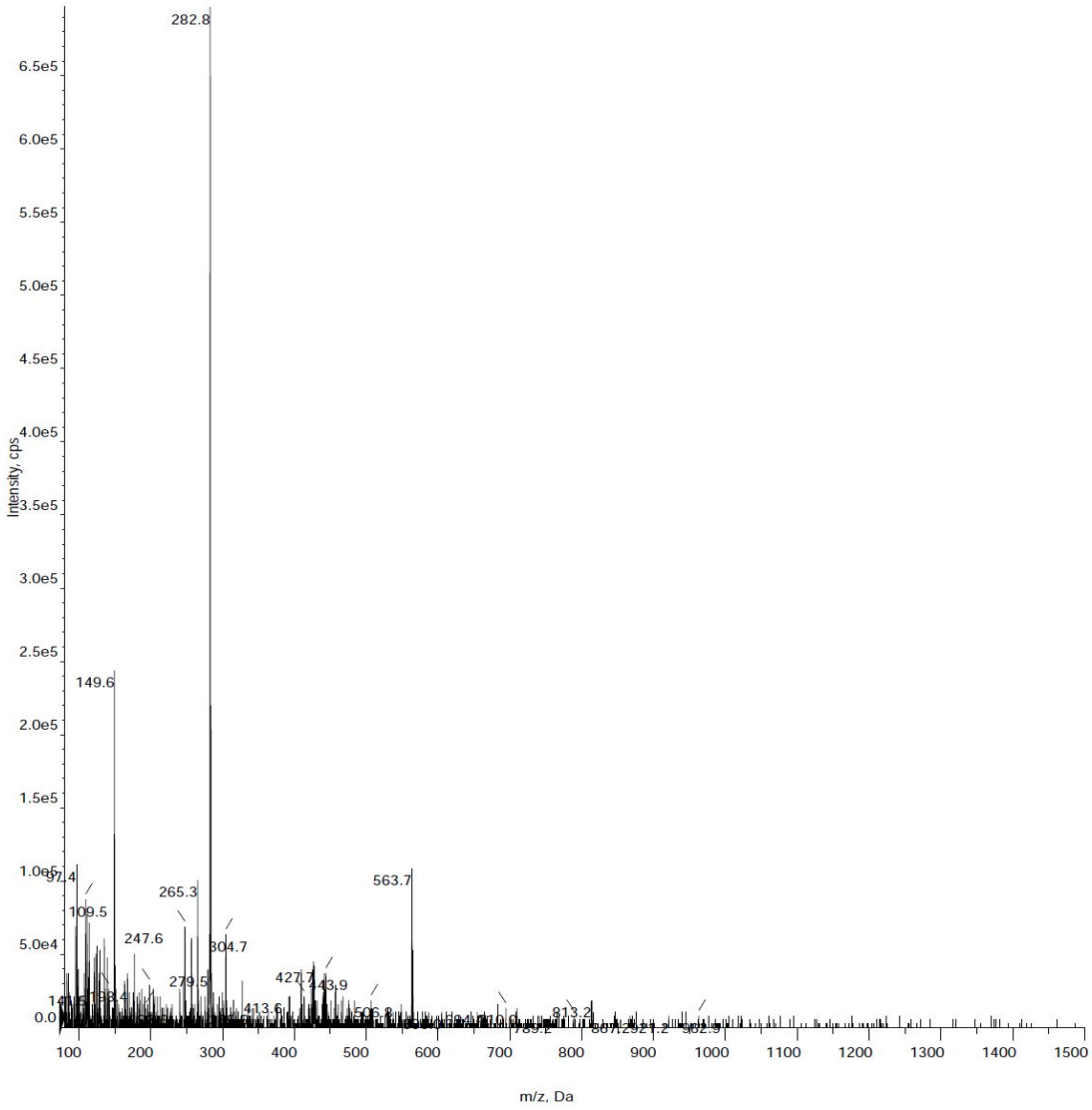

Appendix 42A. The ^{1}H NMR spectrum of 1-O-(Lauroyl)glycerol (**228**) observed at 600 MHz for $CDCl_3$ solution at 25 °C.

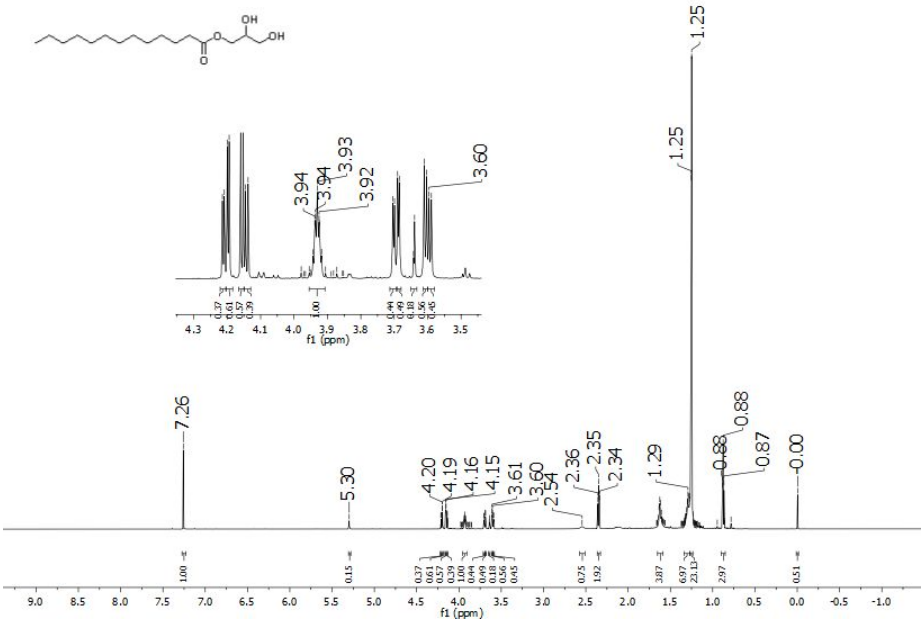

Appendix 42B. The ^{13}C NMR spectrum of 1-O-(Lauroyl)glycerol (**228**) observed at 200 MHz for $CDCl_3$ solution at 25 °C.

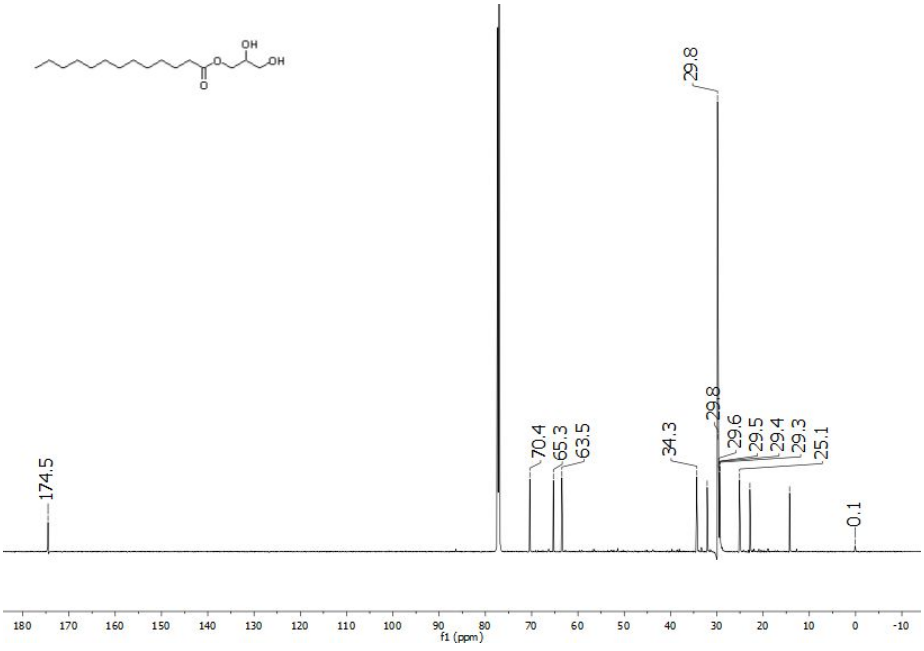

Appendix 43A. The ^{1}H NMR spectrum of *ent*-trachylobane-2α,6β,18,19-tetraol (**229**) observed at 800 MHz for Acetone-d_6 solution at 25 °C.

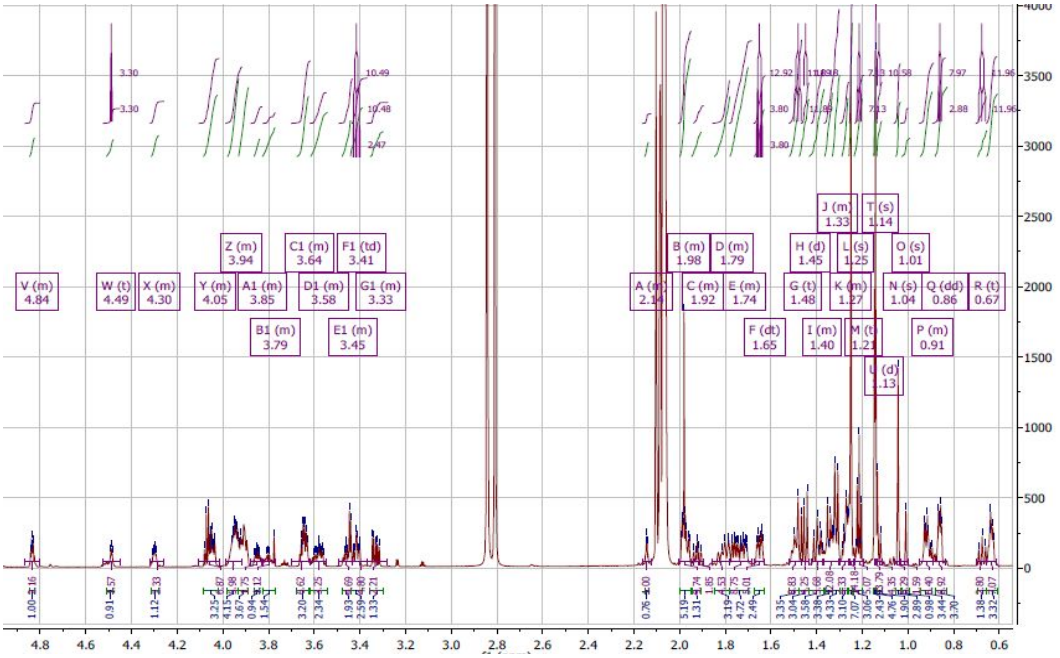

Appendix 43B. The ^{13}C NMR spectrum of *ent*-trachylobane-2α,6β,18,19-tetraol (**229**) observed at 200 MHz for Acetone-d_6 solution at 25 °C.

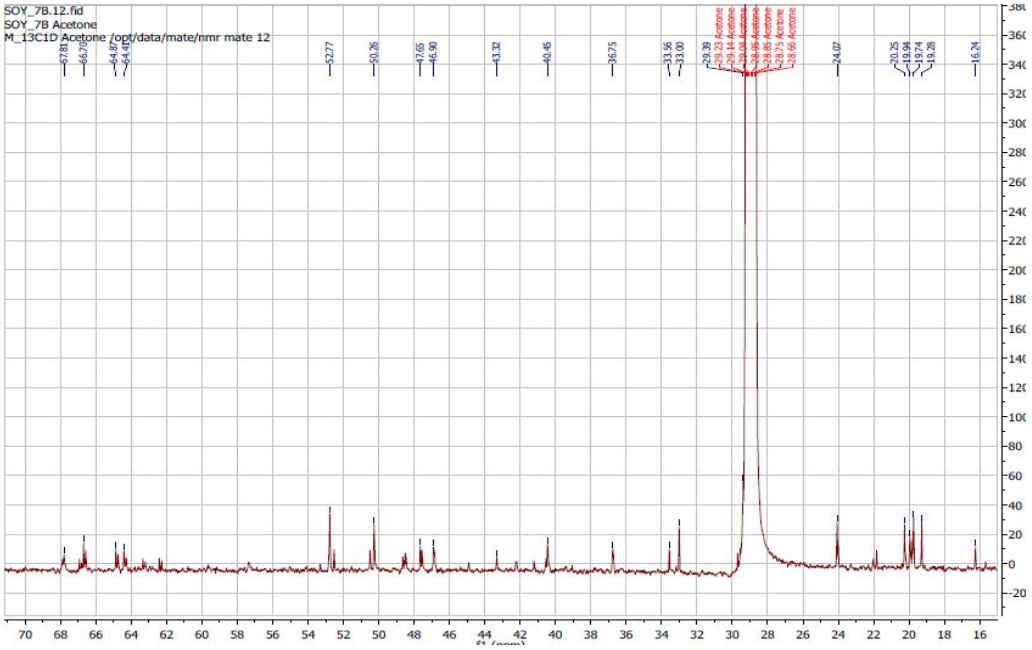

Appendix 43C. The ESIMS spectrum of *ent*-trachylobane-2α,6β,18,19-tetraol (**229**)

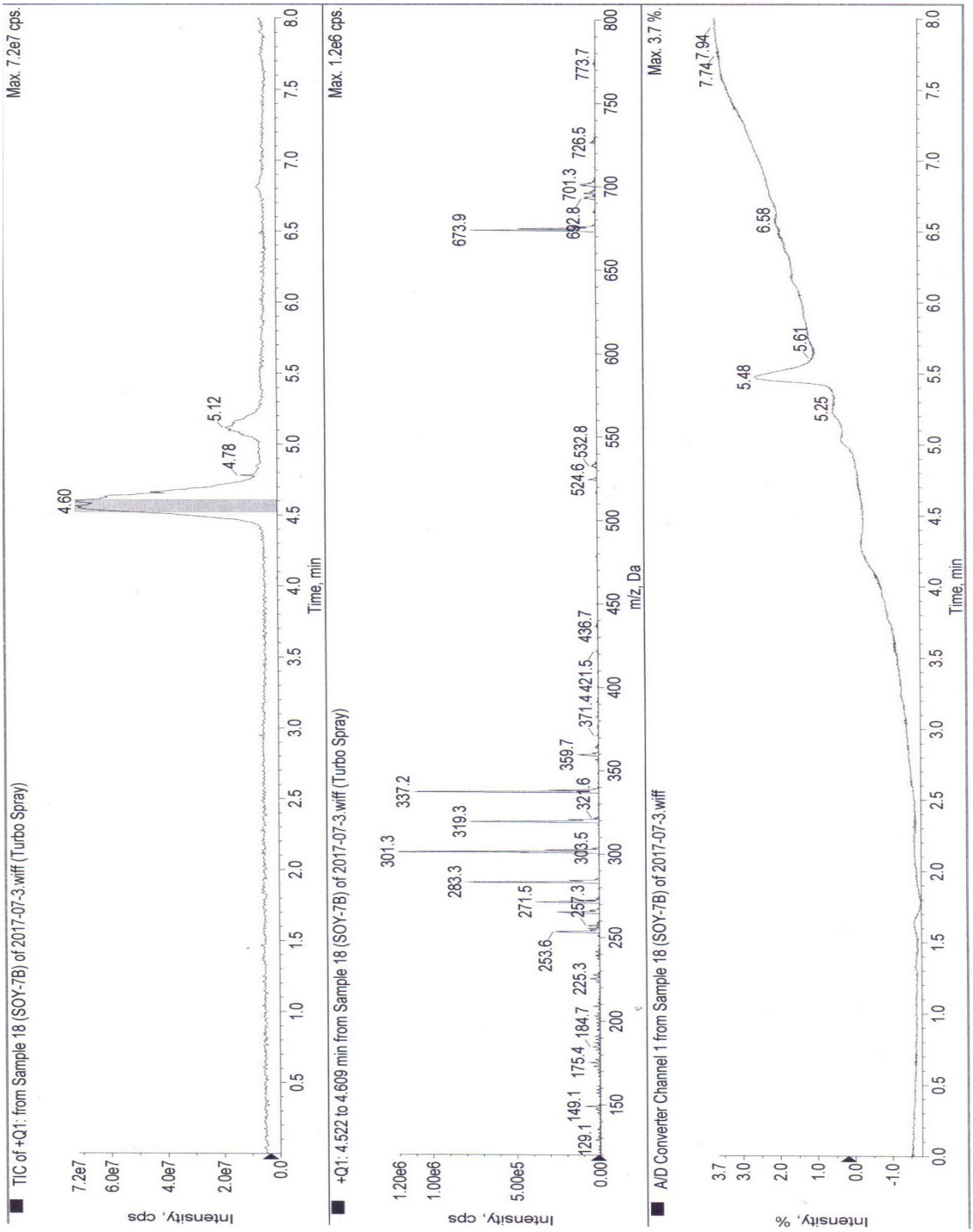

Appendix 44A. The ^{1}H NMR spectrum of *ent*-kauren-16-en-2-one (**230**) observed at 600 MHz for Acetone-d_6 solution at 25 °C.

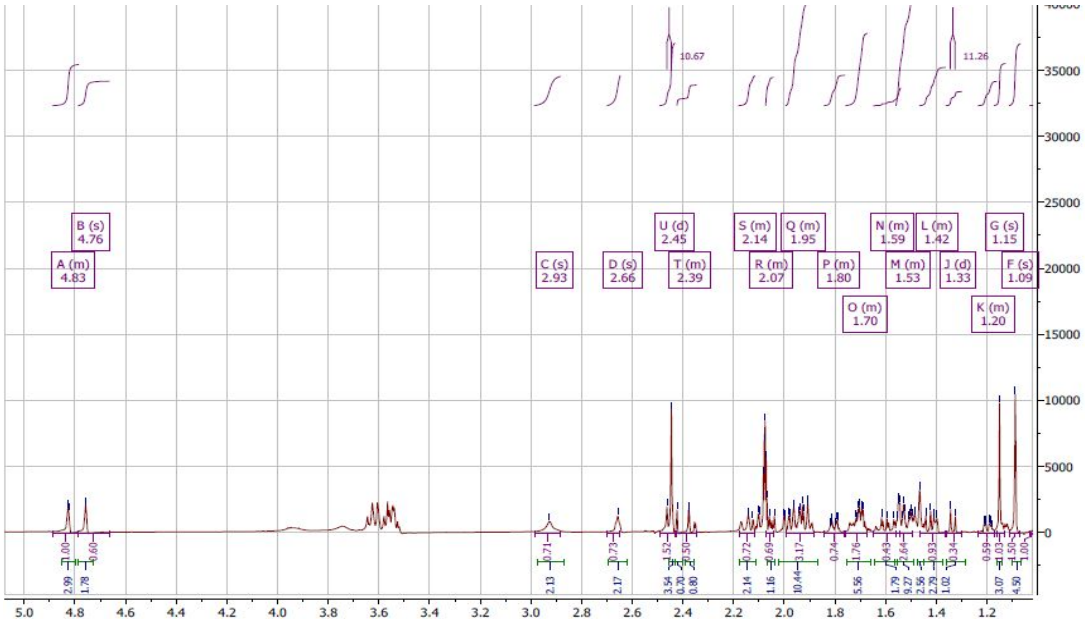

Appendix 44B. The ^{13}C NMR spectrum of *ent*-kauren-16-en-2-one (**230**) observed at 126 MHz for Acetone-d_6 solution at 25 °C.

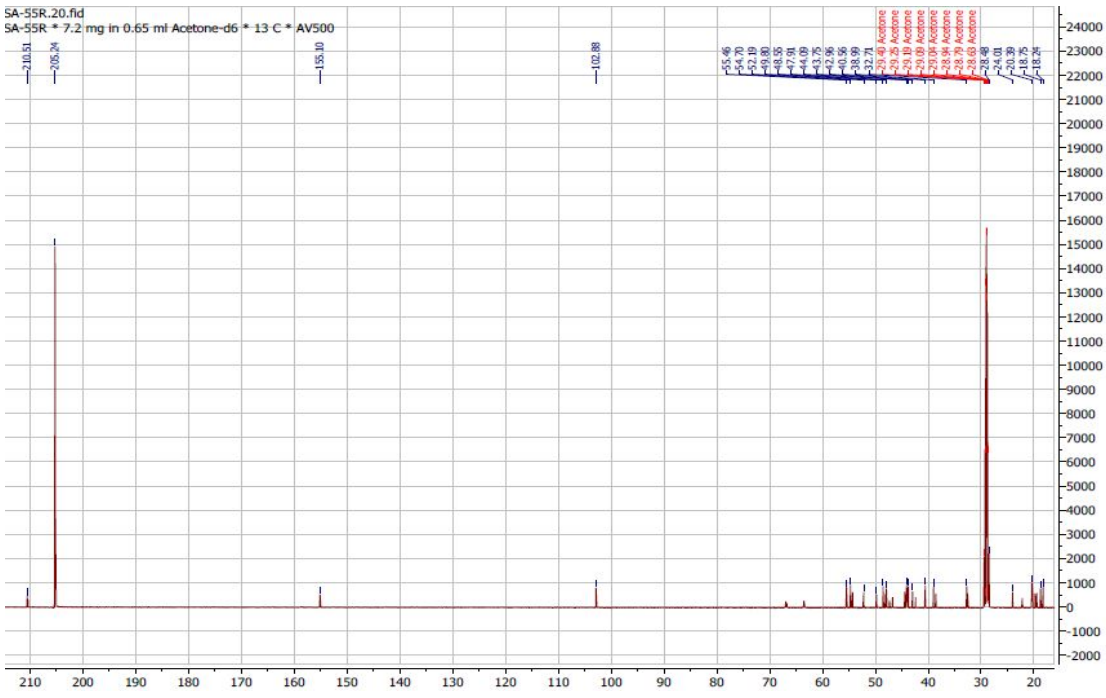

Appendix 45A. The ^{1}H NMR spectrum of friedelin (**231**) observed at 600 MHz for $CDCl_3$ solution at 25 °C.

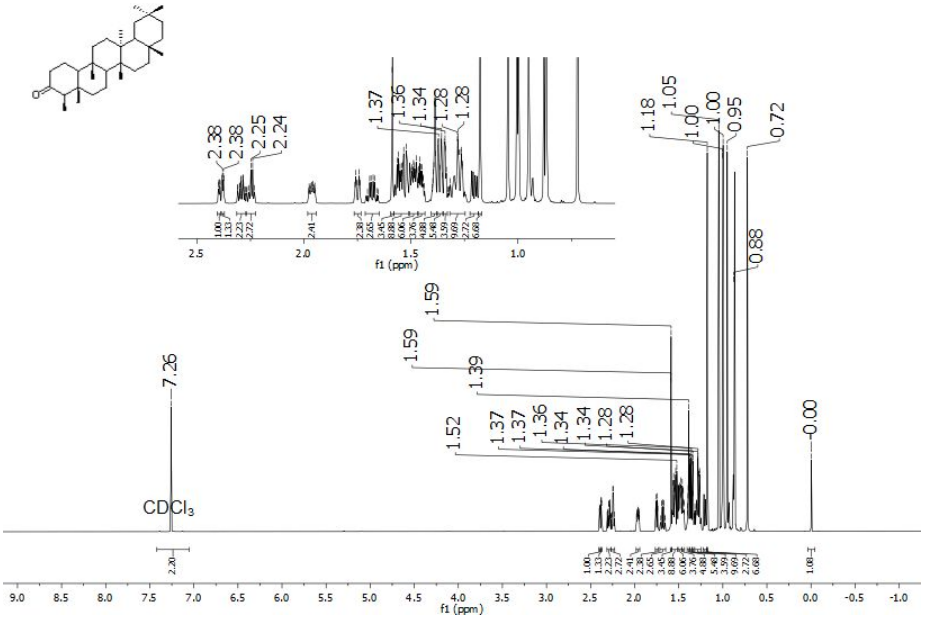

Appendix 45B. The ^{13}C NMR spectrum of friedelin (**231**) observed at 200 MHz for $CDCl_3$ solution at 25 °C.

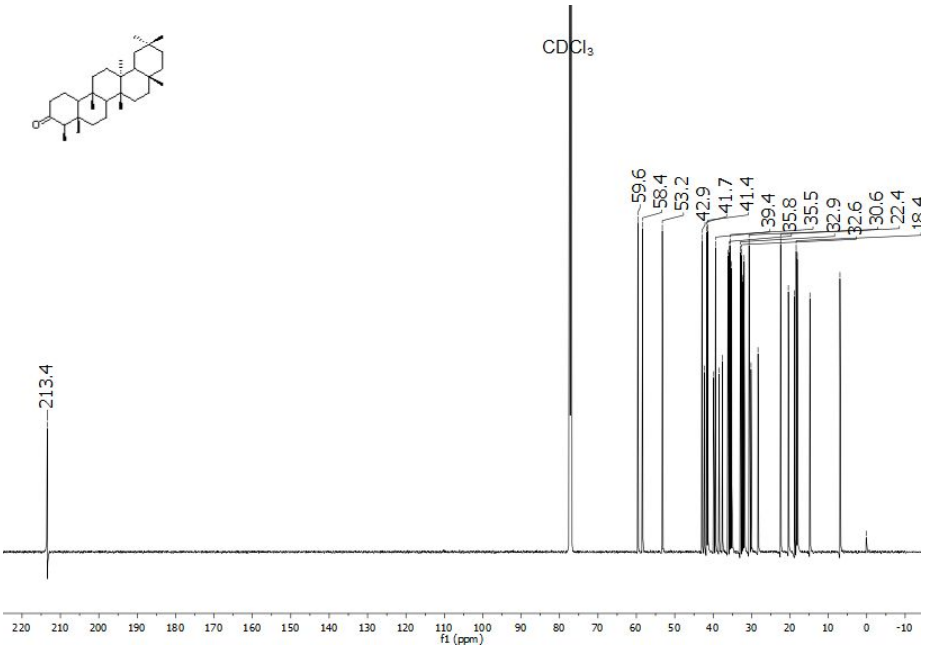

Appendix 45C. The ESIMS spectrum of friedelin (**231**)

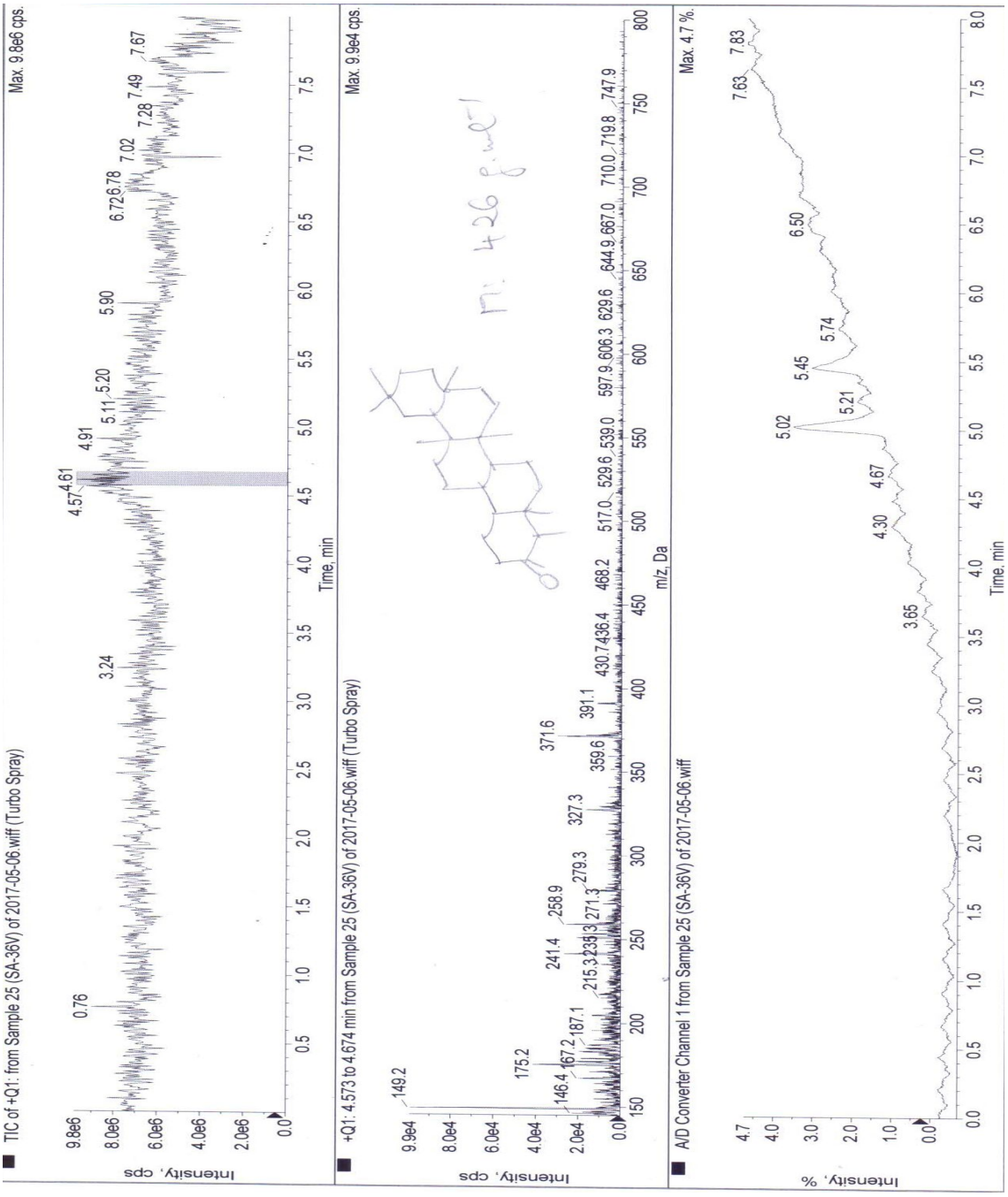

Appendix 46A. The ^{1}H NMR spectrum of 24,25-dihydrolanost-8(9)-en-3-ol (**232**) observed at 600 MHz for $CDCl_3$ solution at 25 °C.

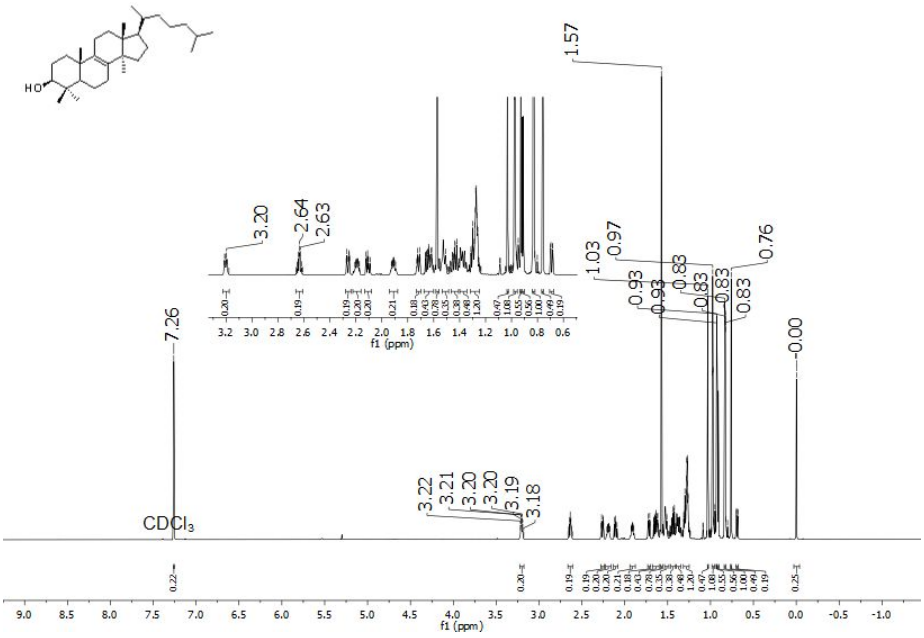

Appendix 46B. The ^{13}C NMR spectrum of 24,25-dihydrolanost-8(9)-en-3-ol (**232**) observed at 200 MHz for $CDCl_3$ solution at 25 °C.

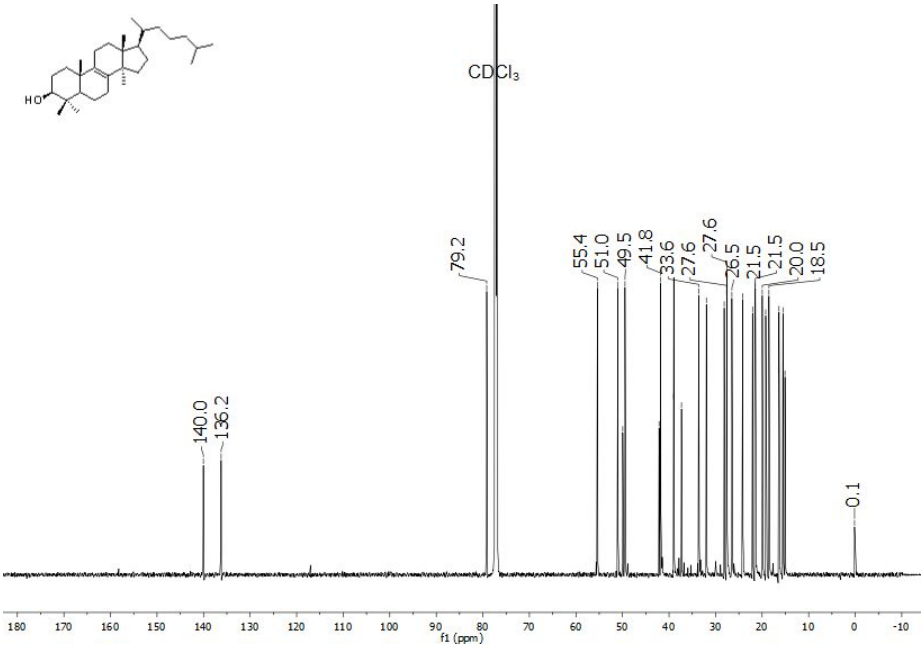

Appendix 47A. The ^{1}H NMR spectrum of (6*R*, 7*R*)-bisabolone (**233**) observed at 600 MHz for $CDCl_3$ solution at 25 °C.

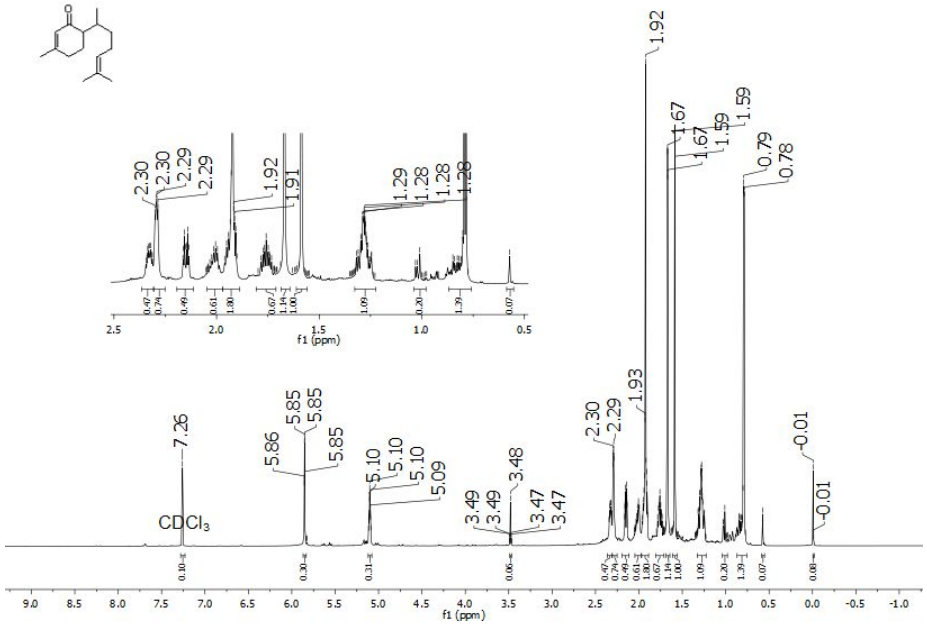

Appendix 47B. The ^{13}C NMR spectrum of (6*R*, 7*R*)-bisabolone (**233**) observed at 200 MHz for $CDCl_3$ solution at 25 °C.

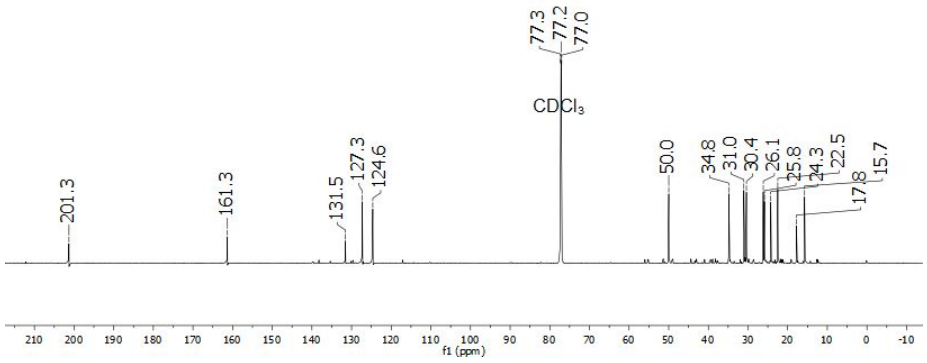

Appendix 47C. The ESIMS spectrum of (6*R*, 7*R*)-bisabolone (**233**)

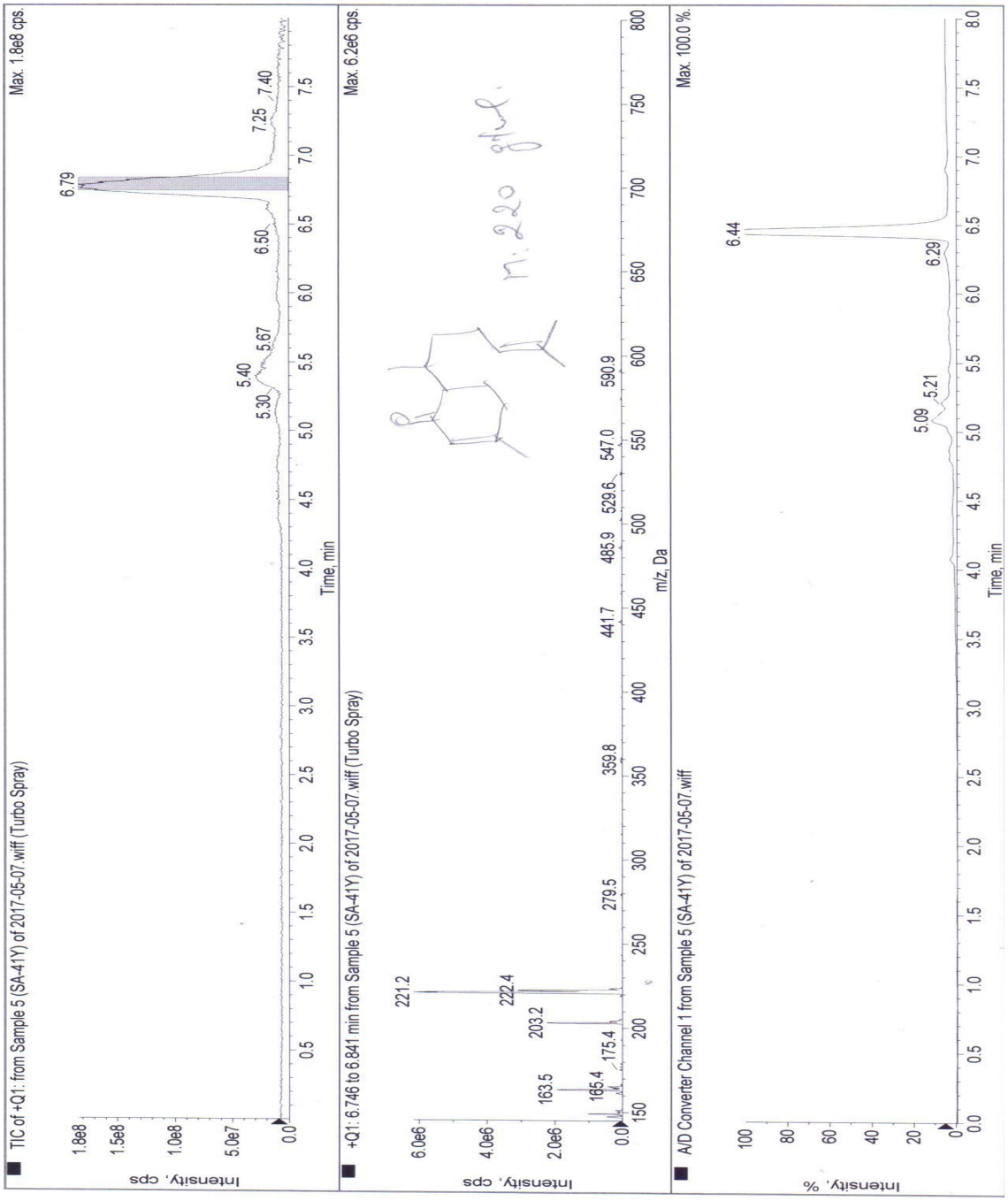

Appendix 3: Spectra for the Compounds Isolated from *Aspilia* Species

Appendix 49A: The ^{1}H NMR spectrum (600 MHz) of 12α-methoxy-*ent*-kaura-9(11),16-dien-19-oic acid (**234**) in $CDCl_3$

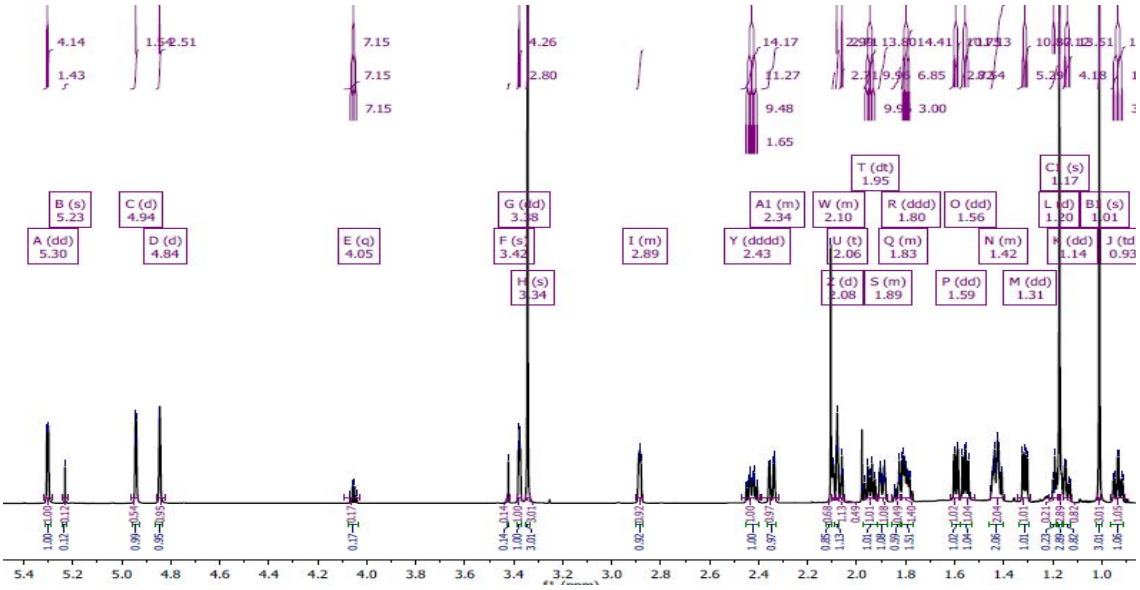

Appendix 49B: The ^{13}C NMR spectrum (200MHz) of 12α-methoxy-*ent*-kaura-9(11),16-dien-19-oic acid (**234**) in $CDCl_3$

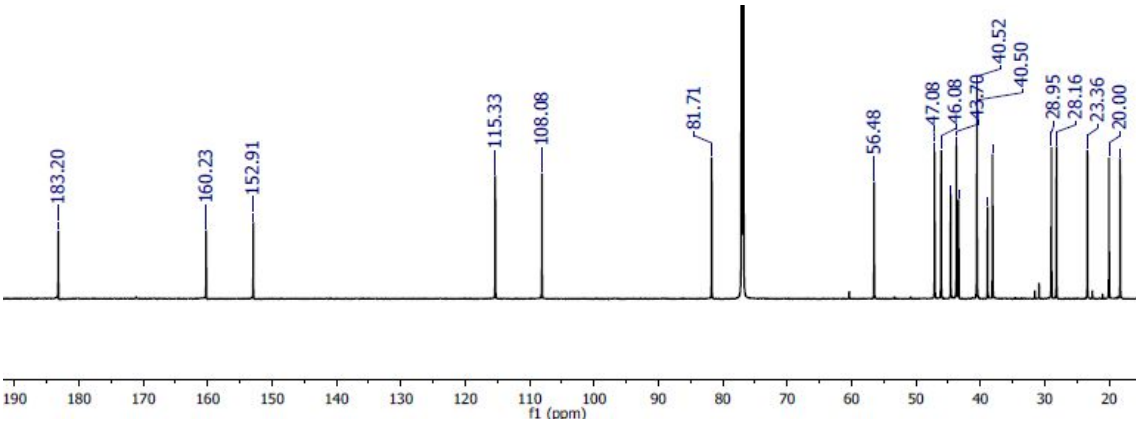

Appendix 49C: The H-H COSY spectrum of 12α-methoxy-*ent*-kaura-9(11),16-dien-19-oic acid (**234**) in $CDCl_3$

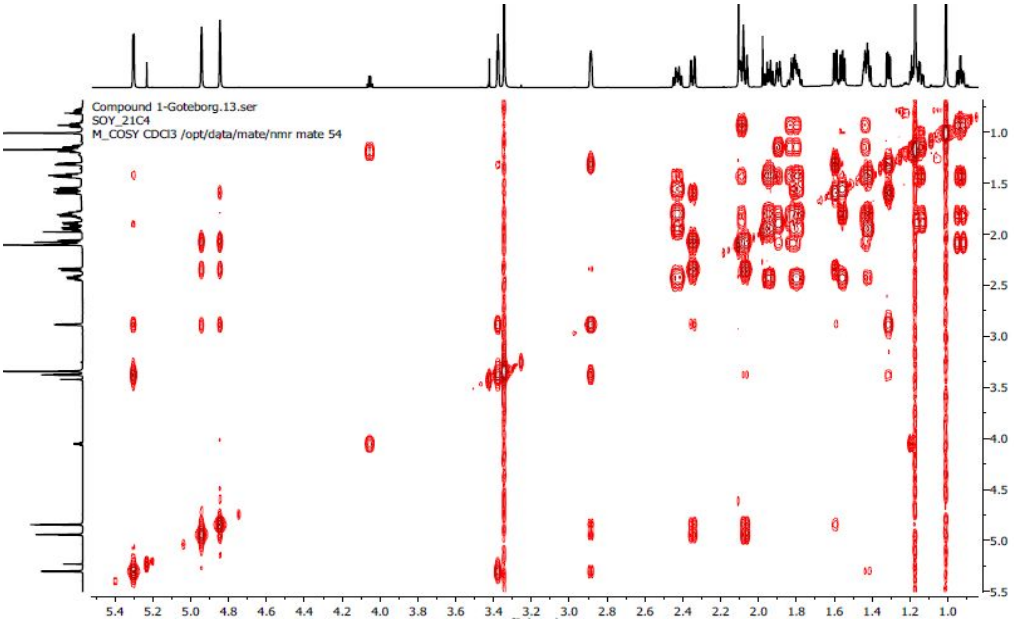

Appendix 49D: The NOESY spectrum of 12α-methoxy-*ent*-kaura-9(11),16-dien-19-oic acid (**234**) in $CDCl_3$

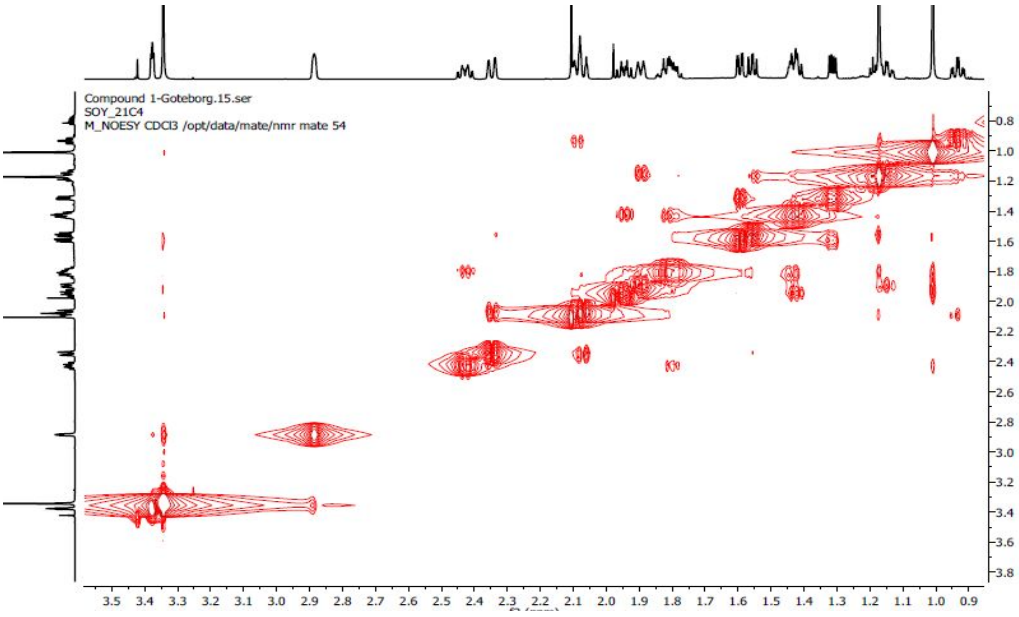

Appendix 49E: The HSQC spectrum of 12α-methoxy-*ent*-kaura-9(11),16-dien-19-oic acid (**234**) in $CDCl_3$

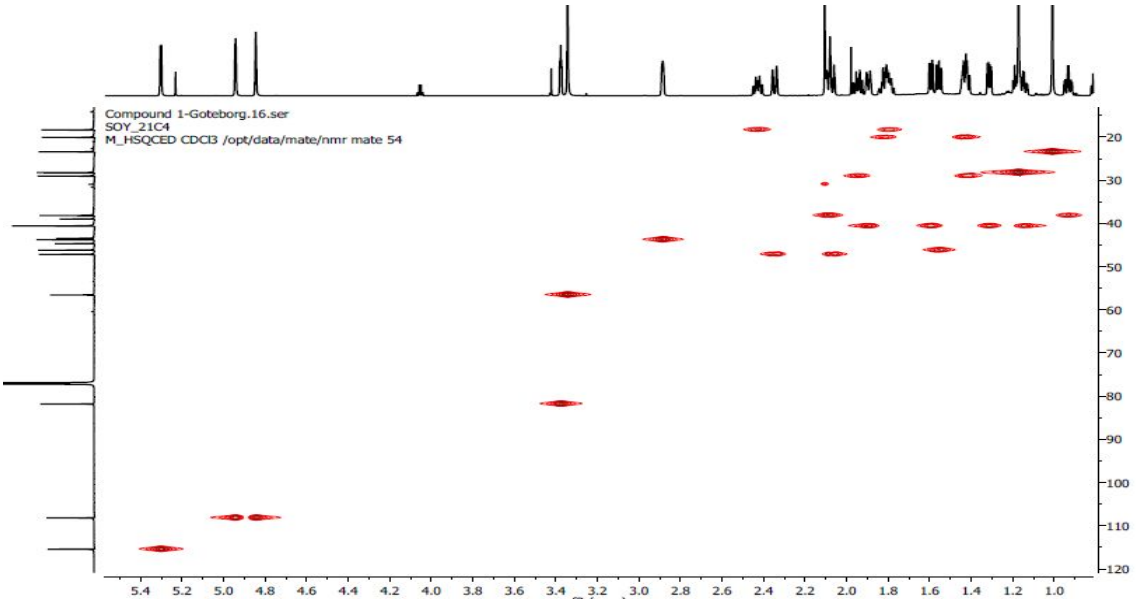

Appendix 49F: The HMBC spectrum of 12α-methoxy-*ent*-kaura-9(11),16-dien-19-oic acid (**234**) in $CDCl_3$

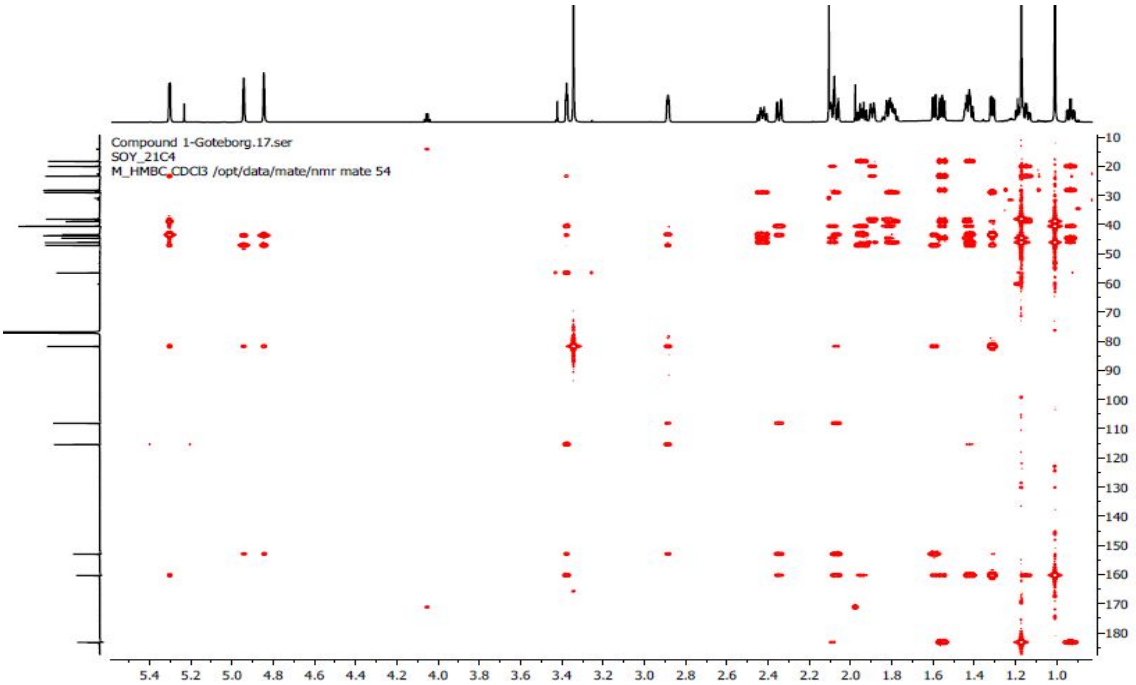

Appendix 49G: The HRESIMS spectrum of 12*α*-methoxy-*ent*-kaura-9(11),16-dien-19-oic acid (**234**)

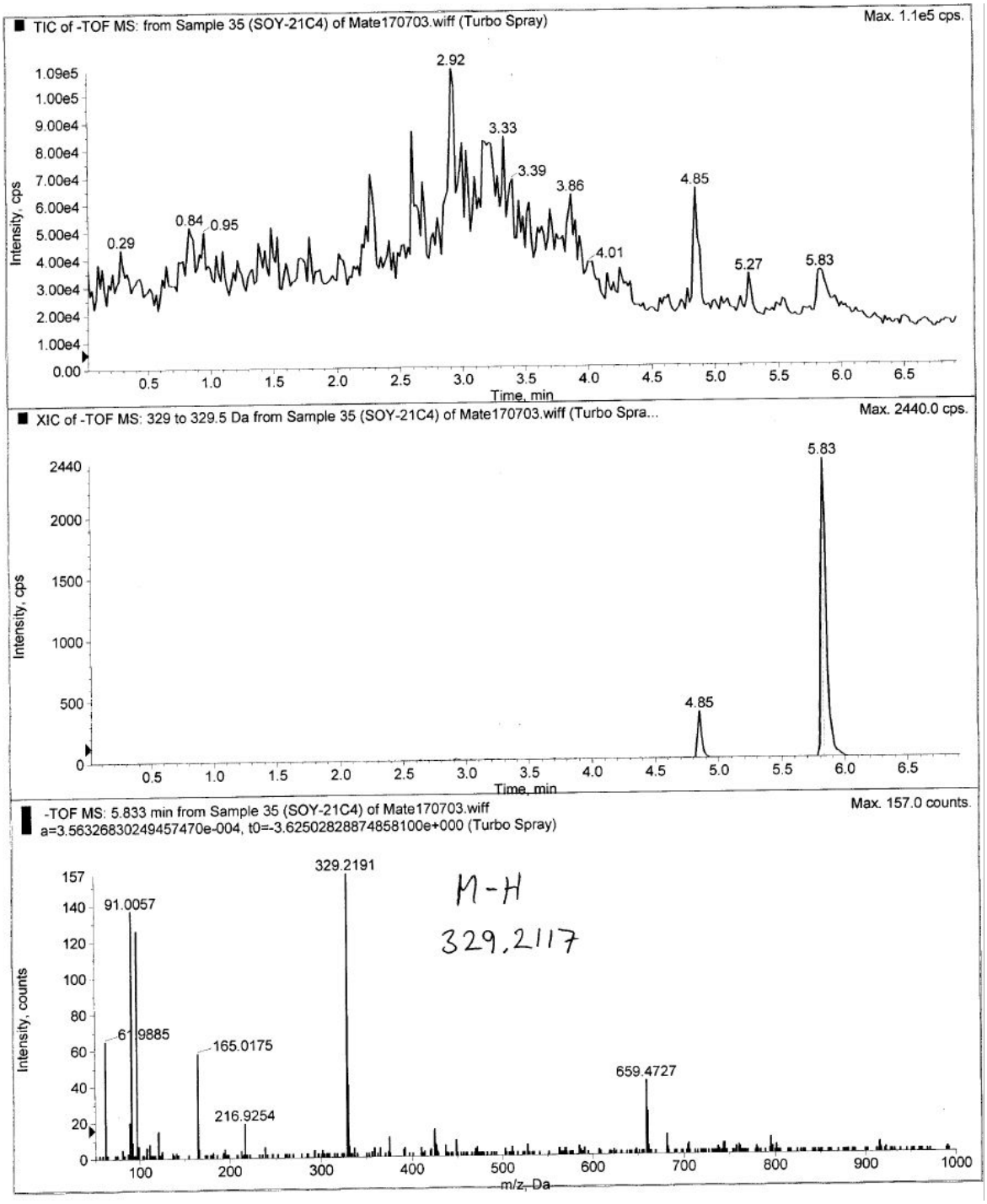

Appendix 50A: The ^{1}H NMR spectrum (600 MHz) of 13β-hydroxy-*ent*-kauran-19-oic acid (**235**) in $CDCl_3$

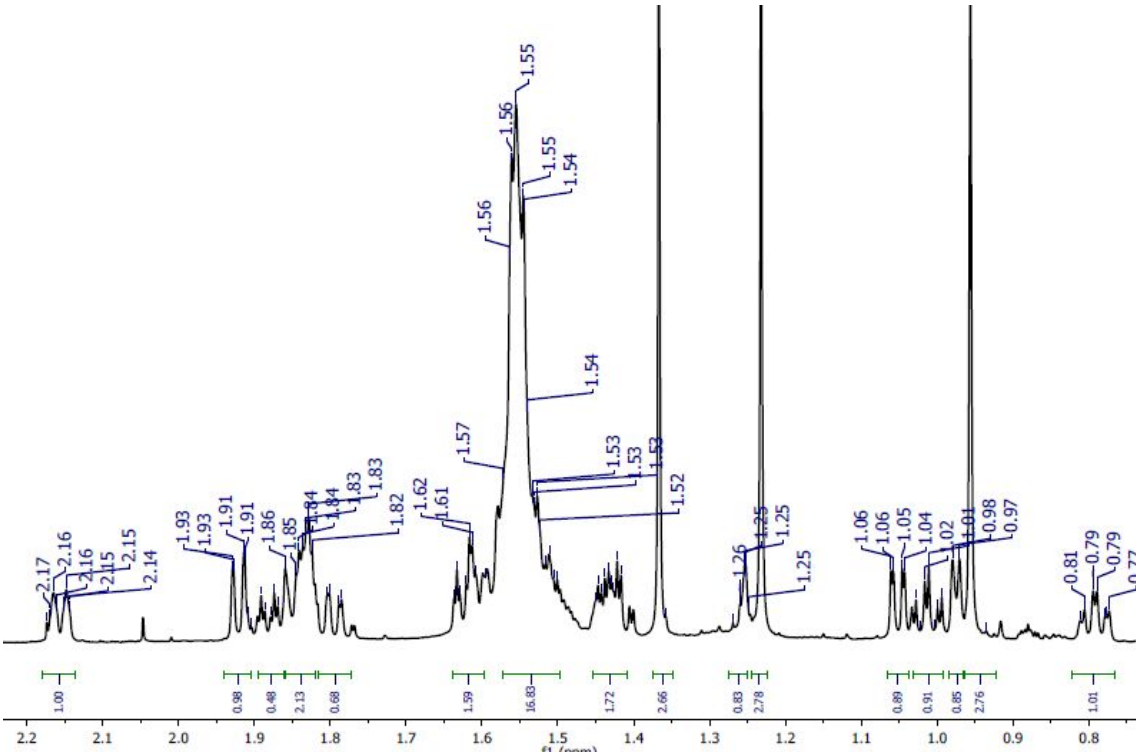

Appendix 50B: The ^{13}C NMR spectrum (200MHz) of 13β-hydroxy-*ent*-kauran-19-oic acid (**235**) in $CDCl_3$

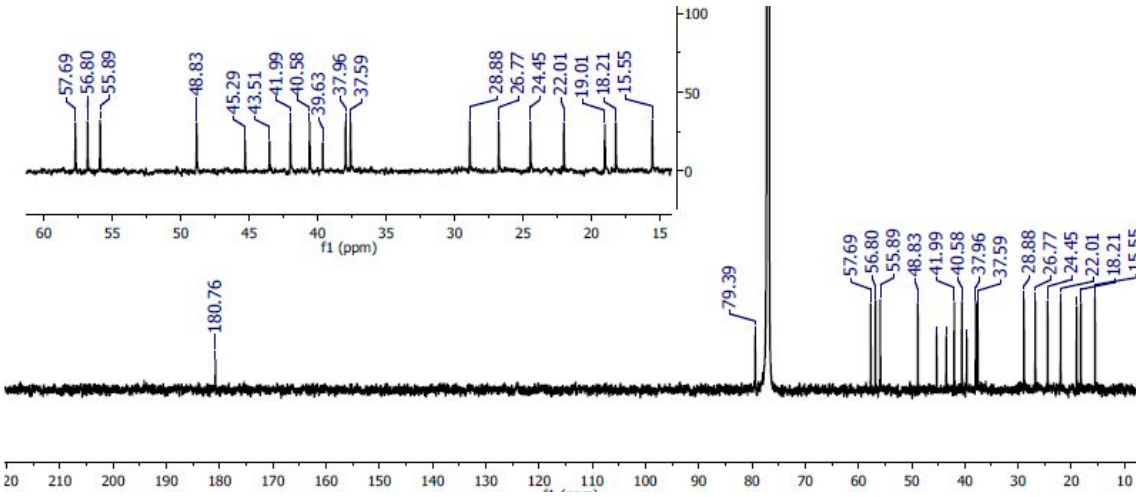

Appendix 50C: The H-H COSY spectrum of 13β-hydroxy-*ent*-kauran-19-oic acid (**235**) in $CDCl_3$

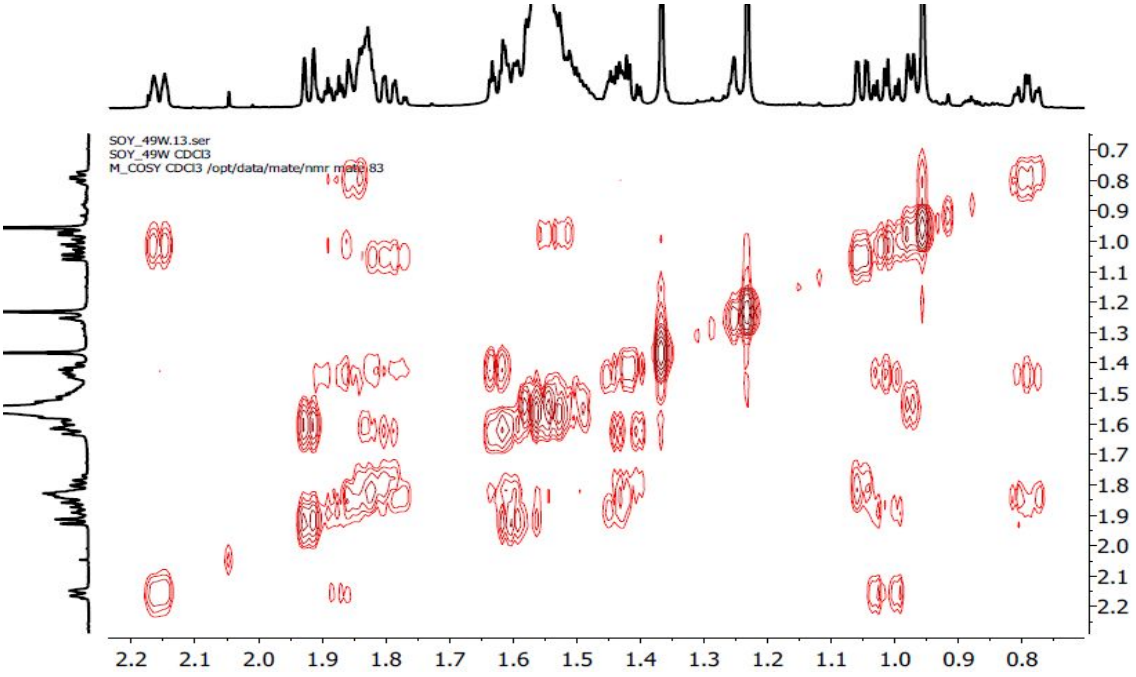

Appendix 50D: The NOESY spectrum of 13β-hydroxy-*ent*-kauran-19-oic acid (**235**) in $CDCl_3$

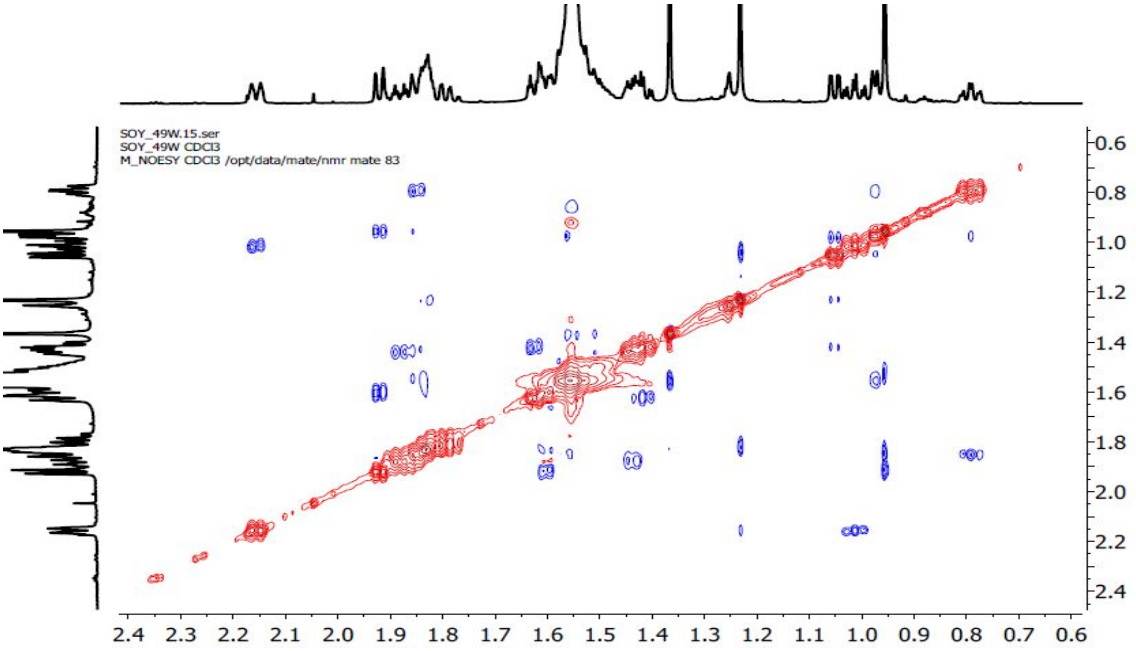

Appendix 50E: The HSQC spectrum of 13β-hydroxy-*ent*-kauran-19-oic acid (**235**) in $CDCl_3$

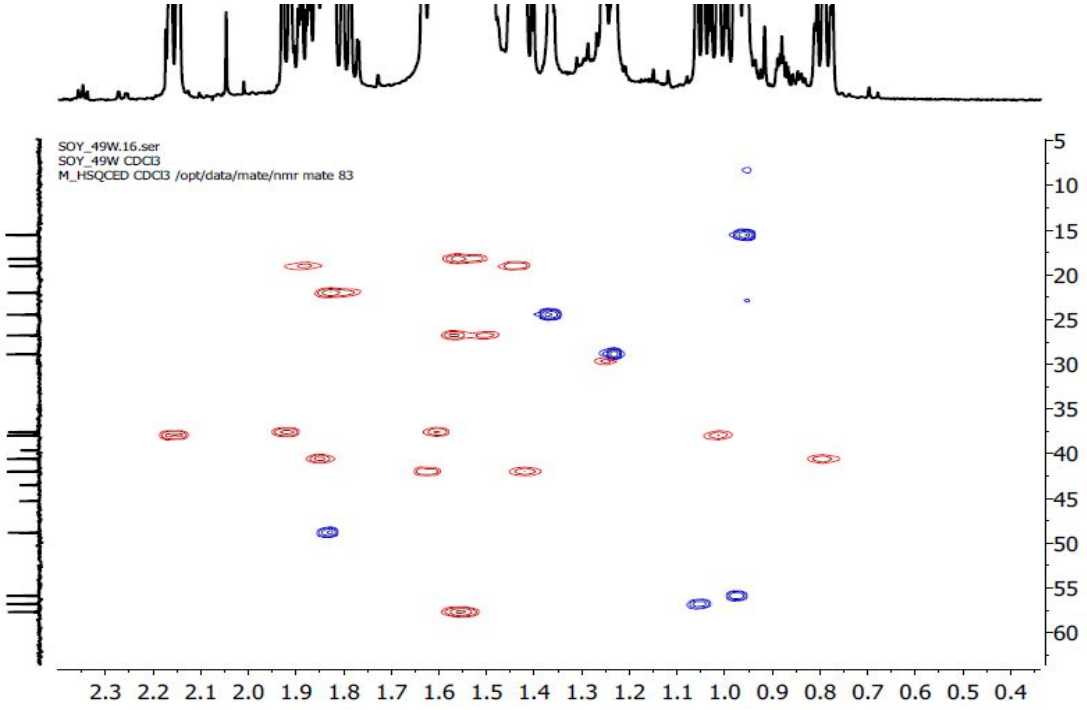

Appendix 50F: The HMBC spectrum of 13β-hydroxy-*ent*-kauran-19-oic acid (**235**) in $CDCl_3$

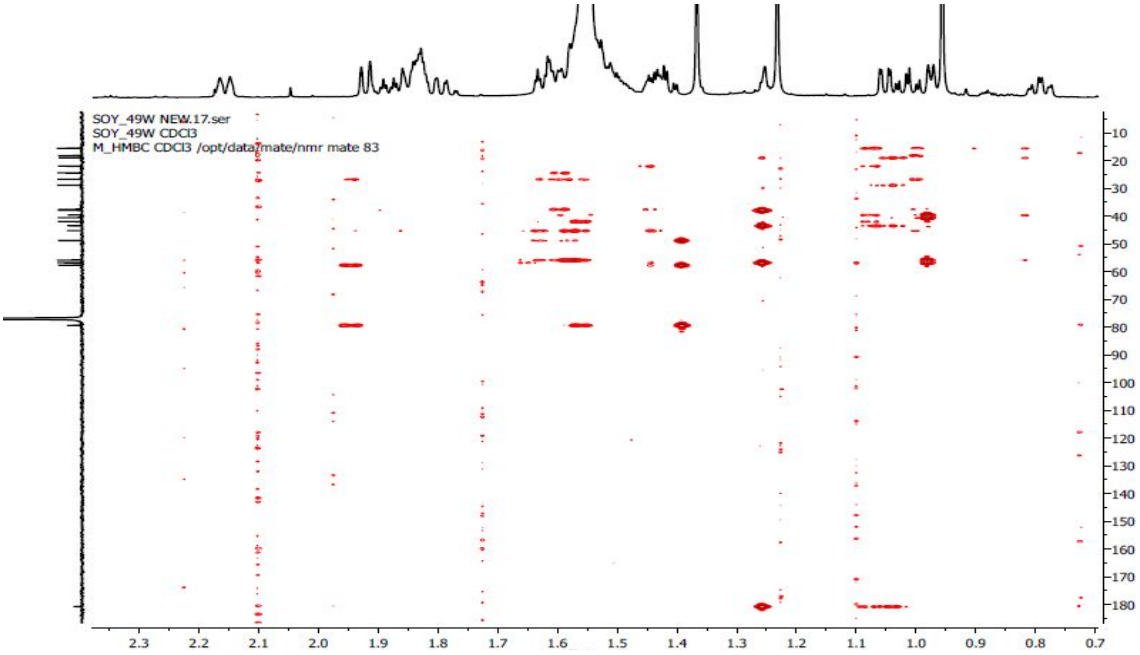

Appendix 50G: The HRESIMS spectrum of 13*β*-hydroxy-*ent*-kauran-19-oic acid (**235**)

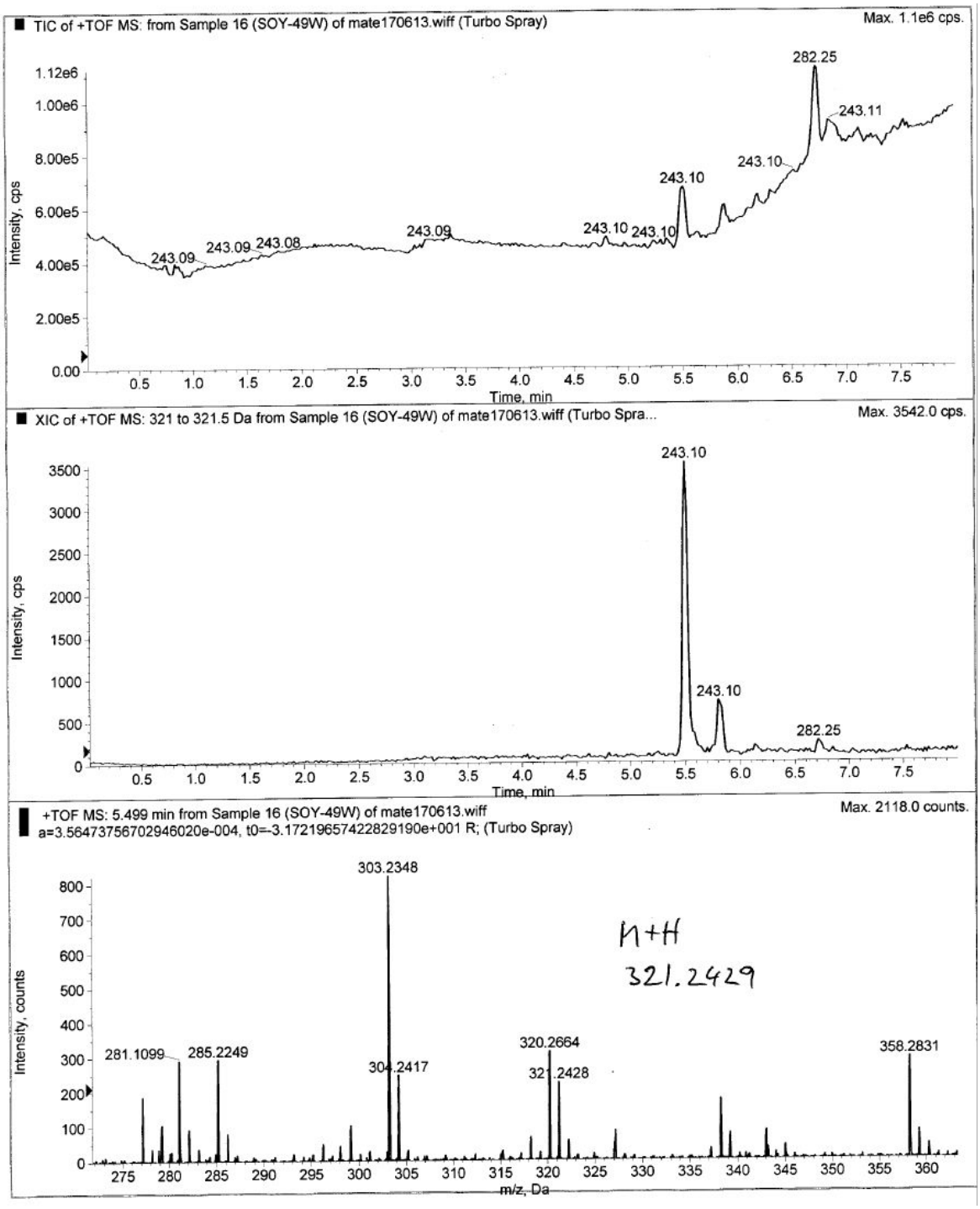

Appendix 51A: The ^{1}H NMR spectrum (600 MHz) of 9*β*-hydroxy-15*α*-angeloyloxy-*ent*-kaur-16-en-19-oic acid (**236**) in CD_2Cl_2

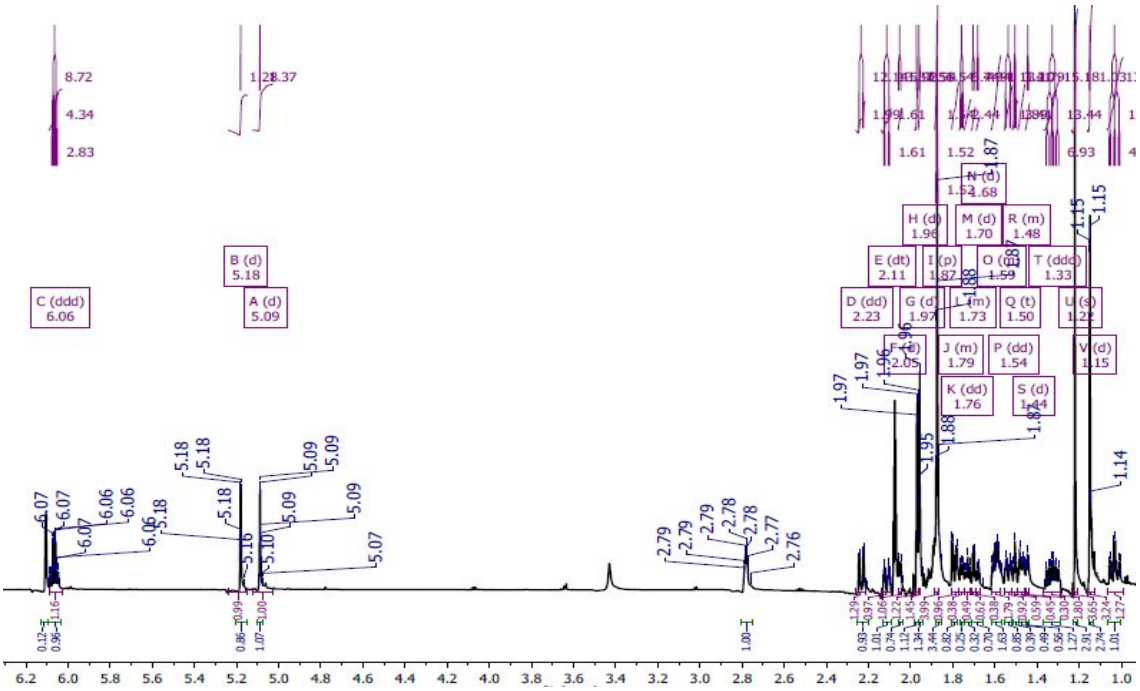

Appendix 51B: The ^{13}C NMR spectrum (150MHz) of 9*β*-hydroxy-15*α*-angeloyloxy-*ent*-kaur-16-en-19-oic acid (**236**) in CD_2Cl_2

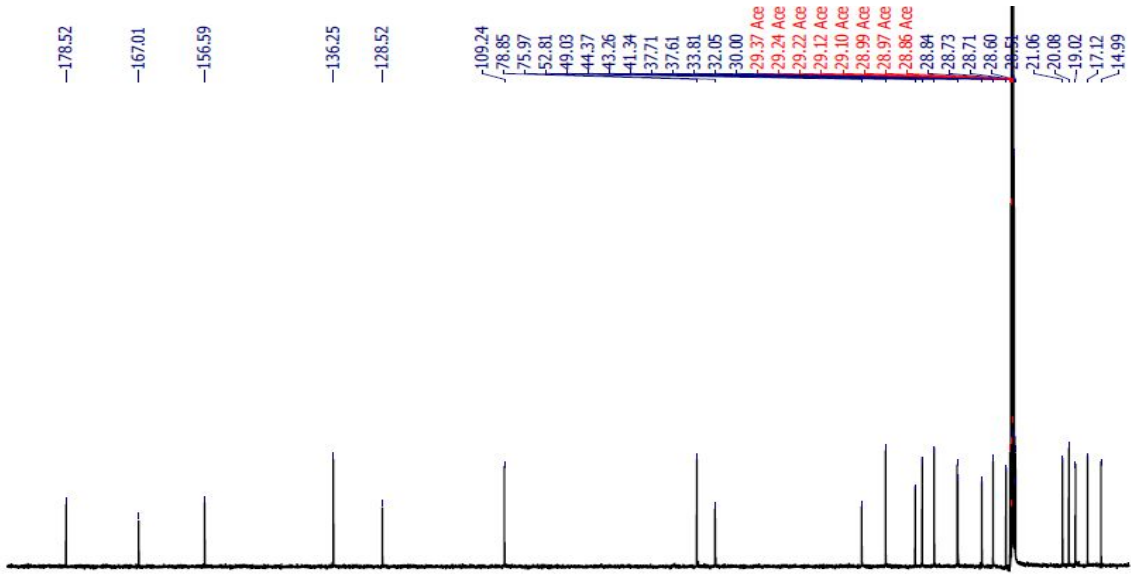

Appendix 51C. The ESIMS spectrum of 9*β*-hydroxy-15*α*-angeloyloxy-*ent*-kaur-16-en-19-oic acid (**236**)

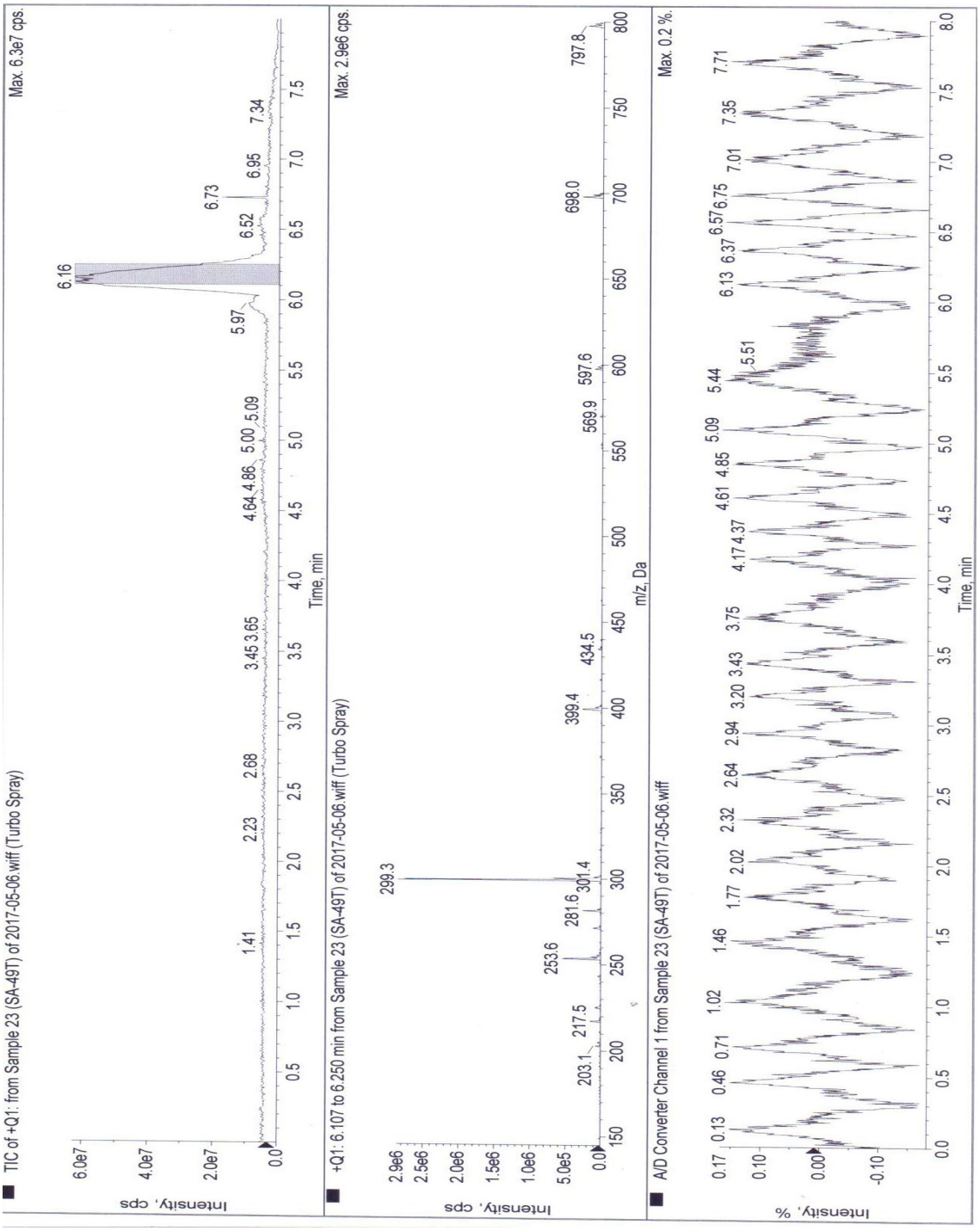

Appendix 52A: The ^{1}H NMR spectrum (600 MHz) of 15α-angeloyloxy-16α,17-epoxy-*ent*-kauran-19-oic acid (**237**) in CD_2Cl_2

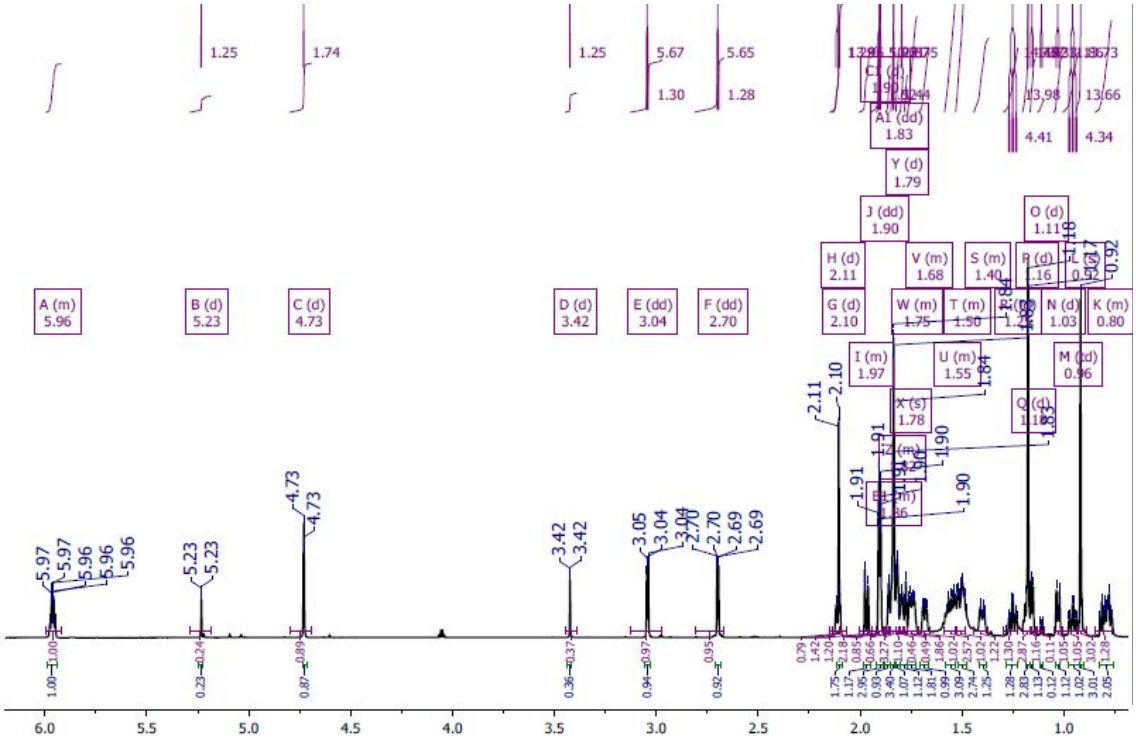

Appendix 52B: The ^{13}C NMR spectrum (150MHz) of 15α-angeloyloxy-16α,17-epoxy-*ent*-kauran-19-oic acid (**237**) in CD_2Cl_2

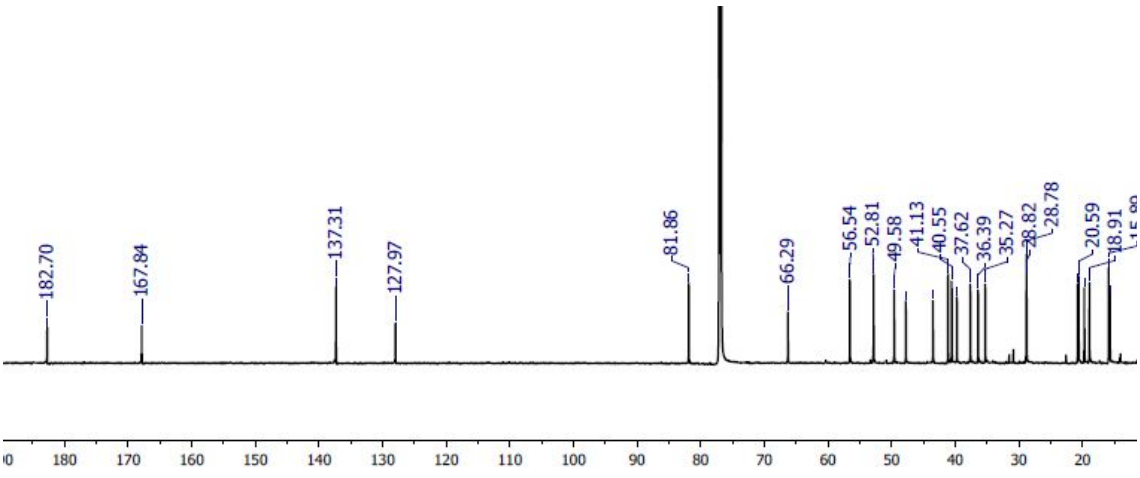

Appendix 52C. The ESIMS spectrum of 15*α*-angeloyloxy-16*α*,17-epoxy-*ent*-kauran-19-oic acid (**237**)

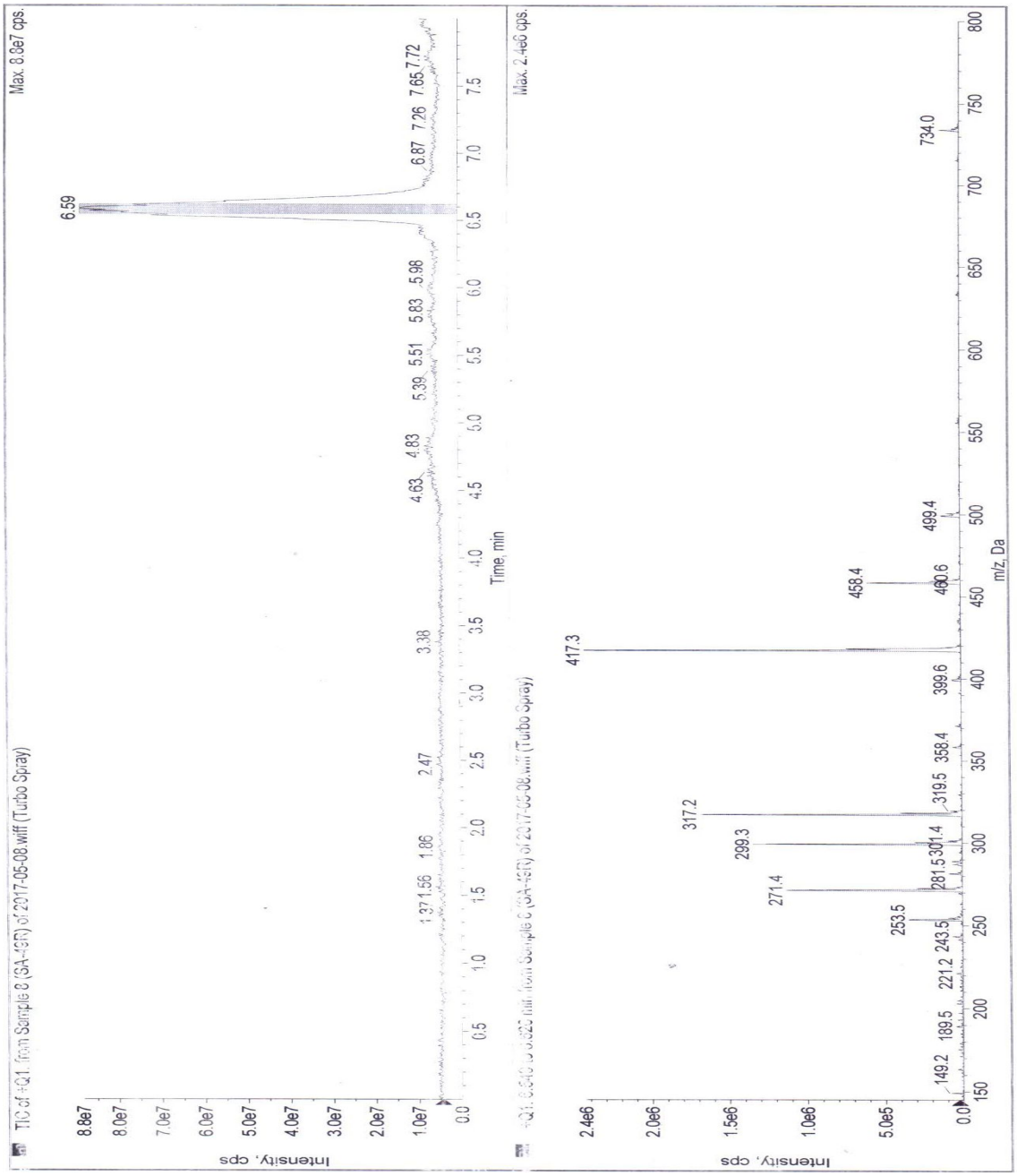

Appendix 53A: The ^{1}H NMR spectrum (600 MHz) of methyl-9β-hydroxy-15α-angeloyloxy-*ent*-kaur-16-en-19-oate (**238**) in CD_2Cl_2

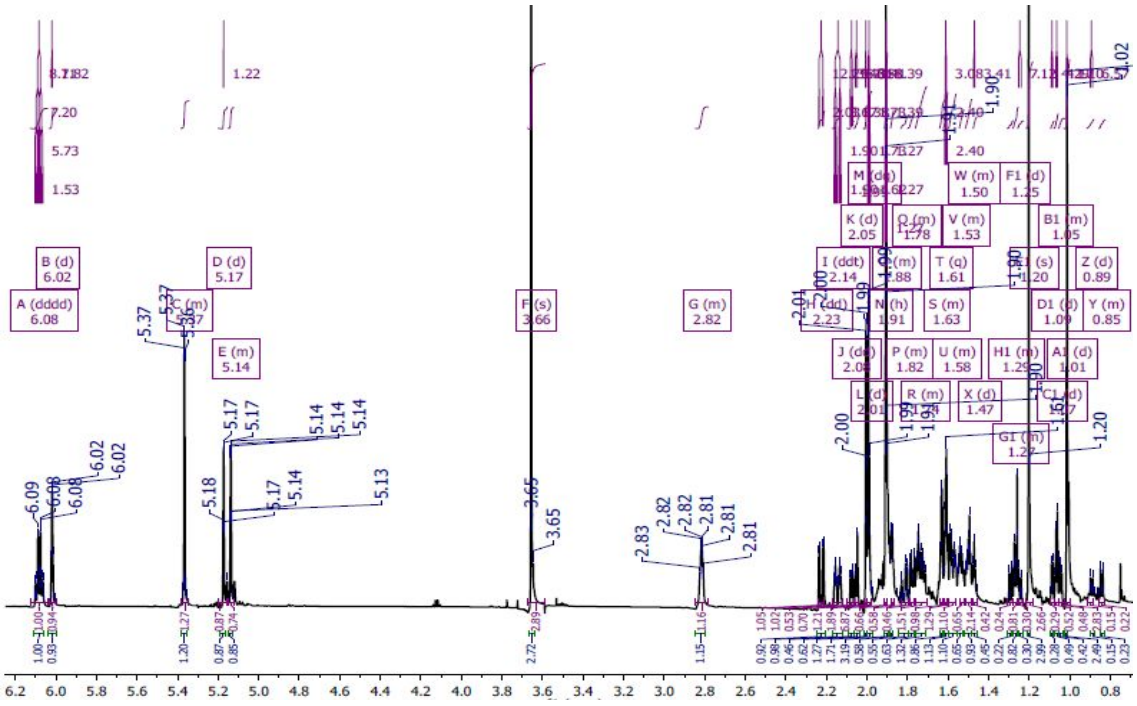

Appendix 53B: The ^{13}C NMR spectrum (150MHz) of methyl-9β-hydroxy-15α-angeloyloxy-*ent*-kaur-16-en-19-oate (**238**) in CD_2Cl_2

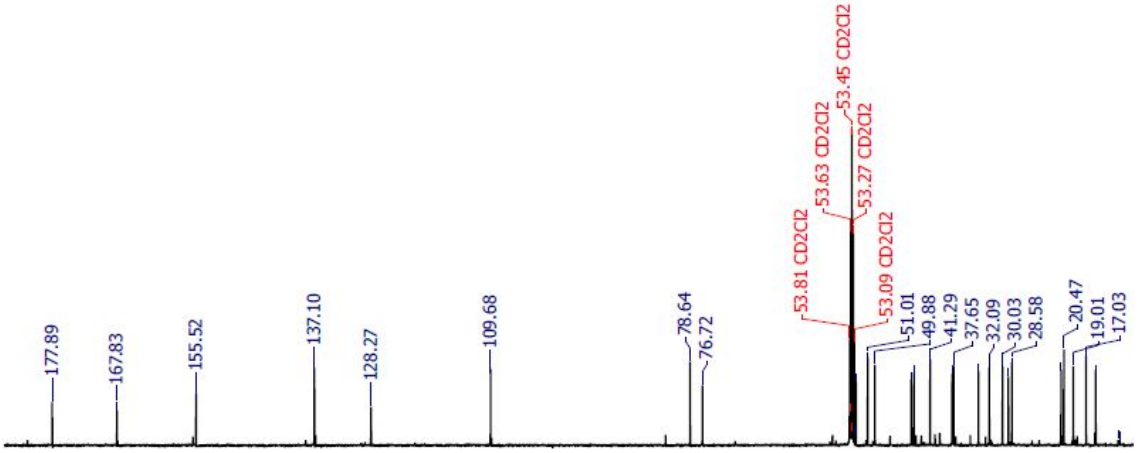

Appendix 53C. The ESIMS spectrum of methyl-9*β*-hydroxy-15*α*-angeloyloxy-*ent*-kaur-16-en-19-oate (**238**)

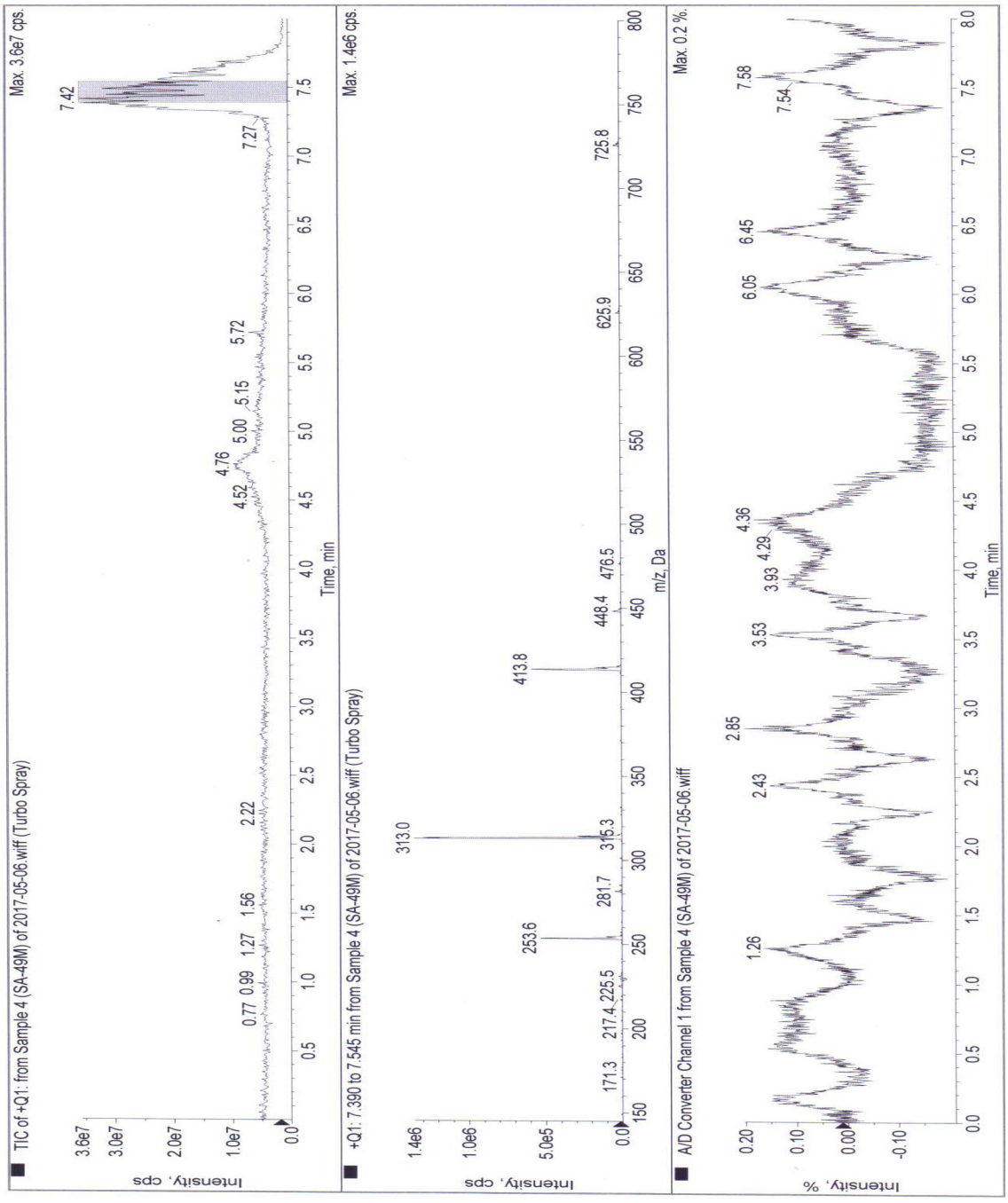

Appendix 54A: The ^{1}H NMR (600 MHz) spectrum of 15α-angeloyloxy-*ent*-kaur-16-en-19-oic acid (**239**) in CD_2Cl_2

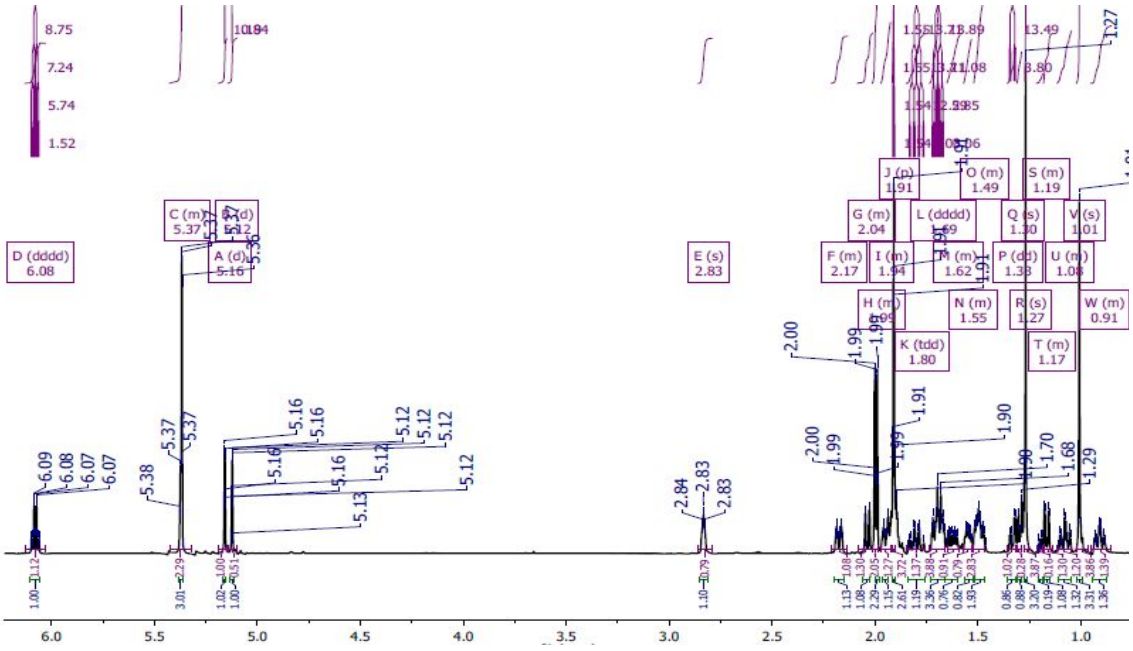

Appendix 54B: The ^{13}C NMR (150MHz) spectrum of 15α-angeloyloxy-*ent*-kaur-16-en-19-oic acid (**239**) in CD_2Cl_2

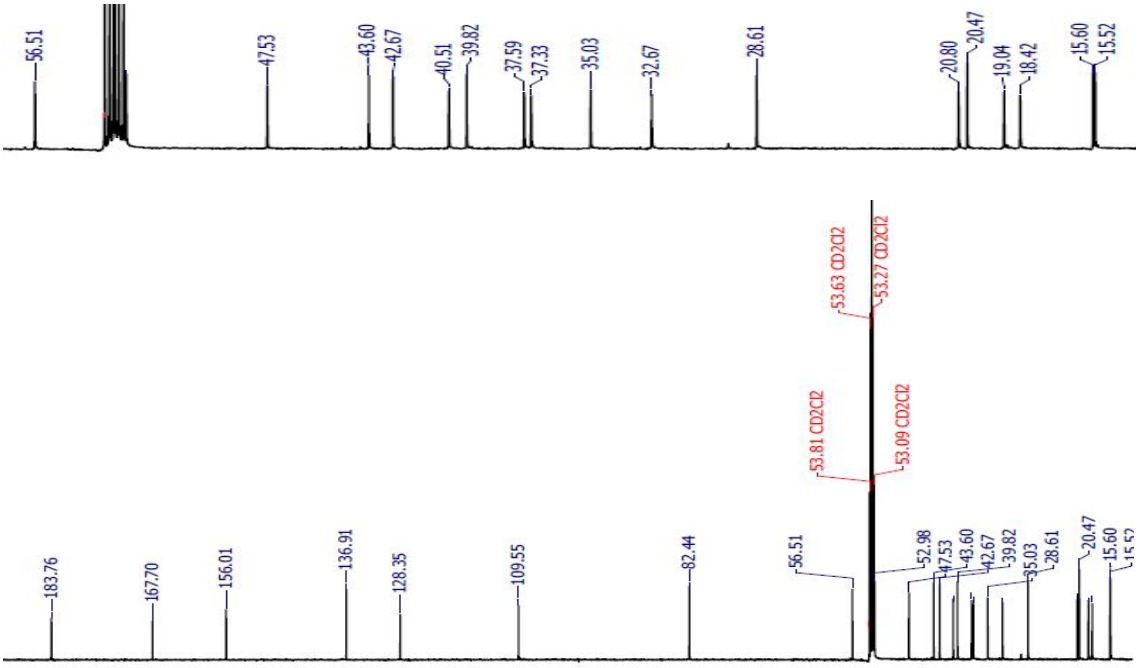

Appendix 73C. The ESIMS spectrum of 15α-angeloyloxy-*ent*-kaur-16-en-19-oic acid (**239**)

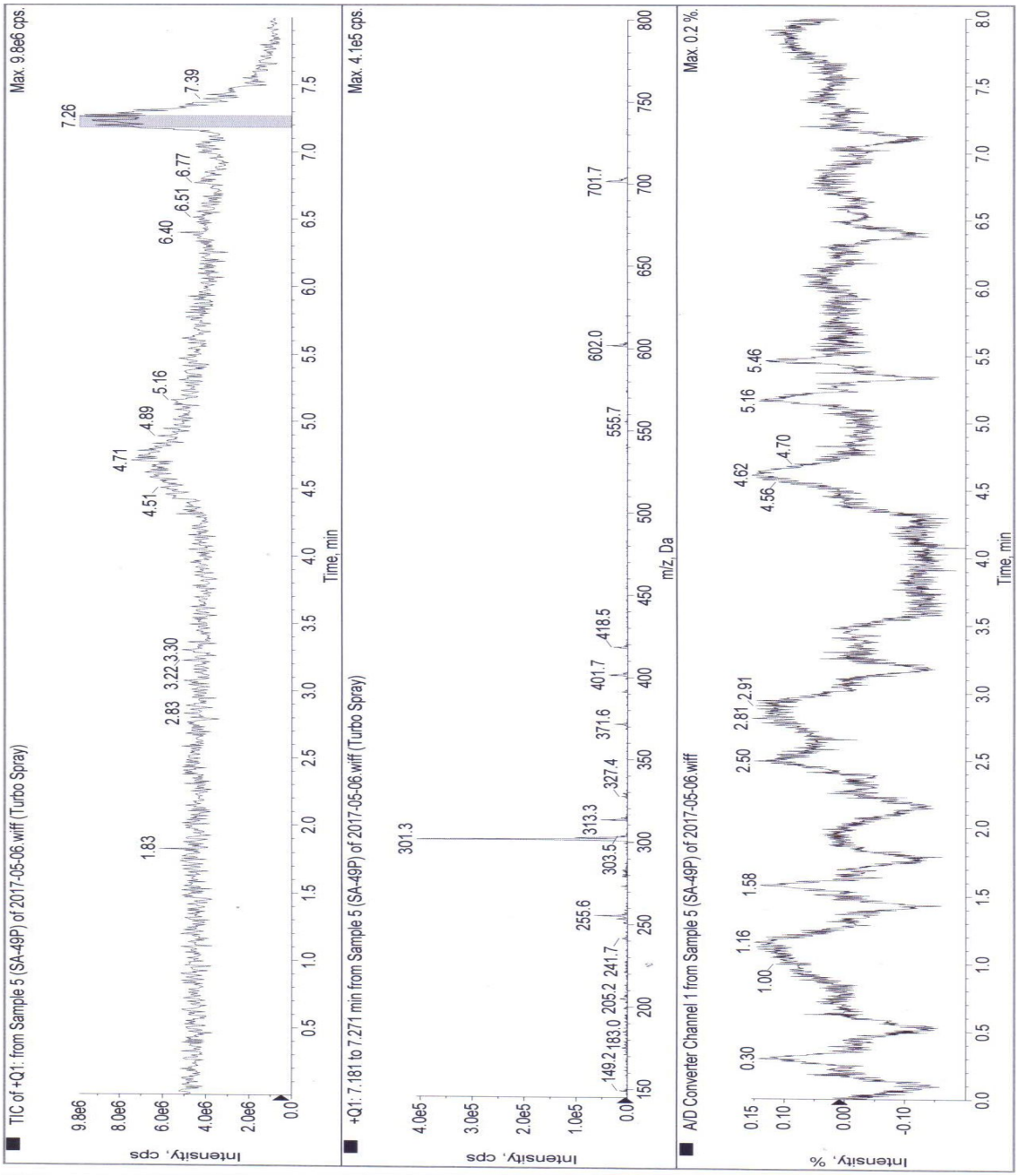

Appendix 55A: The ^{1}H NMR spectrum (600 MHz) of *ent*-kaura-9(11),16-dien-19-oic acid (**240**) in CD_2Cl_2

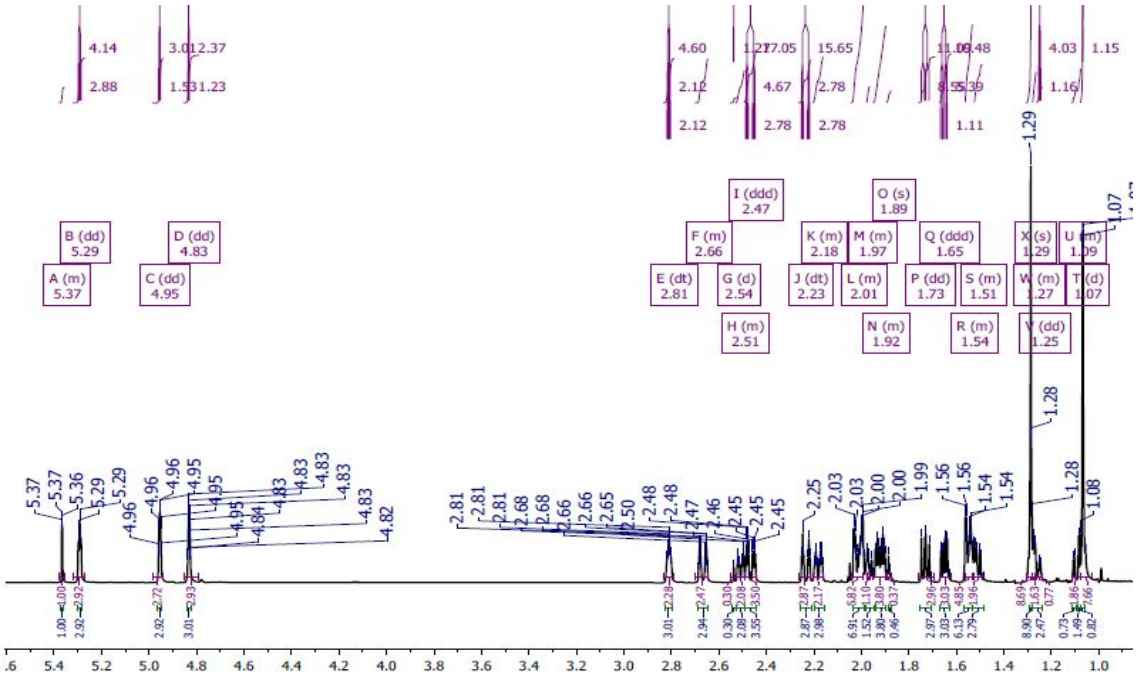

Appendix 55B: The ^{13}C NMR spectrum (150MHz) of *ent*-kaura-9(11),16-dien-19-oic acid (**329**) in CD_2Cl_2

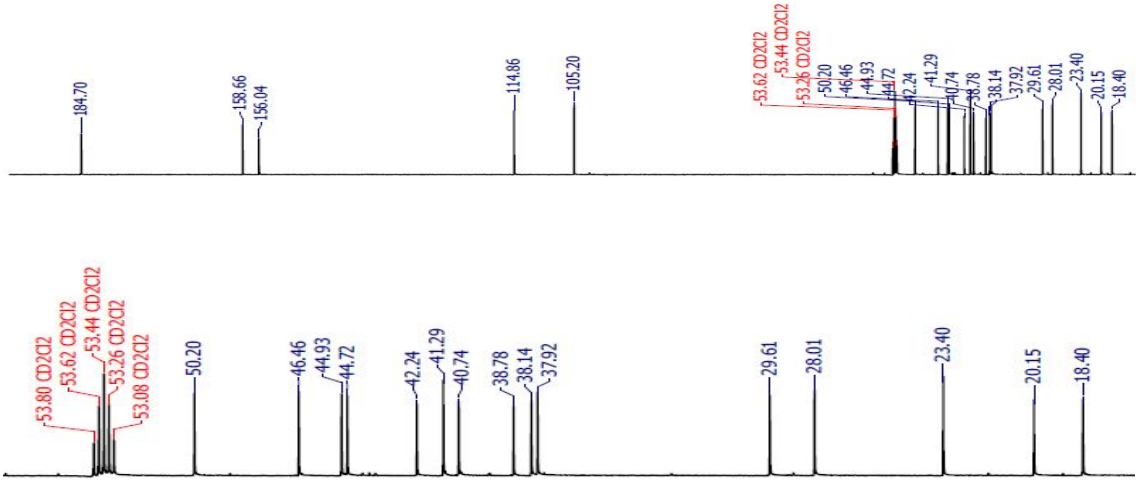

Appendix 55C: The UV graph of *ent*-kaura-9(11), 16-dien-19-oic acid (**240**)

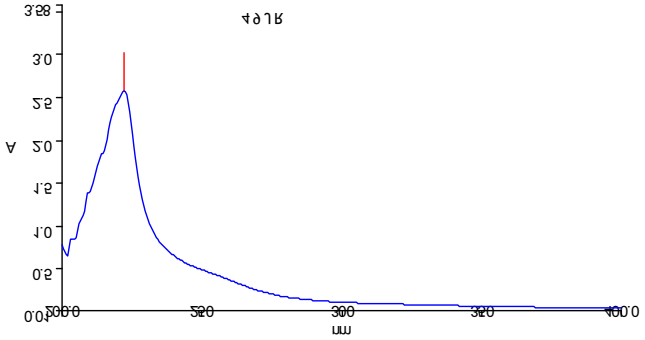

Appendix 56A: The ^{1}H NMR spectrum (600 MHz) of *ent*-kaura-9(11),16-dien-12-one (**241**) in Acetone-d_6

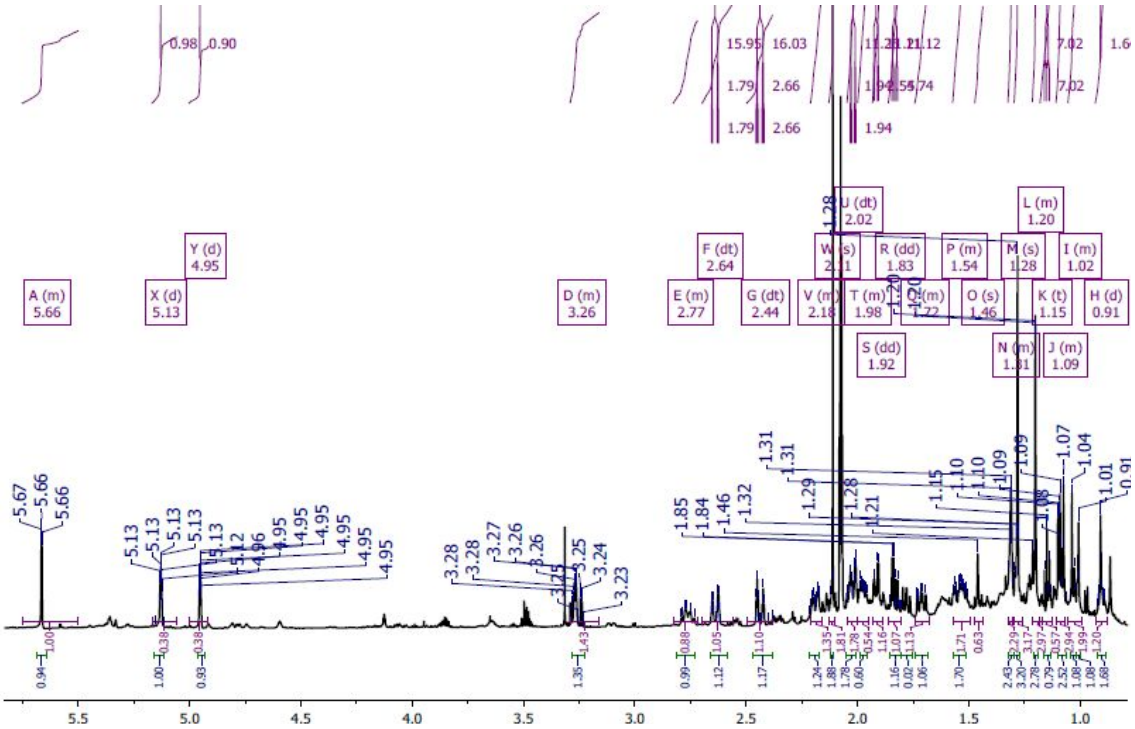

Appendix 56B: The ^{13}C NMR spectrum (150MHz) of *ent*-kaura-9(11),16-dien-12-one (**241**) in Acetone-d_6

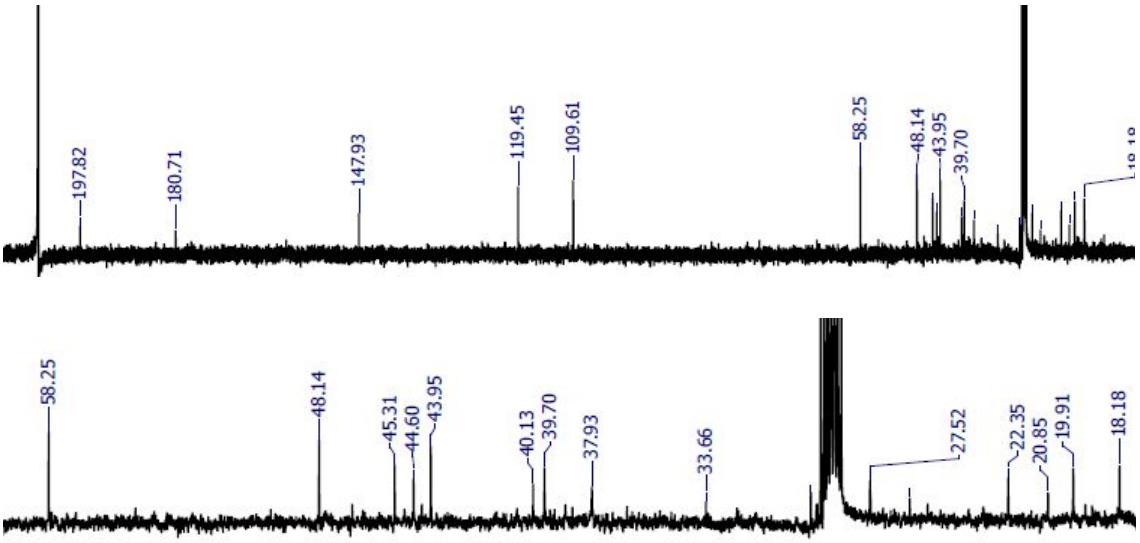

Appendix 56C: The UV graph of *ent*-kaura-9(11),16-dien-12-one (**241**)

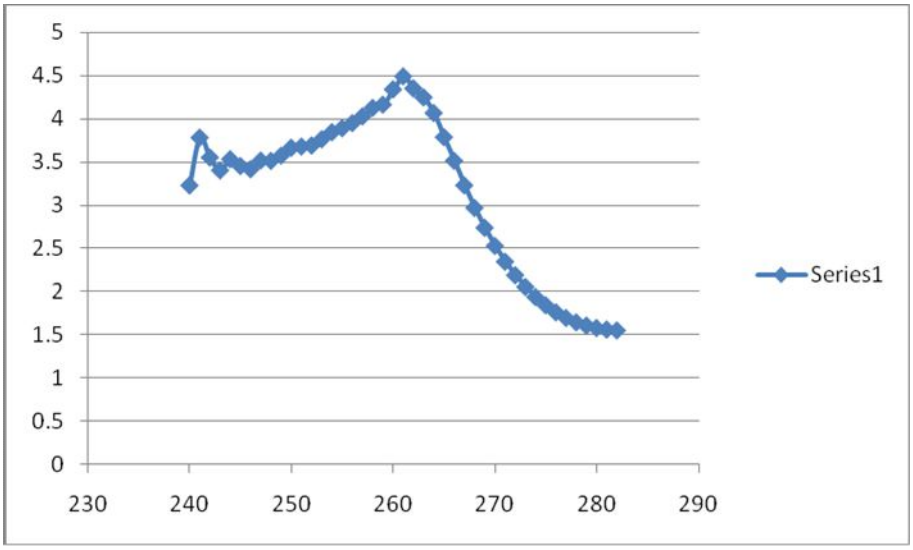

Appendix 57A: The ^{1}H NMR spectrum (500 MHz) of methyl-*ent*-kaur-16-en-19-oate (**242**) in Acetone-d_6

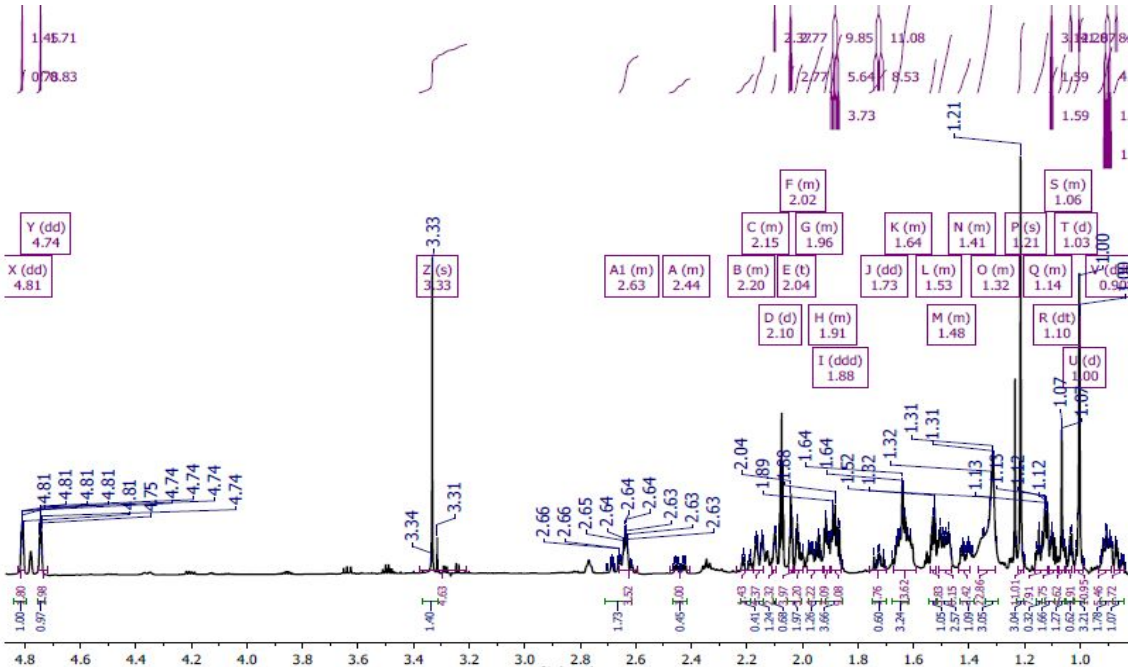

Appendix 57B: The ^{13}C NMR spectrum (125MHz) of methyl-*ent*-kaur-16-en-19-oate (**242**) in Acetone-d_6

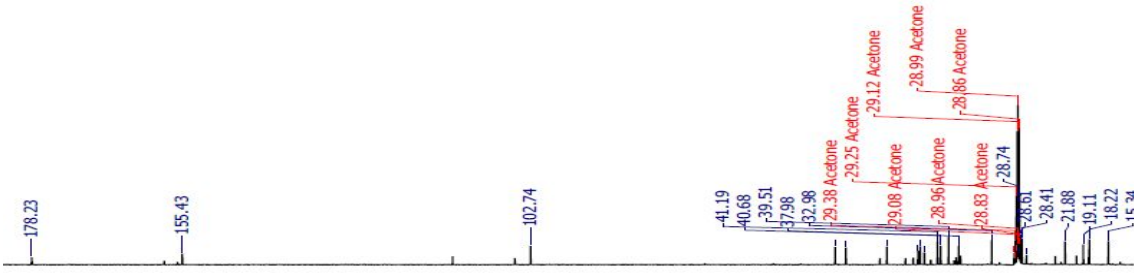

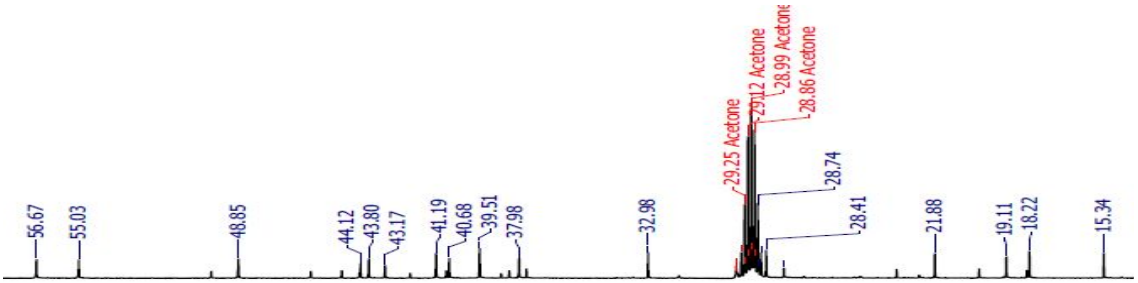

Appendix 57C. The ESIMS spectrum of methyl-*ent*-kaur-16-en-19-oate (**242**)

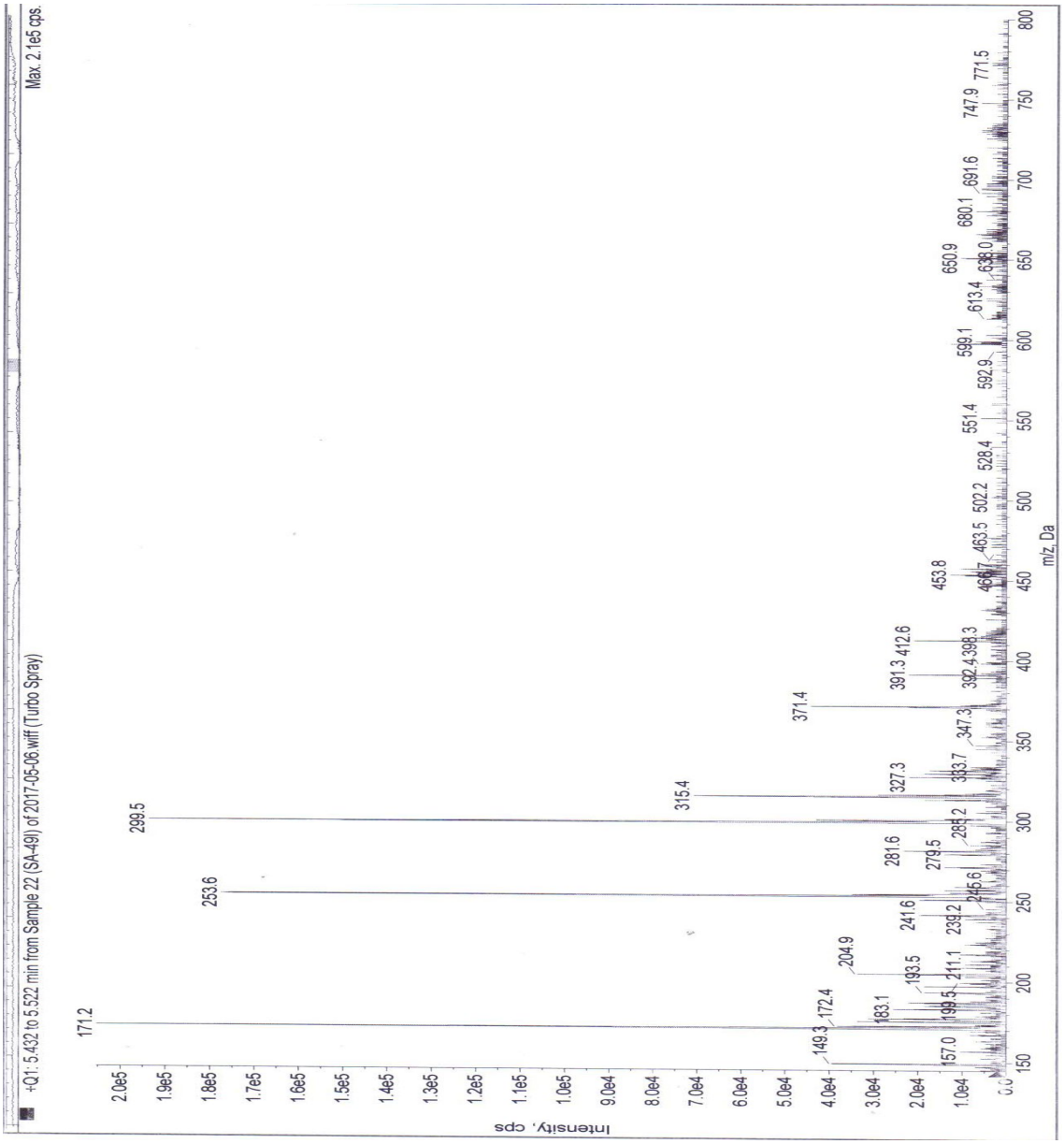

Appendix 58A: The ^{1}H NMR spectrum (600 MHz) of *ent*-kaur-16-en-19-oic acid (**243**) in Acetone-d_6

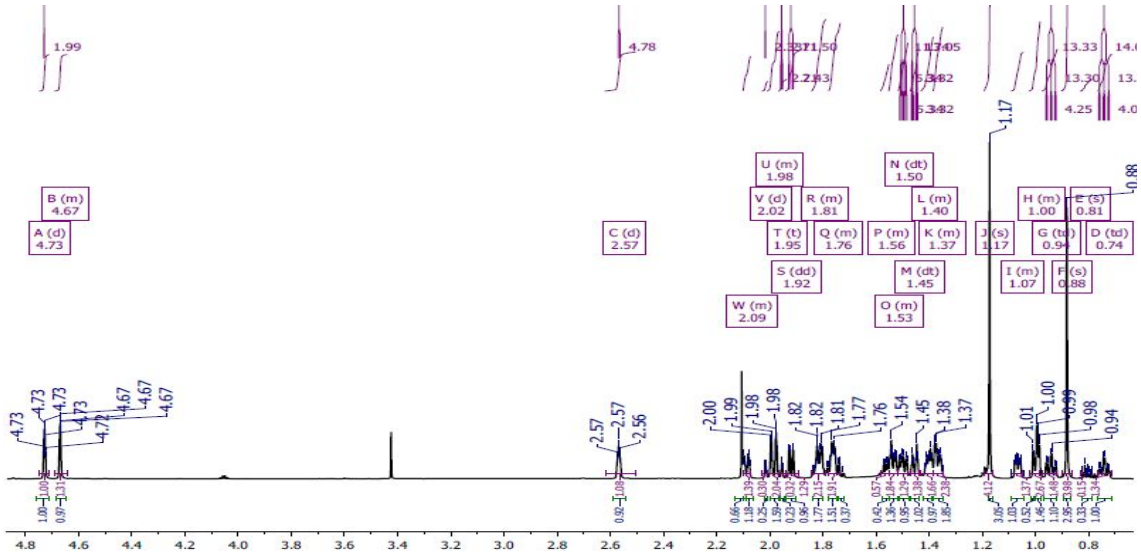

Appendix 58B: The ^{13}C NMR spectrum (150MHz) of *ent*-kaur-16-en-19-oic acid (**243**) in Acetone-d_6

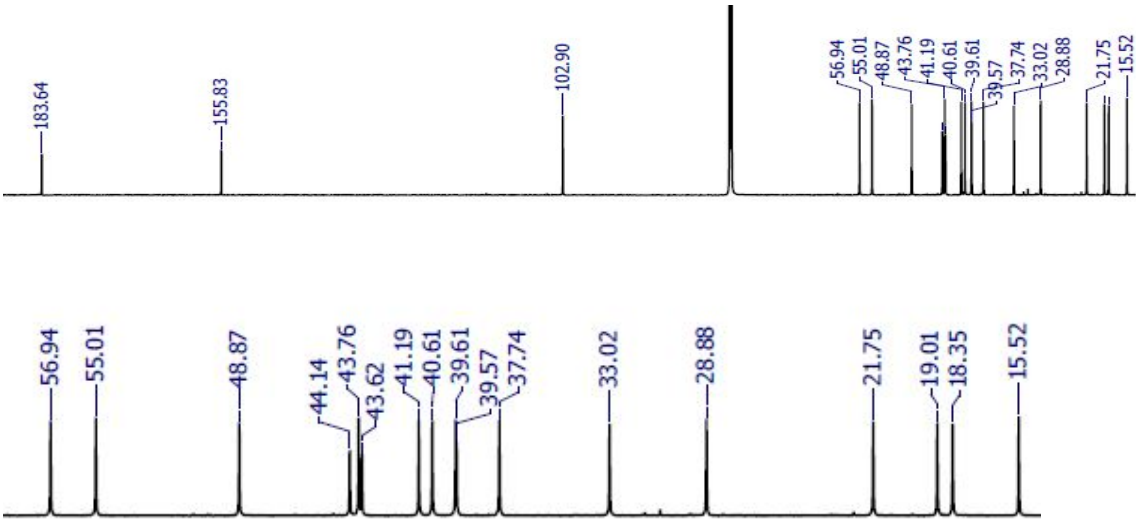

Appendix 58C. The ESIMS spectrum of *ent*-kaur-16-en-19-oic acid (**243**)

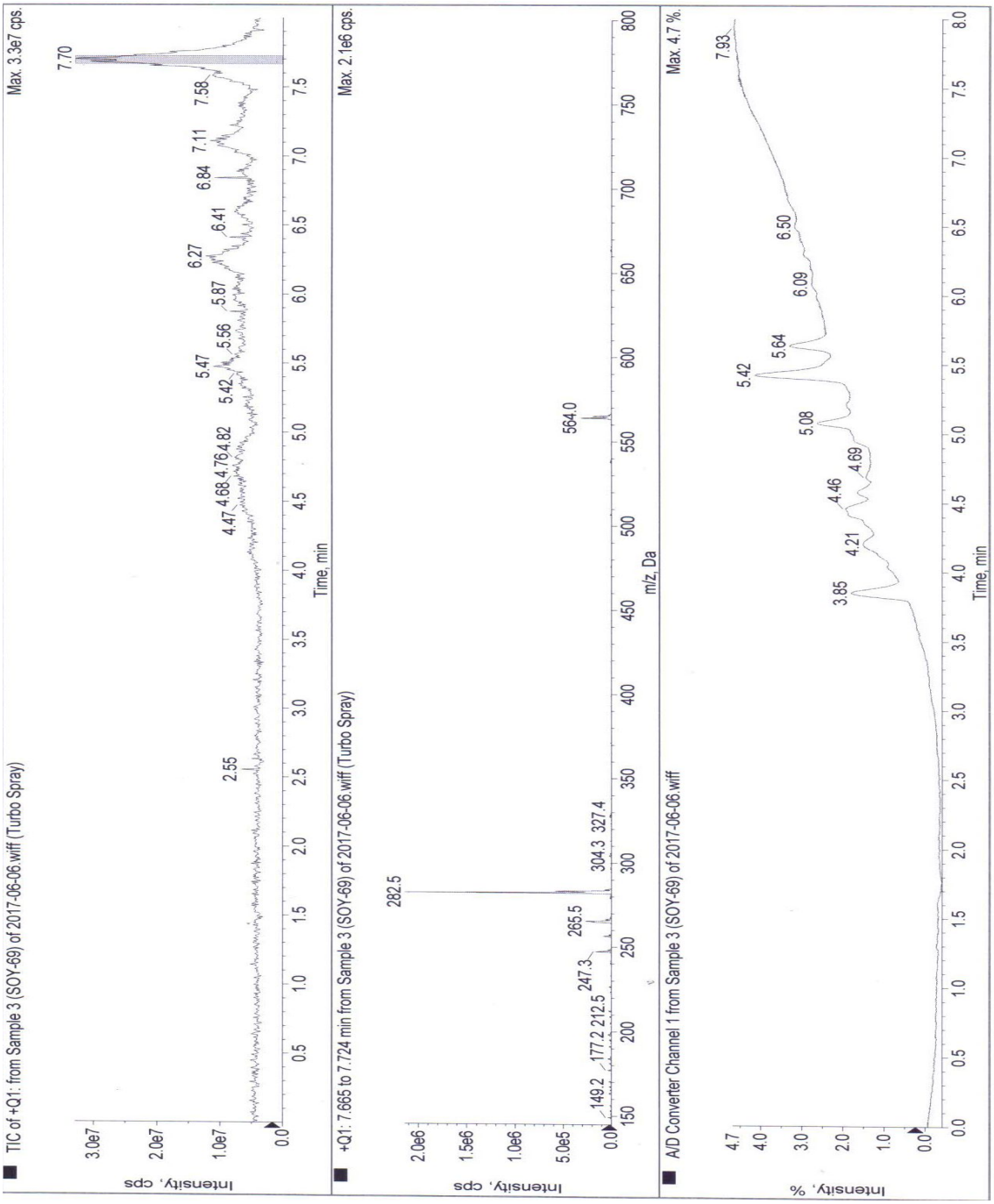

Appendix 59A: The ^{1}H NMR spectrum (600 MHz) *ent*-kaur-16-en-19-ol (**244**) in $CDCl_3$

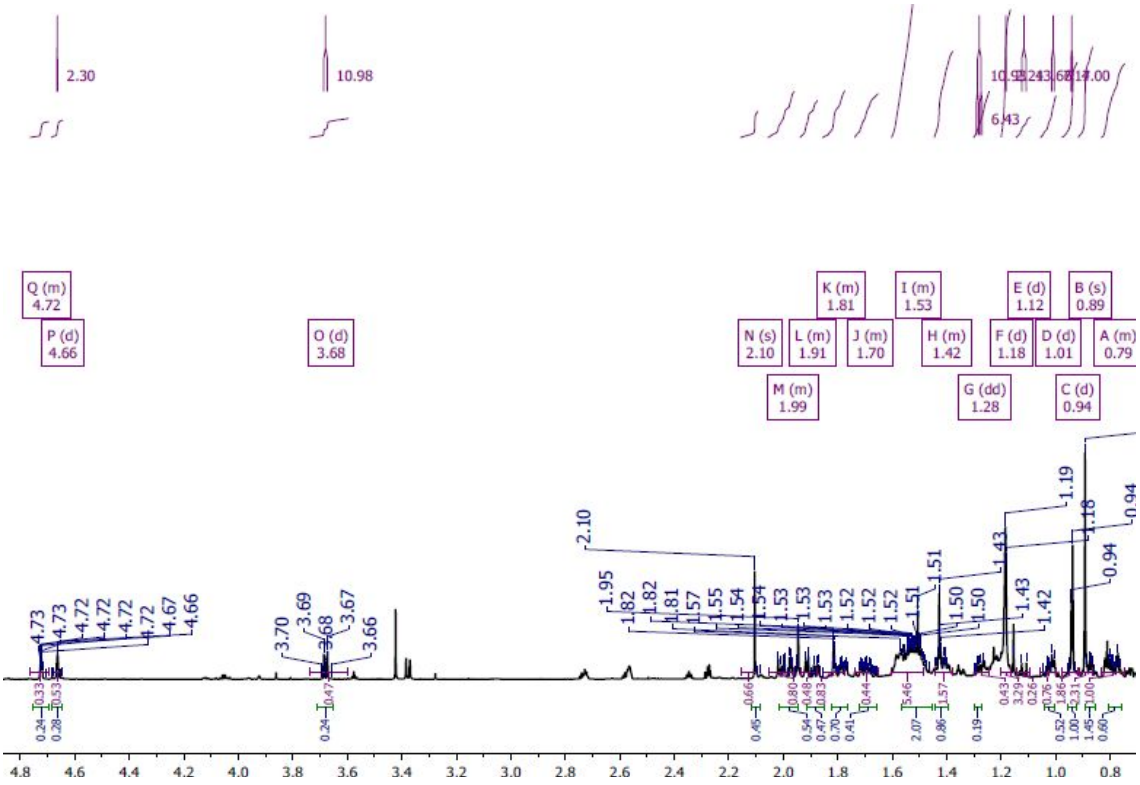

Appendix 59B: The ^{13}C NMR spectrum (200MHz) of *ent*-kaur-16-en-19-ol (**244**) in $CDCl_3$

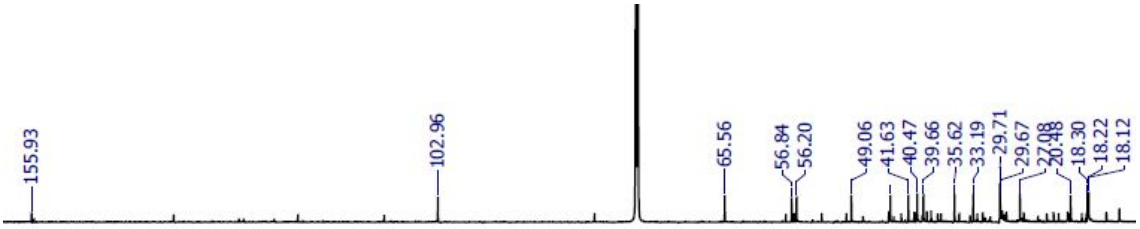

Appendix 60A: The ^{1}H NMR spectrum (500 MHz) of *ent*- kaur-16-ene (**245**) in Acetone-d_6

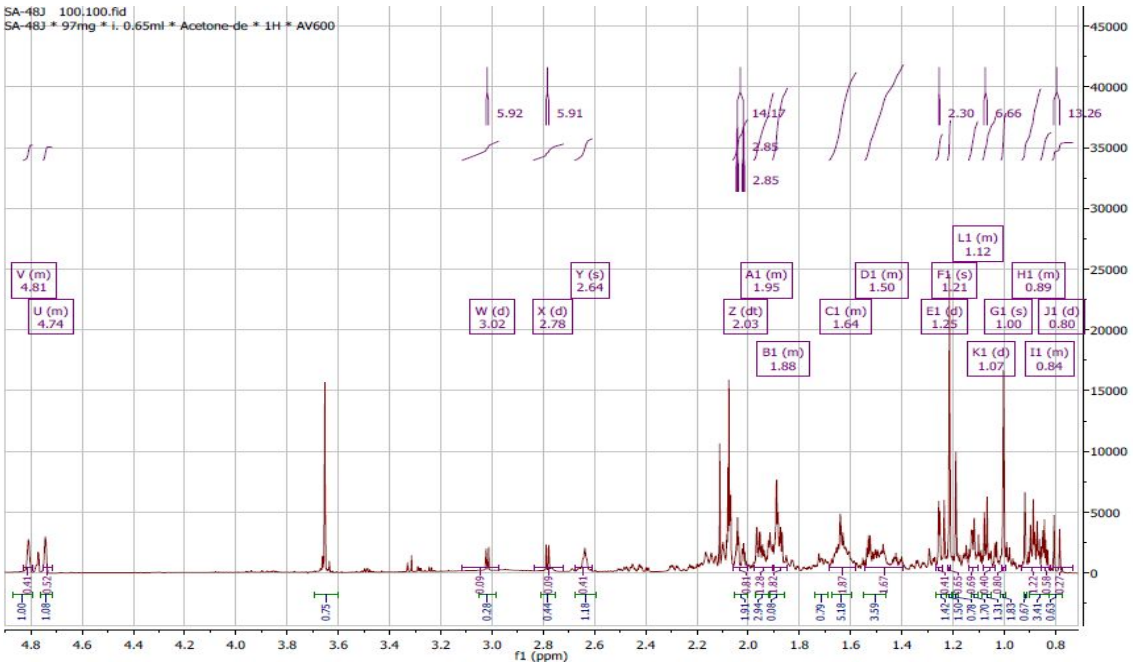

Appendix 60B: The ^{13}C NMR spectrum (125MHz) of *ent*- kaur-16-ene (**245**) in Acetone-d_6

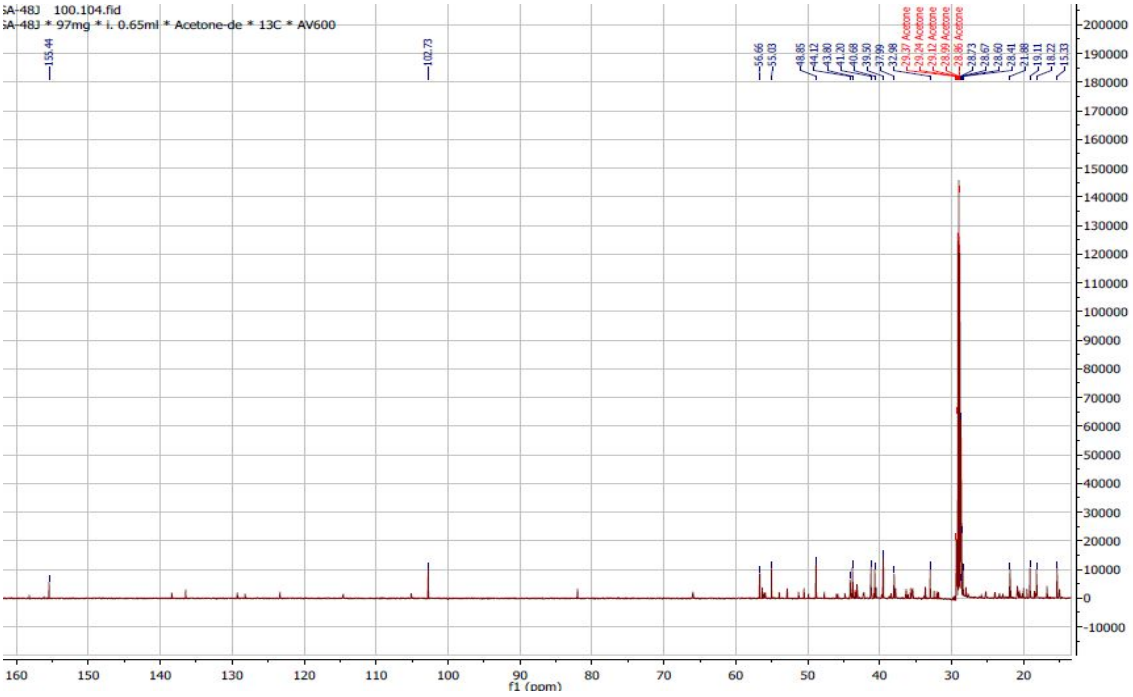

Appendix 61A: The ^{1}H NMR spectrum (600 MHz) of Lanosterol (**246**) in Acetone-d_6

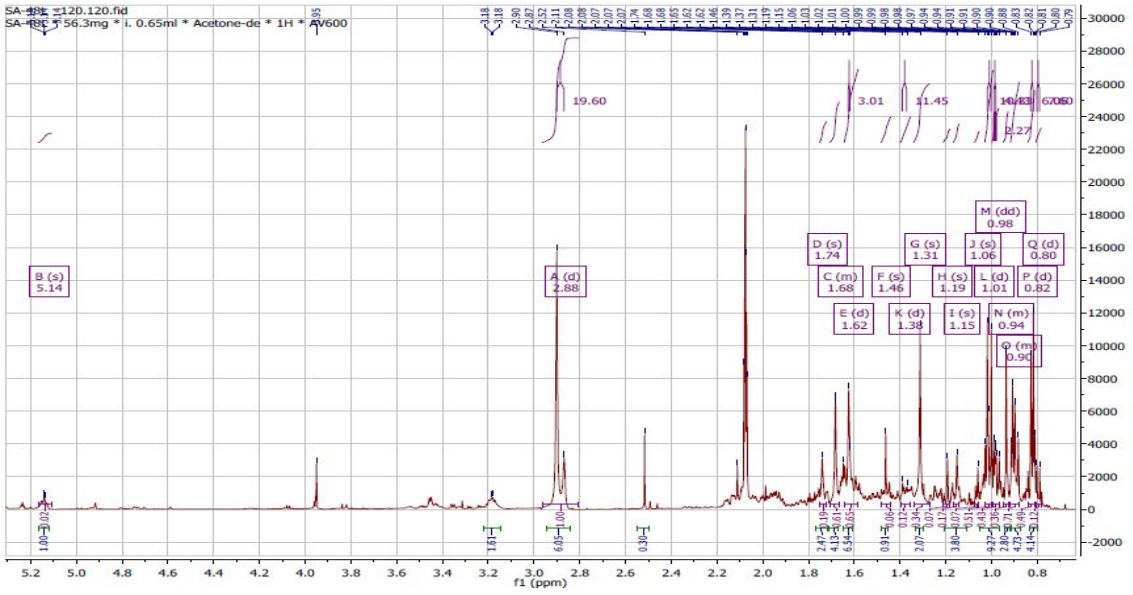

Appendix 61B: The ^{13}C NMR spectrum (150MHz) of Lanosterol (**246**) in Acetone-d_6

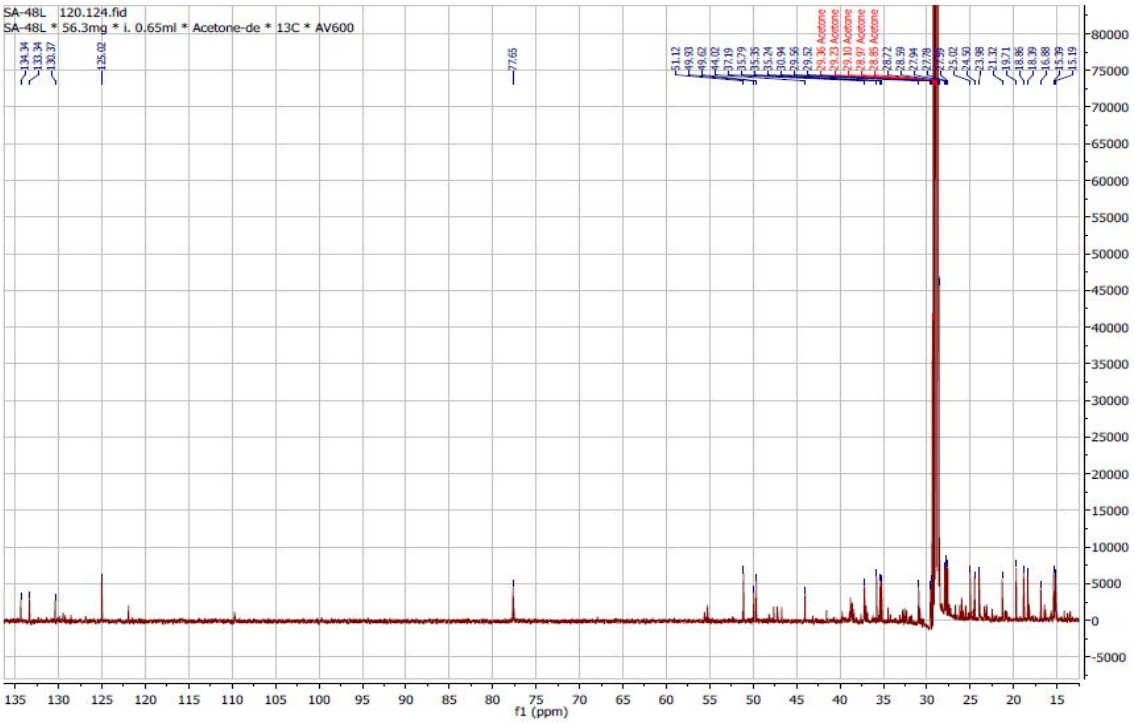

Appendix 62A: The ^{1}H NMR spectrum (600 MHz) of stigmasta-5,22(E)-dien-3β-ol (**247**) in CD_2Cl_2

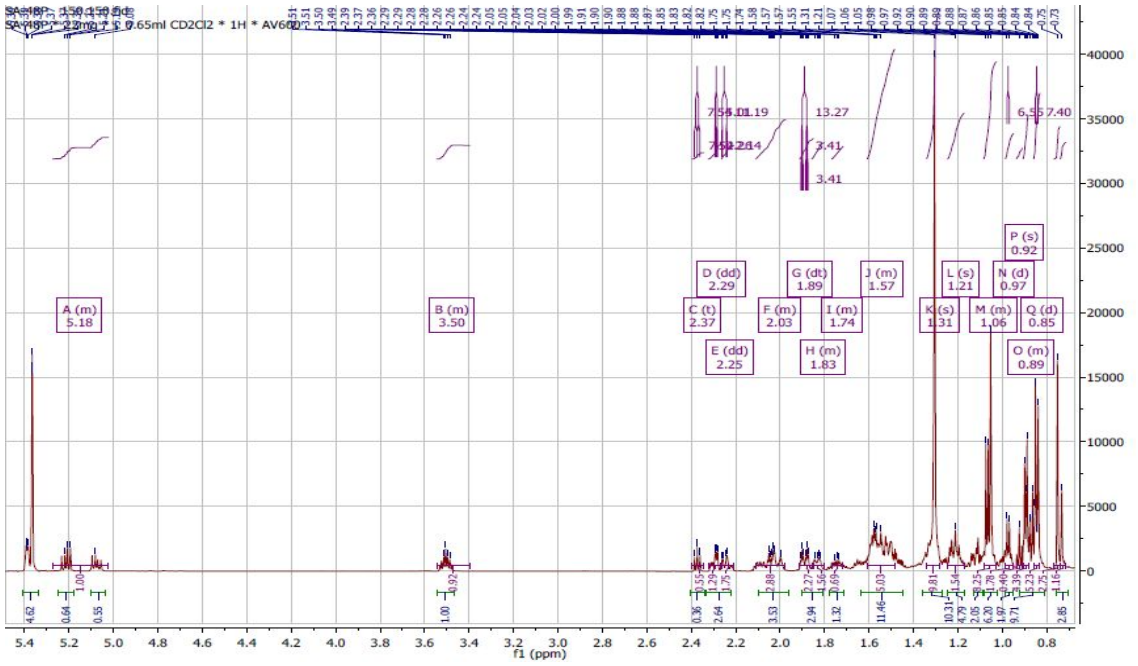

Appendix 62B: The ^{13}C NMR spectrum (150MHz) of stigmasta-5,22(E)-dien-3β-ol (**247**) in CD_2Cl_2

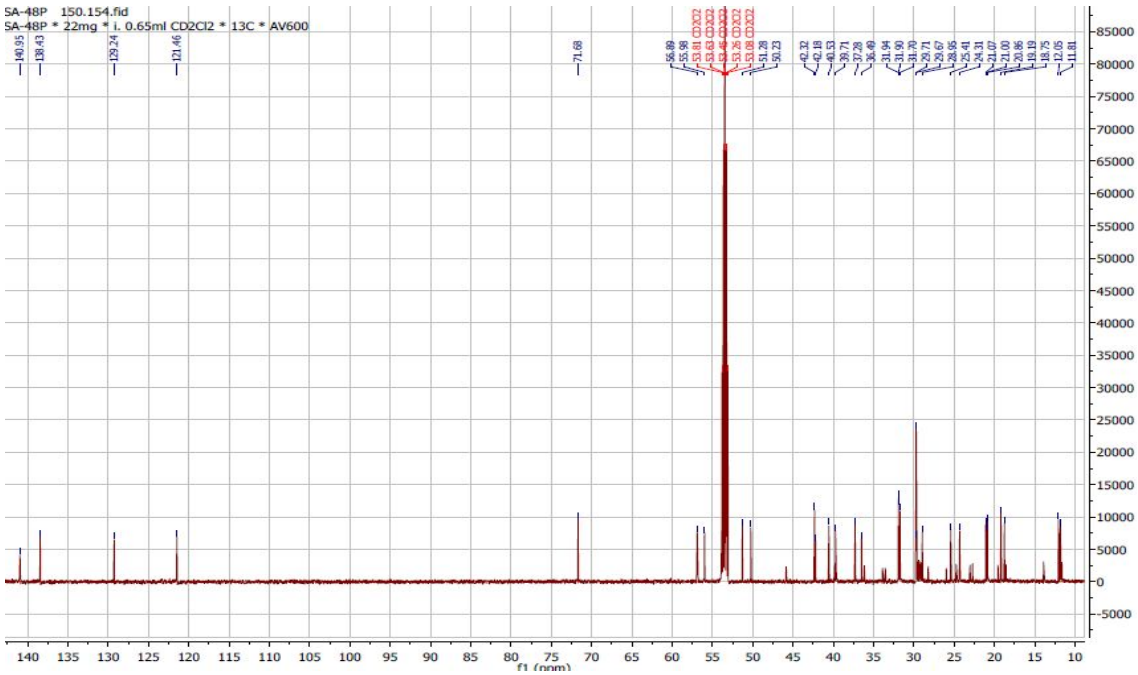

Appendix 63A: The ^{1}H NMR spectrum (600 MHz) of 3β-hydroxy-olean-12-en-29-oic acid (**248**) in DMSO

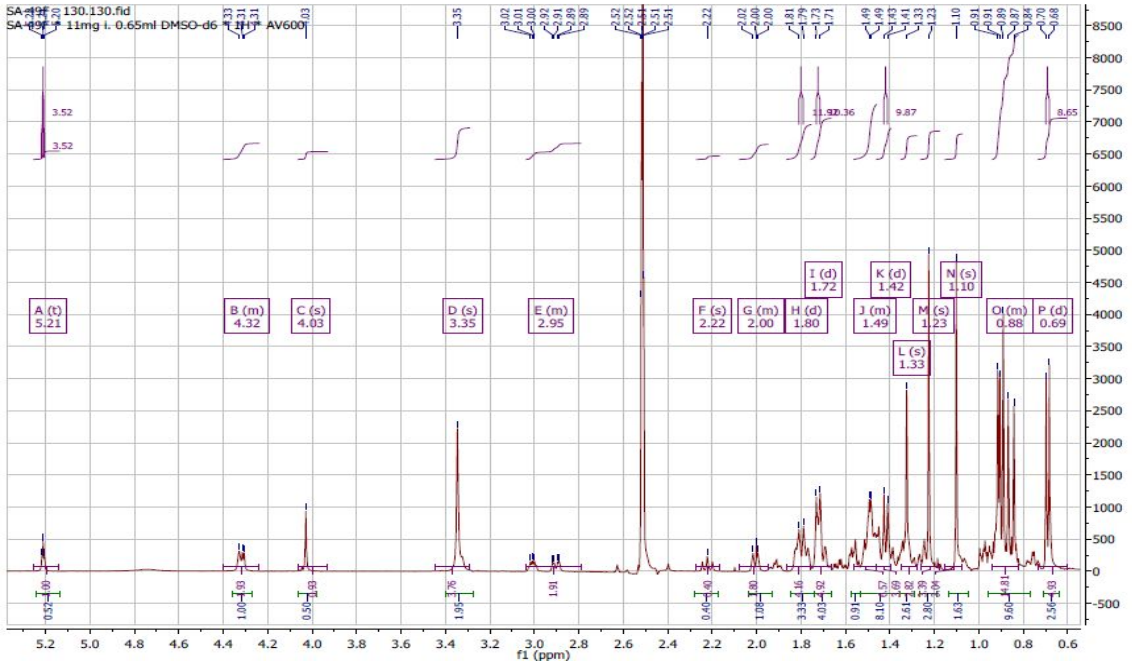

Appendix 63B: The ^{13}C NMR spectrum (150MHz) of 3β--hydroxy-olean-12-en-29-oic acid (**248**) in DMSO

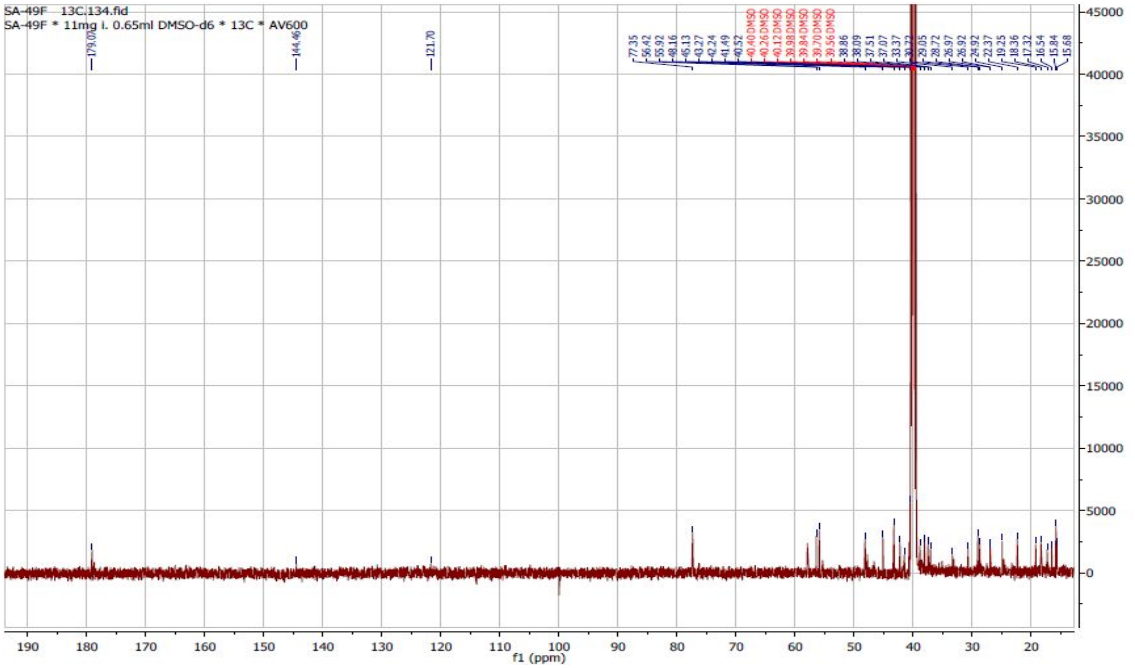

Appendix 64A: The ^{1}H NMR spectrum (500 MHz) of carissone (**249**) in Acetone-d_6

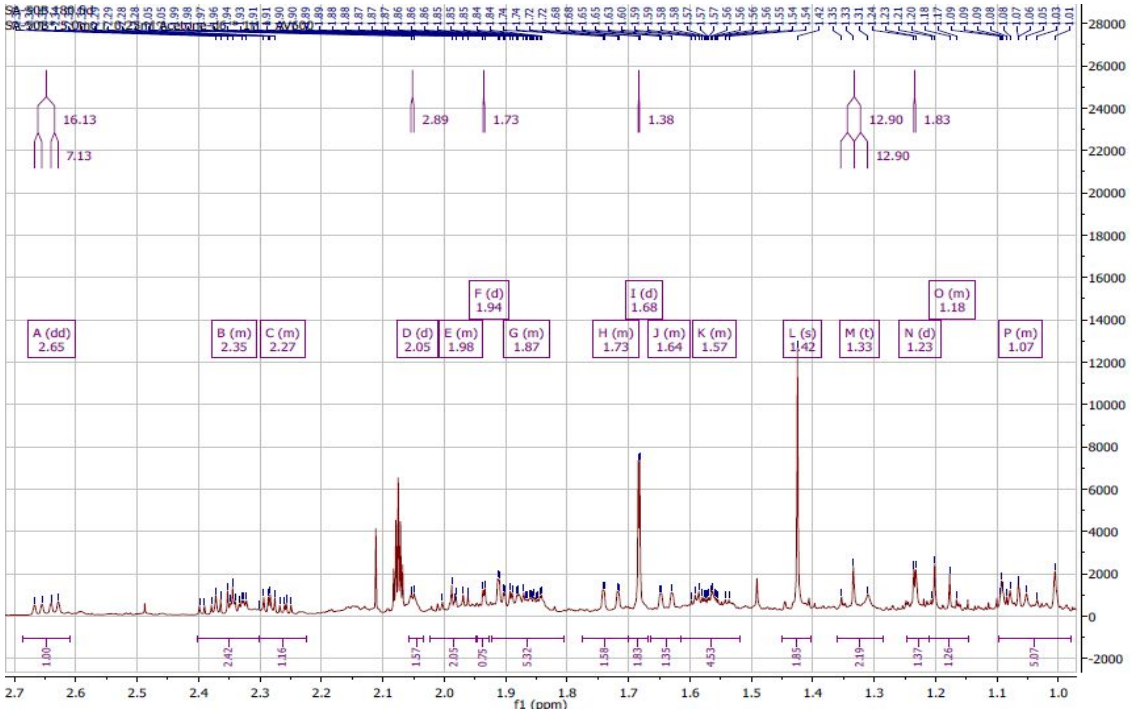

Appendix 64B: The ^{13}C NMR spectrum (125MHz) of carissone (**249**) in Acetone-d_6

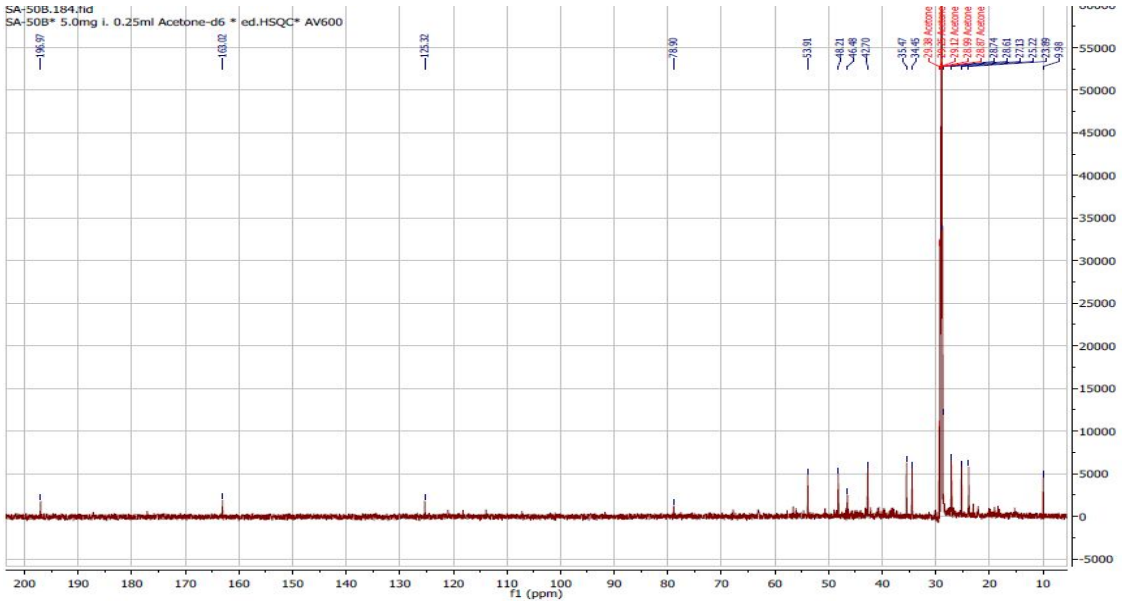

Appendix 65A: The ^{1}H NMR spectrum (600 MHz) of methyl-15α-angeloyloxy-*ent*-kaur-16-en-19-oate (**250**) in CD_2Cl_2

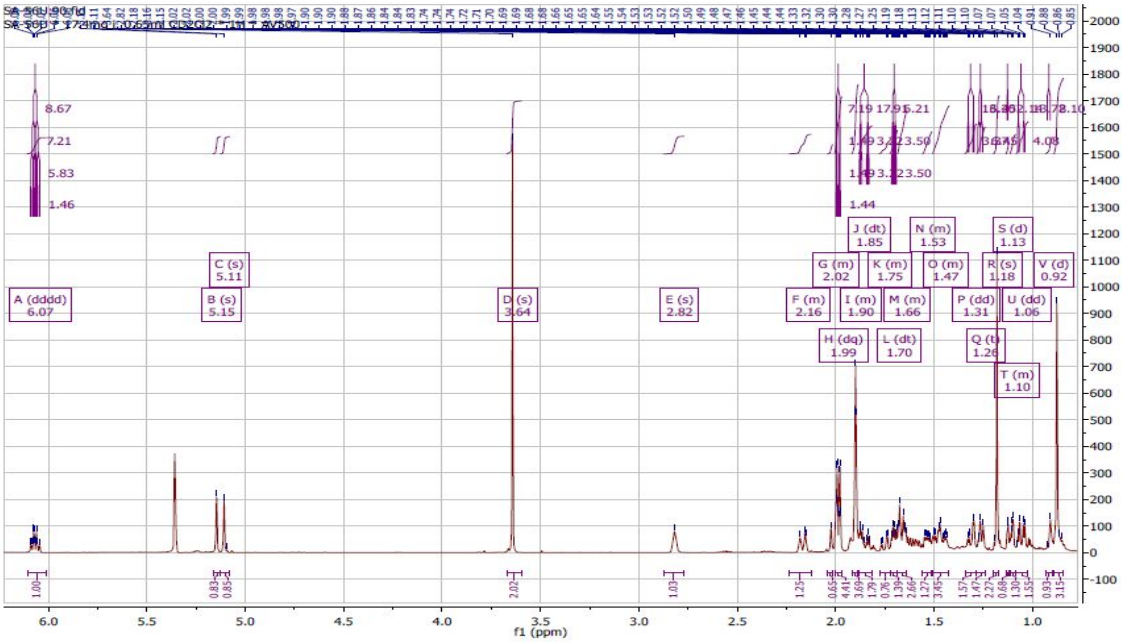

Appendix 65B: The ^{13}C NMR spectrum (150MHz) of methyl-15α-angeloyloxy-*ent*-kaur-16-en-19-oate (**250**) in CD_2Cl_2

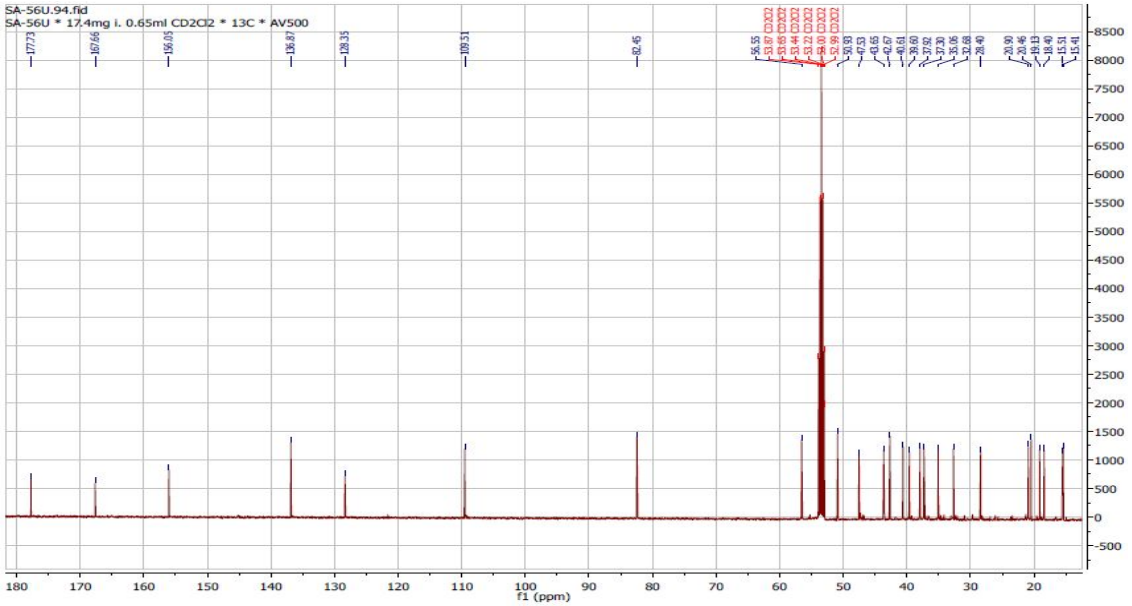

Appendix 66A: The ^{1}H NMR spectrum (800 MHz) of kaura-9(11),16-dien-12-oxo-19-oic acid (**251**) in $CDCl_3$

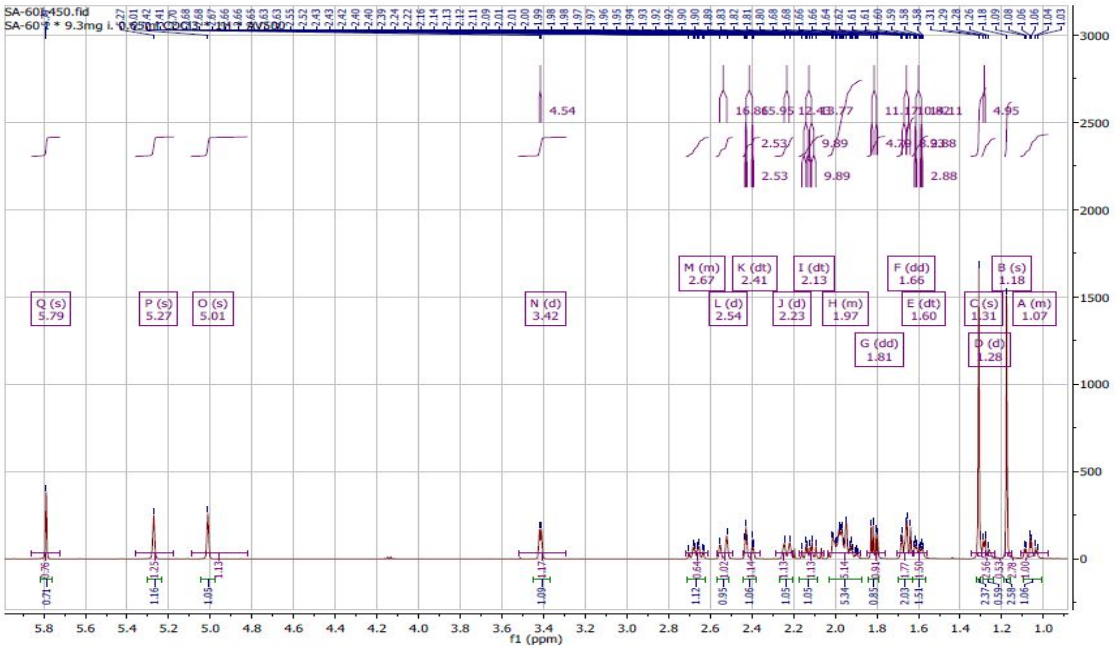

Appendix 66B: The ^{13}C NMR spectrum (200MHz) of kaura-9(11),16-dien-12-oxo-19-oic acid (**251**) in $CDCl_3$

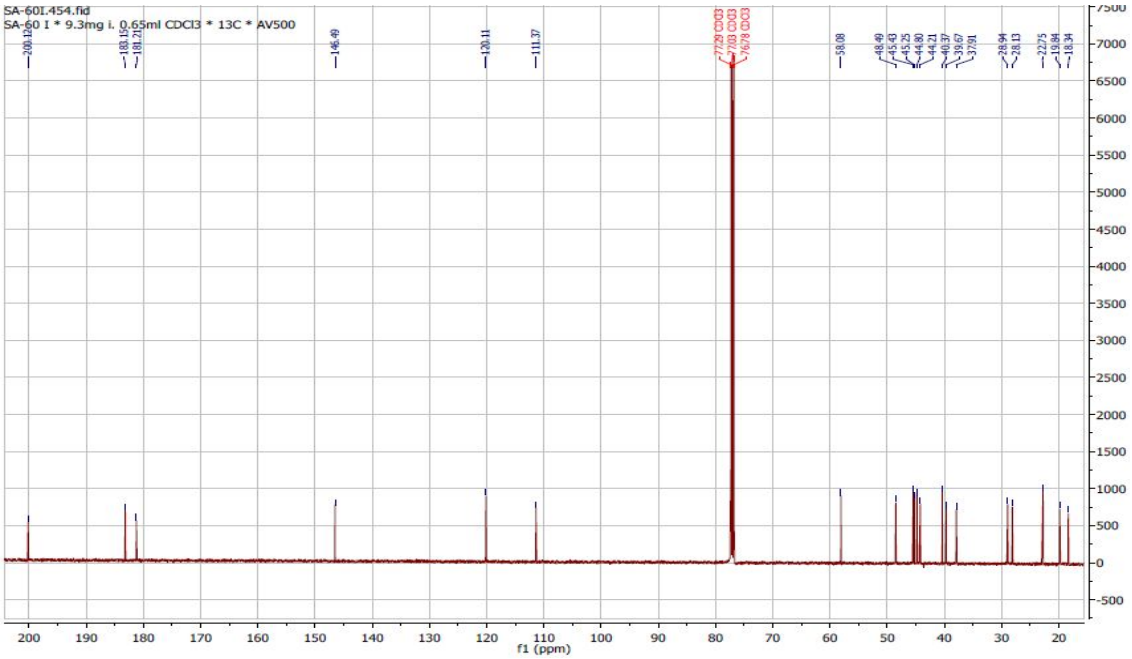

Appendix 67A: The ^{1}H NMR spectrum (500 MHz) of *ent*-kauran-19-oic acid (**252**) in Acetone-d_6

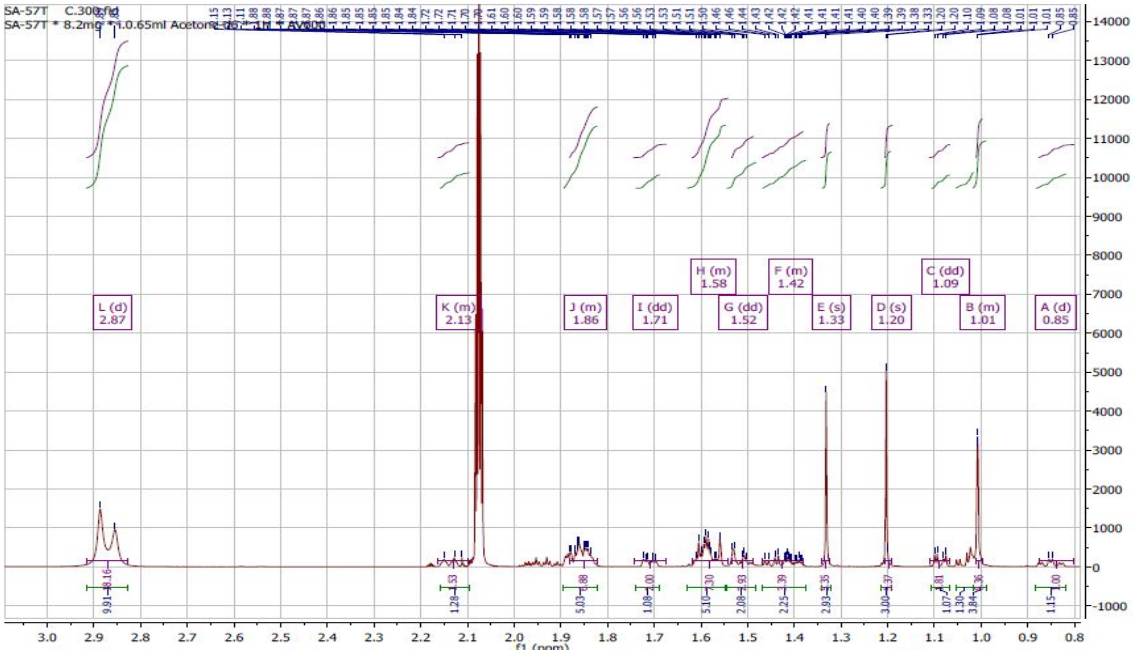

Appendix 67B: The ^{13}C NMR spectrum (125MHz) of *ent*-kauran-19-oic acid (**252**) in Acetone-d_6

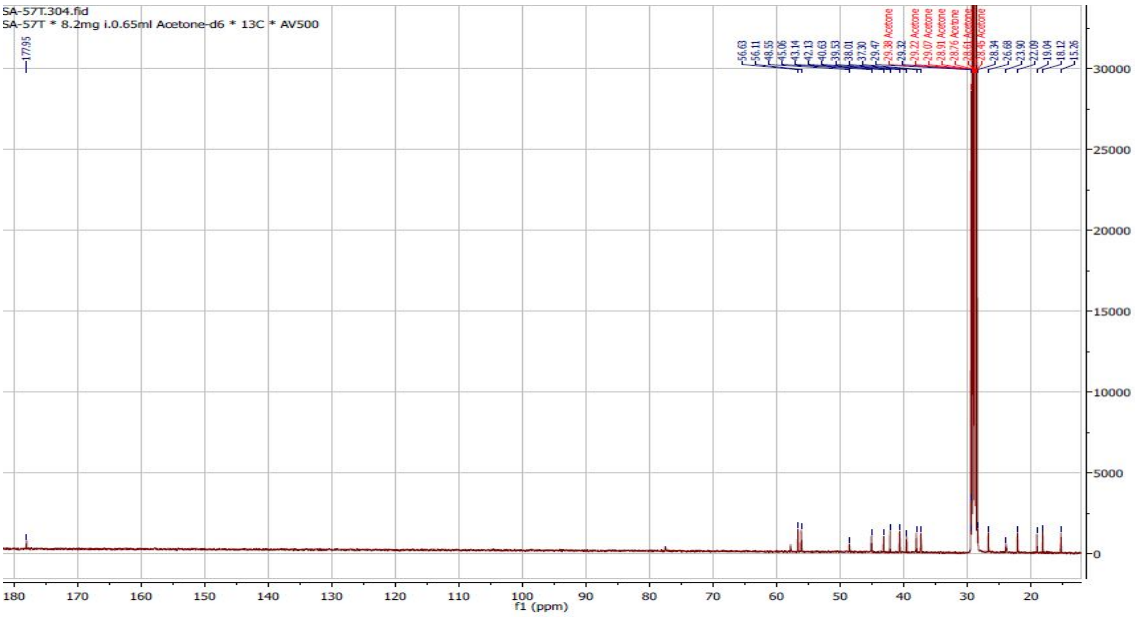

Appendix 68A: The ^{1}H NMR spectrum (500 MHz) of oleanolic acid (**253**) in Acetone-d_6

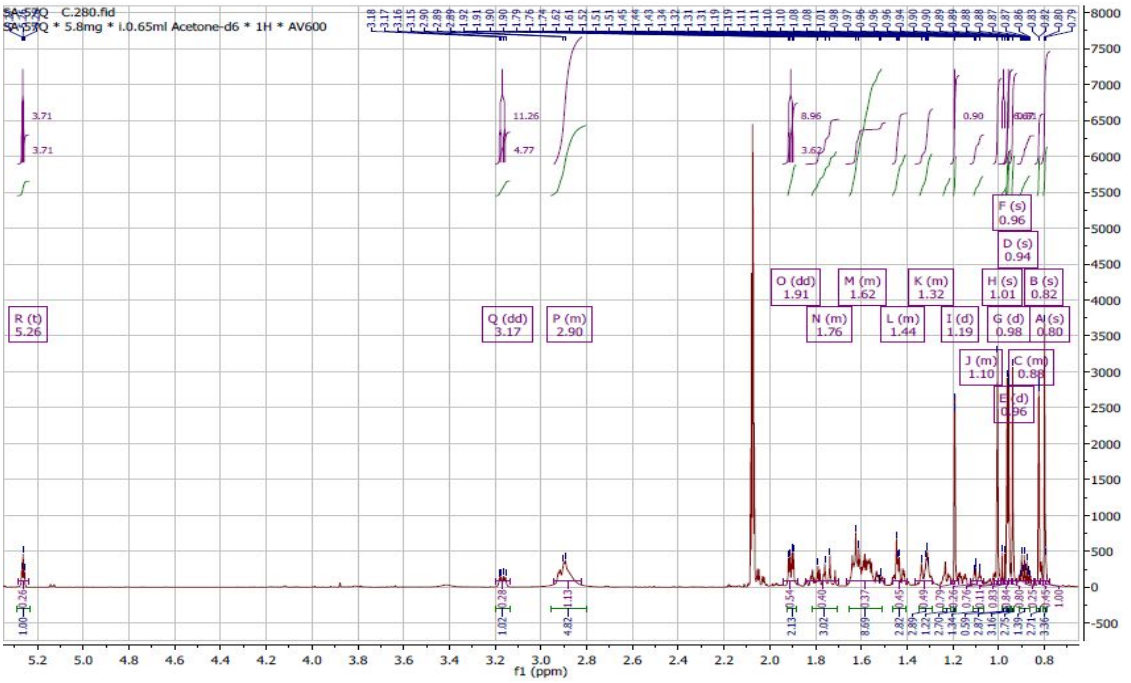

Appendix 68B: The ^{13}C NMR spectrum (125MHz) of oleanolic acid (**253**) in Acetone-d_6

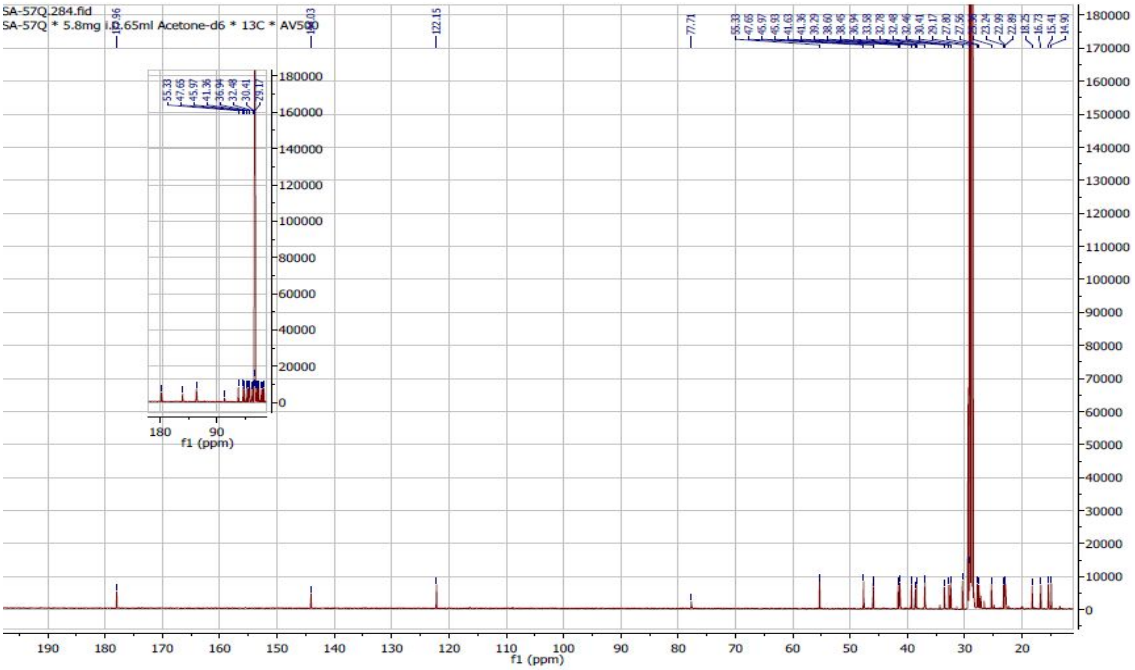

Appendix 69A: The ^{1}H NMR spectrum (600 MHz) of β-amyrin acetate (**254**) in CD_2Cl_2

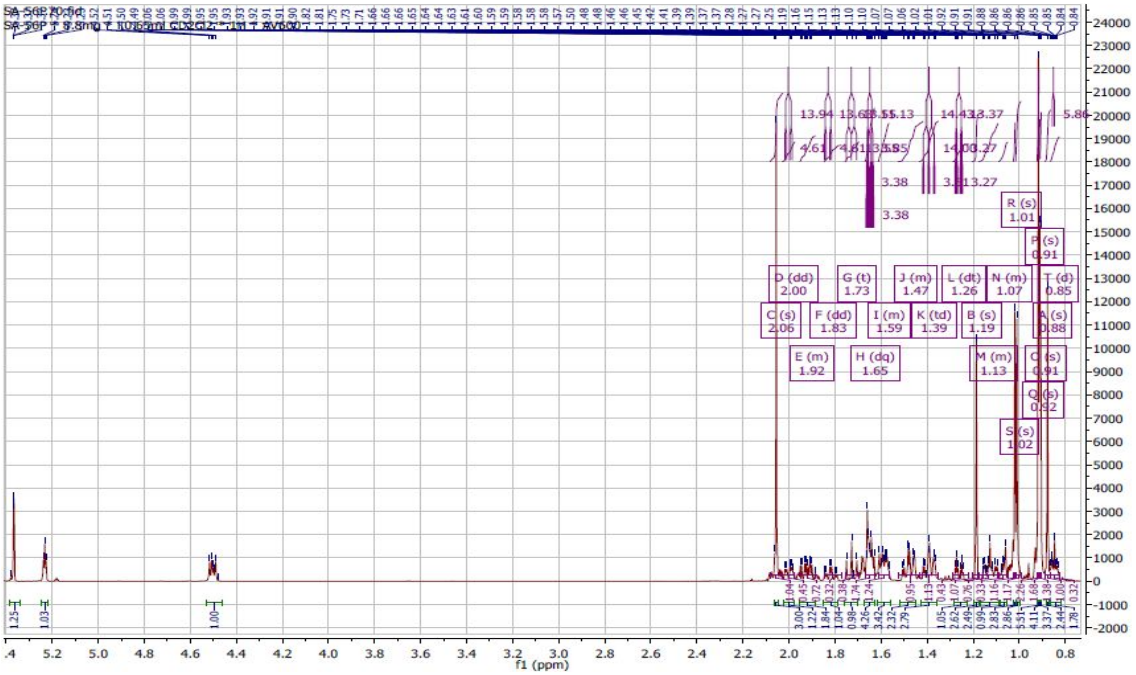

Appendix 69B: The ^{13}C NMR spectrum (150MHz) of of β-amyrin acetate (**254**) in CD_2Cl_2

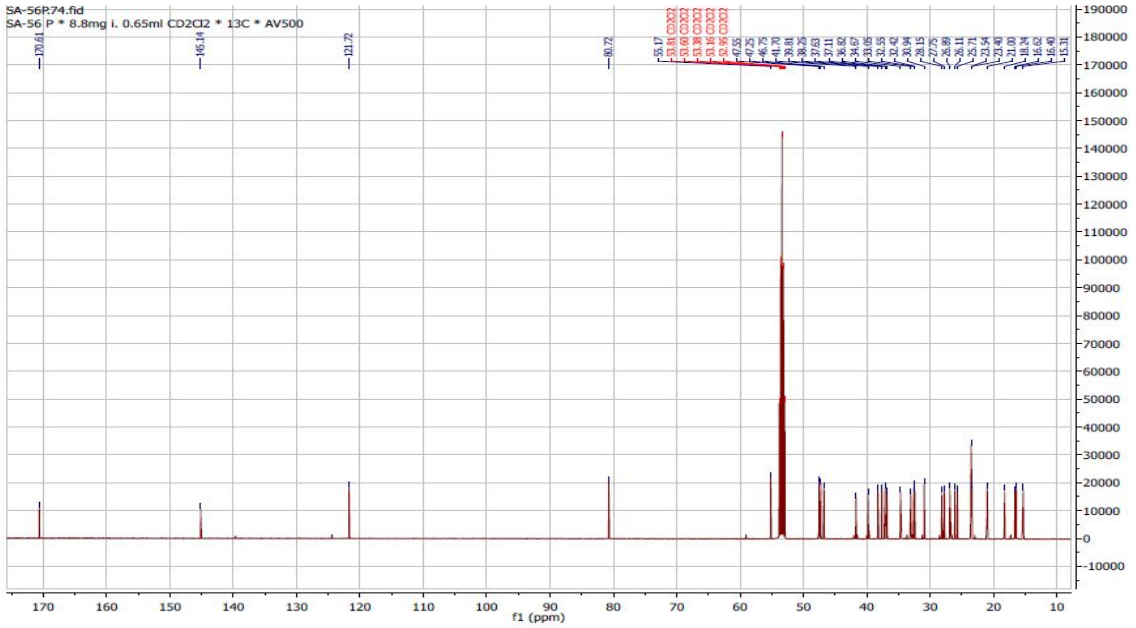

Appendix 69C. The ESIMS spectrum of β-amyrin acetate (**254**)

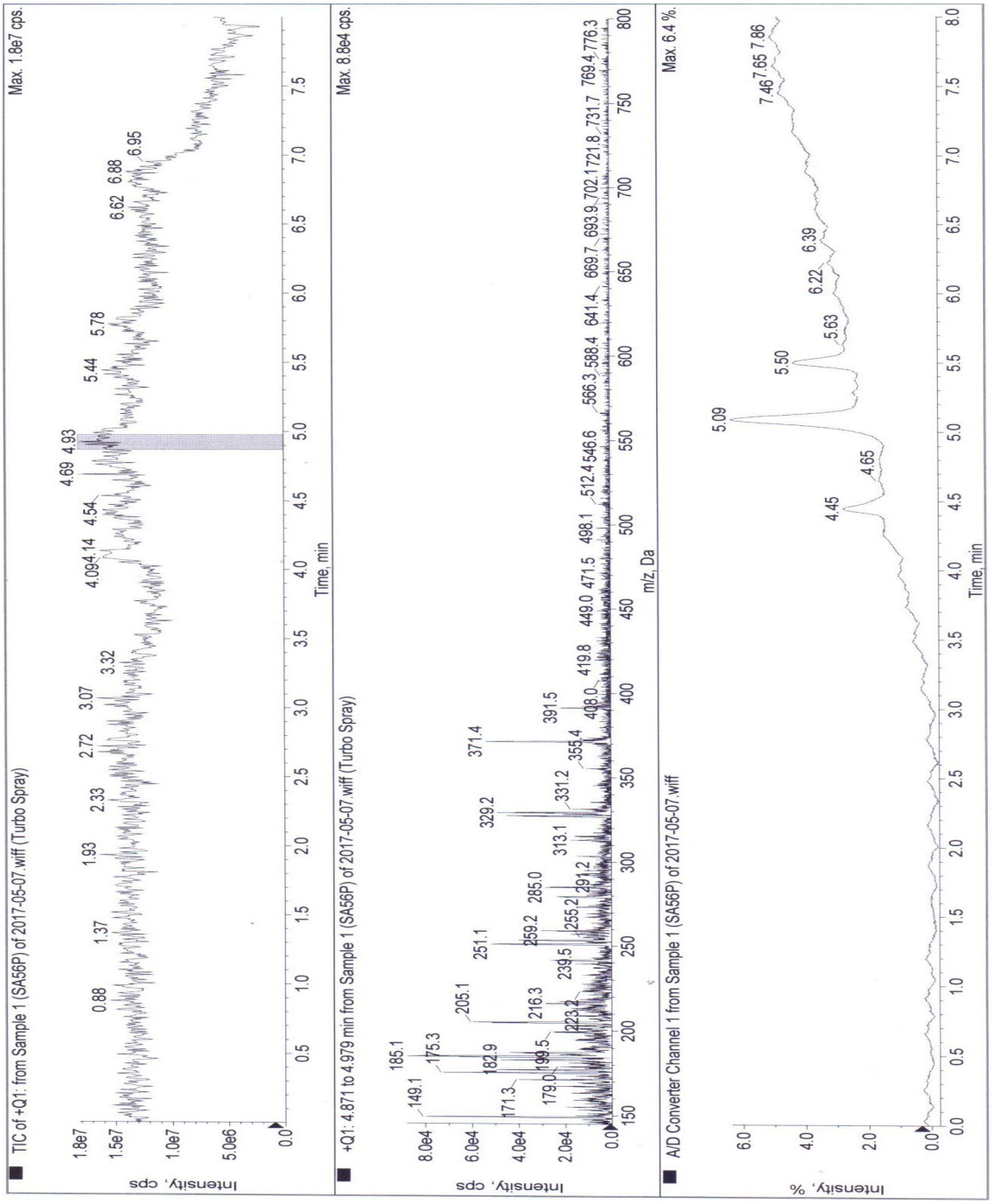

Appendix 70A: The ^{1}H NMR spectrum (600 MHz) of *ent*-kaura-9(11),16-diene (**255**) in CD_2Cl_2

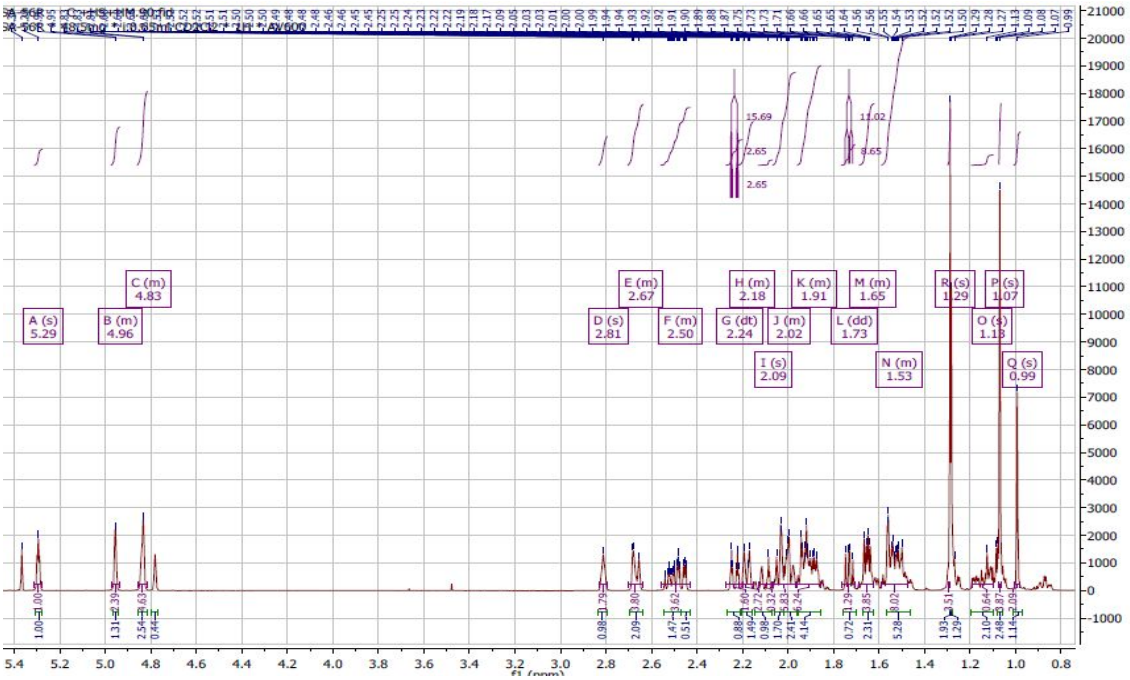

Appendix 70B: The ^{13}C NMR spectrum (150MHz) of *ent*-kaura-9(11),16-diene (**255**) in CD_2Cl_2

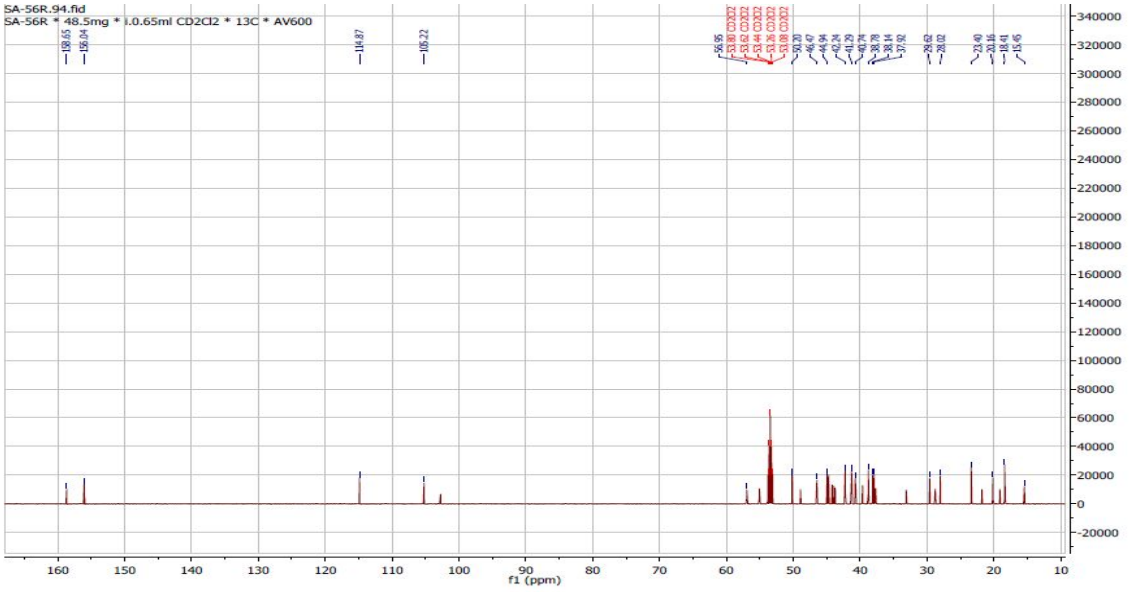

Appendix 71A: The ^{1}H NMR spectrum (600 MHz) of 15β-hydroxy-kaura-9(11),16-diene (**256**) in Acetone-d_6

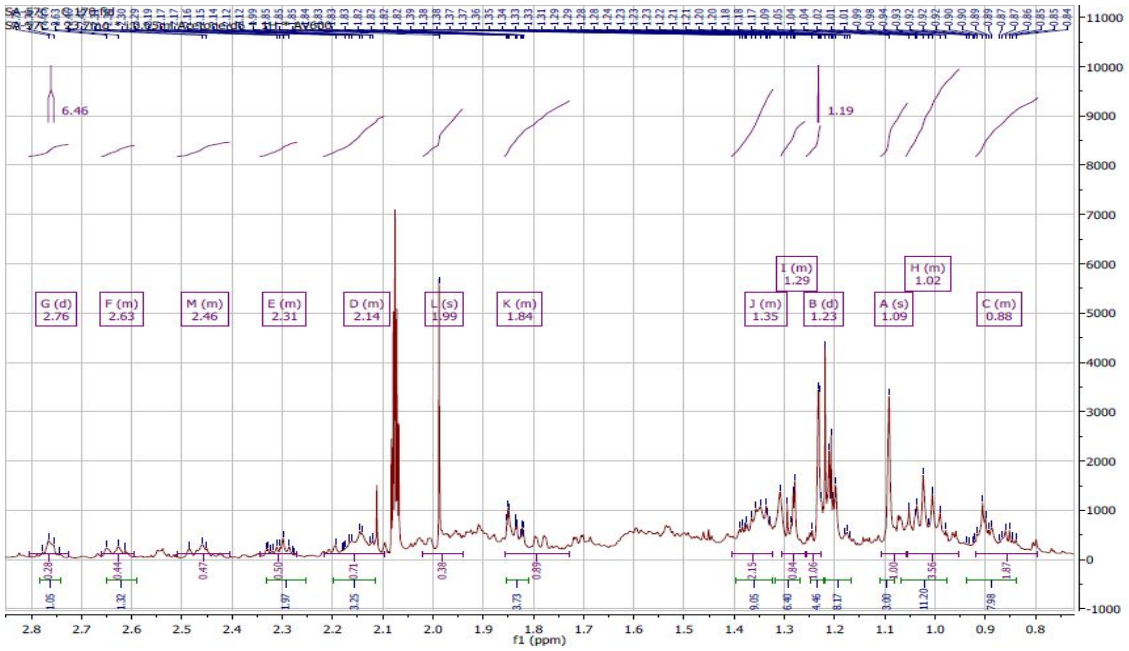

Appendix 71B: The ^{13}C NMR spectrum (150MHz) of 15β-hydroxy-kaura-9(11),16-diene (**256**) in Acetone-d_6

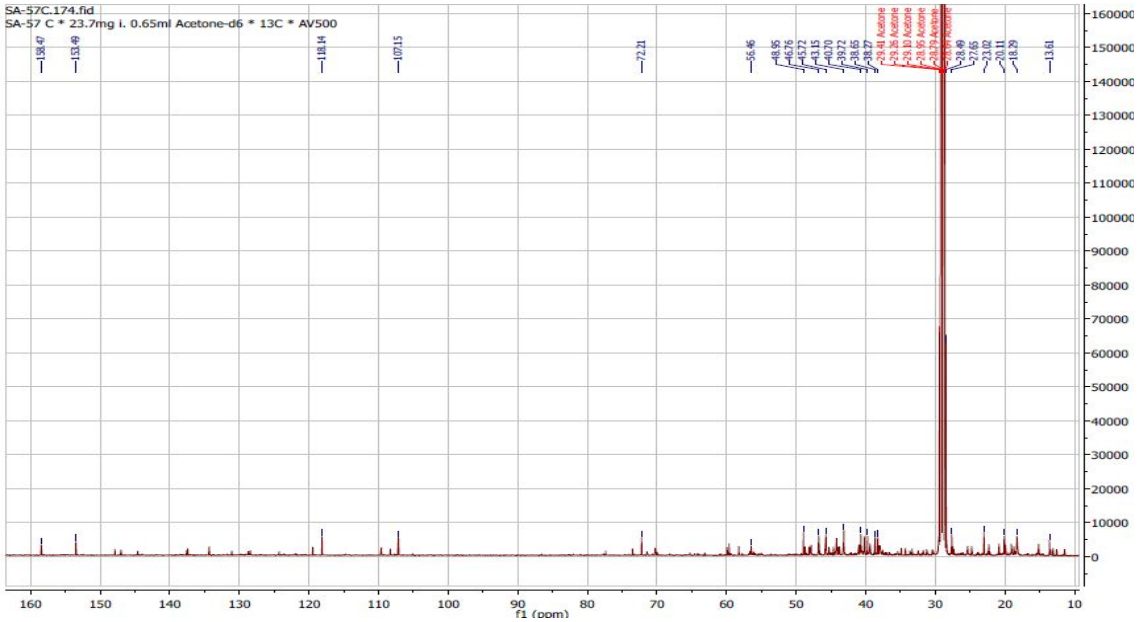

Appendix 72A: The ^{1}H NMR spectrum (500 MHz) of methyl cinnamate (**257**) in Acetone-d_6

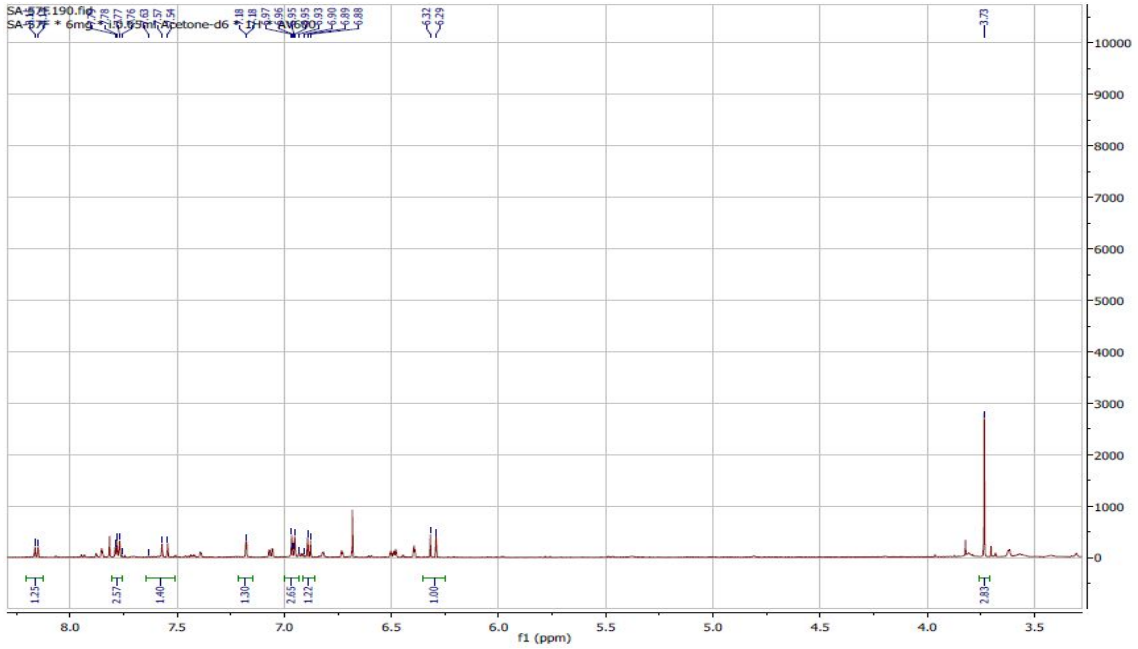

Appendix 72B: The ^{13}C NMR spectrum (125MHz) of methyl cinnamate (**257**) in Acetone-d_6

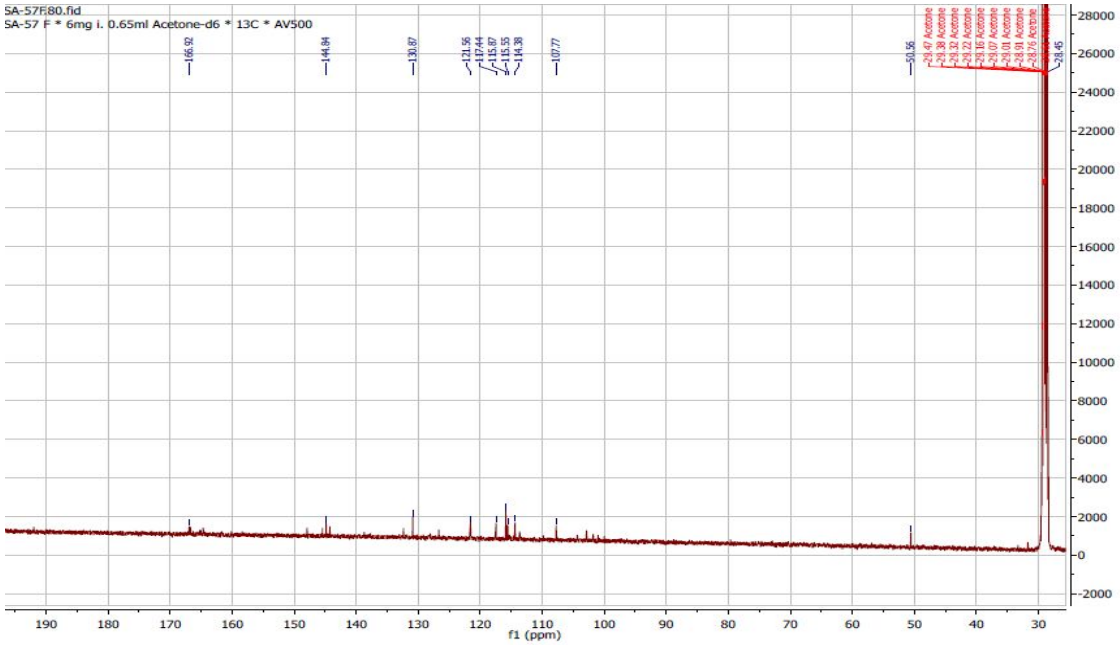

Appendix 4: Spectra for the Derivatized Compounds

Appendix 73A: The ^{1}H NMR spectrum (500 MHz) of 5,7,2',3',4',5'-pentamethoxy-flavone (**258**) in CD_2Cl_2

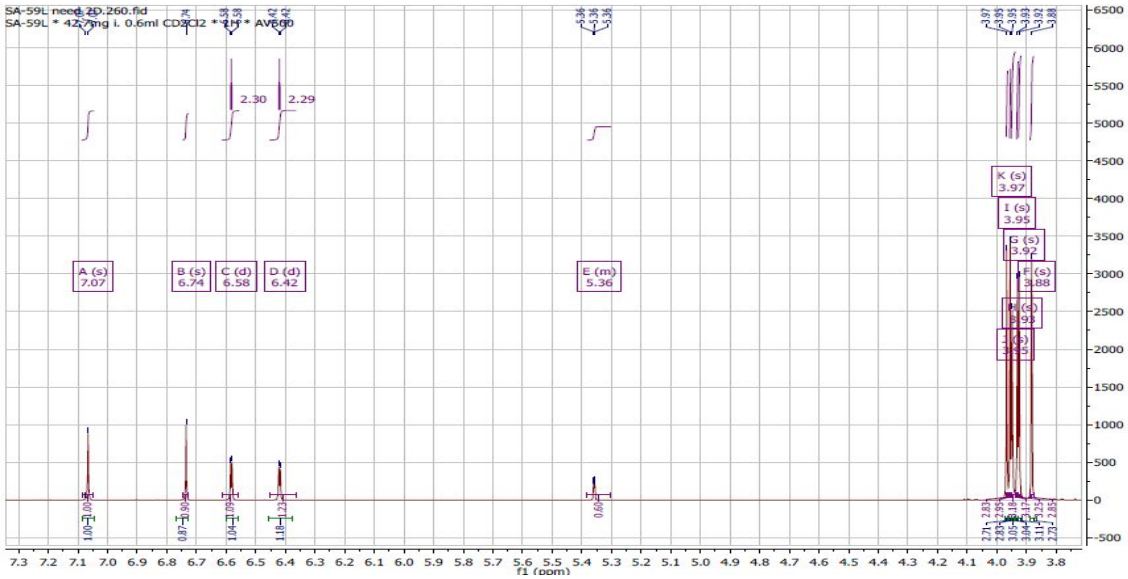

Appendix 73B: The ^{13}C NMR spectrum (125MHz) of 5,7,2',3',4',5'-pentamethoxy-flavone (**258**) in CD_2Cl_2

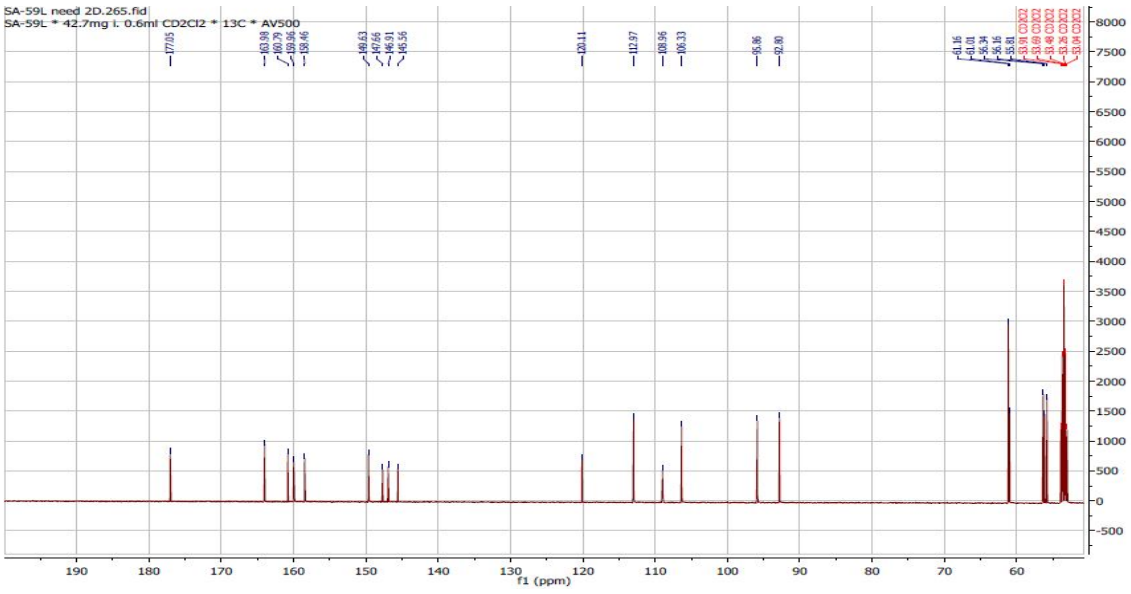

Appendix 73C. The ESIMS spectrum of 5,7,2',3',4',5'-pentamethoxy-flavone (**258**)

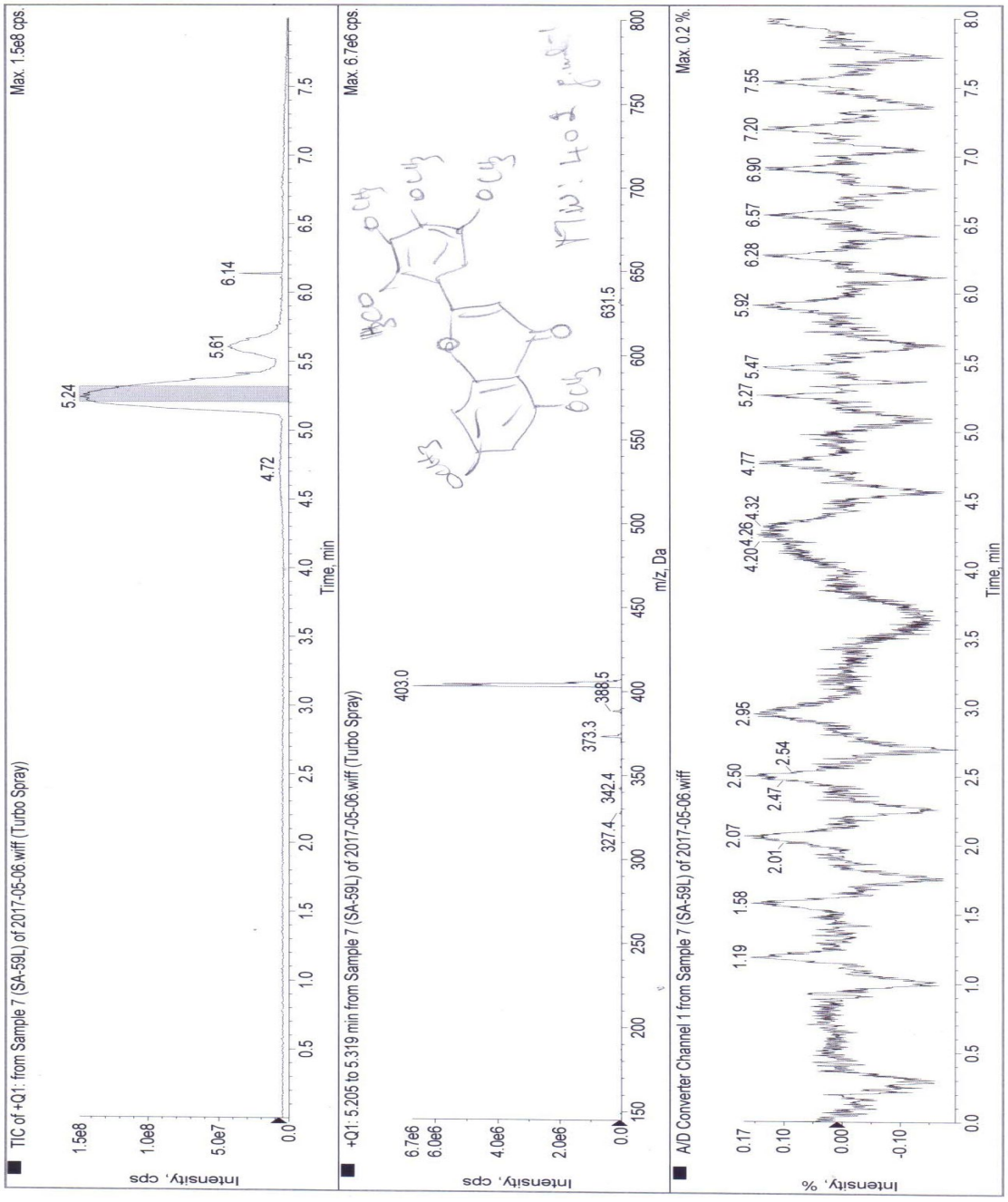

Appendix 74A: The ^{1}H NMR spectrum (600 MHz) of 5-acetyloxy-7,2',3',4',5'-pentamethoxy-flavone (**259**) in Acetone-d_6

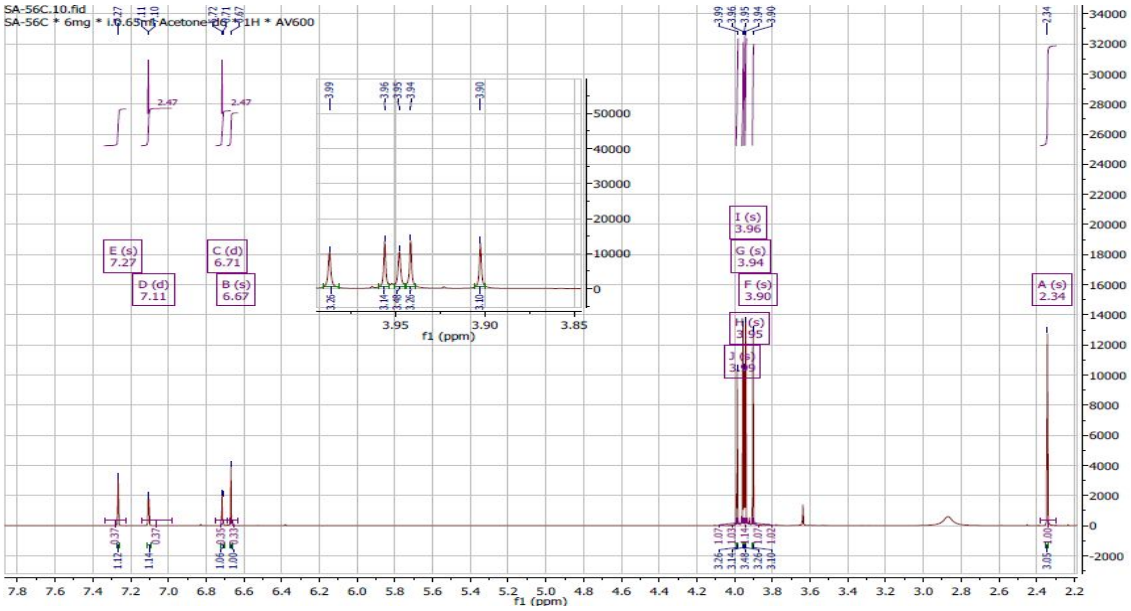

Appendix 74B: The ^{13}C NMR spectrum (150MHz) of 5-acetyloxy-7,2',3',4',5'-pentamethoxy-flavone (**259**) in Acetone-d_6

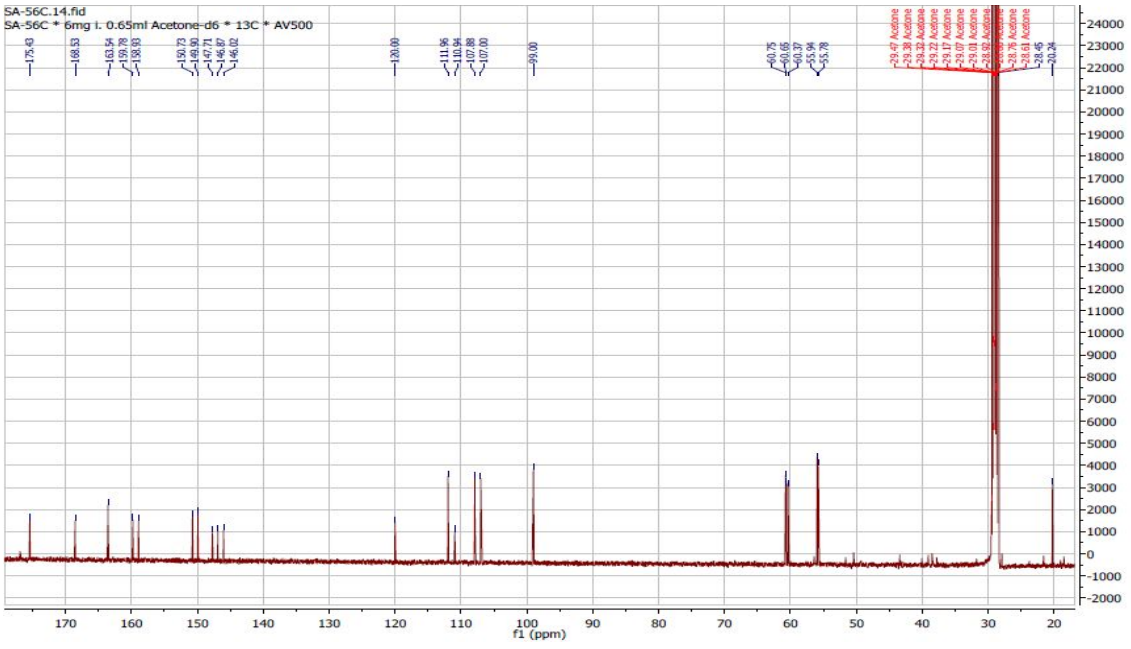

Appendix 74C: The H-H COSY spectrum of 5-acetyloxy-7,2',3',4',5'-pentamethoxy-flavone (**259**) in Acetone-d_6

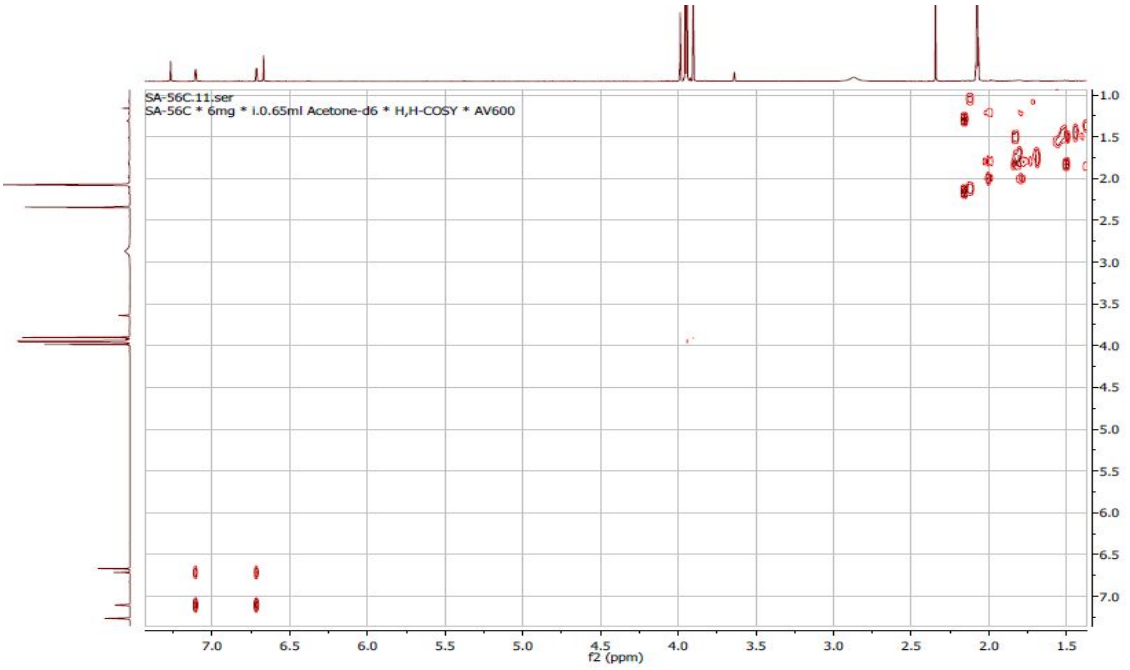

Appendix 74D: The HSQC spectrum of 5-acetyloxy-7,2',3',4',5'-pentamethoxy-flavone (**259**) in Acetone-d_6

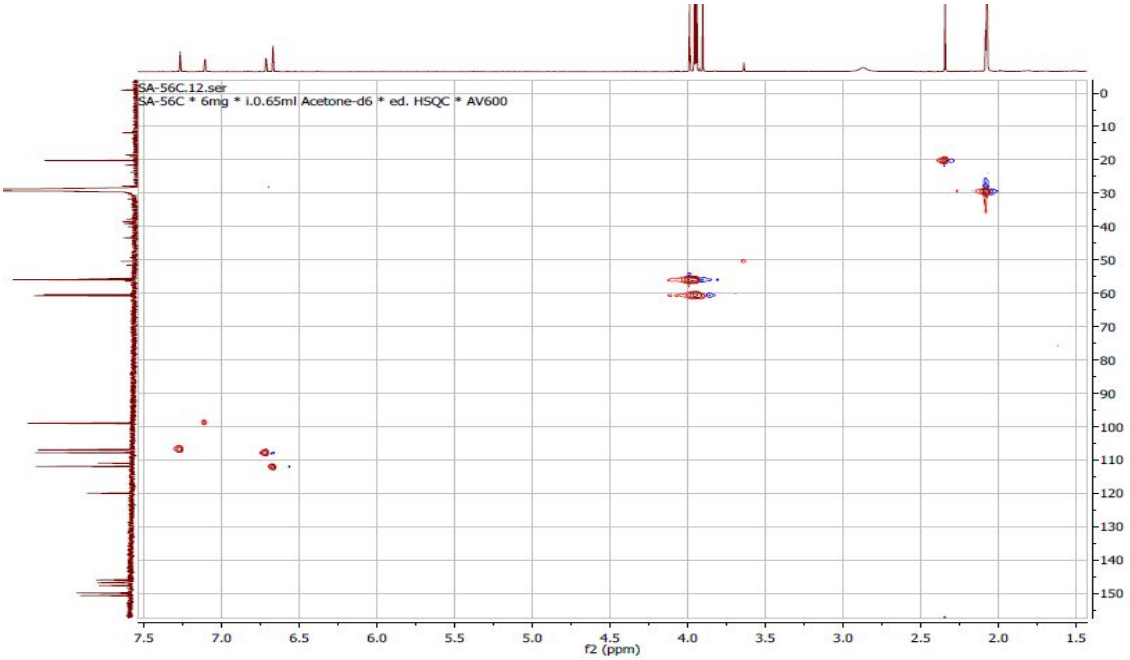

Appendix 74E: The HMBC spectrum of 5-acetyloxy-7,2',3',4',5'-pentamethoxy-flavone (**259**) inAcetone-d_6

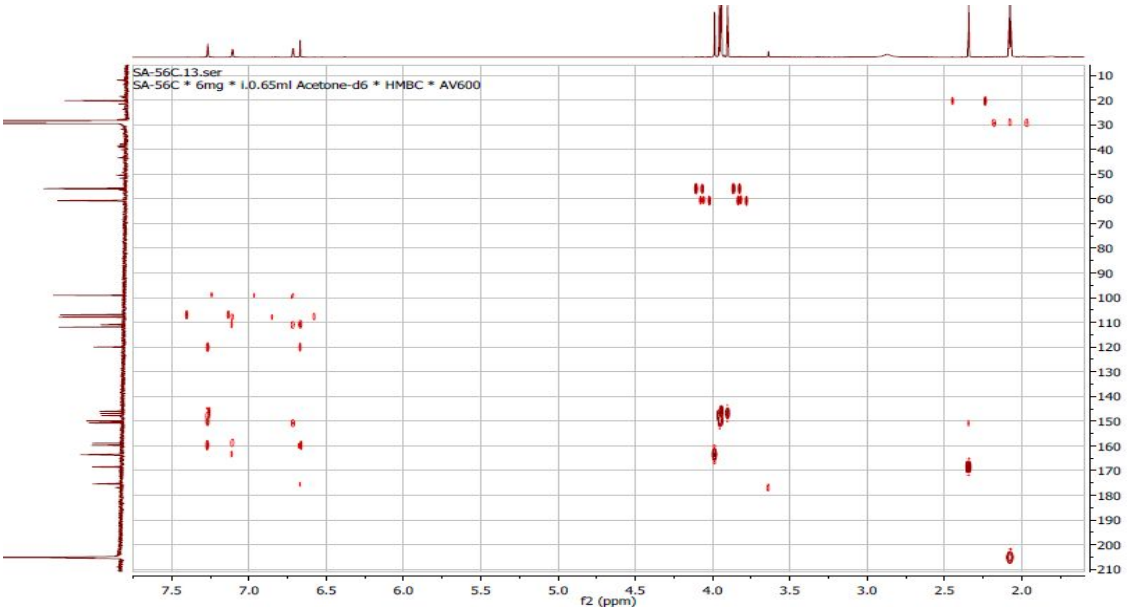

Appendix 74F. The HRMS (ESI) spectrum of 5-Acetyloxy-7,2',3',4',5'-pentamethoxy-flavone (**259**)

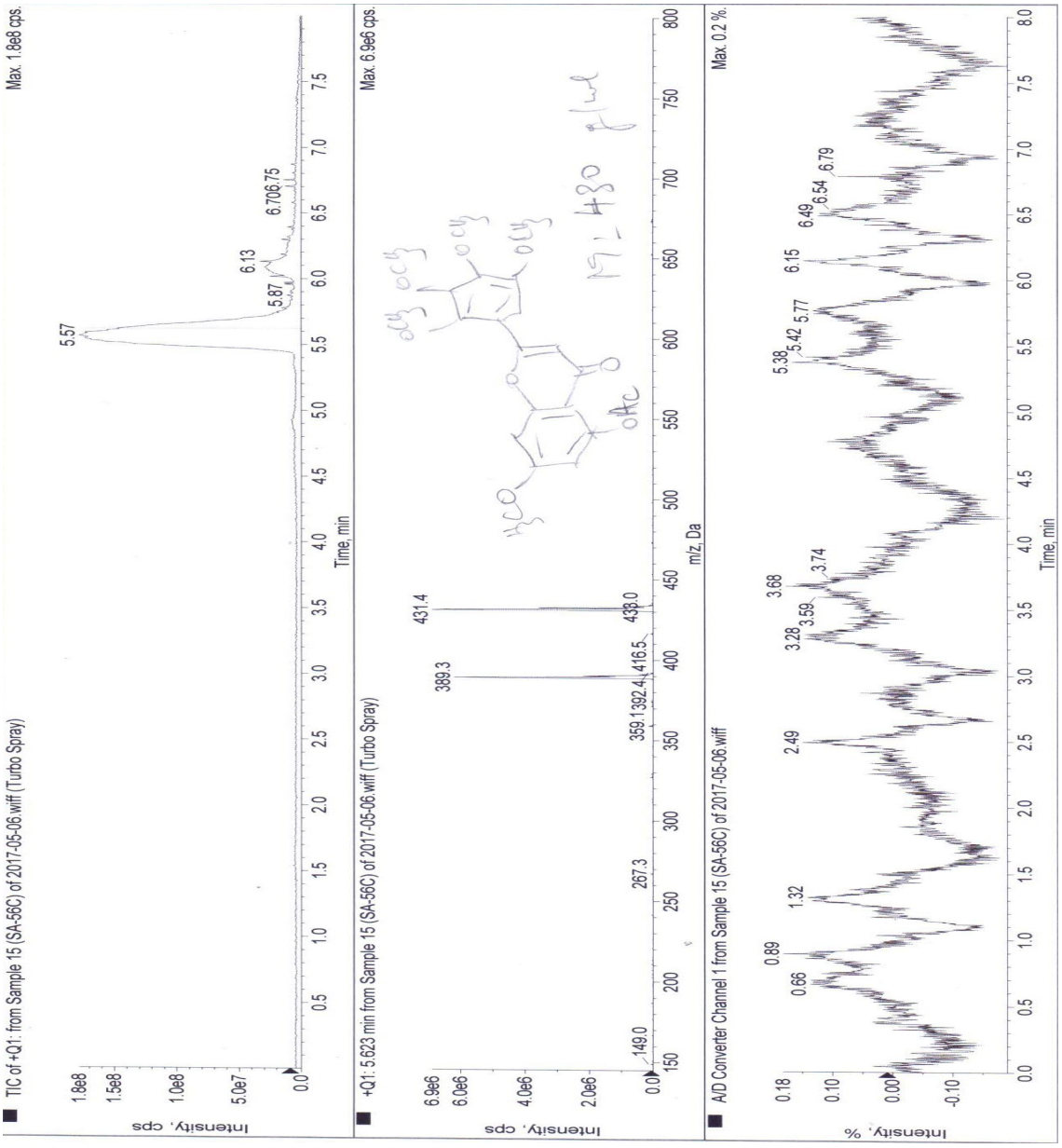

Appendix 75A: The ^{1}H NMR spectrum (500 MHz) of 3-(2,",6"-hydroxy-4-methoxyphenyl)-5-(2',3',4',5'-methoxyphenyl)-1*H*-pyrazole (**260**) in Acetone-d_6

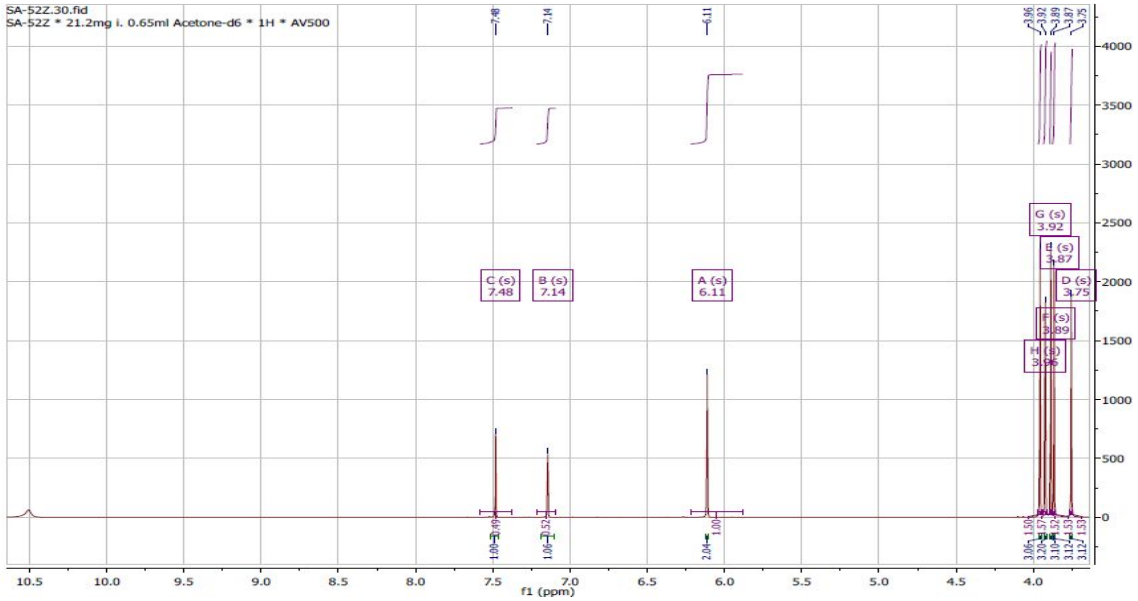

Appendix 75B: The ^{13}C NMR spectrum (125MHz) of 3-(2,",6"-hydroxy-4-methoxyphenyl)-5-(2',3',4',5'-methoxyphenyl)-1*H*-pyrazole (**260**) in Acetone-d_6

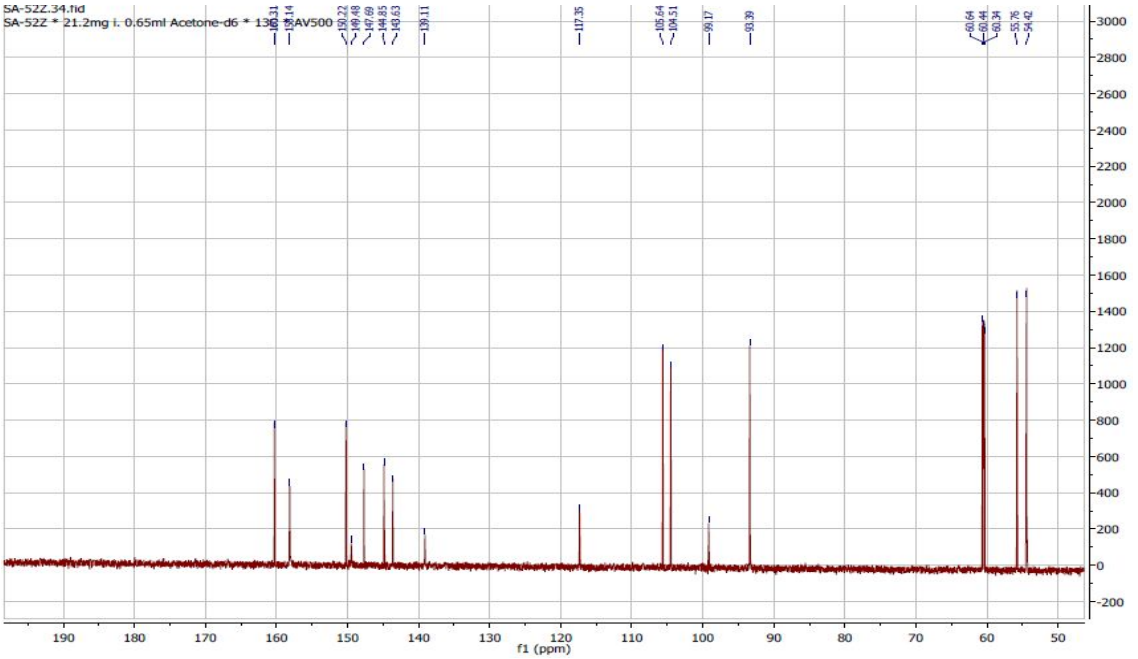

Appendix 75C. The ESIMS spectrum of 3-(2,",6"-hydroxy-4-methoxyphenyl)-5-(2',3',4',5'-methoxyphenyl)-1*H*-pyrazole (**260**)

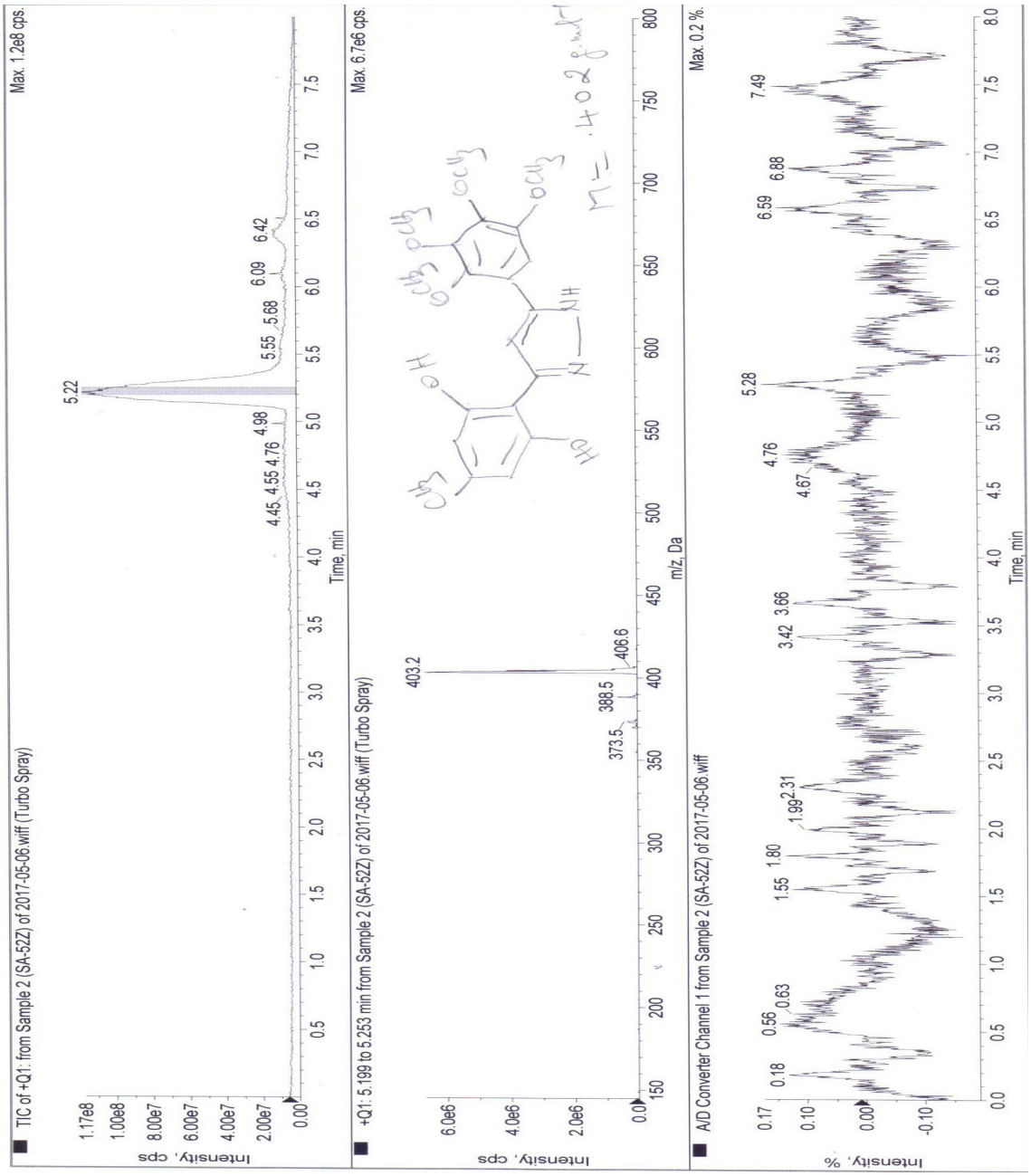

Appendix 76A: The ^{1}H NMR spectrum (600 MHz) of 6,8-dibromo-5-hydroxy-7,2',3',4',5'-pentamethoxy-flavone (**261**) in $CDCl_3$.

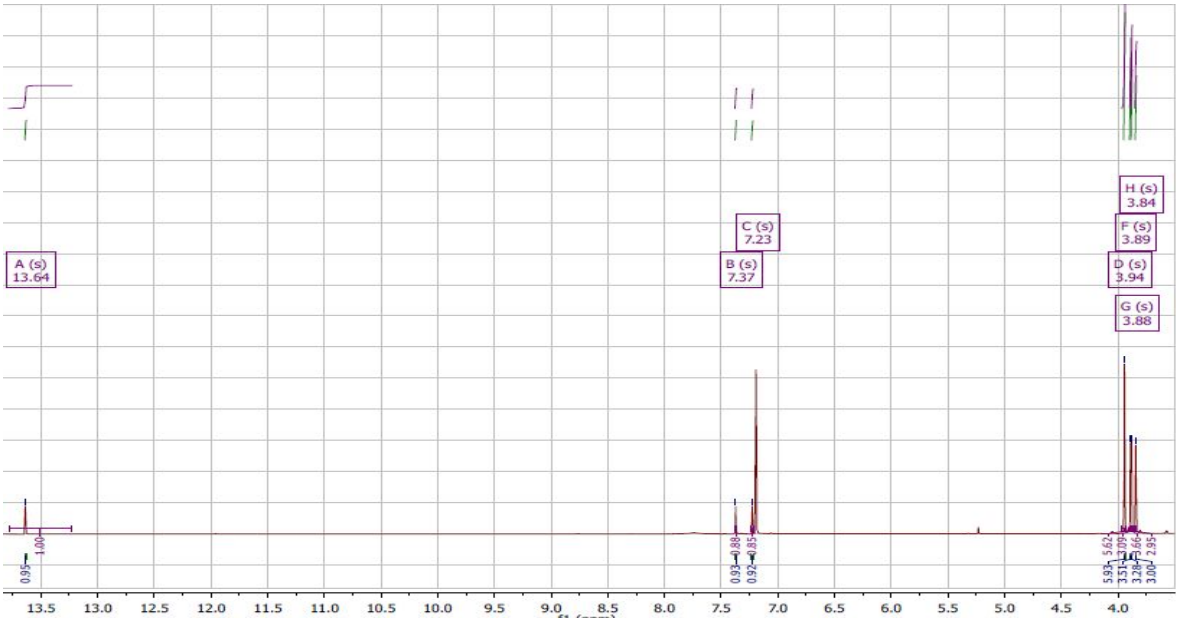

Appendix 76B: The ^{13}C NMR spectrum (200MHz) of 6,8-dibromo-5-hydroxy-7,2',3',4',5'-pentamethoxy-flavone (**261**) in $CDCl_3$

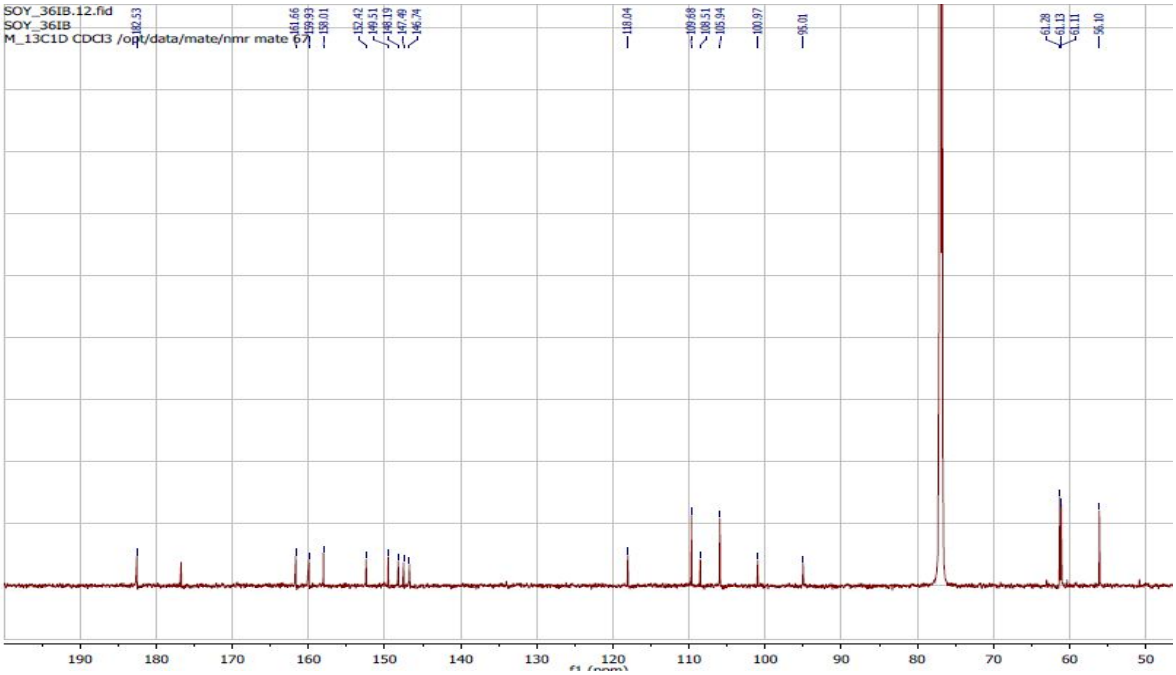

Appendix 76C: The H-H COSY spectrum of 6,8-dibromo-5-hydroxy-7,2',3',4',5'-pentamethoxy-flavone (**261**) in $CDCl_3$

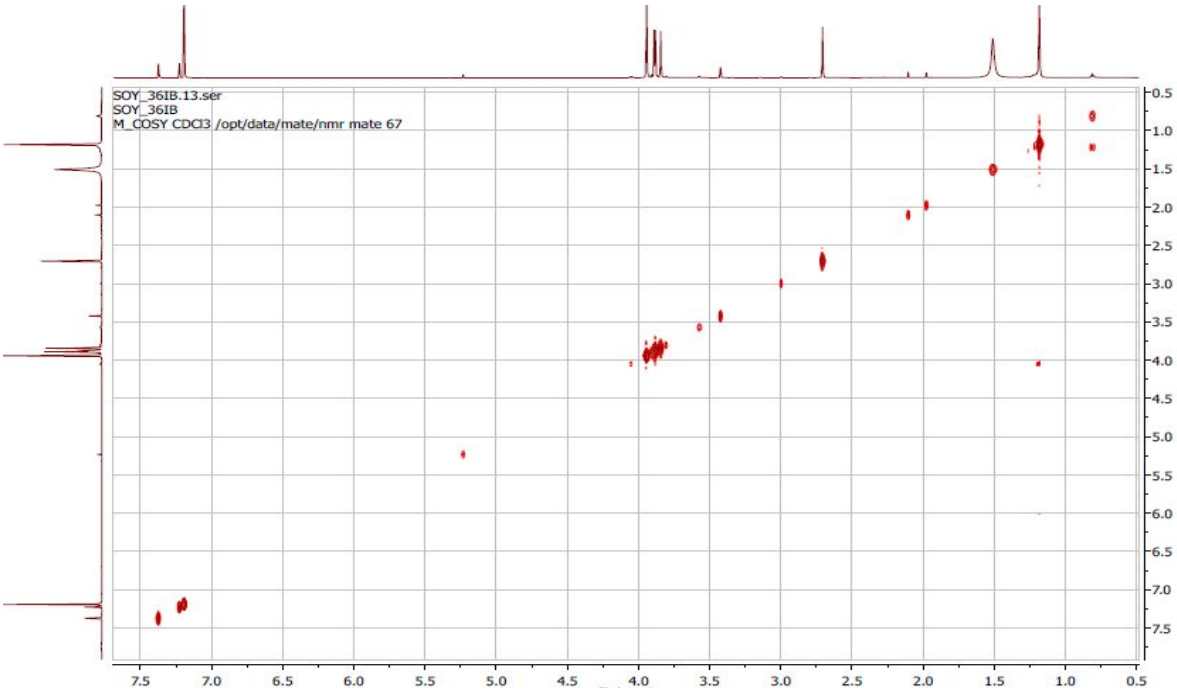

Appendix 76D: The NOESY spectrum of 6,8-dibromo-5-hydroxy-7,2',3',4',5'-pentamethoxy-flavone (**261**) in $CDCl_3$

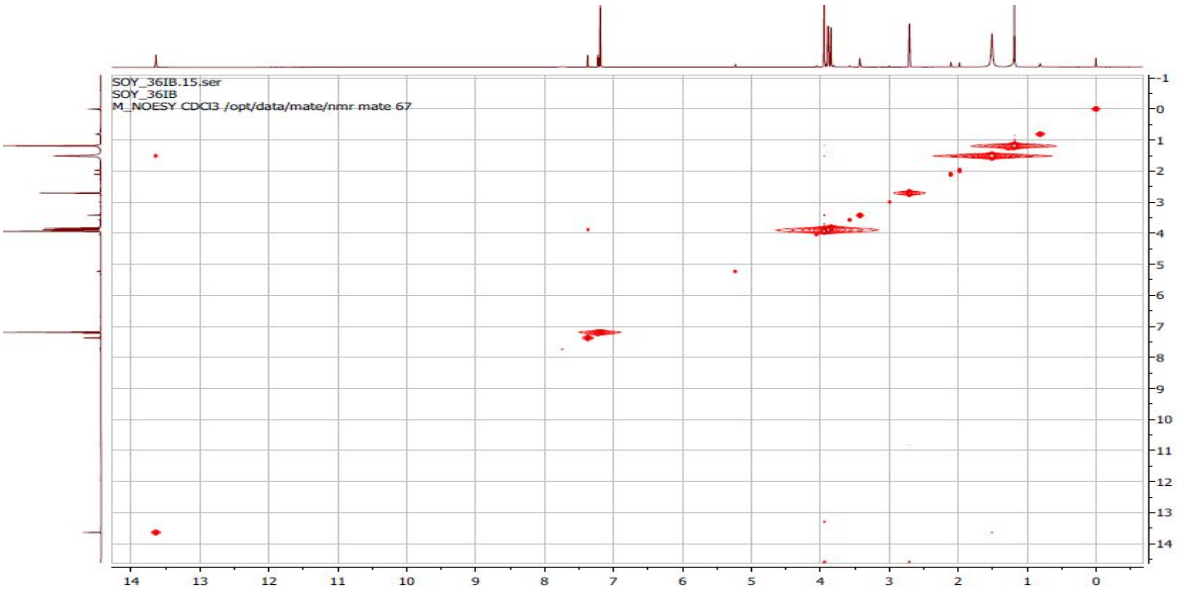

Appendix 76E: The HSQC spectrum of 6,8-dibromo-5-hydroxy-7,2',3',4',5'-pentamethoxy-flavone (**261**) in $CDCl_3$

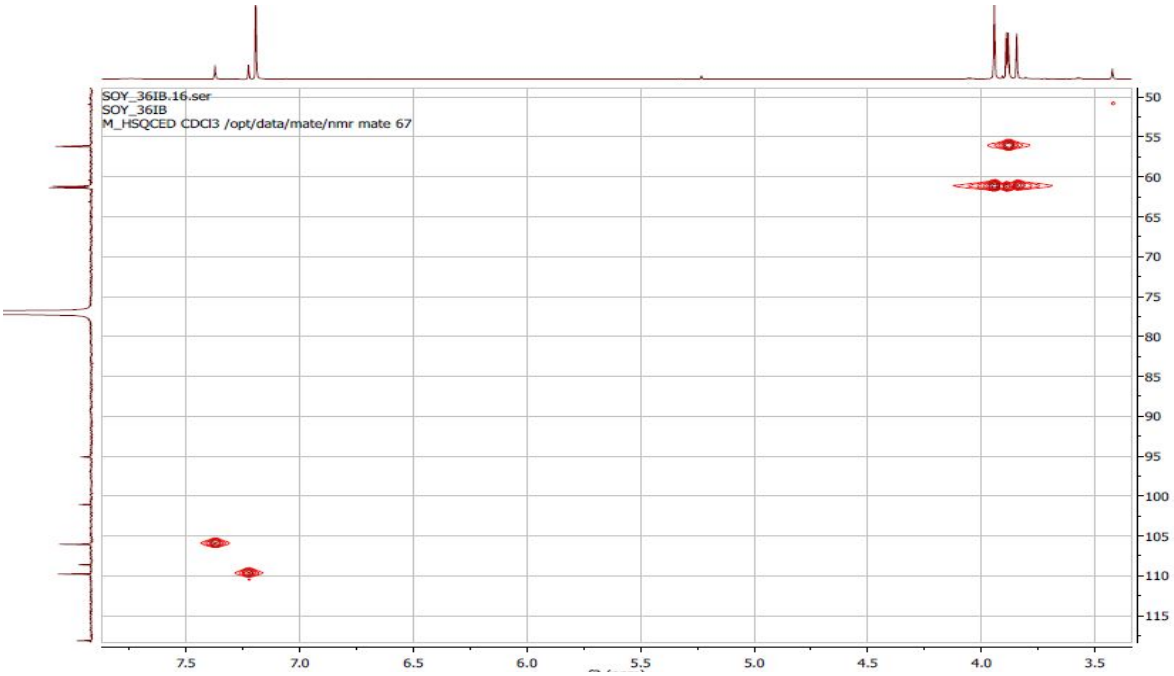

Appendix 76F: The HMBC spectrum of of 6,8-dibromo-5-hydroxy-7,2',3',4',5'-pentamethoxy-flavone (**261**) in $CDCl_3$

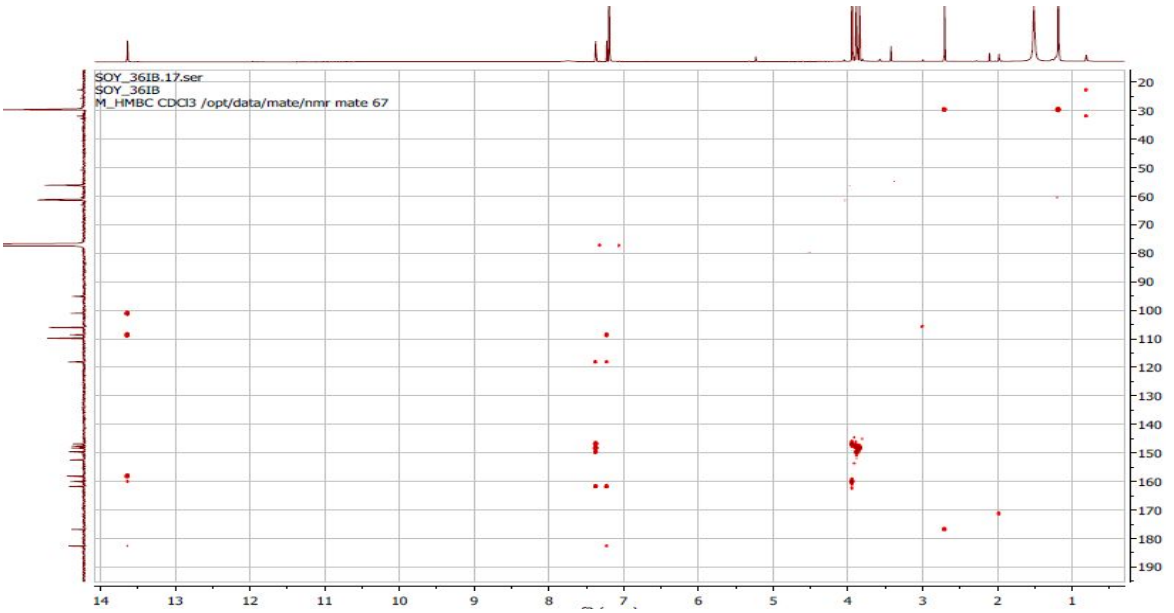

Appendix 76G. The ESIMS spectrum of 6,8-dibromo-5-hydroxy-7,2',3',4',5'-pentamethoxy-flavone (**261**)

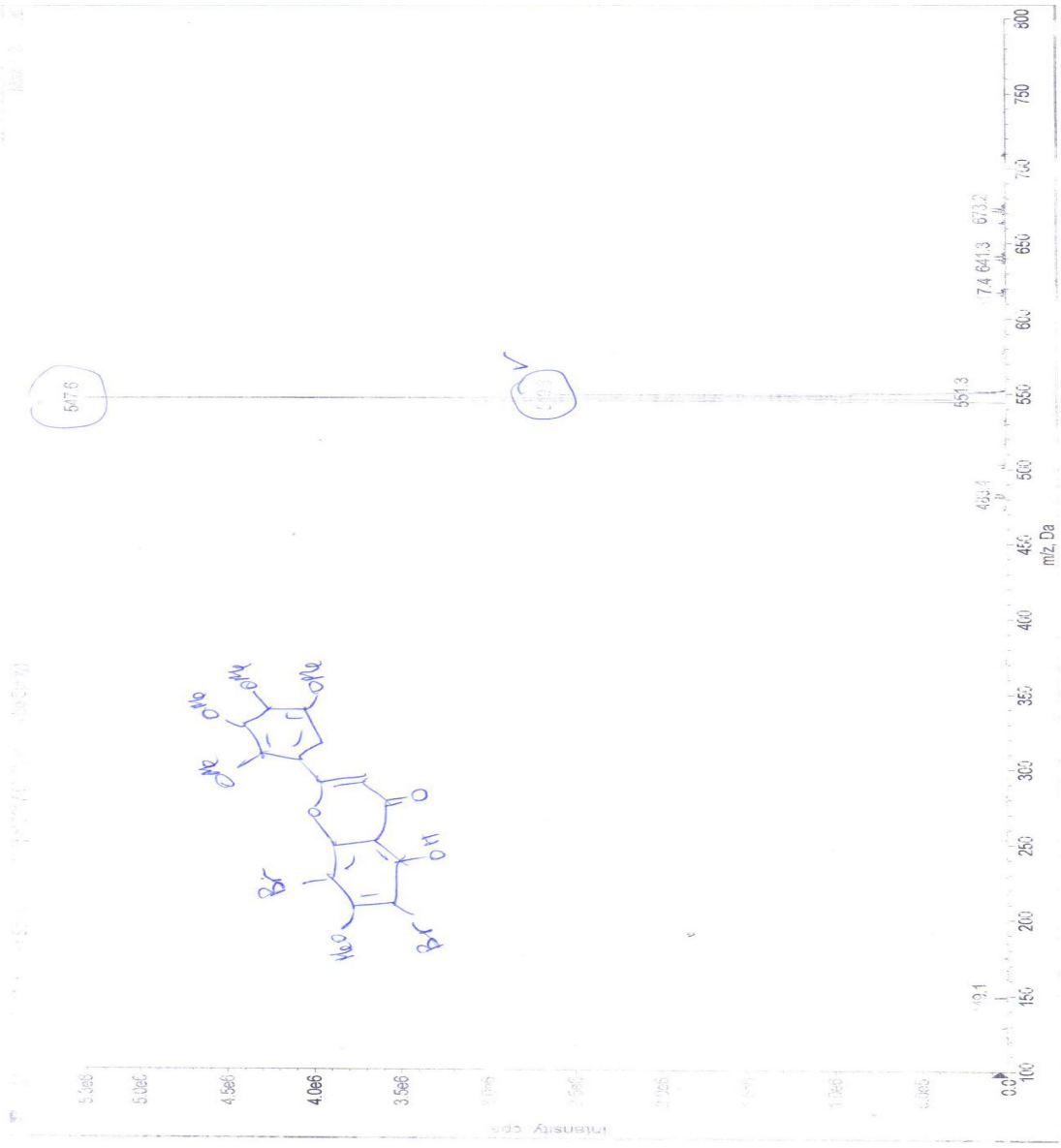

Appendix 77: The ^{1}H NMR spectrum (600 MHz) of 6,8-dibromo- 5,7-dihydroxy-7,2',3',4',5'-pentamethoxy-flavone (**262**) in $CDCl_3$

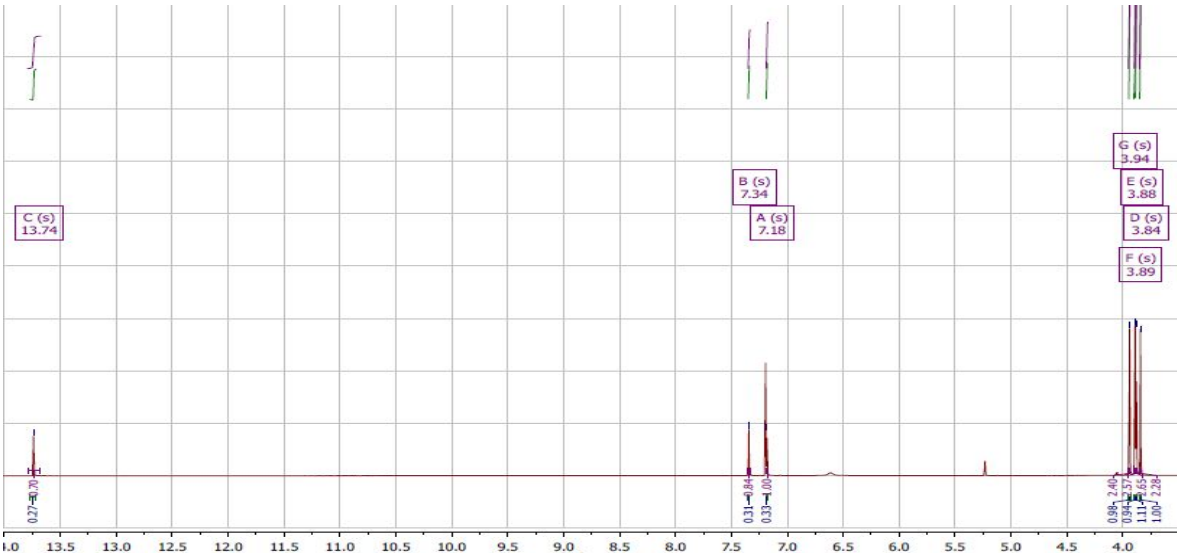

Appendix 77B: The ^{13}C NMR spectrum (200MHz) of 6,8-dibromo- 5,7-dihydroxy-7,2',3',4',5'-pentamethoxy-flavone (**262**) in $CDCl_3$

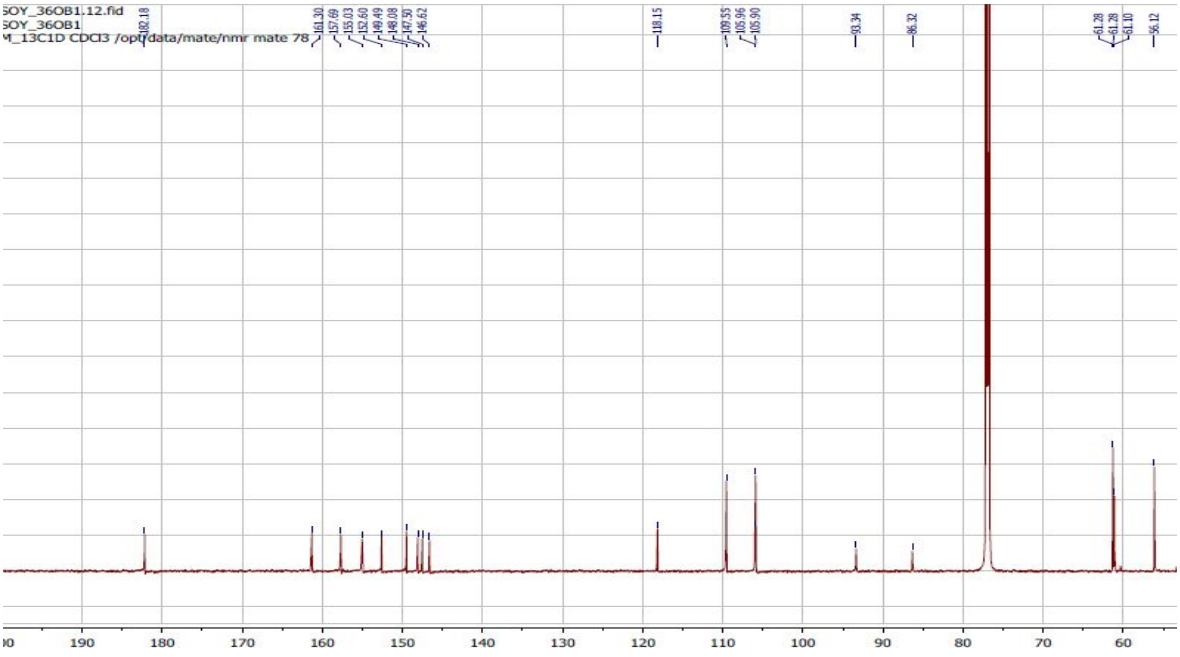

Appendix 77C: The H-H COSY spectrum of 6,8-dibromo- 5,7-dihydroxy-7,2',3',4',5'-pentamethoxy-flavone (**262**) in $CDCl_3$

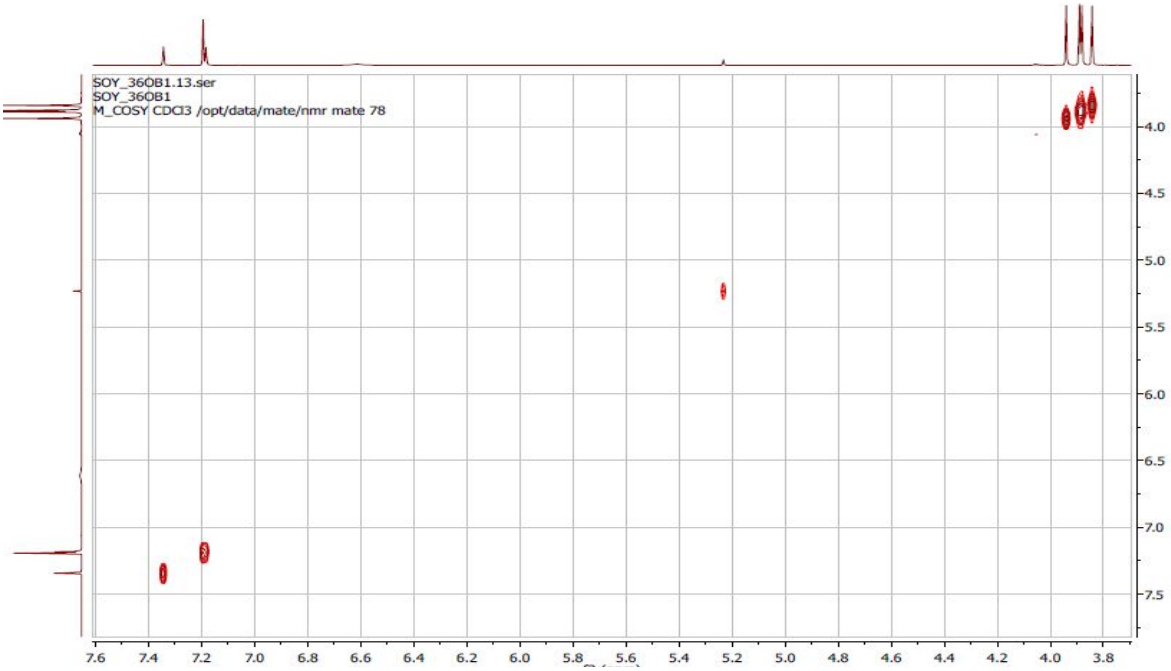

Appendix 77D: The NOESY spectrum of 6,8-dibromo- 5,7-dihydroxy-7,2',3',4',5'-pentamethoxy-flavone (**262**) in $CDCl_3$

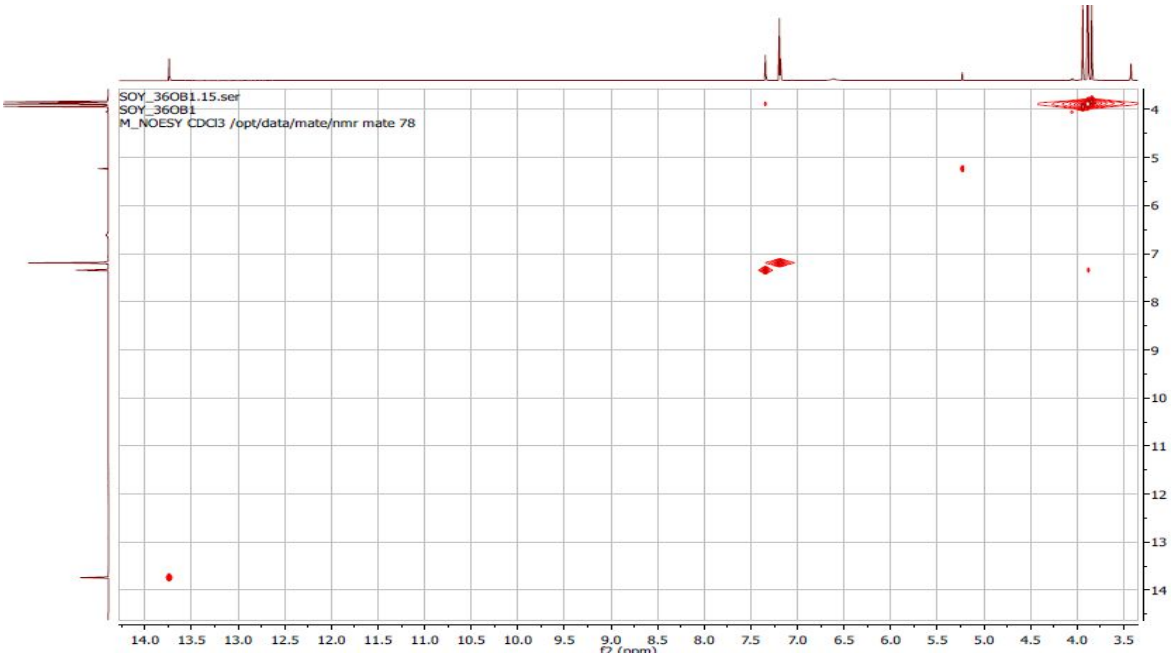

Appendix 77E: The HSQC spectrum of 6,8-dibromo- 5,7-dihydroxy-7,2',3',4',5'-pentamethoxy-flavone (**262**) in $CDCl_3$

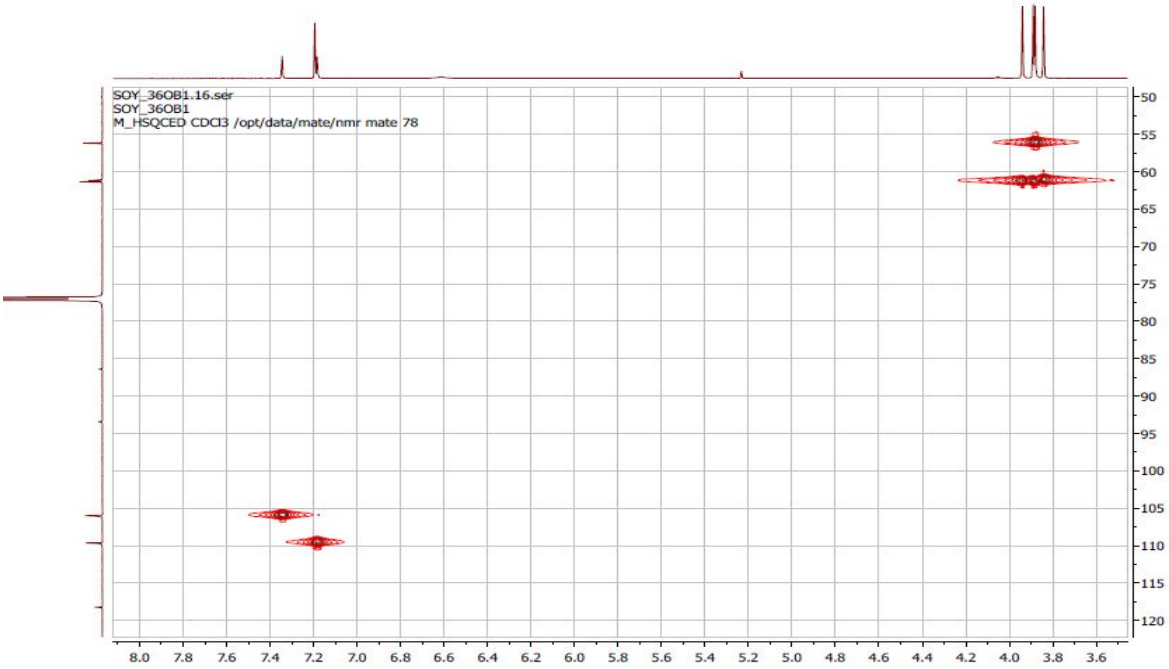

Appendix 77F: The HMBC spectrum of 6,8-dibromo- 5,7-dihydroxy-7,2',3',4',5'-pentamethoxy-flavone (**262**) in $CDCl_3$

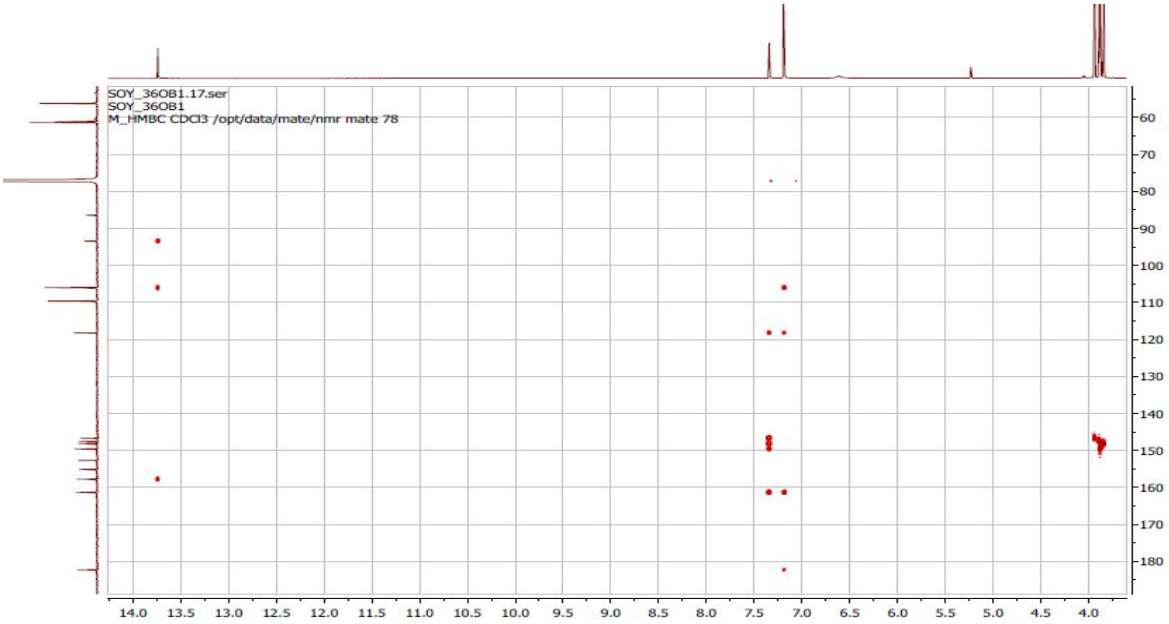

Appendix 78A: The ^{1}H NMR spectrum (600 MHz) of 6β,18,19-trihydroxy-*ent*-trachyloban-2*N*-oxime (**263**) in $CDCl_3$

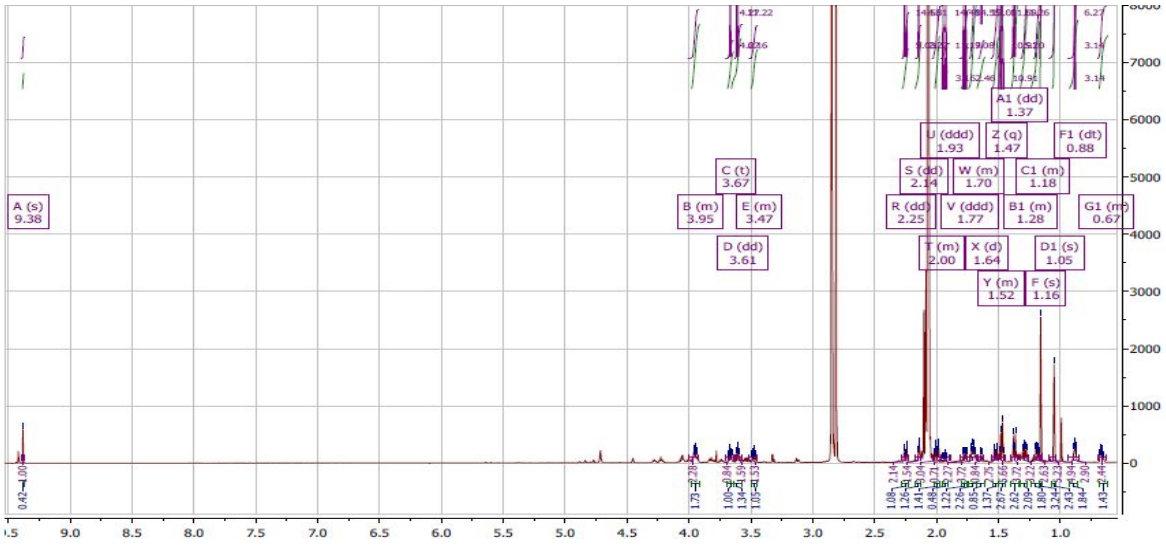

Appendix 78B: The ^{13}C NMR spectrum (200MHz) of 6β,18,19-trihydroxy-*ent*-trachyloban-2*N*-oxime (**263**) in $CDCl_3$

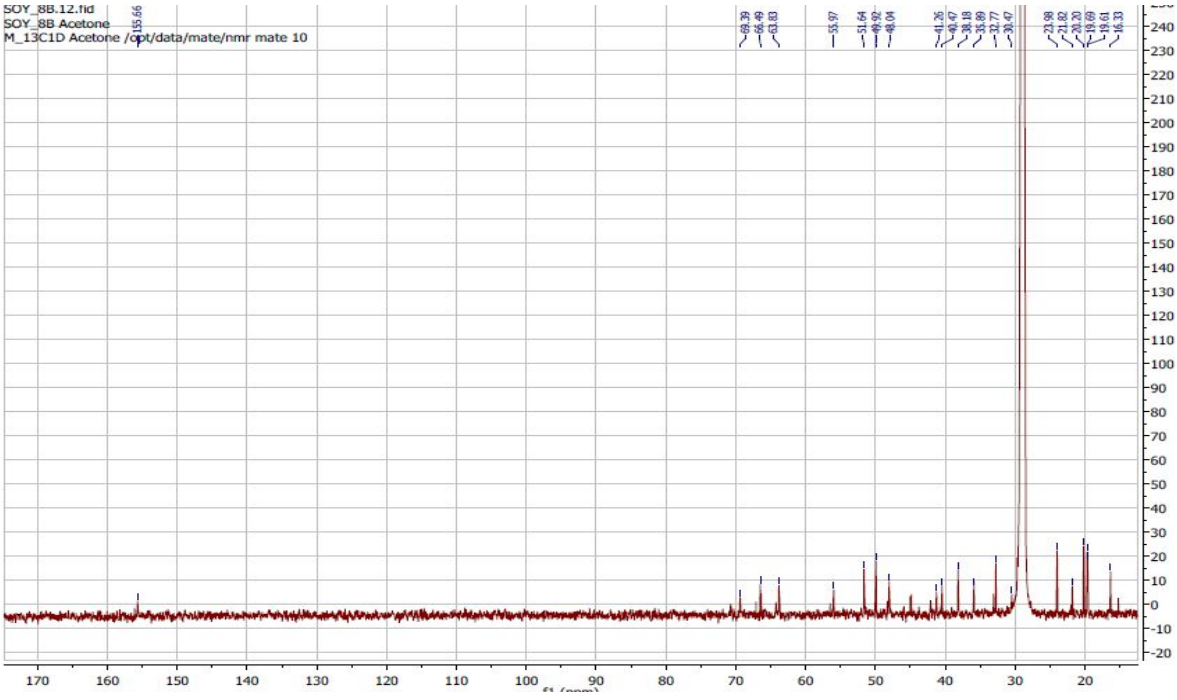

Appendix 78C: The H-H COSY spectrum of 6*β*,18,19-trihydroxy-*ent*-trachyloban-2*N*-oxime (**263**) in $CDCl_3$

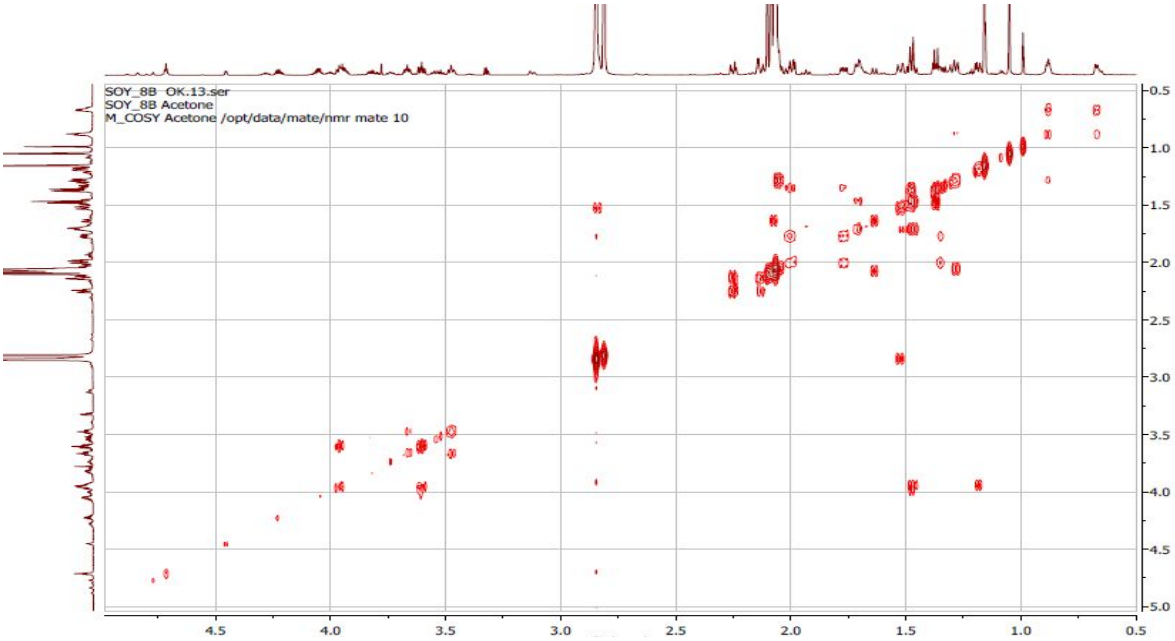

Appendix 78D: The NOESY spectrum of 6*β*,18,19-trihydroxy-*ent*-trachyloban-2*N*-oxime (**263**) in $CDCl_3$

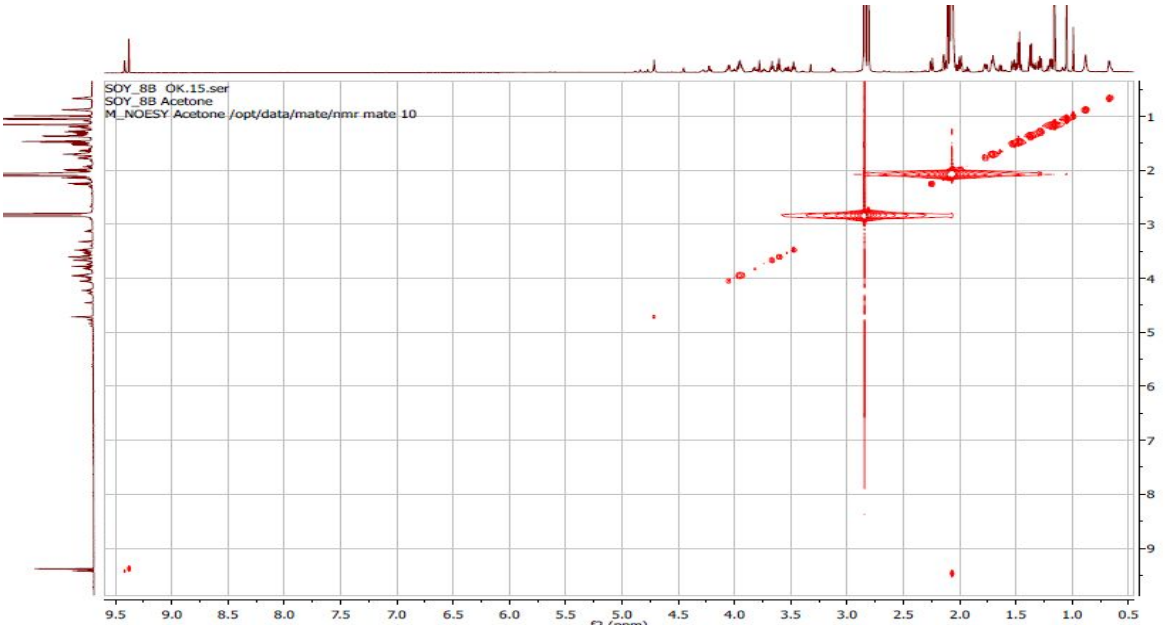

Appendix 78E: The HSQC spectrum of 6*β*,18,19-trihydroxy-*ent*-trachyloban-2*N*-oxime (**263**) in $CDCl_3$

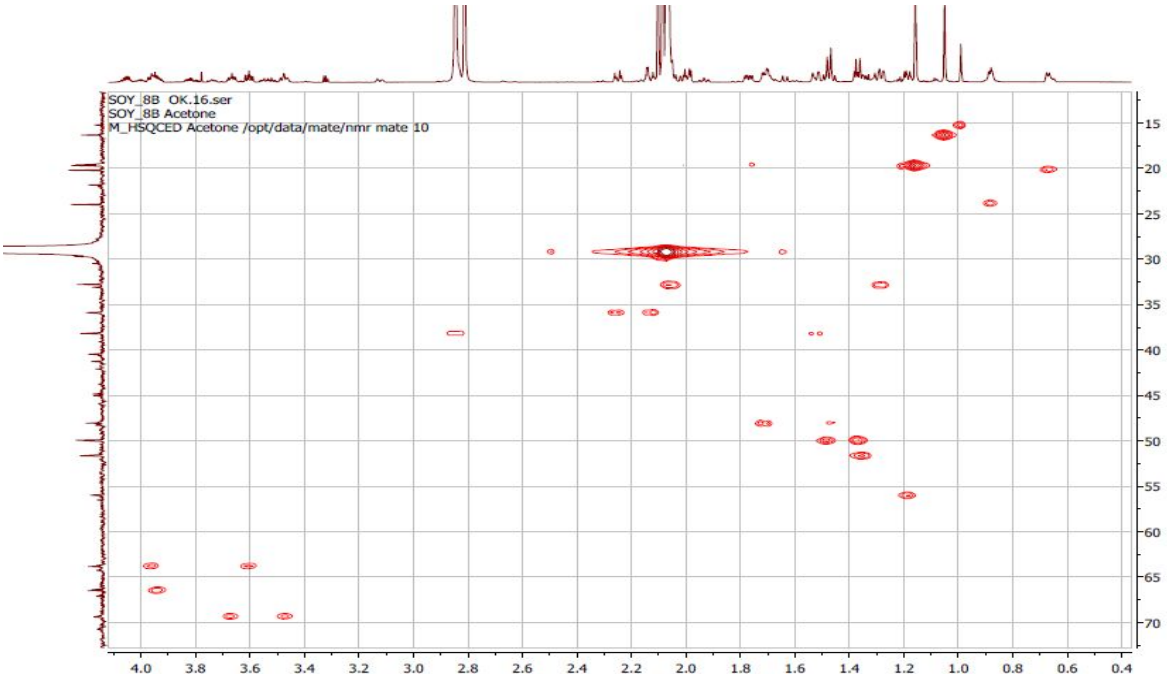

Appendix 78F: The HMBC spectrum of 6*β*,18,19-trihydroxy-*ent*-trachyloban-2*N*-oxime (**263**) in $CDCl_3$

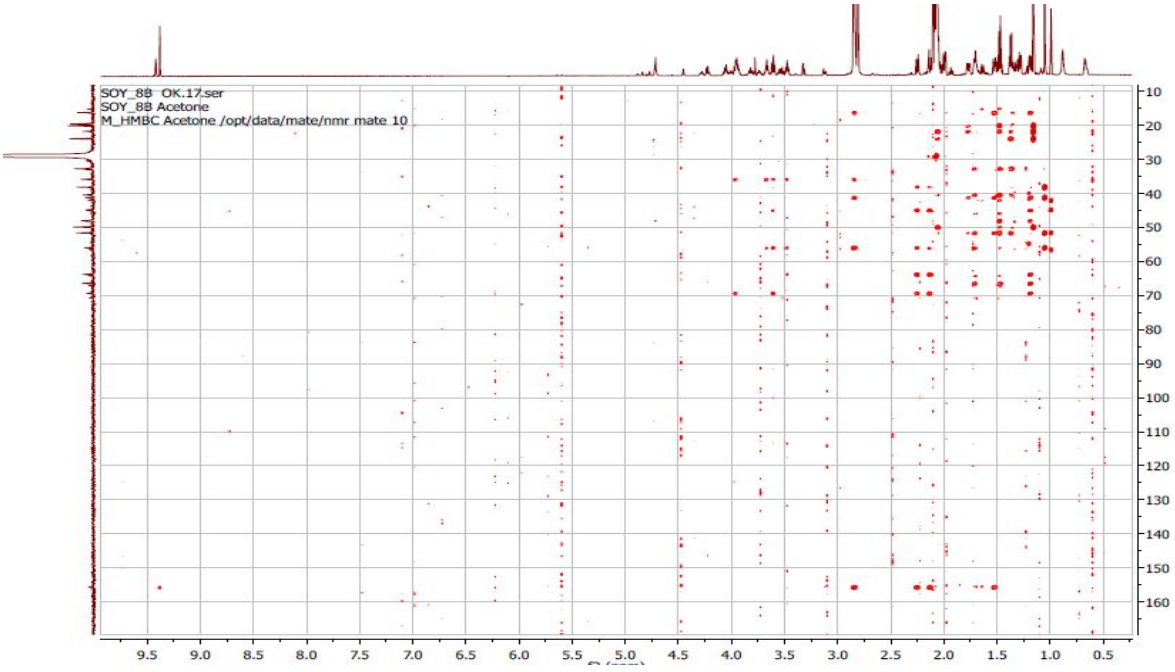

Appendix 78G. The ESIMS spectrum of 6β,18,19-trihydroxy-ent-trachyloban-2N-oxime (**263**)

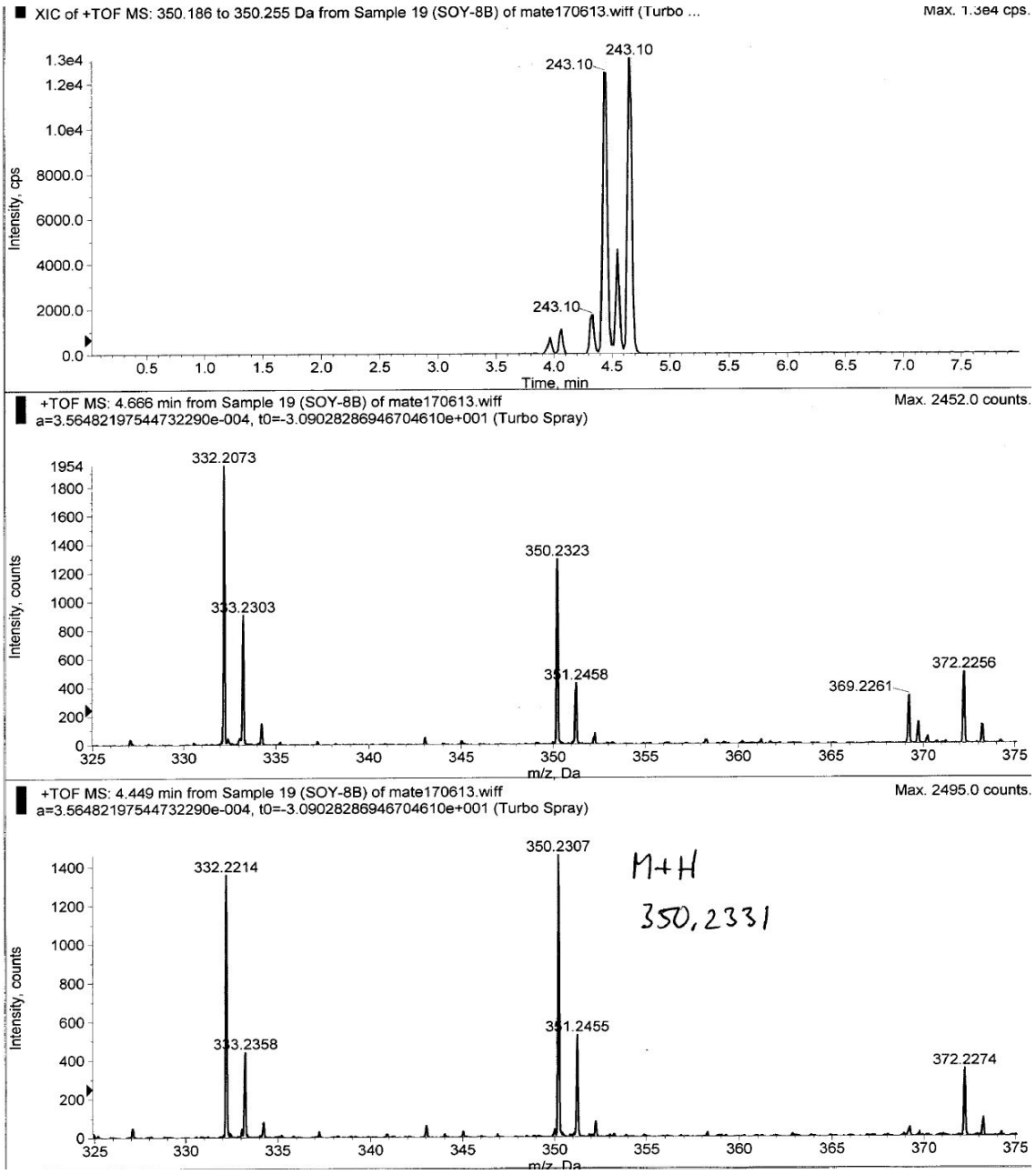

Appendix 79A: The ^{1}H NMR spectrum (600 MHz) of 6*β*-hydroxy-2-oxo-*ent*-trachyloban-18,19-dioic acid (**264**) inAcetone-d_6

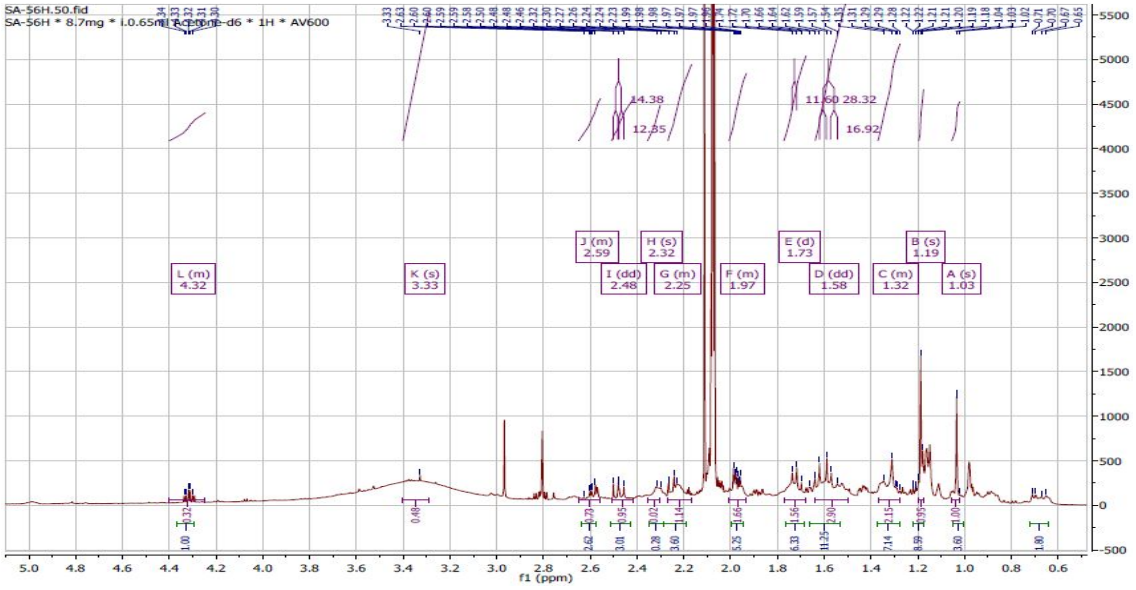

Appendix 79B: The ^{13}C NMR spectrum (150MHz) of 6*β*-hydroxy-2-oxo-*ent*-trachyloban-18,19-dioic acid (**264**) in Acetone-d_6

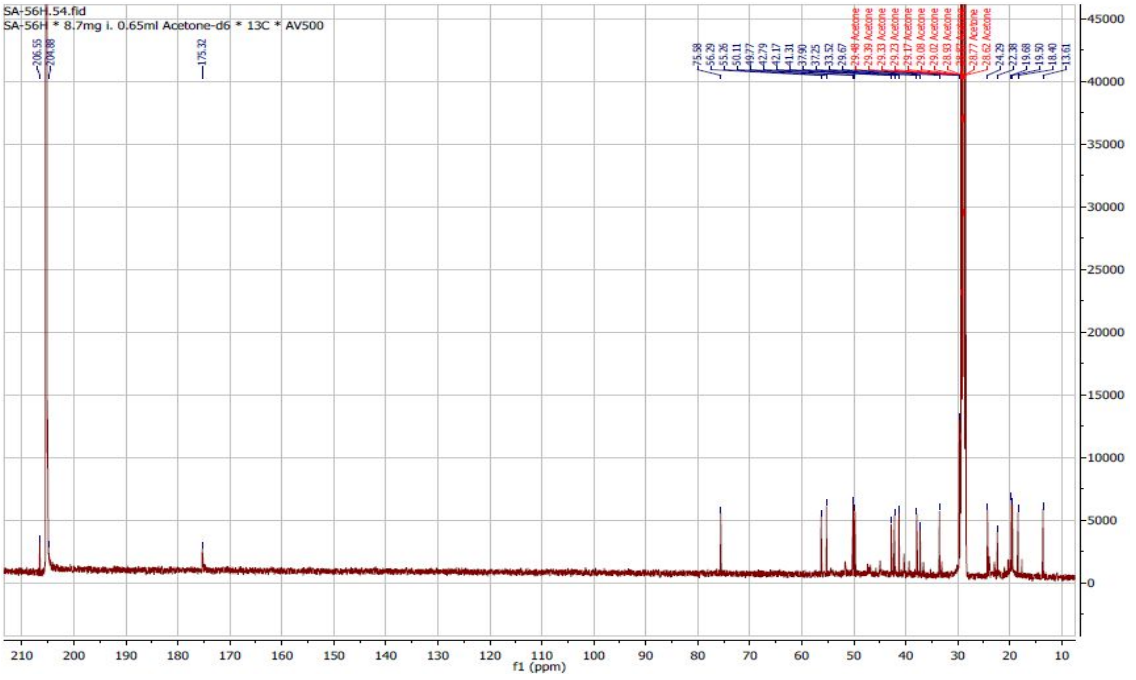

Appendix 79C: The H-H COSY spectrum of 6*β*-hydroxy-2-oxo-*ent*-trachyloban-18,19-dioic acid (**264**) in Acetone-d_6

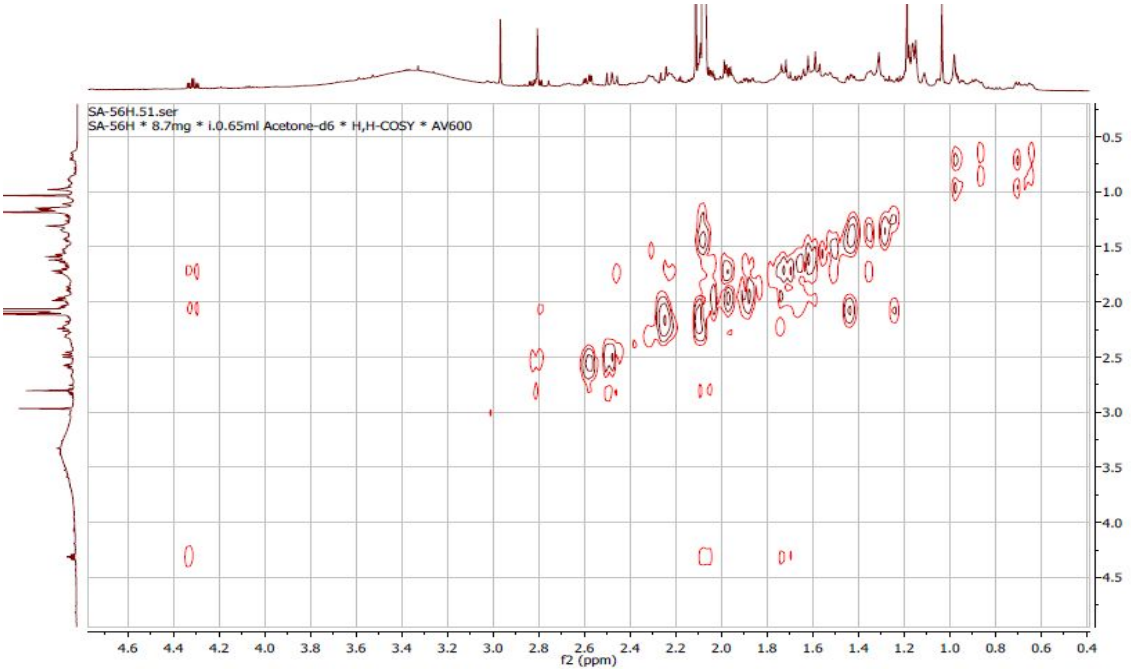

Appendix 79D: The HSQC spectrum of 6*β*-hydroxy-2-oxo-*ent*-trachyloban-18,19-dioic acid (**264**) in Acetone-d_6

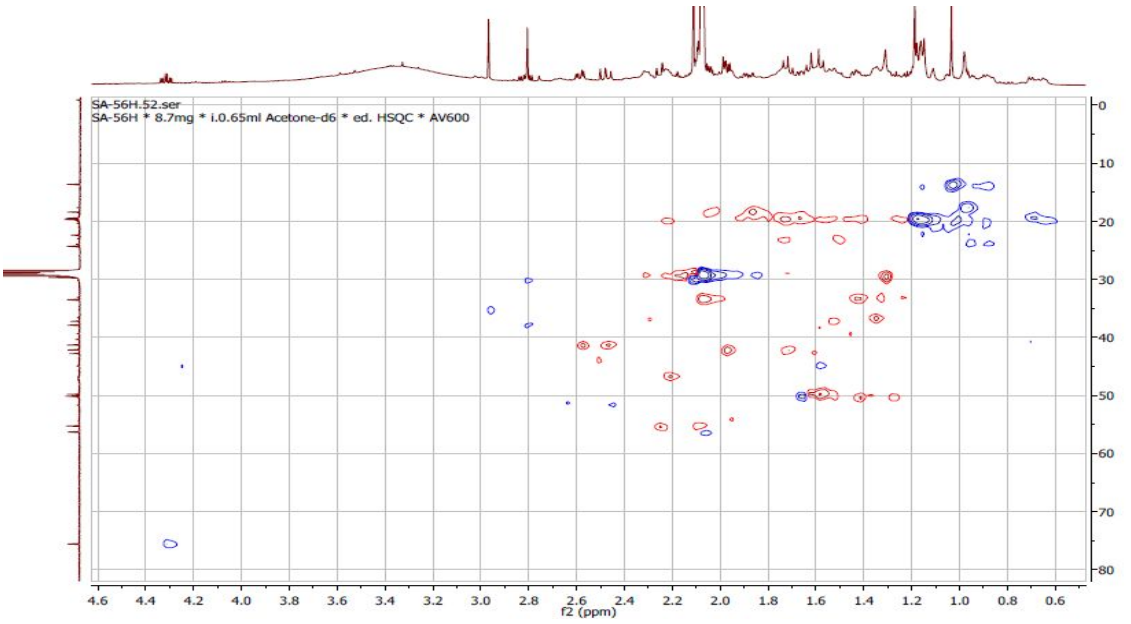

Appendix 79E: The HMBC spectrum of 6*β*-hydroxy-2-oxo-*ent*-trachyloban-18,19-dioic acid (**264**) in Acetone-d_6

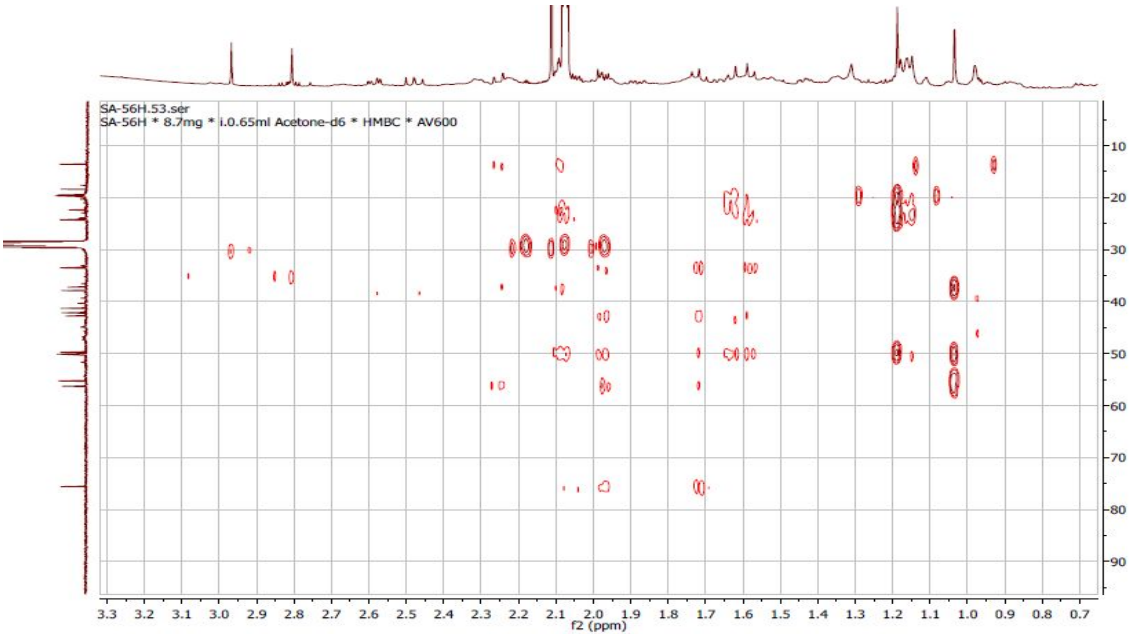

Appendix 80A: The ^{1}H NMR spectrum (600 MHz) of 17-methoxy-ent-trachyloban-6*β*,19-diol (**265**) in $CDCl_3$

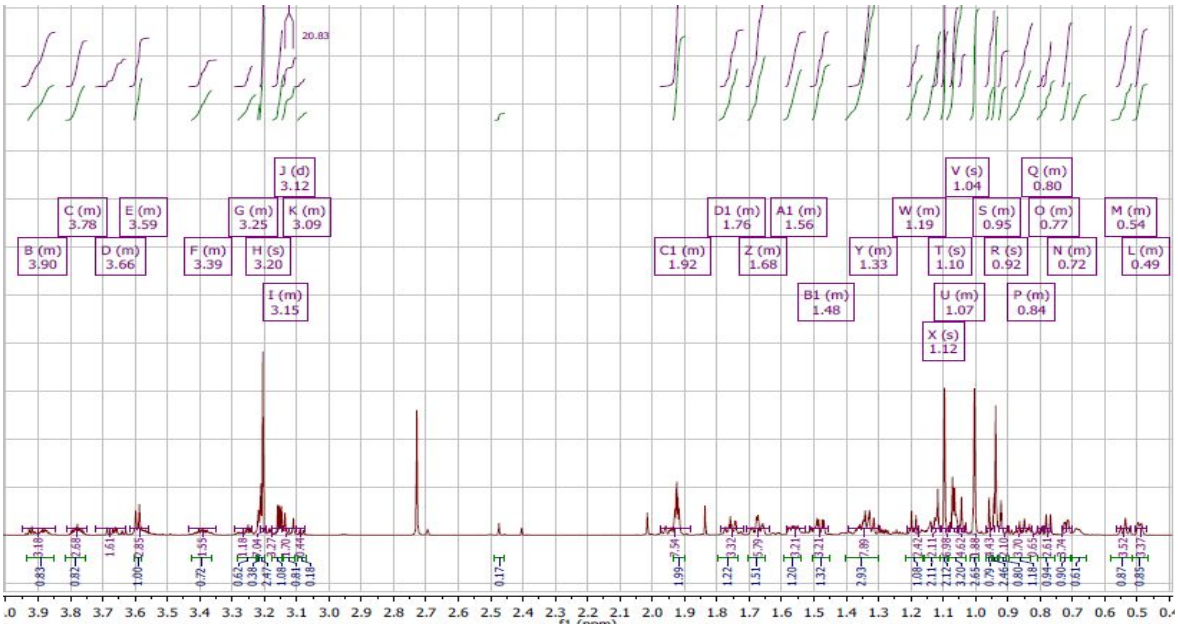

Appendix 80B: The ^{13}C NMR spectrum (200MHz) of 17-methoxy-ent-trachyloban-6β,19-diol (**265**) in $CDCl_3$

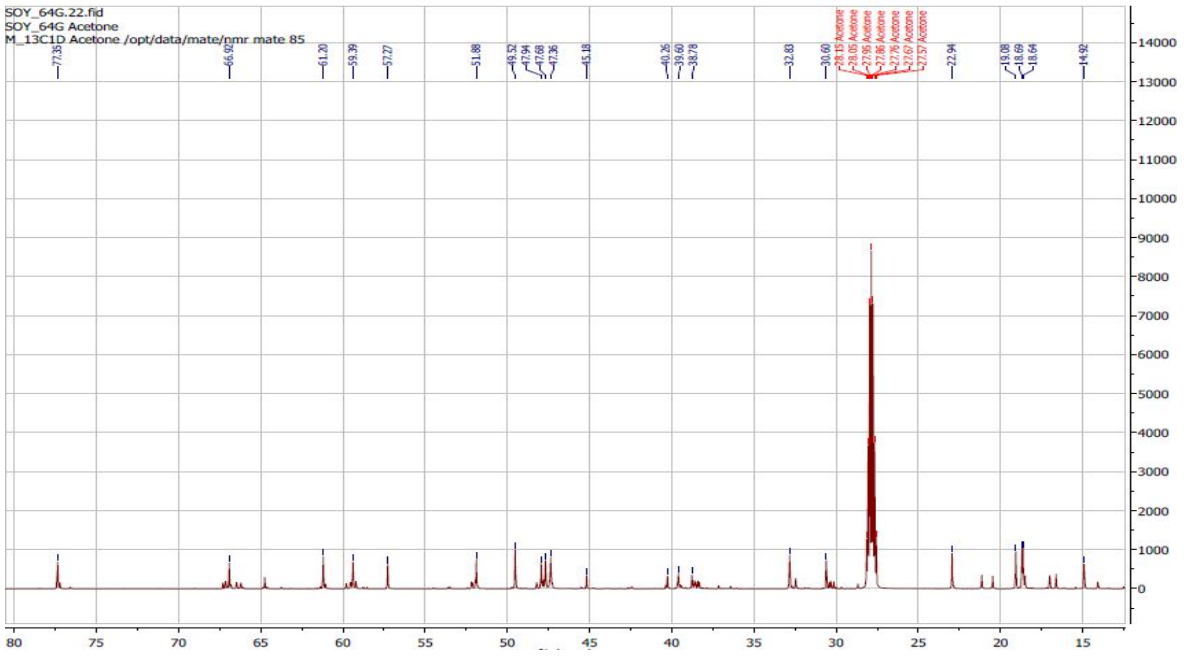

Appendix 80C: The H-H COSY spectrum of 17-methoxy-ent-trachyloban-6β,19-diol (**265**) in $CDCl_3$

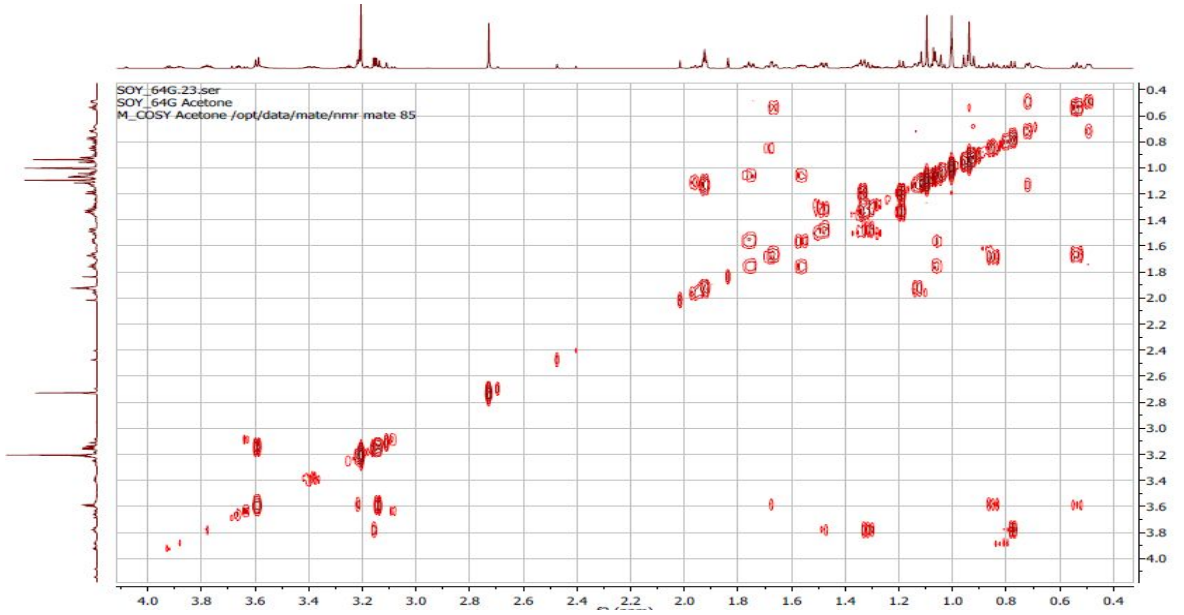

Appendix 80D: The NOESY spectrum of 17-methoxy-ent-trachyloban-6β,19-diol (**265**) in $CDCl_3$

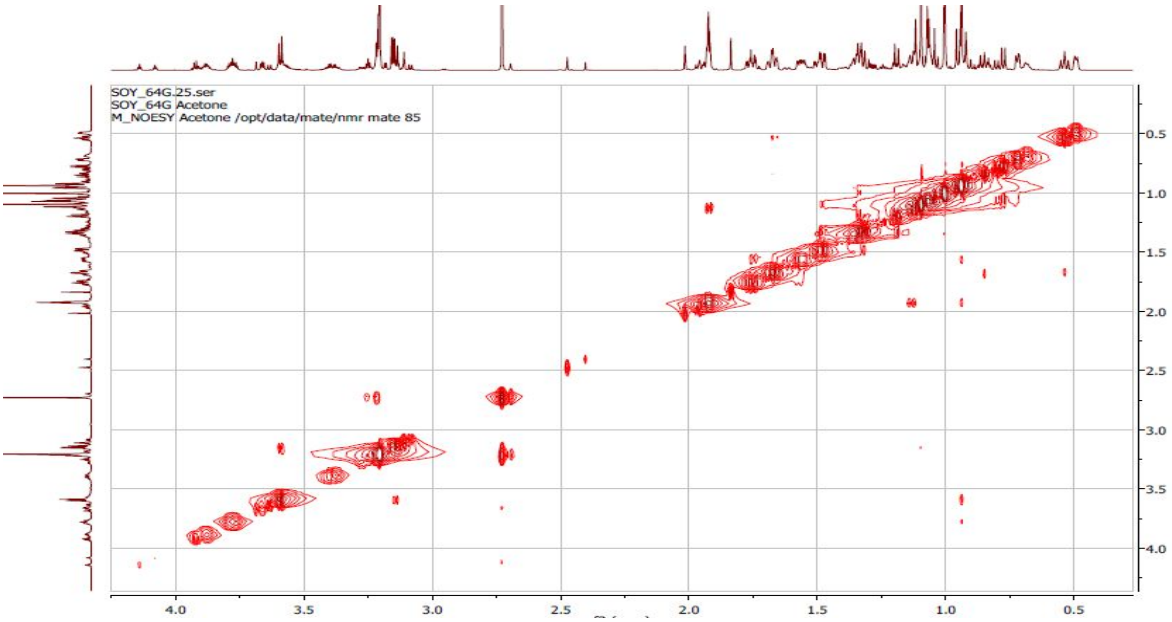

Appendix 80E: The HSQC spectrum of 17-methoxy-ent-trachyloban-6β,19-diol (**265**) in $CDCl_3$

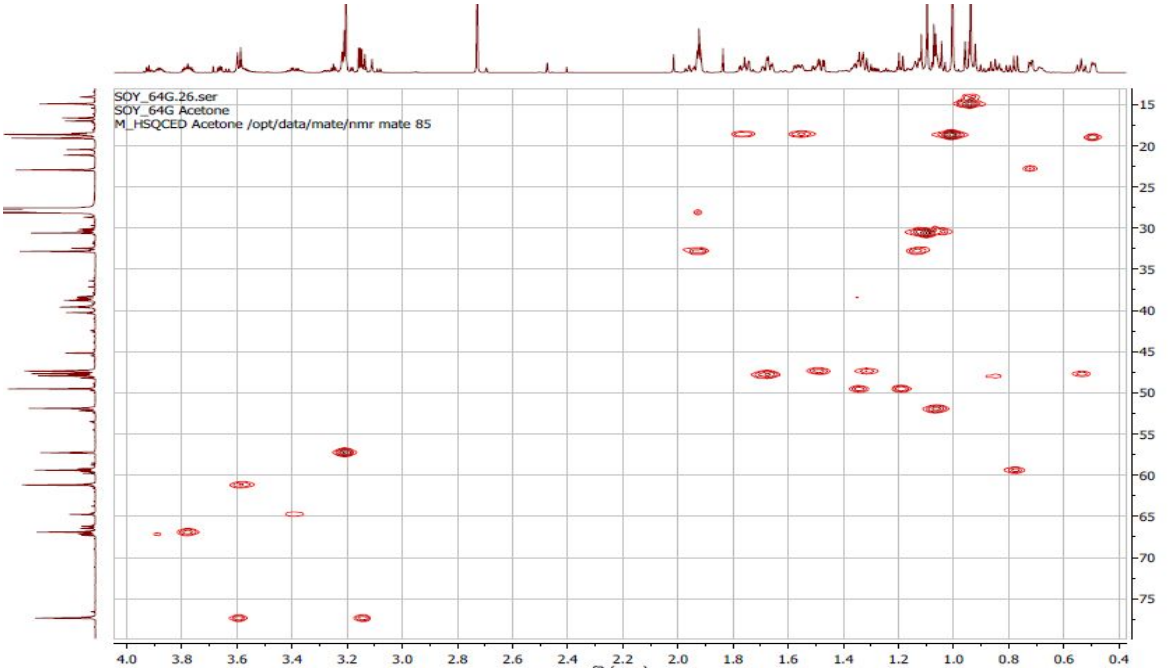

Appendix 80F: The HMBC spectrum of 17-methoxy-ent-trachyloban-6β,19-diol (**265**) in $CDCl_3$

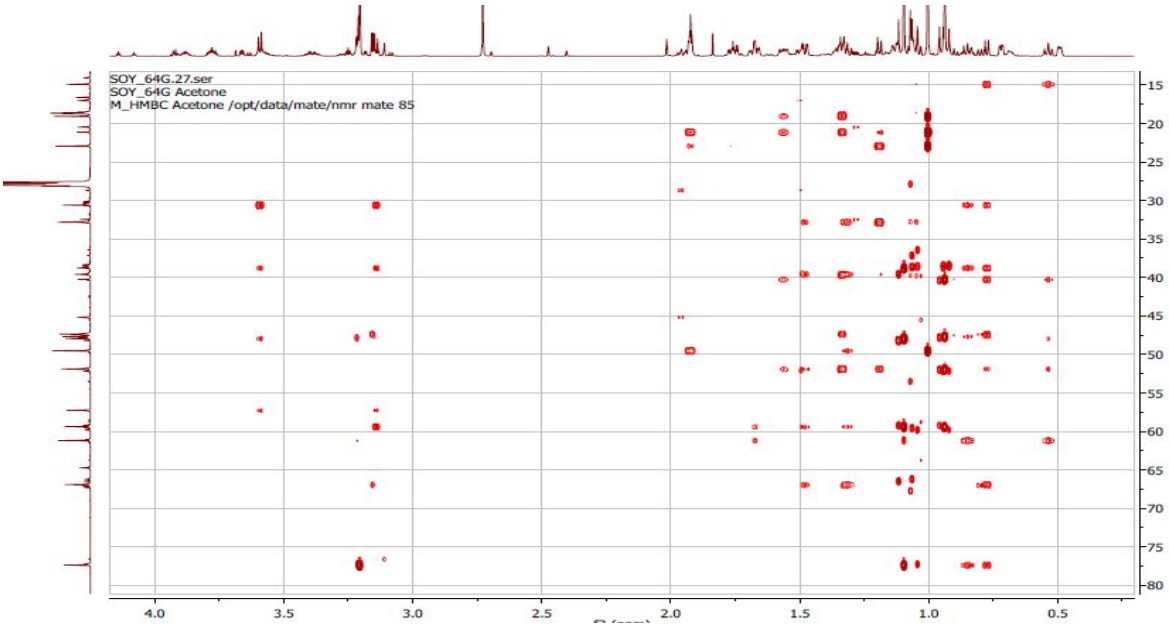

Appendix 80G. The ESIMS spectrum of 17-methoxy-ent-trachyloban-6β,19-diol (**265**)

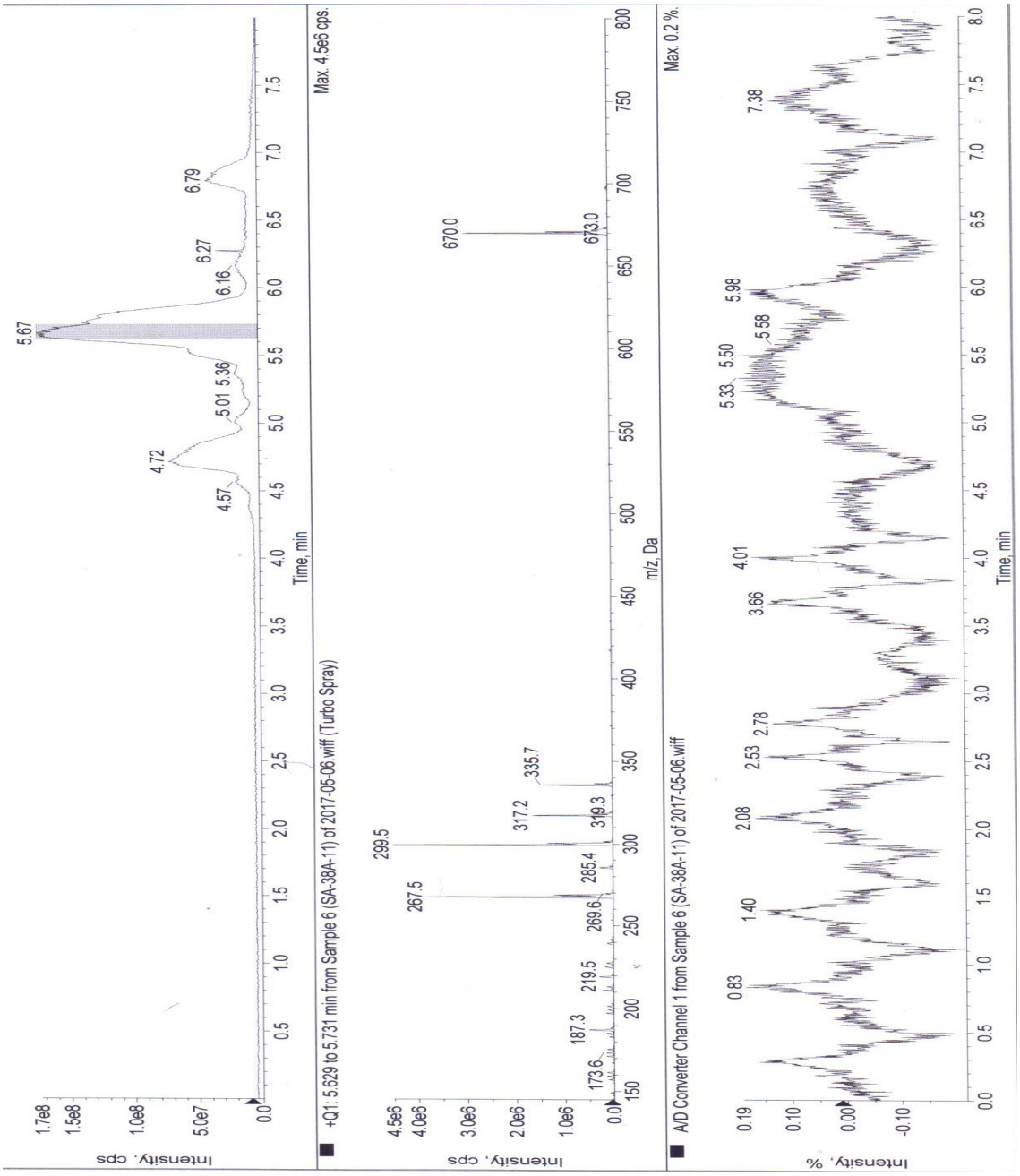

Appendix 81A: ^{1}H NMR spectrum (500 MHz) of 6β,17,19-triacethyloxy-*ent*-trachylobane (**266**) in Acetone-d_6

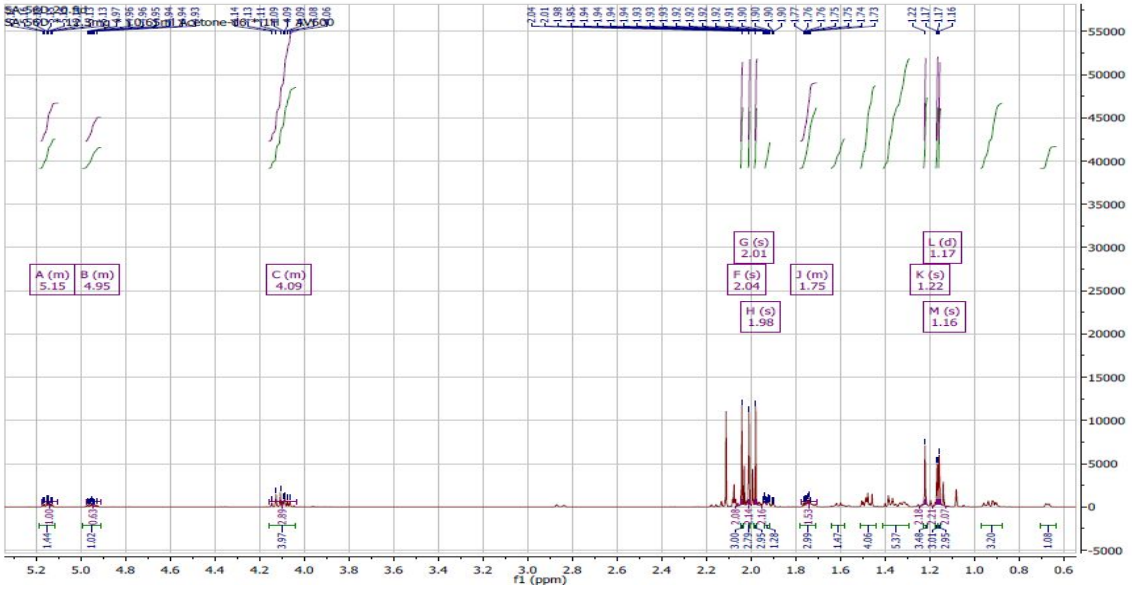

Appendix 81B: The ^{13}C NMR spectrum (125MHz) of of 6β,17,19-triacethyloxy-*ent*-trachylobane (**266**) in Acetone-d_6

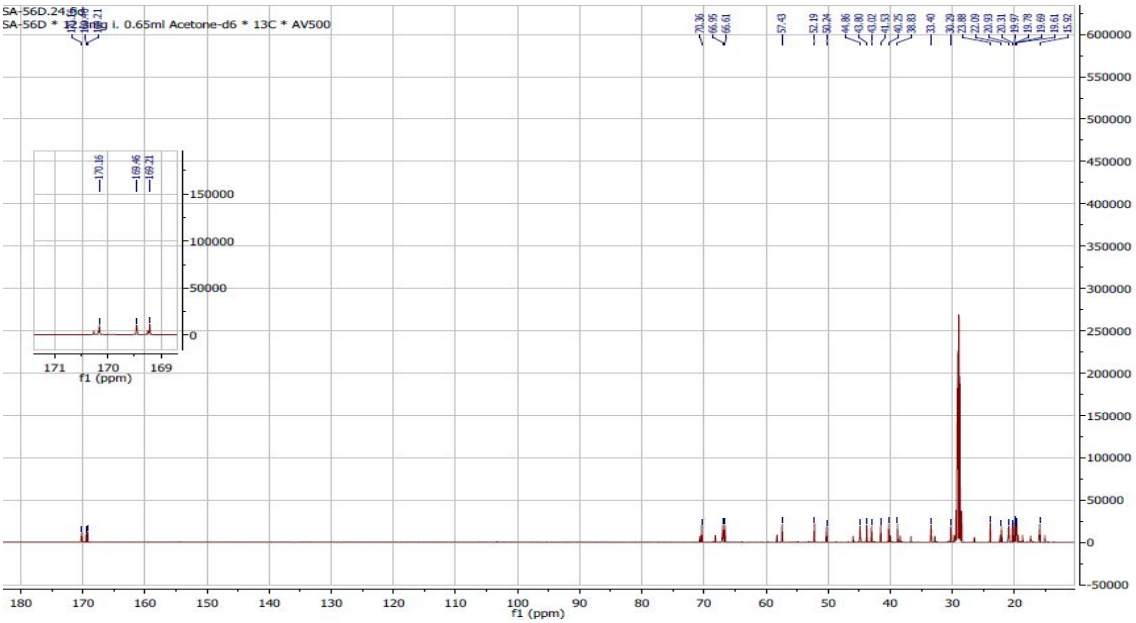

Appendix 81C: The H-H COSY spectrum of of 6β,17,19-triacethyloxy-*ent*-trachylobane (**266**) in Acetone-d_6

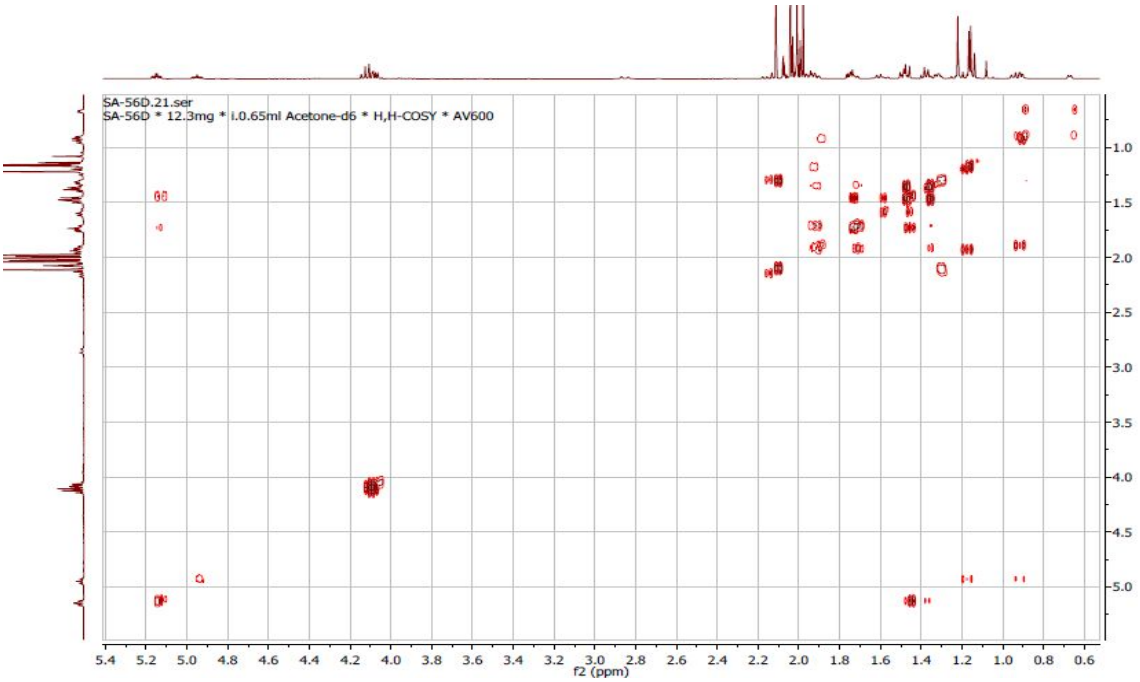

Appendix 81D: The HSQC spectrum of 6β,17,19-triacethyloxy-*ent*-trachylobane (**266**) in Acetone-d_6

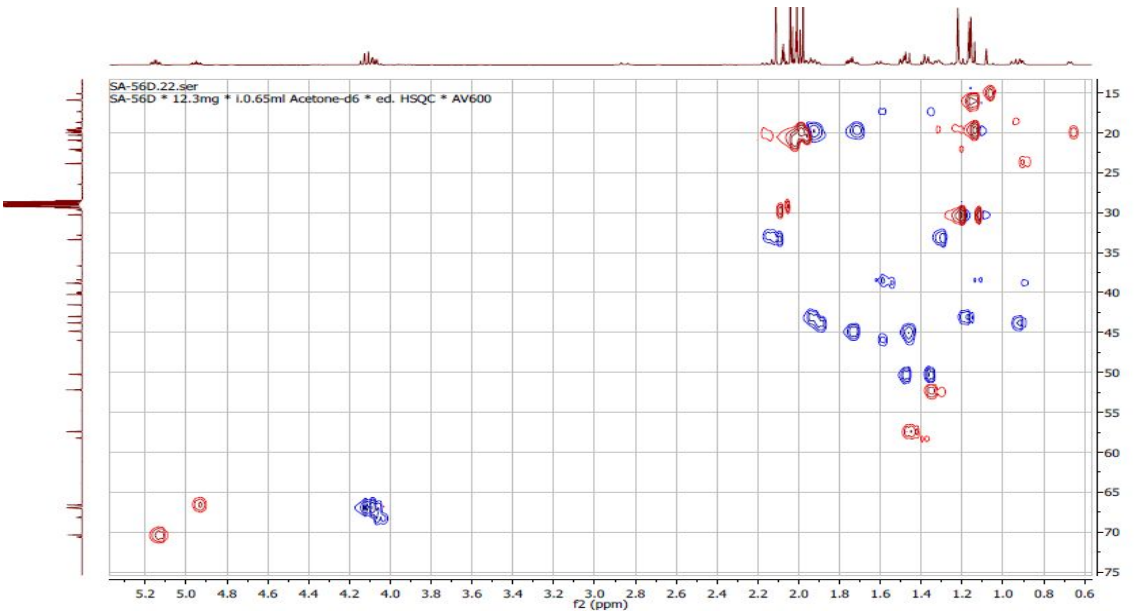

Appendix 81E: The HMBC spectrum of of 6β,17,19-triacethyloxy-*ent*-trachylobane (**266)** inAcetone-d_6

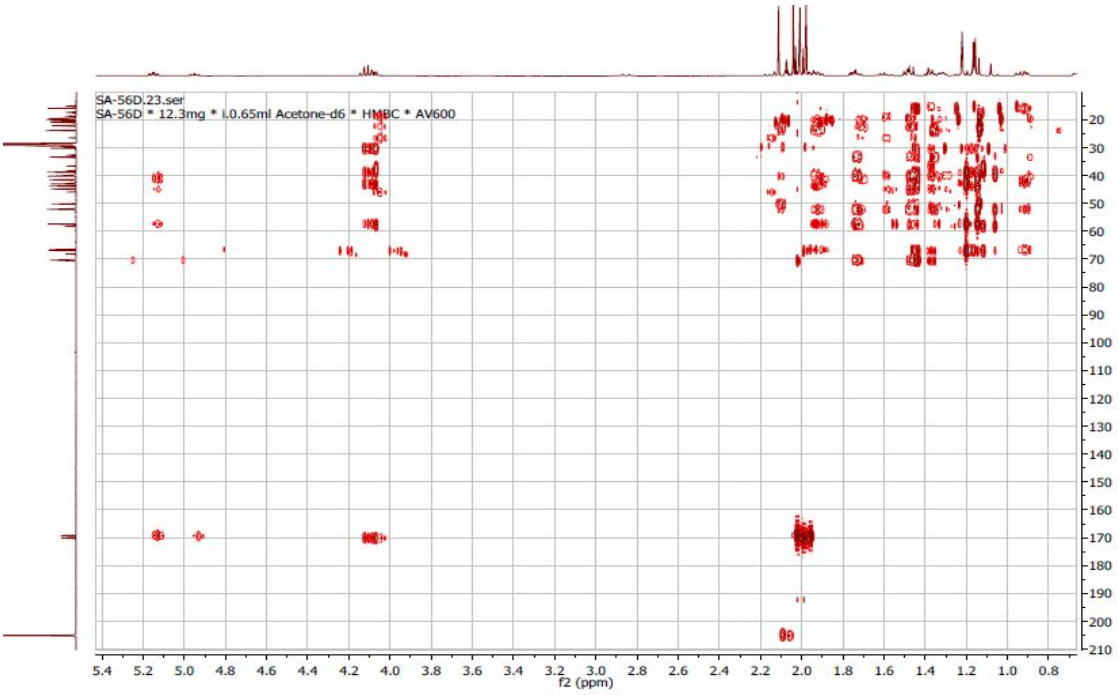

Appendix 82A: The ^{1}H NMR spectrum (500 MHz) of 6β,17,19-triacethyloxy-*ent*-trachylobane (**267**) in $CDCl_3$

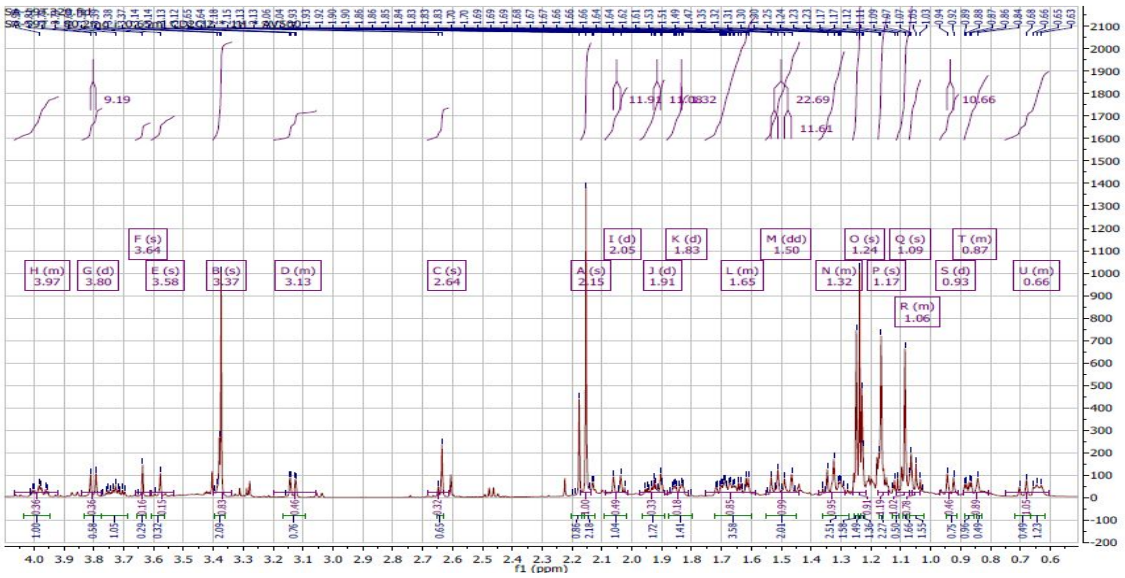

Appendix 82B: The ^{13}C NMR spectrum (125MHz) of 6*β*-methoxy-e*nt*-trachyloban-17,19-diol (**267**) in $CDCl_3$

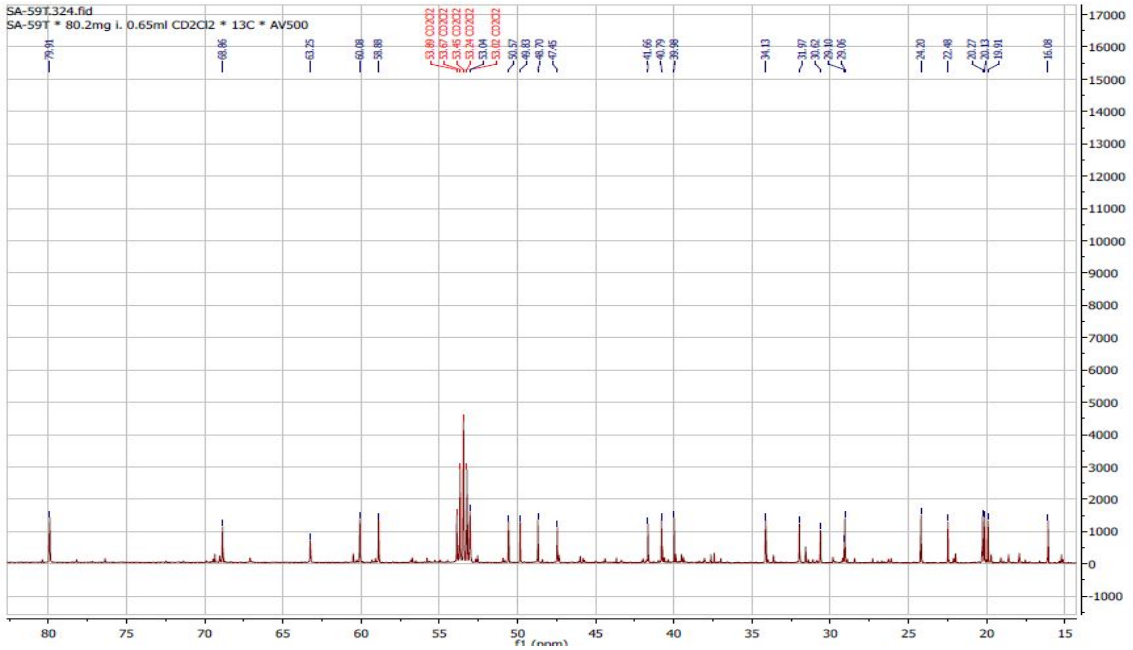

Appendix 82C: The H-H COSY spectrum of 6*β*-methoxy-e*nt*-trachyloban-17,19-diol (**267**) in $CDCl_3$

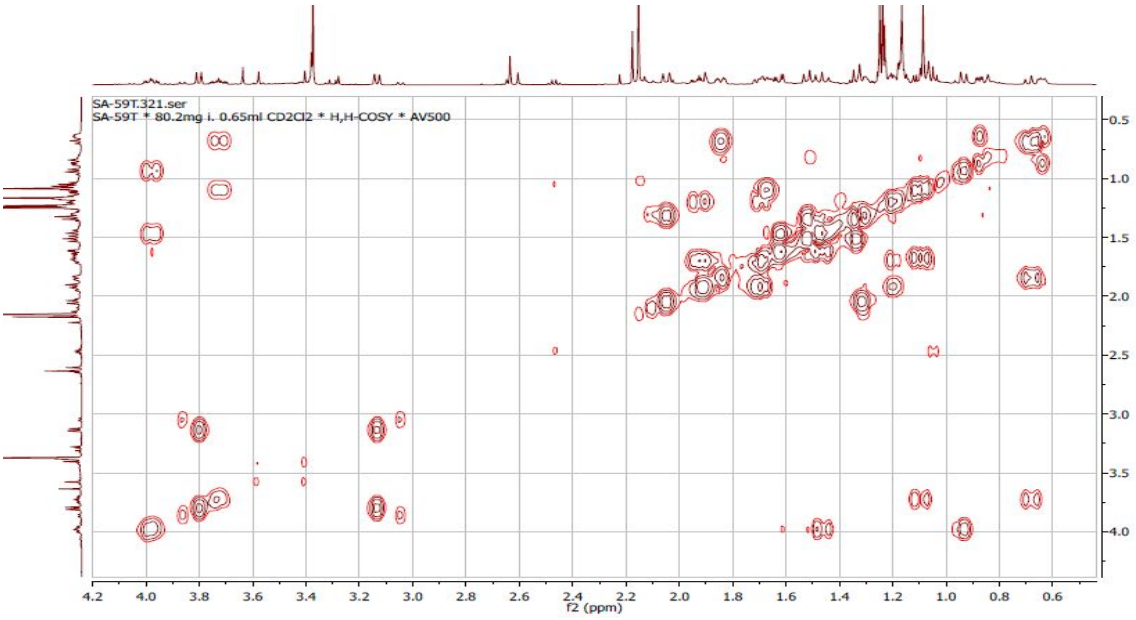

Appendix 82D: The HMBC spectrum of 6*β*-methoxy-e*nt*-trachyloban-17,19-diol (**267**) in $CDCl_3$

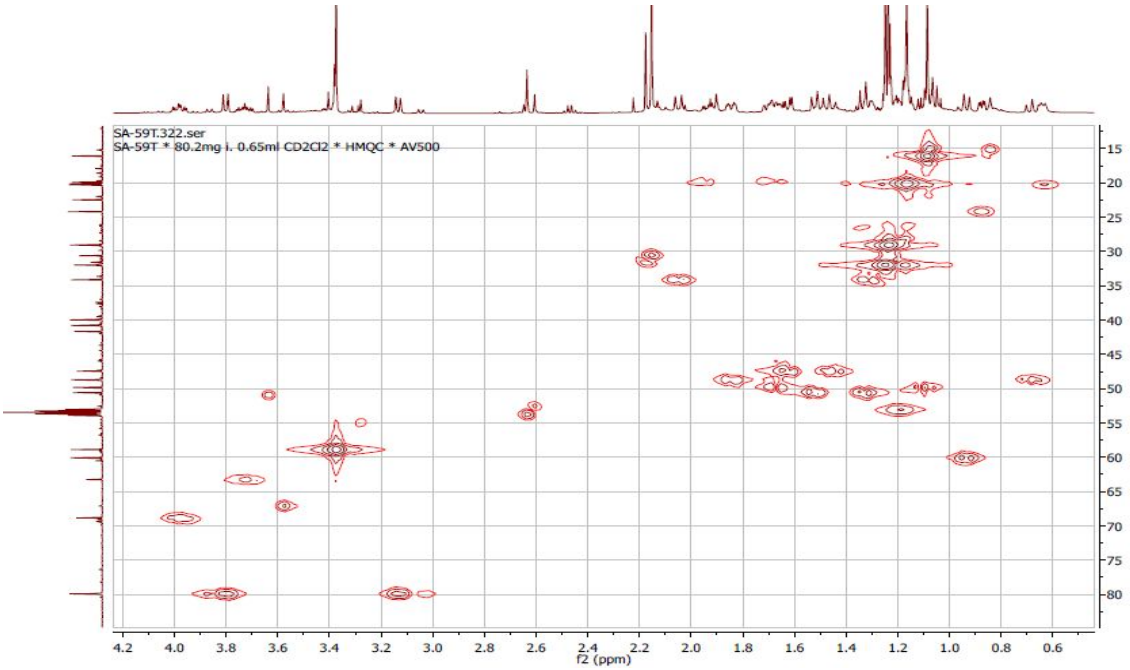

Appendix 82E. The ESIMS spectrum of 6β-methoxy-e*nt*-trachyloban-17,19-diol (**267**)

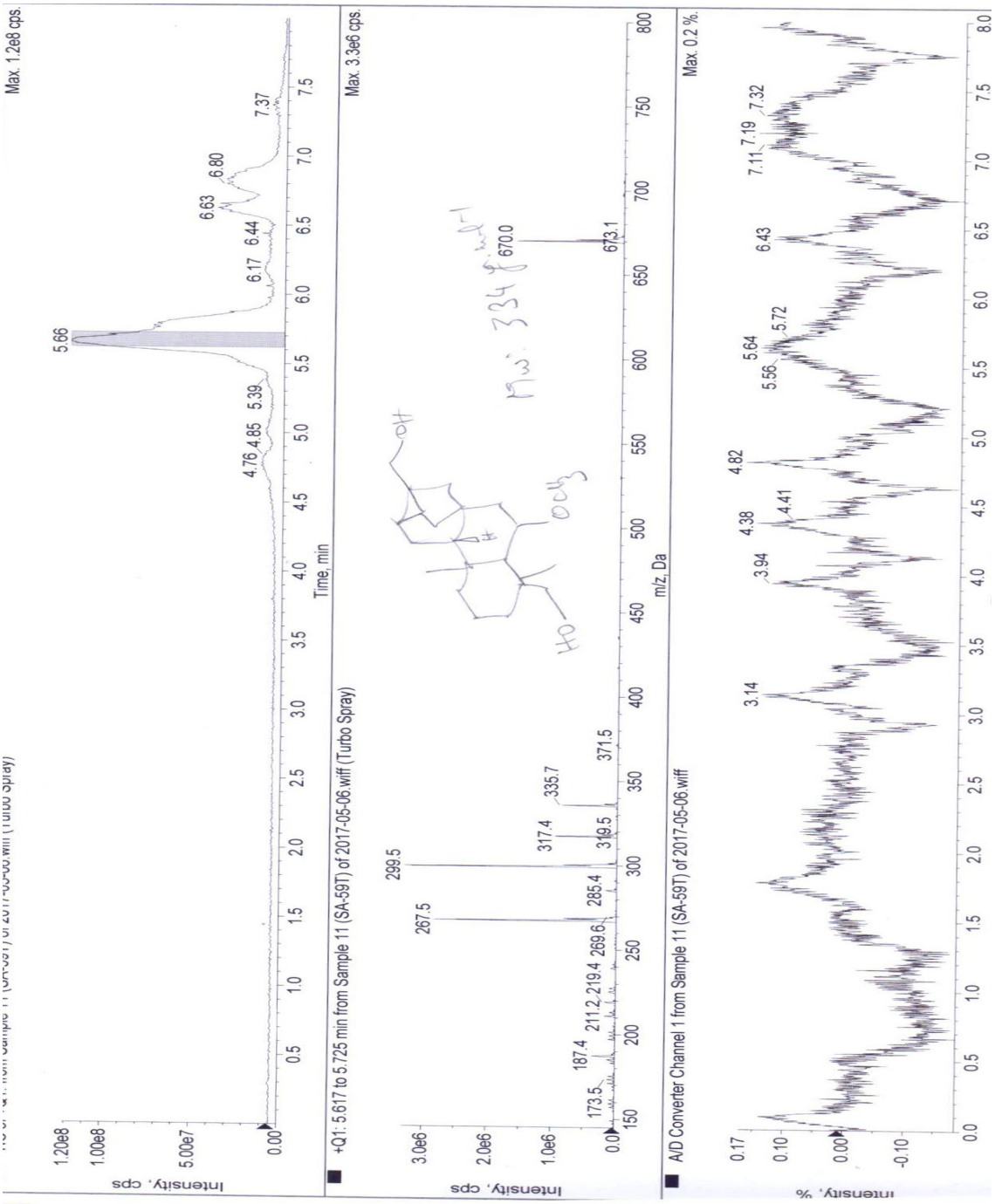

Appendix 83A: The ^{1}H NMR spectrum (600 MHz) of 16*β*-methoxy-*ent*-kaur-9(11)-en-19-oic acid **(268)** in CD_2Cl_2

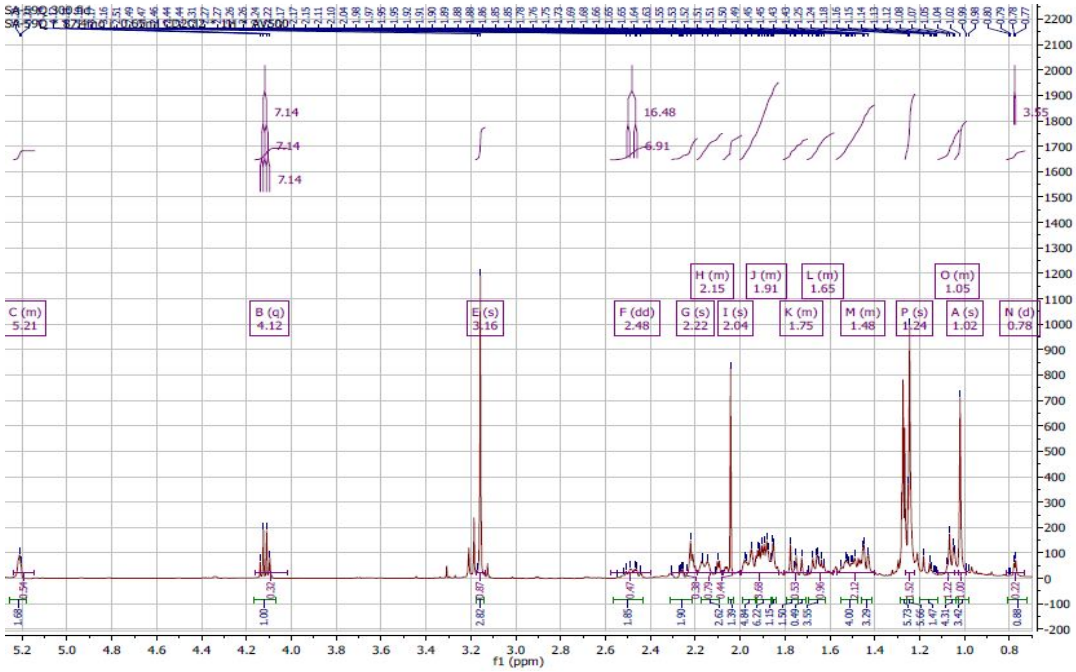

Appendix 83B: The ^{13}C NMR spectrum (150MHz) of of 16*β*-methoxy-*ent*-kaur-9(11)-en-19-oic acid **(268)** in CD_2Cl_2

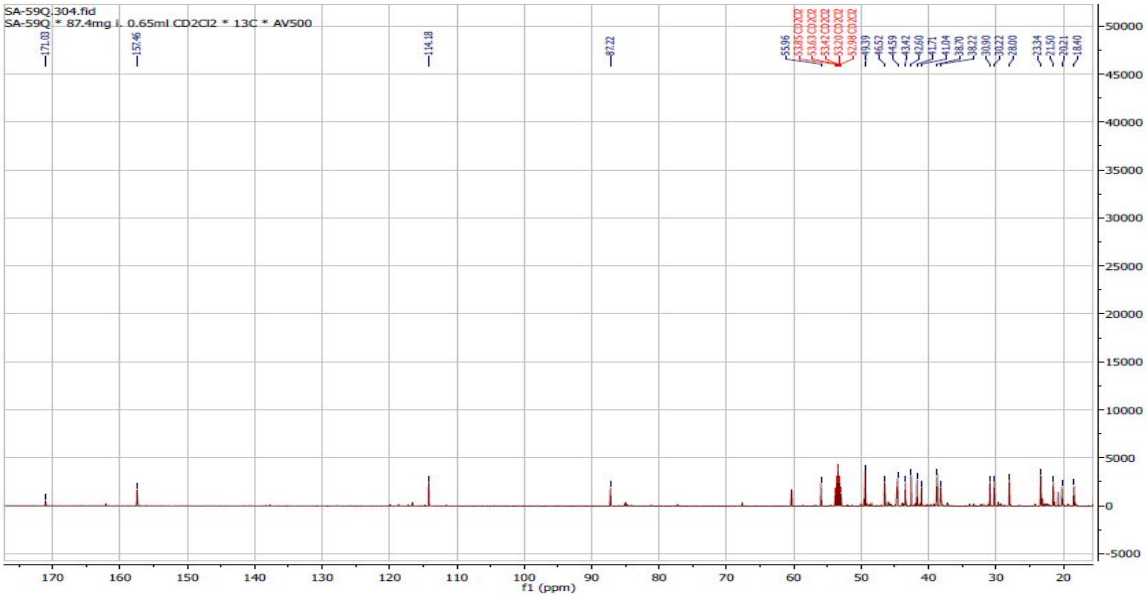

Appendix 83C: The H-H COSY spectrum of 16*β*-methoxy-*ent*-kaur-9(11)-en-19-oic acid **(268)** in CD_2Cl_2

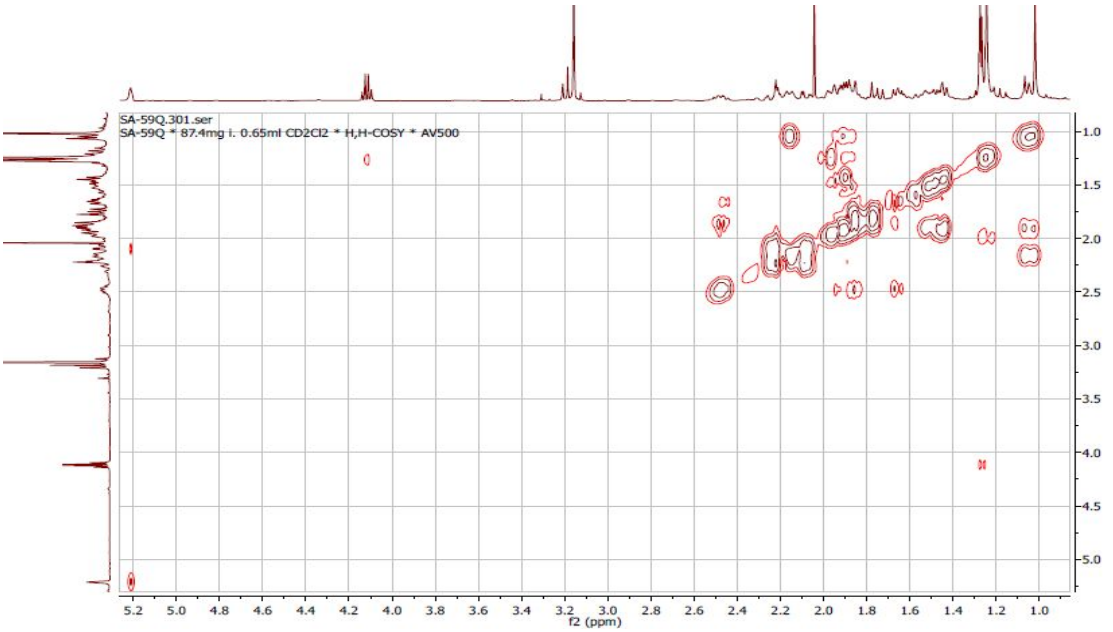

Appendix 83D: The NOESY spectrum of 16*β*-methoxy-*ent*-kaur-9(11)-en-19-oic acid **(268)** in CD_2Cl_2

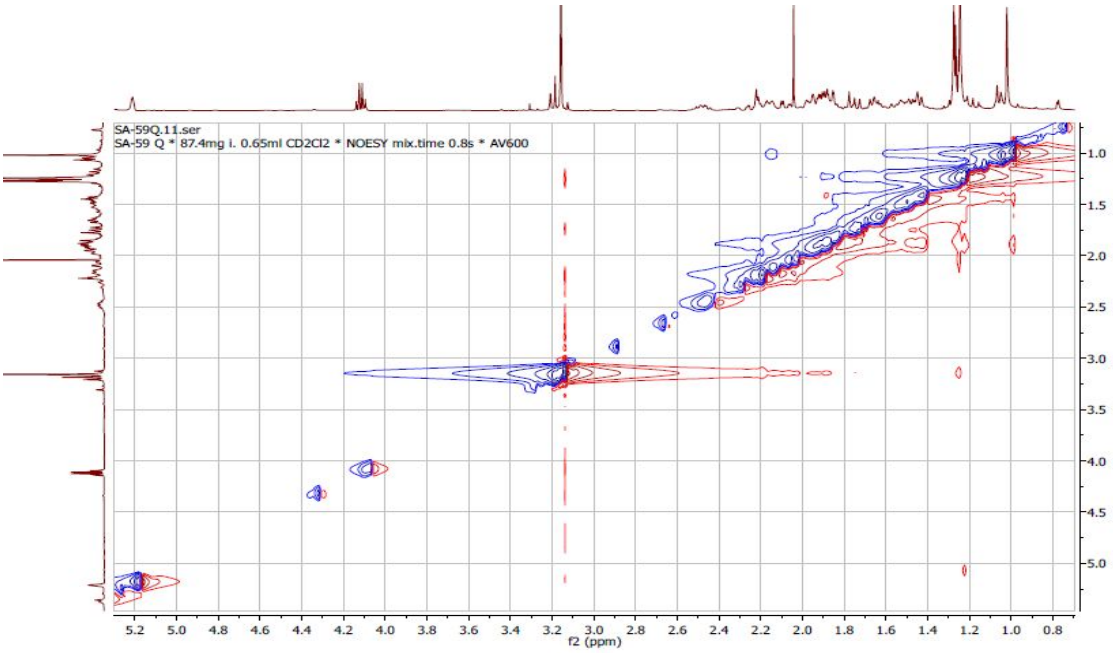

Appendix 83E: The HMQC spectrum of 16*β*-methoxy-*ent*-kaur-9(11)-en-19-oic acid **(268)** in CD_2Cl_2

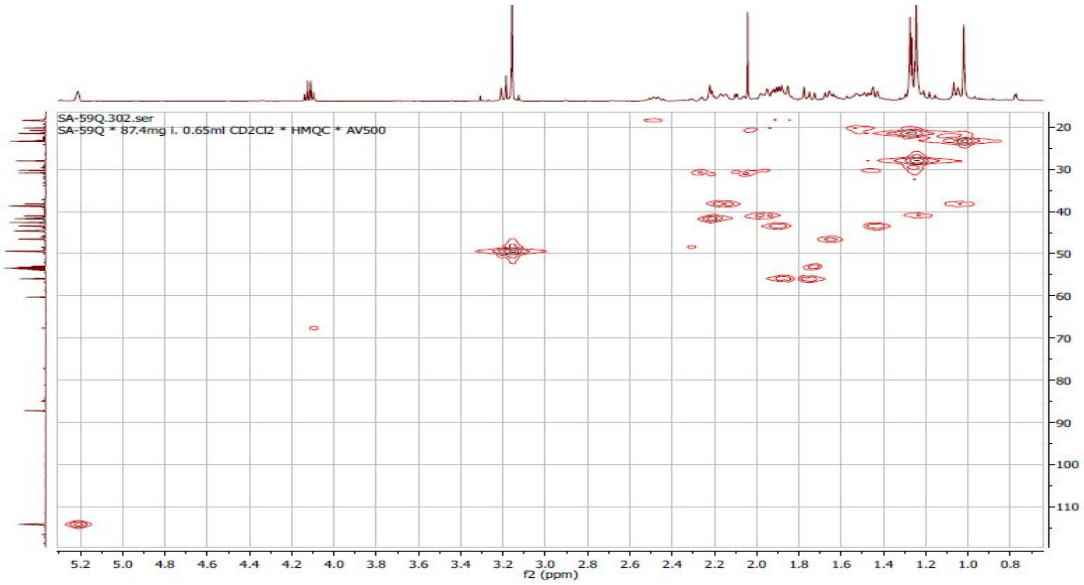

Appendix 83F: The HMBC spectrum of 16*β*-methoxy-*ent*-kaur-9(11)-en-19-oic acid **(268)** in CD_2Cl_2

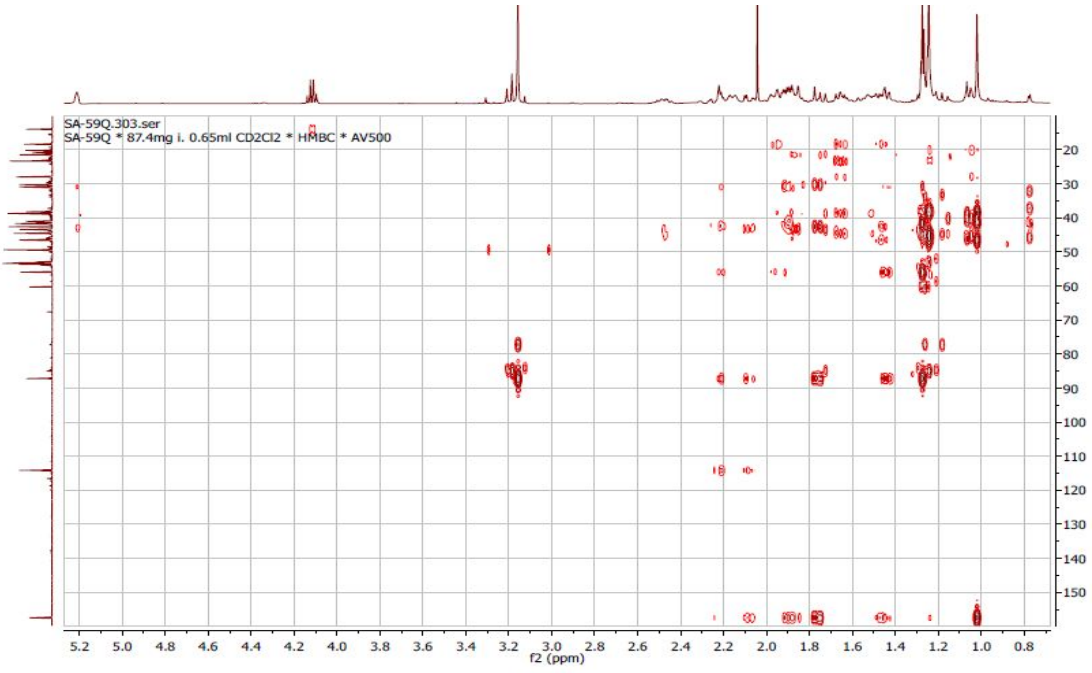

Appendix 83G. The ESIMS spectrum of 16*β*-methoxy-*ent*-kaur-9(11)-en-19-oic acid **(268)**

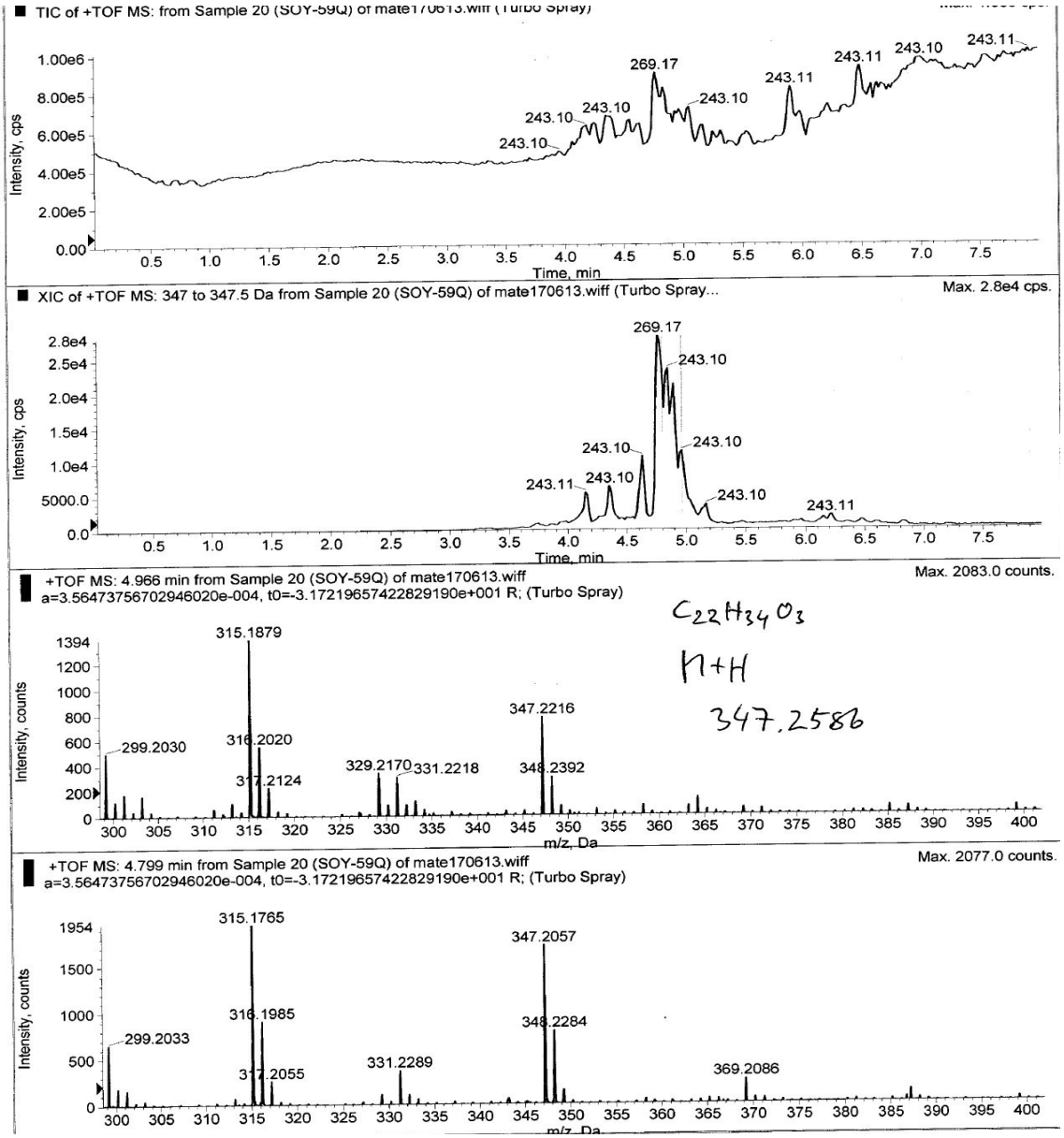

Appendix 84A: The ^{1}H NMR spectrum (600 MHz) of *ent*-kaur-9(11)-en-19-oic acid (**269**) in CD_2Cl_2

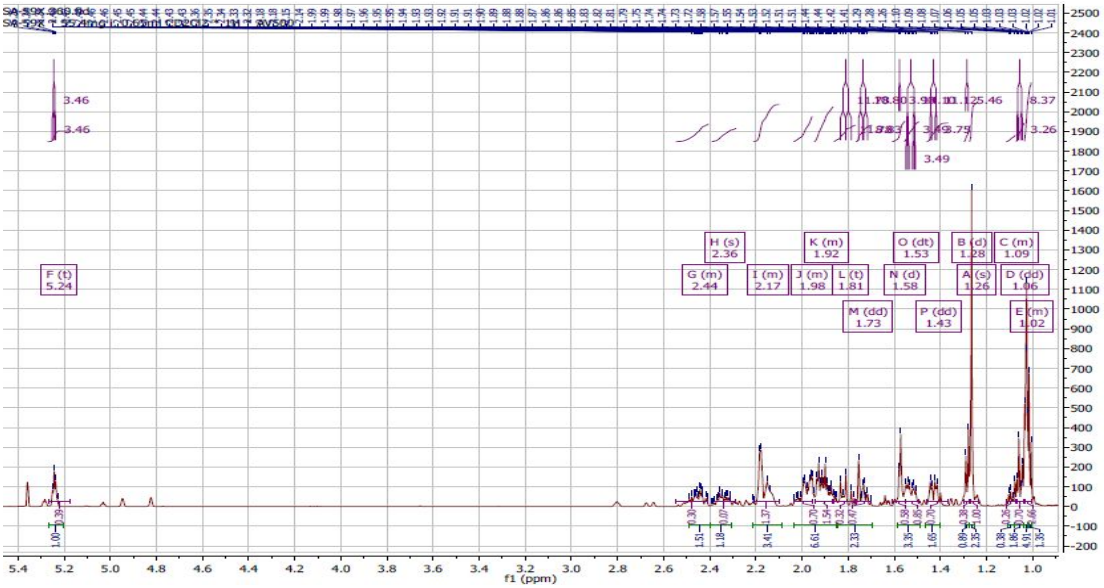

Appendix 84B: The ^{13}C NMR spectrum (150MHz) of *ent*-kaur-9(11)-en-19-oic acid (**269**) in CD_2Cl_2, in $CDCl_3$

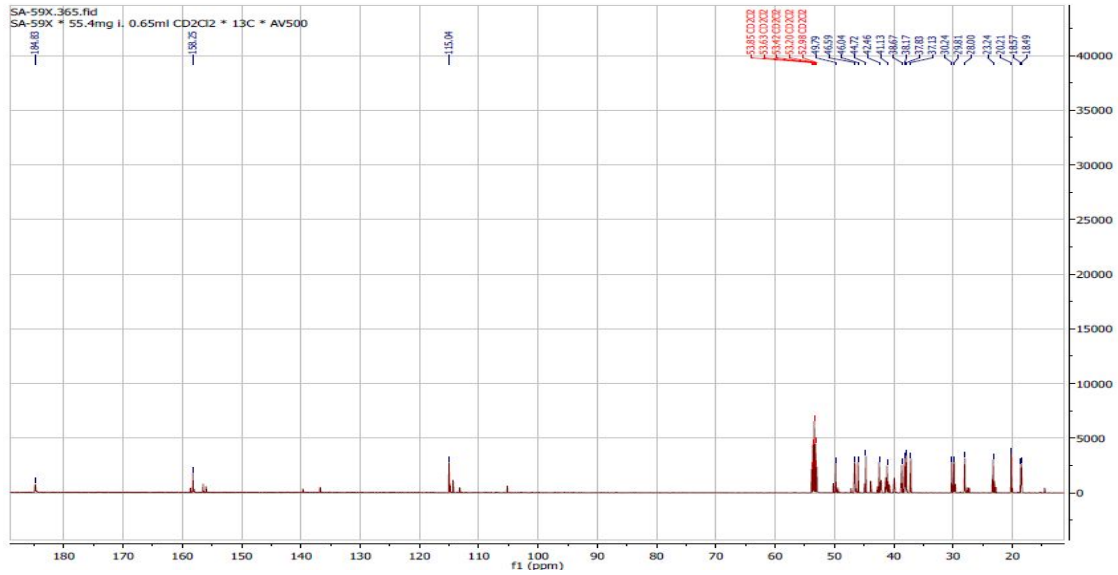

Appendix 84C: The H-H COSY spectrum of *ent*-kaur-9(11)-en-19-oic acid (**269**) in CD_2Cl_2

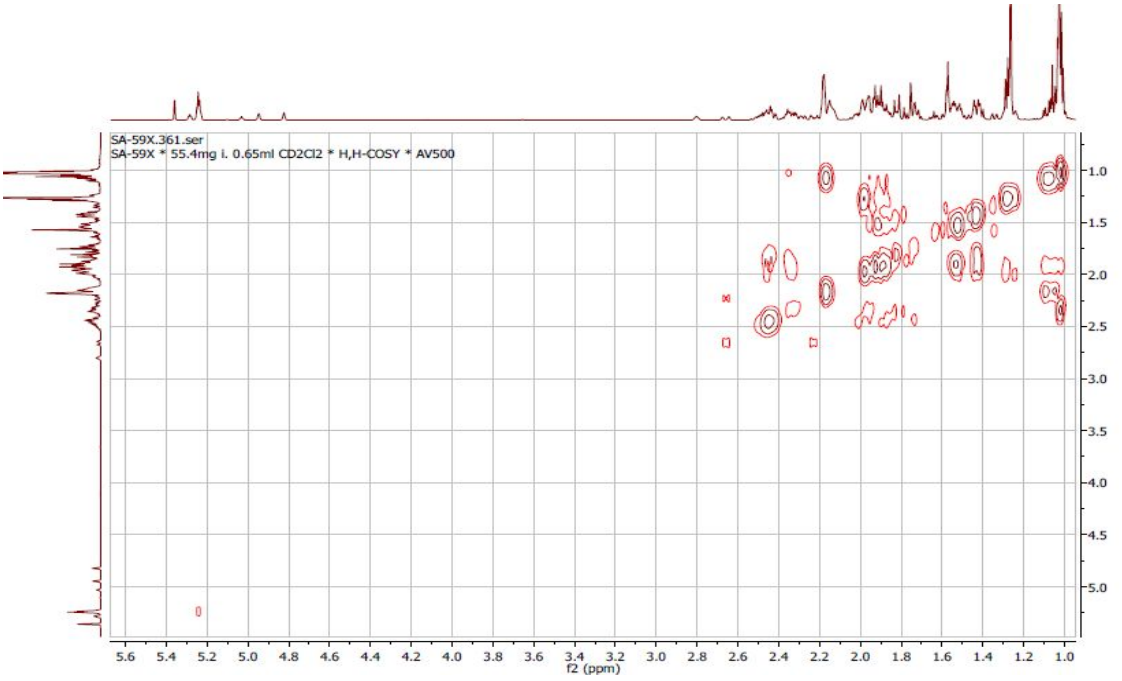

Appendix 84D: The HMQC spectrum of *ent*-kaur-9(11)-en-19-oic acid (**269**) in CD_2Cl_2

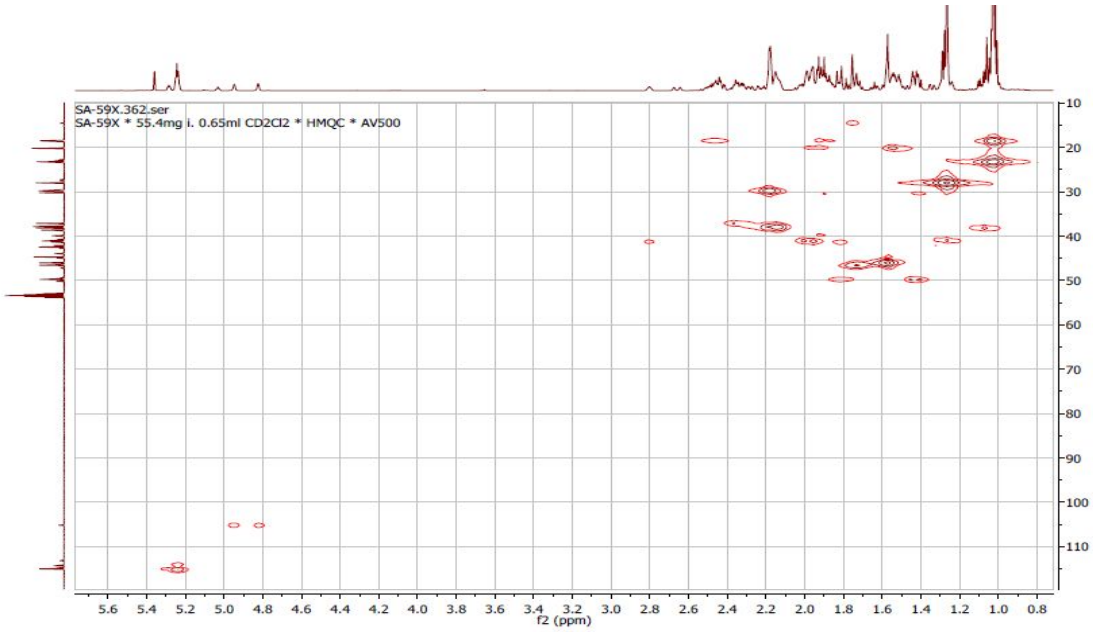

Appendix 84E: The HMBC spectrum of *ent*-kaur-9(11)-en-19-oic acid (**269**) in CD_2Cl_2

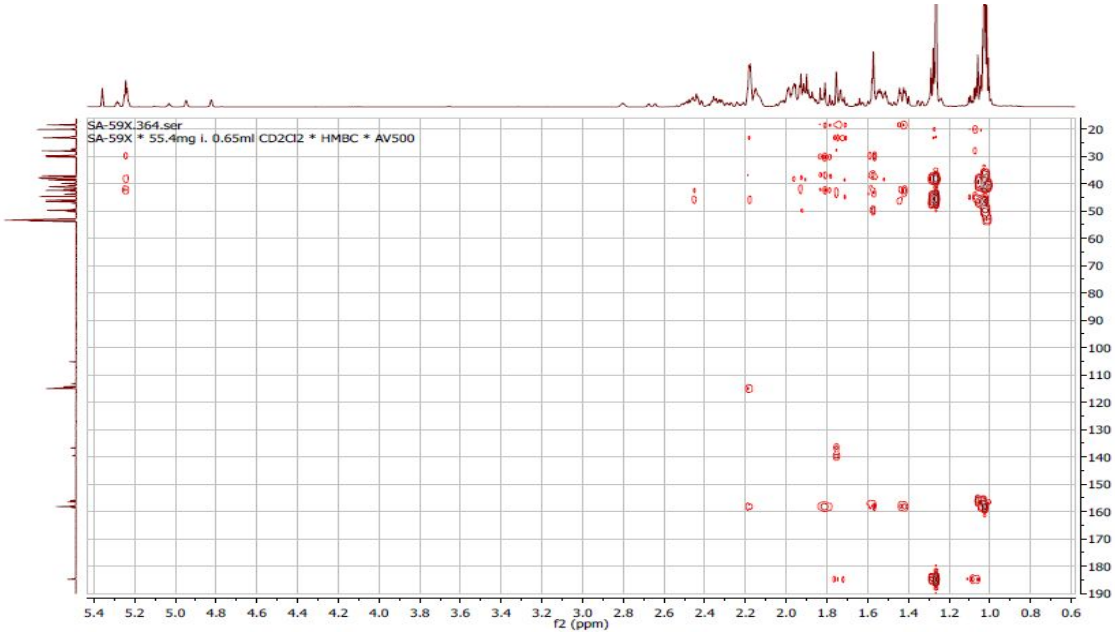

Appendix 85A: The ^{1}H NMR spectrum (500 MHz) of methyl-*ent*-kaura-9(11),16-dien-19-oate (**270**) in CD_2Cl_2

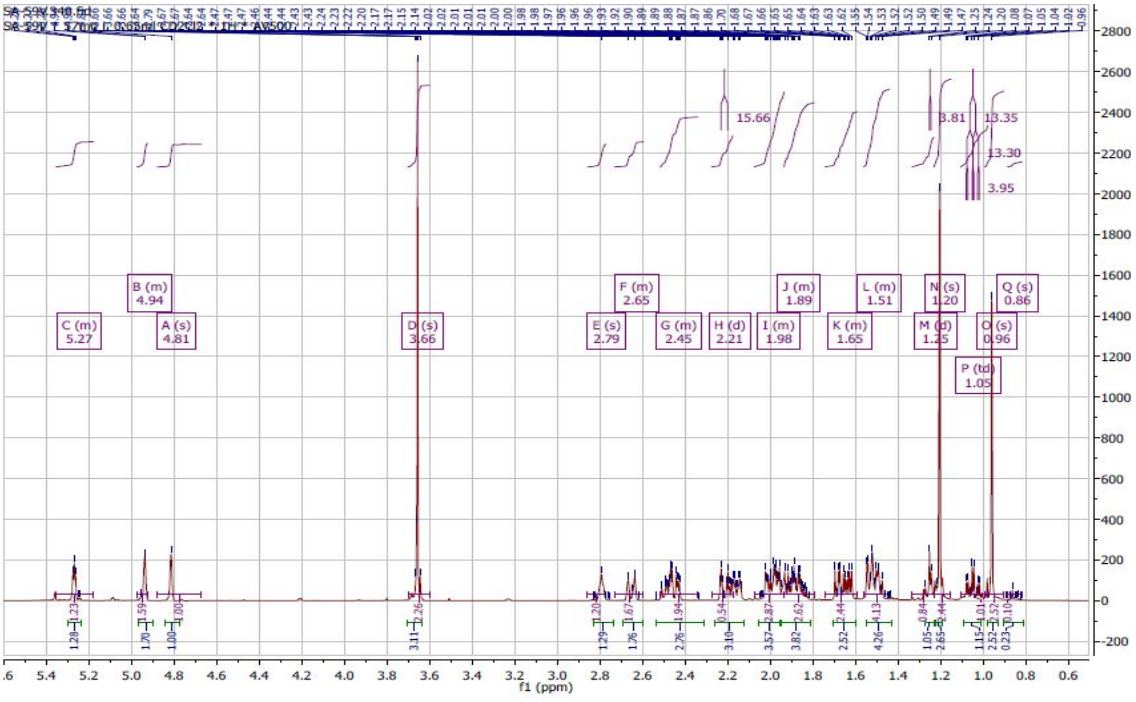

Appendix 85B: The ^{13}C NMR spectrum (125MHz) of methyl-*ent*-kaura-9(11),16-dien-19-oate (**270**) in CD_2Cl_2

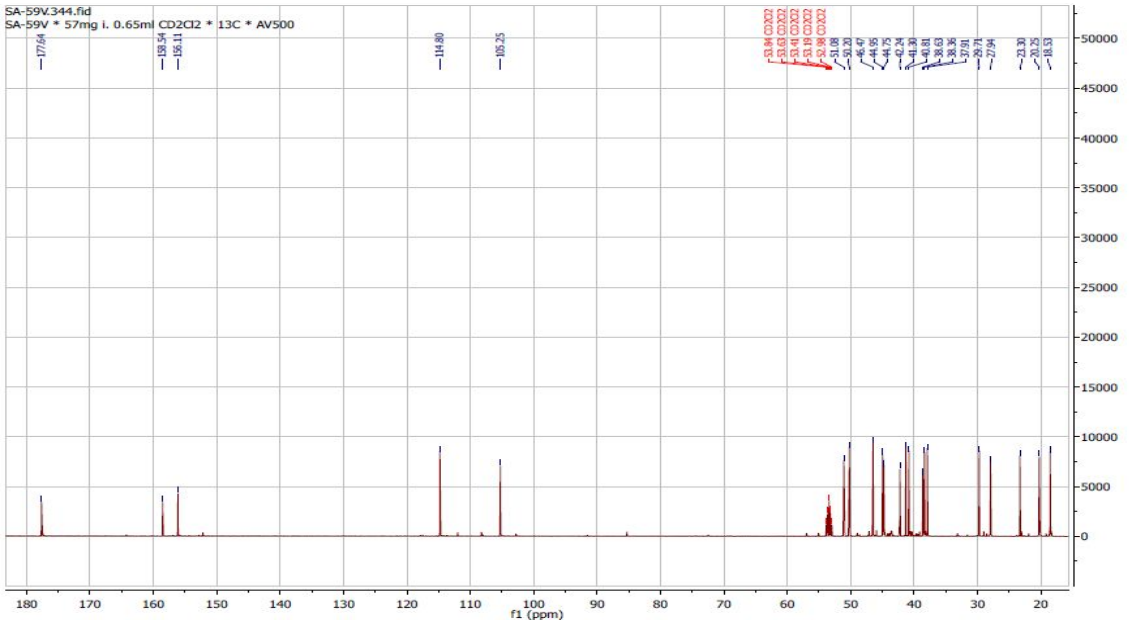

Appendix 86A: The ^{1}H NMR spectrum (500 MHz) of *ent*-kauran-19-oic acid (**271**) in Acetone-d_6

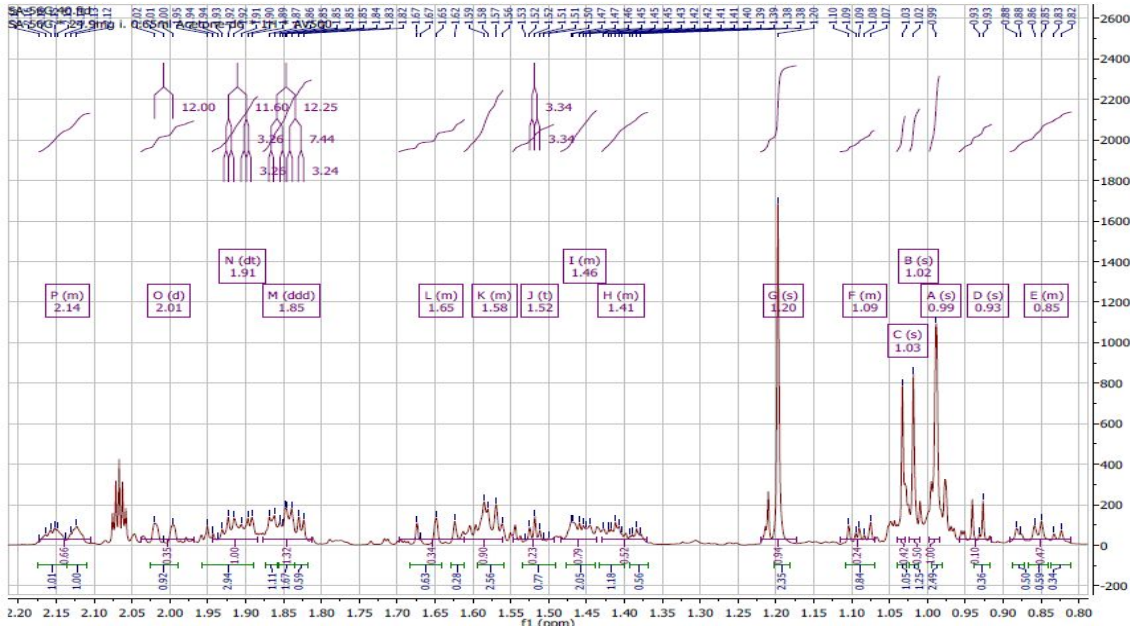

Appendix 86B: The ^{13}C NMR spectrum (125MHz) of *ent*-kauran-19-oic acid (**271**) in Acetone-d_6

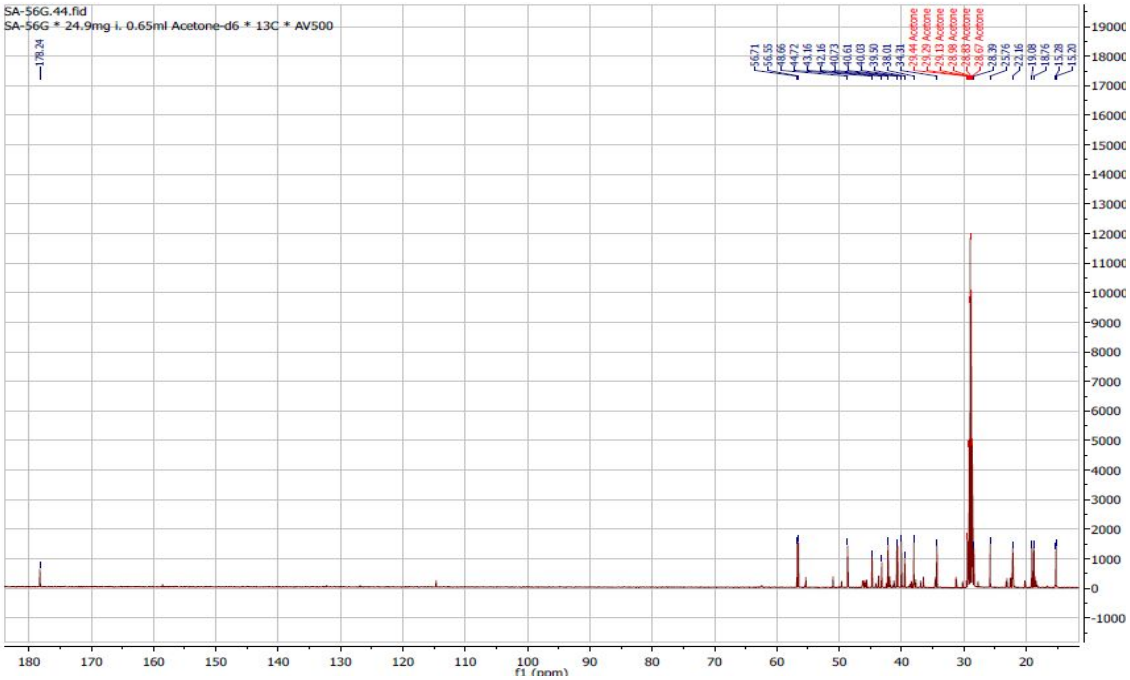

Appendix 86C: The H-H COSY spectrum of *ent*-kauran-19-oic acid (**271**) in Acetone-d_6

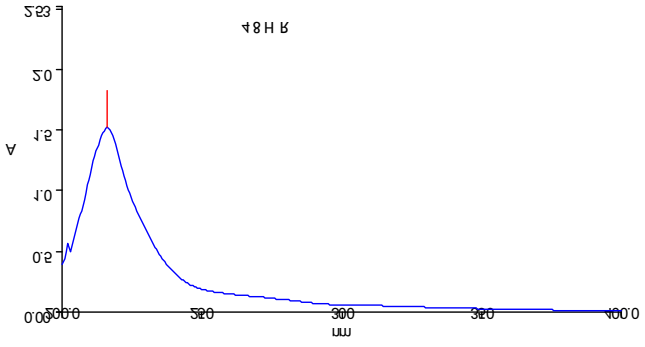

Appendix 4. Crystallographic analysis.

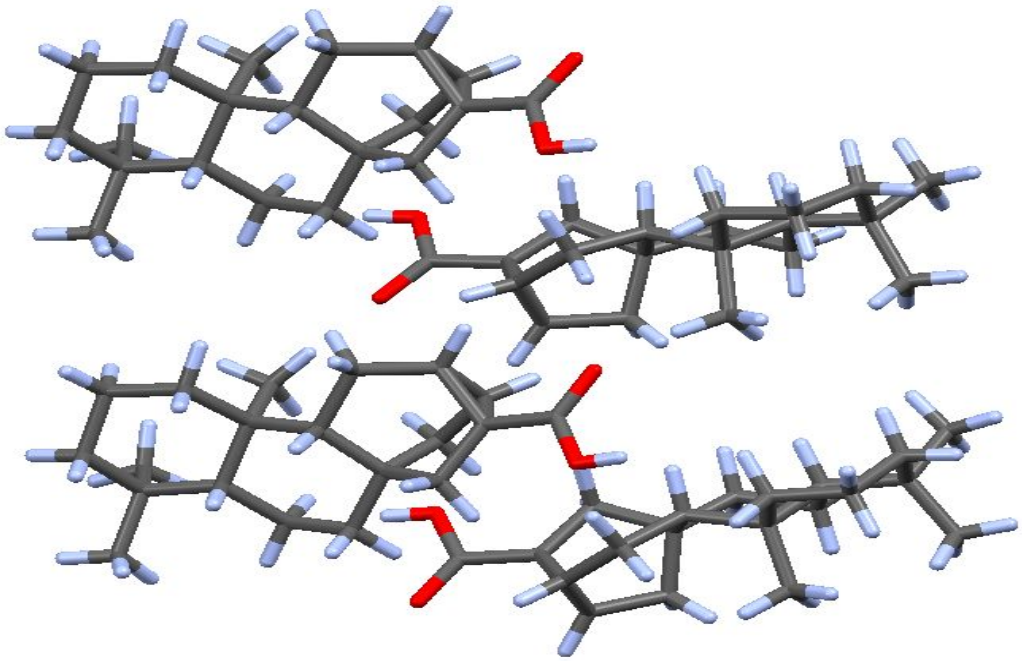

Figure S87 : Crystal structure of compound **205** showing double O-H···O intermolecular hydrogen bonding motifs common for carboxylic acid groups for all four independent molecules in asymmetric unit.

Table S1: Crystal data and refinement parameters for **236**, **237, 238** and **239**.

	236	**238**	**237**	**239**[a]
CCDC number	1868318	1868319	1868321	1868323
Formula	$C_{25}H_{36}O_5$	$C_{26}H_{38}O_5$	$C_{25}H_{36}O_5$	$C_{25}H_{36}O_4$
Formula weight	416.54	430.56	416.54	400.54
T [K]	120(2)	120(2)	170(2)	120(2)
Crystal system	orthorhombic	orthorhombic	hexagonal	monoclinic
Space group (number)	$P2_12_12_1$(19)	$P2_12_12_1$(19)	$P6_522$ (179)	$C2$ (5)
Unit cell dimensions				
a [Å]	8.68202(13)	8.31056(11)	14.07860(10)	11.1698(3)
b [Å]	10.84059(15)	10.89983(12)	14.07860(10)	8.5815(3)
c [Å]	23.5621(3)	25.1640(3)	39.5776(4)	23.5527(8)
β [°]	90	90	90	92.080(3)
V [Å^3]	2217.62(5)	2279.45(5)	6793.58(12)	2256.12(13)
Z	4	4	12	4
ρ_{calc}	1.248	1.255	1.222	1.179
μ [mm^{-1}]	0.684	0.681	0.670	0.618
F(000)	904	936	2712	872
Crystal size [mm]	0.18×0.14×0.13	0.28×0.23×0.09	0.24×0.10×0.09	0.17×0.14×0.03
θrange[°]	3.752 - 74.175	3.513- 74.341	3.794- 74.465	3.756- 73.896
Refl. collected	15950	39010	25659	7630
Independent refl.	4461	4596	4625	4415
R_{int}	0.0281	0.0534	0.0255	0.0243
Reflections[$I>2\sigma(I)$]	4307	4433	4411	3987
Completeness to θ	100.0	100.0	100.0	99.8
Max. /min. transm.	0.952 / 0.933	0.956/ 0.895	0.953/ 0.903	0.984/ 0.937
Restraints / parameters	14 / 280	175 / 343	0 / 279	58 / 281
Goodness-of-fit on F^2	1.027	1.067	1.029	1.047
Final Rindices [$I>2\sigma(I)$]	R1 = 0.0327, wR2 = 0.0856	R1 = 0.0417, wR2 = 0.1153	R1 = 0.0323, wR2 = 0.0863	R1 = 0.0464, wR2 = 0.1224
Rindices (all data)	R1 = 0.0342, wR2 = 0.0872	R1 = 0.0429, wR2 = 0.1167	R1 = 0.0343, wR2 = 0.0881	R1 = 0.0520, wR2 = 0.1285
Flack parameter	0.07(6)	-0.08(7)	0.01(6)	0.1(3)[a]
Largest peak/hole [e.Å^{-3}]	0.376 / -0.181	0.499/ -0.244	0.147/ -0.134	0.282 / -0.199

[a] Refined as a 2-component inversion twin: BASF = 0.14. Standard uncertainty of Flack parameter too high and reliable absolute structure determination was not possible.

Table S2: Crystal data and refinement parameters for **240**, **269** and **252**.

	240	**269**	**252**
CCDC number	1868320	1868324	1868322
Formula	$C_{20}H_{28}O_2$	$C_{20}H_{30}O_2$	$C_{20}H_{32}O_2$
Formula weight	300.42	302.44	304.45
T [K]	120(2)	120(2)	120(2)
Crystal system	monoclinic	orthorhombic	orthorhombic
Space group (number)	$P2_1$ (4)	$P2_12_12_1$ (19)	$P2_12_12_1$ (19)
Unit cell dimensions			
a [Å]	10.67468(12)	17.1810(2)	11.16620(10)
b [Å]	11.35748(12)	17.3156(2)	14.0602(2)
c [Å]	14.10077(16)	23.4406(3)	22.4854(3)
β [°]	99.0578(10)	90	90
V [Å^3]	1688.22(3)	6973.56(15)	3530.19(8)
Z	4 (Z' = 2)	16 (Z' = 4)	8 (Z' = 2)
ρ_{calc}	1.182	1.152	1.146
μ [mm^{-1}]	0.574	0.557	0.550
F(000)	656	2656	1344
Crystal size [mm]	0.30×0.21×0.16	0.42×0.16×0.12	0.23×0.14×0.06
θrange[°]	4.194 - 74.268	3.624 - 76.805	3.708- 74.202
Refl. collected	11890	140940	26113
Independentrefl.	6618	14476	7096
R_{int}	0.0244	0.0607	0.0259
Reflections[$I>2\sigma(I)$]	6366	13376	6706
Completeness to θ	99.8	99.9	100.0
Max. /min. transm.	0.925/ 0.895	0.950/ 0.854	0.965/ 0.909
Restraints / parameters	3 / 403	215 / 867	2 / 403
Goodness-of-fit on F^2	1.035	1.031	1.025
Final Rindices [$I>2\sigma(I)$]	R1 = 0.0340, wR2 = 0.0849	R1 = 0.0517, wR2 = 0.1335	R1 = 0.0383, wR2 = 0.1021
Rindices (all data)	R1 = 0.0355, wR2 = 0.0872	R1 = 0.0555, wR2 = 0.1370	R1 = 0.0408, wR2 = 0.1044
Flack parameter	-0.06(9)	0.10(5)	-0.05(7)
Largest peak/hole [e.Å^{-3}]	0.225/ -0.158	0.337/ -0.329	0.209/ -0.190

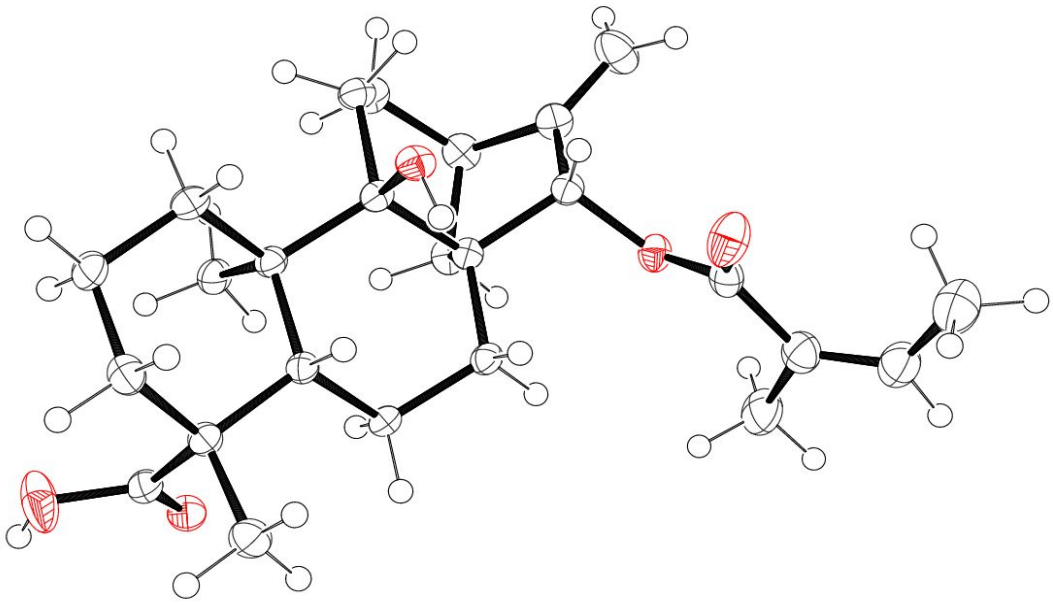

Figure S88. Thermal ellipsoid diagram of **236** (ellipsoid probability 50 %).

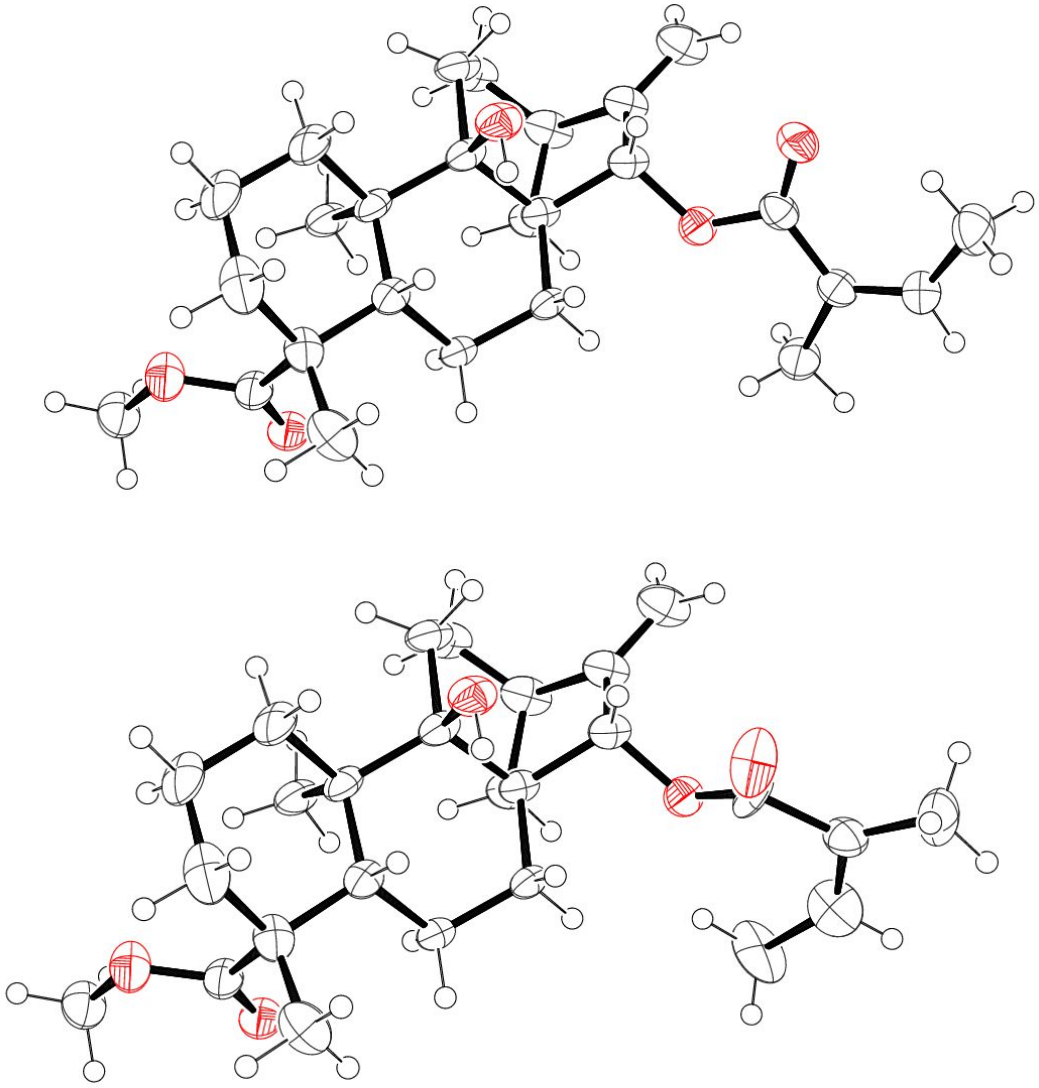

Figure S89. Thermal ellipsoid diagrams of **238** (ellipsoid probability 50 %) showing two different and equal (~1:1) spatial orientations of (*Z*)-2-methylbut-2-enoyl group.

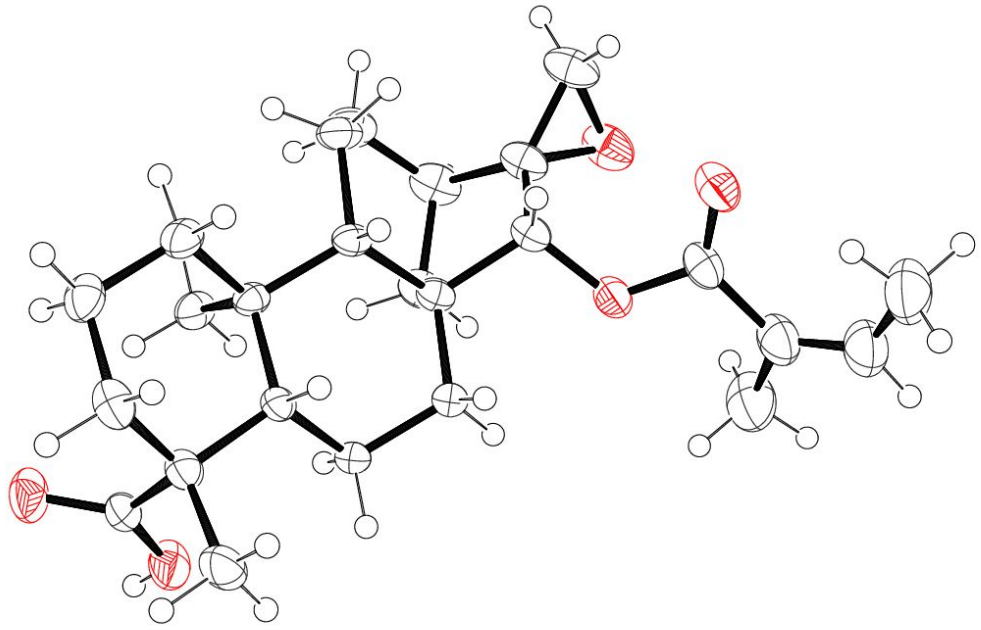

Figure S90. Thermal ellipsoid diagram of **237** (ellipsoid probability 50%).

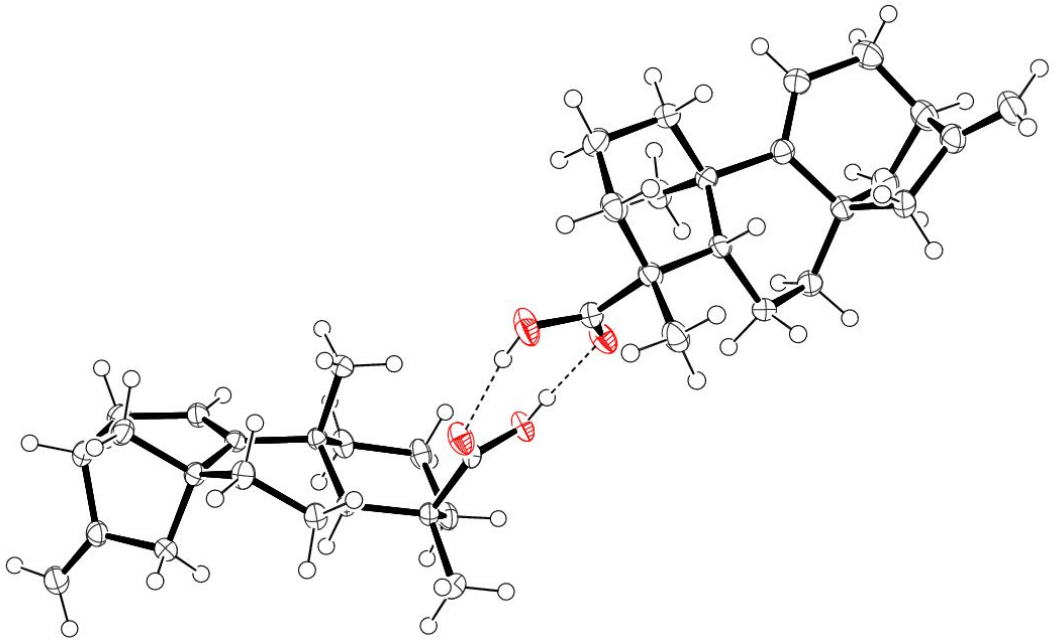

Figure S91. Thermal ellipsoid diagram of **240** (ellipsoid probability 50 %) showing both crystallographically independent molecules in asymmetric unit (AU) and hydrogen bonding (dashed) between them. This corresponds the reported structure by Reynolds. *et. al.* [35].

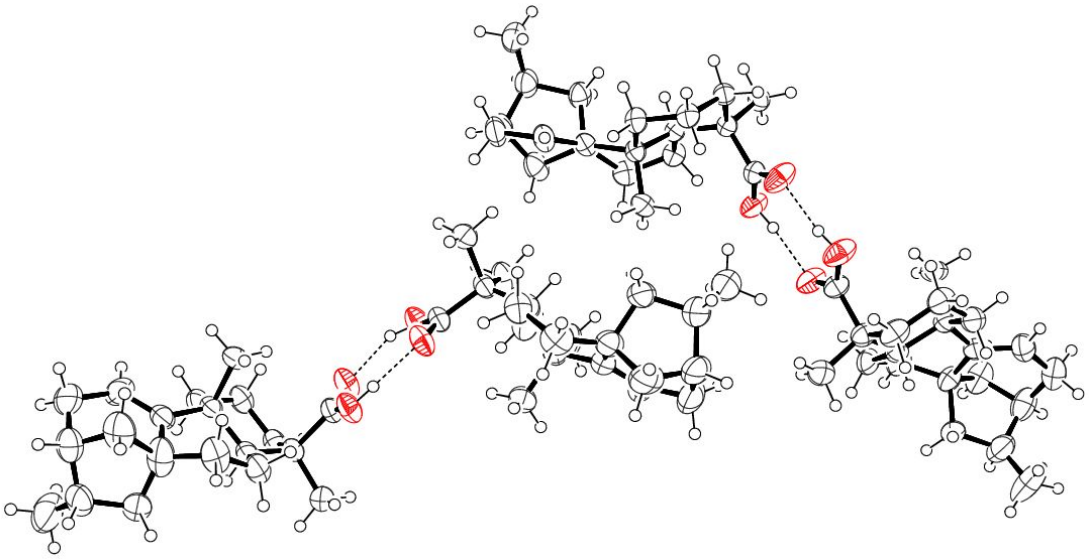

Figure S92. Thermal ellipsoid diagram of **269** (ellipsoid probability 50 %) showing twohydrogen-bonded molecular pairs composed by four crystallographically independent molecules in AU.

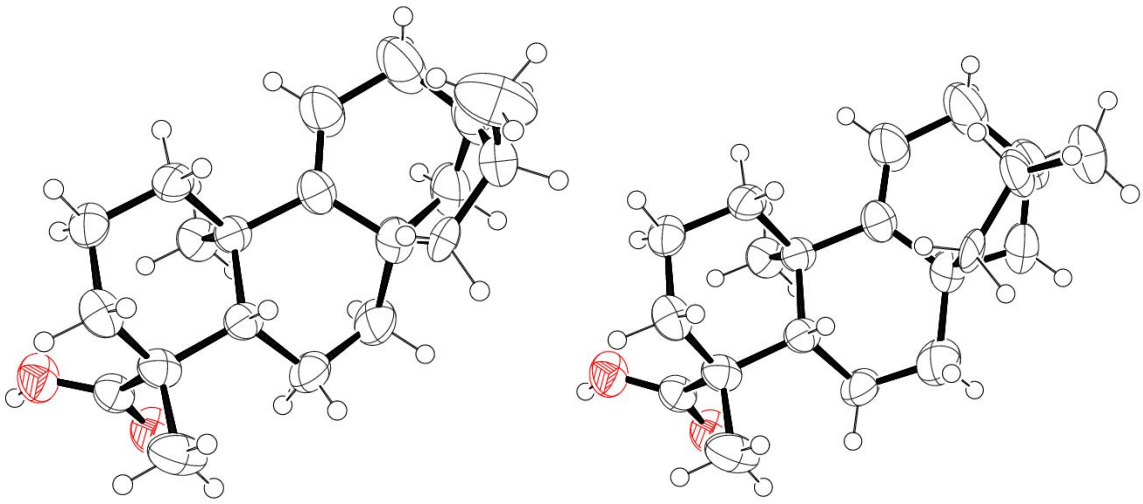

Figure S93. Two different conformations (~90:10 left/right) in aliphatic rings of **269**.

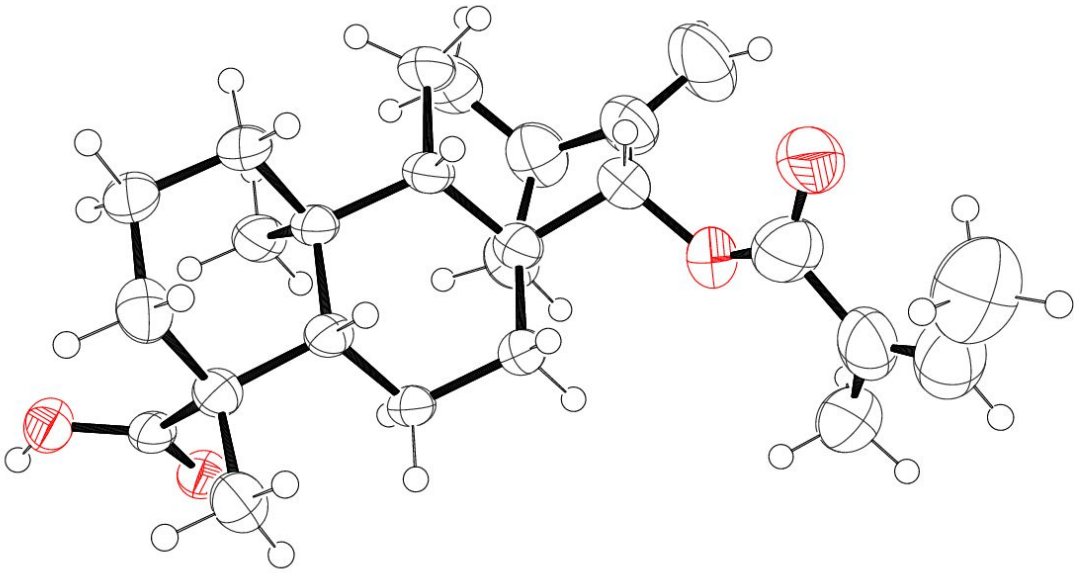

Figure S94. Thermal ellipsoid diagram of **239** (ellipsoid probability 50 %).

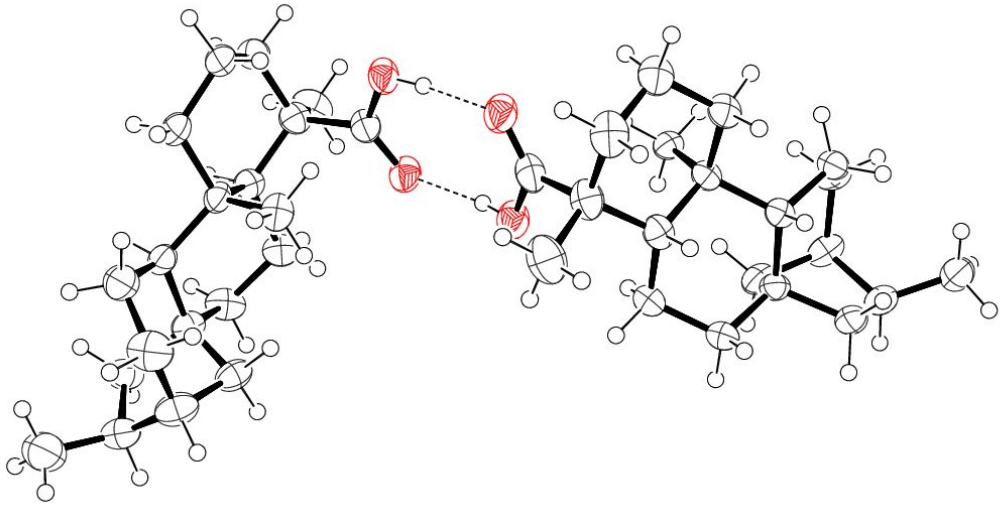

Figure S95. Thermal ellipsoid diagram of **252** (ellipsoid probability 50 %) showing ahydrogen-bonded molecular pair composed by two crystallographically independent molecules in AU.

Table S3. Hydrogen bonding geometries in structures **236**, **238**, **237**, **240**, **269**, **239** and **252**.

D-H...A	*d*(D-H) [Å]	*d*(H...A) [Å]	*d*(D...A) [Å]	<(DHA) [°]
236				
O(19b)-H…O(21)[a]	0.83(2)	1.92(3)	2.690(2)	155(4)
O(9)-H…O(19a)[b]	0.85(2)	2.05(2)	2.835(2)	152(3)
238				
O(9)-H…O(19)[a]	0.90(2)	2.03(3)	2.839(3)	149(3)
237				
O(19b)-H...O(19a)[c]	0.82(6)	1.78(6)	2.594(3)	171(6)
O(19a)-H...O(19b)[c]	0.90(5)	1.74(5)	2.634(3)	176(6)
240				
O(19b)-H...O(19c)[d]	0.85(2)	1.78(2)	2.625(2)	177(3)
O(19d)-H...O(19a)[d]	0.83(2)	1.81(2)	2.637(2)	171(4)
269				
O(19b)-H...O(O19c)[d]	0.84(3)	1.75(3)	2.586(3)	176(11)
O(19a)-H...O(19d)[d]	0.85(3)	1.82(4)	2.658(3)	167(10)
O(19d)-H...O(19a)[d]	0.84(3)	1.84(4)	2.658(3)	163(10)
O(19c)-H...O(19b)[d]	0.85(3)	1.78(5)	2.586(3)	156(10)
O(19f)-H...O(19g)[e]	0.86(2)	1.82(3)	2.662(3)	168(5)
O(19h)-H...O(19e)[e]	0.88(3)	1.79(3)	2.633(3)	162(5)
239				
O(19b)-H...O(19a)[f]	0.81(3)	1.83(3)	2.639(2)	176(10)
O(19a)-H...O(19b)[f]	0.82(3)	1.82(3)	2.639(2)	171(9)
252				
O(19b)-H...O(19c)[g]	0.84(2)	1.79(2)	2.617(2)	170(3)
O(19d)-H...O(19a)[g]	0.84(2)	1.80(2)	2.632(3)	167(4)

[a] -x+1,y+1/2,-z+3/2, [b] -x+1,y-1/2,-z+3/2, [c] -y+2,-x+2,-z+7/6 (half occupancy for H-atom positions), [d] O(19c) and O(19d) atoms of second molecule in AU (half occupancy for H-atom positions), [e] O(19e) and O(19f) are atoms of third as well as O(19g) and O(19h) are atoms of fourth molecule in (AU), [f]-x+1,y,-z+1 (half occupancy for H-atom positions), [g] O(19c) and O(19d) atoms of second molecule in AU

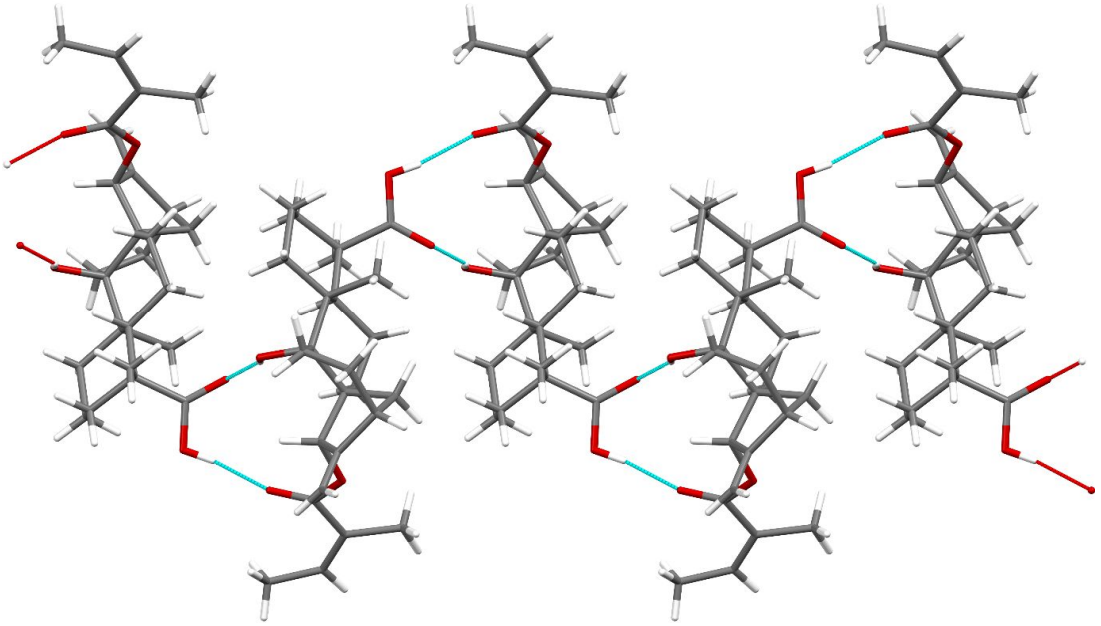

Figure S96. A motif along crystallographic *b* axis formed by O(9)-H···O(19a) and O(19b)-H···O(21) intermolecular hydrogen bonds (viewed along *a*) in **236**. Hydrogen bonding contacts are shown as turquoise (expanded) or red (hanging) stick model.

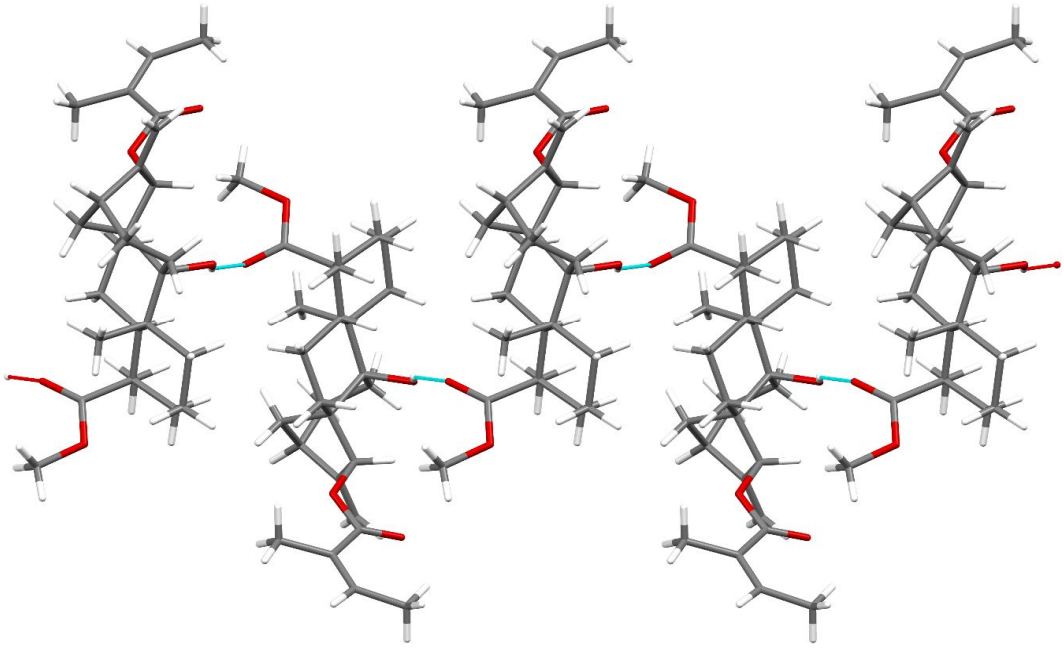

Figure S97. A motif along crystallographic *b* axis formed by O(9)-H···O(19a) intermolecular hydrogen bonds (viewed along *a*) in **238**. Hydrogen bonding contacts are shown as turquoise (expanded) or red (hanging) stick model.

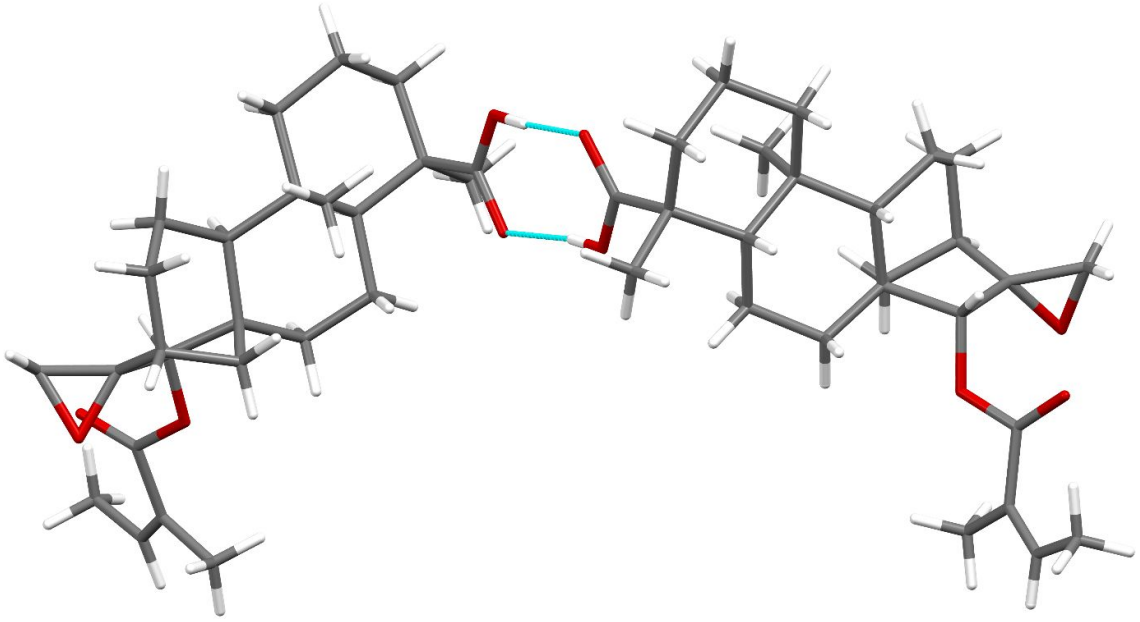

Figure S98. Ahydrogen-bonded molecular pair composed by two molecules of **237**. Hydrogen bonding contacts are shown as turquoise stick model.

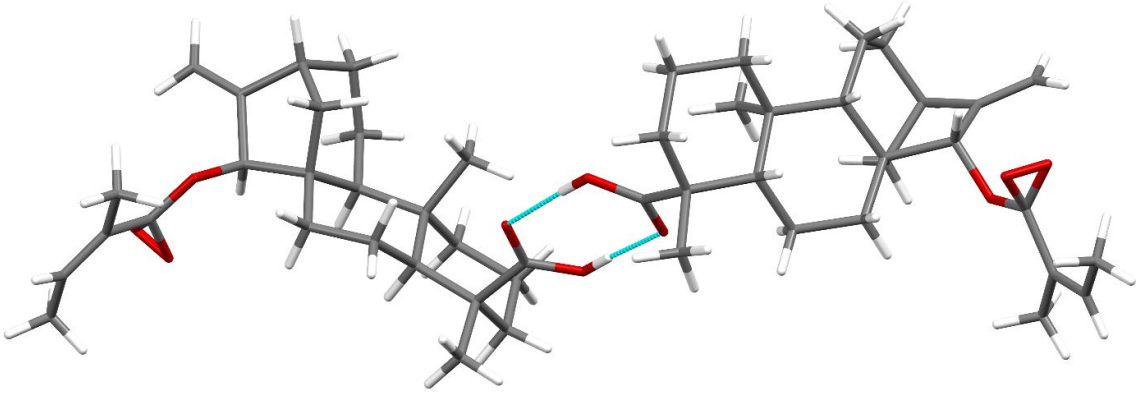

Figure S99. Ahydrogen-bonded molecular pair composed by two molecules of **239**. Hydrogen bonding contacts are shown as turquoise stick model.

Appendix 5: Publications from this PhD work

I. List of Publications and Public Presentations

A. Articles

1. Souaibou Yaouba, Andreas Koch, Eric M. Guantai, Solomon Derese, Beatrice Irungu, Matthias Heydenreich, Abiy Yenesew (2017). Alkenyl Cyclohexanone Derivatives from *Lannea rivae* and *Lannea schweinfurthii, Phytochemistry Letters* **23**, 141-148.

2. Souaibou Yaouba, Arto Valkonen, Paolo Coghi, Jiaying Gao, Eric M. Guantai, Solomon Derese, Vincent K. W. Wong, Máté Erdélyi and Abiy Yenesew (2018). Crystal Structures and Cytotoxicity of *ent*-Kaurane-Type Diterpenois from Two *Aspilia Species, Molecules.*

3. Souaibou Yaouba, Arto Valkonen, Sofia Lindblad, Paolo Coghi, Eric M. Guantai, Solomon Derese, Beatrice Irungu, Jacob O. Midiwo, Vincent K. W. Wong, , Abiy Yenesew and Máté Erdélyi, *Journal of Natural Products* (In preparation).

4. Souaibou Yaouba, Arto Valkonen, Paolo Coghi, Eric M. Guantai, Solomon Derese, Matthias Heydenreich, Vincent K. W. Wong, Máté Erdélyi, Abiy Yenesew, Antimicrobial. Anti-inflammatory and Hypoglycemic Activity of Phytochemicals isolated from *Psiadia punctulata* and their Synthetic Analogues, *Natural Product Research* (In preparation).

B. Book Chapter

1. Solomon Derese, Eric M. Guantai, **Yaouba Souaibou**, Victor Kuete (2017). *Mangifera indica* L. (Anacardiaceae) in "Medicinal Spices and Vegetables from Africa, Therapeutic Potential against Metabolic, Inflammatory, Infectious and Systemic Diseases", *Academic Press*, Elsevier, Oxford OX5 1GB, United Kingdom, ISBN: 9780128092866, 1-694. DOI: 10.1016/B978-0-12-809286-6.00021-2.

C. Public presentations

1. Souaibou Yaouba, Andreas Koch, Eric M. Guantai, Solomon Derese, Beatrice Irungu, Matthias Heydenreich, Abiy Yenesew (2018). Anti-inflammatory and Cytotoxic Phytochemicals from *Lannea rivae* and *Lannea Schweinfurthii.* Paper presented at PACN

Congress 2018. managing resources through chemistry: Wealth not waste, University of Nairobi, Nairobi, Kenya

2. Souaibou Yaouba, Eric M. Guantai, Valkonen Arto, Solomon Derese, Beatrice Irungu, Matthias Heydenreich, Paolo Coghi, Vincent Wong, Máté Erdélyi and Abiy Yenesew (2018). *Ent*-kaurene Diterpenes from *Aspilia pluriseta* and *Aspilia mossambicensis*. Paper presented at NAPRECA Conference, *Utilization of Natural Products for the betterment of the livelihood of Mankind*, Jomo Kenyatta University of Agriculture and Technology, Nairobi, Kenya.

3. Souaibou Yaouba, Andreas Koch, Eric M. Guantai, Solomon Derese, Beatrice Irungu, Matthias Heydenreich, Abiy Yenesew (2018). Phytochemical Investigation of *Psiadia punctulata* for Antimicrobial and Cytotoxic Principles. Paper presented at DAAD Winter school, Technical University of Dortmund. *Natural products: Chromatography, spectroscopy and biological aspects*, TU Dortmund, Dortmund, Germany.

4. Souaibou Yaouba, Matthias Heydenreich, Jacob O. Midiwo, Máté Erdélyi, Abiy Yenesew. New trachylobanes and kaurene diterpenes from *Psiadia punctulata* (2017). Paper presented at Goteborg University, Goteborg, Sweden.

Souaibou Yaouba[1],

II. Publications

A. First paper

Phytochemistry Letters 23 (2018) 141–148

Contents lists available at ScienceDirect

Phytochemistry Letters

journal homepage: www.elsevier.com/locate/phytol

Alkenyl cyclohexanone derivatives from *Lannea rivae* and *Lannea schweinfurthii*

Souaibou Yaouba[a], Andreas Koch[b], Eric M. Guantai[c], Solomon Derese[a], Beatrice Irungu[d], Matthias Heydenreich[b], Abiy Yenesew[a,*]

[a] Department of Chemistry, University of Nairobi, P.O. Box 30197-00100, Nairobi, Kenya
[b] Institut für Chemie, Universität Potsdam, Karl-Liebknecht-Str. 24-25, D-14476 Potsdam, Germany
[c] School of Pharmacy, University of Nairobi, P.O. Box 19676-00202, Nairobi, Kenya
[d] Centre for Traditional Medicine and Drug Research, Kenya Medical Research Institute, P.O. Box 54840-00200, Nairobi, Kenya

ARTICLE INFO

Keywords:
Lannea rivae
Lannea schweinfurthii
Alkenyl cyclohexenone
Alkenyl cyclohexanone
Anti-inflammatory
Cytotoxicity
Antimicrobial

ABSTRACT

Phytochemical investigation of the CH_2Cl_2/MeOH (1:1) extract of the roots of *Lannea rivae* (Chiov) Sacleux (Anacardiaceae) led to the isolation of a new alkenyl cyclohexenone derivative: (4*R*,6*S*)-4,6-dihydroxy-6-((*Z*)-nonadec-14′-en-1-yl)cyclohex-2-en-1-one (**1**), and a new alkenyl cyclohexanol derivative: (2*S**,4*R**,5*S**)-2,4,5-trihydroxy-2-((*Z*)-nonadec-14′-en-1-yl)cyclohexanone (**2**) along with four known compounds, namely epicatechin gallate, taraxerol, taraxerone and β-sitosterol; while the stem bark afforded two known compounds, daucosterol and lupeol. Similar investigation of the roots of *Lannea schweinfurthii* (Engl.) Engl. led to the isolation of four known compounds: 3-((*E*)-nonadec-16′-enyl)phenol, 1-((*E*)-heptadec-14′-enyl)cyclohex-4-ene-1,3-diol, catechin, and 1-((*E*)-pentadec-12′-enyl)cyclohex-4-ene-1,3-diol. The structures of the isolated compounds were determined by NMR spectroscopy and mass spectrometry. The absolute configuration of compound **1** was established by quantum chemical ECD calculations. In an antibacterial activity assay using the microbroth kinetic method, compound **1** showed moderate activity against *Escherichia coli* while compound **2** exhibited moderate activity against *Staphylococcus aureus*. Compound **1** also showed moderate activity against *E. coli* using the disc diffusion method. The roots extract of *L. rivae* was notably cytotoxic against both the DU-145 prostate cancer cell line and the Vero mammalian cell line (CC_{50} = 5.24 and 5.20 μg/mL, respectively). Compound **1** was also strongly cytotoxic against the DU-145 cell line (CC_{50} = 0.55 μg/mL) but showed no observable cytotoxicity (CC_{50} > 100 μg/mL) against the Vero cell line. The roots extract of *L. rivae* and *L. schweinfurthii*, epicatechin gallate as well as compound **1** exhibited inhibition of carageenan-induced inflammation.

1. Introduction

The genus *Lannea* (Anacardiaceae) comprises of about 40 species occurring in tropical Africa and Asia (Kokwaro, 1994). *Lannea rivae* (Chiov) Sacleux is a deciduous shrub or small tree with a flat spreading crown, widely distributed in Eastern Africa including Kenya, Uganda, Ethiopia and Tanzania (Kokwaro, 1994). The stem bark and roots of *L. rivae* are used to treat cough, cold and stomach-ache (Kipkore et al., 2014; Okoth et al., 2016). *Lannea schweinfurthii* (Engl.) Engl. is a small to medium-sized tree distributed in Kenya, Uganda, Tanzania, Malawi, Mozambique, Zambia, Zimbabwe, Swaziland and South Africa (Kindt et al., 2011; Kokwaro, 1994). Infusions of the roots of *L. schweinfurthii* are reported to enhance memory and are also used as a sedative (Seoposengwe et al., 2013). The roots of *L. schweinfurthii* have been reported to show very good radical scavenging activity and the plant was not toxic to human neuroblastoma SH-SY5Y cells at 100 μg/mL (Adewusia et al., 2013).

Lannea species elaborate tetracyclic and pentacyclic triterpenes, bifuran derivatives (Yun et al., 2014), phenolic lipids, alkyl cyclohexenol and alkyl cyclohexenone derivatives (Okoth and Koorbanally, 2015; Queiroz et al., 2003), tannins, benzoic acid derivatives (Islam et al., 2002; Kapche et al., 2007) and flavonoids (Islam and Tahara, 2000; Muhaisen, 2013; Okoth et al., 2013; Reddy et al., 2011; Sultana and Ilyas, 1986). Alkyl phenols, alkenyl cyclohexenones and other phytochemical constituents have been reported from *L. rivae* (Okoth et al., 2016), while the only report on *L. schweinfurthii* is on the biological activity of the crude extract (Adewusia et al., 2013).

In this study, the isolation and characterization of a new alkenyl cyclohexenone derivative (**1**) and a new alkenyl cyclohexanone derivative (**2**) from *L. rivae* along with six known compounds are reported.

* Corresponding author.
E-mail address: ayenesew@uonbi.ac.ke (A. Yenesew).

https://doi.org/10.1016/j.phytol.2017.12.001
Received 9 October 2017; Received in revised form 29 November 2017; Accepted 5 December 2017
1874-3900/ © 2017 Phytochemical Society of Europe. Published by Elsevier Ltd. All rights reserved.

B. Second paper

molecules

MDPI

Article

Crystal Structures and Cytotoxicity of *ent*-Kaurane-Type Diterpenoids from Two *Aspilia* Species

Souaibou Yaouba [1], Arto Valkonen [2], Paolo Coghi [3], Jiaying Gao [3], Eric M. Guantai [4], Solomon Derese [1], Vincent K. W. Wong [3], Máté Erdélyi [5,6,7,*] and Abiy Yenesew [1,*]

[1] Department of Chemistry, University of Nairobi, P. O. Box 30197, 00100 Nairobi, Kenya; yaoubas@gmail.com (S.Y.); sderese@uonbi.ac.ke (S.D.)
[2] Department of Chemistry, University of Jyvaskyla, P.O. Box 35, 40014 Jyvaskyla, Finland; arto.m.valkonen@jyu.fi
[3] State Key Laboratory of Quality Research in Chinese Medicine/Macau Institute for Applied Research in Medicine and Health, Macau University of Science and Technology, Macau 999078, China; coghips@must.edu.mo (P.C.); cubix48@163.com (J.G.); bowaiwong@gmail.com (V.K.W.W.)
[4] Department of Pharmacology and Pharmacognosy, School of Pharmacy, University of Nairobi, P. O. Box 19676, 00202 Nairobi, Kenya; eguantai@uonbi.ac.ke
[5] Department of Chemistry–BMC, Uppsala University, Husargatan 3, 75237 Uppsala, Sweden
[6] The Swedish NMR Centre, Medicinaregatan 5, 40530 Gothenburg, Sweden
[7] Department of Chemistry and Molecular Biology, University of Gothenburg, 40530 Gothenburg, Sweden
* Correspondence: mate.erdelyi@kemi.uu.se (M.E.); ayenesew@uonbi.ac.ke (A.Y.); Tel.: +46-72-999-9166 (M.E.); +254-73-383-2576 (A.Y.); Fax: +254-20-444-6138 (A.Y.)

Academic Editors: Isabel C.F.R. Ferreira and Nancy D. Turner

Received: 11 November 2018; Accepted: 30 November 2018; Published: 4 December 2018

Abstract: A phytochemical investigation of the roots of *Aspilia pluriseta* led to the isolation of *ent*-kaurane-type diterpenoids and additional phytochemicals (**1**–**23**). The structures of the isolated compounds were elucidated based on Nuclear Magnetic Resonance (NMR) spectroscopic and mass spectrometric analyses. The absolute configurations of seven of the *ent*-kaurane-type diterpenoids (**3**–**6**, **6b**, **7** and **8**) were determined by single crystal X-ray diffraction studies. Eleven of the compounds were also isolated from the roots and the aerial parts of *Aspilia mossambicensis*. The literature NMR assignments for compounds **1** and **5** were revised. In a cytotoxicity assay, 12α-methoxy-*ent*-kaur-9(11),16-dien-19-oic acid (**1**) (IC_{50} = 27.3 ± 1.9 μM) and 9β-hydroxy-15α-angeloyloxy-*ent*-kaur-16-en-19-oic acid (**3**) (IC_{50} = 24.7 ± 2.8 μM) were the most cytotoxic against the hepatocellular carcinoma (Hep-G2) cell line, while 15α-angeloyloxy-16β,17-epoxy-*ent*-kauran-19-oic acid (**5**) (IC_{50} = 30.7 ± 1.7 μM) was the most cytotoxic against adenocarcinomic human alveolar basal epithelial (A549) cells.

Keywords: Asteraceae; *Aspilia pluriseta*; *Aspilia mossambicensis*; *ent*-kaurane diterpenoid; X-ray crystal structure; cytotoxicity

1. Introduction

The genus *Aspilia* belongs to the family Asteraceae. The majority of plants in this family are herbaceous, while trees and shrubs are rare [1]. Plants belonging to the Asteraceae family are found worldwide, except Antarctica [2]. They are found in cooler montane habitats or temperate areas in tropical regions, and are not common dwellers of hot lowland tropical rain forests [1,2]. The family of Asteraceae is one of the largest plant families and the richest in vascular plants in the world. The family has about 1,600–1,700 genera and 24,000–30,000 species [1,3,4]. Plants from the genus *Aspilia* (Asteraceae) occur widely in South, South-West, and West Kenya, from the coast to Lake Victoria.

C. Third paper

Cytotoxic Trachylobane and Kaurane Diterpenes from *Psiadia punctulata*

Souaibou Yaouba[†], *Arto Valkonen*, *Sofia Lindblad, Paolo Coghi, Eric M. Guantai*, *Solomon Derese, Beatrice Irungu*, *Jacob O. Midiwo, Vincent K. W. Wong, Abiy Yenesew*, *Máté Erdélyi*

Abstract

Five new trachylobane diterpenes: *ent*-trachyloban-17-oic acid (1), (*rel*)-17-hydroxytrachyloban-20-oic acid (2), (*rel*)-6*β*,18,19-trihydroxytrachyloban-2-one (3), trachyloban-2*β*,18,19-triol (4) and (*rel*)-trachyloban-*2α*,*6α*,19-triol (5), and a new kaurene diterpene: (*rel*)-15*β*,16*α*,17-trihydroxy-trachyloban-19-oic methyl ester (6) have been isolated from the leaves and roots of *Psiadia punctulata* (Asteraceae). In addition, known triterpenes, trachylobane and kaurene diterpenes, sesquiterpenes, fatty acids and flavones were identified from the leaves, roots and stem bark of this plant. The structures were elucidated on the basis of NMR spectroscopy and mass spectrometry. The crystal structures of nine diterpenes are reported through single crystal X-ray crystallography, and showed that the plant produces both "normal"- and *enatio*- trachylobane and kaurane diterpenes. These results are against the assumption that natural trachylobane and kaurene diterpenes belong to the *enantio*-series; and that absolute configuration of such diterpenese should only be proposed based on sound evidence. In a cytotoxicity assay the leaves (CC_{50} = 2.3 ± 0.1 μg/mL) and stem bark (CC_{50} = 9.5 ± 0.1 μg/mL) extracts were active against Vero kidney cancer cell line. Some of the isolated compounds and their derivatives were also tested for cytotoxicity against 2 normal (BEAS-2B and LO_2) and 4 cancerous (A549, Hep-G2, Vero and DU-145) cell lines. Among these, 6*β*,18,19-trihydroxy-*ent*-trachyloban-2-one (3) with CC_{50} value of 6.41±0.2 μM against the Hep-G2 (human liver cancer cell line), and 2*β*,6*β*,19-trihydroxy-*ent*-trachylobane (12) with CC_{50} = 3.4 ± 0.1 μM against DU-145 (prostate cancer cell line) were the most active, without toxicity (CC_{50} >100 μM) towards the normal cell lines, BEAS-2B and LO_2.

Keywords: *Psiadia punctulata,* Asteraceae*,* kaurane diterpene, trachylobane diterpene, cytotoxicity

D. Fourth Paper

Antimicrobial, Anti-inflammatory and Hypoglycemic Activity of Phytochemicals isolated from *Psiadia punctulata* and their Synthetic Analogues

Souaibou Yaouba[a], *Arto Valkonen*[b], *Paolo Coghi*[c], *Eric M. Guantai*[d], *Solomon Derese*[a], *Matthias Heydenreich*[e], *Vincent K. W. Wong*[c], *Máté Erdélyi*[f,g,„,Ω,*], *Abiy Yenesew*[a,*]

Abstract

Three new flavones; 5-acetyloxy-7,2',3',4',5'-pentamethoxy-flavone (**1**); 6,8-dibromo, 5-hydroxy-7,2',3',4',5'-pentamethoxy-flavone (**2**), 6,8-dibromo- 5,7-dihydroxy-7,2',3',4',5'-pentamethoxy-flavone (**3**) and three new trachylobane diterpene derivatives; 6β,18,19-trihydroxy-*ent*-trachyloban-2*N*-oxime (**4**), 2-oxo-6β -hydroxy-*ent*-trachyloban-18,19-dioic acid (**5**), 17-methoxy-*ent*-trachyloban-6β,19-diol (**6**) together with known compounds (**7-9**) have been synthetically derived from the isolated compounds of *Psiadia punctulata*. The structural elucidation has been carried out based on NMR spectroscopy and mass spectrometry. *Ent*-16β, 17-dihydroxykaur-20-oic acid was moderately active against *E. coli* inhibiting 48.48% of bacteria at a concentration of 160 µg/ml. This compound was also the most hypoglycemic agent, reducing the blood glucose to 159.5 ± 24.4 mg/dL after 60 minutes post glucose administration as compared to the drug standard, metformin. 5-hydroxy-7,2',3',4',5'-pentamethoxy-flavone was the most active against carrageenan-induced inflammation reducing the paw volume to 1.38 ± 0.08 ml, 240 minutes post carrageenan administration.

Keywords: *Psiadia punctulata,* Asteraceae, Trachylobane diterpenes, Pyrazole, Antimicrobial activity, Anti-inflammatory activity, Hypoglycemic activity.